Surface-sediment composition and sedimentary processes in the central Arctic Ocean and along the Eurasian Continental Margin

---

Edited by
Ruediger Stein, Gennadij I. Ivanov,
Michael A. Levitan, and Kirsten Fahl

Ber. Polarforsch. 212 (1996)
ISSN 0176 - 5027

Surface-sediment composition and sedimentary processes in the central Arctic Ocean and along the Eurasian Continental Margin

Ruediger Stein
Alfred Wegener Institute for Polar and Marine Research
Columbusstraße, Bremerhaven, Germany
e-mail: rstein@awi-bremerhaven.de

Gennadij I. Ivanov
All-Russian Research Institute for Geology and Mineral Resources
VNIIOKEANGEOLOGIA, St. Petersburg, Russia
e-mail: givanov@sovam.com

Michael A. Levitan
P.P. Shirshov Institute of Oceanology, The Russian Academy of Sciences, Moscow, Russia
e-mail: mlevitan@sedim.msk.ru

Kirsten Fahl
Alfred Wegener Institute for Polar and Marine Research
Columbusstraße, Bremerhaven, Germany
e-mail: kfahl@awi-bremerhaven.de

TABLE OF CONTENT

Preface

The Arctic Ocean and its marginal seas are key areas for understanding the global climate system and its change through time. The deep-water exchange between the Arctic and Atlantic Oceans, for example, is a major driver of the global thermohaline circulation controlling global heat transfer and climate. The permanent Arctic sea-ice cover with its strong seasonal variations in the marginal areas has a strong influence on the earth´s albedo, the marine ecosystem, and the oceanic circulation, which are also all major mechanisms effecting the global climate.

The main goal of numerous past, ongoing, and planned Arctic environmental research projects is a better understanding of the evolution and present state of the Arctic system with emphasis on the questions of how the Arctic will impact the global climate system and how it will be influenced in response. For realistic simulation of climatic models that deal with the future development of the earth climate and take into account the greenhouse effect, it is necessary to reconstruct as quantitatively as possible the Arctic environment in the course of time. The understanding of the natural variability of climate and environment is also absolutely necessary to asses disturbances caused by man on nature in the Arctic environment and Arctic societies.

In the Eurasian Arctic, a huge amount of sedimentological, geochemical, and paleontological data were collected by Russian scientists over the past decades; most of the data, however, was not open for the western literature. Because of the political reorganisation of the former Soviet Union in the most recent past, Russian institutions are getting more and more involved in the international exploration of the Arctic and making their experience, technical facilities, and data available to the international scientific community. Joint American-European-Russian expeditions into the Eurasian continental margin and neighbouring deep sea basins have been carried out during the last years and are also planned for the coming years. The results of international multidisciplinary investigations of material from these expeditions will greatly advance our knowledge on Arctic Ocean paleoenvironment and its relationship to the earth´s climate system.

The major aim of this book is to publish results of - especially Russian - studies dealing with modern sedimentary processes (Fig. 1) and its geological record in the central Arctic Ocean and the adjacent Eurasian shelf seas. For example, the terrigenous sediment supply and its shelf-to-basin transport in the eastern Arctic Ocean is mainly controlled by river discharge, oceanic currents, sea-ice (and iceberg) transport, and down-slope transport. Most of these mechanisms also influence biological processes in the water column as well as at the sea floor (i.e., surface-water productivity, particle fluxes through the water column, benthic activities at the sea floor, organic carbon export and burial, etc.). The understanding of the modern processes controlling the sedimentation is the key of the interpretation of the fossil records and the reconstruction of the paleoenvironmental and paleoceanographic history of the Arctic Ocean.

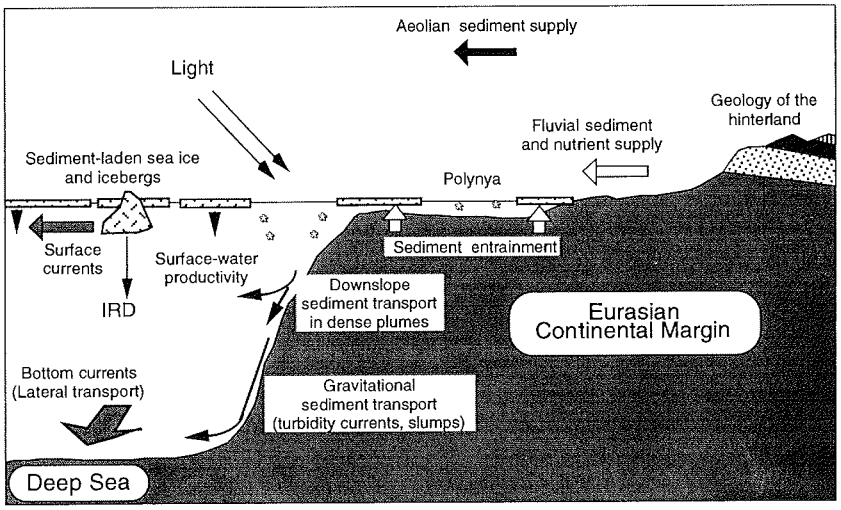

Fig. 1: Summary scheme of factors controlling the sedimentation along the Eurasian continental margin.

The editors made an effort to edit the manuscripts by the Russian authors to make them easier to read. We hope that we have not changed the meanings of the original papers. The papers contained in this report do not necessarily reflect the opinion of the editors.

R. Stein
Bremerhaven
July 1996

OVERVIEWS

THE SEA-ICE COVER OF THE ARCTIC OCEAN AND THE EURASIAN MARGINAL SEAS: A BRIEF OVERVIEW OF PRESENT DAY PATTERNS AND VARIABILITY

J. Kolatschek[1], H. Eicken[1], V. Yu. Alexandrov[2], M. Kreyscher[1]

[1]Alfred-Wegener-Institut, Bremerhaven, Germany
[2]Arctic and Antarctic Research Institute, St. Petersburg, Russia

Abstract

The extent of the Arctic sea-ice cover ranges between 9.3 x 10^6 km^2 in summer and 15.7 x 10^6 km^2 in winter. It controls the exchange between ocean and atmosphere and is of global climatic importance. The mediterranean character of the Arctic Ocean results in the formation of a multi-year ice cover, on average between 3 and 5 m thick. Circulation within the Arctic Basin is mostly wind-driven, with two major circulation systems, the Beaufort Gyre and the Transpolar Drift. Over the American and Eurasian shelves sea ice may entrain significant amounts of particulate matter, which is exported with the ice into the Arctic Basin, eventually released upon ice melting in the European Nordic Seas. Thus, an understanding of the present-day and past patterns of surface sediment distributions requires a thorough knowledge of sea-ice dynamics. Based on a review of the available literature and studies with a large-scale dynamic-thermodynamic sea-ice model, the general drift patterns and their variability as well as their geological relevance are discussed.

1. Introduction

The Arctic Ocean is the only sea with a perennial ice cover. The ice influences the climatology, oceanography, biology as well as the geology of the area to a high degree.

Ice significantly reduces the heat flux between ocean and atmosphere; through its high albedo it has a strong influence on the radiation budget of the entire Arctic. The albedo of open water is as low as 0.10, whereas the ice albedo ranges between 0.6 and 0.8 (Barry, 1996). Thus, over ice surfaces as compared to open water up to eight times as much of the incoming shortwave radiation is reflected, resulting in lower surface temperatures. Furthermore the reduced light availability in the upper ocean greatly reduces primary production.

Through the incorporation and long range transport of sediments, sea ice is a key geological agent in the Arctic (Pfirman et al., 1990; Reimnitz et al., 1993; Nürnberg et al., 1994). Through its control of thermo-haline circulation, driven by ice formation and melting, the Arctic Ocean's ice cover is linked to the climatology of the lower latitudes (Carmack, 1986). Of particular interest in this context is the ice export through Fram Strait and its potential role in controlling deep convection in the Greenland Sea.

The importance of the Arctic sea ice cover is underscored by the drastic changes predicted by global climate models for the ice extent and surface temperature in the Arctic Basin (Mitchell et al., 1990).

The key factors driving these processes are:

- the extent and concentration of sea ice,
- ice thickness,
- ice drift.

Information about the ice extent dates back as far as the historical records of whaling ships and early expeditions. Systematic recording of ice margins began as late as the end of the last century but only for the last 25 years we have an almost complete set of data about sea ice extent and concentration over the whole Arctic (NSIDC, 1995). This became possible through the development of satellite-borne passive microwave sensors, operating independent of cloud cover and light conditions (Gloersen et al., 1992).

Our knowledge of the ice thickness distribution is not as thorough. At the moment only estimates of low spatial and temporal coverage are available. The main data sources are sonar recordings from military submarines taken from underneath the ice, with all the advantages and disadvantages of such a data set (Bourke and McLaren, 1992; Wadhams and Comiso, 1992; Wadhams, 1995). At present, a means for mapping the thickness of the sea ice over a wide area regularly and with good temporal resolution is still lacking.

The data base with respect to sea ice drift is much more extensive. Starting with the drift of Nansen's "Fram" from 1893 to 1895 (Nansen, 1898), up to now a lot of recordings of the drift of ships and stations with the ice through the Arctic exist. In the 1950's drifting radiobeacons and automated radiometeorological stations (DARMS) were deployed by the Soviet Union. Since the 1970's regular buoy deployments have been carried out within the framework of the Arctic Ocean Buoy Program (Colony et al., 1991). Ice drift can also be determined with spaceborne sensors by directly tracking ice features (Holt et al., 1992). A great improvement in recent years is the use of radar sensors, as onboard the satellites of the Russian OKEAN series, the European ERS-1/2 satellites or the Canadian Radarsat. These sensors can penetrate clouds, are independent of solar illumination and are covering a wide swath and/or have a high resolution (Massom, 1991).

2. The Ice Cover of the Arctic Ocean

As mentioned before, most of our knowledge about total ice cover and change of ice concentration is obtained from the series of satellites carrying passive microwave sensors like the SMMR (Scanning Multichannel Microwave Radiometer) onboard the Nimbus 7 satellite and the SSM/I (Special Sensor Microwave/Imager) sensors on the DMSP (Defense Meteorological Satellite Program) satellites. They allow the estimation of total, first-year and multi-year ice concentration with a grid size of 25 km over the whole Arctic.

An analysis of the data collected from 1978 - 1987 (Gloersen et al., 1992) shows that the maximum average ice extent (the area enclosed by the ice edge) is reached in late March with 15.7×10^6 km^2. From this time on ice extent is shrinking to a minimum area of 9.3×10^6 km^2. This value is reached by early September. However, in the central Arctic Ocean the seasonal change in ice coverage only amounts to a small fraction (14 %). Most of it, 86 % of the seasonal variation, takes place in the marginal seas, over the shallow shelf

regions. In winter these areas are usually completely covered with ice, whereas in summer they are mostly ice-free (see Figures 1 and 2).

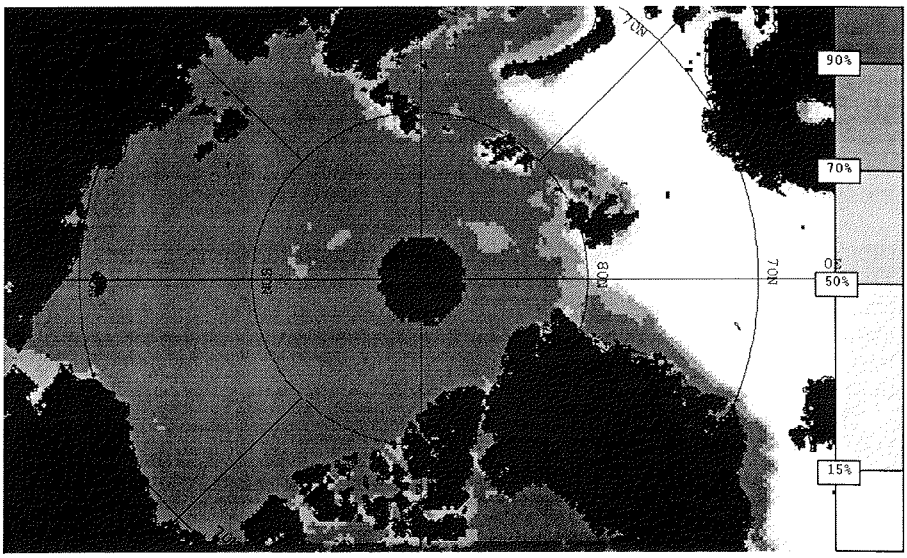

Fig. 1.: Ice concentration in the Arctic in mid-March 1995, derived from SSM/I data. It shows the typical situation in this season with maximum sea ice extent.

Ice formation starts in the Central Arctic where at the end of August a minimum ice concentration of about 85 - 95% is found. With time passing, the freezing area is growing southward in extent. At the end of September ice formation takes place all along the southern ice edge. At this time ice formation also starts from the coasts of Siberia growing northwards, until the zones of ice formation meet. Eicken et al. (in press) have investigated this process in detail for the Laptev Sea. From SSM/I data daily ice area values for this region and estimated duration of the melting season and the start and duration of freeze up were derived. The actual process from beginning of ice formation at the northern ice edge and in the shallow coastal zone until the complete coverage of the Laptev Sea with ice is as short as 2 to 3 weeks (Fig. 3). The time of the start of freezing varies only to a small extent, independent of the very variable summer situation (Fig. 4) which ranges from positions of the ice edge south of 75°N in the years 1979, 1984, 1987 to an observed ice edge at around 80°N in 1995.

Along the Siberian Coast, polynyas develop along the fast ice margin and at Severnaya Zemlya and Franz-Josef-Land, with episodic opening and closing during the entire winter (Zakharov, 1966; Martin and Cavalieri, 1989; Dethleff et al., 1992, Cavalieri and Martin, 1994). Here ice is continuously produced and transported north with prevailing offshore winds and integrated into the Transpolar Drift. Cavalieri and Martin (1994) estimate a total annual

ice production of 848 km^3 in polynyas, which thus contribute significantly to the Arctic Ocean's ice mass balance and are of great importance for salt flux and water mass production.

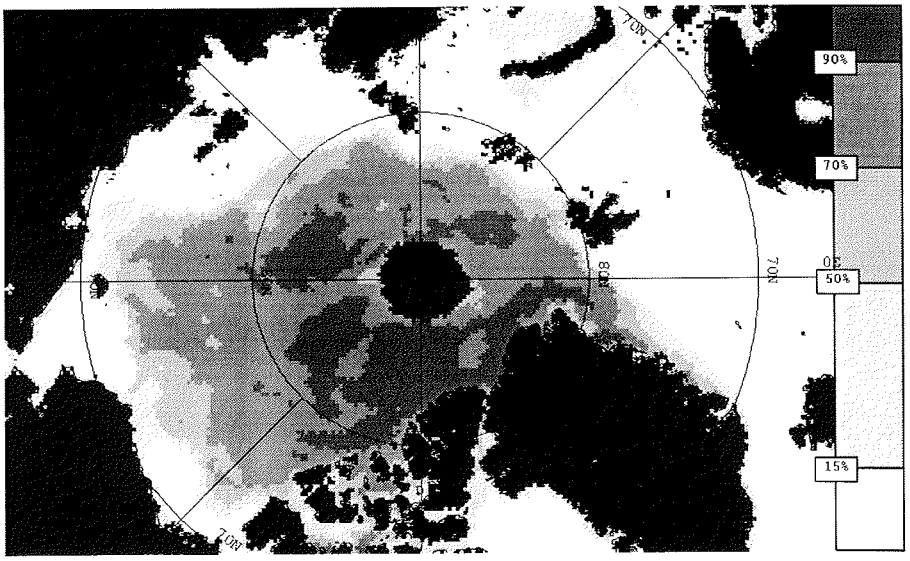

Fig. 2.: Ice concentration in the Arctic at the end of August 1995, derived from SSM/I data. The coastal regions and the marginal seas are partially ice-free.

Furthermore, ice formation in the shallow waters of flaw leads and coastal polynyas in the Laptev Sea has been shown to lead to entrainment of sediments into the ice cover in concentrations of up to several hundred grams per cubic meter (Dethleff et al., 1992; Reimnitz et al., 1994). As important for sediment transport is the entrainment of particulates over shallow shelves during fall freeze-up (Pfirman et al., 1990; Reimnitz et al., 1994; Eicken et al., 1996).

A similar situation is found in the Beaufort Sea (Reimnitz, 1993); because of a comparatively narrow shelf and the persistence of ice through the summer season conditions for the production of sediment-laden ice may not be as favorable, however, as in the Eurasian Arctic (Pfirman et al, 1990; Reimnitz et al., 1994).

At the the end of September, ice in the Kara, Laptev and East Siberian Sea is usually covered with about 5 cm of snow. The snow depth increases to 10 - 25 cm in the Laptev and East Siberian Sea and up to 35 cm in the Kara Sea at the end of the winter season. In the central Arctic there is a rapid snow accumulation in autumn with a layer of 20 cm, then slowly thickening to up to 40 cm in early May (Barry et al., 1993).

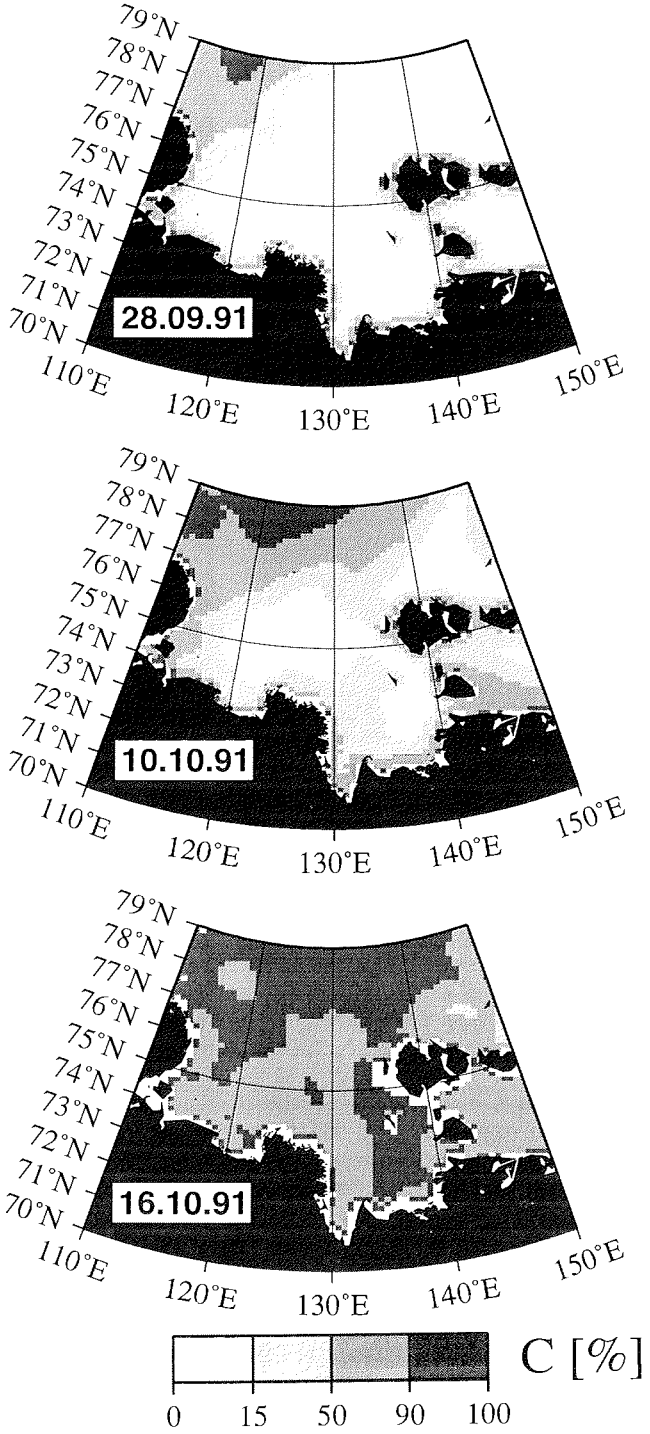

Fig. 3.: Ice concentration maps, derived from SSM/I data, showing the advance of the ice edge during freezing up in the Laptev sea in fall of 1991.

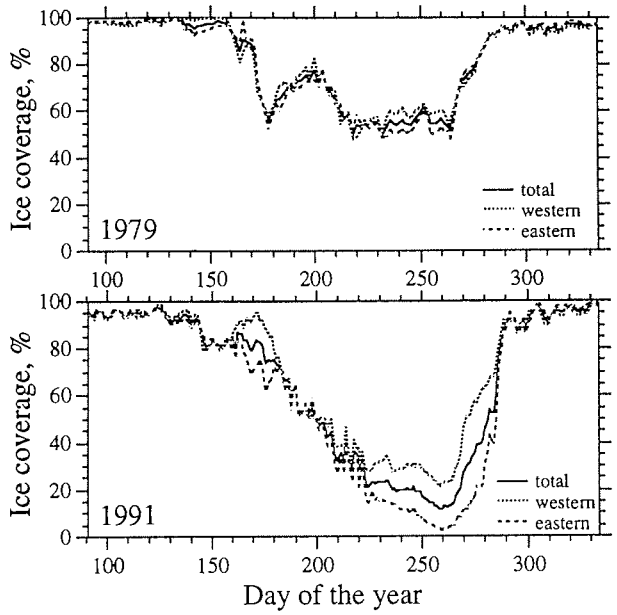

Fig. 4.: Time series showing the development of the ice coverage in the Laptev Sea for the years 1979 and 1991, derived from SSM/I data. Clearly visible is in both cases the fast freeze-up of the area.

Melting starts at the end of May or the beginning of June in the southernmost parts of the Arctic. Usually two weeks after the onset of snow melt, melt puddles begin to appear on the surface of ice floes. The maximum puddle extent is then reached in July with a coverage of 20 - 40%. After that puddles tend to melt through (Barry et al., 1993; Romanov 1993).

Depending on the region, 30 to 40 cm of ice are melted away in one summer season. Ice produced at the end of the winter which has only a thin snow cover and a low thickness has a lower chance to survive the summer than ice which is produced at the beginning of the winter (Romanov 1993).
There is some evidence for a decrease in sea ice area in the years from 1978 to 1987 (Gloersen et al., 1992). The retreat was estimated to 1.8±1.2% with a confidence level of 88.5 %.

Regional trends and variability in the marginal seas dominate (Parkinson and Cavalieri, 1989; Gloersen et al., 1992); because they are usually out of phase, they have only a small influence on the total ice area. There is also some evidence for a shortening of the ice season in some areas (northern coast of Russia and Greenland, Barents Sea, Sea of Okhotsk) countered by a trend to longer ice seasons in the Gulf of St. Lawrence, Labrador, Hudson Bay, Beaufort Sea and eastern Bering Sea) (Parkinson, 1992).

3. Ice Thickness

The bulk of the ice thickness data has been derived from underice sonar measurements from twelve submarine cruises between 1957 and 1987

(Wadhams and Comiso, 1992; Bourke and McLaren, 1992). Mean ice thickness was calculated from averaging over track segments of 50 to 100km of length.

Similar data at fixed locations are provided by upward looking sonars mounted on oceanographic moorings. Some time series exist over fixed locations, but there is, for obvious reasons, no large geographical coverage.

Drilling is by far the most accurate means to estimate ice thickness, but obviously supplies only very limited data sets.

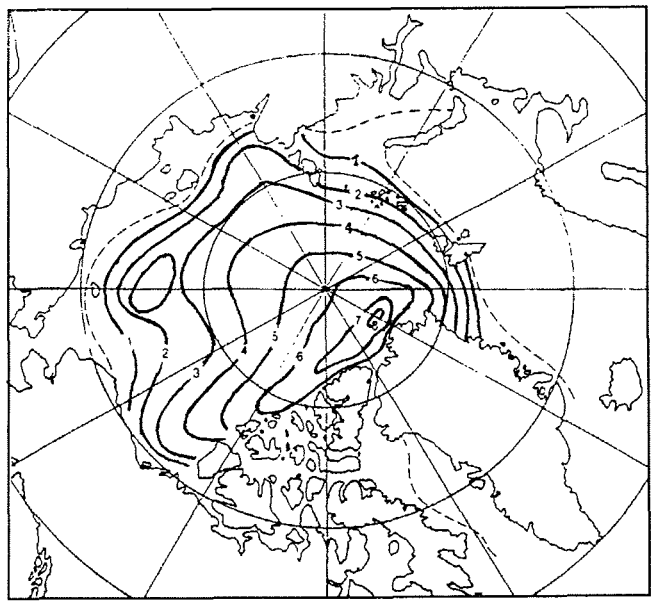

Fig. 5.: Distribution of sea ice thickness in the Arctic in summer (after Bourke and Garrett, 1987).

The overall distribution of sea ice thickness in the Arctic is shown in Figure 5. The lowest values of ice thickness are found in the Eurasian sector of the Arctic, with values between 1 and 2 m, corresponding to the growth of ice during one season. In the direction to the North Pole and to the northern coast of Greenland and the Canadian Arctic Archipelago, ice thickness is continuously increasing. The maximum thickness is reached near the Canadian Archipelago with some 7 to 8 m. Generally ice thickness values are lower by about 0.5 -1 m in summer as compared to winter. Regionally, an increase of ice thickness through transport and compression is possible, as near the Alaskan Coast.

The variability for ice thickness in several years of measurements is lowest in the Transpolar Drift away from the coast, near 0° longitude. The highest variability is observed at the North Greeenland coast (Wadhams, 1990).

With a dynamic thermodynamic sea ice model (Harder, 1996) net freezing rates have been calculated. The model is based on the formulation of Hibler

(1979). Its forcing includes daily surface wind components and monthly means of air temperature, relative humidity and air pressure originating from the European Center for Medium Range Weather Forecasts (ECMWF). The model is described in detail in Harder (1996).

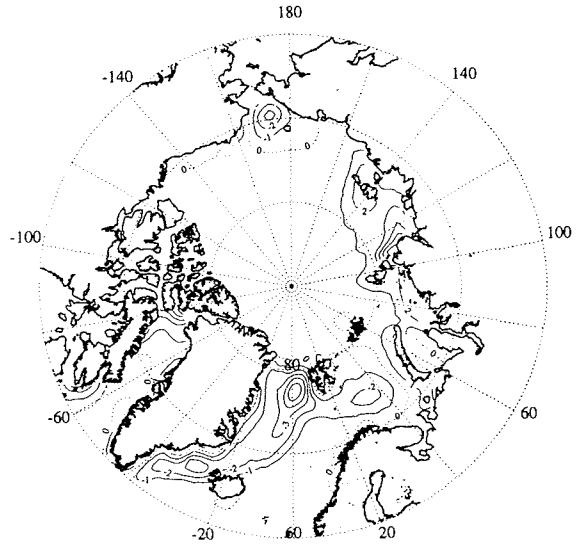

Fig. 6.: Annual mean of net freezing rates from the years 1986-1992 in m/year, calculated with a sea ice model.

The net freezing rate is defined as the difference between ice locally frozen and melted. Figure 6 shows the calculated annual net freezing rate averaged for the years 1986 to 1992. In the central Arctic the ice cover is almost in a stationary state. Approximately the same thickness of ice is melted away in summer which is frozen in winter. The main source regions for ice are the Siberian marginal seas, especially the Kara and the Laptev Sea. There is an annual net ice growth of up to 2 m. The sinks are located in the north of the Bering Strait with net ice melting of 2 - 3 m and, the most important sink, the East Greenland Sea with annual melting rates from 3 to 5 m. The stationary state of the ice thickness distribution is maintained by drift of sea ice from the source regions to the sink regions.

4. Ice drift

4.1. Fundamentals

To accelerate or slow down a body it takes an external force to act. In the case of sea ice, these forces are the wind and ocean currents. Both transfer momentum to the ice through complex interactions. As the earth is a rotating

sphere, the Coriolis force also has to be taken into consideration. All these forces are in changing relations to each other and jointly determine speed and direction of the ice. Considering not a single ice floe in free drift, but a more or less closed area of pack ice, an additional, internal force contributes to the interaction of the ice floes: If floes are pushed together, they react by a resistent force whose strength depends on the ice rheology (Hibler, 1986).

From early observations it is known, as a rule of thumb, that sea ice in the Arctic drifts with about 2 % of the wind speed and at an angle of about 45° to the right of the direction of the surface wind (Nansen, 1898). In a more accurate estimation, the angle to the geostrophic wind is given by 5° (winter) to 18° (summer). An explanation for this seasonal dependence of ice drift could be the different structure of the atmospheric boundary layer which changes the momentum transfer from air to ice or the generally lower ice concentration in summer so that the case of free drift occurs more often (Thorndike and Colony, 1982).

In general the direction of ice drift is governed by the geostrophic wind and thus the distribution of pressure fields in the Arctic and sub-Arctic area. Changes in these patterns do, with a small time shift which is caused by the inertia of the ice, induce changes in the ice drift. From the average pressure gradient one can derive in rough approximation the average ice drift pattern, neglecting the influence of the ocean currents and the internal forces of the pack ice (Colony and Thorndike 1984).

4.2. Patterns of Ice Drift in the Arctic

Averaged over the year, a high air pressure area usually persists north of the Alaskan Coast and an area of lower pressure over the North Atlantic Ocean. This leads to the commonly known pattern of the ice drift as derived by Thorndike and Colony (1982) and Colony and Thorndike (1984) taking into account data of drifting buoys and the geostrophic winds for the years 1979 to 1990 (Fig. 7).

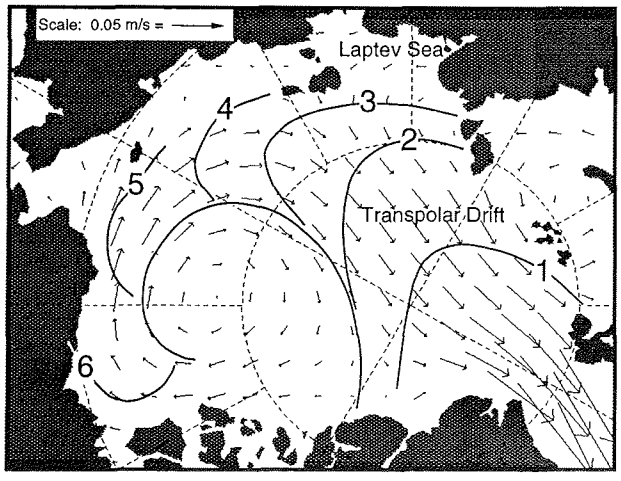

Fig. 7.: Mean field of sea ice drift in the Arctic Ocean, after Rigor (1992).

North of the Alaskan coast the ice cirulates in a big anticyclonic structure, the Beaufort Gyre, corresponding to the high pressure system over the Beaufort Sea. Its diameter is about 700 km. Speed varies from almost zero in the center to 3 cm/s in the marginal zones. During part of the year, reversals in the drift can lead to divergence and the generation of open water in the gyre (Barry et al., 1993). Towards the Siberian Arctic this gyre opens up to a linear structure, the Transpolar Drift. Its origin is in the area of the Chukchi - East Siberian Sea and it leads to the West. Ice drifts with mean velocities of about 2 cm/s past Franz Josef Land and the North Pole, accelerating to mean values of up to 10 cm/s through Fram Strait between Svalbard and Greenland. In the Greenland Sea even higher ice velocities are observed.

It takes 3 to 4 years for the ice to move from East Siberia to Fram Strait, where 20% of the ice area of the Arctic Basin is annually exported (Thorndike, 1986). Ice which gets caught in the Beaufort Gyre remains longer in the Arctic Basin, typically it takes 5 - 10 years for the ice to complete one cycle.

The movement of the ice near Alaska and the Chukchi Sea is parallel to the coast, whereas the direction of the drift in the Laptev Sea is in general away from the coast. For this reason the Laptev Sea and parts of the East Siberian Sea are the most important ice factories of the Arctic (see also Figure 6). Estimates of ice export from the Laptev Sea are in the range from 400 $km^3 yr^{-1}$ (Eicken et al., 1996) to 540 $km^3 yr^{-1}$ (Timokhov 1994). This is more than the export from Barents Sea (40 $km^3 yr^{-1}$), Kara Sea (240 $km^3 yr^{-1}$), East Siberian Sea (150 $km^3 yr^{-1}$) and Chukchi Sea (10 $km^3 yr^{-1}$) together (all numbers from (Timokhov, 1994).

Typically the situation in the summer months deviates more from the average drift pattern than during the rest of the year. Ice velocities are generally lower in the Transpolar Drift which source region is shifted more to the East, to the region of the Bering Strait. North of Greenland lies a zone with ice drift usually directed towards the coast. Here strong ice compression and accumulation of old ice can take place.

4.3. Variability

The mean ice velocity field in the Arctic, averaged over many years, gives only an incomplete image of the real conditions. There are intrinsic limitations of the data set. Usually buoy data from the marginal seas are very sparse. If they exist, they only cover a fraction of the whole year. Also, the drift pattern can be remarkably different from the mean for certain years. In Figures 8 and 9, the mean ice drift in the Arctic is shown for the years 1987 and 1992. These vectors have been calculated with the afore-mentioned dynamic-thermodynamic sea ice model, forced by surface winds, a steady ocean current and taking into account a viscous-plastic sea ice rheology (Hibler, 1979) for the calculation of the internal forces within the ice. Comparison of the model results with real buoy trajectories gave a good agreement between calculation and observation.

The situation in 1987 is very close to the mean drift field derived from Thorndike and Colony (1982). In 1992 the pattern looks different. In east Siberia ice drift is directed from west to east, in the opposite direction of the usually predominant Transpolar Drift. North of the Kara and Barents Sea the velocities are very small. Ice leaving the Arctic Ocean through Fram Strait is originating from the area north of Greenland.

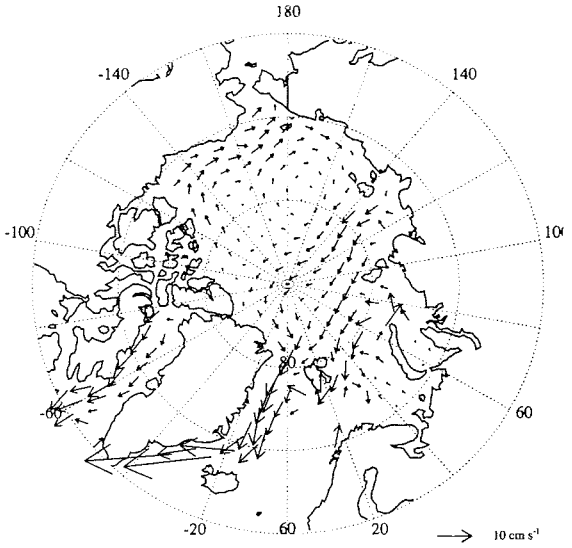

Fig. 8.: Mean sea ice drift in the Arctic for the year 1987, calculated with a sea ice model.

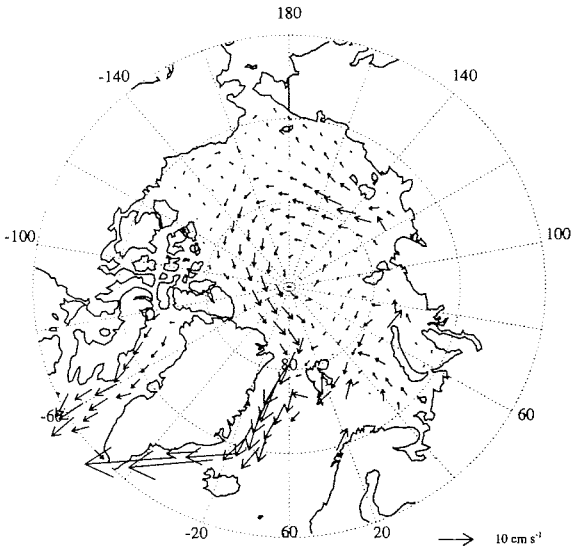

Fig. 9.: Mean sea ice drift in the Arctic for the year 1992, calculated with a sea ice model.

On shorter time scales, drift patterns can change within days or weeks as shown in Figure 10. These vectors have been derived from the location of the multi-year/first-year ice boundary in SSM/I images. During the period from November 1993 to December 1993 the direction of drift in the Laptev and East Siberian Seas is from west to east. In the following period, from December 1993 to January 1994, the ice changed its direction completely, now drifting from east to west, with a small northward component. It is not surprising that the actual trajectory of a buoy or an ice floe can be very complex. Colony and Thorndike (1985) estimate the deviation from daily average motion at 7 cm/s wheras the mean velocity is only 2 cm/s. These high frequency components of the velocity spectrum make the task of backtracking a certain ice floe somewhere in the Arctic to its origin very difficult.

4.4. Local Drift Patterns

Local drift patterns dominate the circulation of ice in the marginal seas, in particular over the Eurasian shelves. Their usually complex patterns cannot be explained by geostrophic winds alone. Within approximately 400 km off the coast winds may be altered by the surrounding topography. But the main reason for a different drift pattern is that the direction of drift is not free any more but governed by the direction of the coastline or by barriers of islands. Also internal forces building up in the pack play a more dominant role.

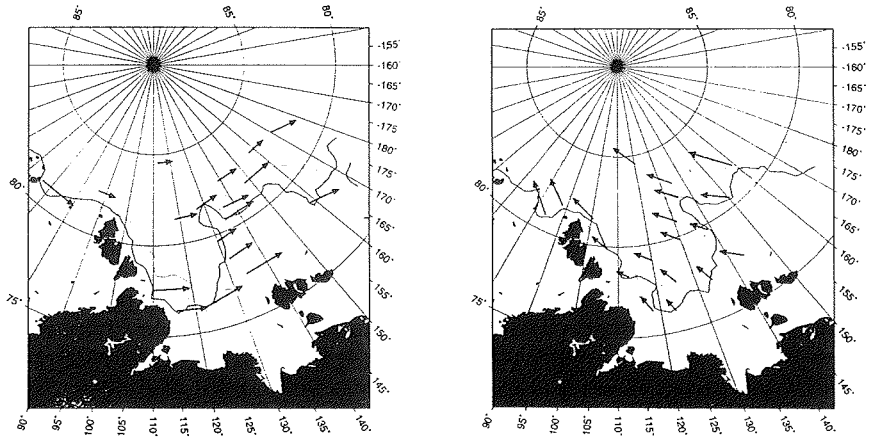

Fig. 10.: Drift pattern in the Eurasian Arctic, derived from the displacement of the multi-year/first-year ice boundary (dotted line) estimated from SSM/I data. Left: Drift from November to December 1993. Right: Drift from December 1993 to January 1994.

Given its overall importance for ice production and sediment dynamics, we will focus in more detail on the Laptev Sea. The Laptev Sea is bounded by the Severnaya Zemlya archipelago in the West and by the New Siberian Islands in the East. Average ice-drift patterns estimated from Rigor and Colony (in press) consists of a gyre, rotating counterclockwise and located at 77°N 120°E

(Fig. 11). This leads usually to a steady inflow of ice from north to south along the coasts of Severnaya Zemlya with an average speed of 2.4 cm/s, building up the Taimyr Ice Massif, a structure which consists of thick ice of mixed age, often lasting through the whole summer season (Timokhov, 1994). In the southern part there is a mixture of movement from west to east along the coast and of a south-to-north component which is responsible for the export of ice into the Transpolar Drift with the average speed estimated at 1.9 cm/s.

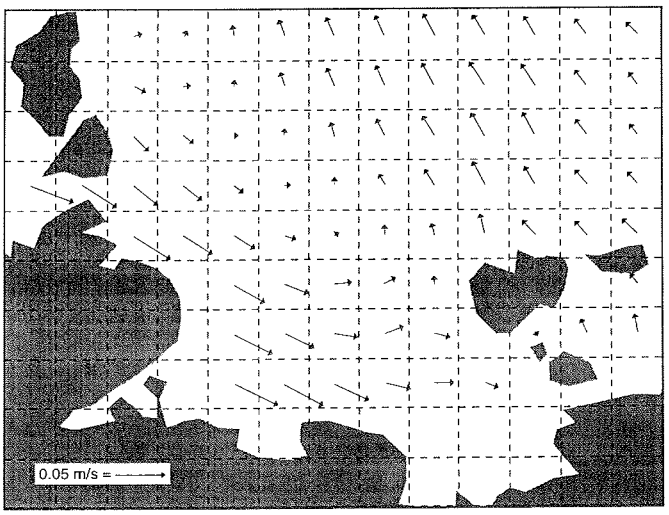

Fig. 11.: Annually averaged velocity field for the Laptev Sea, based on an analysis of the surface pressure field. After Rigor and Colony (in press).

Due to limitations in the data set (only few buoy data in this region are available), the described pattern may only represent a crude approximation. Other investigations suggest that the cyclonic system is not a steady element of the drift pattern in the Laptev Sea and that quite often deviations from this pattern occur (Gudkovich and Nikolaeva, 1963; Bushuev et al., 1967). In winter the drift in the western part of the Laptev Sea is also directed northwards, whereas only in the summer period the cyclonic circulation develops. Gudkovich et al. (1972) estimated the average ice area exported from the Laptev Sea to the Arctic Basin to 355000 km^2 with variations between a maximum ice outflow of 693000 km^2 (in 1942) and a maximum inflow of 198000 km^2 (in 1957). About 90% of the sea ice is exported from the Laptev Sea in the autumn-winter-spring period.

Along the coast in winter a zone of fast ice develops which has a width from 50 km in the west, along the Taimyr Peninsula and broadens towards the East to a width of about 400 km. It is commonly accepted that most of this ice on the shelf melts in spring and summer, so that it contributes very little to the Transpolar Drift.

5. Conclusions

A main goal of this brief overview was to demonstrate the importance of sea-ice processes and variability for the geological environment and in particular the distribution and characteristics of surface sediments in the Arctic realm. Due to the vast extent of the perennial ice cover, biological production and associated particulate fluxes are generally low throughout the interior of the Arctic Basin (Hargrave et al., 1989). Thus, the importance of sediment transport by sea ice and the release from the ice cover in net melting areas, in particular the region of the Greenland Sea (Fig. 6, Hebbeln and Wefer, 1991), becomes all the more important. Likewise, leakage of ice-rafted material to the sea floor within the interior Arctic appears to be of importance for the sediment budget (Wollenburg, 1995), yet has not been quantified or studied in any detail. Ice dynamics in the Eurasian shelf seas and import of ice from the Arctic Ocean may likewise represent a major factor with respect to the surface sediment distribution (Nürnberg et al., 1995, Eicken et al., in press).

It is important to keep in mind, however, that an analysis of the uppermost few centimeters of surface sediments represents an integration over several decades to centuries. The variability in ice drift and ice extent as discussed in this contribution demonstrates, however, that conclusions drawn from observations for individual years or time series extending over a few years are not necessarily comparable to data representative of even the shortest geological time scales. Thus, a shift in the surface wind field may result in "anomalous" ice drift patterns that could transport ice from the Eurasian shelves into the Canadian Basin. If at the same time an increase in net freezing rate and sediment entrainment would induce an increase in sediment transport, an event of comparatively short duration can constitute a sedimentological signal that is not at all representative of long-term conditions.

Given the problems in the interpretation of recent ice-dynamics and sedimentological data, information from the more distant geological past, such as from the last glacial maximum or the previous interglacial will be all the more difficult to derive and interpret based on the sedimentological record alone (cf. contribution by Thiede, this volume). Here, future studies comprising a thorough analysis of the recent sea-ice patterns in conjunction with numerical modelling may provide a better glimpse of the history and importance of the Arctic Ocean's sea-ice cover.

6. References

Barry, R. G. 1996. The parameterization of surface albedo for sea ice and its snow cover. Progr. Phys. Geogr., 20, 63-79, 1996.

Barry, R. G., Serreze, M. C. Maslanik, J. A., Preller, R. H., 1993. The Arctic Sea Ice-Climate System: Observations and Modeling. Reviews of Geophysics,31, November 1993, pages 397-422.

Bourke, R. H. and Garrett, R. P. 1987. Sea ice thickness distribution in the Arctic Ocean. Cold Regions Sci. Technol. 13, 259-280, 1987.

Bourke, R. H. and McLaren, A. S. 1992. Contour Mapping of Arctic Basin Ice Draft and Roughness Parameters. J. Geophys. Res., 97, C11, 17715-17728, 1992

Bushuev, A.V., Volkov, N.A., Gudkovich, Z.M., Loshchilov, V.S. 1967. The results of study on drift and dynamics of the Arctic Basin sea ice cover in spring 1961 - Transactions of AARI, vol. 257, p. 26 - 44. (in russian).

Carmack, E. C. 1986. Circulation and mixing in ice-covered waters. In Untersteiner, N. (ed.), The geophysics of sea ice. Martinus Nijhoff Publ., Dordrecht (NATO ASI B146), 641-712.

Cavalieri, D. J. and Martin, S. 1994. The contribution of Alaskan, Siberian, and Canadian coastal Polynyas to the cold halocline layer of the Arctic Ocean. J. Geophys. Res., 99, 18343-18362, 1994.

Colony, R., and Thorndike, A. S., An estimate of the mean field of Arctic sea ice motion, J. Geophys. Res., 89, 10623-10629, 1984.

Colony, R. L., Thorndike, A. S. 1985. Sea Ice Motion as a drunkards walk, . J. Geophys. Res., 90, 965-974, 1985.

Colony, R. L., Rigor, I., Runciman-Moore, K. 1991. A summary of observed ice motion and analyzed atmospheric pressure in the Arctic Basin, 1979-1990. Applied Physics Laboratory, University of Washington, Seattle, Tech. Memorand. APL-UW TM 13-91.

Dethleff, D., Kleine, E., and Loewe, P., 1994. Oceanic heat loss, sea ice formation and sediment dynamics in a turbulent Siberian flaw lead, in Rep. Ser. Geophys., pp. 35-40,Department of Geophysics, University of Helsinki, Helsinki, 1994

Eicken, H. und Lange, M. A., 1992. Drill hole and ice-core studies of sea-ice thickness in Arctic and Antarctic, Report of the sea ice thickness workshop, 19-21 November 1991, New Carrollton, Maryland, Applied Physics Laboratory, University of Washington, Seattle

Eicken, H., Reimnitz, E., Alexandrov, V., Martin, T., Kassens, H., Viehoff, T. 1996. Sea-ice processes in the Laptev Sea and their importance for sediment export. Continental Shelf Research, 16, in press.

Gloersen, P., Campbell, W. J., Cavalieri, D. J., Comiso, J. C., Parkinson, C. L., Zwally, H. J. 1992. Arctic and Antarctic sea ice, 1978-1987: Satellite passive-microwave observations and analysis. NASA SP-511, National Aeronautics and Space Administration, Washington.

Gudkovich, Z. M., and Nikolaeva, A. Ya., 1963. Ice drift in the Arctic seas and its connection with the ice cover of the Soviet Arctic seas, Transactions of AARI, vol.104, 186p.

Gudkovich, Z. M., Kirillov, A. A., Kovalev, E. G., Smetannikov, A. V., Spichkin, V. A. 1972. The basis of techniques for long-term ice forecasts in the Arctic seas, Gidrometeoizdat, AARI, 348p.

Harder, M., 1996. Dynamik, Rauhigkeit und Alter des Meereises in der Arktis - Numerische Untersuchungen mit einem großskaligen Modell, Ber. Polarforsch., 203, 1996.

Hargrave, B. T., Bodungen, B. v., Conover, R. J., Fraser, A. J., Phillips, G. and Vass, W. P. 1989. Seasonal changes in sedimentation of particulate matter and lipid content of zooplankton collected by sediment trap in the Arctic Ocean off Axel Heiberg Island, Polar Biol., 9, 467-475.

Hebbeln, D., and Wefer, G. 1991. Effects of ice coverage and ice-rafted material on sedimentation in the Fram Strait, Nature, 350, 409-411.

Hibler, W. D. 1979. A dynamic thermodynamic sea ice model. Journal of Pysical Oceanography, 9, (C4): 815-846, 1979.

Hibler, W. D. 1986. Ice Dynamics. In Untersteiner, N. (ed.), The geophysics of sea ice. Martinus Nijhoff Publ., Dordrecht (NATO ASI B146),577-640, 1986

Holt, B., Rothrock, D. A. and Kwok, R., 1992. Determination of sea ice motion from satellite images. In Carsey, F. D.(ed.), Microwave remote sensing of sea ice. Geophysical Monograph 68, American Geophysical Union, Washington, 343-354.

Martin, S., and Cavalieri, D. J., 1989. Contributions of the Siberian shelf polynyas to the Arctic Ocean intermediate and deep water, J. Geophys. Res., 94, 12725-12738, 1989.

Massom, R. 1991. Satellite Remote Sensing of Polar Regions. London, Belhoven Press.

Melling, H., and Riedel, D. A., 1995. The underside topography of sea ice over the continental shelf of the Beaufort Sea inthe winter of 1990, J. Geophys. Res., 100, 13641-13653, 1995.

Mitchell, J. F. B., Manabe, S., Meleshko, V. and Tokioka, T., 1990. Equilibrium climate change and its implications for the future. In Houghton, J. T., Jenkins, G. J., Ephraums, J. J.(ed.), Climate change the IPCC scientific assessment. Cambridge University Press, Cambridge, 131-172.

Nansen, F., 1898. Farthest North, George Newnes Ltd., London, 1898.

NSIDC, 1995. NSIDC Notes, 15, Fall 1995

Nürnberg, D., Wollenburg, I., Dethleff, D., Eicken, H., Kassens, H., Letzig, T., Reimnitz, E. and Thiede, J., 1994. Sediments in Arctic sea ice - implications for entrainment, transport and release. Mar. Geol., 119, 185-214.

Nürnberg, D., Levitan, M. A., Pavlidis, J. A., and Shelekhova, E. S. 1995. Distribution of clay minerals in surface sediments from the eastern Barents and south-western Kara seas, Geol. Rundschau, 84, 665-682.

Parkinson, C. L., Cavalieri, D. J., 1989. Arctic Sea Ice 1983 - 1987: seasonal, regional and interannual variability. J. Geophys. Res., 94, 14199 - 14523.

Parkinson, C. L. Spatial patterns of increases and decreases in the length of the sea ice season in the north polar region 1979 - 1986. J. Geophys. R, 97, 14377 - 14388.

Pfirman, S., Lange, M. A., Wollenburg, I. and Schlosser, P., 1990. Sea ice characteristics and the role of sediment inclusions in deep-sea deposition: Arctic - Antarctic comparisons. In Bleil, U., Thiede, J.(ed.), Geological history of the Polar Oceans: Arctic versus Antarctic. Kluwer Academic Publishers, Dordrecht, 187-211.

Reimnitz, E., McCormick, M., McDougall, K. and Brouwers, E., 1993. Sediment export by ice rafting from a coastal polynya, Arctic Alaska, U.S.A. Arct. Alpine Res., 25, 83-98.

Reimnitz, E., Dethleff, D. and Nürnberg, D., 1994. Contrasts in Arctic shelf sea-ice regimes and some implications: Beaufort Sea and Laptev Sea, Mar. Geol., 119, 215-225, 1994.

Rigor, I. 1992. Arctic Ocean buoy program. ARGOS Newsletter, 44, 1-3, 1992.

Rigor, I. and Colony, R. in press. Sea ice production and transport of pollutants in the Laptev Sea, 1979-1992. Science of the Total Environment

Romanov, I. P., 1993. Ice Cover of the Arctic Basin, St Petersburg 1993

Thorndike, A. S. and Colony, R. 1985. Sea Ice Motion in Response to Geostrophic Winds. J. Geophys. Res., Vol 87, No. C8, 5845-5852.

Timokhov L. A., 1994. Regional characteristics of the Laptev and the East Sibirian seas: climate, topography, icy phases, thermohaline regime and circulation. In: Russian-German cooperation in the Sibirian Shelf Seas: Geo-System Laptev Sea, H.Kassens, H.W. Hubberten, S. Priamikov and R.Stein, editors, Berichte zur Polarforschung, 144, 15-31.

Untersteiner, N. 1990. Structure and dynamics of the Arctic Ocean ice cover. In Grantz, A., Johnson, L., Sweeney, J. F.(ed.), The Arctic Ocean region. Geological Society of America, Boulder, Colorado, 37-51.

Wadhams, P. and Comiso, J. C., 1992. The ice thickness distribution inferred using remote sensing techniques. In Carsey, F. D.(ed.), Microwave

remote sensing of sea ice. Geophysical Monograph 68, American Geophysical Union, Washington, 375-383.
Wadhams, P., 1990. Evidence for thinning of the Arctic ice cover north of Greenland, Nature, 345, 795-797, 1990.
Wadhams, P., 1995. Arctic sea ice extent and thickness. Phil. Trans. R. Soc. Lond., A 352, 301-319, 1995.
Wollenburg, J. 1995. Benthische Foraminiferenfaunen als Wassermassen-, Produktions- und Eisdriftanzeiger im Arktischen Ozean, Ber. Polarforsch., 197, 1-227.
Zakharov, V. F., 1966. The role of flaw leads off the edge of fast ice in the hydrological and ice regime of the Laptev Sea, Oceanology, 6, 815-821, 1966.

ARCTIC PALEOCEANOGRAPHY - QUO VADIS?

Thiede, J.

GEOMAR , Research Center of Marine Geosciences, Kiel, Germany

Introduction: The new Arctic Challenge

Not counting the geographic exploration of the Arctic coast lines by fishermen, commercial traders and a few explorers it is only little more than 100 years ago that systematic investigations of the natural properties of the Arctic Ocean began. It was the German Carl Koldewey who sailed to Fram Strait in 1868 to study the nature of the ice margin, and he was followed by the famous Norwegian Fridtjof Nansen who drifted 1893-1895 (Nansen, 1904) along with the central eastern Arctic Transpolar Drift - on his newly built polar research vessel FRAM - in his attempt to reach the North Pole (Fig. 1). Both men and their crews were driven by the desire to understand the special oceanographic properties of the Arctic Oceans as well as the climatic variability and significance of the Arctic sea ice and its distribution. The motive of modern Arctic research is much the same as more than 100 years ago, but part of our tools and approaches have been improved over the past 100 years in such a way that we stand a much greater chance to succeed than these scientific pioneers.

One of the most important challenges for modern societies is a scientifically based and quantitative attempt to forecast the properties of the global environment in the foreseeable future, in particular since we have learned mainly from geological studies that frequent, fast and dramatic changes of global impact can occur (Bond et al., 1993). We have to assume that a "Greenhouse" effect will lead to a severe perturbation of the natural climate variability in the hundred years to come. One is therefore searching for tools for the early detection of such changes and the Arctic Ocean environment may well be a most suitable one, because
1) its sea ice cover is one of the most sensitive expressions of the modern climate regime, its extreme seasonal fluctuations being a good indicator of its potential instability,
2) through the fresh water influx and the wide permafrost regions it interacts with the wide continental hinterlands both in Eurasia and North America;
3) heat exchange between the Arctic and the North Atlantic oceans controls the NW European climate and on historic time scales is known to fluctuate intensively; and
4) changes in the Arctic may affect the "salt converyor belt" (Broecker, 1994) and thus have an impact on the properties of the entire world ocean.

Time is ripe for some major advances of our understanding of the oceanography of the Arctic Ocean and of its history. This fact is closely tied to some developments over the past years:
1.This book bears witness of the political changes in the countries of the former Soviet Union; relevant Russian institutions are getting increasingly involved in the international exploration of the Arctic. They have accumulated a tremendous experience in Arctic research (Gordijenko, 1967) and are

making their resources, in terms of manpower, technical facilities and data available to the international scientific community.

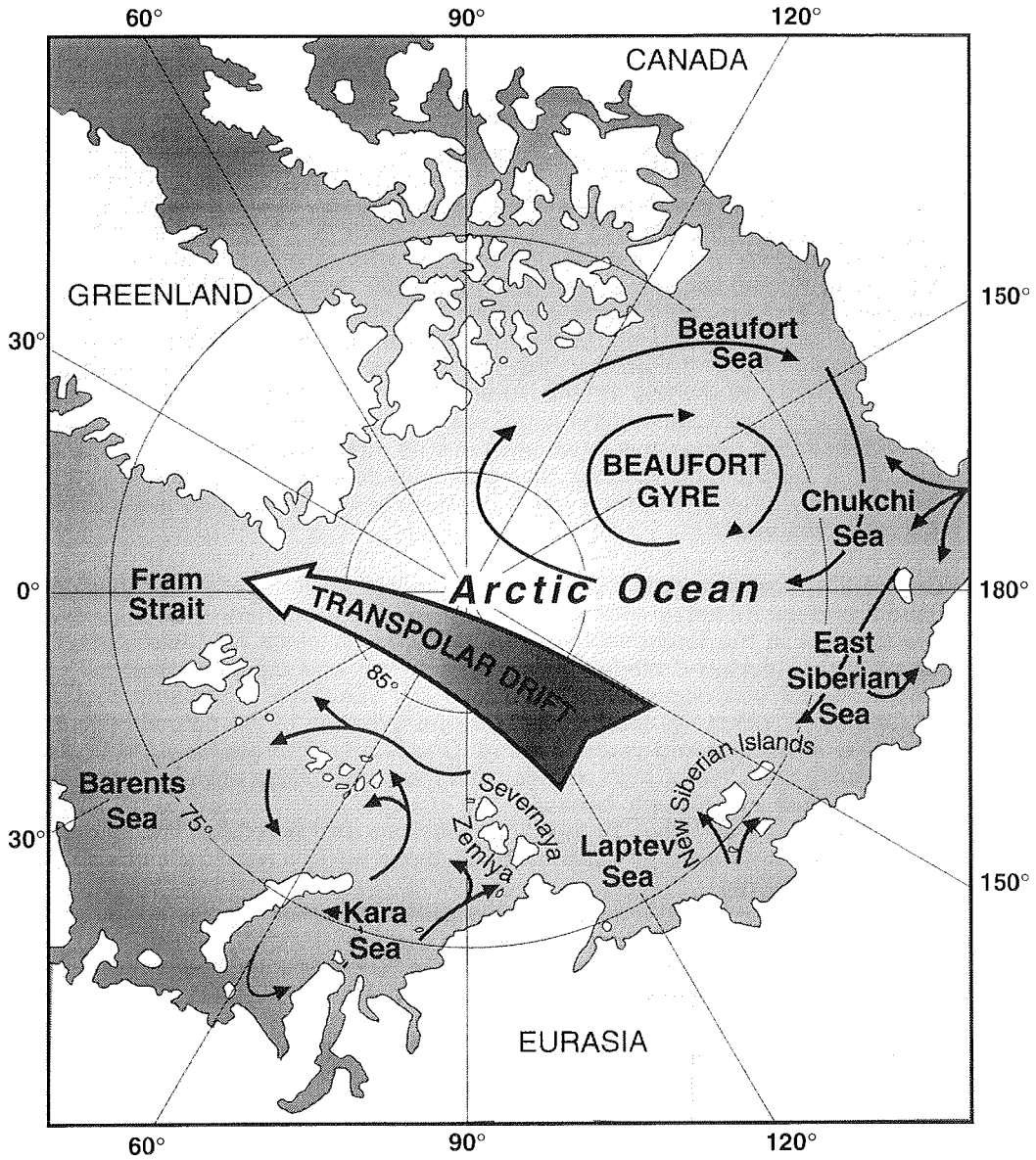

Fig. 1.: Schematic description of the major elements of the circulation patterns of the Arctic sea ice cover (from Kassens et al., 1995).

2. Russia controls a dominant segment of the Eurasian shelf seas which are the largest shelf seas on earth. After these areas were virtually closed to international exploration for a number of decades, they are now increasingly opening up for exploratory scientific work.
3. Shortly before the opening of the Eurasian shelf seas, renewed interest both in North America and in Europe have resulted in a number of major efforts to explore the interior of the Arctic Ocean based on state-of-the-art instrumentation and approach (Gudmandsen, 1980). After the preludes on the Swedish YMER 80-expedition (Schytt et al., 1981) and the German POLARSTERN´s first deep penetration into the eastern Arctic (Thiede, 1988) the Swedish ODEN and POLARSTERN as the first conventionally driven research ice breakers jointly succeeded to reach the North Pole (Anderson et al., 1991; Fütterer, 1992); both ships entered the Arctic Ocean from the NW European Barents Sea. In 1994 the US American POLAR SEAS and the Canadian LOUIS ST. LAURENT crossed the Arctic via the North Pole along their transect from the Bering to the Fram Straits (Aagaard et al., 1996) collecting en route important geologic and oceanographic data and samples. Arctic sea floor sampling is still difficult, but close to be routine provided the availability of suited ships.

These new developments allow for the first time to consider the entire Arctic Ocean including its deep-sea basins and shallow rim areas, both as individual entities and as systems responding to each other. Even though Arctic research is and will be expensive, new avenues for understanding this important compartiment of the global environment which was lagging behind the other oceans in terms of basic and advanced oceanographic knowledge, are opening up, representing a real (grand) challenge for those countries who have a scientific interest in the area.

The Arctic per se also represents one of the most extreme environments on earth, with some very practical consequences. Its increasing use and exploitation require a deep understanding of some of its basic natural properties. Russia is presently developing the Northern Sea Route (Brigham, 1991) requiring long-term forecasts of the ice cover in the Eurasian shelf seas. The Arctic continental margins are known to host large quantities of fossil hydrocarbons, whose exploration and exploitation require special insight into permafrost phenomena and the processes controlling formation and stability of clathrates (Kvenvolden, 1995). If these problems are approached unprudently, enormous damage may arise reaching in its consequences far beyond the local or regional environment which is directly affected. In the next chapters an attempt will be made to define a number of scientific goals where Arctic paleoceanographic studies can make a contribution of particular significance.

The Arctic Ocean as a Monitor of Global Change

Modern society is using our globe at an ever increasing pace, mostly without being concerned about the consequences for future generations. A debate about the possible onset of a "greenhouse effect" has arisen only lately, but satellite based monitoring of changes of the extent and movement of the Arctic sea ice cover (Colony, in press), of its thickness (Wadhams, 1990, Johannessen et al., 1995), as well as of the stability of terrestrial ice sheets

(Andersen and Borns, 1994) has been used to address this problem. A Russian compilation of changes of the sea ice cover during this century (Abramov, 1994) suggests a close correspondence between the sea ice extent and the global mean temperature; this conclusion is supported by Wadhams (1990) data on Arctic sea ice thickness which have been collected from submarines and which suggest a considerable thinning over the past decades.

Sea ice distributions will be continuously monitored in the years to come, and particular emphasis will be paid to seasonally rapidly moving fringes of the sea ice margins. Lately, large sediment concentrations have been observed first in the segment of the Transpolar Drift crossed by the transects from Svalbard to the North Pole where relatively old sea ice is found (Wollenburg, 1993, Pfirman et al., 1990), later also in the area of sea ice formation in the Eurasian shelf seas. Sediment concentrations in sea ice are changing albedo and a long-term monitoring program in the Laptev Sea presently tries to establish the potential variability and climatic significance of the processes of sea ice formation with sediment entrainment (Kassens et al., 1995). The Eurasian marginal seas usually freeze during late September, early October, while during 1995 large tracts of the central Laptev Sea remained ice free with cold surface waters in 7-15 m water depth being underlain by a previously unobserved, +2-+4°C warm subsurface water layers of unknown origin (TRANSDRIFT III Shipboard Scientific Party, in prep.).

Contributions to scientifically based forecasts of the potential change of the global environment will remain for some time one of the major challenges for Arctic research, but we have now taken the first steps to reach one of the prerequisites by establishing a certain basic understanding of the synoptic state of the Arctic oceanography, of its short-term changes as expressed in hydrographic data and of its ability to leave a signal resulting from long-term trends preserved in sea-floor sediments.

The oceanography of the Arctic deep sea has recently - based on measurements from the above listed modern expeditions - been described in a series of papers (Schlosser et al., 1991, Bönisch and Schlosser, 1995). The distribution of the stable light oxygen isotopes in the Arctic surface waters (Bauch et al., 1995) reflect a particularly interesting pattern because they allow to trace the influx of Atlantic and Pacific waters into the Arctic and the interaction of the Arctic Ocean waters with the fresh water influx from the surrounding continents, and because they can be traced through plankton remains in ocean floor sediments. Distributions of the shell material of planktonic foraminifers living in a hitherto poorly defined interval of the upper water column (Carstens and Wefer, 1992), but surprisingly found throughout the Arctic Ocean even under thick sea ice, and their oxygen isotope ratios have recently been mapped (Fig. 2, from Spielhagen and Erlenkeuser, 1994), illustrating the close correspondence of the distributional patterns of the oxygen isotope ratios to surface-water salinities.

Parallel to the advance in oceanography, geoscientific investigations are establishing ocean wide distribution patterns of a number of paleoceanographic proxies (cf. Fig. 2). Beside biogenic remains, terrigenic sediment components such as various minerals allow to identify the long-term and average importance of source regions on the surrounding continents.

Most of the major river systems draining into the Arctic Ocean carry their individual signal in the mineralogy of suspended materials (Wahsner, 1995) which can then be mapped out in its distributional pattern providing a tool to trace the history of these rivers back in time. Sediment accumulations in the marginal seas are known to accumulate fast as compared to the central Arctic Ocean and will provide detailed records of changes.

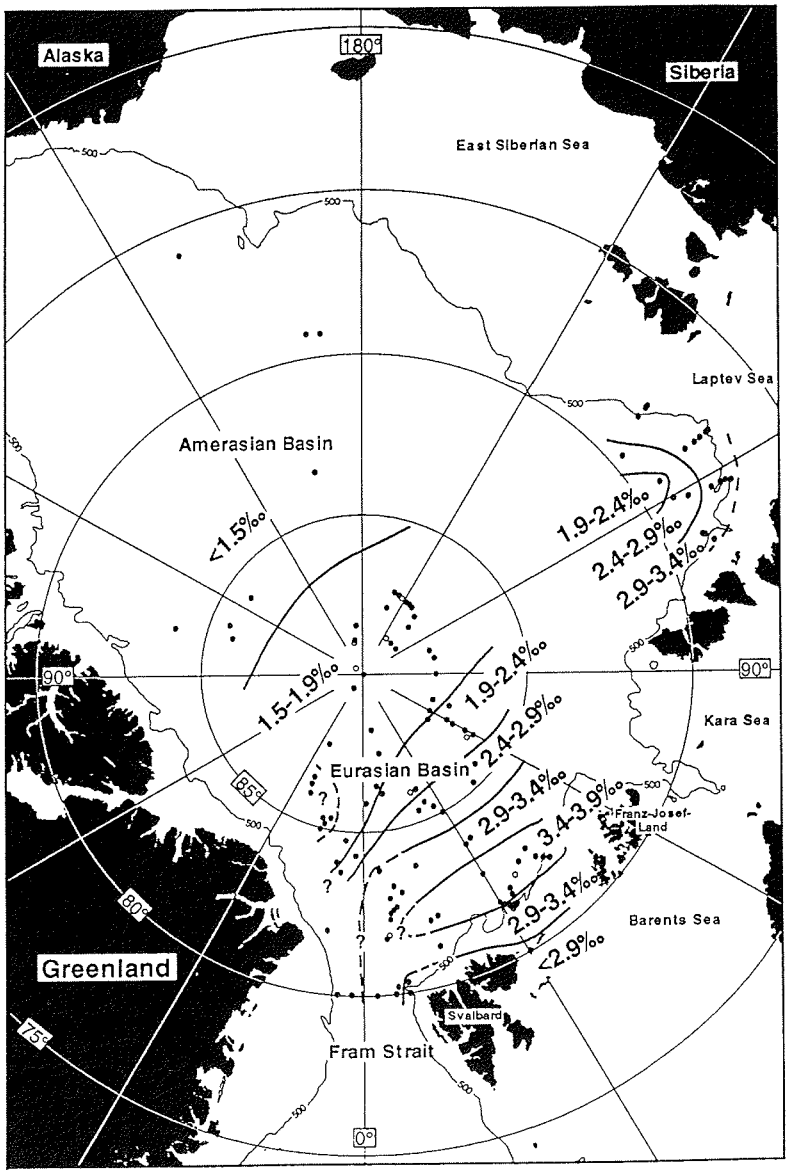

Fig. 2.: Distribution patterns of delta $\partial^{18}O$ isotope ratios in planktonic foraminiferal shell material from surface sediments of the Arctic Ocean (after Spielhagen and Erlenkeuser, 1994).

These ecclectic points selected to address the modern Arctic Ocean and its potential to monitor global change are by no means complete or even representative of the important advances to understand the modern Arctic and the processes controlling its major natural properties. However, they offer a hint that this extremely "Mediterranean" sea whose exploration has been lagging behind the other ocean basins, offers countless challenging new research possibilities in the years to come, and that modern society has the means to do so if the political climate in the circum-Arctic countries stays stable. In addition to much of the detail of the above described properties of the Arctic Ocean major open questions concern the nature and mode of sea ice formation, of the Atlantic influx and its overlying waters, of renewal of the Arctic deep water masses, of the ocean and sea-floor chemistry with respect to its organic carbon (Stein et al., this vol.) and carbonate budgets, of the distributional patterns and life strategies of the endemic plankton and nekton of a low productivity ocean (Nürnberg, this vol.; Stein et al., this vol.), to name a few.

The Chance of Arctic Paleoceanography

The renewed interest in the Arctic Ocean and the novel technical possibilities to visit and sample the areas under the permanent sea ice cover allow to advance in geoscientific problems, too. Even though important for Arctic paleoceanography, the plate tectonic origin of the Arctic deep-sea basins (Lawver et al., 1990) and the particular interesting phenomena of the modern boundary between the Eurasian and North American-Greenland plates will not be considered here. New stratigraphic methods (Eisenhauer et al., 1994), new facilities to obtain ultralong cores (IMAGES, 1994) and to drill the Arctic deep-sea floors (Myhre, Thiede, Firth et al., 1995) as well as to extend the regional core coverage over the entire Arctic permit a new Arctic paleoceanography. The shallow shelf seas around the Arctic rim, however, remain extraordinarily poorly studied at the present time. For the purpose of this book I have chosen to highlight 3 problems, namely the questions of onset of northern hemisphere glaciation, of long- and short-term variability of the ice covers, and the regional patterns of circulation during the last glacial maximum. It is also clear in this perspective that many of the questions which could be posed have to remain open at the present time.

Paleoceanography of the Pre-Glacial Arctic Ocean

The few available fragments of stratigraphic sections representing a pre-glacial depositional environment (Cretaceous to Paleogene in age) represent an Arctic Ocean which was fully marine, but whose gateways to the world ocean are poorly known. The microfossil evidence points to temperate, possibly relatively warm surface waters which were highly productive resulting in the deposition of siliceous oozes (Thiede and NAD Sci. Comm., 1992). The laminated nature of these sediments as well as the occasional occurrence of sapropels (Clark, 1988) points to poorly ventilated bottom waters and henceforth a stable stratification of the water column. As far as the plate tectonic evolution has been resolved (Lawver et al., 1990), prior to the Neogene the Arctic Ocean consisted probably of a series of deep-sea basins separated from each other by the Alpha-Mendeleev and Lomonosov ridges, but with no deep water connection to the adjacent Pacific and North Atlantic Ocean. It must also have had a relatively stable permanent stratification of the

water column which did not permit the deep waters to be renewed. To establish and model patterns and modes of the pre-glacial Arctic oceanography (cf. Clark, 1988) is one of the exciting challenges of the future and requires intense sampling efforts of Mesozoic and Paleogene to lower Neogene sediments on the structural highs which are sufficiently old (mainly Lomonosov Ridge, Alpha-Mendeleev Ridge, Chukchi Plateau, Morris Jesup Rise, Yermak Plateau) and which can be expected to be covered by such deposits. Such sampling will be attempted from the Swedish icebreaker ODEN during summer 1996 (Kristoffersen and Backman, pers. comm.).

Onset of Cenozoic Northern Hemisphere Glaciation

The Cenozoic North Atlantic to Arctic records covering the onset of Cenozoic northern hemisphere glaciation are superior to the Pacific ones because of the stratigraphic details and the spatial resolution of the DSDP and ODP drilling in high latitudes. Since DSDP Leg 38 (Talwani, Udintsev, et al., 1976) it has been well known that 1) the Norwegian-Greenland Sea housed temperate to subtropical surface waters during the Paleogene, 2) indicators of early northern ice covers were not confined to the Quaternary, but also found in unspecified Mio- Pliocene sediments (Warnke and Hansen, 1977), and 3) the history of northern hemisphere glaciation during the latest part of the Cenozoic was much more variable than indicated by the available terrestrial records from Europe and North America, in essence that the deep-sea records were stratigraphically more complete and showed more numerous heavy glaciation events than the corresponding terrestrial ones. Locations drilled to the south of the Greenland-Scotland Ridge during the late phase of DSDP which used a coring technique with often close to 100 % recovery of undisturbed section (Shackleton et al., 1984) later confirmed these results and dated the onset of major northern hemisphere glaciation to 2.4 Ma.

A suite of later ODP legs visited the western North Atlantic with drill sites located to the south of the Greenland Scotland Ridge and in the Labrador Sea. They established the middle to late Miocene onset of glaciation on Greenland (Wolf and Thiede, 1991; Larsen et al., 1994) as well as of an intensification of northern hemisphere glaciation (probably inter alia also on Greenland) approximately 4 Ma. ODP Leg 104 (Eldholm, Thiede, Taylor et al., 1989) drilled a transect across the outer Vøring Plateau off central Norway which allowed a detailed description of the history of the northern extension of the Gulf Stream system, called here the Norwegian Current. As outlined by Jansen and Sjøholm (1991), modest ice-rafting as a sign of incipient glaciation was also observed in upper Miocene sediments on the Vøring Plateau, but the intensification and onset of the highly variable system of alternations of glacials and interglacials observed off S Greenland at 4 Ma, occurred only at 2.6 Ma in the eastern Norwegian-Greenland Sea. During the past 2.6 my the Vøring Plateau area which should react early to warming events was affected by 26 severe glaciations which left dark gray horizons very rich in ice-rafted material (Thiede et al., 1990) in the stratigraphic sequences which over and beyond these intervals mostly represented the products of cold depositional environments, whereas interglacial sediments representing the intrusion of temperate Atlantic waters are exceptional. After ODP Leg 104 it was clear that some kind of a glacial climate mode dominated the entire late Pliocene and Quaternary. Interglacials like the one we are experiencing today are truely exceptional.

The latest and most interesting information on the topic of this paper has been produced by ODP Leg 151 which visited the westernmost Norwegian-Greenland Sea and the approaches to the Arctic Ocean as part of the ODP "North Atlantic-Arctic Gateways" drilling program (Ruddiman et al., 1991). Beside sites on the Iceland Plateau and along the East Greenland continental margins it succeeded to drill the sill depth between the deep Norwegian-Greenland Sea and the Arctic Ocean (Fram Strait) as well to sink wells into the Yermak Plateau which represents an extension of probably volcanic origin of the continental margin of the Barents Sea towards the true Arctic Ocean. The records of the ODP Leg 151 sites (Myhre, Thiede, Firth et al., 1995) contain many examples of the variability of sediment properties in phase with the major orbital Milankovich-frequencies, but it is most astounding to note that the onset of glaciation of these ODP sites of the highest northern latitude ever drilled for scientific purposes seems to occur considerably later than further south (off Greenland), namely only during early Pliocene. Further investigations at key locations in the Arctic Ocean proper are urgently needed to solve this mystery (Thiede and NAD Sci. Comm., 1992).

To use the approach of scientific drilling in the Arctic is expensive and will limit efforts to very few well chosen localities. The problem of the history of the onset of northern hemisphere glaciation will therefore have to be dealt with by means of time series (Imbrie et al., 1992), whereas a set of adequately documented time slices will probably never be available.

Long- and Short-term Variability of the Cenozoic Arctic Ice Cover

Mounting evidence points to the existence of an Arctic sea ice cover for the past several millions years (Thiede and NAD Sci. Comm., 1992, Myhre, Thiede, Firth et al., 1995, Spielhagen et al., subm., cf. Fig. 3). The amount of ice-rafting, however, fluctuated wildly, being relatively monotonous and small prior to 6-700 ka, but revealing four phases of intense ice-rafting (corresponding to O-isotope stages 16, 12, 10 and 6, acc. to Spielhagen et al., subm.) since then (Fig. 3). Other glacial periods such as the last glacial maximum seem to have had a lesser impact on the central Arctic ice-rafting record. These phases of intense ice-rafting have to be related to dynamically changing ice-shields which at variable rates were shedding icebergs transporting these coarse materials probably both from North America/ Greenland as well as on the Eurasian side.

In the near future the facilities to take long sediment cores in the deep central Arctic Ocean will be available. In preparation of scientific drilling into the deep Arctic Ocean floors and with the opportunity of presently available ice breaker capabilities it will be important to plan for a systematic long and large volume sediment coring program with the aim to sample the major structural highs with undisturbed pelagic sediment sequences at locales with relatively high sedimentation rates. At the same time the coring program which could be a contribution to the international IGBP Core Project IMAGES (IMAGES, 1994) should be planned that all major distinct elements of the Arctic sea ice cover and of the surface, intermediate as well as bottom waters are covered.

This approach as well as newly developed stratigraphic techniques (Clark et al., 1986; Eisenhauer et al., 1994) would allow to establish time series for the various compartiments of the Arctic paleoenvironment as well to construct time slices for a number of crucial scenarios such as the pre-O-isotope stage 16

type of ice rafting, the 4 important ice rafting events, for a number of well developed interglacials as well for preglacial and deglacial transitional periods.

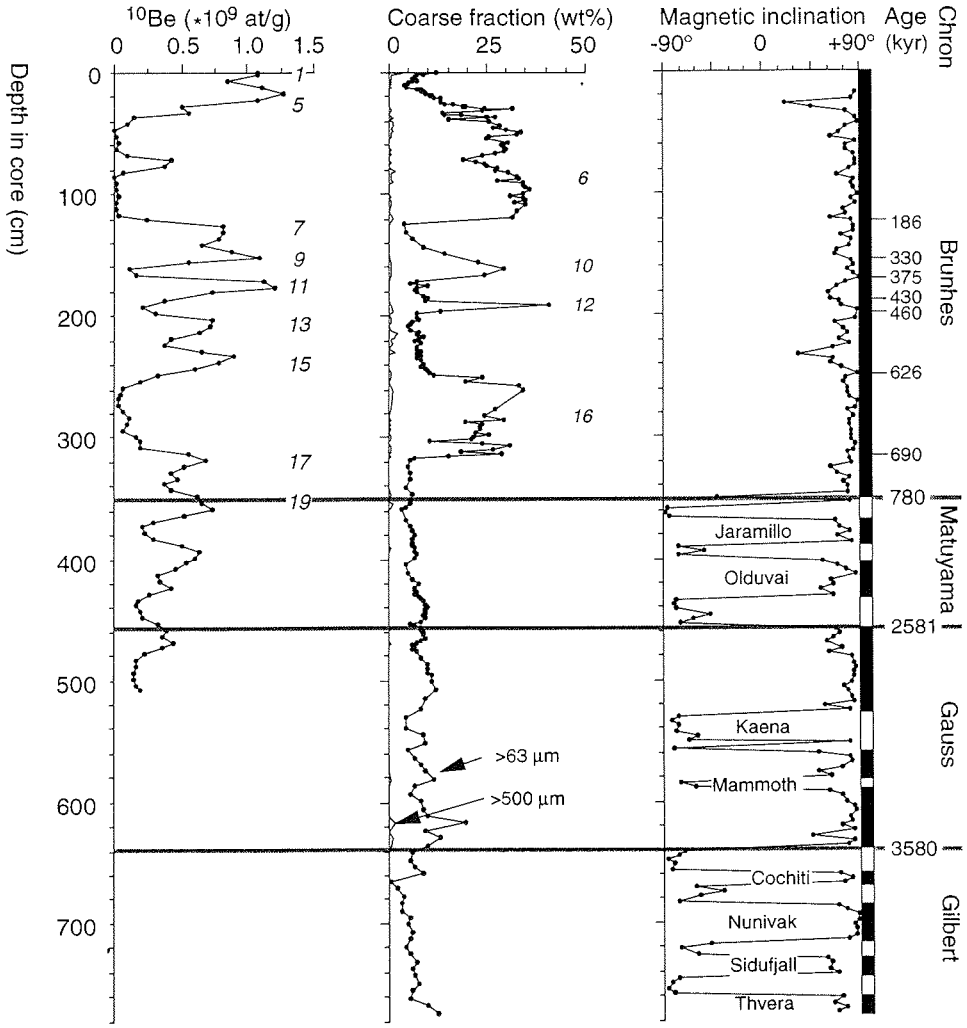

Fig. 3.: Stratigraphy of Core PS 2185 on the crest of the Lomonosov Ridge at 87°32´N 144° 56´E at 1052 m water depth (from Spielhagen et al., subm.). The newly established ^{10}Be stratigraphy together with AMS, ESR, and Amino Acid Dating and on the basis of magnetostratigraphic data have resulted in a temporal resolution comparable to the paleoceanographic records of the Norwegian-Greenland Sea. Henceforth a detailed picture of the paleoceanographic changes of the central Arctic can be deduced from these core materials (Fütterer, 1992).

The Arctic Ocean During the Last Glacial Maximum

In Figure 2 we have shown the distribution of the light stable oxygen isotope values in the shell material of planktonic foraminifers after they have settled down to the sea-floor surface corresponding to the modern or late Holocene situation. By virtue of the relationships between the oxygen isotope ratios and the salinity of the surface waters (under the assumption that these waters in the Arctic Ocean are pretty much isothermal) one can construct the distribution of salinities from these values assuming an average temperature of the surface waters (corresponding to the habitat of the planktonic foraminifers) being at -1.7°C (from Nørgaard-Pedersen, 1996 in prep.). The impact of the high salinities of the Atlantic waters in the south-eastern part of the eastern Arctic Ocean can clearly be shown by means of this approach. Now, by using the stratigraphies (cf. Fig. 3) of as many cores as possible where the last glacial maximum could be identified by a variety of stratigraphic methods one can attempt to construct a similar map for the last glacial maximum. This is shown in Fig. 4 of this report identifying the potential of this method. The oxygen isotope ratios of the planktonic foraminifers reveal isotopic values for the entire Fram Strait area and the area of the Yermak Plateau coinciding well with the values reconstructed for the Norwegian-Greenland Sea as shown by Sarnthein et al. (1995). The obvious difference to the modern or late Holocene is the disappearance of the relatively light values related to the influx of Atlantic waters. Any attempts to estimate salinities based on this method must then show the complete disappearance of the current pattern as could be shown for the modern circulation system we know from the northern Norwegian-Greenland Sea, from the Fram Strait and from the eastern Arctic Ocean adjacent to the Eurasian continental margin. However, the most astonishing aspect of this reconstruction is the emergence of lower salinities in the westernmost Fram Strait and, in particular, in the central and western part of the Arctic Ocean where a similar gradient of decreasing salinities towards a water mass which was much more brackish than the water mass adjacent to the Fram Strait could be identified. The geographic pattern of this gradient has not been identified and described properly because in the moment we do not have access to a sufficiently large number of cores from the entire Arctic Ocean but it is quite clear that a different system has to be assumed for the "glacial" circulation patterns and ice covers in the Arctic Ocean. One of the great challenges for the reconstruction of the Arctic paleoceanography is henceforth (as difficult as it may be) the establishment of as many time slices as possible which can be identified for a sufficiently large number of cores which will decrease in precision and number with increasing sediment age for the Arctic Ocean. It was a lucky coincidence of the first probing attempts to enter the eastern Arctic Ocean by European researchers to identify areas of sedimentation of relatively high temporal resolution and to be able to pin-point this pattern of paleoceanographic variability at all (Boström and Thiede, 1984).

Beside the establishment of time slices great efforts will be devoted to identify areas of ultra-high sedimentation in the eastern Arctic Ocean to be able to resolve its paleoceanographic variability in greater detail than has been hitherto. Particular promising areas can be found along the northern and deeper parts of the continental slope along the entire Eurasian continental margin. Here we find a zone where terrestrial signals mix with oceanic signals and where it will be possible not only to decipher the paleoceanographic history of the oceanic water masses, but also the geological and

environmental history of the shelf areas adjacent to the continental slopes as well as that of the continental hinterlands in northern Europe and in Siberia. Both are areas of great paleoclimatic significance and promising scientific challenge (confer the recently established QUEEN Program of the European Science Foundation). The ultimate goal of these high resolution studies will comprise attempts to describe the history of the ice cover as well as of the oceanic water masses and the other environmental parameters in a temporal resolution of less than 100 years. Promising high sedimentation rate areas have recently been found off the Lena-Delta in the outer Laptev Sea (Spielhagen and Bauch, pers. comm., 1996).

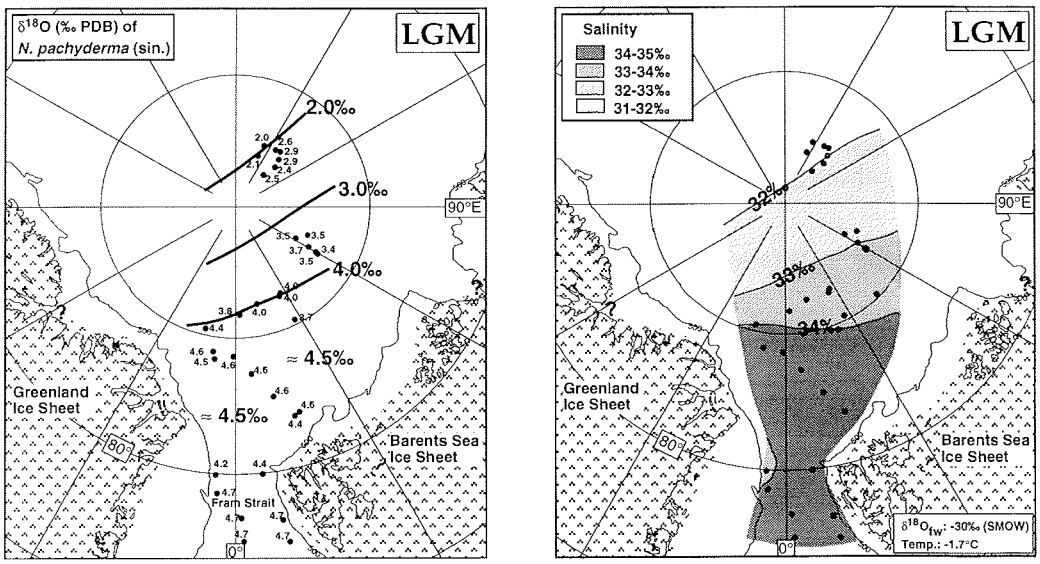

Fig.4.: Surface water salinities in the eastern and central Arctic Ocean (right) during the last glacial maximum (LGM) as reconstructed from oxygen isotope values (left) of planktic foraminifers Neogloboquadrina pachyderma (sin.) (from Nørgaard-Pedersen, in prep.).

The Problem of the Evolution of Polar Marine Biota

Marine biota have developed in the polar seas of both hemispheres. They are adapted to extreme environments and they exhibit in many aspects a great degree of similarity, although only very few bipolar species have been identified hitherto. On the other hand, they are also displaying considerable differences in their composition and nature. Their history is virtually incomparable because Antarctic marine biota adapted to cold extreme paleoenvironments over 30-40 m.y. ago, while the Arctic biota had only 10 - 12 m.y. for this adaptation.

It can be shown that both the southern Ocean as well as the Arctic Ocean were fully marine throughout their Cenozoic history, covering the entire time span of the cooling of surface- und bottom-water masses from the temperate regimes of the early Cenozoic to the extreme and very cold regimes during the latest part of the Cenozoic. All other parameters of the habitat of these biota remained fully marine; it can be assumed that a detailed record of the evolution of the polar biota may provide one of the simplest and most quantitative experiments in evolutionary studies in paleontology.

However, both in the polar waters of the southern hemispheres as well as in the Arctic Ocean the paleontologic record of the marine biota is changing very fast in its composition, because the preservation of the skeletal record of the marine biota in the oceanic sediments documents switches from one fossil group to the other and certain evolutional trends within these. No contiguous evolution of one fossil group covering the entire time span has been produced (maybe with the exception of palynomorphs such as dinoflagellates). A survey how to procede was published by the Nansen Arctic Drilling Science Committee (Thiede and NAD Sci. Comm., 1992) and it will require substantial drilling efforts to resolve this part of the polar life histories.

Modelling Different Arctic Oceans

The Arctic Ocean as a separate ocean basin has been isolated or virtually isolated for deep- as well as shallow-water exchange from the rest of the world ocean for most of the time of its existence. It had a polar position throughout the last 7-80 m.y. and comprised always (as far as can be documented by the available sample record) fully marine environments with highly different temperature regimes as well as a variety of types of ice covers during the latest geological past. It is a major challenge to the modelling community within oceanography to try to model (cf. Clark, 1988) the functioning of an Arctic Ocean in a polar position when surface water masses were temperate, fertile and highly productive while bottom water masses were oxygen deficient and probably stagnant (= ? euxinic). Up to now this stage is only documented by very few cores but it would be challenging to know how it could have functioned in terms of oceanography producing very fertile surface water masses resulting in a siliceous biogenic record.

Modelling efforts will be needed to understand when, where and how incipient ice covers began to develop in the Arctic Ocean and how a variety of types of ice covers as documented by the sediment cores could develop over the Arctic Ocean.

The latest effort which requires an integration of modelling of the terrestrial temperature regime of the ice-sheet record of the continents and shelf seas surrounding the Arctic Ocean as well as of the sea-ice covers will be needed to gain some understanding of the framework condition which led to the highly variable youngest part of the history of the Arctic Ocean.

Based on these modelling efforts one will have to make assumptions and efforts to come up with a scientifically based quantitative assessment of the potential of future environmental change in the Arctic Ocean which will have to

be matched by the observation record collected during these years. The Arctic Ocean per se is representing, indeed, a grand challenge for European polar sciences.

A New Concerted Effort

The new political climate around the Arctic as well as the available technical facilities call for a new and concerted effort of parties who have a scientific and environmental interest in the natural properties of the Arctic seas. At present progress in Arctic paleoceanography is less a question of available techniques of scientific analyses, but rather a problem of organizing (scientifically, financially and politically) the necessary field operations. It is a strange observation that sufficient ship time on ice-breakers and on ice-reinforced drilling platforms is available if necessary financing can be found and that some of the many available tools are sitting idle because of the poor and disconcerted organisation of Arctic science. What should be done?

- There is no detailed geophysical data base from the Arctic which would allow to plan adequately (quality of site locations, safety considerations) for proper locations for scientific drilling or even for taking giant piston cores. A major effort to conduct site surveys in the Arctic deep and shallow areas should immediately be mounted. ODP requirements and procedures provide good examples how this could be achieved.
- The Nansen Arctic Drilling Program (NAD) has been formed at the IGC 1989 and is trying to provide a programmatic framework for scientific drilling in the permanently ice-covered central Arctic (Thiede and NAD Science Committee, 1992). Technical means are available though yet unproven in the Arctic deep sea. The first attempt to use a light drill rig from the Swedish ODEN will be carried out in 1996 (Kristoffersen and Backman, pers. comm., 1995).
- Under the frame of NAD scientific drilling will also be attempted in the shallow shelf, with the aim to sample continent-near sites with extraordinarily high sedimentation rates and henceforth temporal resolution. Selected target areas are the McKenzie Delta where commercial drilling has provided access to a long and very valuable stratigraphic section and new drilling in the Laptev Sea employing mainly Russian scientific institutions and drilling technology. Site survey and safety requirements as well as the political and financial preparation of such drilling will, however, result in considerable delays of the actual drilling.
- New giant piston coring systems can easily be adopted to a number of the available ice breakers and proposals are under preparation for an Arctic IMAGES-program (IMAGES, 1994). Sufficient shallow reflection seismic profiles are already available at present to select coring sites where complete undisturbed young sediments can be found and where outcropping older parts of the stratigraphic sequence can be cored. On the flanks of Lomonosov Ridge, for example, a probably complete Neogene section could be sampled using a stepwise approach, provided ice conditions allow a sufficiently precise positioning of the ice breaker.
- Visits of ice breakers to the North Pole have demonstrated that the Arctic sea ice cover presently is in a state being navigable for sufficiently powerful ships. Provided sufficient preparation and international coordination, synoptic studies of a wide range of oceanographic disciplines can be carried out in the Arctic, in this case a concerted effort to collect high sedimentation

rate young deposits to decipher the paleoceanographic variability of the Arctic and to adequately describe the geologically important properties of its recent depositional environment.

- Ice breakers are sometimes not the most efficient tools to carry out systematic surveys. For several years possibilities have been evaluated to involve (nuclear) submarines or large, long-range AOVs in Arctic sub-ice surveys (swath mapping, side scan sonar surveys, seismic reflection surveys, a wide variety of hydrographic, chemical and biological measurements) should be vigorously persued.

The availability of powerful ice breakers (Russia, Japan, US, Canada, Sweden, Germany, Finland) suitable to support research activities to a range of research communities, the political and financial situation as well as the establishment of relatively large and diversified groups of scientists in government, industrial and academic research institutions represent a golden opportunity to advance Arctic deep-sea research to a level equivalent with the other oceans which should be used by the international scientific community.

Acknowledgments

Many of the ideas described in this short report have been developed in close and intimate intellectual exchange with a small working group at GEOMAR, with colleagues at the Alfred-Wegener-Institute in Bremerhaven and with many international researchers with whom we cultivate an intense scientific exchange. The source of many of these ideas is resulting rather with this entire group than with one individual author and I would like to take the opportunity to acknowledge this free academic and scientific exchange of thoughts between the various communities.

References

Aagaard, K., Barrie, L.A., Carmack, E.C. et al., 1996: U.S., Canadian Researchers Explore Arctic Ocean. - EOS Trans. Amer. Geophys. Un., 77(22):209-210.

Abramov, V.A., 1994: Sea ice variation and biological productivity in the Polar Basin. - In: H. Kassens, H.W. Hubberten, S. Priamikov and R. Stein (eds.) Reports on Polar Research 144:55-68.

Andersen, B.G. and Borns, H.W. (eds.), 1994: The Ice Age World. An Introduction to Quaternary History and Research with Emphasis on North America and Northern Europe During the Last 2.5 Million Years. - Scandinavian University Press, Oslo-Copenhagen-Stockholm, 208 pp.

Anderson, L.G. and Carlsson, M.L. (eds.), 1991: International Arctic Ocean Expedition 1991, Icebreaker ODEN - Cruise Report. - Swedish Polar Research Secretariat, 128 pp.

Bauch, D., Schlosser, P. and R.G. Fairbanks, 1995: Freshwater balance and the sources of deep and bottom waters in the Arctic Ocean inferred from the distribution of $H_2{}^{18}O$. - Prog. Oceanog., 35: 53-80.

Bond, G., Broecker, W., Johnsen, S. et al., 1993: Correlations between climate records from North Atlantic sediments and Greenland ice. - Nature, 365:143-147.

Bönisch, G. and P. Schlosser, 1995: Deep water formation and exchange rates in the Greenland/Norwegian Seas and the Eurasian Basin of the Arctic Ocean derived from tracer balances. - Prog. Oceanog., 35: 29-52.

Boström, K. and J. Thiede, 1984: YMER-80, Swedish Arctic Expedition - Cruise Report for Marine Geology and Geophysics, Sediment Core Descriptions. - Medd. Stockholms Univ. Geol. Inst., 260: 123 pp.

Brigham, L.W., 1991: The Soviet Maritime Arctic. - WHOI Contribution No. 7609, 336 pp.

Broecker, W.S., 1994: An unstable superconveyor. - Nature, 367: 414-415.

Carstens, J. and G. Wefer, 1992: Recent distribution of planktonic foraminifera in the Nansen Basin, Arctic Ocean. - Deep-Sea Res., 39 (Suppl. 2): 507-524.

Clark , D.L., Andree, M. and W.S. Broecker et al., 1986: Arctic Ocean chronology confirmed by accelerator ^{14}C dating. - Geophys. Res. Letters, 13(4):319-321.

Clark, D.L., 1988: Early history of the Arctic Ocean. - Paleoceanography, 3: 539-550.

Colony, R., in press: Seasonal mean ice motion in the Arctic Basin. - Proceedings of the International Conference on the Role of the Polar Regions in Global Change, 19 pp.

Eisenhauer, A. Spielhagen, R.F., Frank, M., Hentzschel, G. et al., 1994: ^{10}Be records of sediment cores from high northern latitudes: Implications for environmental and climatic changes. - Earth Planet. Sci. Letters, 124: 171-184.

Eldholm, O., Thiede, J., Taylor, E. et al., 1989: Proc. ODP, Sci. Results, 104, Ocean Drilling Program, College Station, TX.

Fütterer, D.K. (ed.), 1992: ARCTIC'91: Die Expedition ARK-VIII/3 mit FS "Polarstern" 1991. - Ber. Polarforsch., 107: 267 pp.

Gordijenko, P. (ed.), 1967: Die Polarforschung der Sowjetunion. - Econ-Verlag, Düsseldorf-Wien. 350 pp.

Gudmandsen, P. (ed.), 1980: Eastern Arctic Science. - Workshop Report. - Comm. for Scientific Work in Greenland, Lyngby, Denmark, Jan. 1979. 135 pp.

IMAGES 1994: Pisias, N., Jansen, E., Labeyrie, L., Mienert, J. and N.J. Shackleton, 1994: International Marine Global Change Study. A marine component to the PAGES/PANASH project under joint sponsorship of SCOR and PAGES. PAGES Workshop report, Series 94-3: 37 pp.

Imbrie, J., Boyle, E.A., Clemens, S.C., Duffy, A. et al., 1992: On the Structure and Origin of Major Glaciation Cycles. 1. Linear Responses to Milankovitch Forcing. - Paleoceanography, 7(6):701-738.

Jansen, E. and J. Sjøholm, 1991: Reconstruction of glaciation over the past 6 million years from ice-borne deposits in the Norwegian Sea. - Nature, 349: 600-604.

Johannessen, O.M., Miles, M. and E. Bjørgo, 1995: The Arctic's shrinking sea ice. - Nature, 376:126-127.

Kassens, H., Piepenburg, D., Thiede, J., Timokhov, L., Hubberten, H.W. and S.M. Priamikov (eds.), 1995: Russian-German Cooperation: Laptev Sea System. Ber. Polarf., 176: 387 pp., Bremerhaven.

Kvenvolden, K., 1995: Natural gas hydrate occurrence and issues. - Sea Technology, 36(9): 69-74.

Larsen, H.C., Saunders, A.D., Clift, P.D., Beget, J., Wei, W., Spezzaferri, S. and ODP Leg 152 Scientific Party, 1994: Seven million years of glaciation in Greenland. - Science, 264: 952-955.

Lawver, L.A., Müller, R.D., Srivastava, S.P. and W. Roest, 1990: The opening of the Arctic Ocean. In: Bleil, U. and J. Thiede (eds.): Geological History of the Polar Oceans: Arctic versus Antarctic. - NATO ASI Series C308: 29-62, Kluwer Acad. Publ., Dordrecht.

Myhre, A.M., Thiede, J., Firth, J.V. et al., 1995. Proc. ODP, Init. Repts., 151, 926 pp., College Station, TX (Ocean Drilling Program).

Nansen, F., 1904: The bathymetrical features of the North Polar Seas, with a discussion of continental shelves and previous oscillations of the shoreline, Norwegian North Polar Expedition, 1893-1896. - Sci. Res., 4: 232 pp.

Nørgaard-Pedersen, N., 1996 (in prep.): Paläo-Ozeanographie und Paläoklimatologie des östlichen und zentralen Arktischen Ozeans während der letzten 50.000 Jahre.

Pfirman, S., Lange, M.A., Wollenburg, I. and P. Schlosser, 1990: Sea ice characteristics and the role of sediment inclusions in deep-sea deposition: Arctic-Antarctic comparisons. In: Bleil, U. and J. Thiede (eds.): Geological History of the Polar Oceans: Arctic versus Antarctic. - NATO ASI Series C308: 187-211, Kluwer Acad. Publ., Dordrecht.

Ruddiman, W.F., and JOIDES NAAG-DPG, 1991: North Atlantic Arctic gateways. - JOIDES J., 17: 38-50.

Sarnthein, M., Jansen, E., Weinelt, M., Arnold, M. et al., 1995: Variations in Atlantic surface ocean paleoceanography, 50°-80° N: A time-slice record of the last 30,000 years. - Paleoceanography, 10: 1063-1094.

Schlosser, P., Bönisch, G., Rhein, M. and R. Bayer, 1991: Reduction of deepwater formation in the Greenland Sea during the 1980s: Evidence from tracer data. - Science, 251: 1054-1056.

Schytt, V., Boström, K. and C. Hjort, 1981: Geoscience during the Ymer-80 expedition to the Arctic. - Geol. Fören. Stockholm Förhandl., 103: 109-119.

Shackleton, N.J., Backman, J., Zimmerman, H., Kent, D.V., Hall, M.A., Roberts, D.G., Schnitker, D., Baldauf, J.G., Desprairies, A., Homrighausen, R., Huddlestun, P., Keene, J.B., Katenback, A.J., Krumsiek, K.A.D., Morton, A.C., Murray, J.W. and J. Westberg-Smith, 1984: Oxygen isotope calibration of the onset of ice-rafting and history of glaciation in the North Atlantic region. - Nature, 307: 620-623.

Spielhagen, R.F., Eisenhauer, A., Frank, M., Frederichs, T., Kassens, H. et al. (subm.): Arctic Ocean evidence for Late Quaternary onset of northern Eurasian ice sheet development.

Spielhagen, R.F. and H. Erlenkeuser, 1994: Stable oxygen isotopes in planktic foraminifers from Arctic Ocean sediments: Reflection of the low salinity surface water layer. - Mar. Geol., 119: 227-250.

Talwani, M., Udintsev, G. et al., 1976. Init. Repts. DSDP, 38: Washington (U.S. Govt. Printing Office), 1256 pp.

Thiede, J. (ed.), 1988: Scientific cruise report of the Arctic Expedition ARK IV/3. Ber. Polarforsch., 88: 237 pp., Bremerhaven.

Thiede, J., Clark, D.L. and Y. Herman, 1990: Late Mesozoic and Cenozoic paleoceanography of the northern polar oceans. In: Grantz, A., Johnson, L. and J.F. Sweeney (eds.): The Arctic Ocean region. Geology of North America, Vol. L: 427-458, Boulder, CO.

Thiede, J. and NAD Science Committee, 1992: The Arctic Ocean record: key to global change (initial science plan). - Polarforsch., 61: 102 pp.

TRANSDRIFT III Shipboard Scientific Party (in prep.): EOS, Trans. Amer. Geophys. Union.

Wadhams, P.: 1990: Evidence for thinning of the Arctic ice cover north of Greenland. - Nature, 345: 795-797.

Wahsner, M., 1995: Mineralogical and sedimentological characterization of surface sediments from the Laptev Sea. - In: Kassens, H., Piepenburg, D., Thiede, J., Timokhov, L., Hubberten, H.W. and S.M. Priamikov (eds.): Russian-German Cooperation: Laptev Sea System. Ber. Polarf., 176: 303-313, Bremerhaven.

Warnke, D.A. and M.E. Hansen, 1977: Sediments of glacial origins in the area of DSDP Leg 38 (Norwegian-Greenland seas): Preliminary results from Sites 336 and 344. - Ber. Naturforsch. Ges. Freiburg, 67: 371-392, Freiburg/Breisgau.

Wolf, T.C.W. and J. Thiede, 1991: History of terrigenous sedimentation during the past 10 m.y. in the North Atlantic (ODP Legs 104 and 105, and DSDP Leg 81). - Mar. Geol., 101: 83-102.

Wollenburg, I., 1993: Sedimenttransport durch das arktische Meereis: Die rezente lithogene und biogene Materialfracht. - Ber. Polarforsch., 127: 159 pp., Bremerhaven.

SEDIMENTOLOGY, MINERALOGY, AND GEOCHEMISTRY

TERRIGENOUS SEDIMENT SUPPLY INTO THE ARCTIC OCEAN: HEAVY-MINERAL DISTRIBUTION IN THE LAPTEV SEA

Behrends M.*, Peregovich B.**, and Stein R.*

*Alfred Wegener Institute, Bremerhaven, Germany
**GEOMAR - Research Centre, Kiel, Germany

Abstract

In this study heavy minerals were investigated in sediments from the Laptev Sea and adjacent continental slope to identify sediment source areas and transport processes. Different heavy-mineral assemblages are caused by different source areas. The western part of the Laptev Sea is dominated by high amounts of clinopyroxene which are interpreted as erosion products of Severnaya Zemlya and of the sheet basalt complexes of the Taymyr peninsula, transported by the river Khatanga. Transport vehicel of particels in the area of Severnaya Zemlya are icebergs whereas on the shelf sea ice is controlling the sediment transport into the Arctic Ocean. The eastern part of the Laptev Sea is characterized by amphiboles that are delivered by the rivers Lena and Yana from the Siberian hinterland. An additional source could be erosion products from the New Siberian Islands.

Introduction

The Eurasian parts of the Arctic Ocean are surrounded by wide and shallow shelf areas. Input of sediment and water delivery are controlled by the major Siberian river systems. In the western part of the Laptev Sea, the rivers Khatanga, Olenek, and Anabar are responsible for the sediment supply. In the Eastern Laptev Sea, the rivers Lena and Yana control the sedimentation on the shelf. Different processes and mechanisms are triggering the transport and the distribution of particles of different size in the marginal seas and the adjacent deep sea basins. The most important factors controlling sediment transport are fluvial input, drift of sea ice and icebergs, ocean currents, and gravitational mass flows (turbidity currents and debris flows) (cf. Stein and Korolev, 1994). After entrainment into sea ice, sediment is transported via the Transpolar Drift through the Central Arctic Ocean to the Fram Strait.

To study the present sedimentary environment, surface samples are taken with a giant boxcorer during RV "Polarstern" Cruises ARK-IX/4 (Fütterer et al., 1994) and ARK XI/1 (Rachor, 1996) and RV "Prof. Multanowsky" Cruise "Transdrift II" (Kassens and Dmitrenko, 1995). In order to identify and quantify the different ways of particle flux our investigations are focussed on the sand and silt fractions, which are preferencially transported by ice-rafting. Because of its small grain size, clay is dominantly transported in suspension through ocean currents. Clay and coarser sediment material, on the other hand, are distributed by massflows and, especially, by entrainment into sea ice that is produced on the shelves, mostly in the Laptev Sea.

Methods

The heavy minerals of the subfractions 32 - 63µm and 63 - 125µm were investigated. These subfractions were separated using sodiummetatungstate with a density of 2.83g/cm^3. After 20 min centrifugation, the heavy fraction was frozen in liquid nitrogen. The light minerals were decanted, and the heavy minerals rinsed on filters and dried. The heavy fraction was mounted with Meltmount (n=1,68), optically identified, and counted using a polarisation microscope. On average between 180 - 220 grains were counted on the thin slides.

Results

Amphiboles characterize the eastern part of the Laptev Sea with up to 40 grain% in the silt fraction (Fig. 1) and up to 50 grain% in the fine sand fraction (Fig. 2). In the fraction 32 - 63 µm, the high amphibol contents are concentrated on the outer part of the shelf, near the eastern islands, and towards the continental slope.

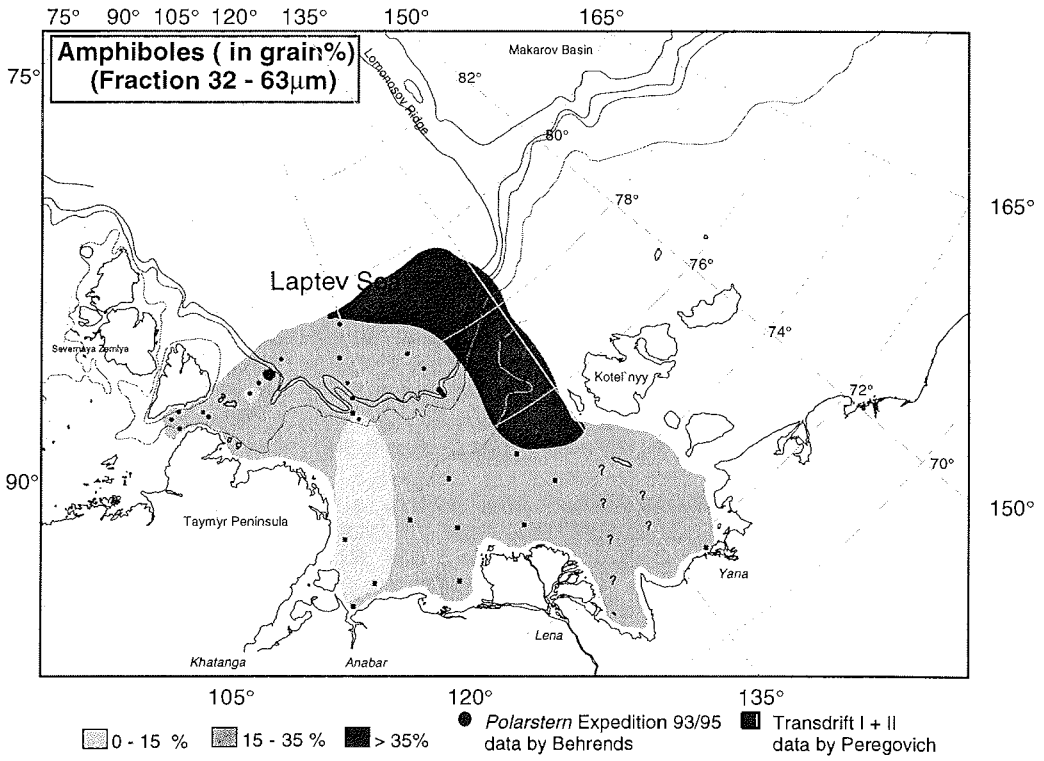

Fig. 1.: Distribution of amphibole in the subfraction 32 - 63 µm.

However, both the silt and the sand fractions show higher contents of amphibole in the eastern part of the shelf. In the sand fraction highest concentrations of up to 35 grain% occur in the eastern Laptev Sea. This tendency of increasing concentrations of amphibole from west to east can be recognized on the shelf as well as on the slope and the adjacent deep sea of Amundsen and Makarov Basins. Off the Khatanga mouth the amphibole concentration is only 0 - 15 grain%. On the shelf close to Severnaya Zemlya as well as in the Vilkitsky Strait amphibole reaches values of up to 15 - 25 grain%.

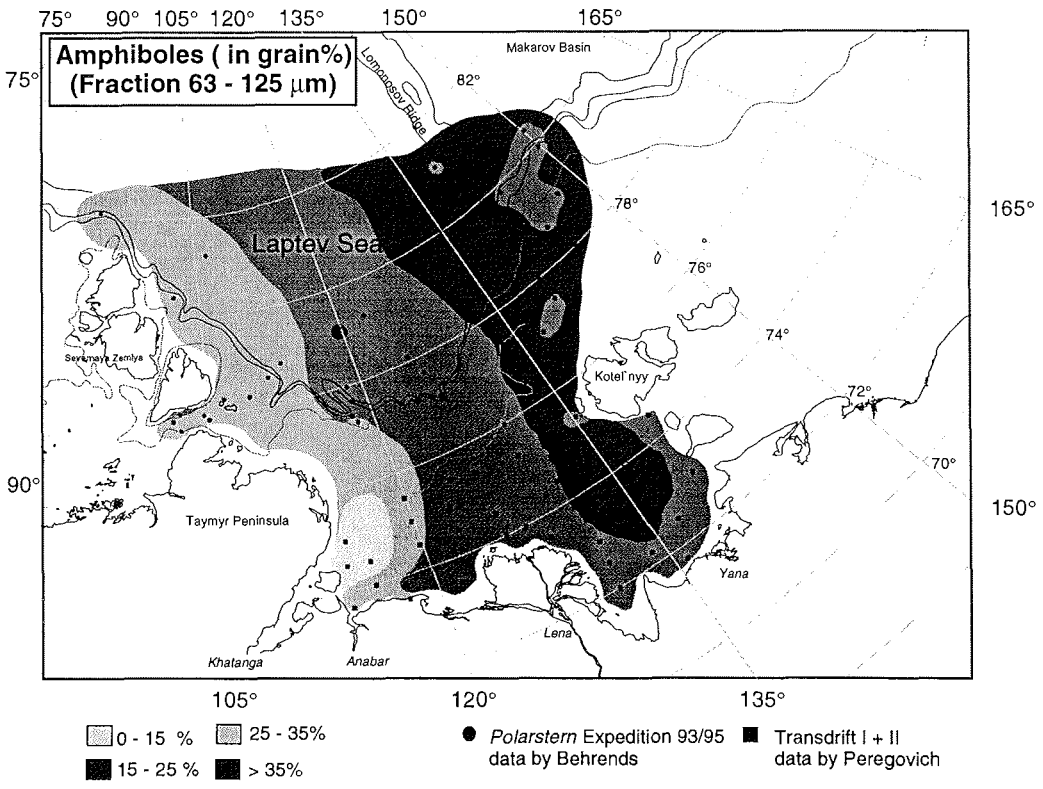

Fig. 2.: Distribution of amphibole in the subfraction 63 - 125µm.

In contrast contents of clinopyroxene of up to 35 grain% are found near the Khatanga outflow and decrease to the east.

Medium concentrations of 15 - 35 grain% and less are found in the terraines of Severnaya Zemlya and the Vilkitsky Strait (Fig. 3 and 4) with decreasing values to the north and to the east as well as towards the New Siberian Islands, where they reach values between 0 - 15 grain%. These trends are reflected in both subfractions.

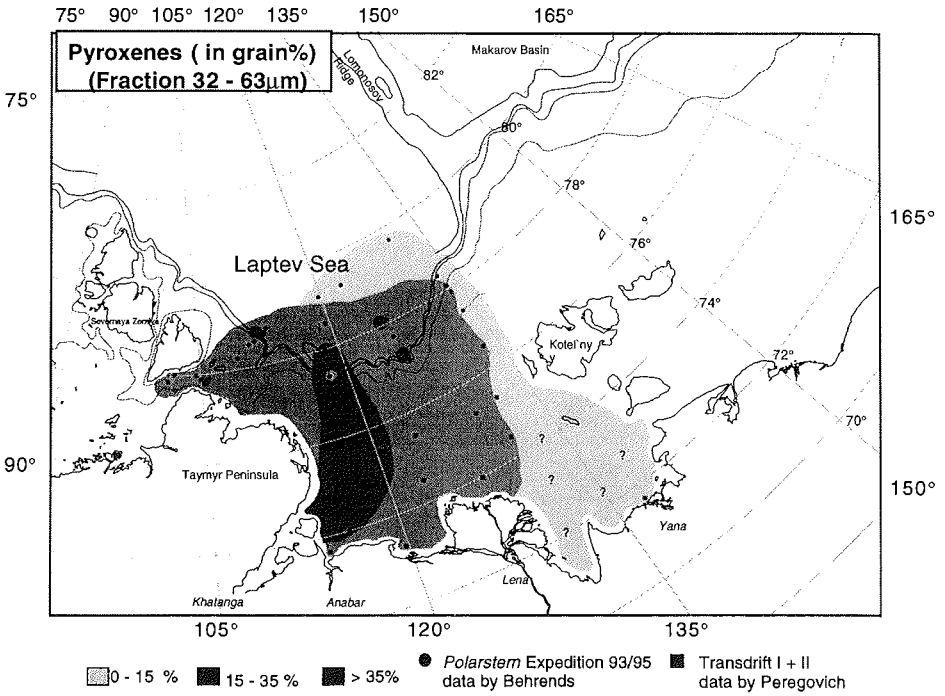

Fig. 3.: Distribution of clinopyroxene in the subfraction 32 - 63µm.

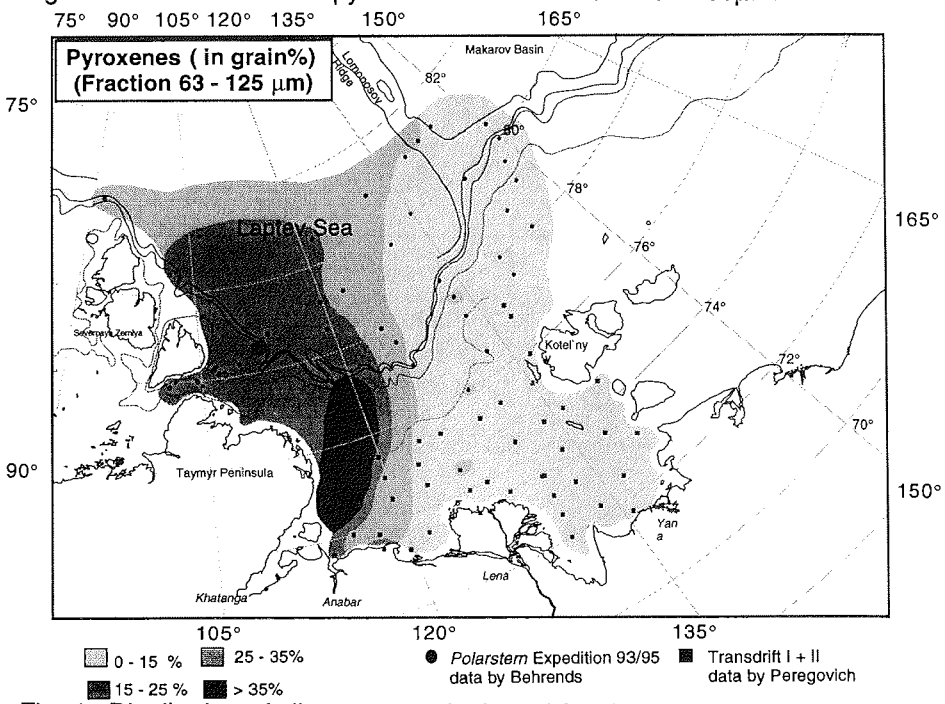

Fig. 4.: Distribution of clinopyroxene in the subfraction 63-125 µm.

Discussion

The sediment supply into the Laptev Sea is mainly controlled by the Siberian river systems. The heavy-mineral distribution in the eastern Laptev Sea is dominated by high contents of amphibole, which is caused by the input of the rivers Lena and Yana. Erosion products from Kotel´nyy Island and sediment supply from the East Siberian Sea may be an additional source of the amphiboles. The input via Vilkitsky Strait and the river Khatanga changes the amphibole-clinopyroxene-epidote assemblage into a clinopyroxene-amphibole-epidote assemblage.

These changes in the heavy-mineral distribution are supported by clay-mineral data (Silverberg, 1972; Wollenburg, 1993; Nürnberg et al., 1994; Wahsner, 1995). The content of illite decreases from east to west and probably has its source area in the Yana and Lena rivers, and the East Siberian Sea.

In both investigated subfractions a slight dilution of clinopyroxene through the input from the Kara Sea via Vilkitsky Strait may be recognized. The clinopyroxene distribution shows a similar pattern as the smectite distribution (Silverberg, 1972; Wollenburg, 1993; Nürnberg et al., 1994; Wahsner, 1995). Smectite is also mainly delivered by the Khatanga river and from the Kara Sea. This implies that smectite and clinopyroxene have similar source regions, for smectite the Taymyr peninsula and the Kara Sea, and for clinopyroxene the Taymyr peninsula, but for a lesser extend the Kara Sea. The medium content of 15 - 35grain% in the Vilkitsky Strait suggests, that clinopyroxene is mainly delivered by the Khatanga. High concentration of this mineral off the river mouth is probably caused by larger amounts of coarser-grained material in this area, that is related to fluvial input (Silverberg, 1972; Wollenburg, 1993; Wahsner, 1995).

In combination and comparison with data of clay minerals, inorganic and organic geochemical tracer, grain size distribution, and IRD-content, heavy-mineral data from long cores from the Laptev Sea and the Central Arctic Ocean will allow the reconstruction of transport processes and pathways, the quantification of sediment budgets, and estimation of flux rates in different areas, and their changes through time.

Conclusion

Heavy-mineral investigations in surface sediments from the Laptev Sea shelf and slope allowed to distinguish between an eastern source area dominated by amphibole and a western source area dominated by clinopyroxene. This knowledge will be extented to analyses of surface sediment and sea-ice samples from the Central Arctic Ocean that will form the reference data set for the ongoing and planned investigations of long sediment cores.

References

Fütterer, D. K., 1994. The Expedition Arctic `93 of RV "Polarstern" in 1993. Berichte zur Polarforschung, 149 : 244 p.

Kassens, H. 1995. The Transdrift II Expedition to the Laptev Sea. In: Laptev Sea System: Expeditions in 1994. Berichte zur Polarforschung, 182: 180 p.

Nürnberg, D., Wollenburg, I., Dethleff, D., Eicken, H., Kassens, H., Letzig, T., Reimnitz, E. and Thiede, J., 1994a. Sediments in Arctic sea ice: Implications for entrainment, transport and release. In: Thiede, J., Vorren, T. and Spielhagen, R.F. (Eds.), Marine Geology. 119: 185 - 214.

Rachor, E.,1996. Scientific Cruise Report of the 1995 Expedition ARK-XI/1 of RV "Polarstern" (Northern Laptev Sea and Adjacant Waters). Berichte zur Polarforschung (in press).

Silverberg, N., 1972. Sedimentology of the surface sediments of the East Siberian and Laptev Seas. PhD thesis, University of Washington.

Stein, R. and Korolev, S., 1994. Shelf-to-basin sediment transport in the eastern Arctic Ocean. Berichte zur Polarforschung, 144: 87-100.

Wahsner, M.,1995. Mineralogical and sedimentological characterisation surface sediments from the Laptev-Sea. In: Kassens,H., Piepenburg, D., Thiede, J., Timokhov,L., Hubberten, H.-W. and Priamokov, S.M. (Eds.) Berichte zur Polarforschung, 176: 303-313.

Wollenburg, I., 1993. Sedimenttransport durch das arktische Meereis: Die rezente lithogene und biogene Materialfracht. Berichte zur Polarforschung, 127: 159 p.

CLAY MINERALS IN SURFACE SEDIMENTS OF THE EAST SIBERIAN AND LAPTEV SEAS

Kalinenko, V.V.[1)], E.S. Shelekhova[1)], M. Wahsner[2)]

[1)]P.P. Shirshov Institute of Oceanology, Moscow, Russia
[2)]Alfred Wegener Institute, Bremerhaven, Germany

Abstract

Surface samples from the East Siberian and eastern Laptev Seas were studied for grain-size and clay-mineral composition. Four facies zones were considered. A kaolinite-chlorite-smectite-illite assemblage is typical for the East Siberian Sea. The Laptev Sea is characterized by a kaolinite-chlorite-smectite-illite set. The composition and distribution pattern of clay minerals reflect the rock composition of source provinces.

Introduction

The modern sedimentation in the East Siberian and Laptev Seas mainly occurs under an ice-covered marine environment. This is reflected in the wide distribution of clayey muds all over the shelf. Clay components dominate in mineral composition of fine-grained sediments. However, they were not sufficiently studied in these regions.

Semenov (1964) mentioned high illite contents in the < 0.001 mm fraction of surface sediments from the East Siberian Sea. Silverberg (1972) performed clay-mineral studies in both seas, which we include in our research. Our and Silverberg´s (1972) clay-mineral data, which were carried out independently in different laboratories but by means of the Biscaye (1965) method, are very closely correlated.

Our research concentrated on the determination of the origin and distribution patterns of clay minerals and their connection with facies and different grain-size types of sediments. We collected the surface and near-surface samples during the cruise of icebreaker "G. Sedov" (1981) along the coastal zone of the East Siberian Sea, in the Laptev Strait, and in the south-eastern part of the Laptev Sea (Fig. 1 A).

Methods

Grain-size analyses were carried out at the P.P. Shirshov Institute of Oceanology according to Petelin (1967). The < 0.001 mm fraction of 27 samples was used for X-ray diffraction of clay minerals. The procedure of sample preparation was described by Ehrmann et al. (1992). Measurements were performed on a Philips PW 1700 diffractometer with Co K-alpha radiation and automatic divergence slit at the Alfred Wegener Institute for Polar and Marine Research. The standard scan was 0.002° per 2 seconds. To distinguish the 3.54 Å peak of chlorite and the 3.58 Å peak of kaolinite the

speed of scanning was lowered down to 0.005° per 2 seconds. Semiquantitative evaluations of illite, smectite, chlorite, and kaolinite were performed according to Biscaye (1965). Molybdenite suspension was added as an internal standard for more accurate evaluations.

Results and discussion

Bathymetry and oceanography

The East Siberian Sea floor is a smooth plain dipping gently to the North and East. The shelf break occurs at a water depth of 50 - 60 m as far as 350 - 400 km north from the coastline (Holmes and Quager, 1974). The study area is situated at depths between 10 - 20 m and not more than 100 km from the shore. The Laptev Sea is also very shallow. Depths of 50 m and less dominate over half of the shelf. In the North, water depths of 50 to 100 m are reached (Dobrovolsky and Zalogin, 1982). Submarine river valleys of Lena and Yana are the main relief features of the eastern Laptev Sea and occupy the largest part of the study area. They comprise a series of depressions with 25 - 45 m in depth (Holmes and Quager, 1974; Semenov and Shkatov, 1977).

The hydrologic situation in the Laptev Sea is strongly affected by a large discharge (525 km^3/year) of relatively warm Lena waters (Gordeev and Sidorov, 1993), accounting for 70 % of the total river water influx (Dobrovolsky and Zalogin, 1982). The surface circulation (Fig. 1 A) is broadly cyclonic (Atlas of Oceans, 1980). The current velocity is only 2 cm/s in the cyclonic gyre but in most of the central (halystatic) zone currents are nearly zero. Due to the barometric situation, the halystatic zone occupies the central northern part of the Laptev Sea or moves closer to Northern Land (Dobrovolsky and Zalogin, 1982). The coastal surface currents are generally weak in both seas (5 - 10 cm/s), but their velocity increases in the Laptev and Long Straits to 50 - 75 cm/s (Silverberg, 1972).

Geologic setting

Following regional sources surrounding the study area, can be distinguished: the Yana-Kolyma Lowland and Chukchi Peninsula are composed by rocks of all ages, but Mesozoic ones predominate (Geology of the UDSSR, 1970). In the Yana-Kolyma province they are covered by 100 m of Quaternary Alluvium, which is very easily washed out by rivers and eroded by the coastal thermoabrasion. In the Chukchi region bedrocks (mainly metamorphic rocks, shales, sandstones) are exposed everywhere. Granitoid massives have the widest distribution among igneous rocks (Geology of the UDSSR, 1970). The Lena River transports terrigenous material supplied from the South of the East Siberian Craton (Galabala, 1987). The river strongly hollows out its left bank, consisting of loose Mesozoic and Paleozoic bedrocks. Most part of the coarse-grained material accumulates mainly in the delta area. In contrast, river suspension spreads over 400 km northward (Holmes and Quager, 1974). The clay particles settle in the most calm areas of the sea within the submerged submarine valleys and other areas. The East Siberian Sea and the Laptev Sea have many similarities considering the sedimentary environment and sediment types. Almost throughout the year a sea-ice cover protects the bottom sediments from storms and waves. The large sedimentary load is transported by rivers: Indigirka (14 x 10^6t/yr), Lena (12 x 10^6t/yr), Kolyma (6 x 10^6t/yr), and Yana (3 x 10^6t/yr) (Milliman and Meade, 1983).

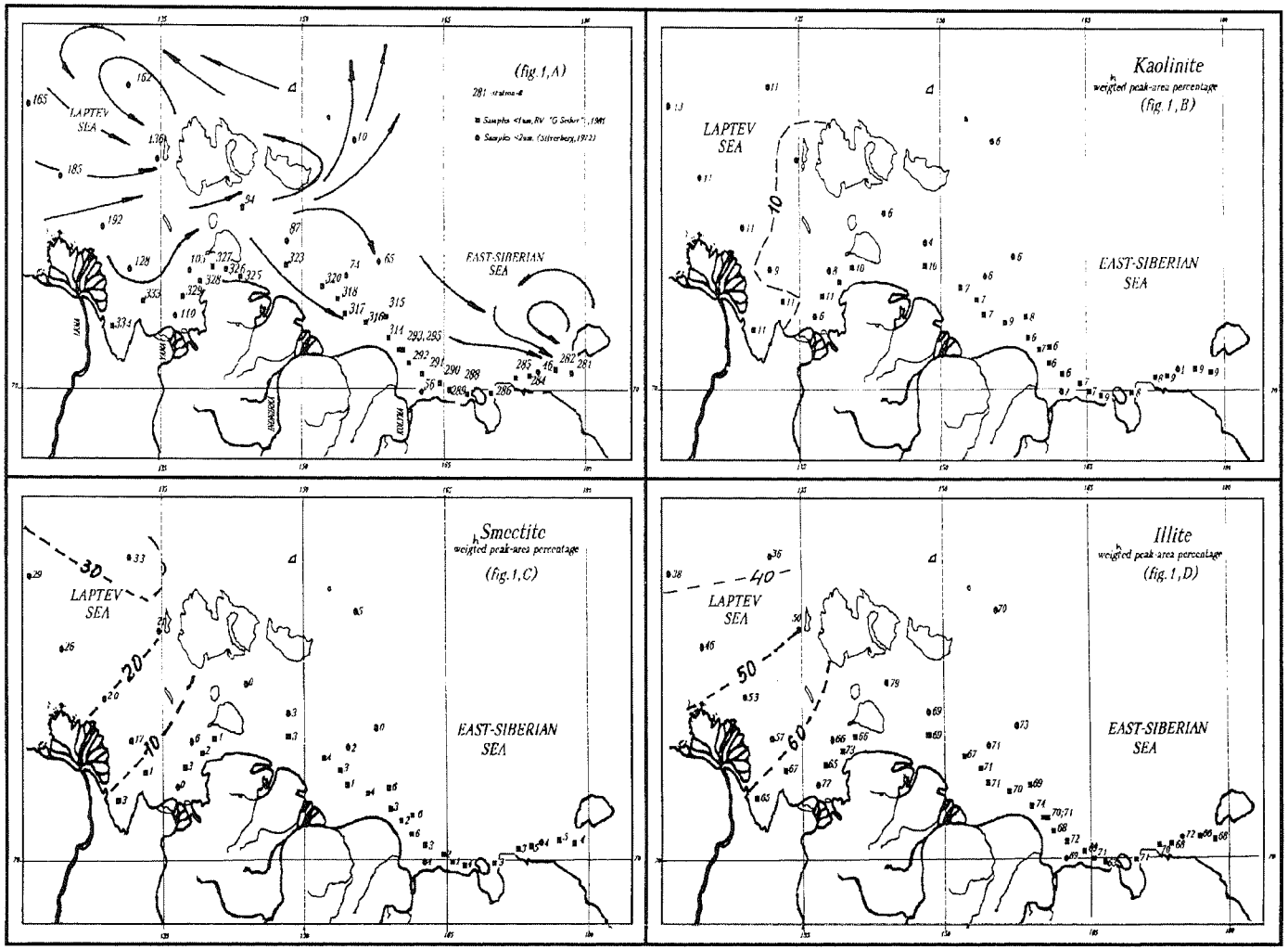

Fig. 1.: Clay minerals in surface sediments of the East Siberian and eastern Laptev Seas: (A) Location of sediment samples analysed for clay minerals and grain-size, and surface circulation pattern (Atlas of Ocean, 1980) (B) Distribution of kaolinite (C) Distribution of smectite (D) Distribuiton of illite.

Under the ice cover clay suspension spreads all over the shelf area and forms the wide fields of monothonous muds. These muds consist of a very high pelite (< 0.01 mm) content with values between 72.2 - 99.5 %. The fraction less than 0.001 mm predominates in the pelite material and accounts for 54 % of this fraction.

The processes of sedimentation in ice-covered environments smooth out all facies features, however, the differences are revealed by means of coarse-grained material, sand (1 - 0.1 mm) and aleuirite (0.1 - 0.01 mm). Mainly, clastic components find their way into clayey muds at the moment of ice melting. At first, ice is differently loaded by terrigenous material in every facies, and these differences are reflected in the sediments. Secondly, the coarse grains concentrate in sediments, when these are affected by storms, waves, bottom currents, and tides.

On the basis of grain-size distribution of surface sediments from the East Siberian and the Laptev Seas we consider four facies zones. The coastal one is divided into three facies subzones (Tab. 1).

Distribution of clay minerals

Illite is the most abundant clay mineral in the surface-layer sediments of the East Siberian and Laptev Seas. However, two provinces can be distinguished (Fig. 1 D). The boundary between both corresponds to 60 % of illite. The first province occupies the entire East Siberian shelf and the most south-eastern part of the Laptev Sea, showing maximum concentrations of 63 - 79 % (average 66 %). The second one is associated with the eastern Laptev Sea, influenced by the Lena River outflow. Here we observe a decrease of illite down to 28 - 57 % (average 46 %). This can be explained by dilution due to higher smectite input and/or by the reduced illite proportion in rocks from nearby sources.

Illite enrichment of the East Siberian Sea reflects the geology of the Yana-Chukchi region. The main source areas for illite are considered to be:

- modern soils and soil-forming rocks of the Yana-Indigirka Lowland, where illite reaches more than 70 % of < 0.00 1 mm fraction (Gradusov, 1976).
- Mesozoic rocks developed on the banks of Yana, Indigirka, and Kolyma rivers (Geology of the UDSSR, 1970).
- Ancient metamorphic rocks, sandstones, and shales, cropping out in the Chukchi region.
- Large areas of granitoid massives widespread over the Chukchi Peninsula.

The smectite content varies from 1 - 3 % to 33 % (Fig. 1 C). The province of high concentrations (17 - 33 %, in average 23 %) is situated in the eastern part of the Laptev Sea, influenced by the Lena terrigenous input. It changes eastward into the province of uniform low amounts of smectite (0 - 6 %, in average 3 %) stretching along the East Siberian coast. The area of smectite enrichment > 30 % coincides with the center of the cyclonic gyre. Due to the shape of the particles smectite has a high buoancy, is transported far seawards, and settles in very calm hydrodynamic areas.

Table 1.: Grain-size composition of sediments from the East Siberian and eastern Laptev Seas.

	stat.	cm	depth m	gravel (%) 5-1 mm	sand (%) 0-0.1 mm	aleurite (%) 0.1-0.05 mm	0.05-0.01 mm	Clay (%) 0.01-0.005 mm	0.005-0.001 mm	<0.001 mm
			OUTER	PART	OF INNER	SHELF	FACIES			
					East	Siberian	Sea			
	314-1	0.1	10	-	0.25	4.62	2.65	9.86	29.14	53.48
	314-2	0-12	10	-	0.25	2.98	2.12	10.12	30.50	54.03
	315-1	0-1	20	-	1.19	3.64	1.23	10.28	30.08	53.58
	315-2	1-7	20	-	0.66	4.44	1.07	0.57	32.34.	51.92
	316-1	0-2	19	-	0.31	4.51	3.81	32.33	23.50	35.54
	316-2	2-16	19	-	0.23	1.75	1.83	24.88	29.39	41.92
	318-1	0-3	17	-	0.77	12.02	4.16	23.06	29.12	30.87
	320-1	0-1	15	-	1.19	15.6	5.86	18,28	22.72	35.93
	320-3	6-16	15	-	0.77	12.41	3.16	14.59	28.27	40.80
	323-2	3-7	16	-	2.51	7.37	2.59	11.44	29.92	45.18
					Laptev	Sea				
	328-1	0-1	28	-	0.67	1.07	0.29	34.21	22.43	41.37
	329-1	1-7	28	-	0.24	0.68	0.10	35.65	27.85	35.48
			COASTAL	SHELF	FACIES					
					East	Siberian	Sea			
a)opened	284.1	0-3	31	-	9.72	4.64	0.17	16.41	23.92	45.14
coast	285-1	0-6	31	.	18.29	9.06	0.48	9.83	18.51	43.82
subfacies	288-1	0-2	26	-	13.76	1.53	0.49	22.55	26.17	35.50
	288-2	2-12	26	-	15.45	2.26	0.73	14.12	21.41	46.03
	289-1	1-5	11	-	25.78	0.82	0.57	11.63	14.49	46.71
b)near-island	293-1	0-1	9	-	1.74	18.67	7.81	14.53	16.57	40.68
subfacies	293-2	1-17	9	-	1.43	22.34	1.36	13.46	16.48	44.93
(Medvezhyi	295-1	0-2	16	-	0.90	10.92	6.48	12.05	24.53	45.12
Island)	295-2	2-16	16	-	0.89	9.66	6.40	16.93	21.88	44.24

Table 1. (continuation): Grain-size composition of sediments from the East Siberian and eastern Laptev Seas.

	stat.	cm	depth m	gravel (%) 5-1 mm	sand (%) 0-0.1 mm	aleurite (%) 0.1-0.05 mm	0.05-0.01 mm	Clay (%) 0.01-0.005 mm	0.005-0.001 mm	<0.001 mm
c)off delta subfacies (KolymaR.)	291-1	0-3	15	-	1.76	28.54	7.36	7.32	12.99	42.03
	291-2	3-17	16	-	1.44	25.61	12.25	9.39	12.67	38.64
	292-1	0-11	11	-	7.65	9.85	1.30	20.25	27.24	33.71
	292-2	1-13	11	-	11.8	10.59	1.54	20.15	22.31	33.61
			BAY FACIES							
					Chaun Bay	East Siberian Sea				
	286-1	0-3	21	-	2.55	1.84	2.45	12.86	38.05	42.25
	286-2	3-10	21	-	3.0	1.98	2.09	12.97	34.71	45.25
	286-3	10-20	21	-	2.43	3.38	1.49	6.16	38.26	48.28
					Buor Khaya Bay, Lapt. Sea					
	333-1	0-3	15	-	0.29	0.06	0.16	18.95	30.18	50.36
	333-2	3-17	15	-	0.23	0.10	0.16	17.36	31.76	50.39
	334-1	0-4	10	-	0.35	0.14	0.35	30.14	27.14	41.88
	334-2	4-15	10	-	0.29	0.14	0.37	35.83	27.67	35.70
			STRAIT FACIES							
					Long Strait					
	281-1	0-2	47	0.78	11.99	13.54	2.22	13.71	18.36	39.40
	282-2	0-2	48	0.71	9.09	11.79	7.21	12.03	21.89	37.28
					Dm.Laptev Strait					
	325-3	5-10	10	-	32.15	17.41	0.89	9.80	12.84	26.91
	326-1	0-5	11	9.96	31.06	12.29	10.37			36.37*
	327-2	0-8	15	2.03	78.12	0.38	0.07			19.40*
								*sum of	pelite	fraction

The very low content along the East Siberian coast is an evidence of minimum smectite occurrence in rocks within Yana-Kolyma and Chukchi regions. Moreover, the smectite contents are typically low in the above mentioned soils and soil-forming rocks, in contrast to the Lena-Anabar Lowland (Gradusov, 1976). The soils of the Chukchi region are characterized by a kaolinite-illite assemblage (Zvereva and Ignatenko, 1983). Pure montmorillonite clays are found in Jurassic coal deposits. Such a sequence of 50 m in thickness was described in the Yakutsk-Vilui depression (Kossovskaya, 1962). However, as mixture with kaolinite and illite, montmorillonite is widespread in clays and in the matrix of sandstones throughout all Mesozoic sequences in the south-east of the craton. Particularly, the source of ferry-montmorillonite is the volcanoclastic Triassic material (Kossovskaya, 1962). Montmorillonite and kaolinite crusis of weathering of 30 m in thickness are found at the base of a Cenozoic sequence in the Lena delta (Galabala, 1987).

Kaolinite is uniformly spread in small amounts (4 - 9 %, in average 6 %) over the East Siberian shelf (Fig. 1 B). A slight kaolinite increase, however, is observed in the eastern Laptev Sea (8 - 13 %, in average 10 %). Kaolinite seems to be transported by the Lena River in combination with smectite. It is found in all rocks from Jurassic to Cretaceous in the east of the East Siberian craton. Horizons of pure kaolinite clay lay under the Upper Jurassic coal deposits (Kossovskaya, 1962; Ivansen, 1991).

Chlorite is found relatively abundant (15 - 25 %). Its distribution pattern does not change much in the East Siberian Sea as well as in the Laptev Sea. Chlorite occurs as a widespread primary constituent of rocks (metamorphic sand stones and shales) and as a product of weathering of other clay minerals. The weighted peak-area percentage in the fraction < 0.001 mm of bottom sediments is nearly reciprocal to that in soil and soil-forming rocks containing about 30 % of chlorite in the Lena River to Vrangel Island region (Gradusov, 1976).

Conclusions

The following assemblage of clay minerals is typical for the East Siberian surface sediments, in order of increasing amount: smectite-kaolinite-chlorite-illite. For the eastern Laptev Sea the following set of clay minerals was observed: kaolinite-chlorite-smectite-illite. The composition and distribution pattern of clay minerals and their assemblages mainly reflect the source rock composition. Facies changes do not play a significant role in the distribution pattern of clay minerals.

Acknowledgment

We sincerely thank D. K. Fütterer for the possibility to process samples in the Geology Department of the Alfred Wegener Institute for Polar and Marine Research. We are grateful to M. A. Levitan for providing helpful discussion and criticism.

References

Atlas of Ocean. Arctic Ocean, 1980. M: Gugk, 196 pp (in Russian).

Biscaye, P.E., 1965. Mineralogy and sedimentation of recent deep-sea clay in the Atlantic Ocean and adjacent seas and oceans. - Geol. Soc. Amer. Bull., 76: 803-832.

Dobrovolsky, A.D. and Zalogin B.S., 1982. Seas of the USSR. M: Moscow Univ. Press 192 pp. (in Russian).

Ehrmann, W.,U., Melles, M., Kuhn, G. and Grobe, H., 199. Significance of clay mineral assemblages in the Antarctic Ocean. - Mar. Geol., 107: 249-273.

Galabala, R.O., 1987. New data about the composition of the Lena delta. - In: Quaternary period of the North-East of the USSR. Magadan, pp. 152-172 (in Russian).

Geology of the USSR, 1970. North-East of the USSR. Geologic description. - M.: Nedra, v. 1, 548 pp; v. 2, 536 pp. (in Russian).

Gordeev, V.V. and Sidorov, I.S., 1993. Concentrations of major elements and tehir outflow into the Laptev Sea by the Lena-River. - Mar. Chem., 43: 33-43.

Gradusov, B.P., 1976. Location of clay minerals in soil-forming rocks and in soils. - M: Nauka, Kora vyvetrivanijy, 15: 131-148 (in Russian).

Holmes, M.L. and Quager, Y.S., 1974. Holocene history of the Laptev Sea continental shelf. - In: Marine geology and oceanography of the Arctic Seas. Berlin, 239-262.

Ivansen, G.V., 1991. Clay minerals of Upper Paleozoic and Mesozoic rocks of Verkhoyansk Fold Zone. - Yakutsk, 95 pp. (in Russian).

Kossovskaya, A.G., 1962. Mineralogy of terrigenous Mesozoic sequence of Vilui depression and Western Verkhoyanje. - Moscow, Academy of Sciences of the USSR Press. Tr. GIN, v. 63, 234 pp. (in Russian).

Milliman, J.D. and Meada, R.H., 1983. World-wide delivery of river sediments to the ocean. - J. Geol., 91: 1-12.

Petelin, V.P., 1967. Grain-size analysis of bottom sediments. - M.: Nauka, 128 pp. (in Russian).

Semenov, Yu. P., 1964. Mineralogical composition of bottom sediments of the East Siberian and Chukchi Seas. - Uch. zapiski NIIGA, Regional geology, 4: 231-239 (in Russian).

Semenov, Yu.P. and Shkatov, E.P., 1977. Geomorphology of the Laptev Sea. - In: Geology of the Sea, L., v. 1, 74-80 pp. (in Russian).

Silverberg, N., 1972. Sedimentology of the surface sediments of the East Siberian and Laptev Seas. - Ph. D. thesis Univ. Washington, 185 pp. (unpub.).

Zvereva, T.S. and Ignatenko, I.G., 1983. Intersoil weathering of minerals in tundra. - M.: Nauka, 230 pp. (in Russian).

STRUCTURE AND LITHOLOGICAL COMPOSITION OF QUATERNARY SEDIMENTS OF THE KARA SEA

Kosheleva V.A. and Yashin D.S.

VNIIOkeangeologia, Russia

Abstract

Based on bottom sampling data, three lithological-stratigraphical complexes (LSC) were distinguished in the late Cenozoic sections of the Kara Sea. The lower and the middle LSC correspond to the Pleistocene stage of the region development, and the upper one includes sediments of the latest (Holocene) transgression. Their compositional and genetic characteristics are presented.

Introduction

Based on the core sampling performed in the Kara Sea by PGO "Sevmorgeologia" (about 4000 core stations incl. 1000 cores of more than 2 m in length), the lithological composition of bottom sediments were studied (Kulikov, 1971; Kulikov et al., 1974; Yashin et al., 1984; Polyan, 1985; Kosheleva and Yashin, 1987; Kosheleva, 1988 a, b, c; Yashin et al., 1988; Yashin and Kosheleva, 1986, 1989, 1994). The obtained samples were subjected to different kinds of analyses (grain size, mineralogy, crystalloptics, geochemistry, chemistry, and paleonatology).

Results and discussion

Similar to the three lithological-stratigraphical complexes (LSC) of bottom sediments in the Barents Sea (Yashin et al., 1985), three LSC were also distinguished in the Kara Sea.

Lower LSC (middle to late Pleistocene)
Sediments of the lower LSC are penetrated by 47 cores in various regions of the Kara Sea. They are built-up by dense grey aleuropelite mictites with coarse detritus of different size and roundness. The coarse detritus is presented by black argillites near Novaya Zemlya, carbonates in the Voronina and St. Anna Troughs, and grey sandstones everywhere. Dark-grey rounded products of very dense clays and coal crumb are observed (Kosheleva and Yashin, 1987).

In shallow water, sediments of the lower LSC are overlain by a thin (0.2 - 1.0 m) sedimentary layer and occasionally eroded. At water depths of more than 200 m, the lower LSC is penetrated is a depth of 1.0 - 3.0 m underneath the bottom surface (Yashin and Kosheleva, 1986; Yashin et al., 1988).

Based on the grain-size data, these sediments are in line with bimodal curves of grain-size composition with median 0.0044 - 0.0074 mm, grading factors of

2.49 - 3.79 and asymmetry values of 0.51 - 1.88 toward the fine fraction (Yashin and Kosheleva, 1989).

Sediments of the lower LSC are aleuropelite or sand-aleuropelite and display allotriomorphic structure, irregular texture, and faulted microtexture of clay components. The main sedimentary component (40 - 70 %) is presented by laths of clay and micaceous minerals which become extinguished at different times, with scattered fine granules of pyrite, quartz, and feldspar. Pyrite granules rarely accumulate around mineral and organic forms. The sediment is characterized by films of black organic matter and rare limonite-hematite pseudomorphs of biogenic and mineral forms (Kosheleva, 1988b, c).

Rock-forming minerals are quartz (40 - 80 %) with traces of corrosion, regeneration, and deformation, and feldspar (20 - 40 %) often leached, albitized, rarely hydromicatized, and sericitized. Mica, rock fragments or carbonates are occasionally observed in noticeable amounts. Heavy minerals constitute 0.5 - 3.68 %, often 1 - 2 % of the sample weight. The main auxiliary minerals controlling the type of discerned terrigenous-mineralogical provinces, are epidote-zoisites, to a lesser extent black ore minerals, pyroxenes, amphiboles, and garnet. Mineral indicators of source rock areas are presented by titaniferous minerals (primarily by sphene), spinel, apatite, tourmaline, zircon, and stress minerals (cyanite, staurolite and sillimanite) (Yashin and Kosheleva, 1986; Kosheleva, 1988 a, c; Yashin et al., 1988).

Authigenic minerals are pyrite, hydrous ferric oxides, quartzine, glauconite, hydromica, and rarely calcite. According to the clay components, the sediments are hydromicaceous except for the Voronin Trough where kaolinite is the main mineral. Moreover, kaolinite-chlorite-hydromicaceous sediments are developed in shallow-water environment near the continent and Severnaya Zemlya Islands. At the Central Kara uplift and in the St. Anna and Novaya Zemlya troughs, sediments are noticeably montmorillonitic (Yashin and Kosheleva, 1989).

The main chemical elements iron, manganese, and biogenic calcium carbonate in sediments of the lower LSC exist in small proportion: 2 - 5 % (more frequently 3 %); 0.1 - 0.3 %; 1.5 - 3.0 % (more frequently 1.8 - 2.0 %), respectively (Kosheleva, 1988c; Yashin and Kosheleva, 1994).

Foraminifera from sediments of the lower horizon in shallow-water environments of Severnaya Zemlya represent poorly preserved single Quaternary forms being probably redeposited (Polyak, 1985).

The analysis of material composition of sediments of the lower LSC together with paleogeographic constructions made for Permian-Mesozoic rocks of this region (Ronkin, 1970; Ronkina and Vishnevskaya, 1977) and its geolgical structure (Geology of the USSR, 1970; Geological structure of the USSR, 1984) suggest that they were formed due to terrigenous products from the nearest source areas built-up by pre-Cenozoic rocks of the upper structural stage, often located in situ. The terrigenous removal from the continent and islands was observed only in shallow water of the paleoshelf (and increased content of resistant minerals). They are probably late Pleistocene in age.

Middle LSC (late Pleistocene)
Sediments of the middle LSC are penetrated by 95 corers in each morphological region of the Kara Sea. Their total thickness in the Novaya Zemlya Basin is usually 0.5 m (occasionally up to 1.8 m). In the South-Western, Western, and Severnaya Zemlya plains it is not over 1.5 m with an average of 1.0 m (Yashin and Kosheleva, 1986; Kosheleva, 1988c).

Based on grain-size composition, the sediments are aleurite clays (52 % of the basin area) and aleurite-clayey mictites (28 %), rarely aleurites and sands. Distribution curves of grain-size composition are commonly bimodal.

Sediments of the middle LSC contain coarse detritus and rounded products of dense clays, characterized by grey colour except for the central Kara Rise and Voronin Trough where they are sometimes brown.

According to the petrographic analysis of thin sections, sediments of the middle LSC show occasionally subhorizontal laminations expressed by yellowish (due to dispersed powered product of hydrous ferric oxides) laminae altered with grey ones. In clay-micaceous products, concentrations of limonite-hematite inclusions as well as organic matter increase. Moreover, columnar hydromicaceous minerals occasionally form star-shaped accumulations around entirely leached minerals.

Rock-forming minerals are analogous to those of the lower LSC. Minerals of the heavy fraction constitute 0.01 - 5.69 % of the sample weight. Their minimum concentrations (up to 1.08 %) are restricted to sediments of the outer and central (middle) shelf as well as to the Severnaya Zemlya shallow-water plain.

The main auxiliary minerals are black ore minerals and pyroxenes, to a lesser extent amphiboles and epidote-zoisites. Other heavy minerals are garnet, zircon, sphene, apatite, titaniferous minerals, mica, tourmaline, spinel, staurolite, and kyanite (less than one percent). Authigenic minerals such as hydrous ferric oxides, ferriginous carbonates, and pyrite (few percents) are observed throughout the sediments of the middle LSC. In the Severnaya Zemlya and Southern plains, pyrite concentrations are up to 14.8 and 30.5 %, respectively. A source of pyrite are very probably not only authigenic processes but also the erosion of pyritized strata by water.

According to clay-mineral data, upper Pleistocene sediments are kaolinite-chlorite-hydromicaceous near the insular and continental parts of the basin, and chlorite-hydromicaceous in the rest area except for the Voronin Trough where they are chlorite-kaolinite. Montmorillonite (10 - 15 %) is observed in sediments of the middle and outer shelf, in areas of sediments of lower Cretaceous rocks (Kosheleva and Yashin, 1987; Kosheleva, 1988c; Yashin and Kosheleva, 1989).

Sediments of the middle LSC within most of the Kara Sea basin are - like in the Barents Sea - similar in composition, textural features, and physical properties, and, thus, in genesis. They represent the upper part of the common sedimentation cycle, and their formation is referred to the end of the late Pleistocene.

Upper LSC (Holocene)
The upper LSC overlies throughout the sea the eroded surface of Pleistocene formations by a thin cover (commonly 0.5 - 1.5 m, less frequently up to 5.0 m and more). Sediments of the upper LSC are characterized by low density, high water content, and variegated granulometric composition.

37.3 % of the water area are occupied by clayey sediments, 33.7 % by aleurite ones, and 19 % and 10 % by differently composed mictites and sands, respectively. Sands contoured by wide bands of various mictites are developed in the coastal areas of continent and islands at small submarine rises and nearly throughout the Southern plain where sedimentation is actively influenced by Ob-Yenisei drainage. Aleurites occupy vast areas in the basin and are confined to the central Kara Rise, Western and Severnaya Zemlya plains, northwestern Pritaimyrsk Plain, and Novaya Zemlya, Yogorsk, Yamal and Gydansk Peninsulas.

Clays nearly entirely fill-up areas in the Novaya Zemlya basin, Voronina and St. Anna Troughs and southern South-Western Plain. Distribution curves of grain-size fractions are generally bimodal, much more rarely with one and three tops, and distinctly reflect bottom hydrodynamic conditions.

Sediments of the upper LSC are variegated in colour: the upper (to 15 cm) oxidized brown and reddish fluid and semi-fluid (bulk density $\approx$ 1,4 g/cm^3, water content > 60 %) sediments overlie the greenish-grey and grey (bulk density 1.46 - 1.48 g/cm^3, water content 43 - 60 %) ones. Foraminifera and mollusk tests, polychaeta tubes, and algae remnants are abundant everywhere. Rarely observed are gravel-pebble products of metamorphic and igneous rocks.

According to the petrographic analysis of aleurite-clayey sediments, their structure and texture are identical to those of Pleistocene sediments, the microtexture is faulted, rarely flocculent. At the same time, concentrations of authigenic pyrite are much lower while those of black organic matter are much higher. Everywhere observed is chemogenic earthy mass of hydrous ferric oxides (Kosheleva, 1988b, c). Rock-forming minerals in the sediments of the upper LSC are feldspar (15 - 40 %) - quartz (40 - 80 %); quartz in the Western plain; micaceous-quartz in some areas of the shallow shelf near the Yamal and Gydansk Peninsulas as well as in the Voronin Trough (Kosheleva, 1988c; Yashin et al., 1988).

The content of heavy minerals is not more than 1.3 % in the troughs and outher shelf. Concentrations of auxiliary minerals are 1 - 5 % in the middle shelf and in the vicinity of the South-Western and Pritaimyrsk shallow plains. Their maximum concentrations are confined to the Southern plain where a vast tongue-shaped sedimentary area containing more than 10 % of heavy minerals extends northeasterly from the Ob and Gydansk Bays. In the rest of the sea, concentrations of heavy minerals show local variations.

The main minerals of the heavy fraction are black ores, epidote-zoisites, pyroxenes, and amphiboles. In most parts of the sea, black ore minerals (> 30 %) are the major auxiliary ones. Their relatively increased concentrations ($\geq$ 20 %) are observed in the rest of the areas. Concentrations of the epidote-zoisite and pyroxene group are rather high (15 - 40 %, more frequently 25 %),

occasionally dominant. For example, epidote-zoisites reach 25 - 30 % in the St. Anna Trough, pyroxenes 30 - 45 % in the Pritaimyrsk plain. Local areas with amphibole concentrations of 30 - 40 % are observed in surficial sediments. Amphiboles are likely of edaphogenic nature here and reflect the composition of closely located pre-Holocene sediments. Very rare authigenic minerals occur in these sediments (Kulikov, 1971; Kosheleva, 1988a).

Holocene sediments of the Kara Sea are iron-free (1 - 3 %) and manganese-free (0,01 - 0,02 %) except for those of troughs and the Western plain, which are poorly ferruginous (5 - 10 %) and poorly manganous (up to 1.7 %) (Yashin and Kosheleva, 1994).

Amorphous silica constitutes 0.5 - 0.94 % in depressed areas of the Central Kara Rise and in troughs. Concentration of calcium carbonate is less than 1 % except for sediments of the Western and Severmaya Zemlya shallow plains where it is up to 30 % due to the abrasion of Paleozoic carbonaceous rocks and the high content of mollusk tests in these sediments.

Concentrations of organic carbon (C_{org}) in Holocene sediments are most commonly 0.5 - 1 % and 1 - 1.5 % (47 % and 38 % of the water area, respectively) (Kosheleva, 1988c; Yashin et al., 1984; Yashin and Kosheleva, 1994). Maximum C_{org} concentrations (1.5 - 2.2 %) occur in the southwestern Kara shelf characterized by the highest sedimentation rate, and in the vicinity of the Voronin Trough where as inflow of biomass-rich waters from the Atlantic is recorded.

In the lowermost part of the upper LSC, brown aleurite clays (average thickness 0.4 - 1.8 m) of relatively high density (1.5 - 1.7 g/cm^3) occur. These sediments contain abundant attachments of organic matter and scarce coarse detritus.

The lithological-geochemical data of sediments of the Kara Sea upper LSC together with physico-chemical and paleontologic data suggest a marine generation during the latest transgression (late Pleistocene-Holocene) the sediments were formed under conditions of polar lithogenesis due to terrigenous products of the nearest source areas built-up of rocks of the upper structural stage. This is especially noticeable for sediments of the outer shelf. In the middle shelf, the nearest source areas are presented primarily by middle-upper Pleistocene sediments being an intermediate sisk of repeatedly rewashed and redeposited underlaying bedrocks. This is indicated by the enrichment of most resistant minerals together with the mainly aleuritic composition. In the shallow shelf, sedimentation was essentially influenced by a removal of terrigenous product from the continent and islands, that is constantly supported by their mineral composition.

Sediments of the upper LSC are coeval with the latest (Holocene) transgression that started at the Kara shelf 10 - 15 thousand years ago.

The distinguished features of bottom sediments are regular in all areas of the Kara Sea. Cross-sections of the studied cores can be easily correlated for every morpholgical region. These complexes may be easily recognized even in the stage of field works.

References

Geological structure of the USSR and distribution regularities of mineral resources, 1984. V. 9. Morya Sovetskoi Arktiki, Leningrad: Nedra.

Geology of the USSR, 1970. V.26. Ostrova Sovetskoi Arktiki. Moscow: Nedra. 548 p.

Kosheleva, V.A. and Yashin, D.S., 1987. Structural and compositional features of Quaternary sediments of the Kara Sea. In: Problemy chetvertichnoi paleoekologii i paleogeografii severnykh morei. II All-Union Conference, abstracts. Apatity. P. 62-63.

Kosheleva, V.A., 1988a. Associations of heavy minerals in late Quaternary sediments of the Kara Sea. In: Geologiya okeanov i morei. VIII All-Union school for marine geology, abstracts. Leningrad. P. 47-48.

Kosheleva, V.A., 1988b. Specific features of petrographic composition of late Quaternary sediments of the Kara Sea. In: Geologiya okeanov i morei. VIII All-Union school of marine geology, abstracts. Leningrad. P. 49-50.

Kosheleva, V.A., 1988c. Abstract of Kandidat Dissertation: Structure and material composition of Pleistocene and Holocene sediments of the Kara Sea. Leningrad: PGO "Sevmorgeologiya". 22 p.

Kulikov, N.N., 1971. Mineral composition of sand-aleurite part of the Kara Sea sediments. In: Geologiya morya. Leningrad. V 1, p. 62-72.

Kulikov, N.N. *et al.*, 1974. Stratification of bottom sediments of the Kara Sea. In: Geologiya morya. Leningrad: NIIGA. V. 3, p. 42-51.

Polyak, L.V., 1985. Foraminifera from bottom sediments of the Barents and Kara Seas and their stratigraphic significance. Abstract of Kandidat Disseration. Leningrad: LGI. 22 p.

Ronkina, Z.Z., 1970. Clay minerals of Jurassic and Cretaceous sediments of the western Yenisei-Khatangsk trough. In: Uchonye zapiski. Regional-naya geologiya. V. 18. Leningrad: NIIGA. p. 71-75.

Ronkina, Z.Z. and Vishnevskaya, T.N., 1977. Terrigenous-mineralogical provinces of the Permian-Mesozoic sediments in the northern Central Siberia. In: Geologiya i neftegazonosnost mezozoiskikh progibov severa Sibirskoi platformy. Leningrad: NIIGA. P. 30-39.

Yashin, D.S. *et al.*, 1984. Organic matter of bottom sediments of the USSR Arcti seas. In: Neftegazonosnost Mirovogo okeana. Leningrad: PGO "Sevmorgeologiya". P. 84-94.

Yashin, D.S., Melnitsky, V.Ye., and Kirillov, O.V., 1985. Structure and material composition of bottom sediments of the Barents Sea. In: Geologicheskoye stroyeniye Barentsevo-Karskogo shelfa. Leningrad: PGO "Sevmorgeologiya". P. 101-115.

Yashin, D.S. and Kosheleva, V.A., 1986. Pleistocene sediments of the Barents-Kara shelf. In: Kainozoi shelfa i ostrovov Sovetskoi Arktiki. Leningrad: PGO "Sevmorgeologiya". P. 56-62.

Yashin, D.S., Kosheleva, V.A., and Polyak, L.V., 1988. Structure and composition of Quaternary sediments of the USSR West-Arctic shelf. In: Geologiya i mineralno-syryevye resursy Evropeiskogo severo-vostoka USSR. All-Union Geological Conference, abstracts. V.II. Syktyvkar. P. 198-199.

Yashin, D.S. and Kosheleva, V.A., 1989. Material composition of "ancient" clays at the shelf of West-Arctic seas. In: Problemy kainozoiskoi paleoekologii i paleogeografii morei SLO. III All-Union Conference, abstracts. Apatity. P. 103-104.

Yashin, D.S. and Kosheleva, V.A., 1994. Geochemical features of late Quaternary sediments of the Kara Sea. In: Geologiya i mineralno-syryevye resursy evropeiskogo severo-vostoka Rossii. XII Geological Conference of Komi ASSR, abstracts. V.II. Syktyvkar. P. 133-134.

THE KARA SEA: A REFLECTION OF MODERN ENVIRONMENT IN GRAIN SIZE, MINERALOGY, AND CHEMICAL COMPOSITION OF THE SURFACE LAYER OF BOTTOM SEDIMENTS

Levitan, M.A.[1], Dekov, V.M.[2], Gorbunova, Z.N.[1], Gurvich, E.G.[1], Muyakshin, S.I.[3], Nürnberg, D.[4], Pavlidis, M.A.[1], Ruskova, N.P.[5], Shelekhova, E.S.[1], Vasilkov, A.V.[1], and Wahsner, M.[4]

[1]P.P.Shirshov; Institute of Oceanology, Moscow, Russia
[2]Sofia State University, Sofia, Bulgaria
[3]Institute of Applied Physics, Nizhniy Novgorod, Russia
[4]Alfred Wegener Institute, Bremerhaven, Germany
[5]Geological Institute, Bulgarian Academy of Sciences, Sofia, Bulgaria

Abstract

Based on bathymetry, physical oceanography, grain-size, and mineral and chemical composition we propose to divide the Kara Sea into two main facies zones: the Western Kara and the Ob-Yenisey zones. The first consists of 2 facies subzones, and the second comprises 4 facies subzones. Facies differences are described. Important to note is that facies changes have little in common with changes of the mineral composition.

Introduction

There are many studies devoted to the recent sedimentation in the Kara Sea (Ul, 1936; Kordikov, 1953; Gorshkova, 1957; Belov and Lapina, 1961; Kulikov, 1961; Gurevich, 1989) using mineralogical and chemical methods which are not comparable to modern ones. Thus, the provenance of heavy and clay minerals is not clear. Also, there are still many questions concerning the distribution of minor elements, boundaries of facies zones and subzones, the possible role of different sources, and pathways and mechanisms of sedimentation. During two expeditions of the P.P. Shirshov Institute of Oceanology to the Kara Sea (12th cruise of RV "Professor Shtockman", 1984, and 49th cruise of RV "Dmitry Mendeleev", 1993), we tried to further investigate the above mentioned problems.

Methods

Figure 1 shows the bathymetry in the area of investigation, the geological stations, and the main surface currents. The bathymetric interpretation is based on all available Russian navigation maps, bathymetric charts, and our "Multibeam" data. Information on the physical oceanography and modern sedimentation processes was received from MARK-IIIB Neil-Brown echo sounder and the Russian variant of the ADCP (Acoustic Doppler Current Profiler)-"AIST" (Muyakshin, 1987).

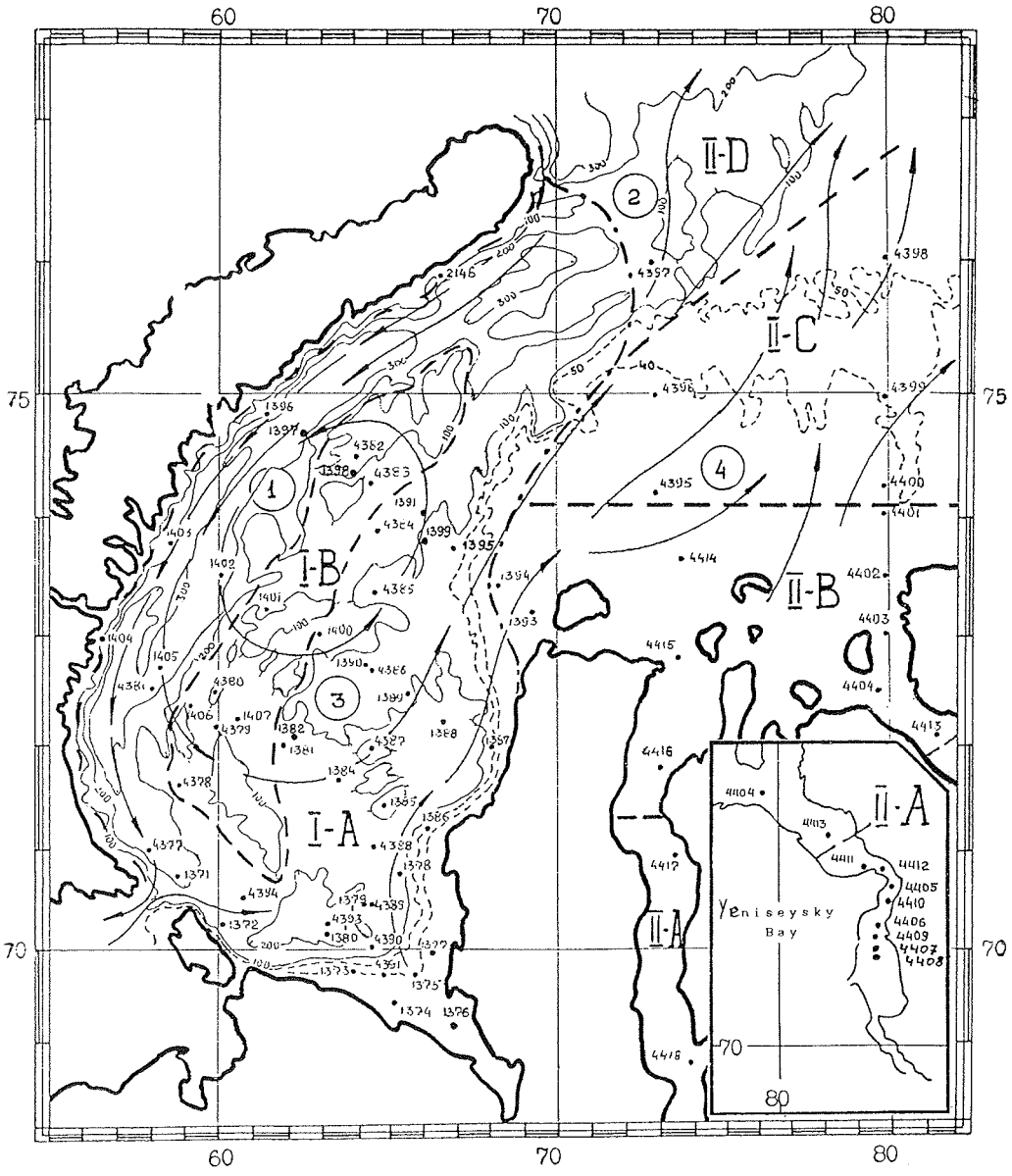

Fig.1.: Bathymetric map of the study area showing geological sampling sites of the P.P. Shirshov Institute of Oceanology. Bathymetry is given in meters. Surface currents are given according to Gorshkov and Faleev (1980). I-A -II-D - facies subzones. Numbers in circles are geomorphological features: 1 - East Novaya Zemlya Trough; 2 - Brusilova Sill; 3 - Western Kara Rise; 4 - Eastern Kara shallow - water Plain.

We obtained sediments and coarse material by gravity and box corers, grab samplers, and benthic trawls. We studied the coarse rock fragments by washing ca. 100 g of surface sediments through 1 - 3 mm sieves. Most grain-size analyses were performed in the analytical laboratory of Shirshov Institute of Oceanology using the water-mechanical method described by Petelin (1967) and decimal scale. For 5 stations along the Yenisey transect, laser grain-size analysis combined with a pipette analysis was applied (Dekov et al. 1993). Three fractions were studied for their mineral composition: 0.05 - 0.1 mm (immersion analysis, separation of heavy and light subfractions by bromoform with n=2.90 g/cm3; analyses were done by Kazakova V.P. and Rudakova A.N.); less than 0.01 mm (XRD, quartz/feldspars ratio, Al_2O_3 as an inner standard, method of Cook et al., 1975); less than 0.001 mm (XRD, clay minerals, method of Lange, 1982). Results of immersion analysis were re-calculated on undeterminable grain-free basis. Methods of chemical analysis were published earlier (Gurvich et al., 1994).

GEOLOGICAL SETTING

The study region is limited by the Novaya Zemlya Hercynian fold belt to the west, the northern part of the West Siberian young craton to the south, and the Taimyr fold belt which consists of a variety of Paleozoic rocks including a number of greenstone transformed basic rocks. A thick sequence of Quaternary poligenetic continental sediments covers the Cretaceous and Paleogene siliciclastic sediments of the northern part of West Siberia. Pre-Cambrian and lower Paleozoic rocks together with Permian-Triassic basic intrusions outcrop on the northern coast of Taimyr Peninsula. The drainage area of the Yenisey river belongs to the vast Tungusian Syneclise filled by Siberian traps of Late Paleozoic to early Mesozoic age. The bathymetry between the western Kara and the Yenisey parts (Fig. 1) reflects a principle difference in the geologial development since Paleozoic times (Senin, 1993). Remnants of Quaternary moraines are known near Novaya Zemlaya and off south-western Yamal (Pavlidis, 1992). There are no moraines in the Ob-Yenisey part of the Kara Sea. This part serves as a main source for sea-ice sediments (Reimnitz et al., 1992). The central part of the Western Kara Sea is occupied by the Western Kara Rise with the crest area in ca. 100m water depth. It is an inverted syncline capped by Paleogene sediments below a Quaternary cover. This rise is surrounded by different types of depressions: the Eastern Novaya Zemlya Trough, the Baidaratzky Depression, and the Peri-Yamal Depression. Below the sequence of Quaternary sediments, these depressions and the Ob-Yenisey shallow-water plain are built-up by Cretaceous siliciclastic rocks.

MODERN ENVIRONMENT AND OCEANOGRAPHY

The Kara Sea basin is strongly influenced by ice conditions: sea ice begins to form in September (to the north) and melts in June-July. Its maximum thickness reaches 1.5 m (Suhovey, 1986). During the navigation period, the Western Kara Sea and the Ob-Yenisey region are significantly different in the temperature and salinity distributions of surface waters (Burenov and Vasilkov, 1994) due to fresh water inflow (up to 1160 km^3 per year) in the eastern part of the basin. The same is true for the water column stratification (Fig. 2). The thickness of the warm low saline surface layer is up to 23 m. A seasonal halothermocline is pronouced in the west, but relatively weakly

developed in the east. Beneath, a cold water mass with a high salinity is established.

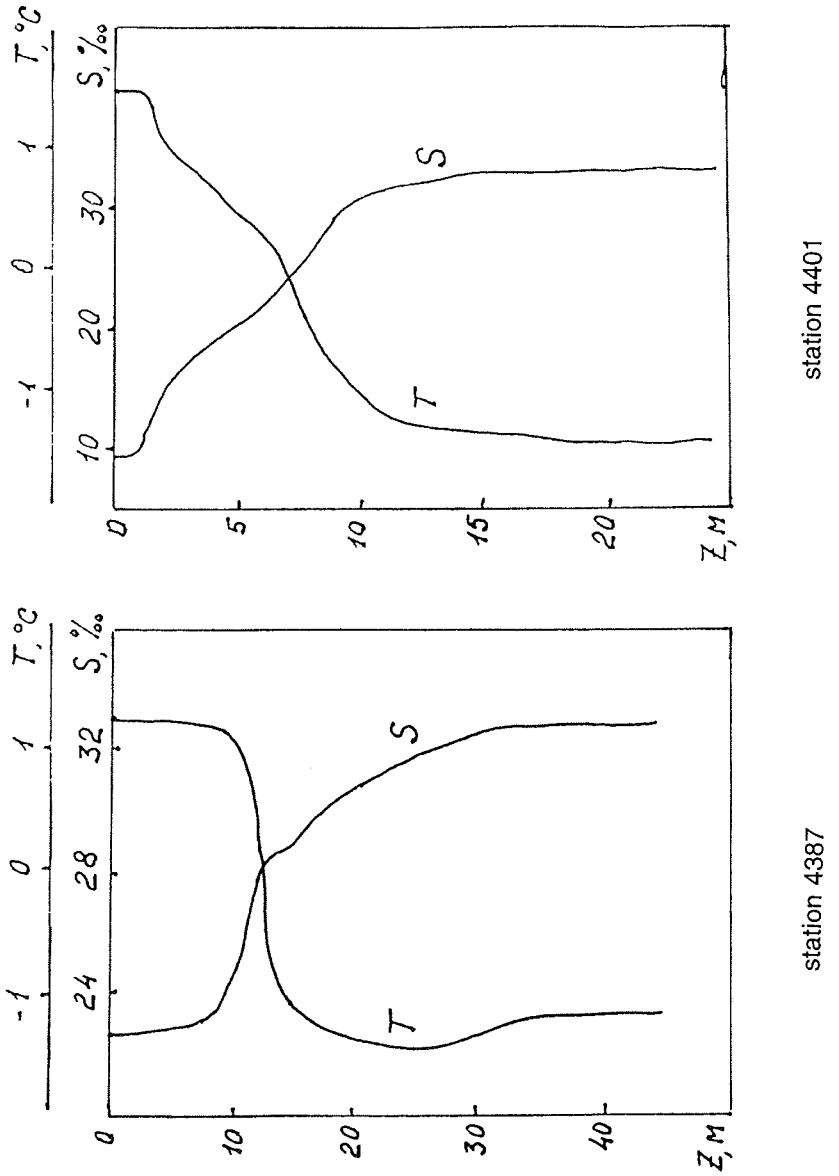

Fig.2.: Typical vertical profiles of temperature and salinity for western (Sta. 4387) and eastern (Sta. 4401) parts of the Kara Sea. September 1993.

Relatively warm Atlantic waters penetrate into the northern part of the Kara Sea below 150 m using the St. Anna and Voronin Troughs. A water mass exchange between the Barents Sea, the Laptev Sea, and the Central Arctic is well proven by the distribution pattern of many planktonic and benthic organisms (Zenkevich, 1963; Polyakova, 1995). The circulation pattern in the western part of the Kara Sea is dominated by a cyclonic gyre (Chaplygin, 1963) (Fig. 1), the average current velocity of which is ca. 10 cm s^{-1}. There are three main types of freshwater in the surface layer of the Ob-Yenisey region: western, central, and eastern surface waters (Moretzky, 1985). They are related to the wind conditions and the amount of fresh water inflow. Consequently, the main currents in this region vary seasonally in direction and velocity.

Results

ADCP back-scattering data point to high concentrations of suspended matter in the water column near the source of sediment matter (Fig. 3). In front of these sources we observe three water layers: the surface and bottom layers (the thickness of each layer is up to 10 m) with highest back-scattering and the intermediate layer with low back-scattering. Such pattern is related to the dominantly lateral spreading of sediment fluxes. We suppose that biogenic particles in the upper layer play the most important role. Winnowing, resuspension, and bottom erosion can play an important role in the formation of the bottom (nepheloid) layer, which consists of cold saline dense brines (Aagaard et al., 1985). Currents in the estuaries of the Ob and the Yenisey mainly flow in a northerly direction, and velocities sometimes reach 60 cm s^{-1}. Further north in the mixing zone of fresh and sea waters, the velocities of currents diminish to ca. 20 cm s^{-1} and orient chaotically. Northwards of this zone, westerly currents dominated with velocities of up to 60 cm s^{-1} in September 1993 (Fig. 3). The annual river load is considered to ca. 25 - 30 mill. tons, coastal abrasion load to ca. 109 mill. tons, and bottom erosion load to ca. 23.6 mill. tons (Saks, 1952; Suzdalsky, 1974; Milliman and Meade, 1983; Leontyev, 1984; Aksyonov, 1987). The amount of suspended matter in the Kara Sea exceeds by far the amount of annually produced sea ice sediments in the Arctic Ocean (Levitan et al., 1995). According to Vedernikov et al. (1994), primary production (September 1993) was 100-360 mg C $m^{-2}d^{-1}$ in the area with a salinity less than 22‰ and 30-80 mg C $m^{-2}d^{-1}$ in the area with a surface water salinity larger than 22‰. Based on geologic and oceanographic data we propose to divide the study area into two main facieszones: the Western Kara area (I) and the Ob-Yenisey area (II).

The first zone is divided into two facies subzones: I-A sediments of depressions and I-B sediments of the Western Kara Rise. The second zone consists of four subzones (from south to north): II-A river sediments; II-B sediments of the mixing zone which is limited by isohalines of the surface waters: 1‰ from the south and 15‰ from the north; II-C sediments of shallow-water areas with intensive bottom erosion ; II-D sediments of the deep-water accumulation zone.

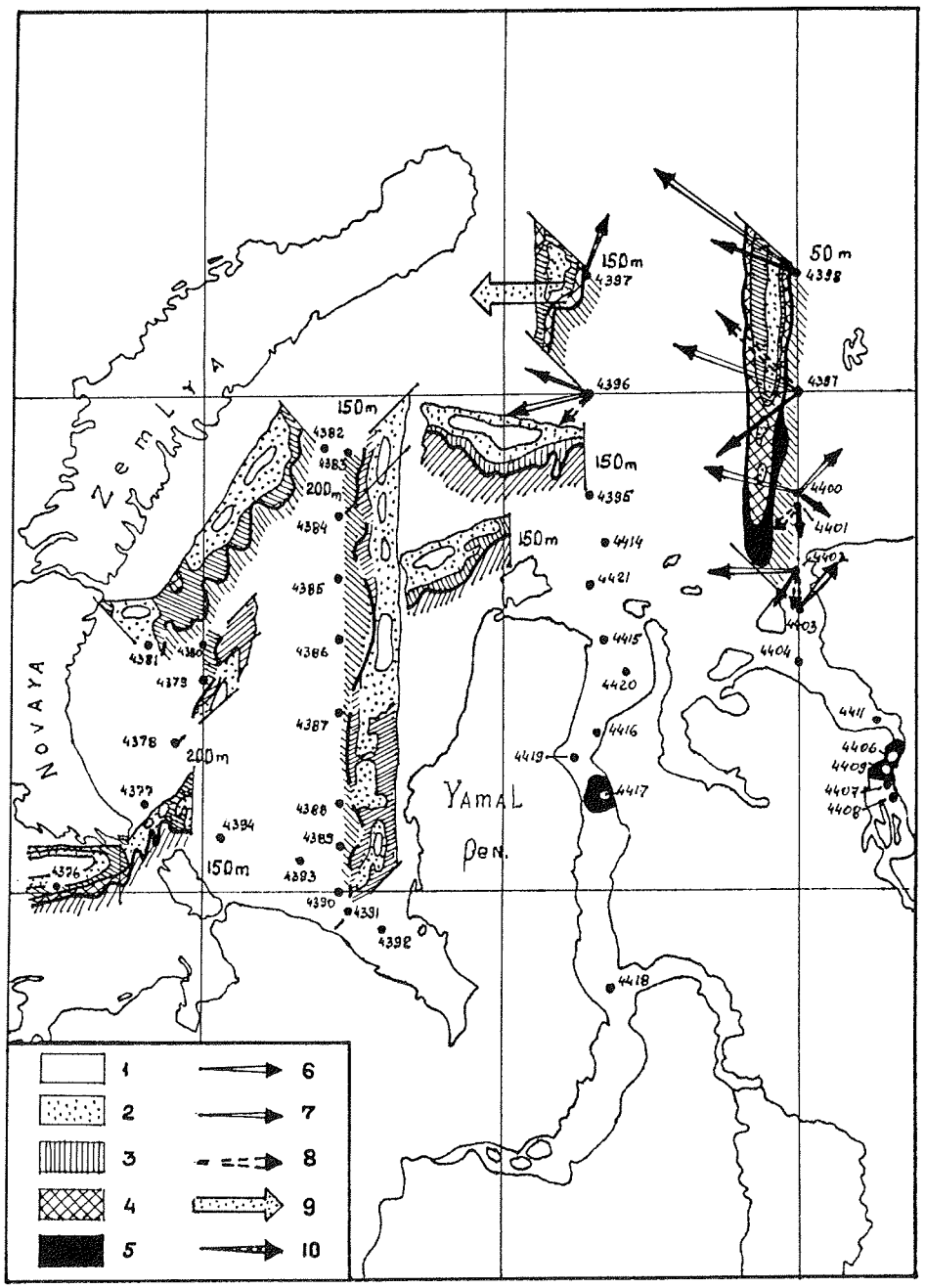

Fig. 3.: ADCP data for back-scattering and currents of the Kara Sea. September 1993. Back-scattering (rel.dB) : 1. < - 78; 2. -78 to -72; 3. - 72 to -66; 4. -66 to -60; 5. > -60. Water depth range for currents (m) : 6. 12 to 18; 7. 18 to 24; 8. 24 to 30; 9. jet stream; 10. 12 to 100. Arrows length 1 cm is 20 cm/s current velocity.

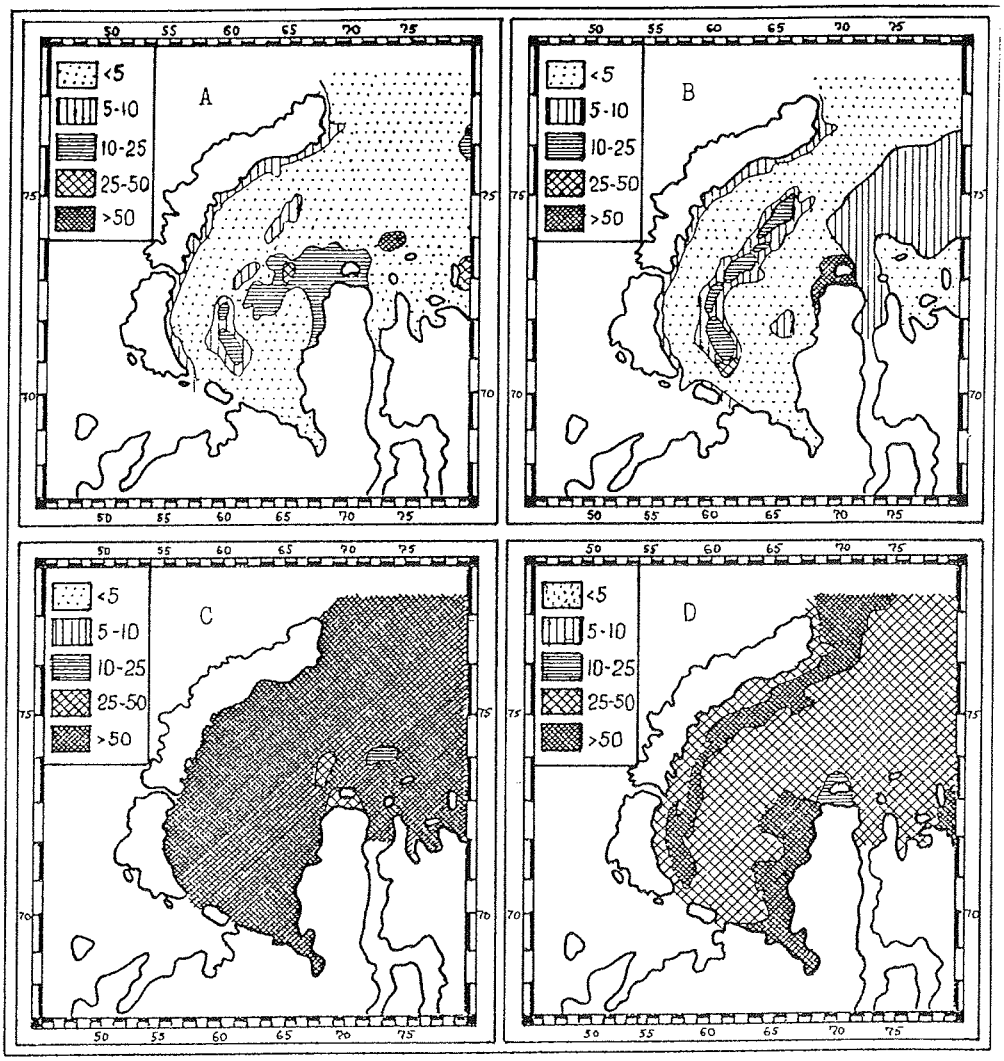

Fig.4.: Distribution of grain-size fractions (wt.%). A - sand (0.1-1.0 mm) ; B - aleurite (0.01-0.1 mm) ; C - pelite (less than 0.01 mm) ; D - subcolloidal (less than 0.001 mm).

GRAIN-SIZE COMPOSITION

In the entire Kara Sea, rock fragments of gravel and pebble size are very rare. Sediments from Sta. 4387, 4388, 4390, 4401, 4403, 4404, 409, 4414, 4415, and 4417 are barren in such fragments. Sometimes well-rounded pebbles of up to 6 cm length were obtained in alluvial deposits (Sta. 4412). Sediments of the Yenisey river are enriched in terrestrial plant debris. Mn nodules with diameters up to 14 cm appear at Sta. 4398, 4399, and 4400. This area coincides with well-known zones of intensive Mn-nodules development in the Kara Sea (Gurevich and Yakovlev, 1993). In conclusion, coarse material can be found in river sediments (II - A subzone) and in sediments of II - C and I - B subzones. Its genesis can be related to fluvial input, bottom erosion, coastal abrasion, ice rafted debris, and Mn-nodule formation and diagenetical processes. In the Kara Sea, sand grains (0.1 - 1.0 mm) play an insignificant role. Their content usually is 5 - 7% in the Western Kara facies zone, and it increases in many alluvial samples (subzone II - A) and subzones of bottom erosion (II - C9). According to Gurevich (1989) and Pavlidis (1992), real sands were exclusively described in narrow belts along the coast of Gydansky and Yamal Peninsula and around the Beliy Island. A distribution of aleurite fractions (0,01 - 0,1 mm) - the most sensitive facies indicator (Fig. 4) - has the same principle feature. The majority of studied samples belongs to clayey muds (classification of Bezrukov, in Lisitzin, 1960) including a number of alluvial sediments. Most samples have two modal grain-size distributions with the main maximum for pelitic (less than 0.01 mm) fractions and a subordinate maximum for coarse aleurite-fine sand fractions (0.05 - 0.25 mm). The same observation was made by Ul (1936) and Kordikov (1953). Interestingly, Pleistocene marine clays from the northern part of the West Siberia zone have similar grain-size compositions (Danilov, 1978). II - A subzone sediments are very different in their grain-size composition. In general they are relatively coarse and have the worst sorting in comparison to other subfacies. There is an improvement of sorting in the Ob-Yenisey zone from south to north.

Above we dicussed the sources of the coarse material. The same holds true for sand to aleurite fractions. An important role (especially for I - B and II - C sediments) plays winnowing and nondeposition of fine fractions caused by bottom currents, tide, storms and wave activity (II - C). We have no further data on the grain-size composition of sea-ice sediments in the Kara Sea but a priori it is obvious that they can include all fractions, though clay and silt normally dominate. Important to note is the comparison between the traditional water-mechanical and the laser grain-size analyses. For example, for II - B sediments (5 stations), the main maximum in the grain-size histogram (laser variant) is 3.8 - 6.2 μm (ca. 30%) and the second one less than 1.9 μm (ca. 7.6%). From our point of view, the most important difference occurs in the fraction less than 1 (2) μm. It can be related to the form of clay particles and electrochemical processes during water-mechanical analyses. Colloidal particles are in bad coincidence with Stoke's law for quartz balls and have very different settling times. This problem should be studied in more detail. It seems that in principle we should study clayey sediments by the laser grain-size analysis.

The lithology was described in details earlier (Levitan et al., 1994). It should be noted that very low $CaCO_3$ contents occur (usually less than 2%), and that

the position of the green/brown boundary varies from some millimeters in the south up to 10 - 14 cm in the north.

MINERALOGICAL COMPOSITION

FRACTION 0.05 - 0.1 mm

Heavy subfraction

This subfraction contains ca. 30 minerals, but only four dominate: hornblende, black ores (magnetite and ilmenite), epidote, and clinopyroxene (Fig. 5, Table 2, Appendix). In general, there is a very significant difference between the western Kara (I) and the Ob-Yenisey (II) facies zones: the average contents of the heavy subfraction are 0.65 and 4.5, respectively; the average epidote/clinopyroxene ratios are 1.7 and 0.3. The Western Kare Sea zone is characterized by black ores, whereas, clinoproxene is the main mineral in the mineral assemblage of the Ob-Yenisey zone. We explain this phenomen by the difference in the source areas. Important to note is the lack of any significant difference between the Ob and Yenisey sediments (Table 2, Appendix). This might be explained by the fact that during Cretaceous to Paleogene times the East Siberian craton served as the main source province for the West Siberia facies zone. These Cretaceous to Paleogene sediments -in turn- served as the main source for the accumulation of Quaternary sediments. Therefore, these two main groups of sedimentary rocks contains a resumbling mineralogical composition of the heavy subfraction. Hornblende and black ores have a relatively better coincidence with the facies subzones than epidote and clinopyroxene.

Light subfraction

There are less minerals in the light subfraction than in the heavy fraction. Three minerals dominate (with the exception of undeterminable grains): acid plagioclase, K-feldspar (mainly orthoclase), and quartz (Fig. 6, Table 2, Appendix). The sum of feldspars is less than the content of quartz (Table 2, Appendix). The role of basic plagioclases and mica is unsignificant. In general, the difference between facies zones I and II is very low (Table 2, Appendix). The same is true for the Ob and Yenisey transects. It seems that K-feldspar is the best facies indicator. There is a close similarity of the K-feldspar distribution in the Western Kara zone with the circulation pattern (Fig. 1). In general, only one assemblage dominates in the study region (Table 2, Appendix). Our data do not coincide with the data of Belov and Lapina (1961) and Kulikov (1961), because they have used the 0.05 - 0.25 mm fraction. But there is a very good similarity between our data and the results of Zagorskaya et al. (1965) for marine Quaternary sediments near the mouth of Yenisey River, as they have used the same fraction: 0.05 - 0.1 mm.

FRACTION LESS THAN 1 mm

For pelitic fractions we observe the same pattern (Fig. 6) as for the light minerals of 0.05 - 0.1 mm fraction: the content of quartz is higher than the content of the sum of all feldspars. Interestingly, the facies zones I and II can be clearly distinguished: in the first zone the quartz/feldspar ratio is higher than in the second one. This may be related to an intensified supply of plagioclases from the East Siberian craton.

FRACTION LESS THAN 0.001 mm

The clay minerals distribution is shown in Figure 7. Their relation to the main facies zones is characterized by a smectite-illite predominace (the average smectite/illite ratio is 1.0) and a relatively high chlorite content (ca. 14 %). The Ob-Yenisey zone has an average smectite/illite ratio of 3.1 and a slightly lower content of chlorite (ca. 10 %). It is suggested that this main difference is due to the influence of the Siberian trap basalts in the hinterland. According to Table 3 (Appendix), there is practically no relationship between the clay mineral distribution pattern and our facies subzones. But if we compare the distribution pattern in the Western Kara zone (Fig. 1), we find a significant similarity.

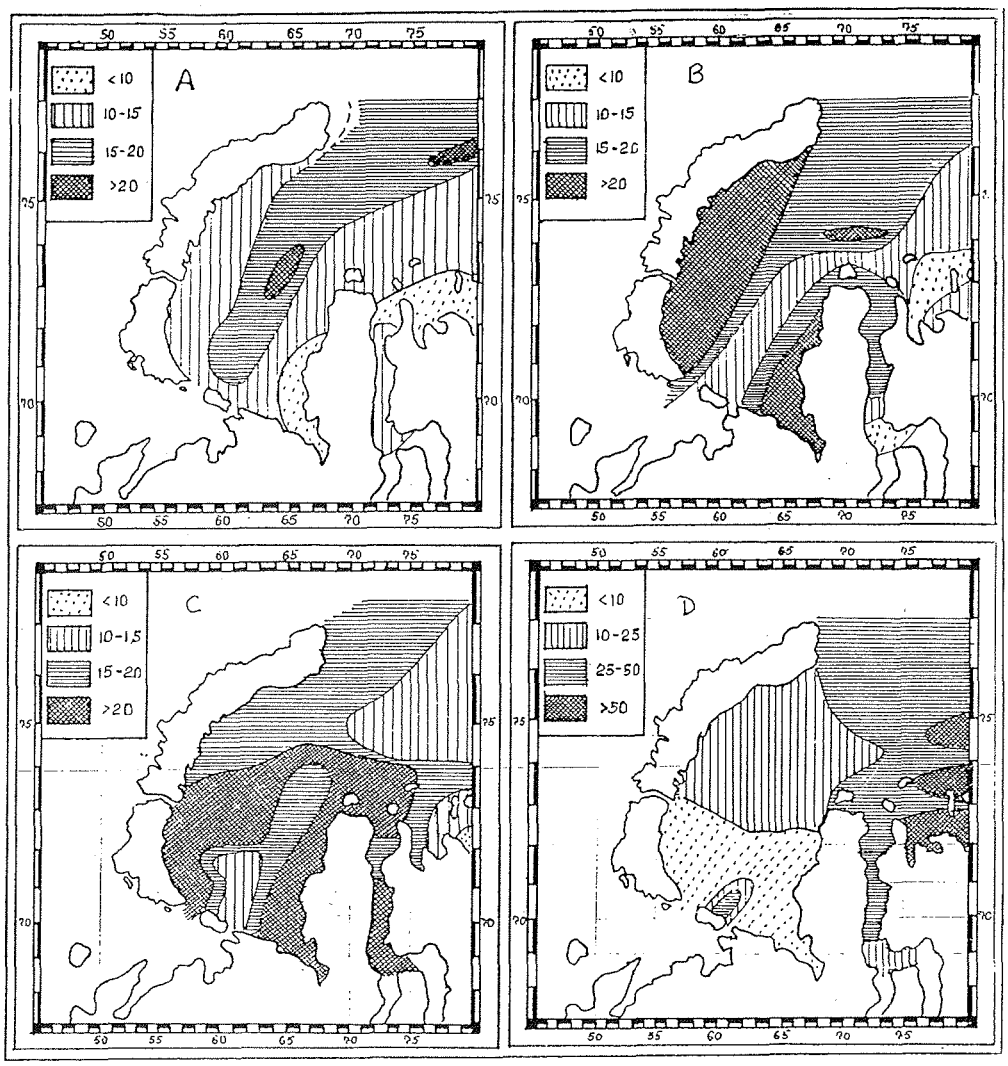

Fig.5.: Distribution of main heavy minerals. (n>2.90 g/cm3), fraction 0.05-0.1 mm (%). A - hornblende; B - black ores; C - epidote; D - clinopyroxene.

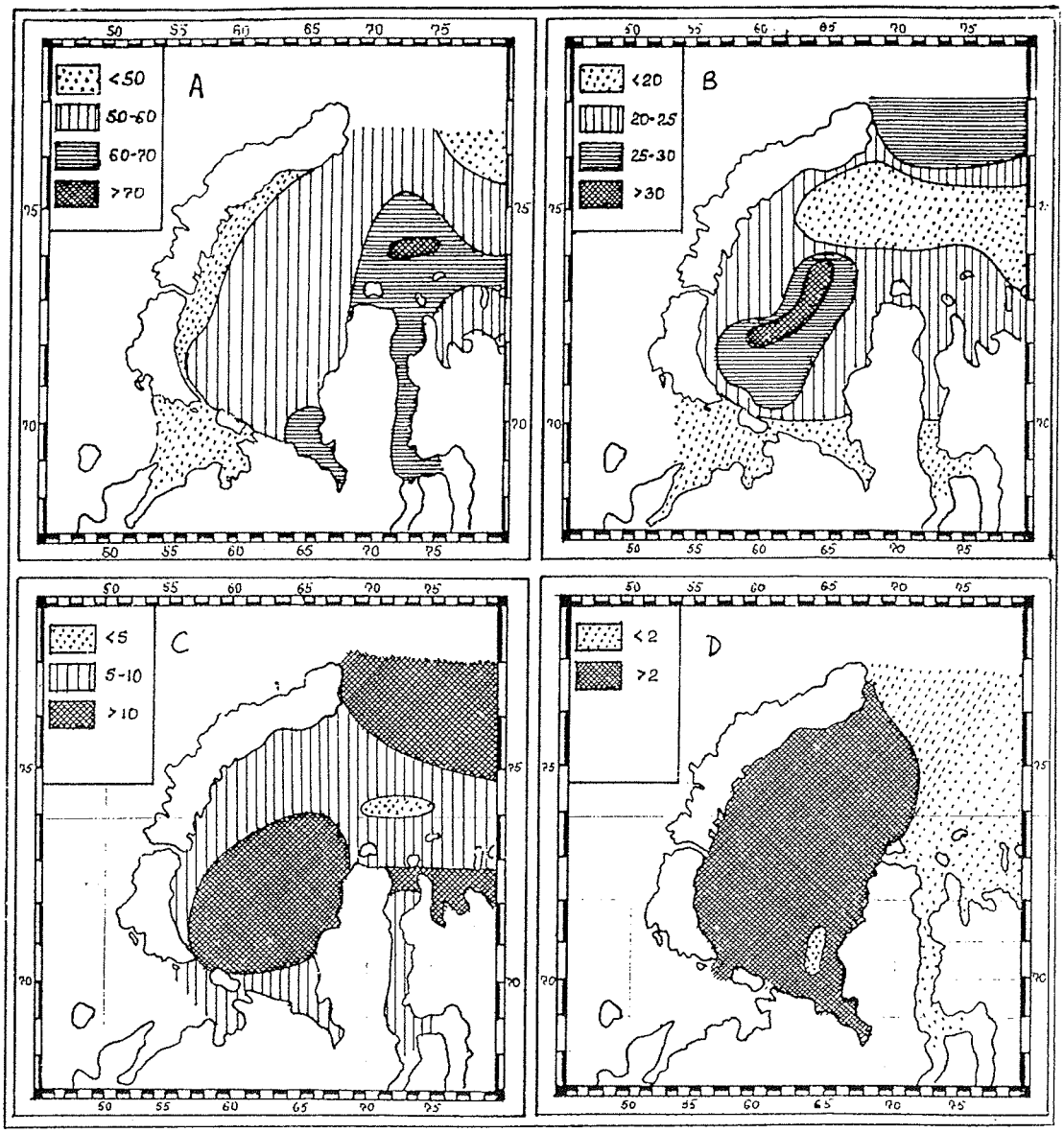

Fig.6.: Distribution of main light minerals (n<2.90 g/cm3), fraction 0.05-0.1 mm (%). A - quartz; B - K feldspar; C - acid plagioclases. D - quartz/feldspar ratio in fraction less than 0.01 mm.

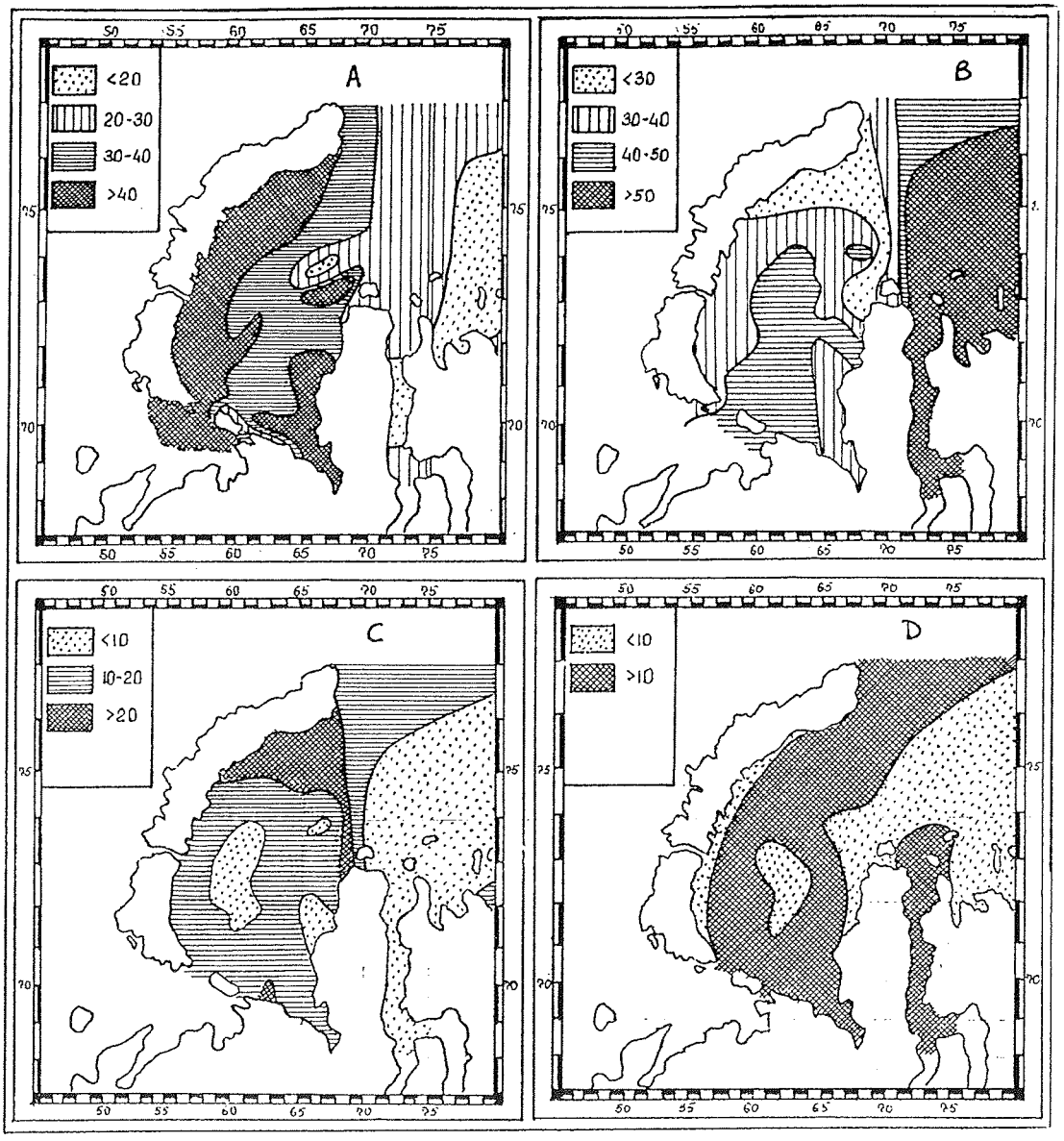

Fig.7.: Distribution of clay minerals (rel.%). Fraction less than 0.001 mm. A - illite; B - smectite; C - chlorite; D - kaolinite.

The strongest currents of the cyclonic gyre can be traced by the kaolinite-chlorite-smectite-illite assemblage and minima of chlorite and kaolinite (Shelekhova et al., 1995). We should notice that our clay-mineral provenance differ significantly from the results of Gurevich (1989), because he has studied clay minerals in the fraction less than 0.005 mm.

CHEMICAL COMPOSITION

The average chemical composition of sediments belonging to different facies zones and subzones is shown in Table 4 (Appendix). If we compare Tables 1 and 4 (Appendix), 3 groups of elements can be differentiated in relation to their grain-size composition. The first group includes those elements, which have a negative correlation with the sand-aleurite to pelite fraction ratio: Al, Ti, Fe, Mn, TOC, P, Zn, Ni, and V. The second group consists of elements with a positive correlation: SiO_2/Ba and SiO_2/Al ratio. The third group includes Co and Cr, and their contents have no clear correlation with grain-size composition. Thus, the connection of chemical and grain-size compositions is a main reason. Some elements have additional factors determining their distribution and concentration. For example, we observe a strong influence of the redox potential on the Mn content in surface layer sediments, or the TOC enrichment of Yenisey sediments relative to the Ob sediments, which is at least partly connected to the flux of debris. It seems that the SiO_2/Al ratio is the best facies indicator among others. We looked through the distribution of Ni, V, and Fe in sediments of the Western Kara zone and did not find any connection with the circulation pattern.

Discussion

We observe pronounced differences between the Western Kara and the Ob-Yenisey facies zones i) through the geological history (Senin, 1993), ii) in relation to Pleistocene glaciations, iii) to environment (physical oceanography and hydrochemistry, primary production, bottom relief), iv) sedimentology, and v) geochemistry. Some of these differences are due to the geological evolution, some to the different sources areas, and some to the influence of river contribution.

The relative role of river input, coastal abrasion, and bottom erosion varies in the different facies zones. We suppose that there is the following sequence in the Western Kara zone (in order of increasing importance): river input-bottom erosion-coastal abrasion. The same sequence of sources for the Ob-Yenisey zone is: coastal abrasion-bottom erosion-river input. We propose (based on bathymetry, bottom topography, and grain-size composition) that bottom erosion is more intensive in the Ob-Yenisey zone than in the Western Kara zone.

In general, sea-ice sediments play an insignificant role in the recent sedimentation. It is reasonable to propose that the composition of sea-ice sediments in the two main facies zones is different (because suspended matter and bottom sediments have different composition).

The main portion of sedimentary matter in the Kara Sea is originating from the East and West Siberia hinterland. The distinct mineral composition of the

Western Kara zone, however, is explained by an additional contribution from the Northern Ural, Vaigach Island, and - especially - from Novaya Zemlya. The similar mineral composition of bottom sediments of the Ob and Yenisey transects is due to the same source areas and to mixing processes of surface currents.

Seasonality of river input, productivity, and physical oceanographic processes in the ice-covered sea and under ice-free conditions, is of great importance in the Kara Sea. We have no data yet for the evolution of this seasonality in the ancient epochs. It is clear that the best regions for such study are the areas adjacent to sources (for example, Baidaratzky Bay and the mixing zones of the Ob and Yenisey rivers) because in these areas the sedimentation rates are the highest.

As we mentioned above, I-A subzone is related to different depressions surrounding the central part of the Western Kara Sea. The facies characteristics of the subzone are related to the deep-water regime (more than 100 m) and the proximity to source provinces. Main parts of the subzone are lying below the relatively strong currents of the cyclonic gyre periphery. Consequently, these sediments are dominantly muds with minor amounts of coarse matter, sand, and aleurite fractions. Their sorting is relatively good. They are enriched in Mn, Fe, Ti; black ores, epidote; illite, chlorite, and -partly- in kaolinite. The SiO_2/Al ratio is very low. According to our grain-size and mineralogical data, this subzone can be divided into four smaller regions: the western (the East Novaya Zemlya Trough), southern, eastern, and northern ones. It seems that sedimentation within the subzone is characterized by "particle by particle" flux.

I-B subzone occurs within the Western Kara Rise in water depths less than 100 m. Partly, it coincides with the core of the cyclonic gyre. It is characterized by slightly higher contents of coarse material, sand, and - especially - aleurite fractions and worse sorting than I-A subzone. Sediments of the subzone are enriched in SiO_2 and Ba, hornblende, K-feldspar, and smectite (?). From our point of view, the main process of "particle by particle" sedimentation is combined with winnowing, which is due to the more active hydrodynamic regime in the bottom waters just above this bathymetric shoal.

Facies subzone II-A occurs in deltas and the southern halves of estuaries of the Ob and Yenisey rivers. It is characterized by fresh waters, strong northerly directed currents, and coarse sediments with very bad sorting (in most cases). Yenisey sediments differ from Ob sediments by a high content of Al, Ti, Fe, Corg, plant debris, heavy subfraction, and clinopyroxene, and by low content of SiO_2, Mn, P, Ba, epidote, and quartz. Sediments of facies subzone II-b belong to the mixing zone of fresh water (from the Ob and Yenisey rivers) and sea water. This zone is limited by the 1‰ and 15‰ isohalines in surface waters in the south and north, respectively. This hydrochemical barrier zone with very specific processes (flocculation of organic matter and coagulation of dissolved (colloidal) and suspended matter, formation of fresh oxyhydrates of Fe and Al, and sharp increase of primary production) (Artemyev, 1993) coincides with the hydrodynamic barrier zone (a strong decrease of current velocities and their chaotic orientation). As a result, we observe a very drastic accumulation of clayey muds with bad sorting. Compared to II-A subzone sediments, these muds are enriched in Al, Fe, Ti, TOC, P, Sr, Ni, V; epidote,

and quartz, and have notably lower contents of the heavy subfraction and black ore minerals.

The water depth for II-C subzone -similar to subzone II-A and II-B- does not exceed a few dozens meters. Salinity in the surface waters changes from 15 to 32-34 ‰. Very strong western currents with velocities of up to 60 cm/s do not allow an intensive recent accumulation of sediments. Thus, this subzone is a region of non-deposition, transit, winnowing, and strong bottom erosion. Sometimes one can observe more ancient Quaternary sediments or outcrops of Cretaceous rocks. Surface layer sediments vary from Recent to relict ones. In general, they are represented by sandy muds with very clear two-modal grain-size distributions and good sorting. Interestingly, these sediments have a very low content of heavy mineral subfraction, epidote, and a high content of black ores, SiO_2, and Ba.

For the characterization of the II-D subzone only one station (4397) is available, which is situated at a water depth of 150m. Nevertheless, it is evident that it is a facies subzone of quite intensive accumulation with very fine clayey muds and the best sorting. The mineral composition (for example, epidote/clinopyroxene and smectite/illite ratios) suggests that these sediments belong to the II facies zone. The most prominent mineralogical feature is an enrichment of K-feldspar, chlorite, and kaolinite. These sediments have a specific chemical composition with very low SiO_2/Al ratios, highest Fe, Mn, P, Sr, and Zn contents, which relate to the highest content of the pelite fractions (Table 1, Appendix).

A boundary between the II-C and II-D subzones differentiates between two types of geochemical behavior of Ba. Southward of this boundary, the coarse fraction is the main carrier of Ba, whereas northward the fine fraction dominates.

If we take into consideration a linkage between the mineral distribution and the circulation pattern in surface waters, we should notice that clay minerals and K-feldspar are the best indicators of surface currents. It is less obvious for hornblende. It seems that most of the heavy minerals, quartz, and acid plagioclases are mainly distributed in the nepheloid layer by dense cold brines.

An important role in the distribution of black ores and the heavy-mineral subfraction (Table 2, Appendix) is played by the differentiation due to specific density differences. Probably, the very low content of basic plagioclases is due to their bad resistivity to weathering processes. In many cases, the distribution of different minerals can be explained by the dilution by other minerals.

Consequently, the mineral distribution patterns are connected with sources, pathways, mineralogical differentiation, and dilution. Facies peculiarities are mainly due to the bathymetry, the lithodynamic regime, and the influence of the river contribution. The best indicators for different facies are the grain-size and chemical compositions. In general, grain-size and mineral compositions are ruled by different processes. That is why there is practically no evident connection between clay minerals and facies subzones (Table 3, Appendix). The same observation was made for the mineral composition of the Lena

River alluvium and sediments from the southern Laptev Sea (Serova and Gorbunova, 1993).

For the chemical composition, we would like to outline the close linkage with the grain-size composition. As most elemental distribution patterns have no similarity with the surface currents, we conclude that the main part of the sediments is accumulated from the nepheloid layer. Geochemical results showed that only up to 10% of the heavy elements as Fe, Ni, Cd, Cr, Co, and Pb in Kara Sea sediments belong to labile forms (Demina and Politova, 1995). Consequently, the main part of these elements is contained in lattice sites of different mineral-carriers. For Cu and Zn, organic matter and oxyhydrates of Fe, respectively, serve as carriers (Demina and Politova, 1995).

It is difficult to evaluate the role of pack ice in the recent sedimentation. There is no doubt about its significance in protecting bottom sediments from wave and storm action for 8-9 month per year.

Conclusion

All results point to the leading role of differentiation processes. There is a wide variety of differentiation: sedimentological, grain-size, mineralogical and geochemical differentiation. Sedimentological differentiation is due to different sources of sediment fluxes, different types of fluxes (vertical and lateral), surface and nepheloid, and different mechanisms of their formation and transformation.

Grain-size differentiation is related to the distance from sources and bottom relief and mainly to lithodynamics in the water column and, especially, in the bottom water layer. Mineralogical differentiation is due to the settling time of the minerals (including their specific density, size, shape, and buoyancy) and their resistivity to mechanical breakage. Geochemical differentiation is combined to grain-size, redox potential, and different carriers of elements (detrital and clay minerals, organic matter, oxyhydrates of Fe and Mn).

Sedimentary systems of the Kara Sea and its main facies zones and subzones are due to different combinations of the above mentioned differentiation mechanisms, their superposition, and relative role each of it.

Acknowledgments

We would like to thank crews of RV "Professor Shtockman" and "Dmitry Mendeleev" for their help during expeditions. This work is supported by Russian Foundation of Fundamental Researches (Grant no. 93-05-9280 for M.A. Levitan, Z.N. Gorbunova, E.G. Gurvich).

References

Aagard K., Swift J.H. and Carmack E.C. (1985). Thermohaline circulation in the Arctic Mediterranean Seas - J. Geophys. Res., 90 (C5): 4833-4846

Aksyonov A.A. (ed.) (1987). Arctic shelf of Eurasia in late Quaternary - Moscow, Nauka, 278 pp (in Russian)

Andrew J.A. and Kravitz J.H. (1974). Sediment distribution in deep areas of the Northern Kara Sea - In: Herman Y. (ed.). Marine geology and oceanography of the Arctic Seas. Springer, Berlin-Heidelberg-New York, pp.231-256.

Artemyev V.E. (1993). Geochemistry of organic matter in river-sea system - Moscow, Nauka, 204 pp (in Russian)

Belov N.A. and Lapina N.I. (1961). Bottom sediments of the Arctic Ocean - Leningrad, Gidrometeoizdat, 152 pp (in Russian)

Bezrukov P.L. and Lisitzin A.P. (1960). Classification of sediments of modern sea basins - Moscow, Transaction of P.P. Shirshov Inst. Oceanol., V. 32, pp. 3-14 (in Russian)

Burenkov P.L. and Vasilkov A.V. (1994). On influence of river inflow at spatial distribution of hydrology charcteristics of the Kara Sea waters - Oceanology, 5:652-661 (in Russian)

Chaplygin E.I. (1963). On currents pattern in the Kara Sea - Transactions of AARI, V.248, pp.49-51 (in Russian)

Cook H.E., Johnson P.D., Matti J., and Zemmels I. (1975). Method of sample preparation and X-ray diffraction data analysis, X-ray mineralogy laboratory - Init.Repts.DSDP, V.28, pp. 999-1008.

Danilov I.D. (1978). Pleistocene of marine subarctic plains - Moscow, MGU, 198 pp (in Russian)

Dekov V.M., Levitan M.A., and Ruskova E. (1993). Methods of grain-size analysis of metalliferous sediments - Oceanology, 2:123-131 (in Russian)

Demina L.L. and Politova N.V. (1995). On the speciation of certain heavy metals in bottom sediments in the estuarine zone of Ob andYenisey rivers (in press) (in Russian)

Geological structure of the USSR and regularities of mineral deposits distribution. V.9. The Soviet Arctic Seas (1984). - Leningrad, Nedra, 280 pp (in Russian)

Gorshkov S.G. and Faleev V.I. (eds.) (1980). World Ocean Atlas. V.3. The Arctic Ocean. USSR Ministry of Defense, Pergamon Press, 189 pp.

Gorshkova T.N. (1957). Sediments of the Kara Sea - Transactions of All-Union Hydrobiol. Soc. , V.8, pp. 66-72 (in Russian)

Gurevich V.I. (1989). Modern sediments - In: Ecology and bioresources of the Kara Sea. Apatity, Acad. Sci. USSR, pp. 6-11 (in Russian)

Gurevich V.I. and Yakovlev A.V. (1993). Mn crusts and nodules of the Kara Sea - In: Co-enriched Mn crusts of the Pacific Ocean, St. Petersburg, VNIIOKEANGEO, pp. 97-111 (in Russian)

Gurvich E.G., Isaeva A.B., Demina L.V., Levitan M.A., and Muravev K.G. (1994). Chemical composition of bottom sediments of the Kara Sea and estuaries of the Ob and Yenisey Rivers - Oceanology, 5:766-775 (in Russian)

Kordikov A.A. (1953). Sediments of the Kara Sea. Transactions of NIIGA, V. 56, 142 pp (in Russian)

Kulikov N.N. (1961). Sedimentation in the Kara Sea - In: Modern sediments of the seas and oceans. Moscow, pp. 437-447 (in Russian)

Lange H. (1982). Distribution of chlorite and kaolinite in eastern Atlantic sediments of North Africa - Sedimentology, 29:427-432.

Leontyev O.K. (1984). About some peculiarities of supply of the sediment matter in the Arctic Ocean - Vestnik MGU, ser.geogr., 1:34-38 (in Russian)

Levitan M.A., Khusid T.A., Kuptzov V.M., Politova N.V., and Pavlova G.A. (1994). Types of upper Quaternary cross-sections of the Kara Sea - Oceanology, 5:776-778 (in Russian)

Levitan M.A., Nürnberg D., Stein R., Kassens H., Wahsner M., and Shelekhova E.S. (1995). On the role of cryosoles in accumulation of Recent bottom sediments in the Arctic Ocean - Repts. Rus. Acad. Sci. (submitted) (in Russian)

Milliman J.D. and Meade R.H. (1983). World-wide delivery of river sediment to the ocean - J. Geol. , 91:1-12.

Moretzky V.N. (1985). Distribution and dynamics of brackish waters of the Kara Sea - Transactions of AARI, 389:33-39 (in Russian)

Muyakshin S.I. (1987). Application of Doppler echolocation for measurements of currents and inner waves - Ph. D. Thesis, Gorky, 23 pp (in Russian)

Pavlidis Yu.A. (1992). Shelf of the World Ocean in late Quaternary - Moscow, Nauka, 272 pp (in Russian)

Petelin V.P. (1967). Grain-size analysis of marine bottom sediments - Moscow, Nauka, 128 pp. (in Russian)

Polyakova Ye.I. (1995). Diatoms of the Eurasian Arctic Seas and their distribution in surface sediments (this Issue) (in Russian)

Reimnitz E., Marincovich L., McCormick M. and Briggs W.M. (1992). Suspension freezing of bottom sediment and biota in the Northwest Passage and implications for Arctic sedimentation - Can. J. Earth Sci. , 29:693-703.

Saks V.N. (1952). Environment of bottom sediments formation in the Arctic Seas of the USSR - Leningrad - Moscow, Glavsevmorput, 140 pp (in Russian)

Senin B.V. (1993). Tectonic structure of the Western Arctic metaplatform - D. Sc. thesis, Moscow, MGU, 65 pp (in Russian)

Serova V.V. and Gorbunova Z.N. (1993). Mineral composition of soils, aerosoles, suspended matter and bottom sediments of the Lena River and the Laptev Sea - In: Arctic estuaries and adjacent seas: biogeochemical processes and interaction with global change. Svetlogorsk, pp. 78-79

Shelekhova E.S., Nürnberg D., Wahsner M., Levitan M.A., and Pavlidis Yu.A. (1995). Distribution of clay minerals in the surface layer of bottom sediments of the south-western part of the Kara Sea - Oceanology, 1 (in Russian)

Suhovey V.F. (1986). Seas of the World Ocean - Leningrad, Gidrometeoizdat, 288 pp (in Russian)

Suzdalsky O.V. (1974). Lithodynamics of shallow water areas of the White, Barents and Kara seas - In: Geology of the Seas, Nedra, No3, pp. 27-33 (in Russian)

Ul G.F. (1936). Rocks of sea bottom and coasts of the Kara Sea. Transactions of NIIGA, 136 pp (in Russian)

Vedernikov V.I., Demidov A.B., and Sudbin A.I. (1994). Primary production and chlorophyll in the Kara Sea in September 1993 - Oceanology, 5:693-703 (in Russian)

Zagorskaya N.G., Yashina Z.I., Slobodin V.Ya., Levina F.M., and Belevich A.M. (1965). Marine Neogene (?) - Quaternary deposits of the land area adjacent to Yenisey River delta - Moscow, Nedra, 92 pp (in Russian)

Zenkevich L.A. (1963). Biology of the Seas of the USSR - Moscow, Acad. Sci. USSR, 740 pp (in Russian)

Appendix

Table 1.: Average grain-size composition of sediments of different facies zones and subzones (wt.%). All fractions are given in mm. S - sum of fractions.

FACIES ZONES	FACIES SUBZONES	GRAVEL			SAND			ALEURITE			PELITE			ΣGr+Sd +Al / ΣPel	Coef.of sorting
		3.0-2.0	2.0-1.0	Σ	1.0-0.05	0.5-0.25	0.25-0.1	Σ	0.1-0.05	0.05 0.01	Σ	0.01-0.005	0.005-0.001 / <0.001 Σ		
WEAST R (I)	I-A (n=19)	0.20	0.12	0.32	0.11	0.88	4.53	5.52	3.73	3.17	6.90	12.86	30.61 / 87.26 43.79	0.15	3.48 (n=10)
	I-B (n=6)	----	0.16	0.16	0.18	0.88	5.22	6.28	7.05	1.65	8.70	10.80	28.75 / 84.86 45.31	0.18	4.07 (n=5)
	Average (n=25)	0.15	0.13	0.28	0.13	0.88	4.69	5.70	4.53	2.80	7.33	12.37	30.16 / 86.69 44.16	0.15	3.68 (n=15)
OBLAST II	II-A (n=7)	0.22	0.16	0.38	0.51	7.48	14.92	22.91	16.10	2.24	18.34	8.59	18.42 / 58.33 31.32	0.70	3.55 (n=7)
	II-B (n=11)	----	0.10	0.10	0.04	0.56	6.54	7.14	5.54	2.75	8.29	12.34	27.22 / 84.39 44.83	0.18	6.53 (n=4)
	II-C (n=3)	----	0.32	0.32	0.11	1.94	28.69	30.74	6.84	0.89	7.73	7.22	20.38 / 61.22 33.62	0.63	3.30 (n=3)
	II-D (n=1)	----	----	----	0.35	0.15	1.24	1.74	2.28	0.45	2.73	14.13	30.69 / 95.53 50.71	0.05	3.21 (n=1)
(II)	Average (n=22)	0.07	0.15	0.22	0.21	2.93	11.99	15.13	8.93	2.23	11.16	10.53	23.64 / 73.47 39.30	0.36	7.23 (n=15)

Table 2.:Average mineral composition of fraction 0.05-0.1 mm from sediments of different facies zones and subzones (%).

FACIES ZONES	FACIES SUBZONES	HEAVY SUBFRACTION							LIGHT SUBFRACTION				
		Content	Horn-Blende (Hbl)	Black Ores (Bor)	Epi-dote (Ep)	Clyno-pyroxene (Mpx)	Ep/Mpx	Assem-blage	Quartz (Q)	K feld-spar (KF)	Asid plag. (Apl)	Q/KF+Apl	Assem-blage
WESTERN KARA (I)	I-A (n=8)	0.7	13.8	19.1	23.2	14.3	1.6	Hbl-Mpx-Bor-Ep	54.0	23.8	9.5	1.7	Apl-Ort-Q
	I-B (n=4)	0.5	15.8	24.1	20.6	9.7	2.1	Mpx-Hbl-Ep-Bor	57.9	27.2	10.9	1.4	- " -
	Average (n=12)	0.65	14.5	20.8	22.3	12.8	1.7	Mpx-Hbl-Bor-Ep	55.0	24.9	10.0	1.7	- " -
OB-YENISEY (II)	II-A (n=9)	6.0	9.6	21.8	12.0	46.8	0.3	Hbl-Ep-Bor-Mpx	52.2	20.4	11.7	1.7	- " -
	II-B (n=6)	4.1	10.0	10.6	17.2	38.1	0.4	Hbl-Bor-Ep-Mpx	62.0	20.4	7.2	2.5	- " -
	II-C (n=3)	1.6	14.1	19.0	12.4	36.9	0.3	Ep-Hbl-Bor-Mpx	62.6	17.7	7.6	2.5	- " -
	II-D (n=1)	2.4	15.4	16.2	17.9	32.0	0.6	Hbl-Bor-Ep-Mpx	56.0	27.0	11.5	1.4	- " -
	Average (n=19)	4.5	11.5	17.5	14.0	41.7	0.3	Hbl-Ep-Bor-Mpx	57.1	20.3	9.6	2.0	- " -
	Ob transect(n=7)	1.7	12.6	17.0	20.4	31.4	0.6	Hbl-Bor-Ep-Mpx	65.5	21.0	7.6	2.5	- " -
	Yenisey tr.(n=12)	5.9	10.9	16.5	10.3	47.7	0.2	Ep-Hbl-Bor-Mpx	52.2	19.8	10.8	1.7	- " -

Table 3.: Average composition of clay mineral assemblages of fractions less than 0.001 mm from sediments of different facies zones and subzones (rel.%).

FACIES ZONES	FACIES SUBZONES	Illite (I)	Smectite (S)	Smectite / Illite	Chlorite (C)	Kaolinite (K)	Assem-blage
WESTERN (I)	I-A (n=35)	36	41	1.1	14	9	KCIS
	I-B (n=8)	38	34	0.9	14	14	(K,C); (S,I)
	Average (n=43)	36	40	1.1	14	10	KC; (I,S)
OB|YENISEY (II)	II-A (n=7)	20	60	3.0	10	10	(K,C); IS
	II-B (n=5)	20	63	3.2	8	9	(C,K); I,S
	II-C (n=4)	19	66	3.5	8	7	(K,C); I,S
	II-D (n=1)	25	49	2.0	13	13	(K,C); I,S
	Average (n=17)	20	62	3.1	9	9	(K,C); I,S
	Ob tran-sect(n=5)	21	59	2.8	10	10	(K,C); I,S
	Yenisey tr.(n=12)	20	63	3.2	9	8	(K,C); I,S

Table 4.: Average chemical composition of sediments of different facies zones and subzones (SiO_2, Al, Fe, C_{org} - in wt.%; Ti, Mn, P, Sr, Ni, Co, Cr, V, Ba - in ppm).

FACIES ZONES	FACIES SUBZONES	SiO_2	Al	Ti	Fe	Mn	C_{org}	P	Sr	Zn	Ni	Co	Cr	V	Ba	$\frac{SiO_2}{Al}$
WESTERN (I)	I-A (n)	59.9 22	7.49 22	4777 23	5.50 23	7244 23	1.10 23	1252 22	352 23	96 23	67 23	20 23	98 23	161 23	554 23	8.00 22
	I-B (n)	62.1 9	7.43 9	4340 9	5.28 9	3930 9	1.09 9	1387 9	344 9	95 9	56 9	19 9	95 9	139 9	597 9	8.36 9
	Average (n)	60.5 31	7.47 31	4654 32	5.44 32	6312 32	1.09 32	1291 31	350 32	95 32	64 32	19 32	97 32	155 32	566 32	8.10 31
OB|YENISEY (II)	II-A (n)	71.4 13	5.31 13	4267 13	3.73 13	1310 13	1.02 12	728 13	272 13	115 13	58 13	21 13	83 13	91 13	658 13	13.45 13
	II-B (n)	60.1 11	7.40 11	4881 12	5.92 12	1265 12	1.48 12	1091 11	345 12	125 12	72 12	24 12	79 12	129 12	545 12	8.12 11
	II-C (n)	67.8 7	5.91 7	3745 7	3.78 7	689 7	0.66 7	489 7	289 7	109 7	55 7	24 7	60 7	98 7	693 7	11.47 7
	II-D (n)	54.8 2	8.27 2	4592 2	7.34 2	14843 2	1.17 2	2145 2	451 2	135 2	88 2	43 2	111 2	179 2	793 2	6.63 2
	Average (n)	65.9 33	6.31 33	4395 34	4.72 34	1962 34	1.12 33	884 33	312 34	118 34	64 34	24 34	79 34	111 34	633 34	10.44 33
	Ob transect (n)	67.1 14	6.08 14	4141 14	4.63 14	3070 14	1.01 13	1051 14	311 14	109 14	63 14	27 14	74 14	108 14	682 14	11.04 14
	Yenisey tr. (n)	64.9 19	6.50 19	4596 20	4.80 20	1087 20	1.20 20	748 19	312 20	126 20	65 20	21 20	82 20	114 20	595 20	9.98 19

Distribution of magnetic susceptibility on the Eurasian shelf and continental slope - implications for source areas of magnetic minerals

Niessen F. and Weiel D.

Alfred Wegener Institute, Bremerhaven, Gemany

Abstract

Dual-frequency, mass-specific magnetic susceptibilities were determined in surface samples from the Kara and Laptev Seas to study the magnetic character and lateral distribution of magnetic grains. Frequency-dependent susceptibility is generally between 0 and 4%. This indicates the presence of magnetic grains larger than 0.03 μm (single and multiple domain) which excludes significant in-situ formation of magnetic crystals in marine sediments. Mass-specific susceptibility ranges from 0.1 to 1.2 $\mu m^3 kg^{-1}$ which suggests a control of susceptibility by ferrimagnetic grains. There is a distal to proximal increase of magnetic susceptibility around Franz Joseph Land (0.1 - 0.6 $\mu m^3 kg^{-1}$). This suggests that volcanic rocks on the archipelago function as an important source area for magnetic particles. Magnetic susceptibility is generally higher in the western (0.4 - 0.6 $\mu m^3 kg^{-1}$) than in the eastern Laptev Sea (0.1 - 0.3 $\mu m^3 kg^{-1}$). This is interpreted to result from an increased input of magnetic grains from the rivers Olenik, Anabar and Khatanga which have metamorphic and volcanic rocks in their catchments.

Introduction

Surface sediments from marine environments are used to study the present imprint of processes on the sedimentary record. Studies of the distribution pattern of sedimentary parameters based on surface sample analysis improves our understanding of past changes in depositional environments. The latter are reconstructed from sediment cores. Magnetic susceptibility is a basic physical property of marine sediments which is often used for high resolution lateral core correlation. In surface sediments, however, measurements of magnetic susceptibilities are rare. In sediments from the Arctic Ocean the present distribution pattern of magnetic susceptibility is practically unknown.

Magnetic susceptibility is commonly used as an indicator of lithological changes. It is defined as the dimensionless proportional factor of an applied magnetic field in relation to the magnetization in the sample. Because ferrimagnetic minerals have a significant higher susceptibility ($k= +10^{-2}$) than most common minerals (-10^{-6} to $+10^{-6}$), changes in susceptibility are normally controlled by variation in the content of ferrimagnetic matter (mostly magnetite, titanomagnetite or maghemite; Thompson and Oldfield, 1986). In marine sediments from high latitude areas, magnetite is mostly derived from terrigenous input and/or volcanic ashes. The sediments of the Arctic Ocean are dominated by terrigenous components. The organic matter content is generally low (0.5 - 2 %, Stein, this vol.). Therefore, significant amounts of

magnetic grains can be expected in the samples. Distribution maps of magnetic susceptibility in surface sediments are thus ideal to study different source regions and the distribution of ferrimagnetic minerals.

Here we present results from the analysis of dual-frequency, mass-specific magnetic susceptibilities of surface sediments collected on the continental shelf and adjacent slope areas of the northwestern Kara and entire Laptev Seas. Frequency-dependent susceptibility can be used to interpret the grain size of magnetic minerals which is indicative of the processes of crystal formation (Thompson and Oldfield, 1986). The determination of mass-specific susceptibility (Dearing, 1994) has the advantage that the results are independent of sample porosity and sample size. This enables the estimation of the content of ferrimagnetic minerals in the surface samples, which, in turn, can be directly compared with equivalent results from sediment cores.

Methods

Surface sediment samples were collected during the cruises ARK-IX/4 (RV "Polarstern"; Fütterer, 1994), TRANSDRIFT I (RV "Ivan Kireyev"; Kassens and Karpiy 1994) and AG 80 (RV "Akademik Golitsin", 1.8.-31.8.1994, Franz Joseph Land). Volume magnetic susceptibilities of freeze-dried samples were measured at high (4.6 kHz, hf) and low (0.46 kHz, lf) frequencies using a MS2B sensor (Bartington Ltd, UK). The per sample measuring time is 10s and data output is in SI units (10^{-5} SI). Each measurement was repeated once and the readings were averaged. Standard containers of 10 cm^3 were used. Because the samples have different volumes the measured volume susceptibility was normalized against sample mass. For our MS2B sensor the simple regression of volume susceptibility against sample mass has been tested using 8 different sample sizes (masses from 3 to 25 g) of a well mixed standard sample. The correlation coefficient is 0.997 and 0.999 for hf and lf, respectively (Fig.1). Mass specific susceptibility ($\mu m^3\ kg^{-1}$) is calculated by volume susceptibility (10^{-5} SI) / (mass (g) * 10). A constant grain density of 2.6 g cm^3 (or 2600 kg m^3 in SI-units) is assumed. Frequency-dependent susceptibility (F-Factor) is calculated as the percent difference of hf relative to lf (Dearing, 1994). For mapping of mass specific susceptibility in surface sediments the hf data were used.

Results and Discussion

Frequency-Dependent Susceptibility

The total variation between hf- and lf-susceptibility (F-Factor, Fig.2) for all samples ranges between -4 and 7 %. Most samples, however, range between 0 and 4 % with a distinct peak at ca. 1.5 %. Differences in the frequency-dependent susceptibility between the two areas are small and insignificant (Fig.2).

Since lf-susceptibility can only be larger than or equal to hf-susceptibility the few negative values have to be attributed to sensor errors. The same may be true for the few values higher than 4% seen in the histogram in Figure 2. This would imply that essentially all samples studied fall within the range of 0 to 4 %.

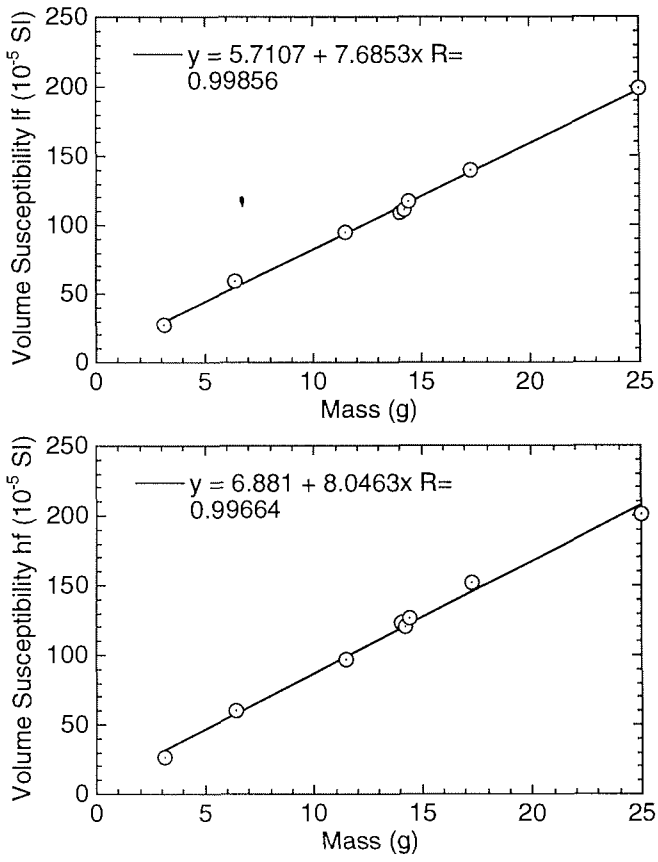

Fig. 1.: Relationship between sample mass and volume susceptibility for different amounts of a standard sample (left hf, right lf).

Frequency-dependent susceptibility can be used to detect the grain size of ferrimagnetic minerals and therefore their magnetic behavior (Dearing, 1994). For example, F-Factors of up to 14% are observed for magnetite grains smaller than 0.035 μm. Such samples are characterized by a superparamagnetic behavior and have strongly increased susceptibilities. Superparamagnetic grains are used as an indication for in-situ formation of magnetic crystals in soils and sediments (Thompson and Oldfield, 1986; Dearing, 1994). In contrast, low F-Factors (between 0 and 2 %) indicate magnetic grain size larger than 0.035 μm and stable single to multidomain behavior.

The low F-Factors of the samples from the Kara and Laptev Seas indicate low to very low contents of superparamagnetic grains. This is important, because significant in-situ formation of ferrimagnetic minerals in the sediments as well as aeolian input of such grains derived from terrestrial soils can be excluded. Thus, the observed low F-Factors suggest a terrestrial source of magnetic grains derived from bedrock erosion.

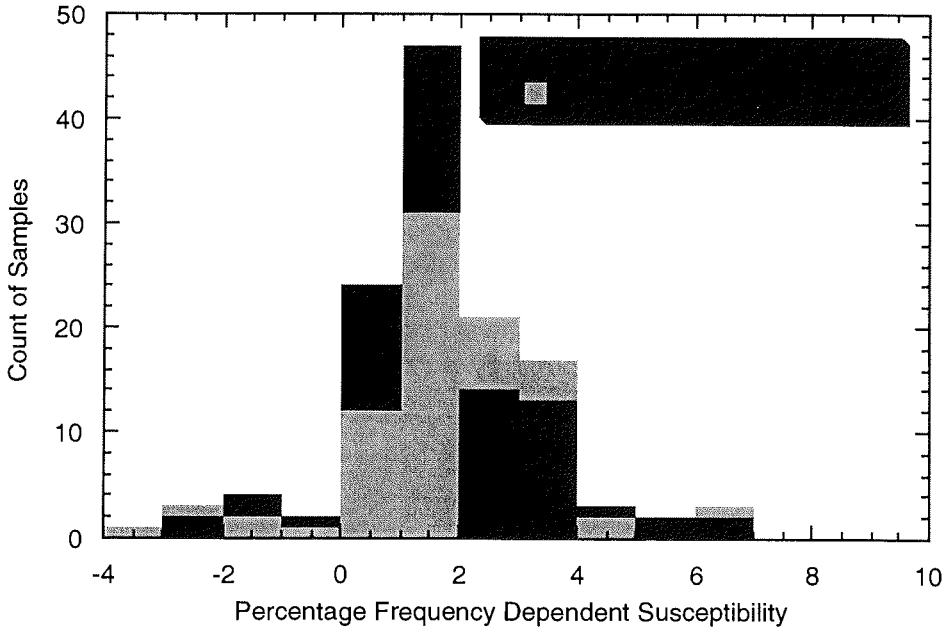

Fig. 2.: Histogram of frequency-dependent susceptibilities.

Mass-specific susceptibility

The total range of mass-specific susceptibilities is about 0.1 to 0.6 ($\mu m^3\ kg^{-1}$) and about 0.1 to 1.2 ($\mu m^3\ kg^{-1}$) for the Kara and Laptev Seas, respectively (Fig. 3, 4). For the Kara Sea the susceptibility distribution map shows a general increase toward the archipelago of Franz Joseph Land (Fig. 3). Values of more than 0.5 ($\mu m^3\ kg^{-1}$) are only found in near-shore areas of the islands. For the Laptev Sea there is an increase toward the Eurasian continent and the New Siberian Islands (Fig. 4). Values higher than 0.4 ($\mu m^3\ kg^{-1}$) are observed predominantly in the western Laptev Sea, including some local patches greater than 1.0 ($\mu m^3\ kg^{-1}$) to northwest and northeast of the Lena Delta.

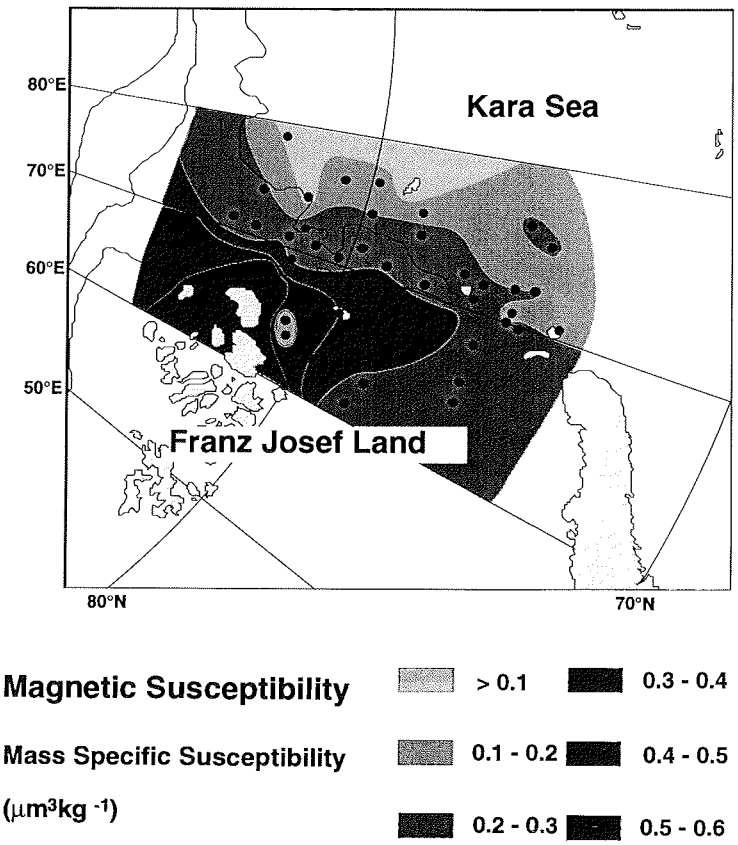

Fig. 3.: Distribution of magnetic susceptibility in the northeastern Kara Sea.

Generally, if mass-specific susceptibility exceeds 0.1 $\mu m^3\ kg^{-1}$, the magnetic carrier of the sample is dominated by ferrimagnetic minerals such as magnetite, titanomagnetite or maghemite. For example, a mass-specific susceptibility of 0.2 to 20 $\mu m^3\ kg^{-1}$ can be explained by a content of 0.1 to 1 mass percent of titanomagnetite in the sediments (Dearing, 1994). The mass-specific susceptibilities of the Kara and Laptev Seas fall well within the above range. This implies that the susceptibility is positively correlated with the content of ferrimagnetic minerals, probably magnetite or titanomagnetite.

The distribution maps support a local terrestrial origin of increased susceptibility in marine sediments. In particular, the archipelago of Franz Joseph Land is indicated as an important source area. Volcanic rocks (basalts and dolerites) exposed on Franz Joseph Land combined with high denudation rates by ice sheets and glaciers are likely to force the export of magnetic particles into the Arctic Ocean.

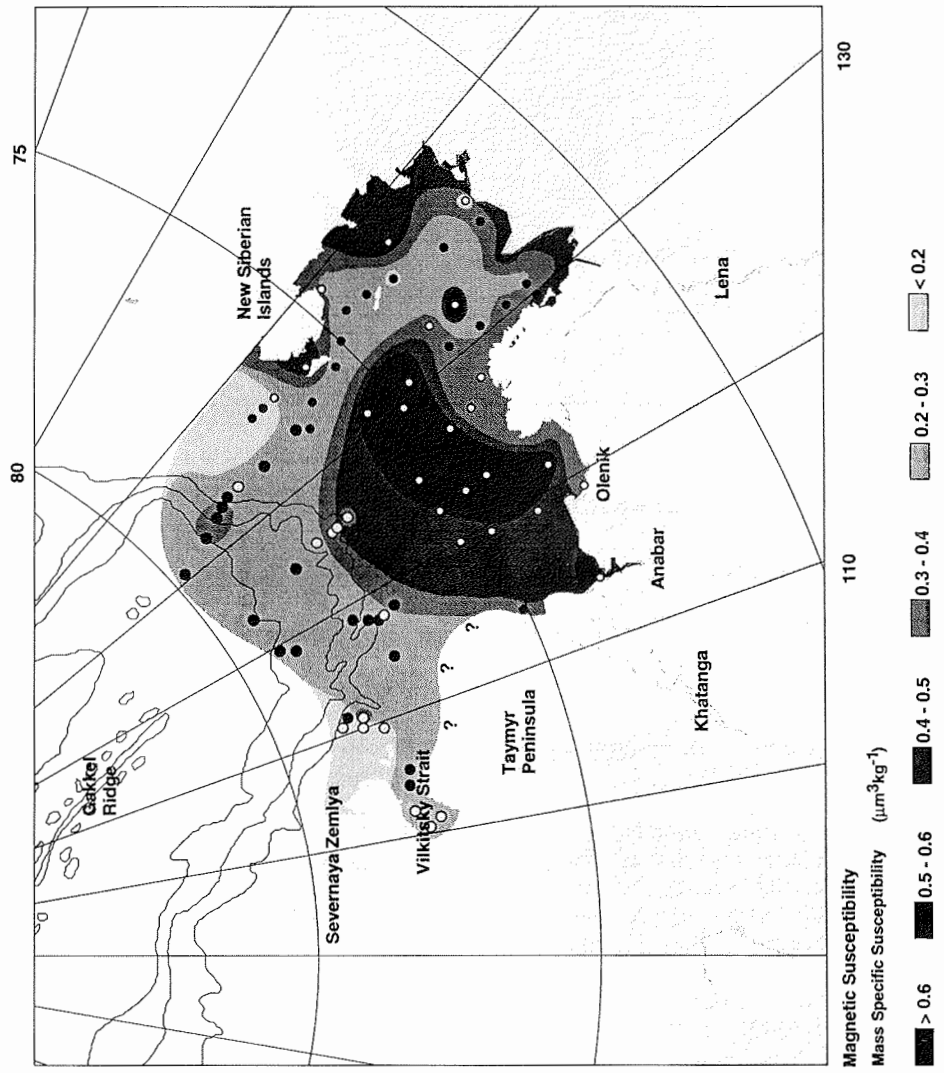

Fig. 4.: Distribution of magnetic susceptibility in the northeastern Laptev Sea.

The distribution observed in the Laptev Sea is interpreted to be largely controlled by river input. Higher susceptibilities in the western part of the Laptev Sea may be related to higher export of ferrimagnetic grains from the rivers Olenek, Anabar and Khatanga. A large Archaen block of crystalline rock is located in both catchments. Additionally, in the Khatanga catchment Triassic volcanic rocks are exposed over a large area and are likely to function as a major source region for magnetite or titanomagnetite. In contrast, the dominance of sedimentary rocks in the catchment of the Lena may be responsible for the lower susceptibility in the eastern area of the Laptev Sea. It is interesting to note that similar west-east gradients in the same surface sediments of the Laptev Sea are also observed for both the clay- and heavy-mineral distributions. The western part is more dominated by smectite and clinopyroxene, the eastern by illite and amphibole (Silverberg, 1972; Wollenburg, 1993; Nürnberg et al., 1994; Behrends et al., this vol.). The authors interpret the pattern to be controlled by input of sediments of different composition mainly from the rivers Lena (eastern province) and Olenik, Anabar, Khatanga and/or the Kara Sea via the Vilkitsky Strait (western province) which is consistent with our results.

The interpretation of the occurrence of isolated patches with high susceptibilities in the Laptev Sea remains speculative. The area is known for high erosion rates. Several islands near the Lena delta have disappeared in historic times (Timokhov, 1994). Increased local input of ferrimagnetic material may thus be the result of surface erosion in areas of submerged islands.

Conclusions

Mass-specific susceptibilities of surface samples of the Kara and Laptev Seas indicate a ferrimagnetic character which can be explained by contents of about 0.1 to 0.5 mass percent of magnetite or titanomagnetite in the samples. Frequency dependent susceptibilities are generally low, and demonstrate single to multidomain behaviour typical for a terrigenous origin of magnetic grains derived from bedrock erosion. The distribution pattern of magnetic susceptibility indicates two possible source areas of ferrimagnetic grains exported into the Arctic Ocean: Franz Joseph Land and the area south of the Taymyr Peninsula in northern Siberia. In both areas volcanic rocks are exposed. This study can help to explain variations in space and time of magnetic susceptibility routinely measured in Arctic Ocean sediment cores.

References

Dearing, J. (1994): Environmental Magnetic Susceptibility. Using the Bartington MS2 System. Chi Publishing, Kenilworth, UK, 104p.

Fütterer, D.K. (1995): The Expedition ARKTIC `93 Leg ARK-IX/4 of RV "Polarstern" 1993. Ber. Polarforsch. 149, 244p.

Kassens, H. and Karpiy, V.Y. (1994): Russian-German Cooperation: The Transdrift I Expedition to the Laptev Sea. Ber. Polarforsch. 151, 168p.

Nürnberg, D., Wollenburg, I., Dethleff, D., Eicken, H., Kassens, H., Letzig, T., Reimnitz, E. and Thiede, J., (1994): Sediments in Arctic sea ice: Implications for entrainment, transport and release. In: Thiede, J., Vorren, T. and Spielhagen, R.F. (Eds.), Marine Geology. 119: 185 - 214.

Silverberg, N., (1972): Sedimentology of the surface sediments of the east Siberian and Laptev Seas. PhD thesis, University of Washington.

Thompson, R. and Oldfield, F. (1986): Environmental Magnetism. Allen and Unwin, Bosten, 227p.

Timokhov, L. A. (1994): Regional characteristics of the Laptev and the East Siberian seas: climate, topography, ice phases, thermohaline regime, and circulation. In: Kassens, H., Hubberten, H. W., Priamikov, S., Stein, R. (ed.), Russian-German Cooperation in the Siberian Shelf Seas: Geo-System Laptev Sea. Ber. Polarforsch., 144, 15-31.

Wollenburg, I. (1993): Sedimenttransport durch das arktische Meereis: Die rezente lithogene und biogene Materialfracht. Ber. Polarforsch., 127.

THE MAIN FEATURES OF MODERN SEDIMENTS IN THE SOUTHERN PART OF THE EAST SIBERIAN SEA

Nikiforov S.L.

P.P. Shirshov Institute of Oceanology, Moscow, Russia

Abstract

During the polar marine cruise of the ice breaker "Georgiy Sedov" new data about modern sedimentation processes within the inner shelf of the East Siberian Sea were obtained. The modern sedimentation processes are closely connected with seabed morphology and terrigenous input. One of the main controlling factor is the intense sea-ice cover causing some lithological anomalies on the shallow parts of the shelf.

Introduction

The East Siberian shelf including its shallow parts is very smooth and separated from the adjacent Chukchi and Laptev Seas. The differences between the seas are related to structural and geological features and lithological and geomorphological peculiarities. The former determine the basic seabed relief, and the latter modify the initial surface subordinating to zonal climatical processes. Within long-lasting ice-cover conditions the seabed morphology is not only formed by wave hydrodynamical effects, but also by under-ice sedimentation. Thus, fine pelite sediments were formed even within the coastal shallow parts. Paleogeographical processes cause some lithological anomalies. These complex processes determine unique structures and specific sediments that have practically no analogues within the Arctic.

Methods

For long time arctic shelves were the main research object of the Laboratory of Shelf Studies, Insitute of Oceanology, Moscow, Russia. In this region more then 10 marine cruises and coastal expeditions were carried out. One of them was devoted to the East Siberian Sea. Unfortunately, the execution was connected with extrem annual ice conditions, and the use of a powerfull ice breaker was necessary. With the ice breaker "Georgiy Sedov", a very long profile within the inner shelf and one detailed poligone in the most interesting key zone with an area about 400 km^2 were performed. The following geological and geomorphological devices were used: gravity corers of various types, echo sounding, and navigation equipment. 45 geological stations with surface and underlying sediment sampling were carried out. During laboratory processing the following analyses were performed: grain-size, mineralogy, and petrography. Besides that, all echo sounding data were analized, and all navigation maps were updated.

Results

Practically all modern sediments within the inner shelf are exclusively fine-grained. Pelite consists up to 95% with a predominance of the finest fraction (less than 0,001 mm). These sediments are characterized by the following average ratios between the main pelite fractions: (0.01 - 0.005 mm): (0.005 - 0.001 mm): (less than 0.001) is 2.0 : 3.5 : 4.5. Sands (with the exception of several cases) are not expressed (usually < 1%). Even in the Arctic such fine grained sediments are rare, and their formation within coastal shallow parts is abnormal and indicates an extremely calm modern sedimentary environment. The grain-size slightly changes in the Dmitriy Laptev Strait where some areas of modern sediments are represented by fine sands (up to 35%) and aleurites (up to 15%) with pelite content about 40 - 45 %.

From a first point of view the input of the large Siberian rivers Indigirka and Kolyma which total input makes about 18.7 - 24.5 mill. tons per year (Spaiher, 1963; Grigoriev, 1966; etc.), significantly influences the sedimentation. In spite of that, the main part of suspended matter falls down in the direct vicinity of the river mouths. Thus, at 70 km off the Indigirka mouth, the aleurite increases up to 20%. A similar situation with sand increasing to 27% was recorded at the same distance from Kolyma mouth.

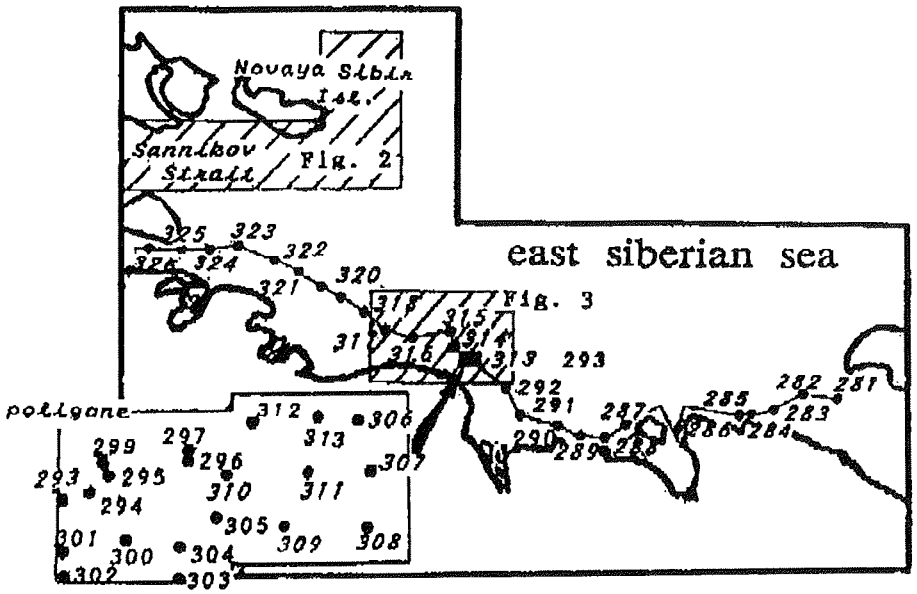

Fig. 1.: The expedition route and geological stations.

The mineralogy of surface sediments is characterized by an epidote and hornblende dominance (except for the Medvezhyi Islands vicinity where black ores are dominant). The heavy-mineral content is usually low (about 0.5%), with some higher values of up to 4.5% within the Dimitriy Laptev Strait caused by hydrodynamical effects. In the group of light minerals quartz (up to 30%) and feldspars (up to 13%) are the most important minerals.

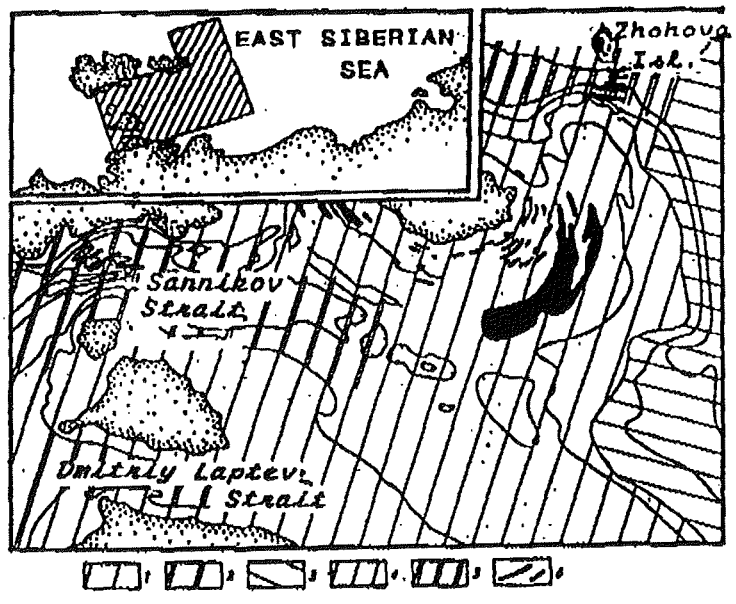

Fig.2.: Geomorphology of the south eastern part of the East Siberian Sea: 1-subhorizontal plain of modern and Pleistocene wave accumulation, 2-accumuation-denudation relief of SannikovaStrait and Dmitriya Laptev Strait, 3-accumulation-denudation relief of the underwater paleo-Indigirka slope, 4-accumulation-denudation relief of the structural depression's slope, 5-subhorizontal accumulative plain of the structural depression's bottom with modern and Pleistocene accumulation pattern, 6-large bars with accumulative forms.

In the seabed morphology we discover a couple of accumulative forms along coastlines of Zhohova Isl., New Siberia Isl., Vilkitskogo Isl., Faddeevskoogo Isl., Zemlya Bunge Isl., and Yakut coastline (Fig. 2). In some cases their sizes are very large - up to 150 km in length and 20 - 30 km in width with 20 - 25 m relative height, and distributed within coastal zones up to 60 km from the

coastlines. Everywhere they parallel the coastlines and have several generations (or series) (Nikiforov, 1984). Within Yakut coastal shallow parts at depths of about 10 - 20 m, we found 9 accumulative generations. Here, in a poligone of about 400 km^2, we performed detailed geological and geomorphlogical studies (Fig. 1, 3). Within this poligone there are two underwater accumulative forms. The southern one has a width of about 7 km and the northern one a width of about 8 km, with relative heights of 12 - 17 m. Their crest and depression floor are flat, and slopes are rather sharp (0.003 - 0.005 in tangence).

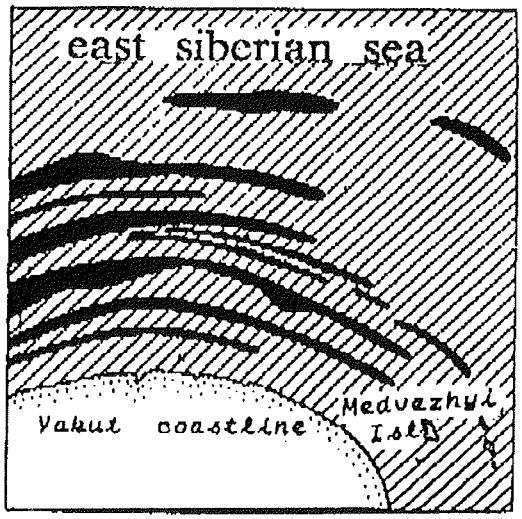

Fig. 3.: The accumulative bar complex along the Yakut shoreline within study poligone.

At the crest we obtained only one type of sediments - very fine pelite with small sand and aleurite admixtures (< 1 - 9 %). These sediments are typical for the inner shelf in general. On the other hand, they do not correspond to the classical distribution in the shallow parts (as in our case at depths of 10 - 20 m) and thus create one of the most interesting and typical anomaly within the East Siberian Sea. Other anomalies are connected with some processes at late Holocene to recent times. Within our poligone we reveal that each element of accumulative forms corresponds to their own type of sediments. The most fine grained sediments with exceedingly high dispertion which were supervised utterly seldom, are advanced on the crests at minimum depths of 10 - 11 m, and the most coarse ones with high content of sands (up to 20%) are found in depressions at maximal depth of about 20 m. No doubt, such correlations between relief and sediments are abnormal (Fig. 4).

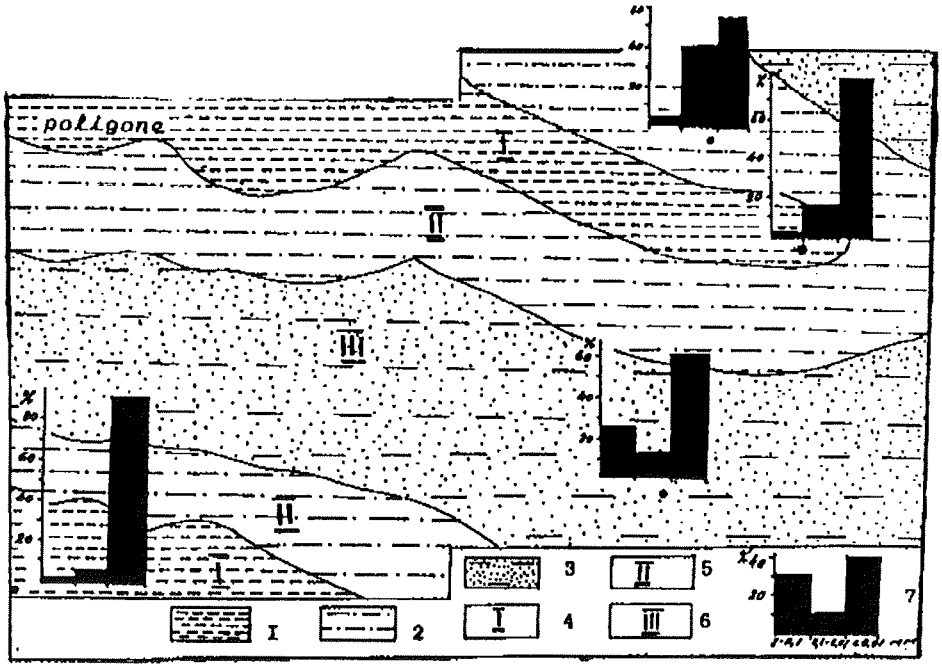

Fig. 4.: Sediment distribution within the the accumulative bar complex in the poligione: 1- fine pelite, 2- pelite with aleurite and some sand admixture, 3- pelite with large sand admixtures, 4- crests of bars, 5- slopes of bars, 6- deression between bars, 7- diagram of grain-size distribution; horizontal axis: sands, aleurite, pelite; vertical axis: percentage of their concentration.

Discussion

One of the key problem was to find out the main causes for the pelite accumulation wide-spread even in the coastal shallow parts. We think that these prosseses are closely connected with the ice regime. Practically all over the year the ice cover is constant and causes a specific long time of under-ice sedimentation with very low hydrodynamical activity, including weak currents extending from the mouths of large rivers. Thus, an enormous amount of fine-grained suspended matter load may have caused the very smooth relief. In such case, the very shallow depth does not influence the sedimentation substantially. During the very short summer and early autumn times, the situation is changed - within the southern parts of the inner shelf many ice floes are spreaded, and large areas of water become ice-free. Hydrodynamics

become more and more intensive and produce some interesting effects in accumulation mounds. We reveal that every relief segment (crests, slopes, and depressions) corresponds to their own lithological type. But in opposite to the normal situation, we found the most fine-grained pelite on the crest and much coarser ones in the deeper depressions. Such abnormal situation is connected with the following. During summer times when the wave activity is most intensive, the pelite sediments of the surface crests suspend first, and erosion occurs. Our results show that in the case of small depths surface sediments raise into the water and are then suspended just at the beginning of the shores. Water immediately looses its transparency. There is formed some kind of muddy-brown suspended pulp (Kalinenko and Nikiforov, 1985). We have recorded the same situation in our poligone where depths do not exceed 20 m. Suspended matter has a very long time of dissipation, even when the storm passes. The lowest part of this suspended cloud has the highest concentration, and the coarse matter is usually dominating here. In the phase of storm degradation coarse matter falls down first and accumulates in the depression as hydrodynamical activity at the crest at this phase of the storm is still high. At the crests at depths of about 10 m hydrodynamical activity is weakening lastly when the density of suspended matter is not very high. Thus, at summer times there is no accumulation at the crests, and we discovered eroded fine-grained pelite there. Accordingly, practically all coarse material is concentrated in the depressions as a result of erosion, resuspension, and specific hydrodynamical separation. On the other hand, we cannot except the possibility of current influence on sediment coarsing in depressions. But unfortunately we have no data about current velocity and other necessary hydrodynamical characteristics.

The next step of our studies is to find out the origin of the discovered accumulative forms of relief. We can offer four variants of their formation: ancient bars, ancient geological structures with modern sediment cover, relief caused by tide (strait) effects, and coastal marshes. Taking into account the discrepancy of geological structures and seabed morphology, weak hydrodynamics of all types, and geomorphological features (i.e., the morphology of the mounds, the taking turns, the correlation with coastline stretching, and the frequency of arrangement), we could make the conclusion that these forms of relief are underwater bars of accumulative geomorphological formations. Their common occurrence is an evidence of their inherit development.

Nowadays it is well known that accumulative bars react to the situation and activity of geological structures. In our case, we could assume the existence of anticlinal and brahyanticlinal flanks there. We know many worldwide-spreaded analogues of bar relief similar to our case. Coastal bars are described along Northern America with length up to 2000 km, Meechken bar within Anadir Bay (up to 90 km), series of bars along Eastern Kamchatka (up to 600 km), Caspian ancient bars with length up to 200 km and up to 100 km wide, and many others.

Conclusions

1. The inner shelf represents a huge shallow-water zone formed by long-lasting under-ice sedimentation with very fine-grained pelite accumulation

even in nearshore. This does not agree with the worldwide conception of sediment (grain-size, mineralogy) distribution in the near-shore shallow parts.

2. Within the inner shelf underwater bars have been wide-spread and represent accumulative forms of relief with inherit origin (fixed by geomorphological features). They rather differ from the adjacent Chukchi region where they are non-inherited. In the East Siberian Sea bars correlate with geological structures and support the possible existence of geological anticlinal and brahanticlinal flanks.

3. Nowadays accumulative bar reliefs are formed by some specific hydrodynamical processes, long-lasting under-ice sedimentation, and short intensive suspension at summer time. As a result, we can see an abnormal surface-sediment distribution.

References

Grigoriev N.F., 1966. Thermofrost sediments of Yakut coastal plain. Moscow, Nauka; 191 pp., Russian.

Kalinalineko V.V. and Nikiforov S.L., 1985. Lithological anomalies within Arctic marine shallow. In: Geology and geomorphology of shelves and continental slopes. Moscov, Nauka; 184 - 194; Russian.

Nikiforov S.L., 1984. Geomorphological structure of the western sector of the East Siberian Sea. Oceanology, v. XXIV,No. 6, 948 - 954; Russian

Shpaiher A.O., 1923. The role of Kolima inputs in hydrological forming of East Siberian Sea (in summer). Scientific papies of AA SRI, v. 264, 31 - 39, Russian, Leningrad.

BIOGENIC BARIUM AND OPAL IN SHALLOW EURASIAN SHELF SEDIMENTS IN RELATION TO THE PELAGIC ARCTIC OCEAN ENVIRONMENT

Nürnberg, D.

GEOMAR, Research Center for Marine Geosciences, Kiel, Germany

Abstract

Data on the distribution of opal and barium in the central Arctic Ocean and adjacent shelf areas are still sparse. The applicability of these parameters for productivity reconstuctions is also not investigated in detail. In contrast to the Southern Ocean, which shows a close correspondance between opal concentrations, biogenic barium, and further proxies for productivity, the Arctic conditions are more complex. On the Eurasian shelves, a correspondance between opal in core-top sediments and dissolved silica in the surface layer apparently exists. The eastern inner Laptev Sea with opal concentrations of about 3% to 6% is significantly different from the western Laptev Sea (0-2%) and the adjacent continental slope (2-3%), which is obviously driven by the enhanced nutrient supply from the Lena and Yana rivers. Similarly, the opal distribution within the Kara Sea with maximum concentrations nearshore (>5%) and decreasing concentrations further offshore generally reflects the nutrient supply from the Yenisey and Ob rivers. Even in the central Arctic Ocean, opal from suspended particulate matter sampled from the surface layer corresponds to concentrations of dissolved silica. However, corresponding surface sediments, the biogenic silica of which ranges between 0% and 6%, exhibit a distribution pattern, which not only depends on surface water characteristics, but also on sediment accumulation rates, preservation, reworking and the presence of siliceous sponges. The applicability for productivity reconstructions, thus, is possible to a certain degree, but largely depends on regional conditions.

In order to infer the marine productivity from barium, the biogenic portion of the total barium (Ba_{bio}) was calculated considering a detrital correction of Ba/Al = 0.0065. Though biogenic barium concentrations are generally low in Arctic shelf sediments (ca. 200 ppm), its distribution pattern resembles the distribution of marine organic matter. A maximum at the ice-edge accompanied by high opal concentrations refers to phytoplankton blooms during the short summer season. In the central Arctic Ocean, the distribution of Ba/Al-ratios initially compares to the distribution pattern of various biological and anorganic-geochemical proxies for marine productivity, but is in fact initiated by varying aluminum fluxes. Surficial occurrences of biogenic barium (> 100 ppm) are restricted to the Yermak Plateau, whereas minima occur in the deep-sea basins, where sedimentation rates are considerably higher.

Introduction

In relation to the world's ocean, the Arctic Ocean is rather low-productive. An extended ice coverage causes a significant reduction of primary productivity

(Subba Roa and Platt, 1984), which is generally reflected in a drastic reduction of the marine Corg-accumulation (Mortlock et al., 1991; Stein and Stax, 1991; Grobe and Mackensen, 1992). That seasonal variations in the ice cover in central parts of the Arctic Ocean leading to open water conditions of considerable duration may cause enhanced primary production rates, which subsequently affect the depositional environment, should be considered.

Especially in the Arctic Ocean, all processes (e.g. insolation, sea-ice, oceanography) driving the enhancement of primary production are closely related and interfinger accordingly. Common geochemical paleo-proxies are the amount of marine organic carbon (e.g. HI-indices, C/N ratios), biogenic barium, and opal. The aim of this study is to prove whether biogenic silica (opal) and biogenic barium can be applied as proxies for paleoproductivity. Core-top sediments from the Eurasian shelf and continental slope were investigated and compared to the central Arctic Ocean deep basins, plateaus and ridges. Processes affecting the barium and opal signal like dissolution, ice effects, sedimentation and primary production rates are subsequently discussed.

Barium in sediments from the Arctic Ocean

Biogenic barium is introduced into the sediment via small barite crystalls, which presumably formed in microenvironments of siliceous plankton during the decay of organic matter (Bishop, 1988). The correlation between TOC and barium in suspended particulate matter further reflects the tight relationship between biological processes in surface water masses and the barium flux to the seafloor. Systematic investigations on the barite accumulation through space and time were recently extended to pelagic areas in the South Atlantic (e.g. Gingele and Dahmke, 1994), the Pacific (e.g. Dymond et al., 1992), and the southern Ocean (e.g. Shimmield et al. 1994, Nürnberg, 1995, Nürnberg et al., subm.).

For the Arctic Ocean, the barium/barite signal and its relation to surface productivity, hydrography and temperature are not yet studied intensively. First investigations were performed by Lloyd et al. (1992) and Falkner et al. (1993). Due to the northward decreasing surface productivity, it is assumed that barium concentrations are generally lower in high northern latitudes compared to southern oceans. Nevertheless, regional differences in biological activity are evident even in the central parts of the Arctic ocean. Whether the dominating terrigeneous supply (Stein et al., 1994) disturbs and/or overprints the biogenic barium/barite signal, is discussed here.

Biogenic silica (opal) in sediments from the Arctic Ocean

The recent distribution of opaline skeletons (e.g. radiolarians, diatoms) is mainly driven by both the presence of nutrients and the oceanic circulation. The occurrence and distribution of biogenic silica (opal) in marine sediments, therefore, is commonly applied to reconstruct marine productivity and surface water circulation patterns (e.g. Mortlock and Froelich, 1989). Investigations of opaline silica in Arctic Ocean sediments were not yet systematically performed. Due to the permanent sea ice cover, the rate of biogenic silica accumulation in Arctic Ocean sediments is believed to be negligible (DeMaster, 1981). Lisitzin (1985) states that the opal accumulation at high latitudes is severely limited by the light factor and the ice cover leading to opal

concentrations commonly < 1% (Lisitzin,1967). According to Ku and Broecker (1965), accumulation rates are estimated to about 0.2-0.3 cm/kyr.

Material and Methods

Element and opal analyses were performed on sediment surface samples (uppermost 1 cm) from the central Arctic Ocean (Nansen, Amundsen and Makarov basins, Gakkel and Lomonosov ridges) and from the Laptev Sea and Kara Sea shelves and continental slopes (Fig. 1). All samples were recovered during RV "Polarstern" expeditions ARK VIII/3, ARK IX/4, and ARK XI/1 in 1991, 1993, and 1995, during RV "Ivan Kireyev" expedition TRANSDRIFT I in 1993, and during RV "Mendeleev" and RV "Logachev" expeditions during 1993 and 1994. The site locations span a water depth range of ca. 4250 m from about 250 m to 4500 m. A few opal analyses were run on suspended particulate matter, which was sampled during ARK VIII/3 from about 11 m water depth by continuous pumping.

Determination of barium

Barium and aluminium analyses were performed by X-ray analyses on a sequential wave-length dispersive Phillipps PW 1400 X-ray fluorescence spectrometer (Univ. Aachen). The accuracy of the barium analyses was checked by both analysing various standards (Govindaraju, Geostandards Newsletter Special Issue 3, 1994) and running replicates applying an acid digest with subsequent measurement by graphite furnace AAS (Fig. 2).

The total barium (Ba_{tot}) in sediments commonly consists of i) Ba_{barite}, which generates within the water column in microenvironments during the decay of organic matter and provides about 75 + 20% of the total barium in suspended particulate material (Dehairs et al., 1980; Wefer et al., 1982), and ii) Babackground, which can be ascribed to siliceous and/or carbonaceous skeletons, organic material (Ba_{bio} without barite) and terrigenous barite (Baterr).

A first approximation of the biogenic portion of the total barium is gained from Ba/Al ratios. There are, however, different normative approaches to distinguish more exactly between the detrital and the biogenic barium (e.g. Boström et al., 1973; Dymond et al., 1992; Gingele and Dahmke, 1994). According to Lea and Boyle (1989), carbonate shells contain maximum 30 ppm Ba. Dehairs et al. (1980) ascribe ca. 120 ppm Ba to siliceous skeletons, and particulate organic carbon accounts for ca. 60 ppm Ba (Martin and Knauer, 1973; Riley and Roth, 1971). According to Dymond et al. (1992), Shimmield et al. (1994) and Stroobants et al. (1991), barium is also significantly contributed from terrigenous matter overprinting the surface productivity signal. This contribution (Ba_{terr}) has to be accounted for when calculating the biogenic portion of the total barium. Since the amount of Ba_{bio} without barite is negligible compared to Ba_{terr}, I followed the normative approach of Boström et al. (1973) to differentiate between detrital and biogenic barium:

(1) $$Ba_{bio} = Ba_{tot} - Ba_{terr}$$

(2) $$Ba_{terr} = Al_{sample} * (Ba/Alumosilicate)$$

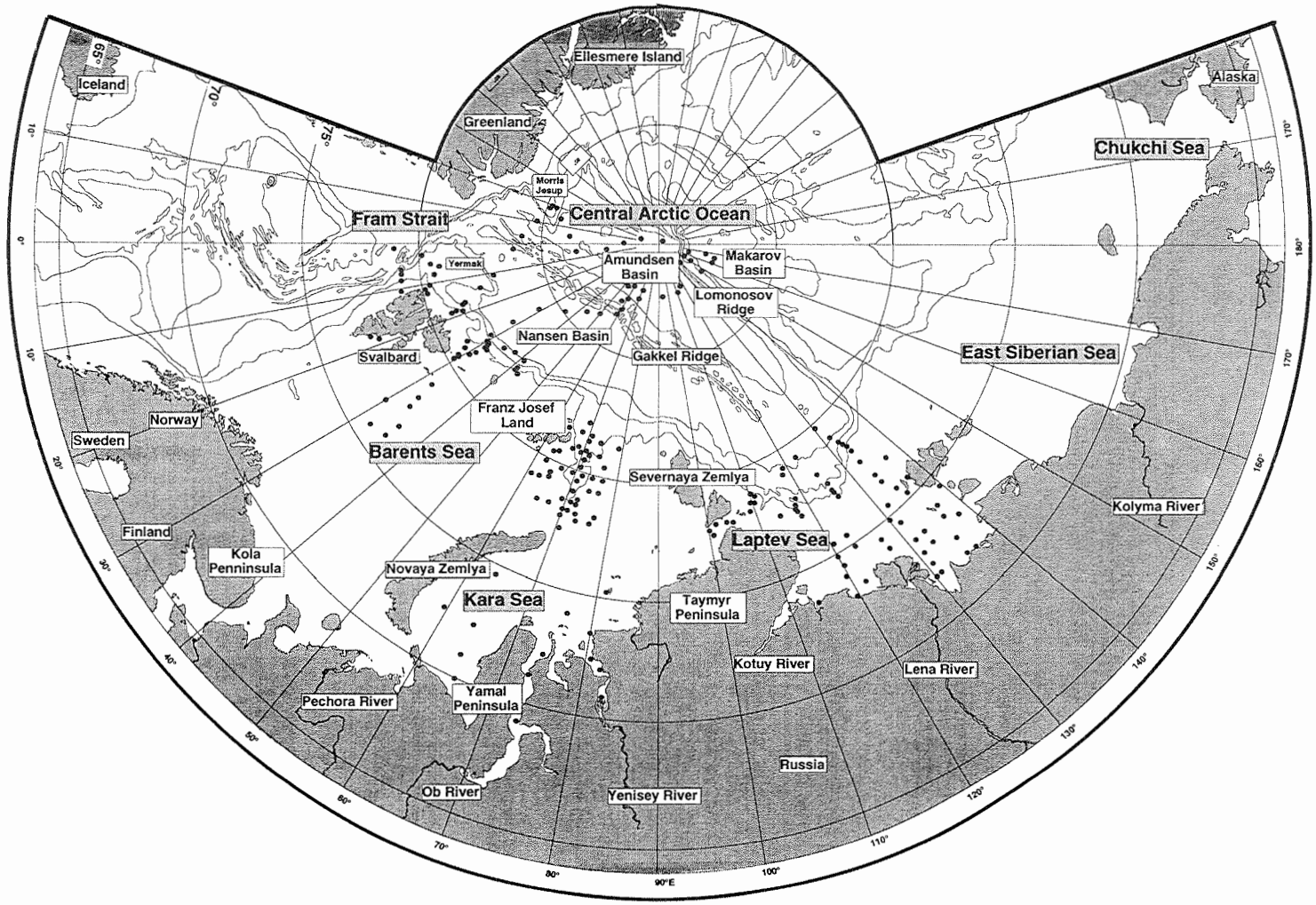

Fig. 1.: Bathymetric chart of the Eurasian Arctic indicating sampling locations.

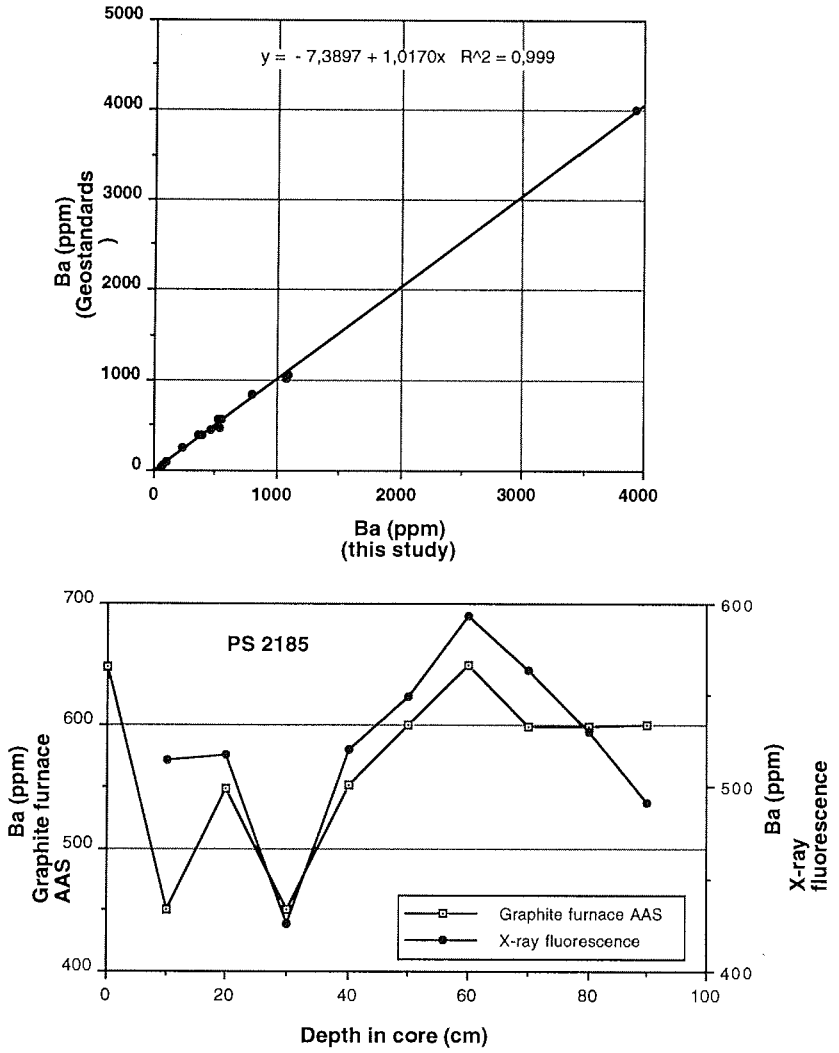

Fig. 2.: The accuracy of the barium analyses by X-ray fluorescence was proved by both analysing various standards (Govindaraju, Geostandards Newsletter Special Issue 3, 1994, left diagram) and running replicates applying an acid digest and subsequent analysis by graphite furnace AAS (done by C.C. Nürnberg, GEOMAR, right diagram).

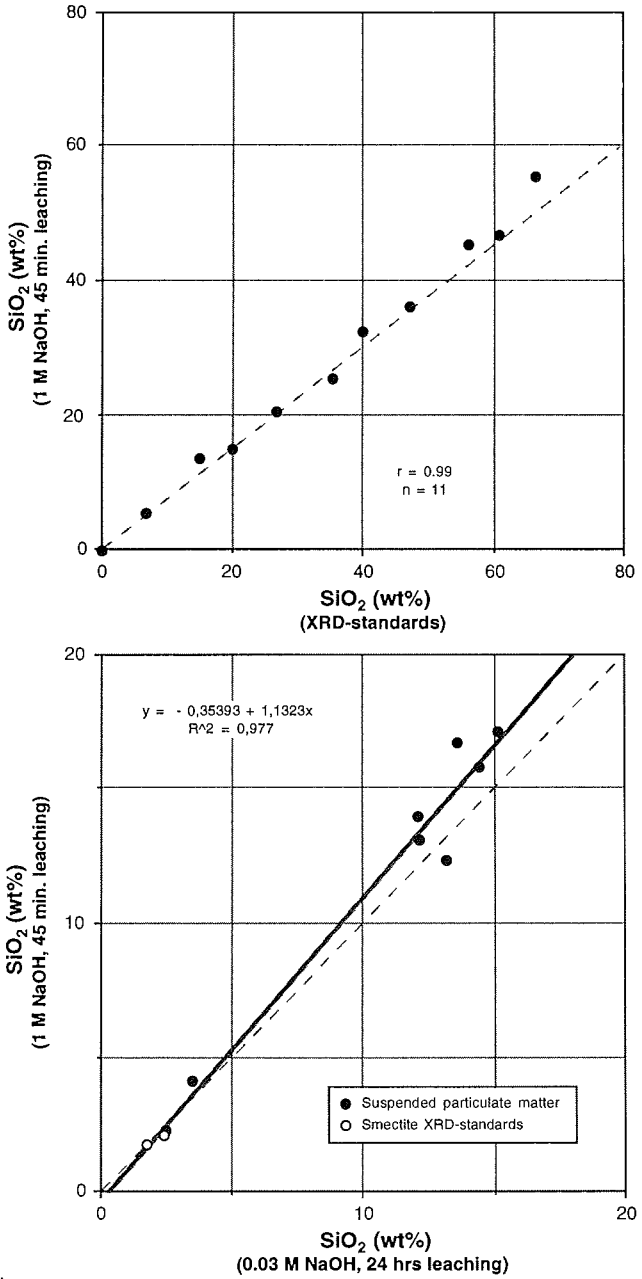

Fig. 3.: Accuracy of opal analyses by the applied automated leaching method. The left plot shows the comparative measurement of opal-standards (Opal-A, sponge spicules) by x-ray diffactometry and by the extraction method. Though the XRD-values are commonly higher, there is a good covariance between both methods. The right diagram compares opal concentrations derived from i) the routinely applied automated leaching (1 M NaOH, 45 min leaching at ca. 85 °C), and ii) 24 hrs leaching with 0.03 M NaOH (kindly carried out by D. Rickert, GEOMAR). Both methods provide comparative results.

This appproach assumes that the total amount of sedimentary aluminium is bound to aluminosilicates. The global average Ba/Alumosilicate ratio ranges between 0.01 and 0.005 (Taylor, 1964; Rösler and Lange, 1972), and according to Wedepohl (1991) it is about 0.0065. In this study, we sticked to the Wedepohl (1991) factor for all Arctic surface samples though regional variations in this factor are apparent. For the quantification of Ba_{bio}, the definition of the Ba/Alumosilicate ratio, however, is of considerable importance, especially when Ba_{tot} is generally low. The higher the Ba/Alumosilicate ratio, the lower (and eventually even negative) the Ba_{bio}.

Determination of biogenic silica (opal)
An automated leaching method according to DeMaster (1981) and Müller and Schneider (1993) was applied to determine biogenic silica (opal) in sediments. The opaline material is extracted from the dry and ground bulk sediment by 1 M NaOH (pH = 14) at ca. 85 °C in a stainless vessel under constant stirring for ca. 45 minutes. The leaching solution is continously analyzed for dissolved silicon by molybdate-blue spectrophotometry. The corresponding absorbance versus time plot is subsequently assessed according to the extrapolation procedure of DeMaster (1981). The autoanalyzer is calibrated by running silicon standard solutions. Both the reproducibility, which is around 0.5 %, and the accuracy were tested by running replicate measurements of samples and silicon standards (Fig. 3).

To further evaluate the applied method, replicate analyses were run by applying 0.3 M NaOH (pH = 12.5) and 24 hrs of leaching. Figure 3 shows that both leaching methods lead to resembling results, whereby the 45 min-leaching procedure with 1 M NaOH commonly exhibits slightly lower opal concentrations. Applying a 1 M NaOH ensures that all biogenic silica, that is siliceous benthos and plankton, is extracted from the sample. Unfortunately, clay minerals can also be affected by such a strong base. In order to assess the silica contribution from clay minerals, pure clay mineral standards and clay mineral mixtures, the composition of which were known, were treated with 1 M NaOH. During all leachings, no more than 1.5% silica were provided by pure smectite, whereas kaolinite and chlorite only contributed < 0.1% silica. The artificial clay mineral mixture (smectite : kaolinite : chlorite = 1:1:1) provided < 0.25% silica.

Results

Central Arctic Ocean
The studies on Arctic Ocean surface sediments exhibit higher opal concentrations than previously estimated by Lisitzin (1967). Bulk opal concentrations range from 1% to about 9%, but do not show a regular distribution pattern (Fig. 4). Since siliceous sponge spicules are common sediment components in central parts of the Arctic, the biogenic opal signal comprises both the benthic and the planktic contribution. Differential leaching of core-top sediments with both 0.1 M and 1 M NaOH provides an estimate of the amount of silica, which can be attributed to siliceous benthos (e.g. sponges). It was concluded that about 50% of the measured opal concentrations account for siliceous benthos. The plankton signal finally preserved in the seafloor deposits is consequently evaluated to range between 1% and 3% all over the study area. Only few exceptions occur on the

Lomonosov and Gakkel ridges, and at selected stations within the Nansen and Amundsen basins. On Morris Jesup Rise and on Yermak Plateau, opal concentrations diminish to < 1%.
Within suspended particulate matter from the surface mixed layer, which is dominated by organic matter (pers. com. C. Joiris, 1994), opal concentrations are significantly higher compared to the seafloor deposits. Opal concentrations of about 2-5% in the vicinity of Svalbard successively raise to >10% further north (Fig. 5).

Within the central Arctic Ocean surface sediments, barium concentrations amount to 420 - 680 ppm. Aluminium representing the terrigenous portion of the bulk sediment ranges between 52% and 98% with maximum concentrations in the deep basins. Resulting Ba/Al ratios range from 44 to 88. The biogenic barium concentrations are mostly negative when applying a detrital Ba/Al ratio of 0.0065. However, on Lomonosov and Gakkel ridges, on Morris Jesup Rise, Yermak Plateau and on the Barents Sea shelf and slope, occurrences of biogenic barium up to ca. 170 ppm are present (Fig. 6).

Laptev Sea area
Microscopic and visual investigations of the Laptev Sea shelf and slope sediments reveal that occurrences of siliceous sponges are rare. Small sponges only occur sporadically (Fütterer, 1994). The opal extracted with 1 M NaOH solution, thus, must be mainly related to siliceous plankton. Opal concentrations within Laptev Sea shelf and continental slope sediments range from undetectable to ca. 6% (Fig. 7). The eastern inner Laptev Sea shelf between the New Siberian Islands, the Lena Delta and the mainland exhibits opal concentrations > 3% to 6%. North and west of this area, opal concentrations diminish to 0-2% being characteristic for the inner western Laptev Sea shelf. The outer shelf and continental slope areas as well as the Strait of Vilkitzky, which are permanently influenced by sea ice, show medium concentrations of 2-3%. In the direct vicinity of the summer '93 ice edge, opal concentrations are enhanced to ca. 3-5% (Stations PS2458, PS2459, and PS2466 at the upper slope).

Barium concentrations range from 327 ppm to 682 ppm, resembling central Arctic Ocean values (Fig. 8). Aluminium values, however, exhibit a much wider range (23 - 87%) than the central Arctic Ocean samples. The Ba/Al ratios lie between ca. 50 and 140, and their distribution is generally opposite to the distribution of elementary aluminum. Occurrences of biogenic barium are generally present though absolute concentrations are below 200 ppm. Exceptionally enhanced concentrations of biogenic barium (251 - 289 ppm) occur in the vicinity of the summer '93 ice edge (Stations PS2457, PS2463 and PS2467) and in front of the main Lena River outflow (Station IK9320, 206 ppm). Here, elementary barium concentrations increase significantly, whereas the aluminum concentrations further decrease. Exclusively terrigenous barium is bound to the near-shore areas and the lower continental slope.

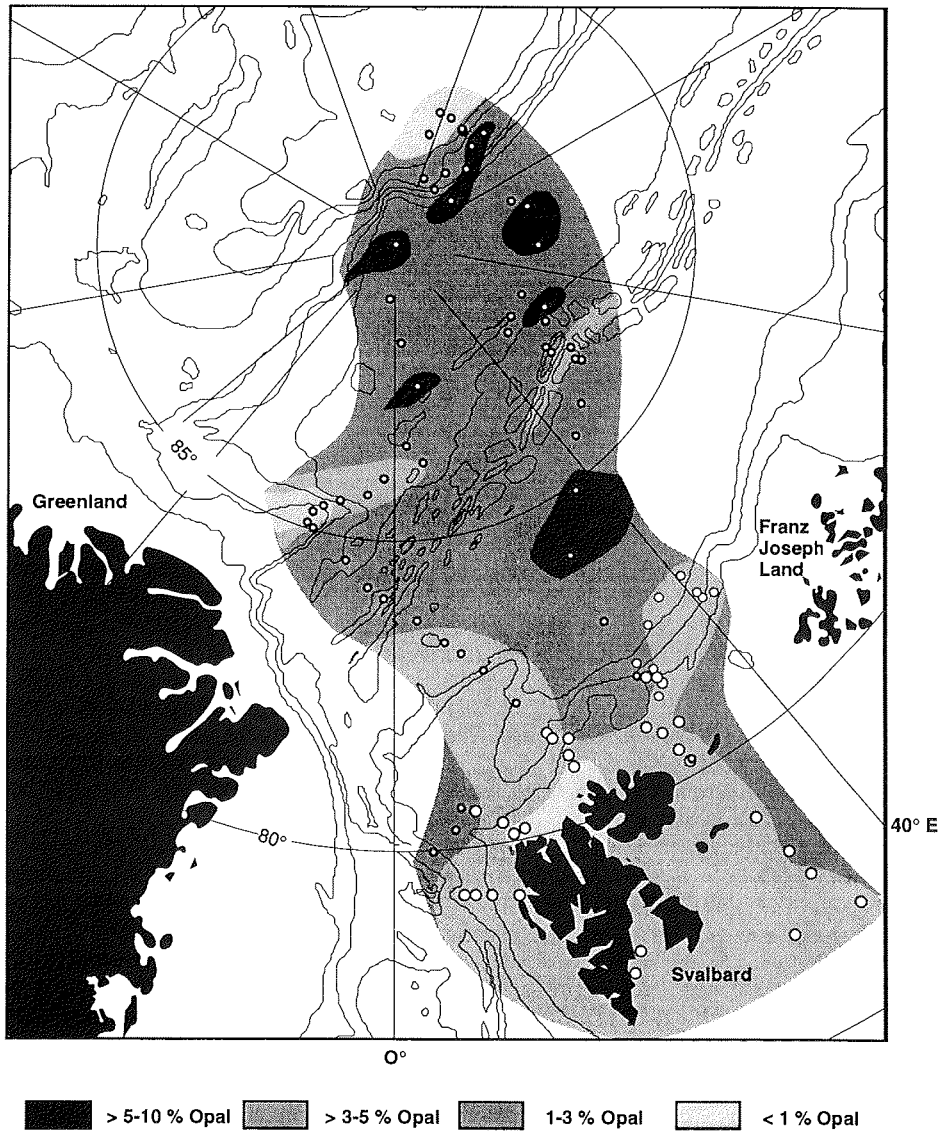

Fig. 4.: Opal in Central Arctic Ocean surface sediments. The distribution pattern of sedimentary opal appears to be strongly influenced by rates of sediment accumulation, preservation effects and reworking processes.

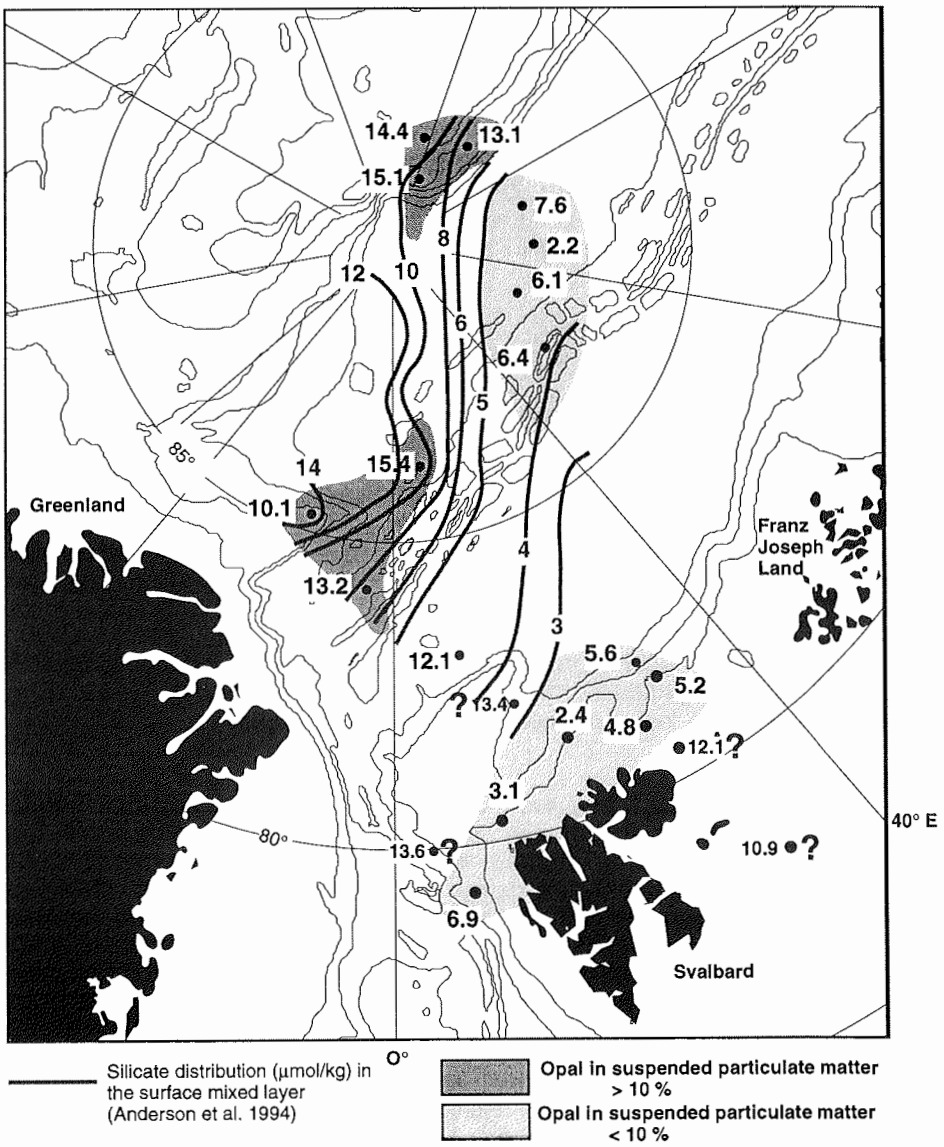

Fig. 5.:
Opal in suspended particulate matter sampled from 11 m below the ship by continuous pumping. Values generally increase from southeast to northwest, thereby showing covariance to concentrations of dissolved silica in the surface mixed layer (Anderson et al., 1994).

Kara Sea area
Figure 9 exhibits the opal distribution pattern in Kara Sea surface sediments. Maximum concentrations (> 5%) appear in the inner bights of the Ob and Yenisey rivers and in the Bay of Kara. Though the sample density in the southwestern Kara Sea is low, it is obvious that the opal concentrations generally decrease with increasing distance from the coast. Within the central St. Anna Trough, opal concentrations are high (3-5%) decreasing on the adjacent slopes.

Barium analyses were only performed on a few samples gained during the RV "Mendeleev" '93 cruise to the southwestern Kara Sea. Barium concentrations range from ca. 310 ppm to 470 ppm. Aluminium concentrations are highest in coastal areas (ca. 70 - 78%). Minimum values occur in central parts of the southwestern Kara Sea (ca. 63-67%). When applying a detrital Ba/Al ratio of 0.0065, no Ba_{bio} is present.

Discussion

Due to the permanent ice-coverage, the modern Arctic Ocean is a low-productive environment, which leads in combination with the well-oxygenated deep-water to a low flux and preservation of marine organic matter in the surface sediments (Stein et al., 1994). Subba Rao and Platt (1984) published primary production rates of 0.004 - 4.9 gC/m2/d for the marginal areas of the Arctic Ocean with maximum values on the shelves, and in bights and fjords. Exceptional high rates occur at ice edges and open waters (e.g. polynyas) (Smith et al., 1985, 1987; Hirche et al., 1991). Regional differences in the distribution patterns of various productivity proxies, thus, should appear. Accordingly, temporal changes within these parameters will supposedly allow to reconstruct the variability of processes driving surface water productivity, e.g. the Arctic pack ice, solar insolation and nutrient supply.

Laptev Sea
An enhanced surface water productivity, which is due to a strong nutrient supply as is typical in front of river systems and in local upwelling areas, may significantly shape the depositional environment in respect to the conservation of productivity proxies (e.g. increased accumulation of organic carbon). The Lena is one of the largest river system dewatering into the Arctic Ocean. Annually, 520 km3 of fresh water (Aagaard and Carmack, 1989) deliver about 21 million tons of suspension load (Korotaev et al., 1994), which accumulates on the Laptev Sea shelf and the adjacant continental slope. Though this is low compared to the ca. 100 million tons/yr of the McKenzie in Alaska (Milliman and Meade, 1983), the estimated high sedimentations rates of about 40-50 cm/ka (Kassens, pers. com.; Nürnberg et al., 1995) are an important prerequisite for the accumulation and conservation of large amounts of (marine) organic matter (e.g. Stein, 1991).

The Lena river run-off is of considerable importance for the hydrochemical and depositional structure in the Laptev Sea. The large brackish surface plume extends up to 200 miles or more northward (Létolle et al., 1993). Approximately 84% of the total outflow is directed to the east and northeast. According to Pivovarov (in Kassens and Karpiy, 1994), the influence of freshwater supply to the Laptev Sea is reflected in the distribution pattern of

dissolved silica in the surface water layer (ca. 5-10 m water depth). Maximum concentrations of about 1400 µg/l were observed near the eastern side of the Lena river mouth during summer 1993, indicating a predominant outflow to the east (Fig. 7). Concentrations gradually decrease with increasing distance from the delta. The Lena river, thus, serves as the major source for dissolved silica in the Laptev Sea (Sidorov, 1993). The fact that i) diatoms represent more than 95% of the total biomass near the mouth of the Lena river (Sidorov, 1993) and ii) bottom waters are always enriched in dissolved silica (Létolle et al., 1993) most probably indicate that the surface depletion results from biological uptake. An enhanced biological activity in the surface layer, which is furthermore indicated by high chlorphyll-a concentrations in the north-eastern Laptev Sea (Knickmeier and von Juterzenka, 1996), is definitely reflected in the bottom sediments east of the Lena Delta with relatively high sedimentary opal concentrations of 3-6% (Fig. 7). The diminishing dissolved silica concentrations to the north and to the west result in correspondingly low opal concentrations in the bottom sediments.

A distinct opal maximum of about 3-5% is observed in the upper Laptev Sea continental slope sediments in 500-1000 m water depth (Stations PS24358, PS2459, PS2466). These sites are situated directly below the summer edge of the pack ice cover, which is relatively stable during summer over years as inferred from satellite imagery (H. Eicken, pers. com. 1995). Surface waters overlying these sites showed drastically enhanced chlorophyll A and phaeopigment concentrations during summer 1993. Nutrients (NO_3, PO_4), in contrast, were significantly depleted (Boetius et al., this vol.) indicating a plankton bloom at the ice edge. Due to the relatively stable position of the summer ice edge, repeated occurrences of plankton blooms are apparently providing enough biogenic silica to be preserved in the surface sediments (Stein and Nürnberg, 1995).

Biogenic barium as an alternative proxy for marine surface water productivity is also enhanced at sites near the ice edge. Here, the terrigenous influence is reduced as infered from the lowered aluminum concentrations, whereas elementary barium is significantly enhanced compared to the remaining Laptev Sea samples. Applying a detrital Ba/Al ratio of 0.0065 (Wedepohl, 1991) for the calculation of biogenic barium, concentrations increase to about 300 ppm, representing the highest Ba_{bio} occurrences in the area of investigation at all (Fig. 8). In this respect, the value of 0.0065 is regarded as convenient, since detrital Ba/Al-ratios derived for inner Laptev Sea surface sediments according to the Rutsch et al. (1994) method lead to a Ba/Al-ratio of 0.0052, whereas the average Ba/Al-mean is about 0.007. The covariance between opal and biogenic barium in addition to other biological parameters apparently reflects i) plankton blooms in the seafloor deposits by geochemical proxies and ii) the relatively permanent summer position of the ice edge. Mapping these parameters should subsequently allow to spatially and temporally reconstruct the changing ice edge position.

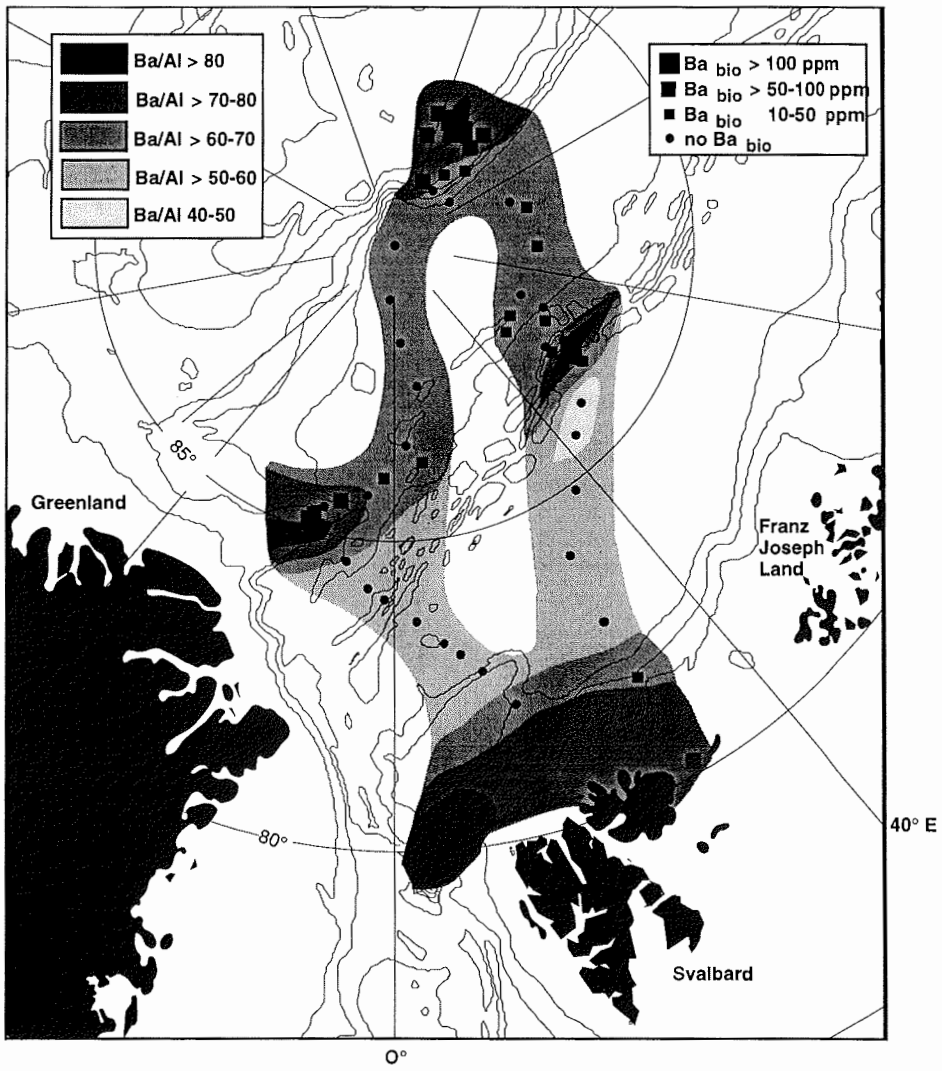

Fig. 6.: Distribution of Ba/Al ratios in central Arctic Ocean surface sediments. When applying a detrital Ba/Alaluminosilicate ratio of 0.0065 (Wedepohl, 1991), considerable occurrences of biogenic barium appear on Gakkel and Lomonosov ridges, Yermak and Morris Jesup plateaus, and in the Makarov Basin (large squares).

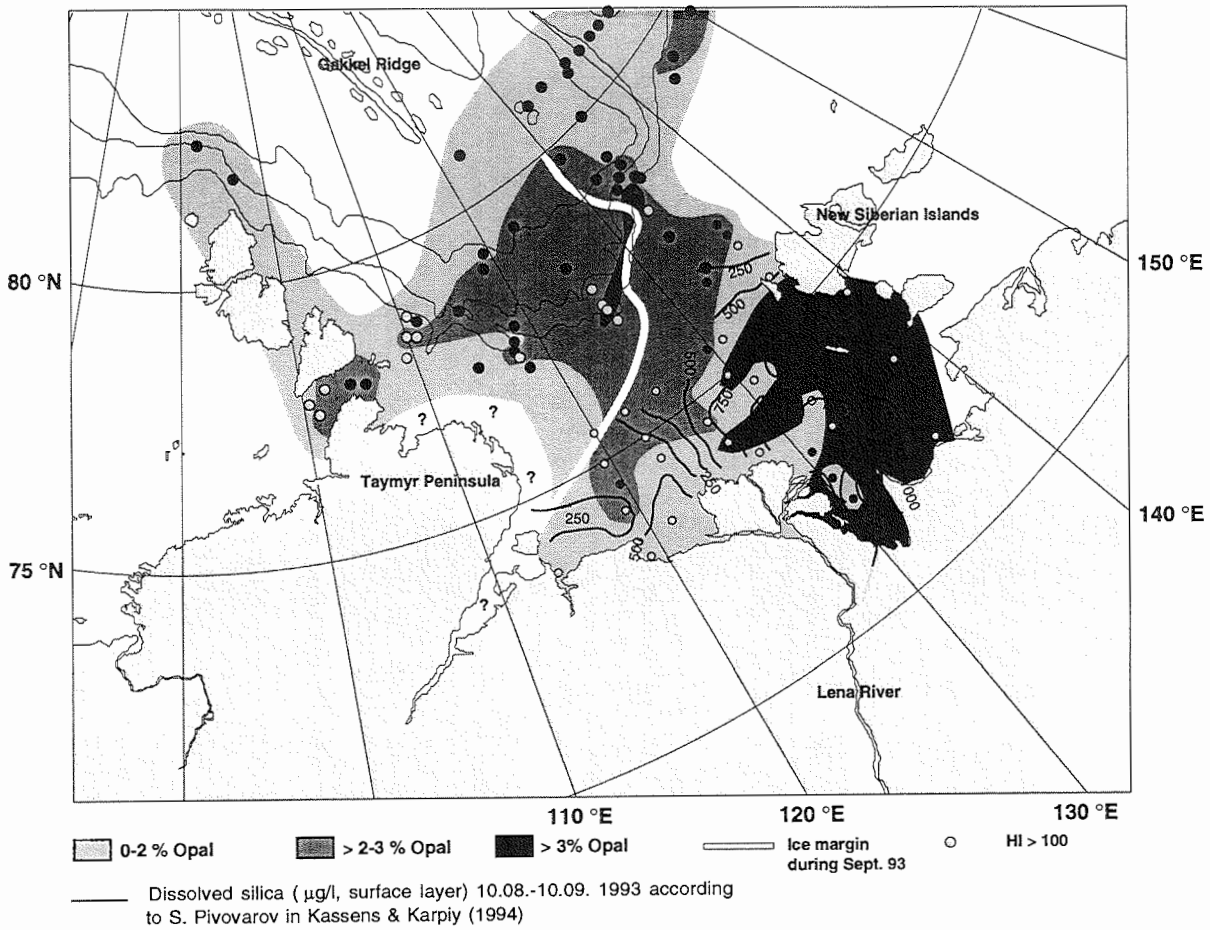

Fig. 7.: Biogenic silica in Laptev Sea surface sediments showing highest concentrations in the eastern Laptev Sea, which must be related to the outflow of Lena River water as deduced from the dissolved silica distribution (Pivovarov in Kassens and Karpiy,1994). Another opal maximum is visible near the ice edge (blue line indicates the ice margin during summer ´93, pers. com. H. Eicken, 1995). Here, both concentrations of plant pigments in the upper water column (Boetius et al., this vol.) and concentrations of biogenic barium (see Figure 8) are enhanced pointing to active plankton growth.

Kara Sea

As could be shown by Stein (this vol.), the inner Laptev and Kara seas are dominated by terrigenous organic material derived from the Siberian hinterland. For the Kara Sea, Franz Joseph Land and Novaya Zemlya are important source areas for the organic material deposited in the St. Anna Trough. Nevertheless, maximum opal concentrations in combination with high TOC values and C/N ratios of about 6 in the center St. Anna Trough (Stein, this vol.) point to an enhanced surface water productivity, which is presumably linked to the outflow of nutrient-rich Yenisey and Ob-river water through the St. Anna Trough.

Central Arctic Ocean

In central parts of the Arctic Ocean, biomass is extremely low (Kröncke, 1994; Boetius et al., this vol.). Nevertheless, towards relatively shallow sites on the Barents Sea slope, and on Gakkel and Lomonosov ridges, numbers of suspension-feeding species (e.g. siliceous sponges) significantly increase (Kröncke, 1994; Fütterer, 1992). Wollenburg (1995) also observes high standing stocks of benthic foraminifers on Yermak and Morris Jesup plateaus, the northern Barents Sea continental slope, and Gakkel and Lomonosov ridges. Mumm (1991) describes enhanced average zooplankton abundances and biomass at the southern margin of the Nansen Basin (northern Barents Sea slope) being five times higher than in the central Arctic region north of 83 °N.

At Yermak Plateau, carbonate contents in addition to enhanced short-chained *n*-alkanes (C_{17} and C_{19}) indicating higher portions of marine organic matter (Schubert, 1995, Schubert and Stein, this vol.), as well as HI-maxima (Stein et al., 1994) witness to a raised primary production due to the intrusion of relatively warm North Atlantic water masses. These water masses, which can be traced far into the central Arctic Ocean, significantly drive the sea ice distribution around Svalbard, and consequently influence the light penetration into the uppermost water layer. Similarly, the intrusion of Pacific water masses via Bering Strait drives the distribution pattern of Pacific diatom assemblages in the Chukchi Sea, the East Siberian Sea, and in parts of the Laptev Sea shelves (Polyakova, 1994), indicating that the hydrographic regime to a large degree influences primary production in the Arctic Ocean. Primary production rates in the Bering Sea are considerably high, being comparable to coastal upwelling areas (ARCSS Workshop Steering Committee, 1990).

In spite of the perennial dense ice-coverage, Morris Jesup Rise is identified as an area of enhanced marine productivity by high standing stocks of benthic organisms, and elevated concentrations of short-chained *n*-alkanes. In addition, Anderson et al. (1994) describe high TOC-concentrations at Morris Jesup Rise within the upper 20-70 m of the water column, which are suspected to initiate plankton growth (Schubert, 1995; Schubert and Stein, this vol.). Enhanced amounts of short-chained *n*-alkanes also appear on the Arctic mid-ocean ridges (Lomonosov and Gakkel ridges) including some sites within the Makarov Basin adjacant to the Lomonosov Ridge slope (Schubert, 1995). Apparently, even in the sea-ice covered central parts of the Arctic Ocean, significant spatial differences in primary productivity occur.

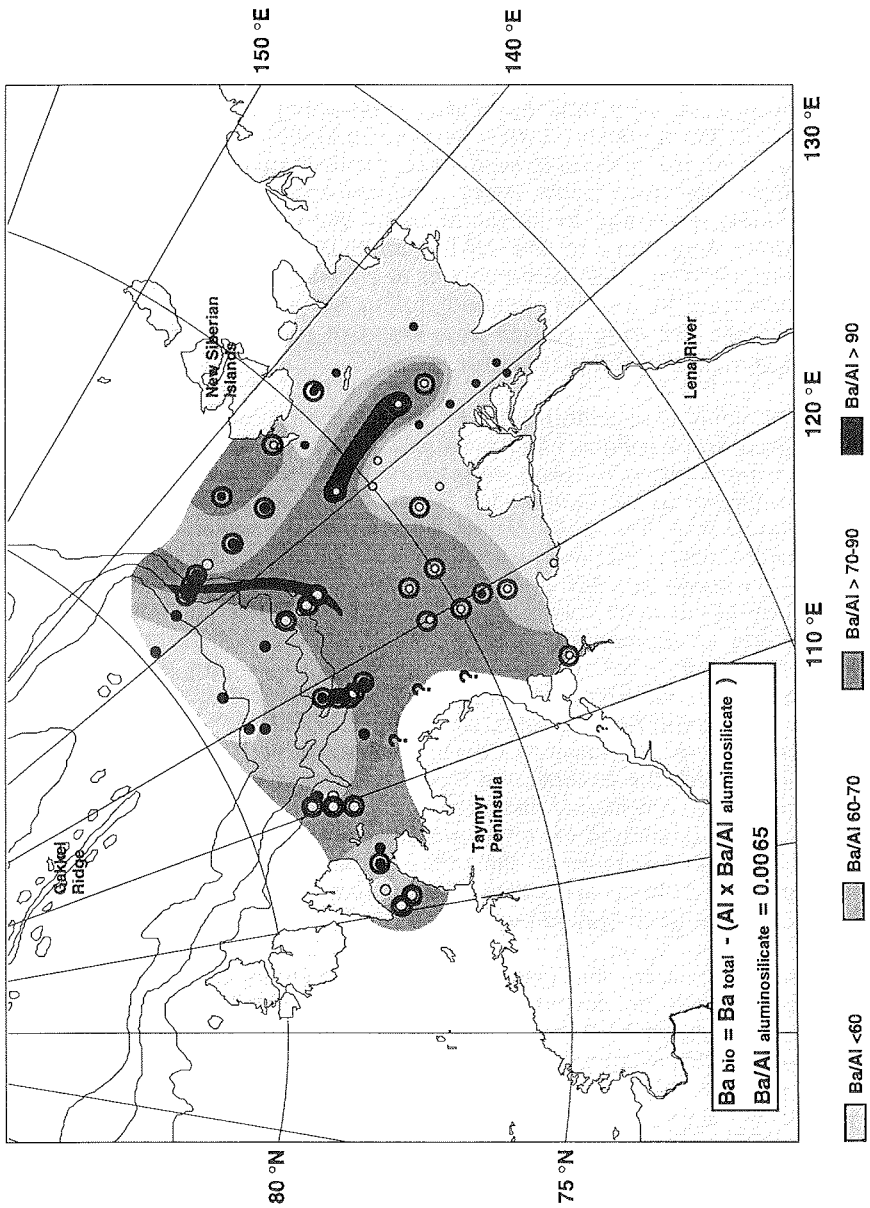

Fig. 8.: Distribution of Ba/Al ratios in Laptev Sea surface sediments. Biogenic barium is calculated according to Dymond et al. (1992) using a detrital Ba/Al ratio of 0.0065 (Wedepohl, 1991). On the shelf, maximum concentrations are related to the ice edge. Lower slope and coastal sediments are dominated by terrigeneous barium. Sites of biogenic barium occurrences (large circles) generally covary with the presence of marine organic matter (HI > 100, white dots; cf., Stein, this vol.).

The above mentioned pattern of marine production requires specific environmental prerequisites. In general, primary productivity in the Arctic Ocean is driven by light (Subba Roa and Platt, 1984; Andersen, 1989), which is strictly related to i) the uppermost water column, ii) sea-ice coverage and iii) snow conditions on the floes. Nutrients are not considered to be limiting factors, since concentrations are generally high in Arctic surface waters (Herman, 1983; Andersen, 1989; Anderson et al., 1994; Heimdahl, 1989) provided by Atlantic and Pacific water masses, Arctic river runoff and sea-ice meltwater (Anderson et al., 1994). Ice coverage is consequently of considerable importance. Wind and tide induced shearing of Beaufort Gyre and Transpolar Drift ice masses (Gordienko and Laktionov, 1969), and the establishment of a sharp oceanographic front separating Eurasian Basin water masses from Canadian Basin water masses (Anderson et al., 1994; Rudels et al., 1994) may lead to temporal open ocean conditions above Lomonosov Ridge. According to the NASA satellite passive microwave observations from 1978 to 1987 (Gloersen et al., 1992), ice density above Lomonosov Ridge may in fact be reduced during summer to about 60%. During summer 1991, for example, ice-free areas of up to 100 km^2 were observed above Lomonosov Ridge (Fütterer, 1992).

Initially, the Ba/Al distribution pattern (Fig. 6) reflects the pattern of enhanced productivity as seen from various other productivity proxies. Enhanced Ba/Al ratios appear on the Arctic mid-ocean ridges including some sites within the Makarov Basin adjacant to the Lomonosov Ridge slope, on Yermak Plateau, and on Morris Jesup Rise. The Ba/Al distribution pattern is inevitably reflected in the Ba_{bio} concentrations (applying a Ba/Alumosilicate ratio of 0.0065), the maxima of which increase to > 100 ppm on the mid-ocen ridges and plateaus, but never reach up to the shelf values of about 300 ppm. When regarding the spatial distributions of elementary barium and aluminum, in particular, it becomes apparent that i) except for Yermak Plateau showing enhanced barium concentrations, total barium does not vary significantly over the entire Eurasian part of the central Arctic Ocean, and ii) at sites with high Ba/Al ratios, aluminum concentrations are lowered due to an apparently reduced flux of terrigenous material. With the exception of Yermak Plateau, spatial differences in the Ba/Al-ratios, thus, are mainly driven by the aluminum flux. The process of barite formation as described for other areas of the world ocean (Bishop, 1988) should of course be active in the entire Arctic Ocean as well. Both, dissolved barium and diatoms are sufficiently present in the surface waters, but the detrital contribution of barium by far exceeds the biotic component.

For Yermak Plateau, instead, the formation of Ba_{bio} in significant amounts is definitely probable. Here, the lowered aluminum values in combination with the significantly enhanced barium concentrations cause high Ba/Al-ratios. Applying an average Ba/Alumosilicate ratio of 0.0065, Ba_{bio} increases to > 100 ppm, and corresponds to high HI-indices, high concentrations of short-chained *n*-alkanes, high standing stocks of benthic foraminifers, and high carbonate and TOC contents. Unpublished downcore records from Yermak Plateau (PS2200) exhibiting a close correspondance between Ba_{bio} and HI-indices further support the finding that barite formation occurres and apparently reflects the temporally changing intrusion of North Atlantic water masses into the Arctic Ocean.

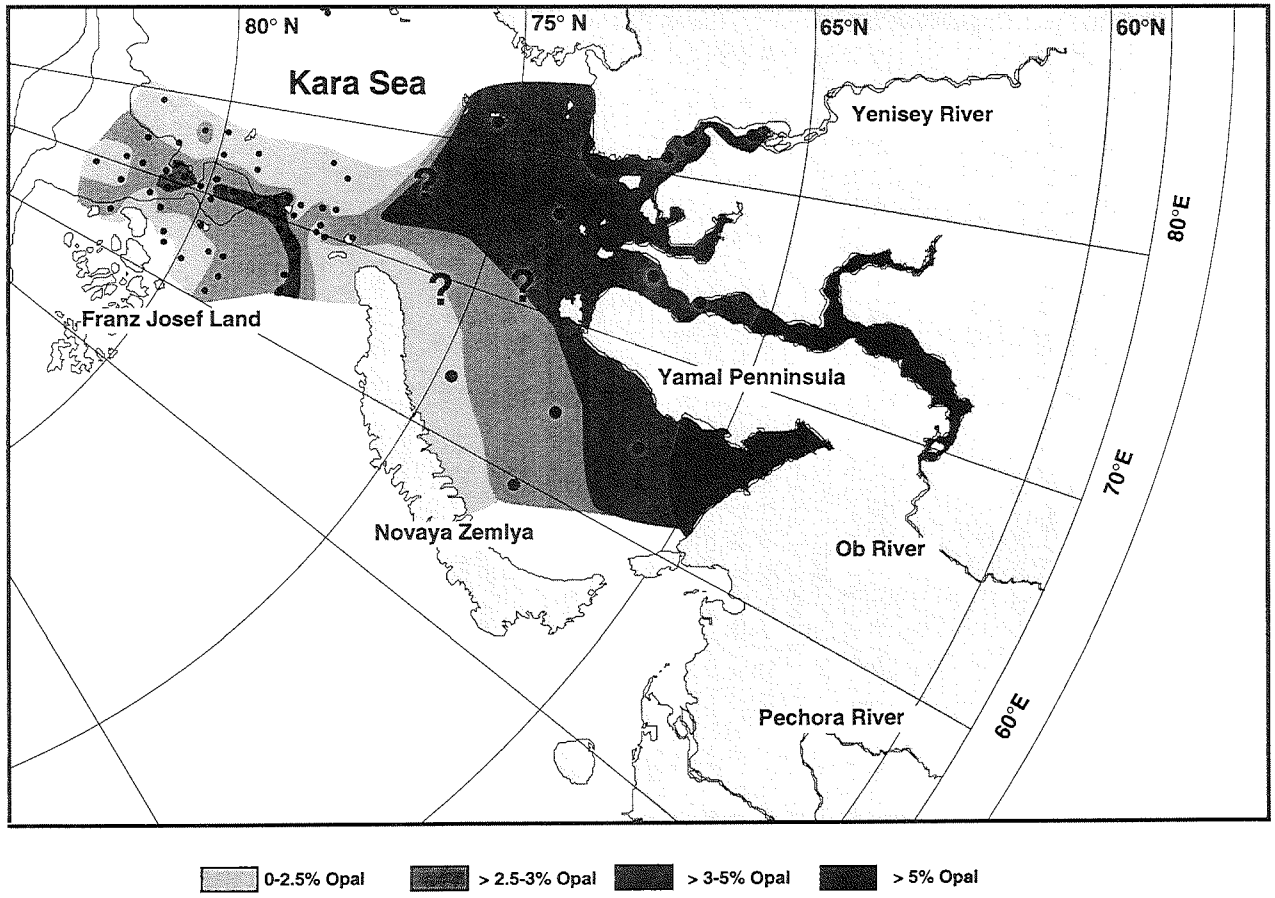

Fig. 9.: Biogenic silica in Kara Sea surface sediments showing highest concentrations i) in coastal areas diminishing with increasing distance from the mainland, and ii) in the center St. Anna Trough.

The opal signal unfortunately does not reflect the conditions described above as it is most likely perturbed by the patchy occurrence of benthic siliceous sponges as well as dissolution and preservation effects. The entire central Arctic commonly has opal concentrations between 3% and 5%. Maximum opal concentrations (- 10%) at a few sites within the deep-sea basins and on the slopes of mid-ocean ridges and plateaus are presumably due to i) the good preservation in high accumulation areas and / or ii) reworking processes. Instead, Morris Jesup Rise, Yermak Plateau, the Barents Sea shelf and the Makarov Basin are extremely low in opal, which points to non-preservation due to low accumulation, winnowing and / or erosion at least for Morris Jesup Rise (Stein et al., 1994). At Yermak Plateau, the low opal concentrations mismatch i) the enhanced levels of other productivity proxies and ii) the relatively high sedimentation rates of about 1.9 cm/kyr (Stein et al., 1994), which should favor opal preservation.

Conclusions

Opal and barium analyses were performed on core-top sediments from Arctic shelf areas and from the central Arctic Ocean deep-sea, mid-ocean ridge and plateau areas. Opal analyses were additionally caaried out on suspended particulate matter from the central Arctic Ocean. Opal concentrations were quantified by a leaching method according to DeMaster (1981) and Müller and Schneider (1993). Barium and aluminum were identified by X-ray fluorescence. The biogenic portion of the bulk barium, which is considered to reflect plankton productivity was calculated according to Boström et al. (1973) applying a detrital Ba/Al ratio of 0.0065.

On the Laptev Sea shelf, a general correspondance between opal in core-top sediments and dissolved silica in the surface layer exists. The eastern inner Laptev Sea characterized by the main Lena outflow, exhibits maximum opal concentrations of about 3% to 6% in accordance with maximum concentrations of dissolved silica. Apparently, accumulation of opal within the Kara Sea is also dependant on fluvial nutrient supply from the Ob and Yenisey rivers. Even in the central Arctic Ocean, opal from suspended particulate matter sampled from the surface layer corresponds to the distribution pattern of dissolved silica. Within the deep central Arctic surface sediments, in contrast, opal preservation is not only influenced by surface water characteristics, but also by accumulation rates, dissolution effects and reworking processes.

In the central Arctic Ocean, the distribution of Ba/Al-ratios compares to various biological and anorganic-geochemical proxies for marine productivity. However, the spatial distributions of elemental barium and aluminum, in particular, suggest that the differences in Ba/Al-ratios and thus, in Ba_{bio}, are intimately related to the differential influx of terrigenous matter. Ba_{bio} formation for sure takes place even in central regions of the Arctic Ocean, however, is effectively diluted by the excessive contribution of detrital barium. At Yermak Plateau lying under the influence of intruding North Atlantic water masses, in contrast, marine productivity is most likely sufficient enough to produce a clear Ba_{bio} signal. The applicability of barium in the central Arctic Ocean is thus extremely restricted.

Acknowledgments

I wish to express my appreciation to the chief scientists and crews of RV "Polarstern", RV "Ivan Kireyev", RV "Mendeleev" and RV "Logachev". Thanks are also due to C.C. Nürnberg and D. Rickert for running some barium and opal analyses. I gratefully acknowledge C. Joiris, who provided the suspended particulate matter samples. S. Pivovarov, Ye. Polyakova, R. Stein, C. Schubert, and Chr. Vogt are kindly thanked for discussion and improving the manuscript. The financial aid of the Ministry for Education, Science, Research, and Technology (BMBF) is gratefully acknowledged. Critical reviews of the manuscript by J. Thiede, Chr. Strobl, and H. Cremer are appreciated.

References

Aagaard, K. and Carmack, E.C. (1989): The role of sea ice and other fresh water in the Arctic circulation. - J. Geophys. Res., 94 (C10): 14485-14498.

Anderson, L.G., Björk, G., Holby, O., Jones, E.P., Kattner, G., Koltermann, K.P., Liljeblad, B., Lindegren, R., Rudels, B., and Swift, J. (1994): Water masses and circulation in the Eurasian Basin: Results from the Oden 91 North Pole Expedition. - J. Geophys. Res., 99 (C2): 3273-3283.

Andersen, O.G.N. (1989): Primary production, chlorophyll, light, and nutrients beneath the Arctic sea ice. In Y. Herman (ed.), The Arctic Seas, New York (Van Nostrand Reinhold): 147-193.

ARCSS Workshop Steering Committee (1990): Arctic Sytem Science: Ocean-Atmosphere-Ice Interactions. Lake Arrowhead Workshop Report, JOI Inc., Washington DC, 132 pp.

Bishop, J.K.B. (1988): The barite-opal-organic carbon association in oceanic particulate matter. - Nature, 332 (24): 341-343.

Boström, K., Joensuu, O., Moore, C., Boström, B., Dalziel, M., and Horowitz, A. (1973): Geochemistry of barium in pelagic sediments. Lithos, 6: 159-174.

Dehairs, F., Chesselet, R., and Jedwab, J. (1980): Discrete suspended particles of barite and the barium cycle in the open ocean. - Earth Planet. Sci. Lett., 49: 528-550.

DeMaster, D.J. (1981): The supply and accumulation of silica in the marine environment. - Geochim. Cosmochim. Acta, 45: 1715-1732.

Dymond, J., Suess, E., and Lyle, M. (1992): Barium in deep sea sediment: A geochemical indicator of paleoproductivity. - Paleoceanogr., 7 (2): 163-181.

Falkner, K.K., Klinkhammer, G.P., Bowers, T.S., Todd, J.F., Lewis, B.L., Landing, W.M., and Edmond, J.M. (1993): The behavior of barium in anoxic marine waters. - Geochim. Cosmochim. Acta, 57, 537-554.

Fütterer, D.K. (ed.) 1992: The Expedition ARCTIC'91 Leg ARK VII/3 of RV "Polarstern" in 1991. Rep. Polar Res., 107/92, 267 pp.

Fütterer, D.K. (ed.) 1994: The Expedition ARCTIC'93 Leg ARK IX/4 of RV "Polarstern" in 1993. Rep. Polar Res., 149/94, 244 pp.

Gingele, F. and Dahmke, A. (1994): Discrete barite particles and barium as tracers of paleoproductivity in South Atlantic sediments. - Paleoceanogr., 9 (1): 151-168.

Gloersen, P., Campbell, W.J., Cavalieri, D.J., Comiso, J.C., Parkinson, C.L., and Zwally, H.J. (1992): Arctic and Antarctic sea ice, 1978-1987: Satellite

passive-microwave observations and analysis. - Washington D.C.: 290 pp.
Gordienko, P.A. and Laktionov, A.F. (1969): Circulation and physics of the Arctic Basin Waters. Ann. International Geophys. Year, 46. New York (Oceanogr. Pergamon): 94-112.
Grobe, H. and Mackensen, A. (1992): Late Quaternary climatic cycles as recorded in sediments from the Antarctic continental margin. In: Kennett, J., und Warnke, D. (Eds.), Neogene Antarctic Glacial Evolution, AGU Ant. Res. Ser., 56: 349-376.
Heimdahl, B.R. (1989): Phytoplankton and nutrients in the waters north-west of Spitzbergen in the autumn of 1979. - J. Plankton Res., 5: 901-918.
Herman, A.W. (1983): Vertical distribution patterns of copenpods, chlorophyll, and production in northeastern Baffin Bay. - Limnol. Oceanogr., 28: 708-719.
Hirche, H.-J., Baumann, M.E.M., Kattner, G., and Gradinger, R. (1991): Plankton distribution and the impact of copepod grazing on primary production in Fram Strait, Greenland Sea. - J. Marine Systems, 2: 477-494.
Kassens, H. and Karpiy, V.Y. (1994): Russian-German Cooperation: The Transdrift I Expedition to the Laptev Sea. Rep. Polar Res., 151/94: 168 pp.
Knickmeier, K. and von Juterzenka, K. (1996): Saisonale Entwicklung der Phytoplankton-Verteilung im Laptevmeer. Terra Nostra, 3/96: p. 32 (Abstract).
Korotaev, V.N., Zaitsev, A.A., Alabyan, A.M., Chalov, R.S., and Sidorchuk, A.Yu. (1994): Hydrological, fluvial and geomorphological investigations in basins of rivers draining into the Laptev Sea. 2nd Workshop on the Russian-German Cooperation "Laptev Sea System", Program and Abstracts, St. Petersburg, Russia, November 21-24, 1994.
Kröncke, I. (1994): Macrobenthos composition, abundances and biomass in the Arctic Ocean along a transect between Svalbard and the Makarov Basin. - Polar Biol., 14: 519-529.
Ku, T.L. and Broecker, W.S. (1965): Rates of sedimentation in the Arctic Ocean. - In M. Sears (ed.), Progress in Oceanography, 4: 95-105.
Lea, D, and Boyle, E.A. (1989): Barium of benthic foraminifera controlled by bottom water composition. - Nature, 338: 751 - 753.
Létolle, R., Martin, J.M., Thomas, A.J., Gordeev, V.V., Gusarova, S., and Sidorov, I.S. (1993): 18O abundance and dissolved silica in the Lena delta and Laptev Sea (Russia). Mar. Chem., 43: 47-64.
Lisitzin, A.P. (1967): Basic relationships in distribution of modern siliceous sediments and their connection with climatic zonation. - Int. Geol. Rev., 9: 631-652.
Lisitzin, A.P. (1985): The silica cycle during the last Ice Age. - Paleogeogr. Paleoclimat. Paleoecol., 50: 241-270.
Lloyd, J., Kroon, D., and Boulton, G. (1992): Paleoceanography of the Spitsbergen margin und deglaciation history of its ice cap. - 4. Int. Conf. Paleoceanography ICP-IV Abstract Volume.
Martin, J.H. and Knauer, G.A. (1973): The elemental composition of plankton. - Geochim. Cosmochim. Acta 37: 1639-1653.
Milliman, J.D. and Meade, R.H. (1983): World-wide delivery of river sediment to the oceans. - J. Geol., 91: 1-21.

Mortlock, M.A. and Froelich, P.N. (1989): A simple method for the rapid determination of biogenic silica in pelagic marine sediments. Deep-Sea Res., 36:1415-1426.

Mortlock, R.A., Charles, C.D., Froelich, P.N., Zibello, M.A., Saltzmann, J., Hays, J.D., and Burckle, L.H. (1991): Evidence for lower productivity in the Antarctic Ocean during the last glaciation. - Nature, 351: 220-223.

Müller, P.J. and Schneider, R. (1993): An automated leaching method for the determination of opal in sediments and particulate matter. Deep-Sea Res. I, 40/3: 425-444.

Mumm, N. (1991): Zur sommerlichen Verteilung des Mesozooplanktons im Nansen Becken, Nordpolarmeer. - Rep. Polar Res., 92.

Nürnberg, C.C. (1995): Bariumfluß und Sedimentation im südlichen Südatlantik - Hinweise auf Produktivitätsänderungen im Quartär. GEOMAR Rep., 38: 105 p., Kiel.

Nürnberg, C.C., Bohrmann, G., Frank, M., and Schlüter, M. (submitted): New productivity estimates based on barium flux in the Atlantic sector of the southern Ocean - Results from 190,000 year records. - Paleoceanogr.

Nürnberg, D., Fütterer, D.K., Niessen, F., Nörgaard-Petersen, N., Schubert, C.J., Spielhagen, R.F., and Wahsner, M. (1995): The depositional environment of the Laptev Sea continental slope - First results from the RV "Polarstern" ARK IX-4 cruise. - Polar Res., 14(1): 43-53.

Polyakova, Ye. I. (1994): The major features of diatom thanatocenoses formation in the bottom sediments of the Eurasian Arctic seas. - Oceanology 34/1, 444-453 (in Russian).

Riley, J.P. and Roth, I. (1971): The distribution of trace elements in some species of phytoplankton grown in culture. - J. Mar. Biol. Assoc., 51: 63.

Rösler, H.J. and Lange, H. (1972): Geochical Tables. - Elsevier, New York: 486 pp.

Rudels, B, Jones, E.P., Anderson, L.G., and Kattner, G. (1994): On the intermediate depth waters of the Arctic Ocean. In O.M. Johannessen, R.D. Muench, and J.E. Overland (eds.), The Polar Oceans and their role in shaping the global environment. Geophysical Monograph 85, Washington D.C., 523 pp.

Rutsch, H.J., Mangini, A., Bonani, G., Dittrich-Hannen, B., Kubik, P.W., Suter, M., and Segl, M. (1995): 10Be and Ba concentrationsin W. African sediments trace productivity in the past. - Earth Planet. Sci. Lett., 133: 129-143.

Schubert, C.J. (1995): Organischer Kohlenstoff in spätquartären Sedimenten des Arktischen Ozeans: Terrigener Eintrag und marine Produktivität. Unpubl. Ph.D. Thesis, Univ. Bremen, 159 pp.

Shimmield, G., Derrick, S., Mackensen, A., Grobe, H., and Pudsey, C. (1994): The history of barium, biogenic silica and organic carbon accumulation in the Weddell Sea and Antarctic Ocean over the last 150,000 years. - In R. Zahn, T.F. Pedersen, M. Kaminski, and L. Labeyrie (eds.), Carbon cycling in the glacial ocean: Constraints on the ocean's role in global change, NATO ASI Series, I: Global Environmental Change, 17: 555-574.

Sidorov, I.S. (1993): Dissolved silica in the coastal waters of the Laptev Sea. In preparation.

Smith, S.L., Smith, W.O., Jr., Codispoti, L.A., and Wilson, D.L. (1985): Biological observations in the marginal ice zone of the East Greenland Sea. - J. Mar. Res., 43: 693-717.

Smith, W.O., Jr., Baumann, M.L., Wilson, D.L., and Aleisee, L. (1987): Phytoplankton biomass and productivity in the marginal ice zone of the Fram Strait during summer 1984. - J. Geophys. Res., 92: 6777-6786.

Stein, R. (1991): Accumulation of organic carbon in marine sediments. Lecture Notes in Earth Sciences, 34, Springer-Verlag Heidelberg, 217 pages.

Stein, R. and Stax, R. (1991): Late Quaternary organic carbon cycles und paleoenvironment in the northern Labrador Sea (ODP-Site 646). - Geo-Mar. Lett., 11: 90-95.

Stein, R., Grobe, H., and Wahsner, M. (1994): Organic carbon, carbonate, and clay mineral distribution in eastern central Arctic Ocean surface sediments. Mar. Geol., 119: 269-285.

Stein, R. and Nürnberg, D. (1995): Organic carbon and biogenic opal in surface sediments from the Laptev sea and the adjacent continental slope. In: H. Kassens, D. Piepenburg, J. Thiede, L. Timokhov, H.W. Hubberten, and S. Priamikov (eds.), Russian-German Cooperation: Laptev Sea System, Rep. Polar Res., 176: 387 pp.

Stroobants, N., Dehairs, F., Goeyens, L., Vanderheijden, N., and Van Grieken, R. (1991): Barite formation in the Southern Ocean water column. - Mar. Chem., 35: 411-421.

Subba Rao, D.V. and Platt, T. (1984): Primary Production of Arctic Waters. - Polar Biol. 3, 191-201.

Taylor, S.R. (1964): Abundance of chemical elements in the continental crust: A new table. - Geochim. Cosmochim. Acta, 28: 1273-1285.

Wedepohl, K.H. (1991): The composition of the upper earth`s crust in the natural cycles of selected metals. - Metals in natural raw materials. - In E. Merian (ed.), Metals and their compounds in the environment, VCH Verlagsgesellschaft mbh; Weinheim.

Wefer, G., Suess, E., Balzer, W., Liebezeit, G., Müller, P.J., Ungerer, C.A., and Zenk, W. (1982): Fluxes of biogenic components from sediment trap deployment in circumpolar waters of the Drake Passage. - Nature, 29 (5879): 145-147.

Wollenburg, J. (1995): Benthische Foraminiferenfaunen als Wassermassen-, Produktions- und Eisdriftanzeiger im Arktischen Ozean. Rep. Polar Res., 179.

LITHOLOGY AND GEOCHEMISTRY OF MODERN SEDIMENTS OF THE CHUKCHI SEA

Pavlidis, Yu.A.[1)], V.I. Ogorodnikov[2)], E.S. Shelekhova[1)], M. Wahsner[3)]

[1)]P.P. Shirshov Institute of Oceanology, Moscow, Russia
[2)]Kiev State University, Kiev, Ukraine
[3)]Alfred Wegener Institute, Bremerhaven, Germany

Abstract

In the present article lithology and geochemistry of modern Chukchi Sea sediments investigated by the P.P. Shirshov Institute of Oceanology and the Arctic and Antarctic Research Institute are considered. Schemes of bottom sediments distribution are compiled according to grain-size data, mineralogy composition, and geochemistry characteristics. It is obvious that sedimentary processes depend on the hydrological environment in the basin, in particular on the Pacific water inflow and sea-ice cover.

Introduction

The Chukchi Sea shelf occupies an area known as "Beringia". Special attention was paid to this region due to the episodic existence of "Beringian land bridge" from Asia to northwestern North America troughout the early and middle parts of the Quaternary (Hopkins, 1973). The processes of modern sedimentation were studied by Pavlidis (1982, 1992) and Logvinenko and Ogorodnikov (1980).

Under the "modern sediments" we understand the surface layer of the sediment column, influenced by hydrogenic processes and active bioturbation. Usually this layer has signs of oxidation reflected in the sediment colour. The thickness of surface layer sediments in the Chukchi Sea (except for its coastal zone) varies between 1 and 10 cm. The series of samples presented and discussed here were collected during different cruises organized by the P.P. Shirshov Institute of Oceanology (Moscow) in 1978 - 1981, and by the Arctic and Antarctic Research Institute (St. Petersburg) in 1967 - 1976 (Fig. 1).

Methods

Surface sediments (0 - 10 cm) were sampled by gravity corers and grab-sampler "Ocean-50". To analyse the composition of the sediments a diverse set of methods was applied. 350 grain-size analyses were carried out by means of the method adopted by Petelin (1967). Terrigenous components of 200 samples were studied in the fraction 0.1 - 0.05 mm. The coarser fraction was divided into heavy and light minerals by bromoform with a specific density of 2.9 g/cm^3. Clay minerals were determined in the < 0.001 mm fraction (12 samples) and in the < 0.002 mm fraction (7 samples) at the Alfred Wegener Institute for Polar and Marine Research (Germany).

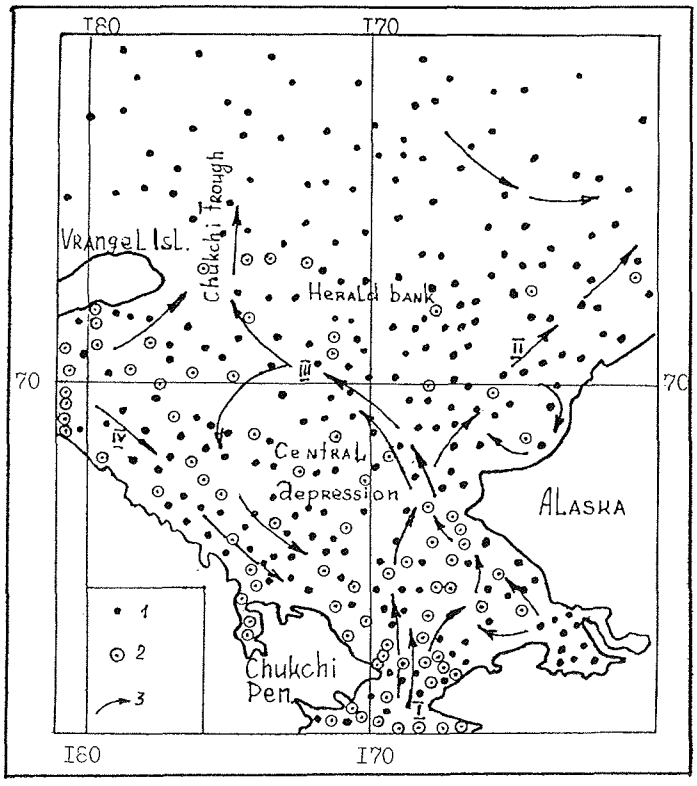

Fig.1.: Circulation pattern and sampling locations in the Chukchi Sea (Coachman et al., 1975). Stations: 1 - stations of Arctic and Antarctic Research Institute (St. Petersburg, Russia); 2 - stations of P.P Shirshov Institute of Oceanology (Moscow, Russia); 3 - currents: Pacific waters (I), Alaskian Branch (II), Herald Branch (III), East Siberian Sea waters (IV)

Results and discussion

The Chukchi Sea is a flat plain with average gradients between 0.002 - 0.0003 mm. Depths vary from 20 m to 58 m (Pavlidis, 1982). The central Chukchi Depression, the Chukchi Trough, and the Herald Bank are the main features of this region (Fig. 1).

The two main surface current systems in the Chukchi Sea (Fig. 1) are the inflow of relatively warm saline Pacific waters through the Bering Strait (nearly 150 cm/s) and the inflow of cold polar waters from the East Siberian Sea (nearly 30 cm/s) (Coachman et al., 1975). Pacific waters can be divided into two branches, one of which turns to the north-east along Alaska toward the Herald Bank. The system of prevailing surface currents forms a cyclonic gyre

in the centre of the sea relating the to the central Chukchi Depression. Pacific waters transport between 110 mill. and 154 mill. tons per year of terrigenous and biogenic suspension through the Bering Strait. In contrast, the contribution of the river-transported material is relatively low. The annual sedimentary flux into the Chukchi Sea is as follows (Pavlidis, 1982):

- Transport of terrigenous components through the Bering Strait: 50 mill. tons per year;
- Transport of biogenic material (diatom phytoplankton) through the Bering Strait: 60 mill. tons per year. However, only 10 % of this amount is accumulated as biogenic opal at the sea floor.
- Contribution of coastal abrasion: 4.5 mill. tons per year;
- River suspension: 3.5 mill. tons per year.

Lithology and mineralogy

The distribution of grain-size types of sediments is mainly influenced by bottom topography and the prevailing currents (Fig. 2).

The pelite and aleuritic-pelite muds predominate. Fine-grained sedimentation occupies the central Chukchi Depression, an area of about 150.000 km^2 (Pavlidis, 1982). The common feature of these pelite muds is the high degree of dispersion. The fraction < 0.001 mm reaches about 50 % of the pelite one (< 0.001 mm), but together they comprise 98 % of the total sediment. The deposition of these very fine muds in the central Chukchi Depression is related to the core of the cyclonic gyre.

The highest content of the heavy-mineral subfraction (2.5 - 3.4 %) is found within coastal areas, in the zone of active hydrodynamics. Seaward values are lower, and to the north of the sea they decrease down to 0.3 - 0.5 %. High contents also exist on top of the banks (2.7 - 2.9 %) decreasing to 0.7 - 1.0 % toward the base of the banks.

The main heavy minerals are epidote, clynopyroxene, hornblende, magnetite, and ilmenite. Maximum concentrations of clinopyroxene (18.9 - 24.7 %) are associated with the tuffs of Alaska. Hornblende is abundant (13.7 - 20.8 %) in the bottom sediments due to the wide distribution in rocks from nearby sources. Black ores are concentrated in the nearest coastal areas (23.7 - 25.7 %). The mineral composition of the modern sediments in the Chukchi Sea characterizes this region as a hornblende-epidot-clinopyroxene province.

Quartz (22.4 - 48.5 %) and feldspars (16.9 - 42.0 %) dominate in the light sub-fraction.

The following composition (range and average) of clay minerals was determined in the fractions < 0.001 mm and < 0.002 mm: illite (45 - 69 %; 58 %), chlorite (16 - 39 %; 22 %), smectite (0 - 20 %; 10 %), kaolimite (0 - 13 %; 8 %).

The results reflect that the clay composition of the surface sediments occur within the peripherical north-western part of the Chukchi Sea. According to Naidu et al. (1982), the smectite content increases to 20 - 30 % in the centre of the sea, but illite decreases to 38 - 48 %. Smectite enrichment is related to the halistatic circulation in this area and closely correlated with the distribution pattern of the clayey muds in the central Chukchi Depression.

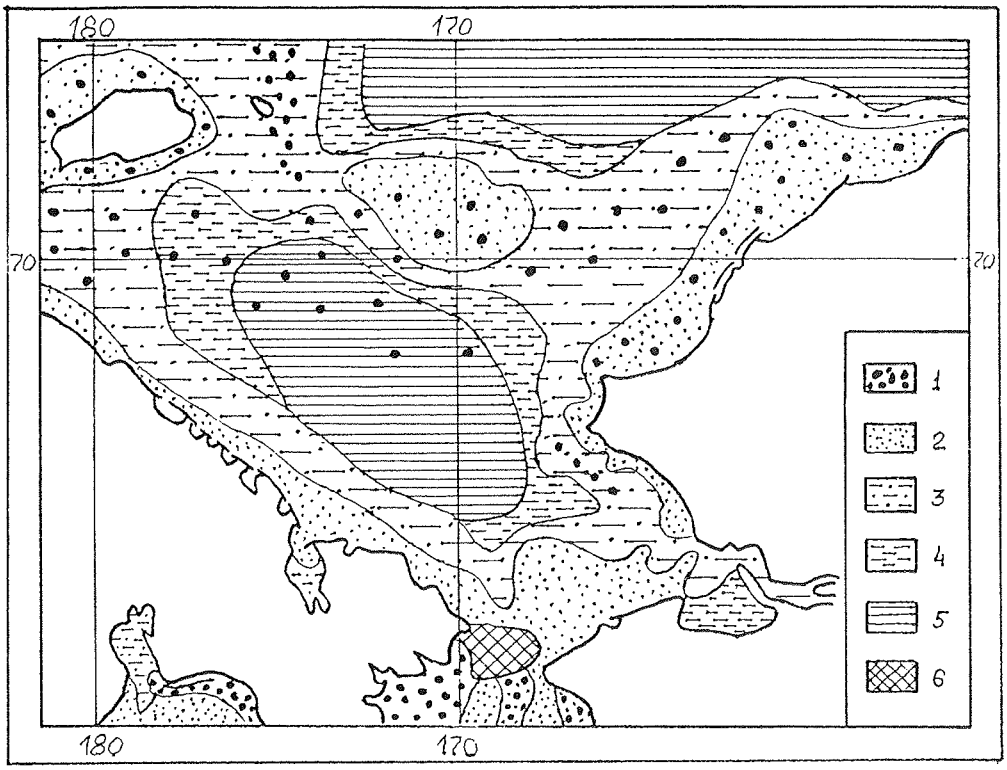

Fig.2.: Grain-size composition of modern sediments. 1) gravel pebbles; 2) sand; 3) sandy aleurite; 4) aleuritic mud; 5) mud; 6) bedrocks.

Geochemistry

$CaCO_3$

In modern Chukchi Sea sediments $CaCO_3$ is usually low (1 - 2 % and less). A slight enrichment (> 2 %) is related to the Pacific warm waters (Fig. 3). Bulk carbonate is represented by mollusk shell debris with dissolution features and by foraminifers.

Biogenic silica

One of the main components in bottom sediments of the Chukchi Sea is biogenic silica (Fig. 3). It is mainly produced by diatoms and is deposited as diatom frustules. Silica accumulation is much higher in the Chukchi Sea than in other Arctic seas. The water exchange between the Pacific Ocean and the Chukchi Sea is the principal source of dissolved silica. The highest contents of $SiO_{2biog.}$ are found in the central Chukchi Depression and in the Chukchi

Trough (3 - 10 % and > 10 %, respectively) (Fig. 3). These areas are situated underneath the Herald Branch of Pacific waters. The sediments in the north of the sea are characterized by lower contents of SiO_{2biog} (1 - 3 %) due to the sea-ice cover.

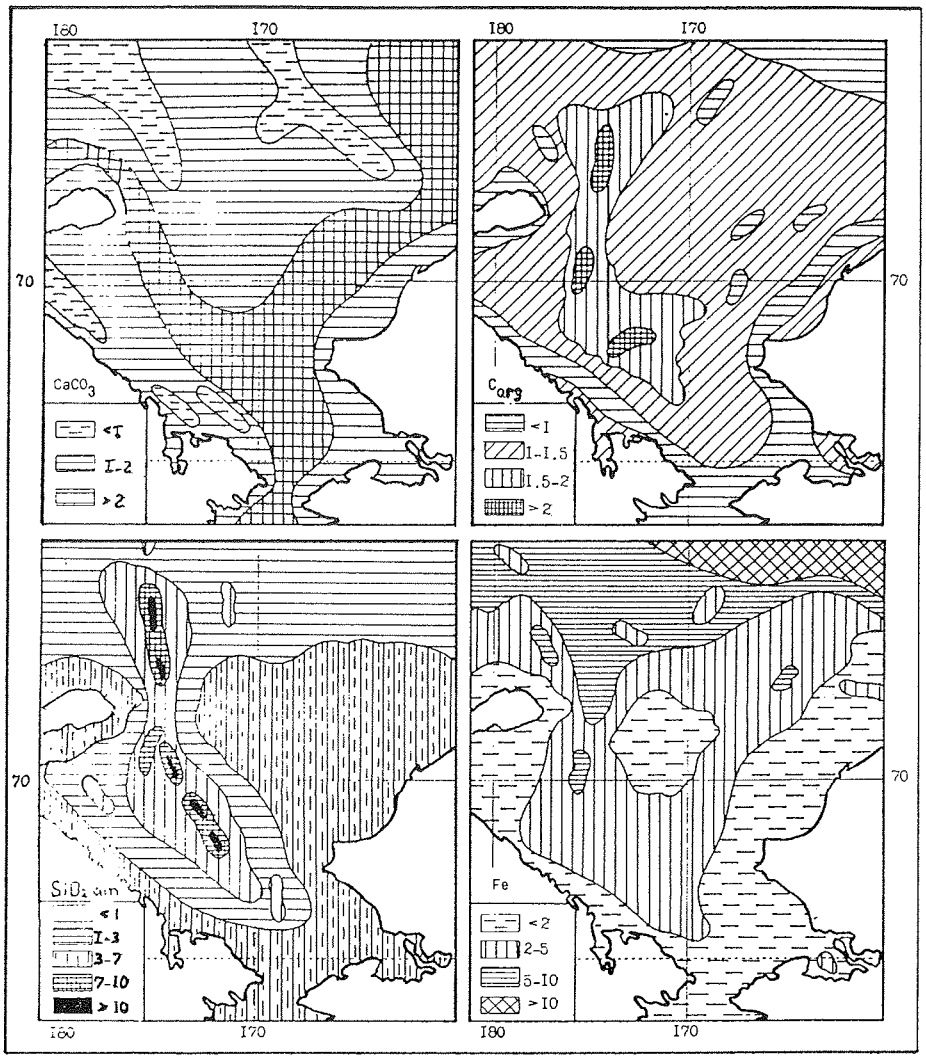

Fig. 3.: Distribution of some chemical components in surface sediments.

Organic carbon (C_{org})

The productivity of plankton and the influx of C_{org} as dissolved humus compounds and plant detritus are the main sources of C_{org} in bottom sediments. The major part of C_{org} is transported by Pacific waters, however, relatively high amounts are also concentrated in mouth areas of the largest rivers (Fig. 3). The highest C_{org} contents (1.5 - 2 % and more) occur in muds of

the central Chukchi Depression. The lowest ones (< 1 %) are found among sandy sediments. Zones of high C_{org} content are closely associated with high SiO_{2biog} accumulation in the basin. The C_{org}/SiO_{2biog} is relatively constant and may vary from 0.1 to 0.4 (in average 0.2).

Iron (Fe)
The Fe distribution pattern in bottom sediments is controlled by the grain-size and the relief. The highest content of Fe (> 10 %) is found in pelite muds (Fig. 3). Significant portions of Fe are accumulated in the central part of the sea, where the Pacific waters are divided into branches. In this halystatic zone, the fine-grained particles accumulate because the current velocity decreases.

In the central part of the shelf, the distribution pattern of Fe is positively correlated to that of SiO_{2biog} and C_{org}. Some amounts of Fe are assimilated by diatom plankton and deposited after its death (Rusanov and Ogorodnikov, 1979). However, the maximum Fe content occurs in outer shelf parts and along the continental slope, where C_{org} and SiO_{2biog} contents are low. Here the relatively warm Chukchi waters meet with polar Arctic ones, saturated by oxygen. This causes the rapid oxidation of Fe compounds and its transition into hydroxides.

Conclusions

The modern sedimentation in the Chukchi Sea is mainly influenced by the inflow of warm Pacific waters transporting the dominant part of terrigenous and biogenic suspension.

The relief and the hydrology of this basin influence the grain-size distribution. The modern sediments of the Chukchi Sea are mainly terrigenous, except in the central part where they are slightly siliceous. The relatively high SiO_{2biog} accumulation distinguishes the Chukchi Sea sediment composition from that of other Arctic seas. The prevalence of fine-grained fractions (especially pelites) over most parts of the Chukchi shelf is a result of a ice-covered marine environment typical for Arctic seas.

Acknowledgment

The financial support of the Russian Foundation of Fundamental Research Grand No. 94-05-16202 is greatly acknowledged.

References

Coachman, L.K., Aagaard, K., and Tripp, R.B., 1975. Bering Strait. The Regional Physical Oceanography. -I nst. of Washington. Press. Seattle and London, 195 pp.

Hopkins, D.M., 1973. Sea level history of the Beringia during the past 250.000 years. Quatern. Res., 7: 520-540.

Logvinenko, N.V. and Ogorodnikov, V.I., 1980. Modern bottom sediments of the Chukchi Sea shelf. - Oceanology, V. 20, N4: 681-687 (in Russian).

Naidu, A.S., Creager, J.S., and Mowatt, T.C., 1982. Clay mineral dispersal patterns in the north Bering and Chukchi Seas. - Mar. Geol., 47: 1-15.

Pavlidis, Yu.A., 1982. Sedimentary environment in the Chukchi Sea and facies of its shelf. - In: Problems of geomorphology, lithology and lithodynamics of the shelf. M.: Nauka, pp. 47-76 (in Russian).

Pavlidis, Yu.A., 1992. Shelf of the World Ocean in the Last Pleistocene. M.: Nauka, 272 pp. (in Russian).

Petelin, V.P., 1967. Grain-size analysis of bottom sediments. M.: Nauka, 128 pp. (in Russian).

Rusanov, P.P., 1982. Seasonal events in life-cycle of plankton of Arctic seas. - In: Plankton of Arctic seas. M.: Nauka, pp. 132-202 (in Russian).

LITHOLOGY OF MODERN SEDIMENTS IN THE EASTERN BARENTS SEA

M.A. Pavlidis

P.P. Shirshov Institute of Oceanology, Moscow, Russia

Abstract

A new database of geomorphology, sedimentology, lithology, and hydrodynamical processes, which were obtained from sediments taken during cruises of the Institute of Oceanology Moscow within the Barents Sea since 1982, show the main features of modern sediments and principal peculiarities of its distribution in the shelf area. They were the basis for compilation of new maps and morpholithodynamical investigations.

Introduction

The surface layer of the Barents Sea bottom sediments (thickness up to 5 - 10 cm) which are controlled by modern physical, geographical, and lithodynamical processes are of significant interest for studies of sedimentary processes occuring along the Arctic glacial shelves.

The geographic situation and climatic features of this region together with the geological structure of the adjacent land cause the obvious dominance of terrigenous sedimentation in the basin. In contrast to the eastern Arctic seas of Eurasia which are characterised by the circumcontinental distribution of sedimentary matter, the western Arctic seas including the Barents Sea are distinguished by a non-uniform sediment distribution. This is related to the complexity of the interaction of different natural processes controlling the sedimentation, e.g., currents, hydrodynamic regime, ice regime, and relief. Thus, the main purpose of this work is to define the composition and peculiarities of accumulation of modern bottom sediments in the Barents Sea to reveal common distribution laws of main lithological types of sediments within the shelf area.

Material and methods

This paper is based on a large data set obtained from sediments taken during several cruises of research vessels of P.P. Shirshov Institute of Oceanology in the Barents and Kara Seas in 1982 - 1990. Sampling of bottom sediments was conducted by means of corers and grab samplers of various systems. Processing of grain-size data was realized using Petelin technique (1967). We used the classification of modern marine sediments, offered by Bezrukov and Lisitzin (1960). Thus, lithological types of Barents Sea sediments were proposed on the basis of percentage values according to grain-size content instead of median diameter of particles (Klyonova, 1960). The division of sediments on grain fractions was conducted on the base of decimal scale with

base $10^{1/10}$ progression. Received data were processed with special software for statistics ("CSS-1", "STATGRAF", "LOTUS").

For compiling lithological maps, data on hydrology, geology, and sediment dynamics were received at more than 240 stations (Fig. 1); data on geomorphology, echo sounding, and seismoacoustics using "Parasound" and "Multibeam", were used too.

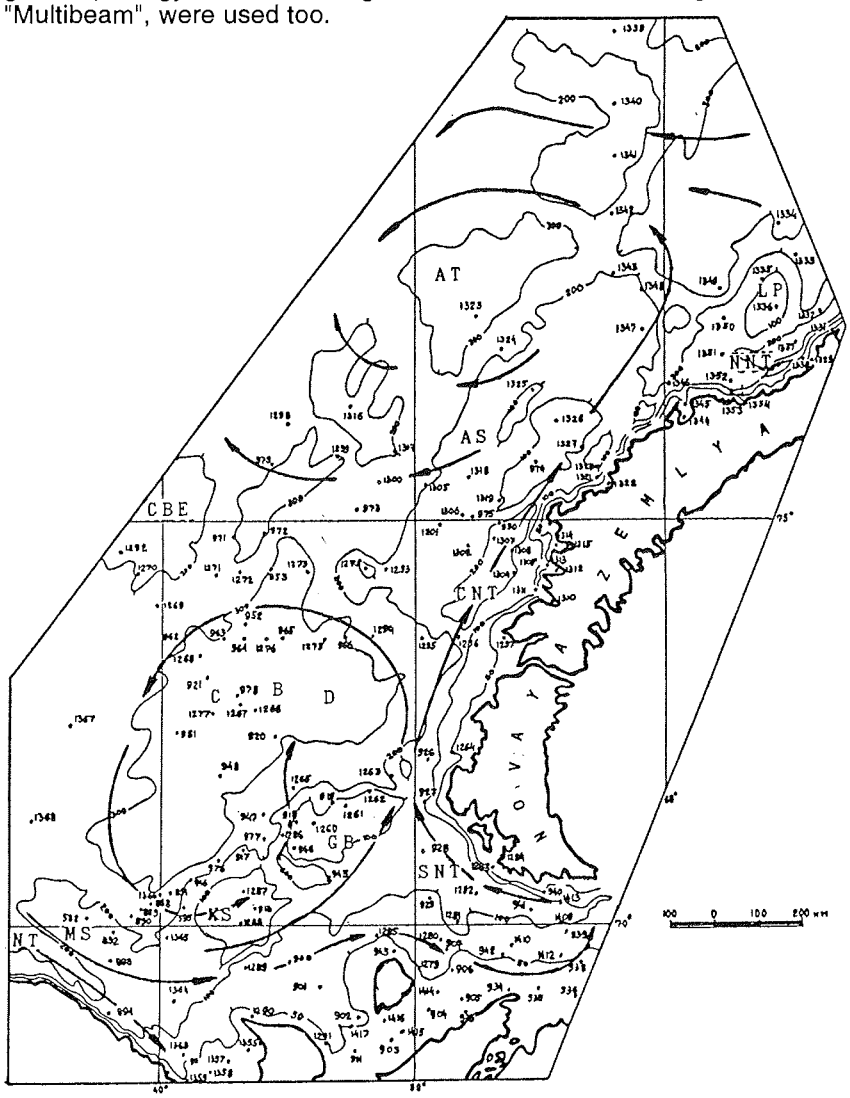

Fig. 1.: The bathymetry map of the eastern part of the Barents Sea with the main current system and the positions of geological stations. NT - Nordkapsky Trough; AT - Albanova Trough; NNT - the northern part of Novozemelsky Trough; CNT - the central part of Novozemelsky Trough; SNT - the southern part of Novozemelsky Trough; CBD- Central Depression of the Barents Sea; MS - Murmansky Swell; AS - Admiralteisky Swell; CBE - Central Elevation of Barents Sea; KS - Kaninsky Shallow; GB - Gusianya Bank; LP - Litke Plateau.

Results and discussion

The Barents Sea shelf entirely belongs to the Arctic polar zone of glacial type (Aksyonov, 1987). Typical is a considerable prevalence of terrigenous matter in the sediments, which is supplied from the land where physical weathering processes dominate. $CaCO_3$ content (represented mainly by molluscs and brachiopods shells) is low in shelf sediments. The areas of shell material accumulation (Gusinaya Bank, Petchorsky Basin, etc.) are insignificant. Thus, they are not reflected in our maps.

The Barents Sea has some main sources of sediment material. On one hand, there are external sources which include the following five largest areas (USSR Geology, 1970; Aksyonov, 1987): Kolskaya, Timano-Pechorskaya, Novozemelskaya provinces, Franz-Josef Land archipelago, and Spitsbergen archipelago. According to Medvedev and Potehina (1990), the role of Novozemelskaya province is most important as it supplies more than 50 % of sedimentary matter to the basin. Main processes of mobilization and transport of sedimentary matter in these provinces are physical weathering, coastal erosion, fluvial transport, and glaciers (for the northern provinces). On the other hand, an important source of sedimentary matter for modern sediments are ancient sediments and bedrocks of the Barents Sea. Here, the various hydrodynamic processes and wave erosion not only denudate but also re-distribute sedimentary matter all over the shelf area. According to Kalinenko (1985), the ratio of external and inner sources is approximately 50:50 on volume.

The distribution pattern of main grain-size fractions in Barents Sea bottom sediments is presented in Figure 2. It is obvious that the concentration of each fraction changes significantly. The material accumulation depends not only on the distance from the source area, but mainly from the morphological control of bottom relief and hydrodynamic factors.

On the basis of our classification scheme, eleven lithological types can be distinguished among modern Barents Sea sediments - from rough boulders, gravels, and pebbles to very fine clayey muds. There are also sediments of mixed grain-size composition containing all spectra of grain-size fractions with less than 50 % of each fraction (Fig. 3).

The coarses matter (boulders, gravels, and pebbles) distribution on the shelf area is insufficient. According to our data, predominantly pebble-sized sediments with up to 52% of material coarser than 10 mm occur in the vicinity of Kolguev Island where they accumulate mainly due to coastal denudation of the island, as well as in narrow coastal areas off Novaya Zemlya at Admiralteisky Peninsula, in the mouths of Mashigina and Sulmeniova Bays where coarse material is supplied by small mountain streams and as a result of exaration activity of island glaciers. In other parts of the basin the dissemination of pebbles and gravels (less often boulders) has a rather sporadic character. From our point of view, this is connected with bottom erosion of basal moraines which are described to a distance of up to 400 km from assumed glacial centers (from Novaya Zemlya, Franz-Josef Land, etc.).

Among sandy sediments of the Barents Sea, we distinguish "pure" sands (> 90 % of sand fraction from total sediment composition), sands with pelite and

(or) coarse material admixture, and aleuritic, pelite-aleuritic and aleuritic-pelite sands (Fig. 3).

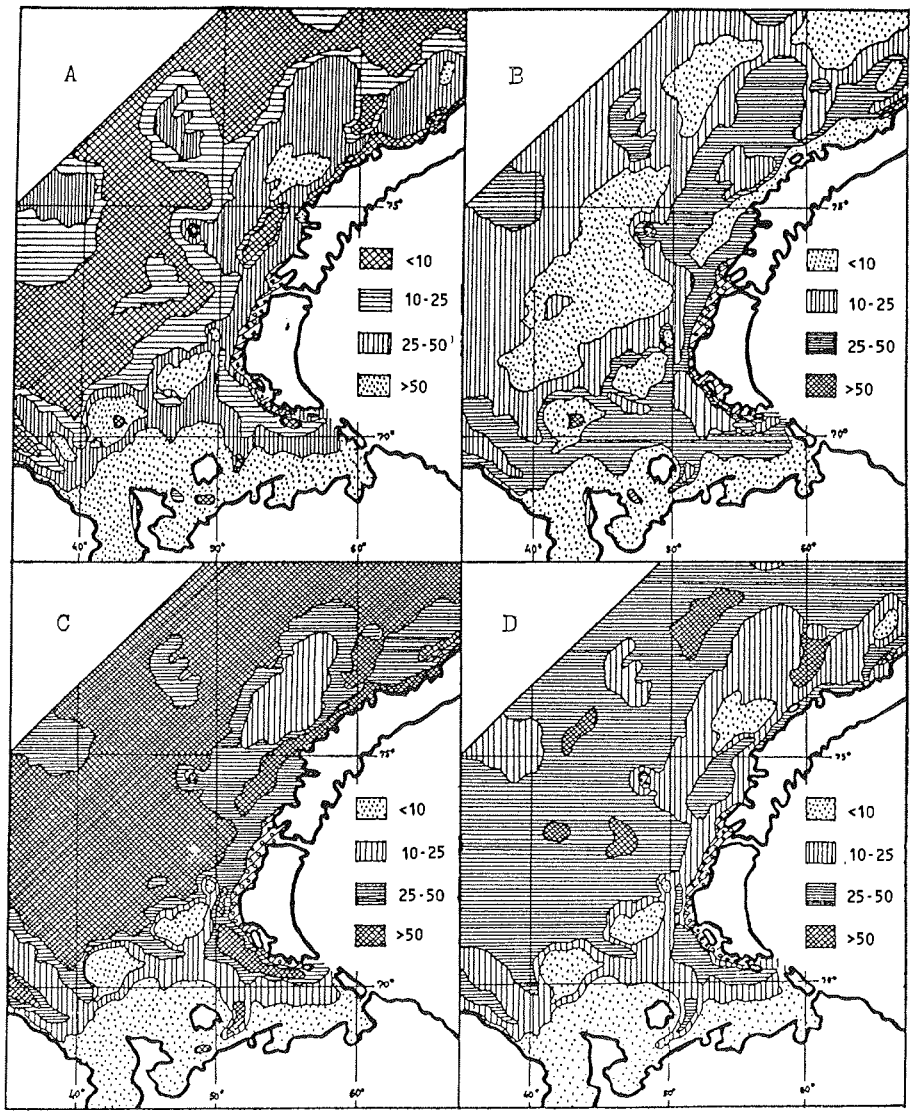

Fig. 2.: Grain-size distribution pattern in sediments of the eastern Barents Sea (wt. %). A - sand (1.0 - 0.1 mm); B - aleurite (0.1 - 0.01 mm); C - pelite (< 0.01 mm); D - colloid pelite (< 0.001 mm).

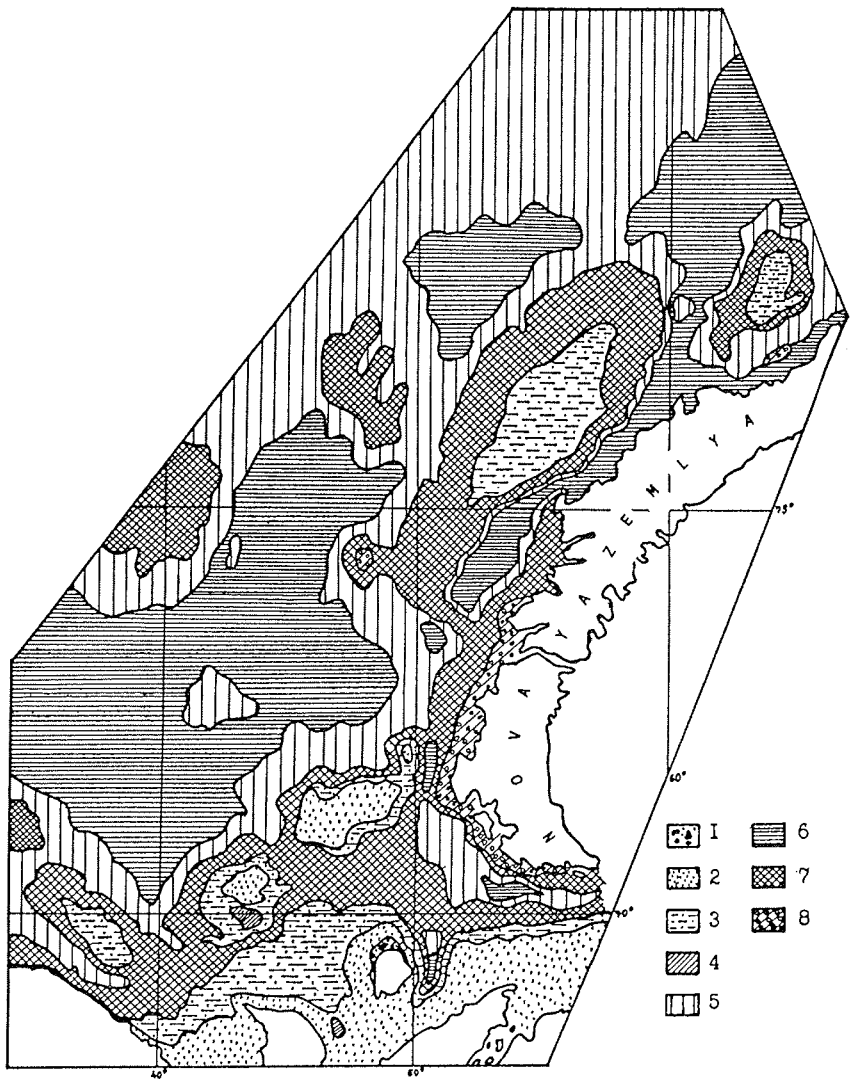

Fig. 3.: Distribution of lithological types of surface sediments in the eastern Barents Sea. 1 - boulders, pebbles, gravels; 2 - sand; 3 - aleuritic, aleuritic -pelite and pelite-aleuritic sand; 4 - aleurite; 5 - sand-aleuritic, aleurite-sandy mud; 6 pelite mud; 7 - sediments of mixed grain-size composition; 8 - Late Quaternary basal tills (moraines).

The "pure" sands are mainly described within the coastal areas. They form a band of sediments from Kola Peninusala coast bending around Kanin Peninsula and Kolguev Island to Vaigach Island. Besides that, sandy sediments cover the flat crests of two underwater elevations (Kaninsky Shallow and Gusinaya Bank) which morphologically separate the shallow continental part of the shelf from the central part of the basin (the Barents Sea Depression, Central Elevation, Samoilova Trough, etc.). The water-depth limit of "pure" sand distribution is restricted to 50 m. The exception is the area of the eastern coast of Kolguev Island where sandy sediments are exchanged by pelitic muds at the depth much less than 50 m in the "wave shadow" of the island.

Sands with admixtures of fine and coarse material are distributed on the shelf more widely and are met practically on all crests of underwater ridges and rises, except for Central and Ludlovsky elevations (Fig. 3). The depth of formation of such sandy sediments is 80 - 100 m in the southern part of the sea and 100 - 120 m in the eastern part - in the area of Admiralteisky Swell and Litke Plateau. The increase of depth is connected with the total deepening of the basin floor from the south to the north and with increasing bottom current velocity (Tantsura, 1973).

Grain-size data show that the fine-sand fraction prevails among sandy deposits (Table 1). The highest concentration (67.63 %) of fine sand occurs in sediments of the Petchorsky Basin.

As a component of terrigenous matter in sediments of the Barents Sea, aleurite is very widespread - from 0.65 % to 94.27 %. However, as original type, aleurite sediments are very rare and only occur in several places - on Kaninsky Shallow and at the southern coast of Kolguev Island (Fig. 3). The greatest concentration of aleurite material is described in sediments in depths from 80 to 200 m, which are typically for slopes of underwater elevations and small depressions. But as admixture, the aleurite material is present in various proportions in almost all shelf sediments.

The grain-size data show that within the aleurite fractions coarse aleurite (0.1 - 0.05 mm) prevails. Its content nearly always exceeds the content of fine aleurite (0.05 - 0.01 mm) fraction in 2 - 3 times (Table 1). The reason of this is not clear yet.

The most widespread sediments on the Barents Sea shelf are pelites (with a predominance of the fraction less than 0.01 mm). They include different lithological types such as: aleurite-sandy pelite muds, aleuritic pelite muds, sandy pelite muds, and pure pelite muds consisting more than 90 % of pelitic particles. These sediments are most wide-spread distributed in the central part of the Barents Sea and in all deep-water depressions. As an exception, these sediments are also accumulated near the coast of Northern Island of Novaya Zemlya in its bays and gulfs, where their formation is related to melting of glaciers mainly in spring and summer time.

The area of pelite sediments is much more extended than the area of sandy and especially aleurite sediments and consists of more than 60 % of the investigated part of the Barents Sea shelf (Fig. 3).

Table 1: Grain-size composition of the surface sediments of the eastern part of Barents Sea.

The place of sample selection	NN stati-ons	Depth (m)	Hori-zon (m)	Gravel (mm)	Sand (mm)			Aleurite (mm)		Pelite (mm)		
				>1.0	1.0-0.5	0.5-0.25	0.25-0.1	0.1-0.005	0.05-0.01	0.01-0.005	0.005-0.001	<0.001
							S A N D S					
Continental Shallow	900	63	0-6	0.98	2.09	15.47	46.52	25.05	2.53	Σ 7.36		
	902	55	0-5	8.52	4.46	14.87	53.79	13.78	0.70	Σ 3.88		
(southern and	1412	37	0-7	2.81	1.54	9.25	67.63	10.24	2.13	0.75	1.93	3.72
eastern part)	1415	45	0-2	1.25	1.59	16.08	35.14	4.76	2.73	8.68	16.75	
Gusinaya Bank	891	170	0-5	.....	1.05	8.29	57.45	9.18	1.26	5.22	8.63	8.92
and Kaninsky	917	98	0-5	0.92	1.25	13.51	75.46	4.96	0.37	Σ 3.53		
Shallow	918	68	0-3	0.77	1.54	26.41	67.57	2.07	0.05	Σ 1.39		
	1288	118	0-12	0.32	0.91	7.93	42.28	35.35	2.20	1.44	3.35	6.22
Admiralteisky	1318	167	0-3	1.40	0.53	6.99	58.98	13.75	0.73	3.59	4.98	13.55
Swell	1325	100	0-2	15.74	0.07	3.65	47.39	17.26	3.20	1.39	5.25	6.03
	1326	95	0-4	4.65	1.11	10.98	47.55	10.22	2.63	3.54	6.02	13.20
Litke Plateau	1336	90	0-4	4.10	1.97	11.00	38.32	6.55	1.63	3.61	13.32	19.42
							A L E U R I T E S					
Kaninsky Shallow	913	100	0-4	3.25	0.38	3.17	23.20	57.20	4.58	Σ8.23		
Continental Shallow	1417	54	0-3	.....	.....	0.17	0.65	48.60	45.67	2.71	0.08	2.12
							P E L I T E M U D S					
Central part	1268	330	0-5	0.24	0.19	0.71	3.79	2.94	1.75	14.06	26.28	50.04
of the	1273	312	0-4	0.94	0.47	1.72	4.06	3.59	4.45	18.89	30.52	35.36
Barents Sea	1300	280	0-2	0.65	0.11	0.22	0.65	0.54	0.11	10.88	35.08	53.76
	1323	345	0-2	.....	0.08	0.16	1.45	2.98	2.01	9.41	27.62	56.29
Fiords and gulfs	1310	24	0-3	0.84	0.19	0.41	0.97	2.03	2.08	20.00	27.68	45.80
of Novaya Zemlya	1322	26	0-3	0.70	0.10	0.10	0.97	0.60	8.16	18.98	23.44	47.65
Nordkapsky Trough	1370	200	0-4	1.25	0.23	0.70	4.91	12.07	1.54	13.01	22.79	43.50
Pechorsky Basin	1414	45	0-2	.....	.....	0.30	1.16	5.80	17.15	11.20	25.81	38.58
							SEDIMENTS OF MIXED GRAIN-SIZE COMPOSITION					
Continental	1289	45	0-10	0.40	0.71	6.79	35.34	37.26	3.82	1.22	4.23	10.23
Shallow	1281	88	0-2	0.69	1.03	7.81	30.37	30.29	5.07	4.99	7.78	11.97
Central part	1265	175	0-10	0.27	0.89	6.21	30.08	18.76	2.11	4.91	5.93	30.84
of the	1294	215	0-2	0.51	0.98	6.47	42.05	22.84	1.32	2.47	7.73	15.63
Barents Sea												
Central Elevation	1292	140	0-1	3.24	1.01	3.76	33.44	17.08	11.86	3.17	8.41	18.00
Ludlovky Elevation	1316	170	0-3	1.80	0.46	1.27	22.47	22.01	9.62	6.54	10.31	25.52
Admiralteisky	1301	148	0-2	12.05	0.58	2.04	11.52	16.04	5.54	8.34	18.81	25.08
Trough	1324	271	0-2	0.18	0.09	1.02	32.94	44.17	1.84	2.00	7.80	9.96
	1343	167	0-3	0.32	0.07	1.51	35.62	30.94	6.36	5.88	6.33	12.97
Litke Plateau	1333	175	0-5	8.54	4.74	17.69	26.57	13.38	2.09	5.39	8.15	13.45

Significant percentages of fine material in the basin is explained by three main reasons: first, main share of terrigenous flow to the basin belongs to fine material and its main source is Novaya Zemlya (Medvedev and Potehina, 1990); second, hydrodynamical conditions in the basin are such that surface currents can transport only fine pelite material and the more coarse matter is accumulating in considerable volume in coastal zones; third, the current system in the Barents Sea has a cyclonic nature, and fine material is not removed out of the shelf limits (Tantsura, 1973).

The grain-size composition of pelite sediments (< 0.01 mm fractions) shows that the 0.01 - 0.001 mm fraction is dominant (up to 70 % from the total mass of pelite muds) (Table 1). The content of colloidal fraction (less than 0.001 mm) does not exeed 30 %. However, in some cases as, for example in the Central Depression, its concentration reaches 56 - 57 %. This fact is especially important because such sediment is the most active accumulator of organic matter and different sorts of anthropogenic pollutants. The presence of coarse sandy material and even gravels and pebbles (less often boulders) in fine pelite material (see Table 1) allows to conclude about the combination of two independent processes of accumulation in the central part of the Barents Sea: the stable background sedimentation of fine matter as the main part of mud formation and sea-ice melting which determines the presence of coarse components in the pelite matrix.

In the Barents Sea shelf area, sediments of mixed grain-size composition (Fig. 3) are widely distributed. According to their lithological and dynamical properties and because of the practically total absence of aleurite sediments, they occupy a transitional position between fine and coarse sediments. This type is more often found on slopes of underwater elevations and depressions, for example, Admiralteisky Swell, Litke Plateau, and the Central Depression between 80 and 200 m in depth (Table 1).

Conclusions

The consideration of sediment distribution pattern and accumulation processes on the shelf permits to make a conclusion about rather significant facial diversity. Under more detailed consideration of sediment distribution features in the shelf area the following regularities may be established:

1. The sediment distribution of profiles of the underwater slope is controlled by hydrodynamics laws (Zenkovitch, 1962). The shallow part of shelf and crests of underwater elevation correspond to more coarse - grained sediments, whereas the deeper part and depressions consist of pelites.
2. The various shelf areas are distinguished by the character of sediment distribution. The southern and southeastern parts are characterized by a patchy (mosaic) sediment distribution. In the eastern part, the sediment distribution has a more linear character and is mainly caused by the linear distribution of bottom relief features. In the central deep (up to 400 m) part of the basin, the mode of sedimentation is more calm and the areal distribution of fine-grained sediments predominates.
3. The sediment accumulation is mainly controlled by the bottom relief, hydrodynamical factors, and the ice regime. The distance from the source areas is of secondary importance.

Acknowledgments

The paper is supported by Russian Foundation of Fundamental Research (grant No. 94-05-9703).

References

Aksyonov, A.A., 1987. The Eurasian Arctic shelf in Late Quaternary time. Moscow, Science: pp. 215 (in Russian).

Bezrukov, P.L., Lisitzin, A.P., 1960. Classification of sediments of modern sea basins. Moscow, Transact. of Inst. of Oceanol., T-32: pp. 3-14 (in Russian).

Kalinenko, V.V., 1985. The sedimentation characteristics in central part of the Barents Sea / Geology and Geomorphology of shelves and continental margins. Moscow, Science: pp. 101 (in Russian).

Klyonova, M.V., 1960. Geology of the Barents Sea. Moscow, Science: pp. 367 (in Russian).

Medvedev, V.S. and Potehina, E.V., 1990. Supply by the Novaya Zemlya island' modern glaciers of fine material to the Barents Sea / The modern sedimentation processes in the World Ocean shelves. Moscow, Science: pp. 102-110 (in Russian).

Petelin, V.P., 1967. Grain-size analysis of marine bottom sediments. Moscow, Nauka: pp. 128 (in Russian).

Tantsura, A.I., 1973. Seasonal changing of Barents Sea currents. PINRO, V. 34: pp. 102-112 (in Russian).

USSR Geology, 1970. The Soviet Arctic Islands. Moscow, Nedra, T-26: pp. 547 (in Russian).

LITHOLOGY OF BOTTOM SEDIMENTS OF THE CENTRAL WHITE SEA

Shcherbakov, F.A.

P.P. Shirshov Institute of Oceanology, Moscow, Russia

Abstract

The distribution of the grain-size types of the bottom sediments of the White Sea is described. It is connected with the circulation pattern, ice regime, river input, and wave action. According to the geographical situation the White Sea belongs to the Barents Sea basin and hence to the Arctic Ocean. Three main parts are distinguished: the Northern, the Central, and the Southern part (Nevessky et al., 1977).

Material and Methods

The modern (late Holocene) layer of White Sea bottom sediments is represented by a wide spectrum of terrigenous types differing by grain-size composition. The samples of these deposits were received during a joint expedition performed by the Biological Department of the Moscow State University and the Institute of Oceanology of the Russian Academy of Sciences in the central part of the White Sea (Shcherbakov and Semionova, 1990). Sediments were obtained on stations (Fig. 1) by means of grab sampler "Ocean-0.25". Samples were selected from the surface layer of 2 - 3 cm thickness and stored under wet condition. Grain-size analysis was carried out in the Analytical Laboratory of the Institute of Oceanology, using the technique described by V.P. Petelin, 1967. Water analysis was conducted by adding a dispergator (Tripolyphosphat Na) on fractions selected by pipette. A control of particle size was carried out under the microscope.

The separation into sediment fractions was performed as shown in Table 1. The content of the major sediment-forming component should not be less than 50% of the weight of the sample. Other components are considered as admixtures that are reflected in the names of types; they are arranged as adjective in the order of increased abundance in the sediment composition. The classification includes: purely clay (more than 70% clay particles); aleurite clay and sandy clay (more than 10% aleurite or sandy particles); aleurite clayey mud (from 50% to 70% pelite particles); aleurite clayey mud with sand (sand more than 30%). Among sediments containing more than 50% of aleurite particles, pure aleurite (more than 70% particles of 0.1 - 0.01 mm size), aleurite - sand - clay (more than 50% aleurite, other sand and pelite), and aleurite - sandy with clay and gravel (not less than 20% particles with size more than 1.0 mm) were distinguished. A group of sand (more than 50% of sandy particles with pelite and small admixture of aleurite and more coarse particles) is represented by pure sand (more than 70% of sandy particles), sand with aleurite as well as sand- ravel sediments containing nearly fifty - fifty of sand and gravel particles. A significant proportion of the bottom sediments

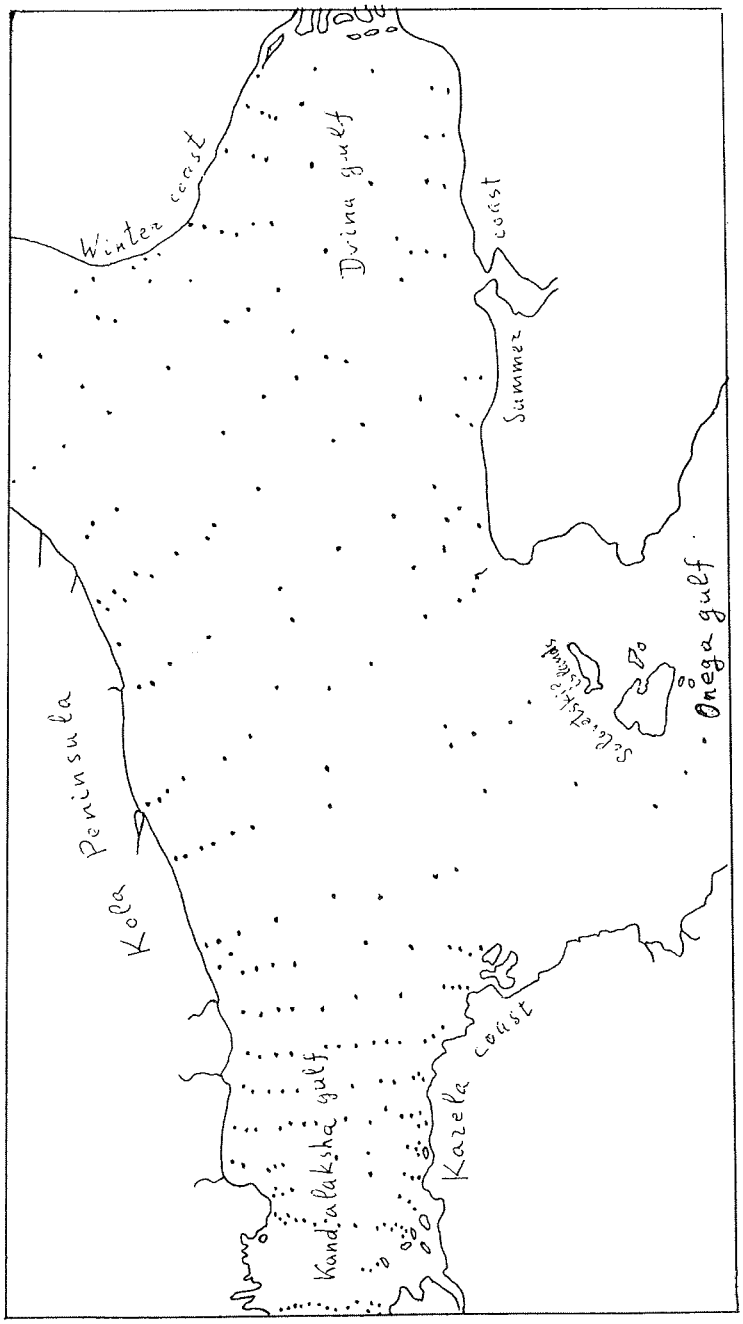

Fig. 1.: Position of sampling stations in the White Sea.

of the White Sea are so-called " mixed sediments" containing no more than 50% of any fraction. Among them there are sand - aleurite - pelite sediments with large (more than 40%) content of pelite, sand - aleurite - clay sediments with plenty of sand and aleurite particles (not less than 60% particles of more than 0,01 mm size) as well as sand - aleurite - clay sediments with plenty of pelite and with gravel.

Table 1.: Decimal grain-size scale.

Gravel mm	Sand mm			Aleurite mm		Clay mm
	coarse	middle	fine	coarse	fine	
> 1	1.0-0.5	0.5-0.25	0.25-0.1	0.1-0.05	0.05-0.01	<0.01

Results and discussion

The distribution of grain-size types of modern bottom sediments in the central part of the White Sea are presented in Figure 2. In general, the White Sea is characterized by a so-called "circumcontinental distribution" of the different types. The central depression is covered by an extensive field of clay with high content of fraction <0.001 mm, which is surrounded by more and more coarse sediments toward the coast: sands, gravel, and, less often, boulders. A typical feature for inner seas is the zone of constant wave effects on the sea floor, disposed in the basin along the most opened coasts at a depth of ca. 20 m. A large influence on bottom sediment composition and their distribution has the ice regime of the White Sea. First of all, it controls the wide-spread distribution of mixed sediments outside the wave zone. These sediments consist of subcolloidal fractions of pelite and aleurite and are enriched in ice-rafted debris. Especially, a wide band of such sediments occurs along the northern coast of the basin, which may be connected with the drift of ice from the eastern part of "Gorlo". The rather wide-spread distribution of aleurite can be related to climatic conditions and sediment mobilization on land (prevalence of processes of mechanical weathering). The presence of sand-aleurite and especially gravelly material as a large admixture in clay, is mainly connected with ice melting. Therefore, the details of the spatial distribution of such coarse admixture reflect general patterns of surface-water circulation in the White Sea. As shown in Figure 2, there are four large areas of accumulation of most fine-grained aleurite in the basin depression. From our point of view, they mark a halistases in the central part limited by branches of "circumcontinental" currents (Fig. 2). Underneath such branches, bands of aleurite sediments occur at the bottom surface. Along to the northeastern (Winter) coast of Dvensky Bay, there are fields of pelites and aleurites connected with Northern Dvina River load. Here one can observe a very sharp transition from sandy sediments near the southeastern coast and gravel sediments near the nothwestern coast (wave zone), to aleurite and sand-aleurite- clay sediments in the upper part of the shelf. At the southwestern coast of Dvinsky Bay the sandy and sandy-gravelly sediments cover a considerably wider zone of the shelf. As shown in Figure 2 the field of fine aleurite was formed in the central part of the bay, fixing the presence of halistatic circulation formed by branches of coastal currents. The influence of ice melting is reflected in the sandy sediments which sometimes are enriched in gravel.

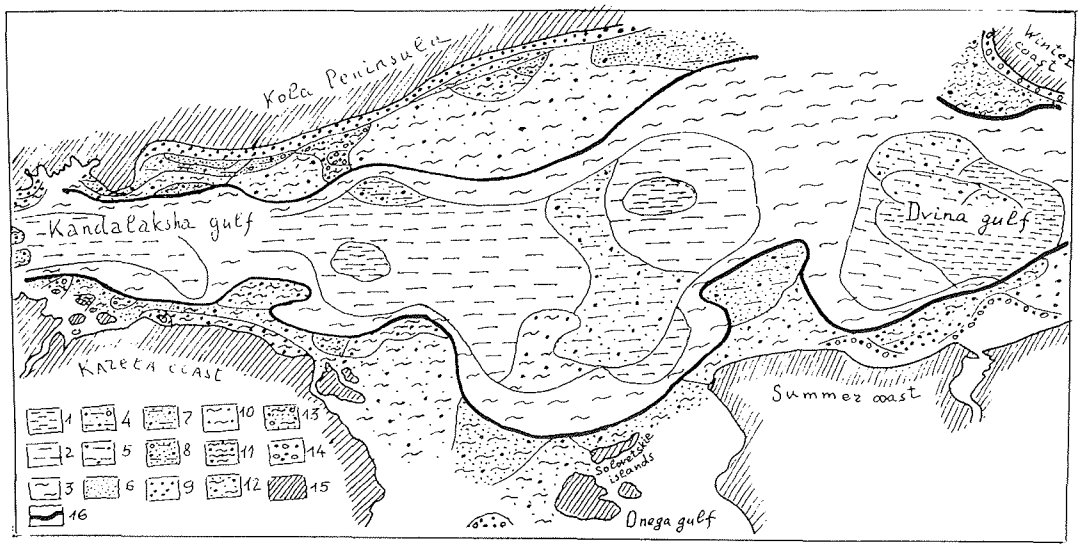

Fig. 2.: Distribution of grain-size types of modern sediments from the central part of White Sea. 1 - clay (>90% of pelite); 2 - aleuritic clay (>70% of pelite); 3 - aleurite clay (>50% of pelite); 4 - sand - aleurite - clay with a number of gravel grains; 5 - aleurite clay with sand (>50% of pelite); 6 - aleurite (>70% of 0,1 - 0,01 mm fraction); 7 - sandy - clay aleurite (>50% of 0,1 - 0,01 mm fraction); 8 - sandy aleurite with clay and gravel (>50%of 0,1 - 0,01 mm fraction); 9 - sand (>70% of 1,0 - 0,1 mm fraction); 10 - sand with clay (>50% of 1,0 - 0,1 mm fraction); 11 - sand - aleurite - clay with pelite (>40% of pelite and about 60% particles more than 0,01 mm); 12 - sand - aleurite - clay sediment with plenty of sand and aleurite particles; 13 - sand - aleurite - clay sediments with plenty of pelite and gravel; 14 - sand with gravel; 15 - land; 16 - boundary of clay-sediment distribution.

Acknowledgments

This article is supported by the Russian Foundation of Fundamental Researches (Grant No. 94-05-9703)

References

Nevessky E.N., Mednev V.S., and Kalinenko V.V. (1977). The White Sea sedimentogenesis and the history of the development during the Holocene. Moscov, Nauka, 235 pp., (Russian).

Petelin V.P. (1967). The grain-size analysis of marine bottom sediments. Moscov, Nauka, 128 pp., Language: Russian

Shcherbakov P.A. and Semionova N.L. (1990). The bottom sediments type and biovenoses of the central part of the White Sea. In: Modern sedimentation processes on shelves of the World Ocean. Moscov, Nauka, 126 - 134, (Russian).

AEROSOL SIZE DISTRIBUTION OVER THE LAPTEV SEA IN JULY-SEPTEMBER 1995: FIRST RESULTS

Smirnov V.V.[1], Shevchenko V.P.[2], Stein R.[3] Lisitzin A.P.[2], Savchenko A.V.[1] and ARK XI/1 *Polarstern* Shipboard Scientific Party

[1]Institute of Experimental Meteorology, Obninsk, Russia
[2]P.P.Shirshov Institute of Oceanology, Moscow, Russia
[3]Alfred Wegener Institute, Bremerhaven, Germany

Abstract

Aerosol size distribution in the marine boundary layer over the Laptev Sea was studied from 20 July until 10 September 1995 during the RV *Polarstern* expedition ARK XI/1. Measurements were carried out at 63 sites by means of a photoelectrical counter PC-218. Particles larger than 0.5 μm were counted. In general, there were much more particles within the size fraction from 0.5 to 1 μm than larger particles. For areas where open water occupied more than 30-50 %, there is possitive correlation between wind speed and the concentration of particles larger than 0.5 μm. This could testify the input of sea-salt particles from the sea-surface microlayer. During the formation of fog, an increase of concentration of particles with a size from 2 to 5 μm was registered.

Introduction

Over the two past decades it has become apparent that the atmospheric input of particulate matter into surface waters plays an important role in the oceanic biogeochemical cycling of many chemical elements (Lisitzin, 1978; Duce et al., 1991). Numerous studies have shown that aerosols in the Arctic are of importance for atmospheric chemistry and climate (Rahn, 1981; Barrie, 1986; Leck et al., 1996). But up to now aerosols of the Russian sector of the Arctic were studied little (Vinogradova, 1994; Shevchenko et al., 1995).

To estimate fluxes of aerosols into the surface waters and the role of aerosol supply in the modern sedimentation in the Ocean we have to know the concentrations of particles in the air and a deposition velocity which depends on particle size (Duce et al., 1991). Aerosol size distributions in the Central Arctic were only studied in the Summer of 1991 during the International Arctic Oceanic Expedition onboard the Swedish icebreaker *Oden* (Covert et al., 1996).

The present study aimed to obtain continuous and representative measurements of marine aerosol particle spectra in the range from 0.5 to 10 μm in the Laptev Sea and to study their dependence on meteorological parameters: wind speed and direction, temperature, visibility etc.

Methods

Measurements of aerosol size distribution were carried out in the period from 20 July to 10 September 1995 during the RV *Polarstern* expedition ARK XI/1

into the northern Laptev Sea area. The positions of 63 sites where aerosol measurements were carried out, are shown in Figure 1. These remote sites were characterized by the absence of industrial plants in a radius of more than 1000 km. Aerosol size spectra were measured by photoelectric counter PC-218 (Royco Instr. Inc., USA) on the deck over the bridge approximately 20 m above the sea surface. At each site 3 parallel measurements of concentrations of particles in the ranges 0.5 to 1; 1 to 2; 2 to 3; 3 to 5; and 5 to 10 μm were carried out. The relative error of measurements by PC-218 is less than 10% (Smirnov, 1993). Data on the temperature, wind speed and direction, and visibility were obtained from ship´s meteorological service.

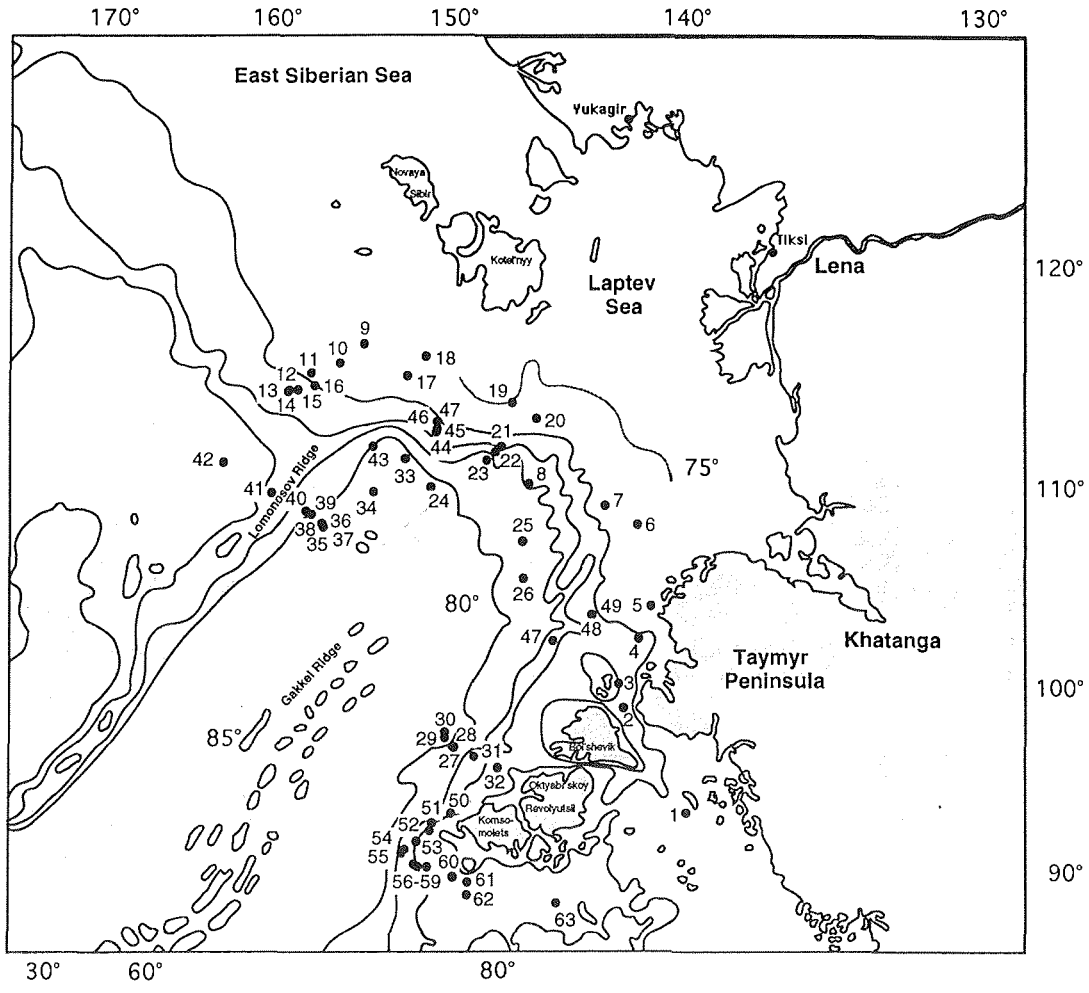

Fig.1.: Location of sites where aerosol size distributions have been measured in the Laptev Sea from 20 July to 10 September 1995 during ARK XI/1 Expedition of RV *Polarstern*.

Results and discussion

As compared with the Antarctic, the surface air in the Arctic region is more polluted (Barrie, 1986), but as compared to Obninsk, Russia, the Arctic air is much cleaner (Smirnov, 1993), although the number aerosol concentrations (N) of particles with D>0.5 μm turn out to be equal: N=4 to 8 cm^{-3} (Table 1; Fig. 2). For comparison, in arid regions of Tadjikistan N=20 to 100 cm^{-3} (Gillette et al., 1992). The form and variability of the aerosol size spectra at different regions of the Arctic and Antarctic as well as in mountain and forest-steppe regions do not differ significantly. The term „polar aerosol" would, probably, define only the geographical features.

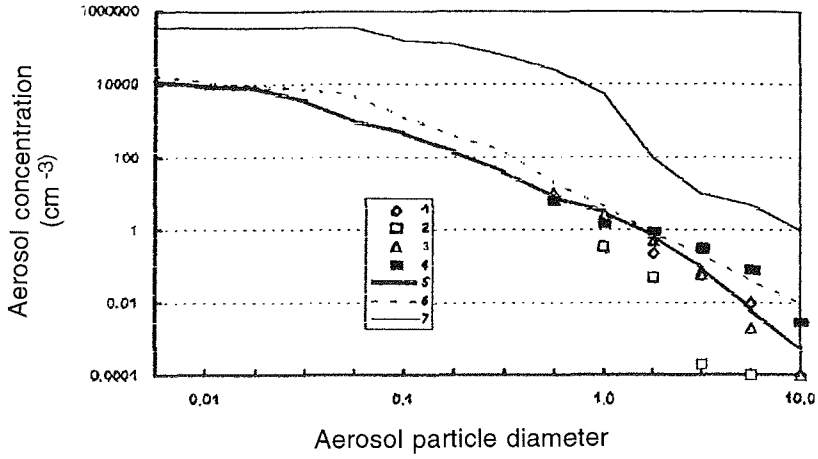

Fig.2.: Averaged cummulative size spectrum of the atmospheric aerosols from RV *Polarstern* cruise 20 July-10 September 1995 (1-4) and other regions (5-7): 1- the Laptev Sea, all days (see also Table 1); 2-clear days; 3-stormy days; 4-foggy days; 5-Arctic, Franz-Joseph Archipelago, the Spring 1994; 6-Obninsk, Russia, May 1994; 7-the Aral Sea dry bed, Kazakhstan, dust storm, 30 May 1992.

Table 1.: Mean values of marine aerosol concentrations, wind direction and speed, and air temperature during the ARK XI/1 cruise of RV *Polarstern* (20 July -10 September 1995).

	Aerosol concentration (cm^{-3})						Wind		Visi-	T
	D>0.5 μm	>1 μm	>2 μm	>3 μm	>5 μm	>10 μm	Direc -tion	Speed m/s	bility m	°C
All days	8	2	0.22	0.06	0.01	0.0001	180°	8.6	8000	-2.2
Clear days	6.2	0.33	0.05	0.0002	0	0	190°	8.1	8600	-4.2
Stormy days	10.6	2.7	0.5	0.06	0.002	0	180°	14	9900	+0.5
Foggy days	7	1.5	0.8	0.33	0.08	0.003	195°	5.4	1000	-2.5

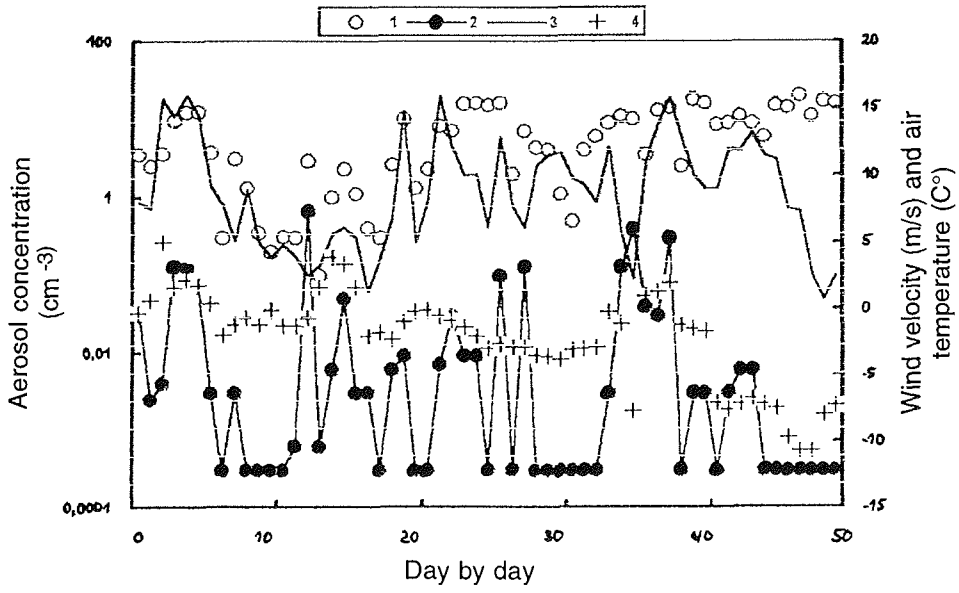

Fig.3.: Day by day variation of the number concentration of aerosol particles with diameter D>0.5 μm (1) and D>3.0 μm (2), wind speed in m/s (3), and air temperature in ºC (4) during RV *Polarstern* cruise in the Laptev Sea from 20 July to 10 September 1995.

In general, concentrations of small particles (0.5 to 1 μm) are much higher than concentrations of large particles (Table 1; Fig. 2). In areas where open water occupies more than 30-50%, the concentration of particles larger than 0.5 μm increases with the increase of wind speed (Fig. 3). This could testify the input of sea salt particles from the sea surface microlayer by wind and the importance of sea salt for the chemical composition of marine aerosols, as it has been shown by O´Dowd and Smith (1993). Strong winds (> 10 m/s) stimulate the grows of the concentration of coarse fraction (D> 5μm). In the north-eastern part of studied area at times when wind speed was more than 8 m/s, the concentration of aerosol particles (D>0.5 μm) was 1.05 to 11.23 cm^{-3} (in average 6.52 cm^{-3} for 10 sites), but at Site 17 and a wind speed of 3.3 m/s we only found 0.09 cm^{-3}. In foggy days we observed an increase of the concentration of particles with D=2 to 5 μm (Table 1; Fig. 2).

In future investigations the results of this study could be used for the estimation of fluxes of aerosols at the surface of arctic seas.

Acknowledgments

We thank the Russian Foundation for Basic Research for financial support (grant RFBR N 96-05-65907). We are grateful to the crew of the RV *Polarstern* for all assistance.

References

Barrie, L.A. (1986). Arctic air pollution: an overview of current knowledge. Atmos. Environ., Vol.20, p.643-663.

Covert, D.S., Wiedensohler, A., Aalto, P., Heintzenberg, J., McMurry, P.H. and Leck, C. (1996). Aerosol number size distributions from 3 to 500 nm diameter in the arctic marine boundary layer during summer and autumn. Tellus, Vol. 48B, p.197-212.

Duce, R.A., Liss, P.S., and Merrill, J.T. (1991). The atmospheric input of trace species to the world ocean. Global Biogeochemical Cycles, Vol.5, p.193-259.

Gillete, D.A., Gomes, L., and Smirnov, V.V. (1992). A generalized model on arid aerosol spectrum. In: Fukuta, N. and Wagner, P.E. (Eds.), Nucleation and Atmospheric Aerosols. Deepack Publ., Hampton, p.461-464.

Leck, C., Bigg, E.K., Covert, D.S., Heintzenberg, J., Maenhaut, W., Nilsson, E.D. and Wiedensohler, A. (1996). Overview of the atmospheric research program during the International Arctic Ocean Expedition of 1991 (IAOE-91) and its scientific results. Tellus, Vol. 48B, p.136-155.

Lisitzin, A.P. (1978). Processes of oceanic sedimentation. Moscow, Nauka, 392 p. (in Russian).

O'Dowd, C.D. and Smith, M.H. (1993). Physico-chemical properties of aerosols over the Northeast Atlantic: Evidence for wind-speed-related submicron sea salt aerosol production. J. Geophys. Res., Vol.98, p.1137-1149.

Rahn, K. A. (1981). Atmospheric, riverine and oceanic sources of seven trace constituents to the Arctic ocean. Atmos. Environ., Vol. 15, p.1507-1516.

Shevchenko, V.P., Lisitzin, A.P., Kuptzov, V.M., Ivanov, G.I., Lukashin, V.N., Martin, J.M., Rusakov, V.Yu., Safarova, S.A., Serova, V.V., Van Grieken, R. and Van Malderen, H. (1995). The composition of aerosols over the Laptev Sea, the Kara, the Barents, the Greenland and the Norwegian Sea. In: Kassens, H. et al. (Eds.), Russian-German Cooperation: Laptev Sea System. Berichte zur Polarforschung, 176, p.7-16.

Smirnov, V.V. (1993). Ionization in the troposphere. Gidrometeoizdat, St.Petersburg, 312p. (in Russian).

Vinogradova, A.A. (1994). Microelements in the composition of arctic aerosol (review). Physics of the Atmosphere and Ocean, Vol.29, p.417-437.

SURFACE SEDIMENTS OF THE NORTH-WESTERN BARENTS SEA

Solheim A.[1)] and Elverhøi A.[2)]

[1)] Norwegian Polar Institute, P. O. Box 5072, Majorstua, N-0301 Oslo, Norway
[2)] Department of geology, University of Oslo, P. O. Box 1047, Blindern, N-0301 Oslo,Norway.

Abstract

The Barents Sea was covered by a marine based ice sheet during the Late Weichselian, and this is reflected in the present-day sediment distribution. Main processes responsible for the surface sediment distribution are winnowing from the bank areas with subsequent redeposition in troughs, and deposition from sea ice. Sedimentation rates are generally low, 3-5 cm/ky, but may increase to 30 cm/ky in glacier proximal areas close to Svalbard. Based on a number of both published and unpublished studies, this paper presents a short summary of the surface sediment characteristics in the north-western Barents Sea.

Introduction

The Barents Sea covers an area of approximately 1.2 million km^2, and is the largest present-day epicontinental sea (Fig. 1). With an average water depth of approximately 250 m, it is a relatively deep shelf sea, and at present around two thirds of the area are influenced by sea ice and icebergs. The presence of a marine based ice sheet covering most or all of the Barents Sea during the Late Weichselian maximum, at 18-20 ka, now seems well established (Elverhøi and Solheim, 1983a; Solheim and Kristoffersen, 1984; Vorren and Kristoffersen, 1986; Vorren et al., 1988, 1989; Solheim et al., 1990). The retreat of the Barents Sea ice sheet most likely took place in a rapid, stepwise manner, starting at around 15 ka, partly as a response to an increasing eustatic sea level (Jones and Keigwin, 1988; Elverhøi et al., 1990, 1993; Solheim et al., 1990).

The present-day distribution of unlithified sediments in the Barents Sea is a direct response of the latest glacial history. In general the Quaternary cover of the northern Barents Sea is less than 10-15 m thick, and often 5 m or less. Several local accumulations form exceptions from this (Solheim and Kristoffersen, 1984; Solheim et al., 1990). The thickness increases to several hundred meters towards the shelf break in the west, and to generally more than 50 m in the southern Barents Sea (south of approximately 74°N). In general, the sediment stratigraphy contains 3-4 units (Fig. 2), starting with a basal layer of overconsolidated diamicton (Unit D) (undrained shear strength, Su, >150 kPa), interpreted to represent Late Weichselian basal till. Above this, a layer of slightly overconsolidated diamicton (Unit C) (Su = 30-100 kPa) is observed in several cores, interpreted as a deformation till (Nyland Berg, 1991; Solheim et al., 1990).

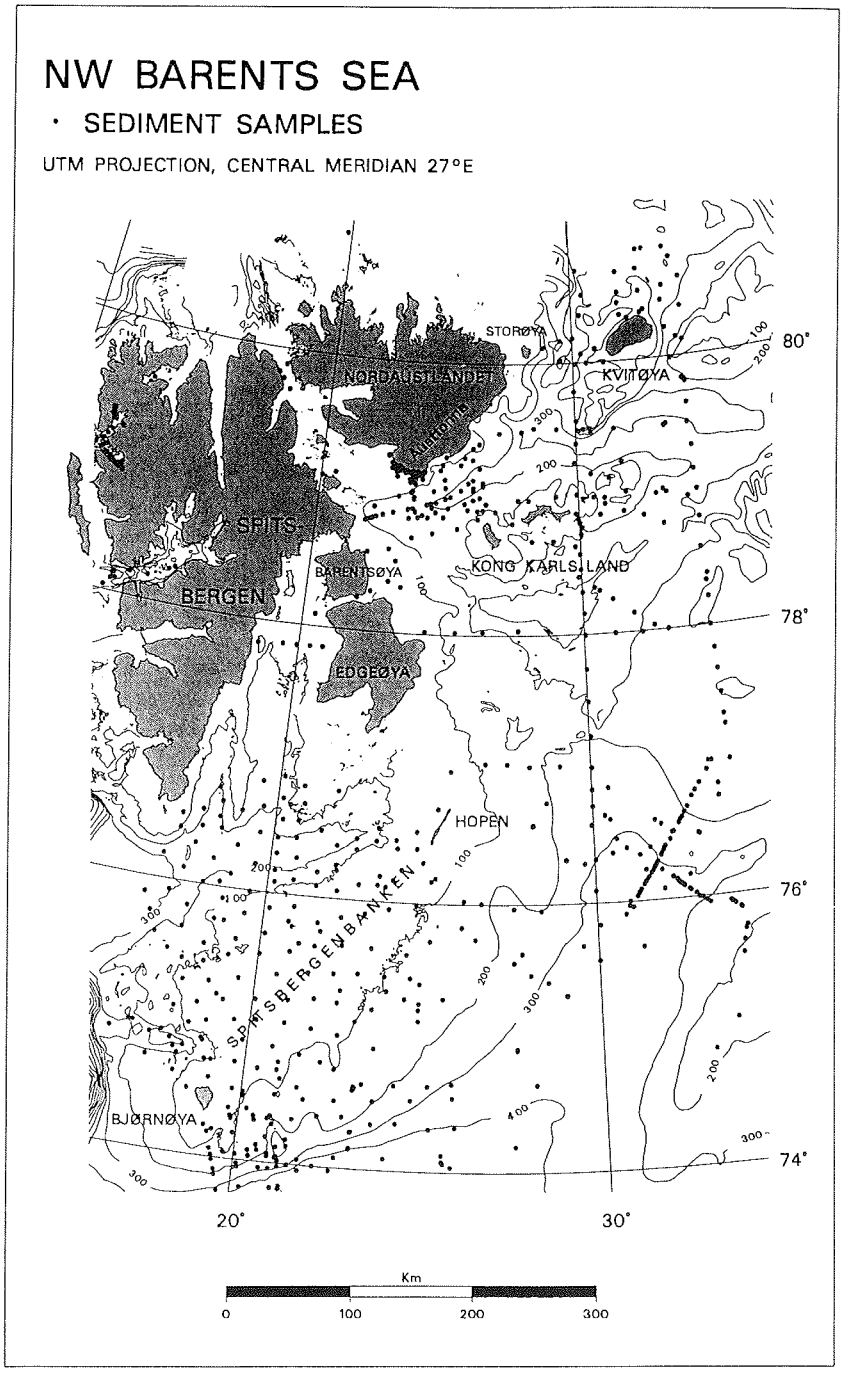

Fig. 1.: Map showing the northwestern Barents Sea, with the Norwegian Polar Institute's sampling locations shown. Bathymetry in 100 meter contours.

The tills are covered by a layer of IRD-rich glacial marine sediments (Unit B), interpreted to be deposited proximal to the retreating Late Weichselian ice sheet. A thin veneer of Holocene, mostly fine-grained deposits (Unit A) cover these units. The present paper focuses on Unit A, and aims at summarising the present knowledge of the Holocene deposits and sedimentary environments of the north-western Barents Sea (north of 74°N and west of 35°E). We will briefly present the main studies and the main results obtained. For details, however, the reader should consult the different publications and studies cited in this contribution.

Data base and main studies

Elverhøi and Solheim (1983b) presented a surface sediment distribution map of the western Barents Sea, north of 72°N, based on approximately 400 sample locations. Of these, the majority were samples taken for "geochemical sniffing" purposes by the Norwegian Petroleum Directorate, and had only shipboard observations of sediment texture, with no grain size analyses carried out. This data base was extended by 168 sample stations in 1983 and 1987 (Elverhøi and Solheim, 1983c; Solheim et al., 1988a), but again with approximately half the stations for "sniffing" purposes, with only shipboard observations available. Main tools for sediment sampling have been dredges and grab samplers in shallow, hard bottom areas, while 3 m and 6 m gravity corers have been the principal tools in deeper waters. 61 vibrocorer stations were added to the database in 1987, giving more data on the overconsolidated till underlying the postglacial sediments.

The sediment cores are accompanied by approximately 35000 km of single channel seismic data, most of which also have 3.5 kHz echo sounder coverage. In addition, about 2000 km of side scan sonar records support the regional interpretation of sea floor characteristics of the Barents Sea.

Since Elverhøi and Solheim's (1983b) map of the surface sediment composition of the western Barents Sea, no new regional compilation has been published. However, several local studies have been performed in the north-western Barents Sea, which involves analyses of the surface sediment composition. In addition, several graduate student have also analysed data of relevance to this topic and reported the results in their theses. Some key studies, both published and unpublished, include: Bjørlykke et al. (1978), Forsberg (1983), Elverhøi and Solheim (1983a, 1983b, 1987), Pfirman (1985), Wensaas (1986), Larssen (1987), Solheim et al. (1988b), Solheim and Elverhøi (1990), Solheim (1991), Russwurm (1990), Nyland Berg (1991), and Elverhøi et al. (1989, 1990, 1992).

Since the analyses summarised in this paper are compiled from studies over more than 15 years, several different analysis techniques and instruments have been used. The grain size analyses have been performed by dry sieving of the > 63 μm fractions (Table 1, Appendix), while the fine fractions have been analysed by either fractionation, falling drop apparatus (Moum, 1966) or by Xray methods in a Micrometrics Sedigraph 5000D Particle Size Analyser. The mineralogical content of the surface samples have been determined by Xray diffraction of oriented samples of the bulk <63 μm fractions, and/or the <

2 µm fractions. Details of the analyses may be found in the different reports and publications cited in the text.

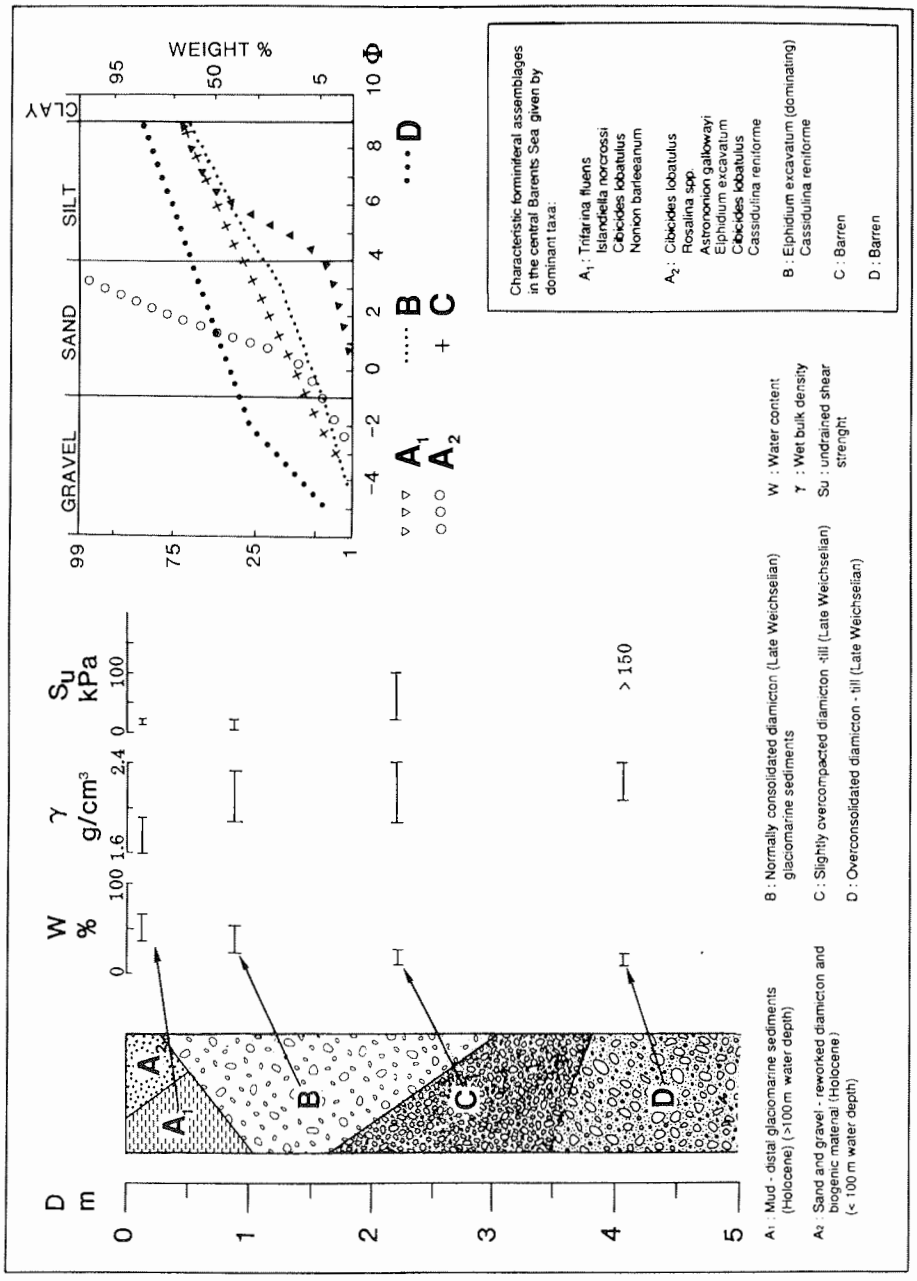

Fig. 2.: Generalized lithological section of the Late Cenozoic sediments in the northwestern Barents Sea. From Elverhøi et al. (1993), based on data from Elverhøi and Solheim (1983a), Solheim et al. (1988b, 1990), Elverhøi et al. (1990), Russwurm (1990) and Nyland Berg (1991).

A common effect seen in the grain size distribution is a bimodality, with the coarse silt fraction apparently missing. This has been interpreted as partly resulting from methodology, caused by the two different methods used for the > 63 μm and < 63 μm fractions, respectively, but partly also a real effect of the "terminal grade" of the underlying Mesozoic sand- and siltstones (Nyland Berg, 1991). The relative importance of the two has not been examined in detail.

Sedimentary processes

The deposition proximal to the heavily glaciated north-eastern Svalbard is dominated by output of suspended sediments from the glaciers. However, studies off the Austfonna ice cap on Nordaustlandet (Fig. 1), show that the suspended sediments are mainly entrained in the coastal waters, and very little, probably considerably less than 10%, is transported beyond 10 km off the coast (Pfirman and Solheim, 1989). Similar conditions are also recorded in other glacial environments. Syvitski (1989) estimated that 70% of the sediment load may be deposited within 500 m off an ice front. In addition to the proximal mud deposition, the glaciated areas of Svalbard also supply IRD, which is found in somewhat higher concentrations in the surface sediments of the north-westernmost Barents Sea than in central and southern regions.

In more ice distal regions, comprising the main part of the Barents Sea, the most important sedimentary processes involve deposition from sea ice and winnowing from the shallow banks with redeposition of fines in troughs deeper than 200 - 250 m. Estimates of the sediment input indicate that approximately 50% of the surface sediments are transported in by sea ice, and that most of this originate on the Russian shelf (Elverhøi et al., 1989). Main winnowing agents are strong currents in the zone of the oceanic polar front, down-slope currents related to winter brine formation on the banks (Midttun, 1985) and tidal- and storm effects, particularly in the shallowest banks (Pfirman, 1985). In addition, iceberg gouging may enhance the resuspension of sediments on the banks, particularly in the northern areas, both in the gouging process proper, but also by creating a trough-and-berm topography, which may have relief of several meters, making the sea floor more vulnerable to winnowing. Present-day icebergs may reach depths of 120-130 m, although the majority if the icebergs have keel depths of less than 90 m (Elverhøi and Solheim, 1983b; Solheim et al., 1988b, Solheim, 1991).

Sedimentation rates

Based on ^{14}C ages in the Holocene sediments and extrapolation using lithological changes in the cores, Elverhøi et al. (1989) calculated average sedimentation rates for various areas of the northern Barents Sea. Average Holocene sedimentation rates for the major part of the region is 3-5 cm/ky. In the northernmost region the rates vary from 10-20 cm/ky, with the highest variation found in the proximity of the glaciated areas of north-eastern Svalbard. Locally, immediately off Nordaustlandet, average rates of 30 cm/ky may be found, but these are directly related to proximal and ice front processes (Solheim, 1991). Spitsbergenbanken and the shallow banks around Kong Karls Land and Kvitøya are characterised by net erosion.

Surface sediments

Three main classes of surface sediments are mapped in the northern Barents Sea; mud, diamicton (sandy, pebbly mud) and sand and gravel (Elverhøi and Solheim, 1983b; Elverhøi et al., 1989). The division between areas dominated by the different sediment types follows the bathymetry, to a large extent (Fig. 3). Over large areas, the 200 m contour defines the approximate boundary between mud (below) and diamicton (above). Deviations from this pattern are relatively common, however, and diamictons are for instance found down to 300 m water depth on the southern flank of Spitsbergenbanken, while fine grained mud is mapped to shallow depths north-east of Edgeøya (Fig. 3).

Sandy and gravelly lag deposits prevail on the shallow banks around the islands of Kong Karls Land and Kvitøya, and on Spitsbergenbanken. In the latter area, carbonate form the main constituent of the coarse grained deposits, which contain up to 90% shell fragments (Bjørlykke et al., 1978; Forsberg, 1983; Elverhøi et al., 1989). The fossil content of the sands and gravels on Spitsbergenbanken indicate a transition from soft-bottom conditions (*Mya truncata*) to hard-bottom conditions (barnacles) during the Holocene, possibly following shallowing caused by glacioisostatic rebound and winnowing by waves and currents (Bjørlykke et al., 1978). Side scan sonar data show ripples in carbonate sand on the sea floor of Spitsbergenbanken.

In the deeper parts of the Barents Sea, fine grained, olive grey mud prevails. The mud is generally homogeneous, bioturbated by polychaets and contains monosulphides at 15-20 cm sediment depth (Elverhøi and Bomstad, 1980). The muds get a more dark grey colour towards the north, and the content of dropstones also increases when approaching the glaciated regions of north-eastern Svalbard.

In general, the muds have a median diameter in the clay fraction, with the clay content increasing with depth. The diamictons have a median diameter in the medium-coarse silt fraction, and the clay content in these sediments appears depth independent.

Typical clay mineral assemblages form the northern Barents Sea surface sediments consist of illite, chlorite, kaolinite, smectite and random mixed-layer smectite-illite. With the exception of smectite, this assemblage is characteristic for most of the Mesozoic and Tertiary rocks of Svalbard, and for clasts found in Quaternary tills in the Barents Sea, probably reflecting the underlying bedrock (Elverhøi et al., 1988, Antonsen et al., 1991). Smectite on Svalbard is restricted to the early Cretaceous Helvetiafjellet formation in the eastern parts of the archipelago. Recent investigations have shown very high smectite contents in the sediments being discharged from the Russian rivers that drain into the Kara Sea (S. L. Pfirman, pers. commun., 1995). Transport with sea ice from this area, as well as from areas further east along the Russian Shelves (Forsberg, 1987) is not unlikely.

Non-clay minerals in the bulk <63 μm fraction are dominated by quartz and feldspars, but show large variations in particularly the calcite and dolomite content. These are mainly related to proximity to outcropping calcareous rocks of Carboniferous - Permian age, particularly in the north (Elverhøi et al., 1988).

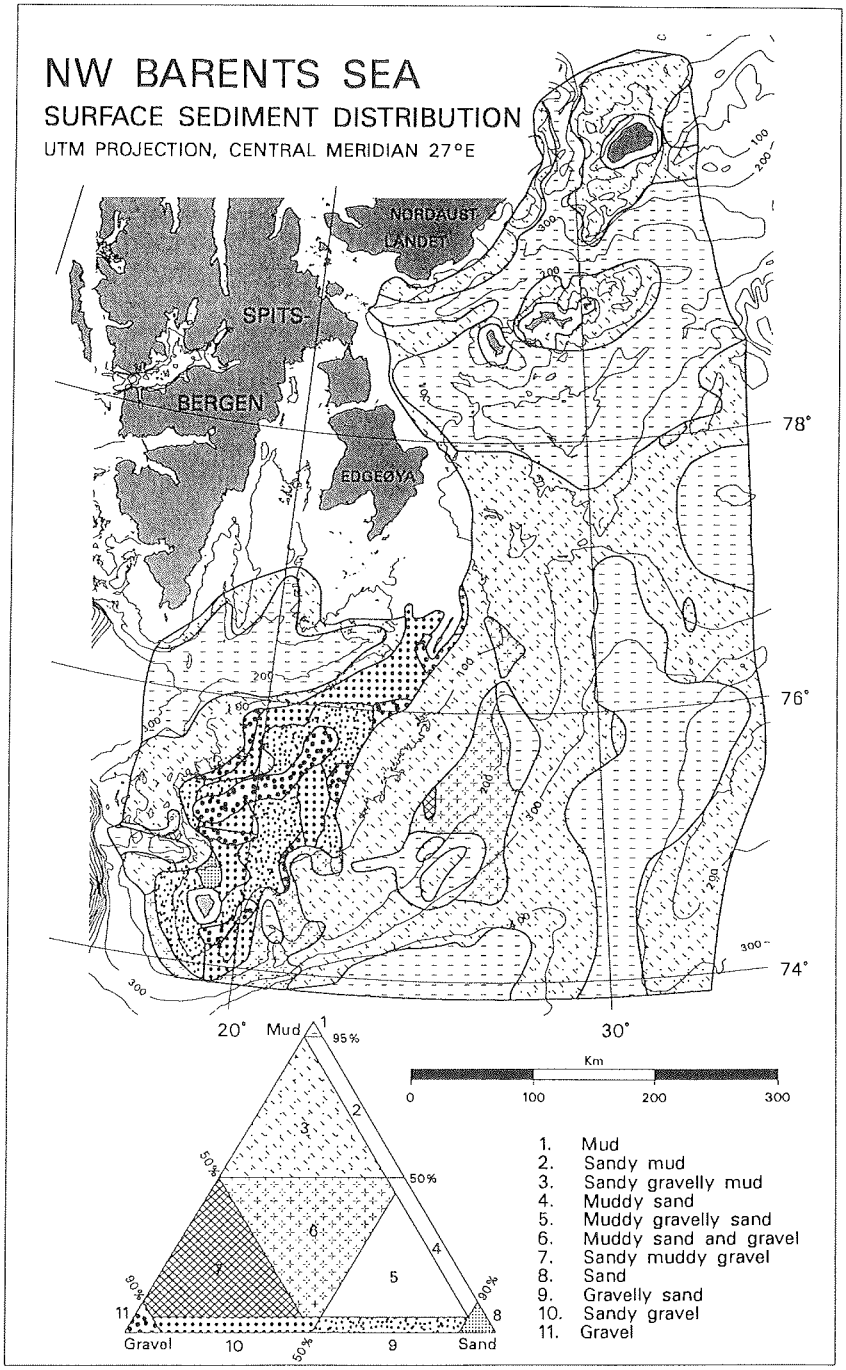

Fig. 3.: Map showing the surface sediment distribution in the northwestern Barents Sea. Note that in areas of poor core coverage (Fig.1), unpublished shipboard observations from the Norwegian Petroleum Directorate have been used as a supplement. Bathymetry in 100 meter contours. (Modified from Elverhøi and Solheim, 1983b).

Summary

The northern Barents Sea in general has a thin (< 15 μm) cover of unlithified sediments. The Holocene part of this sediment cover was deposited at rates varying from 3-5 cm/ky up to 30 cm/ky, locally. The most important Holocene and present-day processes include transport with and deposition from sea ice, as well as current- and wave related winnowing from the shallow areas with redeposition at depths greater than 200-250 meters. High rates of deposition takes place in the ice proximal environment, where suspended sediments are directly supplied from north-eastern Svalbard. The texture of the surface sediments reflect the processes, with primarily muds in the deeper areas and sandy- and gravelly lag deposits and diamictons dominating the shallower areas and the glacier proximal environment.

Acknowledgments

Terje Sundberg is acknowledged for preparing the maps and tables presented in this paper from the Norwegian Polar Institute marine geological data base. Carl Fredrik Forsberg kindly reviewed the manuscript prior to submission. This is the Norwegian Polar Institute contribution no. 297.

References

Antonsen, P, Elverhøi, A., Dypvik, H. and Solheim, A., 1991. Shallow bedrock geology of the Olga Basin area, north-western Barents Sea. A.A.P.G.Bull., 75, 1178-1194.

Bjørlykke, K., Bue, B. and Elverhøi, A., 1978. Quaternary sediments in the northwestern part of the Barents Sea and their relation to the underlying Mesozoic bedrock. Sedimentology, 25, 227-246.

Elverhøi, A. and Bomstad, K., 1980. Late Weichselian glacial and glaciomarine sedimentation in the western central Barents Sea. Norsk Polarinstitutt Rapportserie, 3, 29pp.

Elverhøi, A. and Solheim, A. 1983a. The Barents Sea ice sheet - a sedimentological discussion. Polar Research 1 n.s., 23-42.

Elverhøi, A. and Solheim, A., 1983b. The physical environment, Western Barents Sea; Surface sediment distribution. Norsk Polarinstitutt Skrifter, 179 A, 21pp.

Elverhøi, A. and Solheim, A., 1983c. Marin geologiske og -geofysiske undersøkelser i Barentshavet 1983 - Toktrapport. Norsk Polarinstitutt Rapportserie, 14, 116pp.

Elverhøi, A. and Solheim, A., 1987. Shallow geology and geophysics of the northern Barents Sea, (with special reference to possibilities for and detection of submarine permafrost). Norsk Polarinstitutt Rapportserie, 37, 68pp.

Elverhøi, A., Antonsen, P., Flood, B., Solheim, A. and Vullstad, A. A., 1988. The physical environment, western Barentrs Sea, 1:1.500.000, Shallow bedrock geology. Norsk Polarinstitutt Skrifter, 179 D.

Elverhøi, A., Pfirman, S. L., Solheim, A. and Larsen, B. B., 1989. Glaciomarine sedimentation in epicontinental seas exemplified by the northern Barents Sea. Marine Geology, 85, 225-250.

Elverhøi, A., Nyland-Berg, M., Russwurm, L. and Solheim, A., 1990. Late Weichselian ice recession in the central Barents Sea. In Bleil,U. and Thiede,J. (eds.) Geological history of the polar oceans: Arctic versus Antarctic. Kluwer Academic Publishers, The Netherlands, 289-307.

Elverhøi, A., Solheim, A., Nyland Berg, M. and Russwurm, L., 1992. Last interglacial-glacial cycle, Western Barents Sea. LUNDQUA Report vol.35, 17-24.

Elverhøi, A., Fjeldskaar, W., Solheim, A., Nyland Berg, M., and Russwurm, L., 1993. The Barents Sea Ice Sheet - a model of its growth and decay during the last maximum. Quaternary Science Reviews, 12, 863-873.

Forsberg, C.F., 1983. Sedimentation and early diagenesis of the late Quaternary deposits in the central Barents Sea. Unpubl. thesis, Univ. of Oslo, 120pp.

Forsberg, C.F., 1987. The Late Weichselian - Holocene transition in the Barents Sea: sedimentological and early diagenetic studies. Polar Research, 5 n.s., 289-290.

Jones, G.A. and Keigwin, L.D., 1988. Evidence from Fram Strait (78°N) for early deglaciation. Nature 336, 56-59.

Larssen, B.B., 1987. En sedimentologisk undersøkelse av pertikulært materiale i havis fra Framstredet, Arktis. Unpubl. Cand. Scient. thesis, Univ. of Oslo, 148pp.

Moum, J., 1966. falling drop used for grain size analysid of fine-grained materials. Norwegian Geotechnical Institute, Publ. 70.

Midttun, L., 1985. Formation of dense bottom water in the Barents Sea. Deep-Sea Research, 32, 1233-1241.

Nyland Berg, M., 1991. Sedimentologiske og geofysiske undersøkelser av sen-kenozoiske sedimenter på sydøstskråningen av Spitsbergenbanken, det nordlige Barentshav. Unpubl. Cand.scient. thesis, Univ. of Olso, 203pp.

Pfirman, S.L., 1985. Modern sedimentation in the northern Barents Sea: Input, dispersal and deposition of suspended sediments from glacial meltwater. Unpublished Ph.D.thesis, Woods Hole Oceanographic Institution and The Massachusetts Institute of Technology, 375pp.

Pfirman, S.L. and Solheim, A., 1989. Subglacial meltwater discharge in the open-marine tidewater glacier environment: Observations from Nordaustlandet, Svalbard Archipelago. Marine Geology, 86, 265-281.

Russwurm, L., 1990. Sedimentologiske og geofysiske undersøkelser av sen-kvartære sedimenter, nordlige Barentshav. Unpubl. Cand. scient. thesis, Univ. of Oslo, 182pp.

Solheim, A. and Kristoffersen, Y., 1984. The physical environment, Western barents Sea; Sediments above the upper regional unconformity: thickness, seismic stratigraphy and outline of the glacial history. Norsk Polarinstitutt Skrifter, 179B, 26pp.

Solheim, A.,Elverhøi, A. and Finnekåsa, Ø., 1988a. Marinegeophysical/geological cruise in the northern Barents Sea 1987 - Cruise report. Norsk Polarinstitutt Rapportserie, 43, 113 pp.

Solheim, A., Milliman, J.D. and Elverhøi, A., 1988b. Sediment distribution and sea floor morphology of Storbanken; Implications for the glacial history of the northern Barents Sea. Canadian Journal of Earth Sciences, 25, 547-556.

Solheim, A. and Elverhøi, A.,1990. Recent and Late Weichselian glacial geology of the northern Barents Sea. In: Kotlyakov,V.M. and Sokolov,V.E. (eds.) Arctic research: Advances and prospects. Proceedings of the

conference of Arctic and Nordic countries on coordination of research in the Arctic, Leningrad, December 1988, Part 2, Moscow, "Nauka", 44-55.

Solheim, A., Russwurm, L., Elverhøi, A. and Nyland Berg, M., 1990. Glacial geomorphic features: direct evidence for grounded ice in the northern Barents Sea and implications for the pattern of deglaciation and late glacial sedimentation. Geological Society of London, Special Publication. 53,253- 268.

Solheim, A., 1991.The depositional environment of surging sub- polar tidewater glaciers: A case study of the morphology, sedimentation and sediment properties in a surge-affected marine basin outside Nordaustlandet, northern Barents Sea. Norsk Polarinstitutt Skrifter, no.194, 97pp

Syvitski, J.P.M., 1989. On the deposition of sediment within glacier-influenced fjords: Oceanographic controls. Marine Geology, 85, 301-330.

Vorren, T. O. and Kristoffersen, Y., 1986. Late Quaternary glaciation in the south-western Barents Sea. Boreas, 15, 51-59.

Vorren, T. O., Hald, M. and Lebesbye, E., 1988. Late Cenozoic environments in the Barents Sea. Paleoceanography, 3, 601-612.

Vorren, T.O., Lebesbye, E., Andreassen, K. and Larsen, K.B., 1989. Glasigenic sediments on a passive continental margin, as exemplified by the Barents Sea. Marine Geology, 85, 251-272.

Wensaas, L., 1986. Sedimentologiske og sedimentpetrografiske studier av kvartære sedimenter i det nordlige Barentshav. Unpubl. Cand. Scient. thesis, Univ. of Oslo, 178pp.

Appendix

Table 1.: Core locations from which grain size analyses (GRZ) have been performed in the upper 10 cm of the sediment. A x under XRD marks that Xray diffraction analysis has been performed for either the bulk <63m fraction, the <2m fraction or both, also in the upper 10 cm of the core.

Station	Position		Water depth	GRZ	XRD
	North	East	(m)		
NP71_4	74° 03.00'	21° 06.96'	310	x	x
NP71_12	74° 19.26'	25° 07.98'	370	x	x
NP71_14	74° 20.46'	23° 33.00'	231	x	x
NP71_16	74° 22.68'	22° 04.98'	196	x	x
NP71_20	74° 22.98'	19° 42.96'	73	x	x
NP71_30	74° 38.46'	25° 03.96'	260	x	x
NP71_35	74° 29.58'	18° 30.30'	60	x	x
NP71_37	74° 43.20'	19° 03.48'	114	x	x
NP71_39	74° 41.76'	20° 21.96'	73	x	x
NP71_41	74° 34.80'	21° 28.98'	130	x	
NP71_56	75° 01.38'	21° 42.96'	55	x	x
NP71_58	75° 05.88'	22° 55.98'	100	x	x
NP71_62	75° 13.26'	20° 59.88'	50	x	x
NP71_66	75° 04.86'	17° 48.00'	105	x	x
NP71_68	75° 17.88'	18° 41.46'	35	x	x
NP71_72	75° 26.28'	21° 28.98'	34	x	x
NP71_80	75° 39.00'	23° 15.96'	68	x	x
NP71_81	75° 39.48'	22° 23.46'	58	x	
NP71_86	75° 30.48'	19° 09.00'	62	x	x
NP71_90	75° 34.08'	18° 23.40'	124	x	x
NP71_92	75° 41.76'	21° 07.38'	50	x	x
NP71_93	75° 45.96'	20° 52.50'	30	x	x
NP71_96	75° 51.78'	22° 18.00'	46	x	x
NP71_98	75° 56.76'	23° 42.96'	47	x	
NP71_99	75° 59.16'	24° 32.46'	70	x	x
NP71_100	76° 11.16'	25° 06.00'	72	x	x
NP71_102	76° 14.46'	24° 01.98'	55	x	
NP71_107	76° 12.48'	22° 01.98'	87	x	x
NP71_115	76° 27.48'	22° 34.98'	176	x	x
NP71_126	75° 40.20'	17° 39.90'	192	x	x
NP71_132	76° 04.86'	20° 12.96'	146	x	x
NP71_139	76° 33.00'	20° 13.98'	172	x	x
NP71_152	76° 25.68'	17° 47.76'	215	x	x
NP71_155	75° 55.38'	17° 06.66'	306	x	x
NP71_166	76° 52.20'	20° 08.10'	132	x	x
NP71_170	76° 42.18'	25° 06.00'	30	x	x
NP77_13	73° 39.36'	19° 46.92'	416	x	
NP77_14	73° 38.34'	20° 24.36'	495	x	
NP77_15	73° 47.88'	20° 15.18'	370	x	

Station	Position		Water depth	GRZ	XRD
	North	East	(m)		
NP77_29	73° 44.46'	20° 51.06'	493	x	
NP77_30	73° 48.78'	21° 02.10'	465	x	
NP77_38	73° 49.80'	21° 15.12'	499	x	
NP77_39	73° 48.54'	21° 15.18'	504	x	
NP77_44	74° 19.98'	20° 46.98'	206	x	
NP77_48	74° 44.22'	18° 05.04'	270	x	
NP77_49	74° 50.58'	17° 49.98'	326	x	
NP77_54	74° 51.54'	16° 06.84'	387	x	
NP80_7	75° 19.08'	29° 01.44'	335	x	x
NP80_10	75° 33.90'	27° 30.72'	225	x	x
NP80_13	75° 34.50'	30° 00.54'	450	x	x
NP80_14	75° 50.22'	30° 04.56'	310	x	x
NP80_15	76° 05.46'	29° 59.16'	310	x	x
NP80_16	76° 19.32'	30° 00.78'	280	x	x
NP80_17	76° 34.86'	29° 56.46'	280	x	x
NP80_19	77° 00.54'	30° 01.68'	230	x	x
NP80_22	77° 02.52'	27° 18.54'	140	x	
NP80_23	77° 01.44'	28° 01.62'	160	x	x
NP80_29	78° 01.92'	28° 44.88'	300	x	x
NP80_30	78° 02.04'	27° 41.16'	230	x	x
NP80_31	78° 01.50'	26° 25.80'	175	x	x
NP80_32	78° 01.02'	25° 26.76'	135	x	x
NP80_36	78° 42.36'	23° 39.84'	125		x
NP80_37	78° 44.70'	24° 26.58'	150	x	x
NP80_38	78° 47.04'	25° 23.52'	120	x	x
NP80_39	78° 51.42'	26° 09.78'	107	x	x
NP80_44	78° 49.26'	30° 00.30'	130	x	
NP80_45	78° 44.28'	30° 02.58'	125	x	
NP80_46	78° 38.94'	29° 47.82'	230	x	
NP80_48	78° 28.86'	29° 58.56'	280	x	x
NP80_50	78° 09.18'	30° 01.98'	325	x	x
NP80_52	77° 59.64'	32° 03.00'	200	x	x
NP80_53	78° 00.12'	32° 57.90'	125	x	x
NP80_55	78° 12.66'	34° 29.16'	250	x	
NP80_56	78° 23.04'	34° 32.40'	100	x	
NP80_57	78° 34.74'	34° 25.14'	210	x	
NP80_58	78° 48.24'	34° 30.66'	330	x	
NP80_59	79° 00.60'	34° 33.12'	305	x	
NP80_60	79° 00.60'	33° 22.02'	345	x	
NP80_62	79° 00.12'	30° 59.64'	225	x	
NP80_64	79° 15.78'	29° 53.10'	320	x	
NP80_65	79° 10.92'	30° 30.60'	85	x	
NP80_66	79° 09.06'	23° 39.42'	80	x	x
NP80_67	79° 06.24'	23° 40.98'	80	x	x
NP80_69	79° 00.36'	23° 40.44'	135	x	x
NP80_71	78° 52.38'	24° 00.84'	178	x	x

Station	Position		Water depth	GRZ	XRD
	North	East	(m)		
NP80_84	79° 24.30'	29° 58.92'	320	x	x
NP80_85	79° 34.26'	30° 02.40'	250	x	x
NP80_86	79° 47.40'	29° 59.46'	142	x	x
NP80_87	79° 59.46'	30° 06.30'	255	x	x
NP80_88	80° 10.74'	30° 01.14'	275	x	x
NP80_89	80° 20.94'	30° 21.06'	275	x	x
NP80_90	80° 29.76'	30° 28.86'	225	x	x
NP80_91	80° 40.50'	30° 14.22'	295	x	
NP80_93	80° 30.00'	32° 04.08'	140	x	
NP80_101	80° 48.48'	33° 03.24'	170	x	
NP80_102	80° 48.66'	33° 19.74'	170	x	
NP80_104	80° 43.80'	34° 31.62'	180	x	
NP80_105	80° 34.68'	34° 50.82'	149	x	x
NP80_106	80° 31.50'	34° 03.60'	165	x	x
NP80_107	80° 25.02'	33° 56.76'	185	x	x
NP80_108	80° 21.72'	34° 45.42'	275	x	
NP80_109	80° 12.96'	34° 00.30'	260	x	
NP80_111	80° 08.34'	34° 26.34'	215	x	
NP80_112	79° 59.28'	34° 05.88'	197	x	x
NP80_113	79° 50.04'	34° 28.98'	214	x	
NP80_114	79° 39.06'	34° 33.60'	340	x	
NP80_115	79° 30.42'	34° 29.40'	300	x	
NP80_116	79° 20.10'	34° 33.18'	262	x	
NP80_118	79° 30.60'	33° 36.96'	280	x	x
NP80_119	79° 29.94'	33° 32.04'	307	x	x
NP80_121	79° 29.16'	30° 35.40'	175	x	
NP80_124	79° 30.96'	29° 14.94'	330	x	x
NP80_125	79° 31.50'	28° 20.46'	330	x	
NP80_126	79° 30.00'	27° 51.24'	285	x	x
NP80_127	79° 29.40'	26° 58.14'	130	x	x
NP80_128	80° 01.26'	29° 30.12'	265	x	x
NP80_131	79° 59.88'	31° 17.16'	115	x	x
NP80_134	77° 40.50'	34° 29.52'	165	x	
NP80_137	77° 15.60'	34° 30.54'	125	x	x
NP80_140	74° 51.96'	33° 08.46'	162	x	x
NP81_136	79° 08.16'	23° 34.74'	109	x	
NP81_216	79° 11.22'	22° 55.68'	81	x	
NP82_224	79° 18.42'	22° 37.98'	21	x	
NP82_225	79° 18.24'	22° 34.86'	36	x	x
NP82_226	79° 18.48'	22° 35.34'	36	x	x
NP82_229	79° 09.18'	22° 57.72'	55	x	x
NP82_230	79° 12.66'	23° 07.44'	81	x	x
NP82_231	79° 13.38'	23° 05.34'	83	x	x
NP82_232	79° 11.64'	23° 47.10'	82	x	x
NP82_233	79° 10.68'	23° 47.22'	101	x	x

Station	Position		Water depth (m)	GRZ	XRD
	North	East			
NP82_234	79° 09.72'	23° 43.92'	79	x	x
NP82_235	79° 09.00'	23° 37.20'	106	x	x
NP82_237	79° 02.40'	23° 32.88'	105	x	x
NP82_239	79° 09.84'	23° 54.84'	87	x	x
NP82_241	79° 13.20'	22° 53.52'	57	x	x
NP82_253	78° 55.26'	22° 10.44'	124	x	x
NP82_317	78° 55.44'	25° 46.14'	142	x	x
NP82_320	78° 53.88'	23° 44.10'	181	x	x
NP82_321	79° 00.48'	23° 04.56'	99	x	x
NP82_323	79° 15.24'	22° 45.24'	39	x	x
NP82_324	79° 14.52'	22° 47.82'	43	x	
NP82_326	79° 14.70'	22° 48.24'	45	x	
NP82_327	79° 15.18'	22° 44.22'	44	x	x
NP83_20	75° 33.48'	34° 13.98'	174	x	
NP83_21	75° 43.98'	34° 22.98'	191	x	
NP83_23	76° 49.50'	34° 02.58'	130	x	
NP83_24	76° 44.10'	34° 01.20'	127	x	
NP83_25	77° 00.06'	33° 48.66'	165	x	
NP83_26	79° 11.46'	23° 58.56'	70	x	
NP83_27	79° 10.86'	23° 58.80'	75	x	
NP83_28	79° 10.08'	23° 56.88'	73	x	
NP83_29	79° 08.46'	23° 57.96'	91	x	x
NP83_31	79° 11.58'	23° 22.50'	92	x	
NP83_34	79° 12.48'	23° 06.18'	78	x	
NP83_35	79° 11.70'	23° 03.60'	96	x	
NP83_37	79° 12.00'	23° 12.78'	57	x	
NP83_38	79° 14.40'	22° 48.90'	42	x	
NP83_39	79° 13.26'	22° 46.26'	43	x	
NP84_1	78° 55.26'	26° 21.06'	102	x	
NP84_2	78° 54.96'	26° 08.64'	110	x	
NP84_3	79° 00.90'	26° 13.44'	168	x	
NP84_4	78° 59.82'	25° 58.14'	172	x	
NP84_5	78° 58.14'	25° 38.46'	182	x	
NP84_6	79° 04.02'	25° 29.46'	219	x	
NP84_7	79° 07.26'	25° 45.84'	220	x	
NP84_8	79° 06.12'	26° 20.82'	232	x	
NP84_9	79° 07.38'	26° 20.34'	246	x	
NP84_10	79° 06.72'	26° 20.52'	260	x	
NP84_11	79° 03.90'	25° 58.32'	225	x	x
NP84_13	79° 08.64'	25° 57.12'	248	x	x
NP84_14	79° 13.92'	26° 12.18'	266	x	
NP84_15	79° 13.92'	26° 12.18'	212	x	
NP84_16	79° 15.30'	25° 27.90'	124	x	x
NP84_17	79° 18.54'	25° 36.42'	112	x	x
NP84_18	79° 22.62'	25° 56.16'	128	x	x

Station	Position		Water depth	GRZ	XRD
	North	East	(m)		
NP84_19	79° 17.58'	25° 56.10'	90	x	
NP84_20	79° 24.66'	26° 10.92'	68	x	
NP85_1	78° 49.14'	21° 52.20'	50	x	
NP85_2	78° 49.62'	21° 56.28'	60	x	
NP85_3	78° 49.98'	22° 04.20'	71	x	
NP85_4	78° 50.40'	22° 08.28'	90	x	
NP85_5	78° 50.88'	22° 15.96'	110	x	
NP85_6	78° 51.90'	22° 31.32'	125	x	
NP85_7	78° 53.10'	22° 54.30'	141	x	
NP85_8	78° 54.90'	23° 27.48'	155	x	
NP85_9	78° 55.32'	23° 37.80'	170	x	
NP85_10	78° 57.24'	24° 10.68'	185	x	
NP85_11	78° 57.72'	24° 19.74'	200	x	
NP85_12	78° 58.26'	24° 31.50'	215	x	
NP85_13	79° 10.98'	23° 28.08'	91	x	
NP85_14	79° 08.10'	23° 32.10'	109	x	
NP85_15	79° 03.00'	23° 36.12'	105	x	
NP85_16	78° 59.58'	23° 40.02'	134	x	
NP85_17	78° 51.36'	23° 50.88'	178	x	
NP85_18	78° 51.60'	24° 13.14'	168	x	
NP85_19	78° 51.90'	24° 50.04'	164	x	
NP85_20	79° 00.06'	24° 53.46'	216	x	
NP85_21	79° 03.36'	24° 25.80'	158	x	
NP85_22	79° 04.92'	24° 53.16'	180	x	
NP85_23	79° 12.72'	24° 40.02'	134	x	
NP85_25	79° 18.48'	24° 52.44'	52	x	
NP85_26	78° 50.88'	23° 30.42'	153	x	x
NP85_28	79° 01.02'	25° 04.98'	218	x	x
NP85_29	79° 08.58'	24° 50.58'	157	x	x
NP87_18	74° 36.93'	23° 00.53'	122	x	
NP87_20	75° 07.35'	24° 43.94'	148	x	
NP87_23	75° 17.08'	24° 18.55'	140	x	
NP87_25	75° 17.59'	25° 25.88'	191	x	

BULK MINERALOGY IN SURFACE SEDIMENTS FROM THE EASTERN CENTRAL ARCTIC OCEAN

Vogt, C.

Alfred Wegener Institute, Bremerhaven, Germany

Abstract

This study focusses on the investigation of surface sediments collected during the international ARCTIC´91 and ARCTIC´93 expeditions with RV "Polarstern" to the Eurasian Basin of the Arctic Ocean and the adjacent slopes of the Barents, Kara and Laptev Seas. The bulk mineralogy of surface samples was evaluated to study the distribution of quartz, calcite, dolomite, and feldspars with respect to transport mechanisms, source areas, and sedimentation processes.

Introduction

The dissimilarities of the western and eastern coastal and shelf regions of the Arctic Ocean and their hinterland as well as the different dominant transport mechanisms (e.g. eolian, fluvial, ice, gravitational or current transport) should lead to detectable differences in the sedimentological record through space and time. This study focusses on the mineral assemblages in the Central Arctic Ocean surface sediments and their implications on transport processes and source areas. In 1991 the international ARCTIC´91 (ARK-VIII/3) expedition (Fütterer, 1992) collected a unique sample set in the Eurasian Basin, while in 1993 RV "Polarstern" performed a sampling program on the northern Barents Sea slope east of Svalbard and in the Kara and Laptev Sea (ARCTIC'93 / ARK-IX/4, Fütterer, 1994). Mineralogical data of 126 surface sediment samples (Table 1, Appendix; Fig. 1) are presented to describe the distribution of certain minerals in relation to the present sedimentation regime. The oceanographic circulation of the Eurasian Basin is dominated by the northeast-southwest Transpolar Drift that transports huge amounts of sea ice from the Siberian shelves to the Fram Strait, and the influx of warmer water of Atlantic origin around north Svalbard by the West Spitsbergen Current. Mid depth and bottom currents influence especially the Gakkel and Lomonosov Ridge regions (Anderson et al., 1994). Gravitational transport is active on the continental slopes surrounding the deep sea basin (Fütterer, 1994; Stein et al., 1994)

At present the Eurasian Arctic basin is predominantly covered by sea-ice which is produced in the Laptev Sea area (Nürnberg et al., 1994 and references therein). During this process shelf sediment is incorporated and transported via the Transpolar Drift to the main ablation areas in Fram Strait and Greenland Sea. Sea-ice sediments color the ice and influence the albedo and consequently the heat budget of the Arctic region. Thus, the amount of sediment entrained into sea-ice is one important factor influencing the Arctic system which is crucial to global climate. Sediments of the Laptev and Kara

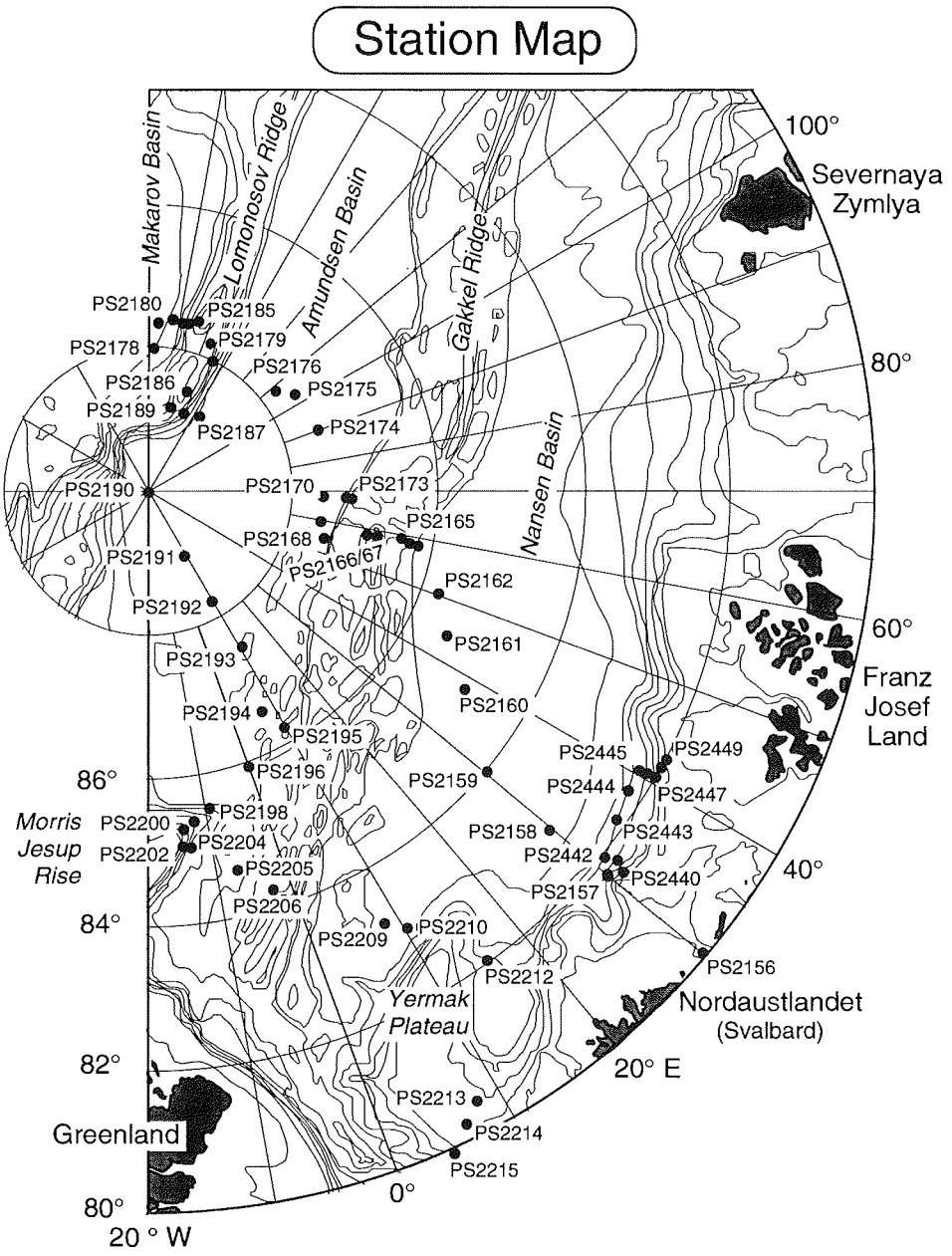

Fig.1.: Station map of investigated surface samples of the ARK VIII/3 and ARK IX/4 expeditions in the Eurasian Basin.

Sea shelf that are main areas of sea-ice formation contain very high amounts of the clay mineral smectite (up to 70 %, Wahsner and Shelekova, 1994) which was also found in sea ice sediments (max. 40-60 %, Wollenburg, 1993, Nürnberg et al., 1994). The sea ice sediments and the Laptev Sediments are also rich in quartz which is a main constituent in Eurasian Basin sediments (Lapina, 1965; Wollenburg, 1993; Stein and Korolev, 1994; Vogt et al., 1994).

The occurrence of dolomite and detrital calcite in glacial deposits of the Arctic Ocean can be related to local source areas of Proterozoic and Paleozoic platform carbonates of the Alaskan and the Canadian Arctic (Darby et al., 1989; Bischof et al., subm.). From these regions, sometimes very coarse detrital particles ("dropstones") are transported by icebergs into the central Arctic Ocean (Clark et al., 1980, Darby et al., 1989). Distribution variations of these minerals may thus help to reconstruct intensity, source areas and transport paths of icebergs in the eastern Central Arctic Ocean revealing changes in the Beaufort Gyre-Transpolar Drift surface current system and/or the intensity of iceberg-production by the North American and Greenland ice shields.

The northern Barents Sea slope is influenced by gravitational downslope transport into the Nansen Basin. Surface sediments in this area of the basin reveal higher kaolinite contents linkable to Franz-Josef-Land source regions (Stein et al., 1994; Nürnberg et al., 1995). On the other hand Canadian source regions could deliver kaolinite together with quartz through glacial erosion of ancient sand-, silt- and claystones to the Alpha Ridge, Canada Basin (Dalrymple and Maass, 1987) adjacent to the Eurasian Basin.

Methods and sampling

Bulk ground multicorer (MUC) and giant box corer (GKG) samples were measured with a Phillips PW 1710 X-ray diffractometer (Arctic´91 samples) and a Phillips PW 1830 (Arctic'91 GKG and Arctic´93 samples). To evaluate the bulk mineralogy, unoriented non-textural specimens and pressed powder pellets, respectively, were prepared. They were measured with a cobalt ka-radiation from 2 to 100° 2Q with a 0.02 step/ 1 sec mode. All mineral contents are expressed as percent of bulk sediment. The quartz content was determined by using the Qualit software package (Emmermann and Lauterjung, 1990). The dolomite content equals the peak intensity of 2.89 Å-peak divided by the sum of calcite (3.03 Å) and dolomite (2.89 Å) peak intensities times the carbonate content (Stein et al., 1994; Stein, this vol.). The dolomite percentages were additionally cross-checked applying the Qualit software package. The calcite content is calculated as carbonate minus dolomite content assuming that other carbonate minerals are of minor importance. To gain information about feldspar contents the quartz/feldspar-ratio (Qz/Fsp) was calculated by dividing the intensity area of the quartz 4.26 Å-peak by the sum of the feldspar 3.18 and 3.24 Å-peak intensity areas.

Results and Discussion

In Figure 2, the quartz content distribution in the Eurasian Basin is shown. Quartz contents range from 14% (PS2160) to 81% (PS2480), Qz/Fsp-ratios

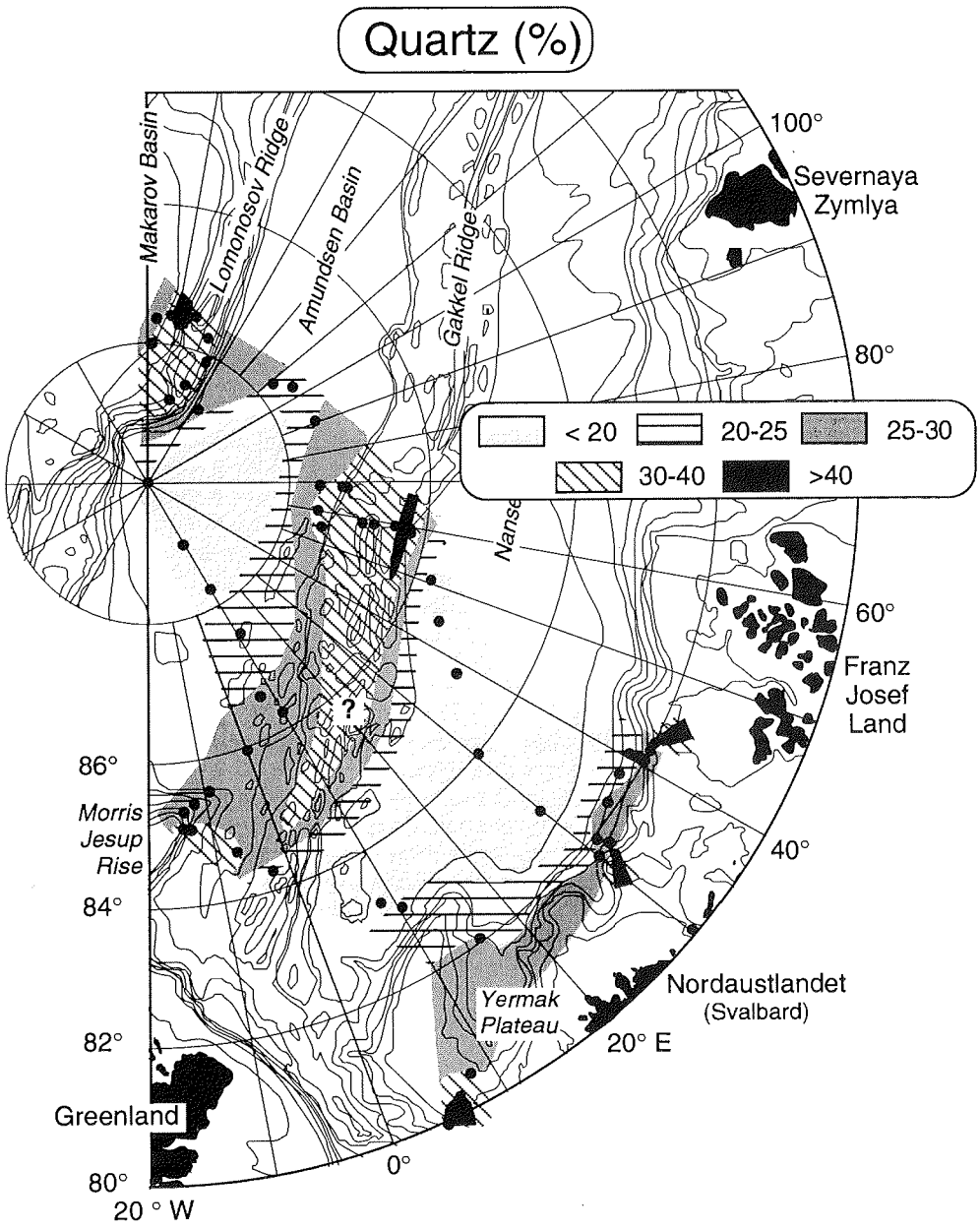

Fig.2.: Distribution map of quartz content in surface sediments in the Eurasian Basin.

from 0.23 (PS2212-5) to 0.82 (PS2449). At several stations MUC and GKG samples were investigated revealing some differences especially of the quartz content between surface samples of the same station. Regarding the changing positions during station work (Table 1, Appendix), one can deduce the patcheness of Arctic Ocean sediments. Despite these observations many MUC and GKG samples of a particular station show very similar mineral contents. The highest amounts of quartz can be found on the Eastern Gakkel Ridge, on the Lomonosov Ridge, at two stations on the outer Barents Sea shelf, and in the vicinity of Severnaya Zemlya in the Western Laptev Sea. As Figure 3 reveals, the high quartz contents are related to higher amounts of coarse material in these regions. The silty clay sediments of the Nansen and Amundsen Basin yield very small coarse fraction contents (Fig. 3, c.f. Stein et al., 1994), and the quartz percentage is also low. At the Lomonosov Ridge and the Eastern Gakkel Ridge high bottom current speeds were measured (Anderson et al., 1994). Hence, winnowing of the fine fraction may have resulted in increased quartz values in the residual sediment. Although the Morris Jesup Rise and the slope of the Yermak Plateau show high coarse fraction contents medium amounts of quartz (25-35%) were recorded. At the Morris Jesup Rise it is even lower than in the adjacent basins (Fig. 2). The sedimentation at the stations of the western transect seemed to be influenced by some other transport processes.

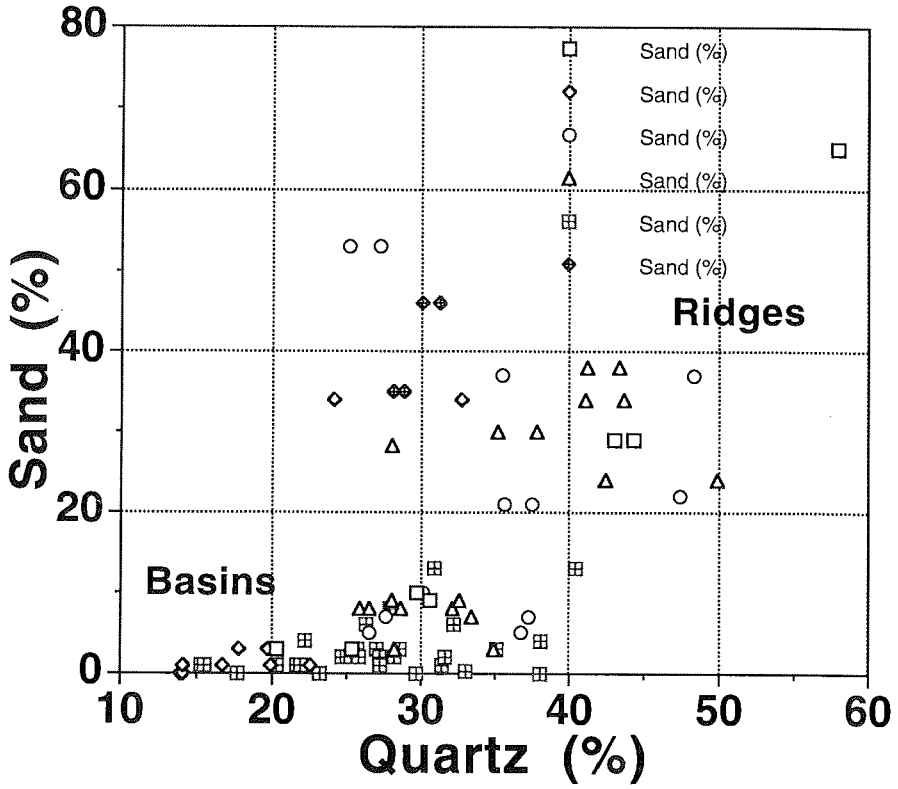

Fig.3.: Plot of quartz content (% bulk sample) vs. sand content (% fraction > 63 µm, carbonate-free samples; Stein et al., 1994, PS24** unpubl. data, Wahsner) of Eurasian Basin samples.

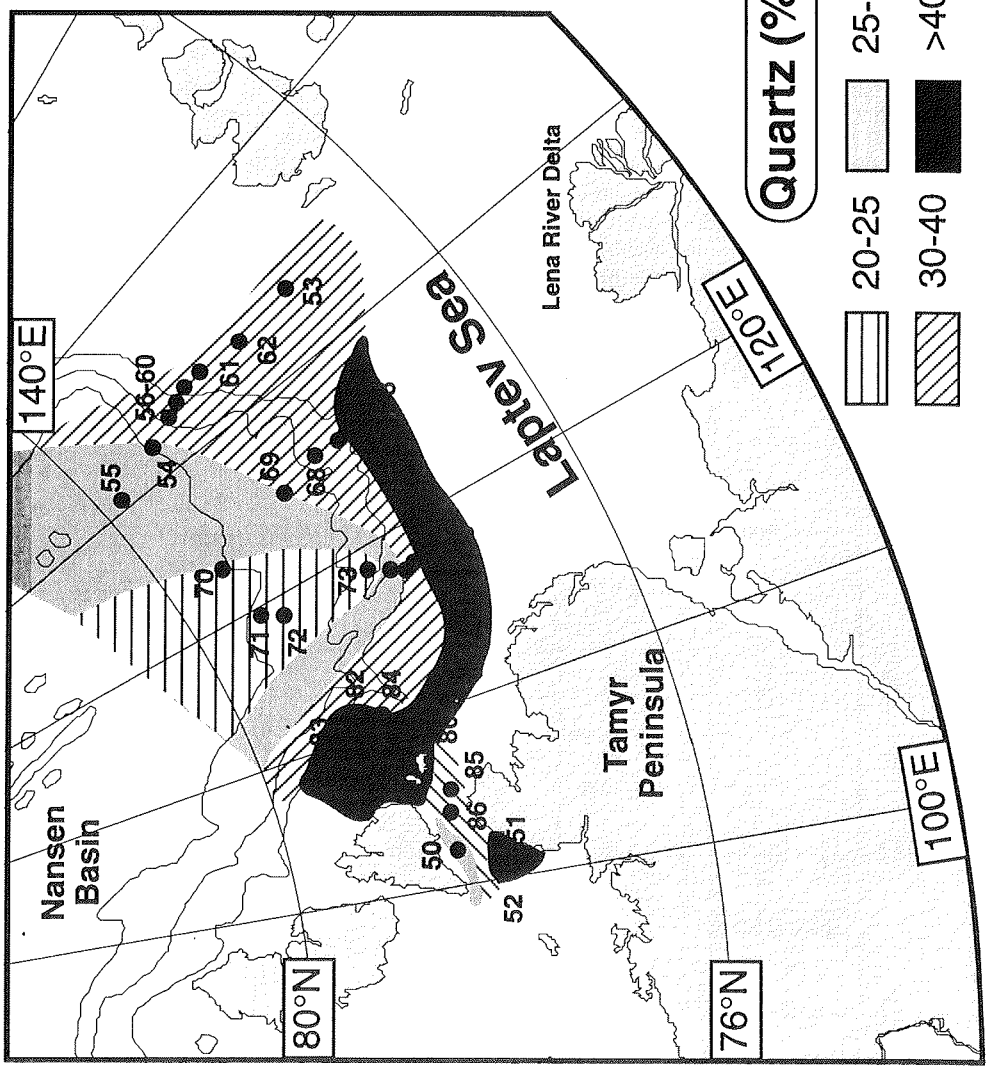

Fig.4.: Distribution map of quartz content in surface sediments of the Laptev Sea shelf and continental slope area (station numbers PS24**, c.f. Fütterer, 1994).

First measurements of Laptev Sea slope sediments express a deminishing of the quartz content towards the deep Nansen Basin (Table 2, Appendix; Fig. 4, about 40% at the upper slope and outer shelf to 25-30% in the deep Nansen Basin). This is probably related to a decreasing transport energy of downslope movement (cf., Selley, 1988).

Similar to quartz, the Qz/Fsp ratio increases to greater than 0.5 values on the eastern Gakkel Ridge and the Lomonosov Ridge. The Qz/Fsp ratio of sediments not influenced by ridge top sediment processes in these regions, is usually below 0.5 (Table 1, Appendix) showing a relatively high influx of feldspar minerals. The area between Morris Jesup Rise and Yermak Plateau is characterized by higher Qz/-Fsp-ratios above 0.5. Although the absolute quartz content is lower than at the eastern transect, the feldspar contents appear even lower, resulting in higher QZ/Fsp ratios. The northern Barents Sea slope reveals the lowest Qz/Fsp-ratios, which may indicate a comparatively high input of feldspar from the Barents Sea shelf region into the Nansen Basin.

Calcite values range from 0 (PS2160) to 25% (PS2202), with highest amounts on the Morris Jesup Rise and the Yermak Plateau (Table 1, Appendix; Fig. 5). The deep-sea basins reveal the lowest calcite contents. The Laptev Sea continental slope yields only minor amounts of carbonates (0-2%; Stein, this vol.), mainly constituted of dolomite.

High dolomite contents (between 3 and 17%, Fig. 6, Table 1, Appendix) are measured in the sediments of the northernmost region including the Lomonosov Ridge, the Morris Jesup Rise, and the part of the Amundsen Basin between both ridges. All other investigated samples yield dolomite contents between 0 and 3 %. The highest dolomite value of 17% at station PS2181 was mainly produced by carbonate dropstones in the surface sediment. The XRD-measurement of some carbonate dropstones of this surface sediment (kindly provided by N. Nørgaard-Petersen, GEOMAR) revealed a dolomite content of 80-85% with some minor amounts of calcite, quartz, and clay minerals. Dolomite joined by terrigenous calcite can also be observed in the fine fraction of these sediments (Vogt and Stein, 1994). Dalrymple and Maass (1987) relate these fine grained terrigenous carbonates to the grinding process of glaciers in soft sediments of the Canadian Arctic like the Paleozoic platform carbonates.

In Figures 5 and 6 the distribution of calcite and dolomite contents illustrate two important processes in the Eurasian Basin. While high dolomite contents in the northernmost surface sediments can be clearly correlated to dropstone sedimentation in this region, the high amounts of calcite in the Yermak Plateau area mirror the influx of warm North Atlantic surface waters that keep open-water conditions and trigger higher production of carbonate shells and tests (Stein et al., 1994). The distribution of high dolomite values does not only correlate to the grain size distribution but is also restricted to the northernmost regions of the study area including the Morris Jesup Rise. Hence, it indicates the input of detrital carbonate which presumably derived from the Canadian Arctic region. According to Darby et al. (1989) and Bischof et al. (subm.) the Canadian Arctic is the source region for this material. A minor increase of dolomite content can be sighted at the Barents Sea slope between Svalbard and Franz Josef Land. Regarding the abundance of rechristallized Upper

Paleozoic age carbonates in the North and Northeast of Svalbard (Winjes, 1988; Sigmond, 1992) and the present oceanographic setting (Anderson et al., 1994) these carbonates should originate from Svalbard and adjacent shelf regions (cf., Solheim and Elverhoi, this vol.).

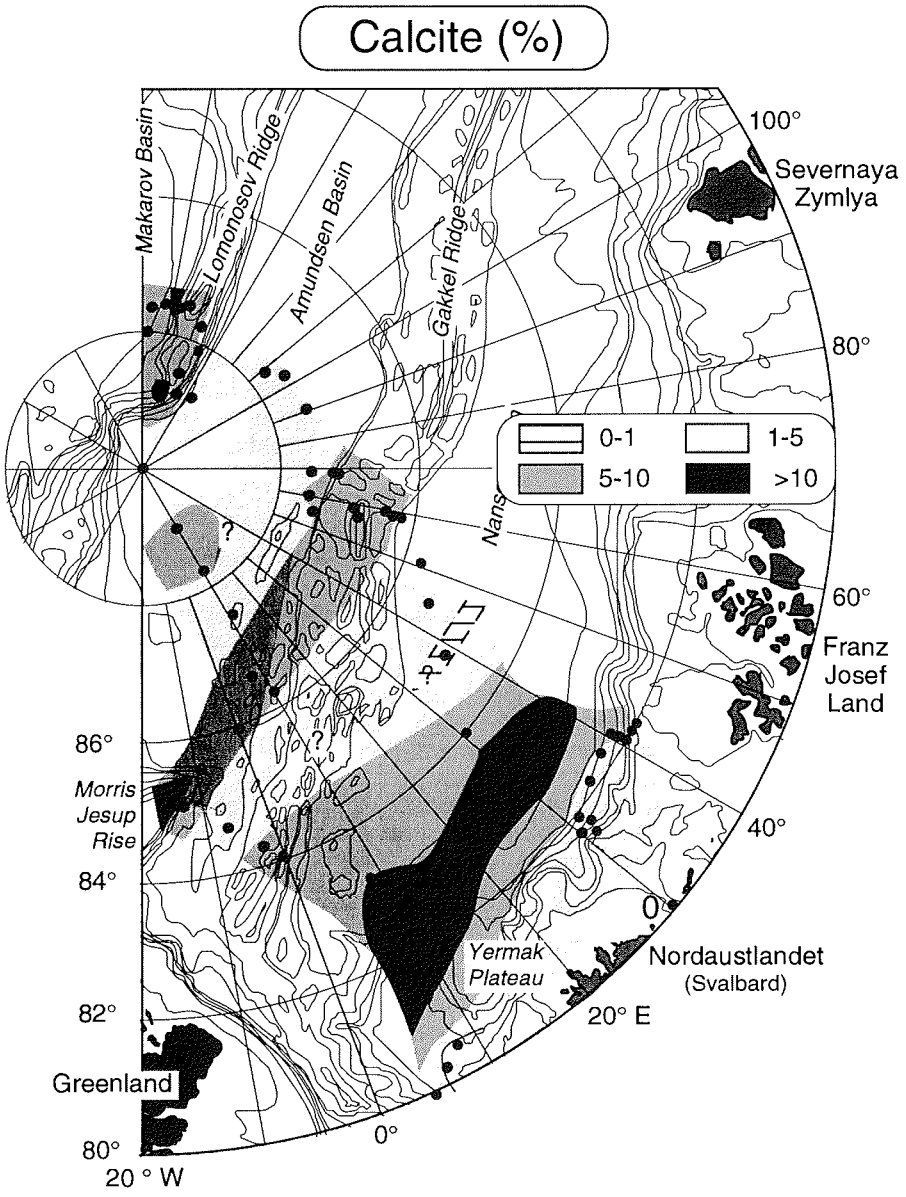

Fig.5.: Distribution map of calcite content in surface sediments in the Eurasian Basin.

The high calcite values of the Morris Jesup Rise (up to 25%, PS2202) and Lomonosov Ridge areas (max. 11%, PS2182) can partly be related to dropstone deposition. In the Morris Jesup Rise sediments, plenty of carbonate dropstones were found (pers. comm. N. Nørgaard-Petersen, 1994). Despite the terrigenous input, higher amounts of calcitic test were observed on the Lomonosov Ridge (e.g., benthic foraminifera; Wollenburg, 1995) indicating an increased productivity and/or transport from the Siberian shelves. Wollenburg (1995) found an increased amount of (sea)ice-rafted shallow water benthic foraminiferas.

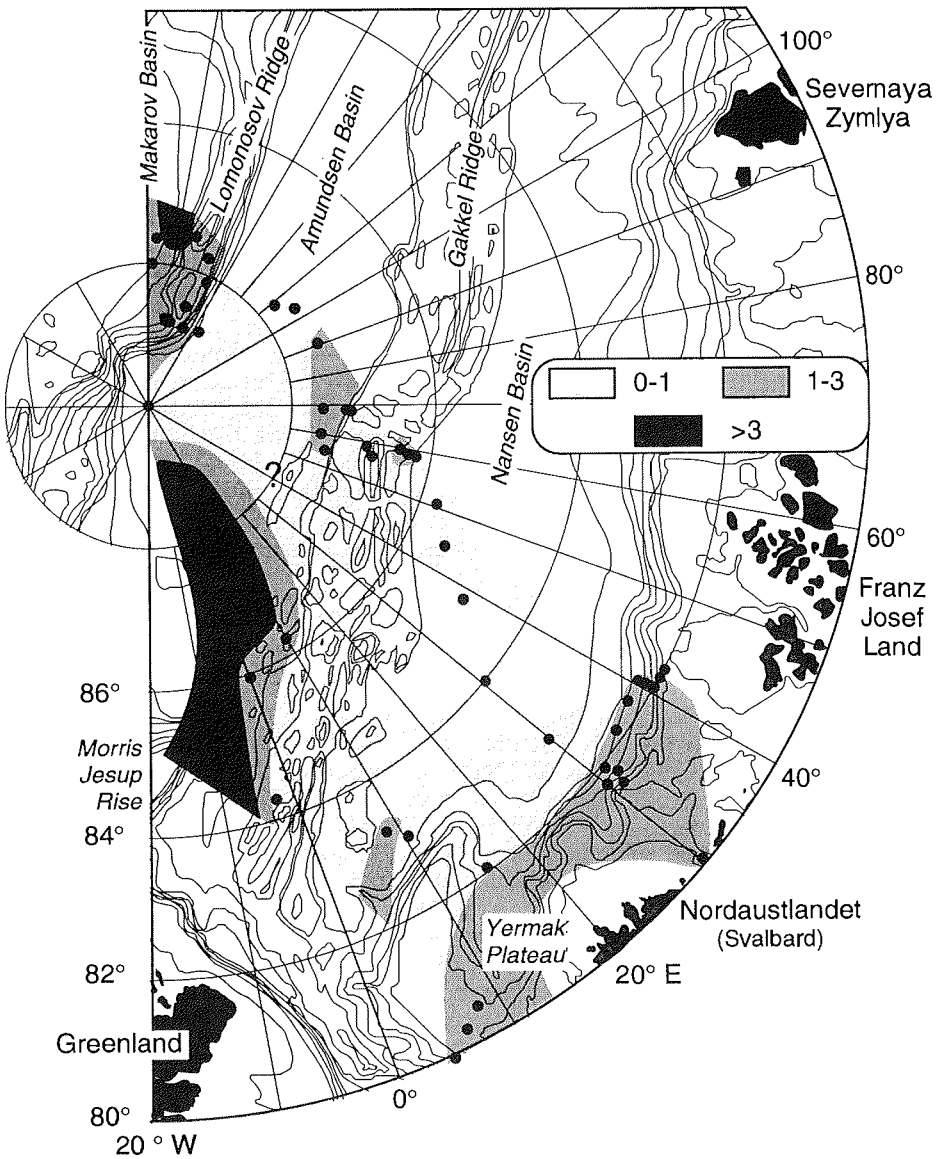

Fig.6.: Distribution map of dolomite content in surface sediments in the Eurasian Basin.

In the Yermak Plateau area high calcite contents (17%, PS2210; 11%, PS2212) occur together with higher amounts of calcitic shells (Stein et al., 1994; Wollenburg, 1995). The occurrences reflect higher productivity of the North Atlantic waters intruding the Arctic Ocean via the Fram Strait. In the deep-sea basins, in particular the Nansen Basin, carbonate deminishes to 0 % (PS2160) mainly by dilution from terrigenous material and by some dissolution (Pagels, 1991). The dominant components of the basin sediments are clay minerals reaching up to 60% of the bulk sediment (Stein et al., 1994). At present the illite group constitutes up to 65 % of the clay minerals in eastern Central Arctic region (Stein et. al., 1994).

Further investigations will extent the data base in the Eurasian Basin and on the shelves. We will concentrate on the recognition of other significant minerals relating source areas to depositional centers. The collection of more sedimentological and mineralogical data of the source regions will require an enhanced international cooperation with scientists of the Arctic surrounding countries.

Acknowledgments

The author wishes to thank M. Wahsner, D. Nürnberg, C. Schubert and R. Stein for technical assistance and data discussion. N. Nørgaard-Petersen (GEOMAR, Kiel) kindly provided picked carbonate dropstones of the northernmost cores. J. Lauterjung (Geoforschungszentrum Potsdam) helped with the software package Qualit and the evaluation of mineral contents. J. Wollenburg (AWI) shared her knowledge of foraminiferas of the investigated area. Thanks are due to captain and crew of R.V. "Polarstern" during cruises ARK VIII/3 and ARK IX/4 who made it possible to sample under the harsh conditions of the Arctic region.

References

Anderson, L.G., G. Björk, O. Holby, E.P. Jones, G. Kattner, K.P. Koltermann, B. Liljeblad, R. Lindegren, B. Rudels, and J. Swift (1994). Water masses and circulation in the Eurasian Basin: Results from the Oden 91 North Pole Expedition, Journ. Geophys. Res., 99 (2), p. 3273-3283.

Bischof, J., D.L. Clark, J.-S. Vincent (subm.). Significance of Arctic Ocean dropstones for the definition of Pleistocene surface currents and the continental glaciations in the Arctic North America, Journ. Sed. Res.

Clark, D.L., R.K. Whitman, K.A. Morgan, and S.D. Mackey (1980). Stratigraphy and glacial-marine deposits of the Amerasian Basin, Central Arctic Ocean, Geol. Soc. Am. Spec. Pap., 181, 57 pp.

Dalrymple, R.W. and O.C. Maass (1987). Clay mineralogy of late Cenozoic sediments in the CESAR cores, Alpha Ridge, central Arctic Ocean, Can.J.Earth.Sci, 24, p. 1562-1569.

Darby, D.A., A.S. Naidu, T.C Mowatt, and G. Jones (1989). Sediment composition and sedimentary processes in the Arctic Ocean,In: The Arctic Seas, Y. Herman (ed), van Nostrand Reinhold Company, New York, p. 657-720.

Emmermann, R. and J. Lauterjung (1990). Double X-Ray analysis of cuttings and rock flour: a powerful tool for rapid and reliable determination of borehole lithostratigraphy, Scientific Drilling, 1, p. 269-282.

Fütterer, D.K. (1992). ARCTIC´91: The expedition ARK-VIII/3 of RV "Polarstern" in 1991, Berichte zur Polarforschung, 107, 267 pp.

Fütterer, D.K. (1994). The expedition ARCTIC´93, Leg ARK-IX/4 of RV "Polarstern" 1993, Berichte zur Polarforschung, 149, 244 pp.

Nürnberg, .D., I. Wollenburg, D. Dethleff, H. Eicken, H. Kassens, T. Letzig, E. Reimnitz, and J. Thiede (1994). Sediments in the Arctic sea ice: Implications for entrainment, transport and release, Mar. Geol., 119, p. 185-214.

Nürnberg, D., M.A. Levitan, J.A. Pavlidis, and E.S. Shelekhova, (1995).. Distribution of clay minerals in surface sediments from the eastern Barents and southwestern Kara seas. *Geol. Rund*, 84, p. 665-682.

Lapina, N.N., 1965: The determination of distribution paths of sediments, based on mineralogical investigations of marine deposits (example Laptev Sea). Uchennye Zapiski NIIGA, Ser. Region. Geol., Vol. 7, p. 139-157 (in Russian).

Pagels, U. (1991). Sedimentologische Untersuchungen und Bestimmungen der Karbonatlösung in spätquartären Sedimenten des östlichen Arktischen Ozeans, GEOMAR Report, 10, 106 pp.

Selley, R.C. (1988). Applied sedimentology, Academic Press, London, 446 pp.

Sigmond, E.M.O. (1992). Bedrock map of Norway and adjacent ocean areas. Scale 1:3 million. Geol. Surv. Norway.

Spielhagen, R.F. and H. Erlenkeuser (1994). Stable oxygen and carbon isotopes in planktic foraminifers from the Arctic Ocean surface sediments: Reflection of the low salinity surface water layer, Marine Geology, 119, p. 227-250.

Stein, R., H. Grobe, and M. Wahsner (1994). Organic carbon, carbonate, and clay mineral distribution in the Eastern Arctic Central Ocean, Marine Geology, special issue of "ICP-IV-92, 119, p. 269-286.

Stein, R. and S. Korolev (1994). Shelf-to-basin sediment transport in the eastern Arctic Ocean. Berichte zur Polarforschung, 144, p. 87-100.

Vogt, Chr., F. Lindemann, and M. Antonow (1994). Sediment distribution in the Laptev Sea, In: Kassens, H. and Karpiy, V.Y. (eds.): Russian-German Cooperation: The Transdrift I expedition to the Laptev Sea, Berichte zur Polarforschung,151, p. 66-73.

Vogt, Chr. and Stein, R. (1994). Terrigenous sediment input into the Eurasian Arctic Ocean :Bulk and clay mineralogy as tracers of the transport and sedimentation processes, Abstracts Sediment '94 Conference, Greifswald, Germany.

Wahsner, M. and E.S. Shelekova (1994). Clay mineral distribution in Arctic deep sea and shelf surface sediments. Greifswalder geologische Beiträge, A 8 29, p. 234 (abstract).

Wollenburg. I. (1993). Sediment transport by the Arctic Sea Ice: The recent load of lithogenic and biogenic material, Berichte zur Polarforschung, 127, 159 pp.

Wollenburg, J., 1995. Benthische Foraminiferenfauna als Wassermassen-, Produktivität- und Eisdriftanzeiger im Arktischen Ozean. Berichte zur Polarforschung, 179, 227 pp.

Winsnes, T.S. (1988). Geological map 1: 1 000.000. Bedrock map of Svalbard and Jan Mayen, Nor. Polar. Temakart 3, 12 pp.

Appendix

Table 1.: Station list and quartz, calcite, and dolomite contents expressed as percentage of bulk sample, and quartz (4.26Å)/feldspar (3.23+3.19Å)-ratio of the surface sediments in the Eurasian Basin (c.f. Fütterer, 1992). Multicorer samples are high-lighted.

Eurasian Basin/ Barents Sea Slope

Station	Long. (Deg.Min.Sec)	Lat. (Deg.Min.Sec)	Water Depth (m)	Quartz (%)	Calcite (%)	Dolomite (%)	Qz4.26/Fsp	Station	Long. (Deg.Min.Sec)	Lat. (Deg.Min.Sec)	Water Depth (m)	Quartz (%)	Calcite (%)	Dolomite (%)	Qz4.26/Fsp
PS2156-1	80°05.2'N	30°13.8'E	258	29.7	0.0	6.2	0.37	PS2185-3	87°32.0'N	144°22.9'E	1051	28.0	5.5	3.1	0.36
PS2157-3	81°45.3'N	29°54.9'E	2875	22.5	4.2	1.5	0.54	**PS2185-4**	87°32.0'N	144°28.9'E	1051	32.6	6.9	2.3	0.51
PS2157-4	81°45.4'N	29°57.9'E	2900	19.9	8.1	3.2	0.26	**PS2186-3**	88°30.8'N	140°21.8'E	2004	28.6	4.7	1.8	0.38
PS2158-1	82°46.5'N	29°55.5'E	3800	17.8	12.1	0.0	0.34	PS2186-5	88°30.9'N	140°29.4'E	2036	26.5	3.7	6.3	0.28
PS2159-4	83°56.9'N	30°17.1'E	4010	19.7	9.7	0.7	0.33	PS2187-1	88°44.1'N	126°51.5'E	3813	17.7	2.1	1.0	0.35
PS2160-3	84°52.6'N	37°53.5'E	4029	13.9	0.0	0.0	0.49	**PS2187-5**	88°45.5'N	127°12.6'E	3898	38.1	1.3	0.4	0.46
PS2161-4	85°26.3'N	44°18.2'E	4005	14.1	2.6	0.0	0.33	PS2189-1	88°46.9'N	144°33.0'E	1018	41.1	10.7	0.0	0.46
PS2162-1	85°47.7'N	50°49.6'E	3981	14.1	2.4	0.5	0.26	**PS2189-3**	88°46.8'N	144°47.9'E	1064	43.6	6.8	4.8	0.60
PS2163-2	86°14.5'N	59°14.0'E	3047	27.6	7.7	0.6	0.32	PS2190-3	89°59.0'N	84°44.7'W	4240	21.9	2.3	1.0	0.24
PS2164-2	86°20.2'N	59°12.6'E	2004	47.4	5.9	1.4	0.64	**PS2190-5**	89°57.8'N	110°49.1'E	4267	21.7	1.1	0.7	0.45
PS2164-4	86°20.1'N	59°16.0'E	2030	37.3	5.5	2.8	0.39	**PS2191-1**	88°59.6'N	09°00.7'E	4346	15.5	4.9	3.2	0.33
PS2165-3	86°26.4'N	60°04.3'E	1794	48.3	7.4	1.5	0.51	PS2192-1	88°15.7'N	09°52.7'E	4375	15.3	6.6	3.4	0.29
PS2165-5	86°26.1'N	60°08.4'E	1911	35.4	9.8	1.5	0.45	PS2193-2	87°31.1'N	11°15.5'E	4337	24.7	2.3	4.1	0.31
PS2166-1	86°51.6'N	59°41.9'E	3618	36.8	5.1	0.0	0.54	PS2194-1	86°35.6'N	07°29.3'E	4326	31.4	6.8	5.0	0.41
PS2166-2	86°51.6'N	59°45.9'E	3636	26.5	6.3	0.0	0.38	PS2195-4	86°13.7'N	09°35.6'E	3873	25.7	6.3	1.5	0.32
PS2167-2	86°56.1'N	59°04.5'E	4425	25.1	1.7	1.0	0.34	PS2196-2	85°57.1'N	00°06.9'E	3958	24.5	5.6	2.4	0.28
PS2167-3	86°56.0'N	59°08.3'E	4427	27.2	1.7	0.0	0.33	**PS2196-3**	85°56.4'N	00°00.6'E	3888	27.2	4.2	2.3	0.38
PS2168-1	87°30.6'N	55°56.0'E	3846	37.8	3.6	1.1	0.31	PS2198-1	85°33.9'N	09°03.5'W	3767	30.9	5.7	3.2	0.38
PS2168-3	87°31.1'N	56°15.0'E	3685	35.6	4.6	0.7	0.62	**PS2198-4**	85°33.6'N	08°56.8'W	3818	40.4	7.7	2.8	0.74
PS2170-1	87°35.4'N	60°46.0'E	4226	26.3	4.2	1.6	0.31	PS2200-2	85°19.6'N	14°00.0'W	1074	28.1	18.9	4.4	0.45
PS2170-4	87°35.8'N	60°53.7'E	4083	32.2	5.6	0.0	0.48	**PS2200-4**	85°19.4'N	14°00.3'W	1072	28.8	17.2	3.9	0.60
PS2171-1	87°35.1'N	68°58.7'E	4384	25.8	6.2	0.0	0.35	PS2201-1	85°25.3'N	12°08.6'W	1353	18.7	16.6	3.4	0.37
PS2171-2	87°35.6'N	69°12.0'E	4384	28.2	3.4	2.5	0.46	PS2202-2	85°06.4'N	14°22.7'W	1083	31.2	24.8	4.2	0.44
PS2172-3	87°15.9'N	68°41.6'E	4480	35.1	5.6	0.0	0.50	**PS2202-4**	85°06.3'N	14°23.4'W	1083	30.0	7.7	2.9	0.48
PS2173-1	87°18.4'N	69°19.3'E	4558	27.0	3.7	2.7	0.31	**PS2204-3**	85°03.5'N	13°02.1'W	3899	28.5	6.6	4.1	0.48
PS2174-2	87°29.5'N	90°43.2'E	4427	25.1	1.8	1.8	0.45	**PS2205-1**	84°38.6'N	06°46.0'W	4283	33.0	2.9	4.0	0.56
PS2174-4	87°29.1'N	91°20.3'E	4426	25.3	2.2	1.9	0.33	**PS2206-4**	84°16.7'N	02°30.3'W	2993	18.9	6.6	0.8	0.65
PS2175-3	87°35.4'N	103°43.6'E	4411	23.2	4.3	0.0	0.30	PS2209-1	83°13.5'N	08°34.4'E	4046	16.7	11.5	1.8	0.35
PS2175-4	87°36.0'N	103°47.6'E	4411	29.7	3.2	0.0	0.47	PS2210-1	83°02.7'N	10°07.5'E	3949	24.1	11.8	1.7	0.33
PS2176-2	87°46.2'N	108°32.5'E	4396	27.2	1.7	1.1	0.42	**PS2210-3**	83°02.3'N	10°05.4'E	3806	32.7	16.8	0.3	0.63
PS2176-4	87°46.6'N	108°10.0'E	4364	20.3	3.8	0.0	0.27	PS2212-5	82°04.0'N	15°46.0'E	2485	20.3	13.2	0.5	0.23
PS2177-1	88°02.2'N	134°55.1'E	1388	22.2	5.4	0.8	0.33	**PS2212-6**	82°03.8'N	15°43.0'E	2439	25.3	11.5	2.2	0.43
PS2177-3	88°02.2'N	134°50.7'E	1390	38.1	5.1	0.3	0.62	PS2213-1	80°28.4'N	08°12.3'E	897	30.6	1.2	2.2	0.38
PS2178-2	88°00.2'N	159°14.0'E	4009	28.3	5.8	0.0	0.34	PS2214-1	80°16.1'N	06°37.6'E	552	55.3	0.7	2.7	0.48
PS2178-4	88°01.3'N	159°35.1'E	4008	33.4	5.3	1.3	0.42	**PS2214-4**	80°17.2'N	06°34.7'E	562	44.3	0.3	3.4	0.59
PS2179-1	87°44.8'N	138°01.7'E	1230	28.2	3.1	2.8	0.31	PS2215-1	79°41.7'N	05°20.4'E	2045	58.0	3.0	1.9	0.47
PS2179-3	87°45.0'N	138°09.4'E	1228	34.9	4.6	1.4	0.75	PS2440-4	81°13.0'N	30°36.7'E	196	56.5	0.4	3.5	0.44
PS2180-1	87°37.6'N	156°40.5'E	4005	27.9	3.8	2.5	0.34	PS2441-3	81°28.3'N	30°53.9'E	589	27.8	1.3	2.1	0.33
PS2181-3	87°35.8'N	153°22.5'E	3331	32.1	6.6	3.2	0.38	PS2442-4	81°43.0'N	30°20.9'E	2915	25.6	4.1	2.2	0.34
PS2181-4	87°35.9'N	153°29.0'E	3418	25.9	7.5	17.3	0.49	PS2443-2	82°12.2'N	34°36.8'E	2464	25.8	4.8	1.8	0.54
PS2182-1	87°34.5'N	151°07.2'E	2489	37.8	10.8	4.5	0.36	PS2444-1	82°29.2'N	37°44.4'E	2566	20.0	4.7	2.0	0.36
PS2182-4	87°34.7'N	151°29.9'E	2619	35.2	9.2	3.0	0.52	PS2445-3	82°45.8'N	40°14.5'E	2995	20.9	6.6	2.2	0.37
PS2183-1	87°36.1'N	148°49.8'E	2016	41.2	4.5	2.2	0.36	PS2446-3	82°23.9'N	40°53.6'E	2025	24.3	5.3	1.8	0.42
PS2183-3	87°36.3'N	149°00.4'E	2022	43.3	5.2	3.2	0.51	PS2447-4	82°09.9'N	42°02.7'E	1024	22.7	3.5	2.8	0.41
PS2184-1	87°36.7'N	148°08.4'E	1640	42.4	8.1	3.6	0.32	PS2448-3	82°07.4 'N	42°32.2'E	534	19.5	5.7	3.4	0.33
PS2184-3	87°36.7'N	148°15.2'E	1674	49.8	5.6	4.9	0.43	PS2449-3	82°01.4'N	43°34.6'E	286	65.6	2.9	0.0	0.82

Table 2.: Station list and quartz content expressed as percentage of bulk sample of the surface sediments of the Laptev Sea shelf to Nansen Basin area (Fütterer, 1994).

Laptev Sea

Station	Long. (Deg.Min.Sec)	Lat. (Deg.Min.Sec)	Water Depth (m)	Quartz (%)	Station	Long. (Deg.Min.Sec)	Lat. (Deg.Min.Sec)	Water Depth (m)	Quartz (%)
PS2450-2	78°02.0'N	102°18.5'E	145	28	PS2468-3	77°41.6'N	125°53.6'E	1991	35
PS2451-2	77°42.4'N	102°17.3'E	143	58	PS2469-3	77°03.6'N	125°00.0'E	2332	30
PS2452-2	77°53.5'N	101°35.5'E	132	57	PS2470-4	79°13.0'N	122°54.4'E	3233	25
PS2453-2	76°30.5'N	133°21.3'E	38	34	PS2471-3	79°09.3'N	119°46.9'E	3048	25
PS2455-3	79°32.1'N	130°32.1'E	3429	27	PS2472-3	78°40.0'N	118°44.3'E	2620	22
PS2456-2	78°29.0'N	133°00.1'E	2520	36	PS2473-3	77°58.9'N	118°34.3'E	1927	22
PS2457-2	78°23.5'N	133°09.6'E	2130	37	PS2474-2	77°40.2'N	118°34.5'E	1497	36
PS2458-3	78°10.0'N	133°23.7'E	981	29	PS2475-1	77°31.9'N	118°27.4'E	1108	29
PS2459-2	78°05.9'N	133°30.8'E	517	31	PS2476-3	77°23.5'N	118°11.5'E	524	29
PS2460-3	78°04.3'N	133°36.5'E	191	36	PS2477-3	77°14.8'N	118°33.2'E	193	39
PS2461-2	77°54.6'N	133°33.3'E	73	34	PS2478-3	77°10.3'N	118°42.6'E	101	41
PS2462-3	77°24.3'N	133°33.4'E	54	34	PS2480-2	78°15.7'N	109°14.7'E	51	81
PS2463-3	77°01.8'N	126°24.8'E	93	45	PS2481-2	78°28.4'N	110°47.3'E	101	49
PS2464-2	77°28.8'N	125°54.2'E	2025	28	PS2483-2	78°45.8'N	112°42.2'E	1216	43
PS2465-3	77°11.0'N	126°13.4'E	1025	32	PS2484-2	78°34.9'N	111°23.2'E	235	34
PS2466-3	77°08.1'N	126°21.2'E	552	41	PS2485-1	77°54.0'N	105°05.0'E	229	33
PS2467-3	77°05.0'N	126°13.4'E	284	41	PS2486-2	77°59.4'N	104°35.6'E	122	33

MARINE GEOLOGICAL INVESTIGATIONS OF SURFACE SEDIMENTS IN THE FRANZ-JOSEF-LAND AREA AND THE ST. ANNA TROUGH

M. Wahsner*, G. Ivanov', and G. Tarasov°,

*Alfred-Wegener-Institute, Bremerhaven, Germany
'VNIIOkeangeologia, St. Petersburg, Russia
°Murmansk Marine Biological Institute, Murmansk, Russia

Introduction

Geological processes in the Arctic Ocean are strongly influenced by the permanent sea-ice cover which reacts very sensitvely on changes in temperature and climate. The feedback on related geological, oceanographic, and biological processes is presently not fully understood. Therefore, strong efforts have to be made to study the "fingerprints" of potential global climate changes in this sensitive area.

In order to study the Arctic Ocean sedimentation it is necessary to consider the close interaction between processes on the shelf, the continental slope, and the deep sea. The broad and shallow shelf areas situated along the eastern margin of the Arctic Ocean are supplied with an enormous amount of fresh water and suspended sediments by the major Siberian river systems Ob, Yenisey, and Lena. They are the most dynamic areas in the Arctic Ocean because of seasonal changes in the ice coverage and river discharge. The formation of huge ice shields and subsequent strong sea-level changes in the past had important impacts on these shallow marginal seas and the continental slope. As a consequence sediment supply from distinct source areas could be intensified or diminished. Besides this, ocean currents and the drift ice pattern of the Arctic Ocean were strongly influenced by changing sea levels. These processes and different supply mechanisms from varying source areas are reflected in the mineralogical and geochemical composition of the deep-sea sediments.

As shown by different investigations on clay minerals in the Arctic Ocean (Dalrymple and Maass, 1987; Clark et al., 1989; Darby et al., 1989; Stein et al., 1994; Nürnberg et al., 1995), the clay mineralogy can be a valuable indicator of sediment sources and transport pathways. This is of special importance in polar and subpolar regions, where physical weathering processes dominate and chemical and diagenetic alteration are negligible. In general, the clay mineralogy of Arctic Ocean sediments reflects the source mineralogy of the landmasses and shelf areas surrounding the central Arctic Ocean basins (Darby et al., 1989). To understand the supply and transport mechnisms of the sediments into the deep ocean and to interpretate mineralogical changes within the sediment cores it is necessary to investigate the clay composition of the shelf sediments surrounding the Arctic Ocean (e.g. Elverhoi et al., 1989; Elverhoi et al., 1995).

The input of warm, saline Atlantic water entering the Artic west of Spitsbergen and through the St. Anna Trough, and the supply of fresh water from rivers and

run-off over the broad, shallow shelves characterize a major part of the oceanographic conditions in this area. Together with the changing ice coverage these water masses have a strong influence on the sedimentation. The St. Anna Trough represents an area of special interest discussing these processes. Oceanographic measurements and ice observations have shown, that a mixing of the warmer Atlantic water coming via the Barents Sea and shelf waters from the Kara Sea, took place before these mixed waters enter the deep Arctic basins along the Eurasian continental slope via the St. Anna Trough (Rudels et al., 1994). On the other hand, surface currents east of Franz-Josef-Land transport Arctic surface waters from the Nansen Basin into the St. Anna Trough area and into the northern Barents Sea (Dickson et al., 1970). Therefore, sediment transport in this region could be interpreted only in consideration of these mixtures and movements of water masses.

There are three main processes transporting the shelf sediment particles into the deep sea: (1) Transport in suspension via distinct current systems in the water column, (2) gravitational flows (turbidity currents, debris flows), and (3) sea-ice or ice-berg transport. One aim of geological investigations in the Barents and Kara seas is to study these major processes controlling the sediment flux from the shelves to the deep-sea floors and to identify different source areas and transport pathways of the terrigenous material. The St. Anna Trough area is one of the key areas to characterize these geological processes in the Eurasian part of the Arctic Ocean. This morphological particularity along the Kara Sea slope exhibits a sedimentation regime with a close interaction of the above mentioned oceanographic and geological processes.

The investigations of sediment samples from the St. Anna Trough area were carried out within the frame of intensive clay mineral analyses from different shelf areas and the deep sea in the Eurasian part of the Arctic Ocean (Wahsner et al. 1995, Stein et al., 1994, Wahsner 1995). The expeditions with RV "Prof. Logachev" and RV "Akademik Golitsin" could make an important contribution to complete the sample network in the shelf areas and to interpretate the geological and oceanographic processes.

Sampling and methods

The expedition into Franz-Josef-Land area with RV "Akademik Golitsin" in August 1994 (Fig. 1) was part of a Russian-German cooperation. The geological sampling program focussed on the area of the St. Anna Trough and around some southern islands of Franz-Josef-Land. In addition, some sample locations on the islands of Franz-Josef-Land could be carried out. Two years ago there was already a first expedition to Novaya Zemlya and Franz-Josef-Land within the scope of the cooperation between the Murmansk Marine Biological Institute (MMBI) and the Alfred-Wegener-Institute for Polar and Marine Research (AWI). During that cruise sampling was carried out along the western coast of Novaya Zemlya, along a transact at about 60° E to Franz-Josef-Land, and inbetween the islands (Nürnberg and Groth, 1993). The sampling program in 1994 represents a useful completion to the former cruises, because the sampling sites could extend more to the east of Franz-Josef-Land and, because of good ice conditions, two transects crossing the St. Anna Trough at about 80° N could be carried out.

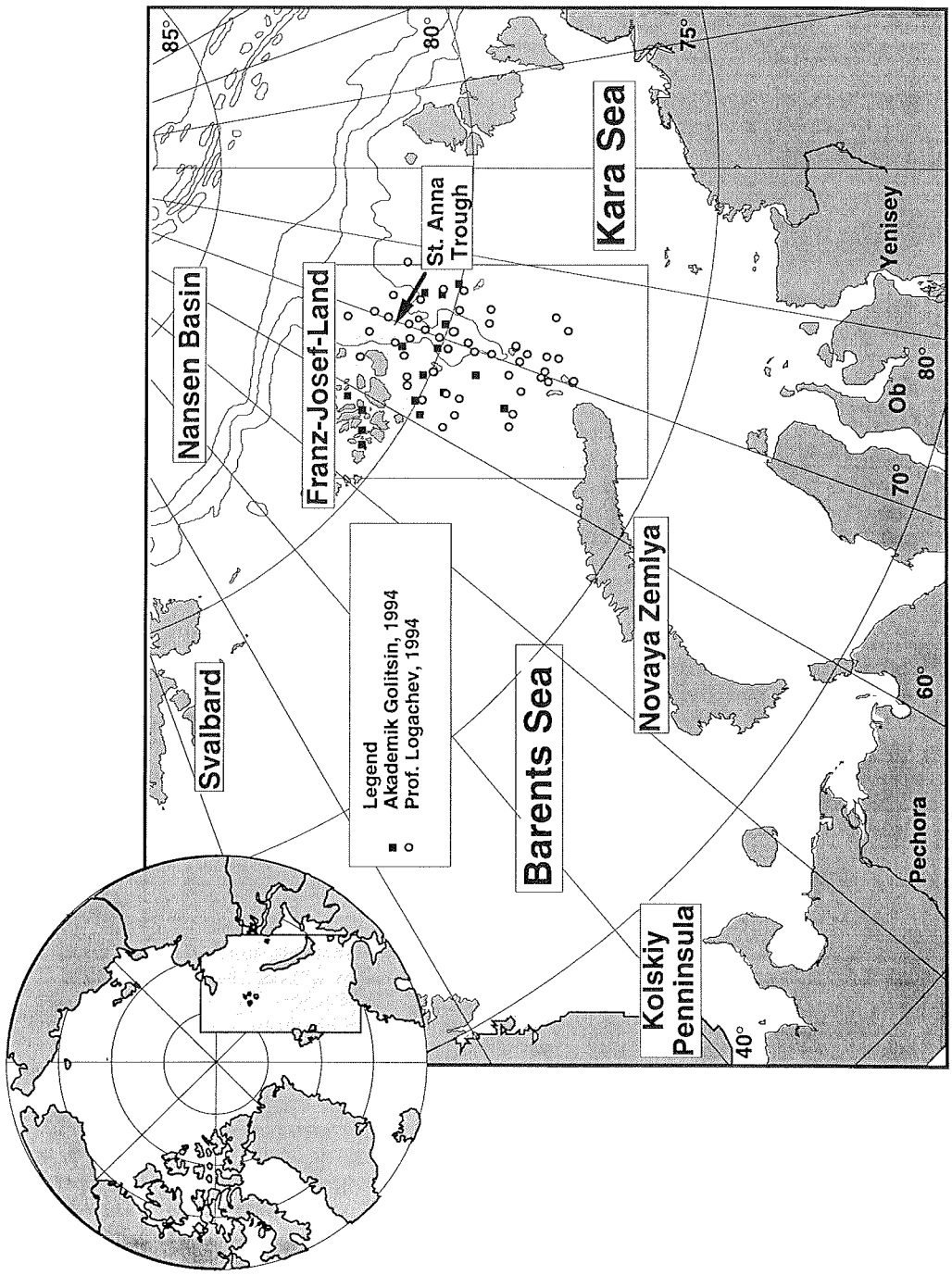

Fig. 1.: Station map of the two expeditions of RV "Akademik Golitsin" and RV "Prof. Logachev" in 1994.

Nearly at the same time the Russian vessel "Prof. Logachev" from VNIIOceangeologia in St. Petersburg also worked in the St Anna Trough area to obtain sediment samples and to carry out oceanographic and geophysical measurements. Stations between 77° N up to about 82° N were carried out during that cruise (Fig. 1). Results of investigations of surface sediment samples from both cruises will be presented and discussed in this paper.

During the cruise of RV "Akademik Golitsin" 10 stations were carried out on two transects crossing the trough at about 80° N. Ice conditions were very good, and it was possible to extend the sampling profile until 75° E. Four sampling stations were carried out within the Franz-Josef-Land archipel, in the deep troughs between the islands. In addition, sediment samples from 8 different islands along the beaches, in moraines, and from an outcrop of mesozoic rocks were taken. Three stations were carried out on the way back to Murmansk (Fig. 1). The geological working program focussed on the sampling of surface and near-surface (up to 30 cm depth) sediments from the ocean floor. At three stations also longer cores up to 150 cm were recovered. The deepest station in the St. Anna Trough was sampled at about 600 m. During the cruise of RV "Prof. Logachev" 70 geological stations (Fig. 1) could be carried out, where surface and near-surface samples were taken with a box corer and a grab sampler, and longer cores with a gravity corer.

In total, 76 surface samples and 10 samples from land locations were investigated with regard to grain sizes and clay minerals. To remove the organic carbon, each sample was shaked in a 5% hydrogenic peroxide solution for about 24 hours. After wet sieving of the sand fraction (> 63 µm) silt and clay was separated by the Atterberg settling method. Sodium pyrophosphate (1%) was used to avoid coagulation of clay particles, and the clay fraction (> 2µm) was treated with $MgCl_2$ to provide a unique cation charging. Free ions were removed by centrifuging the clay at least two times. The dried clay fraction was carefully ground in an agate mortar. For measuring the clay texture preparations were carried out by vakuum filtration. To support quantitative measurements an internal standard of 1ml of 0.4% molybdenite suspension was added to 40 mg of clay during resuspension of the sample. This suspension was sucked onto a membran filter by vakuum filtration. After drying, the clay cakes were transfered onto aluminium platelets. This preparation technique (see Ehrmann et al., 1992) leads to highly texturated , low particle-size segregated clay films with a thickness of about 50 to 100µm (10mg/cm^2, see Petschik et al., in press)

All samples were measured with a Philips PW 1820 goniometer, equipped with CoKa radiation, a theta-circle-integrated automatic divergence slit, a graphite monochromator, and an automatic sample changer. At first, "air-dried" samples were measured by a step scan with 2 seconds counting for each angle between 1-18°2θ with a step size of 0.02°. After vaporisation with ethyleneglycol at 50° C for at least 1 day, samples were measured between 2-40° 2θ with the same step size. In addition, the area between 28 and 30.5° 2θ was measured with steps of 0.005° to seperate the (002) peak of kaolinite minerals from the (004) reflections of chlorite minerals.

For the semi-quantitative calculations the relative clay mineral content (rel%) of smectite, illite, kaolinite, and chlorite were determined using the integrated peak areas of their basal reflections, weightened by empirically estimated

factors after Biscays (1965). For the calculation of smectite and illite, the 17Å line (after removal of the chlorite 14Å line) and the 10Å line, respectively, were used. Kaolinite at 3.57Å - 3.58Å and chlorite at 3.53Å - 3.54Å were identified from the slow scan by their intensity ratios. The share of the respective mineral was transformed to the 7Å peak of both minerals, following Biscaye (1965).

First results and discussion

First descriptions of the sediments from RV "Akademic Golitsin" cruise show that they mainly consist of fine grained, clayey and silty material. Coarser material and "dropstones" could be observed only in minor amount. The oxidized, brownish-colored layers of the sediment surfaces mainly reaches a few cm. Only in the deepest parts of the St. Anna Trough they reach up to 30 cm, depending on lower sedimentation rates. In the shallower channels inbetween the islands, the sediments are very rich in organic material indicated by gray to black colors and a high concentration of long tube worms (Polychaeta).

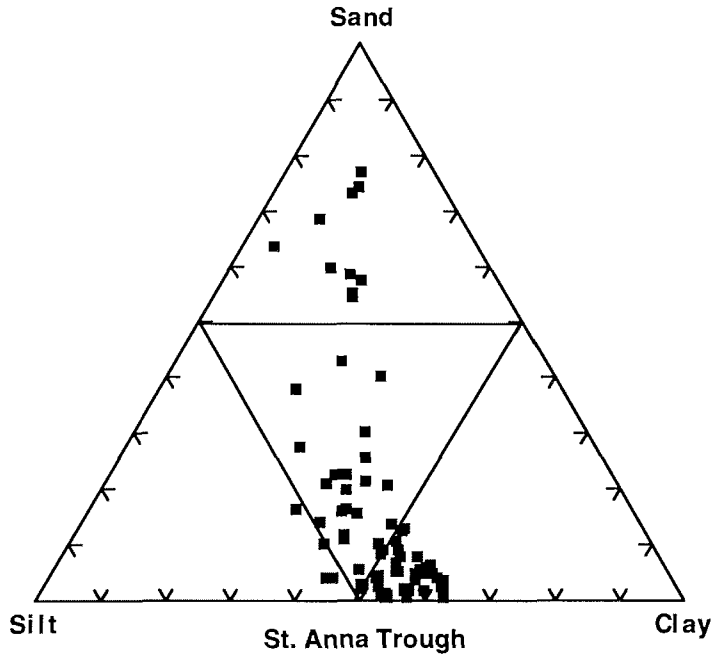

Fig. 2: Sand, silt, and clay distribution of surface sediments from the St. Anna Trough area plotted in a triangular diagram (only marine samples).

The grain-size distribution of the surface sediments (Fig. 2) shows, that only very few samples contain more than 50% sand (>63µm). These are samples from stations near the islands of Franz-Josef-Land and east of the St. Anna Trough, where north of Vize Island shallow water depths between 20 and 100m exist. The silt concentration (2-63µm) normally varies between 30 and 50%. Only north of Vize Island the values decrease down to 11%. Clay (<2µm) shows the opposite trend to sand. High values, up to 60%, occur in the deeper trough area, lower values along the slopes (30-50%), and on the western and eastern topographic highs (10-30%). South of the St. Anna Trough, in direction to Novaya Zemlya, also lower values down to 30% clay exist.

The 10 samples from land locations mainly consist of relatively coarse-grained material with sand contents between 30 and 100%. Only two soil samples are more fined-grained with 90% silt and clay.

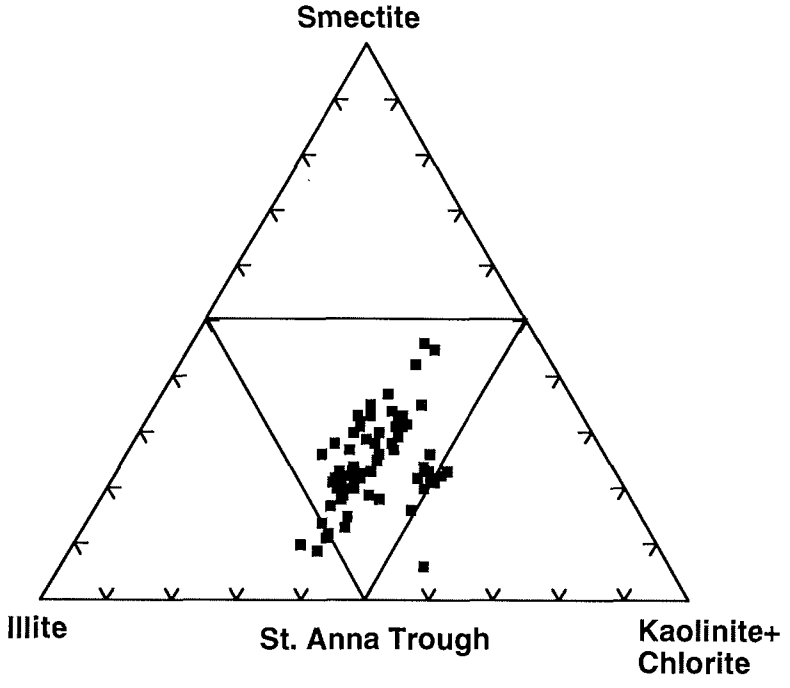

Fig. 3: The smectite, illite, and kaolinite+chlorite distribution of surface sediments plotted in a triangular diagram (only marine samples).

The clay composition (smectite, illite, and kaolinite+chlorite) of the investigated sediments are plotted in Figure 3. It is obvious, that illite and smectite show a large concentration range, whereas the kaolinite+chlorite values vary only between 40 and 50%. These variations depend on distinct differences between the eastern and western part of the trough. The smectite

concentration (Fig. 4a) varies between 10 and 40%. Highest values exist along the western slope with up to 30-40% smectite. Lowest values of smectite occur east of the Franz-Josef-Land islands and south-east of the trough in the northern part of the Kara Sea. Illite (Fig. 4b) shows the opposite trend to smectite. High contents (up to 60%) in the eastern part of the trough and in the northern part of the Kara Sea, and lower occurrences (about 20%) in the western part and south of Franz-Josef-Land. The kaolinite distribution (Fig. 4c) distinctly reflects the supply from the islands of Franz-Josef-Land. Values up to 35% were measured in the surface samples southeast of the islands. Lowest concentrations of kaolinite were measured east and southeast of the St. Anna Trough, with only 10% kaolinite in the clay fraction. Chlorite concentrations (Fig. 4d) show smaller variations but are relatively high in comparison to the surrounded Kara Sea shelf (maximum values up to 25%), the Barents Sea (10-20%), and the Central Arctic Ocean (up to 25%). In the eastern part of the trough and especially in the south, the chlorite concentration reaches 35%, in the western part it reaches about 15 to 20%.

The clay composition of the 10 land samples differs strongly. Soil samples have a relatively high content of smectite minerals (up to 80%), whereas the samples from Mesozoic rock outcrops along the beaches have high kaolinite contents between 70 and 90%. Illite values are relatively low in all samples (5 and 40%). Chlorite concentrations vary from 0 to 30%.

The distribution pattern of the clay minerals shows, that there exists no direct connection between the smectite-rich shelf sediments from the inner Kara Sea and the St. Anna Trough. In contrast, smectite (Fig. 4a) reflects a decrease in direction to the eastern Kara Sea. The high smectite content in the inner Kara Sea with up to 70% in the surface sediments (Wahsner and Shelekova, 1994; Levitan et al., this volume) in front of the Ob and Yenisey deltas results from the suspension supply of these two rivers. Both river systems drain huge sheet basalt complexes in the Siberian hinterland, where erosion and weathering of the basalt leads to the formation of smectite. Current measurements have shown that there exists a strong sediment transport from the eastern Kara Sea to the east, through the Vilkitsky Strait into the western Laptev Sea. In this area also relatively high values of up to 40% smectite were measured (Wahsner 1995).

The data from the St. Anna Trough show, that the most important material supply probably takes place from the western Kara Sea and not from the eastern part. The oceanography of the western part is characterized by a cyclonic surface current (Nürnberg et al., 1995, Levitan et al. this volume). Within this current system sediment transport to the north is possible along its eastern branch. Material from the western region with low smectite and higher illite occurrences (Wahsner and Shelekova, 1994, Levitan et al., this volume) therefore could be transported to the north and to the St. Anna Trough. This is also supported by the higher chlorite concentrations in the western Kara Sea and in the south of the St. Anna Trough. The enrichment of smectite on the western slope of the St. Anna Trough is probably caused by local smectite-rich rock outcrops or sediments. The clay mineral data explain the distinct differences between the eastern and western part of the St. Anna Trough. The western area is more influenced from Franz-Josef-Land (kaolinite) and from the geological situation in the northern Barents Sea (smectite-rich rocks).

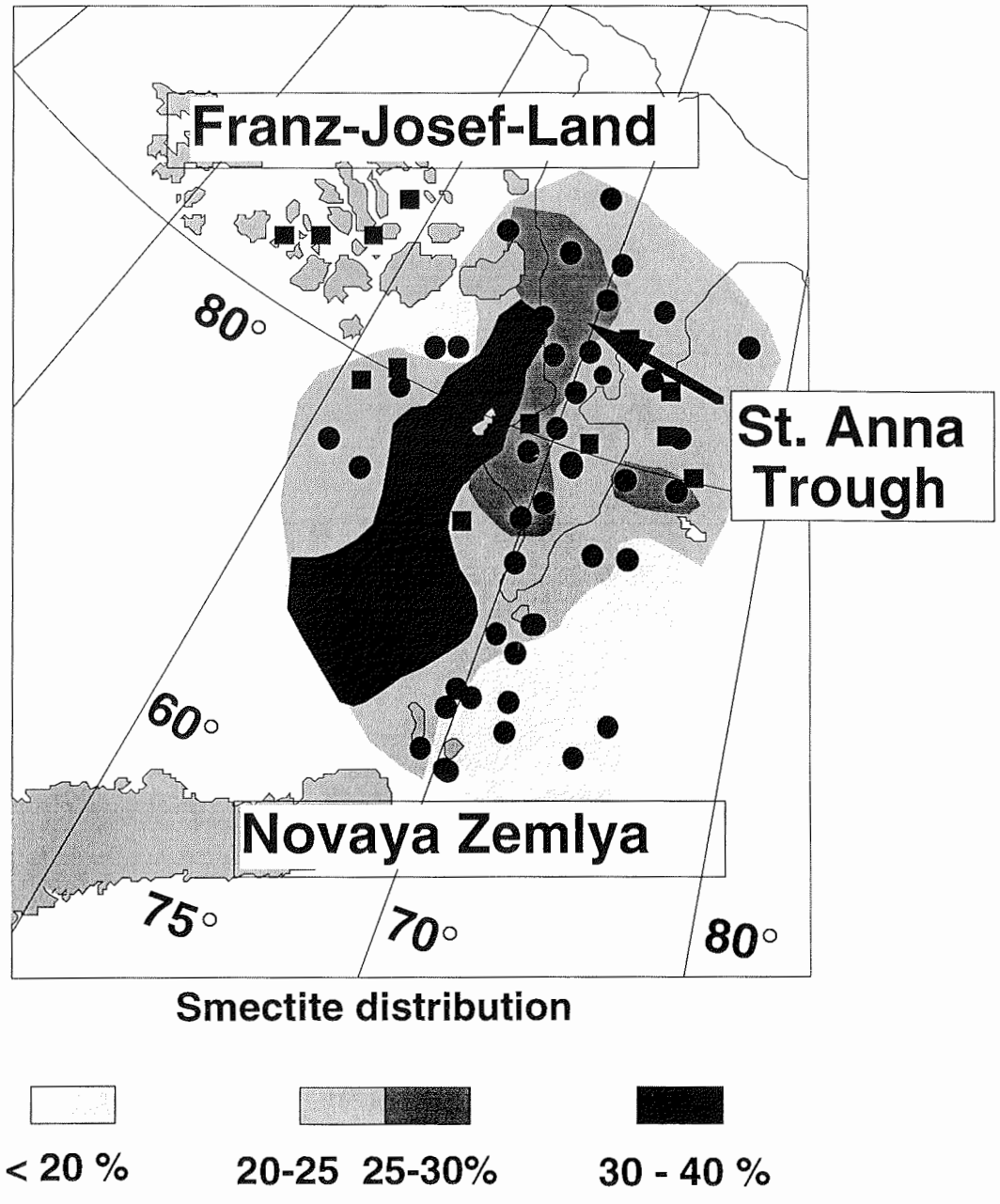

Fig. 4a.: Distribution map of the clay mineral smectite.

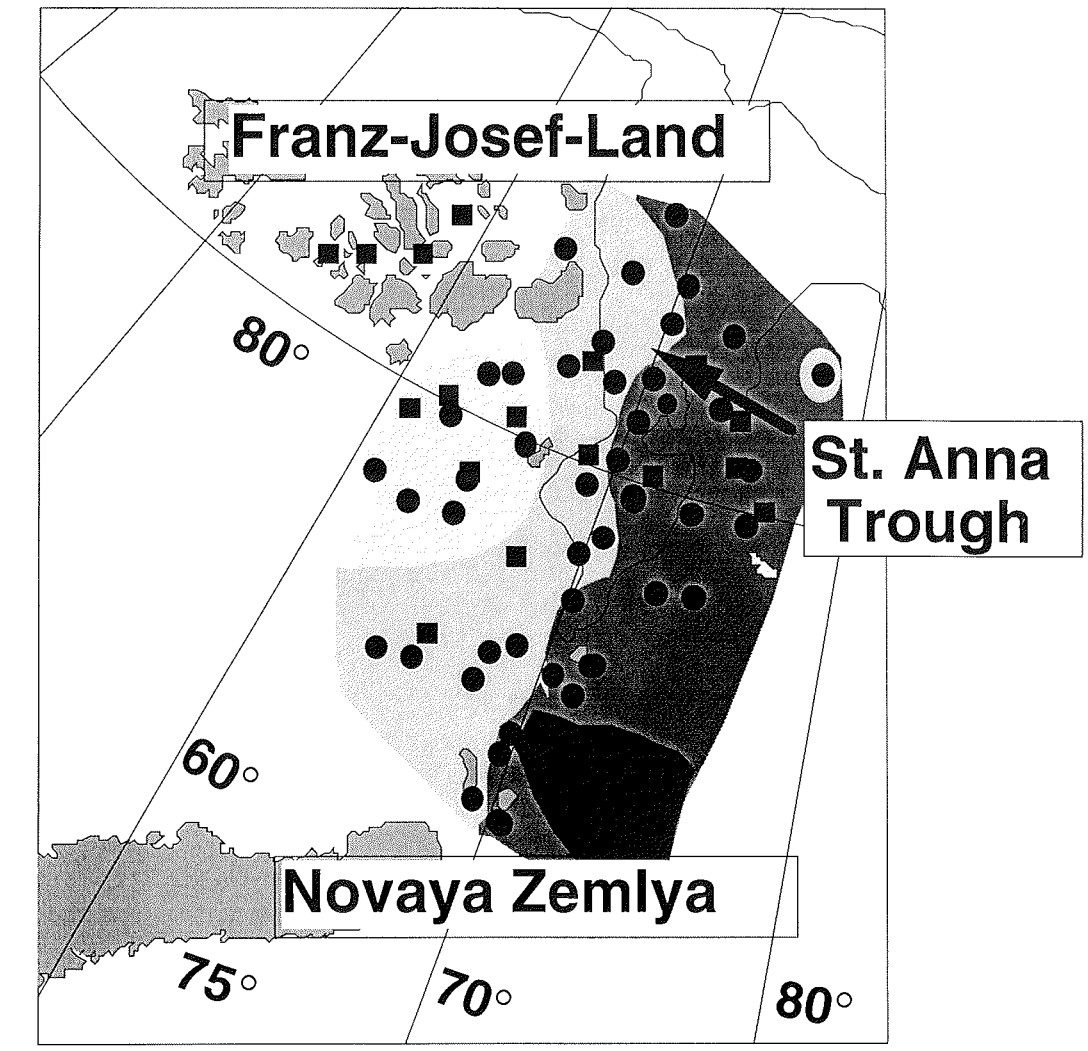

Illite distribution

20 - 30 %

30 - 40 %

40 - 50 %

> 50 %

Fig. 4b.: Distribution map of the clay mineral illite.

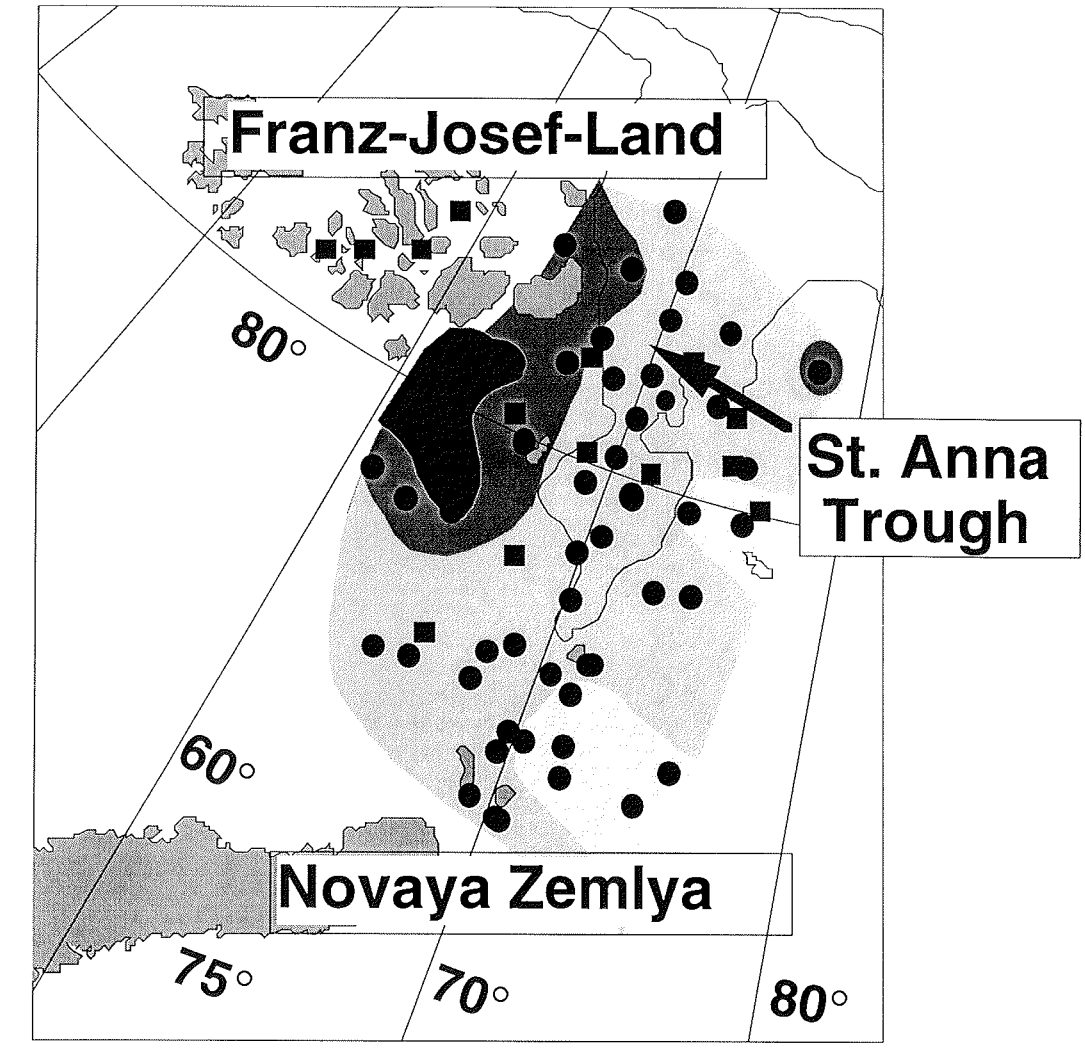

Fig. 4c.: Distribution map of the clay mineral kaolinite.

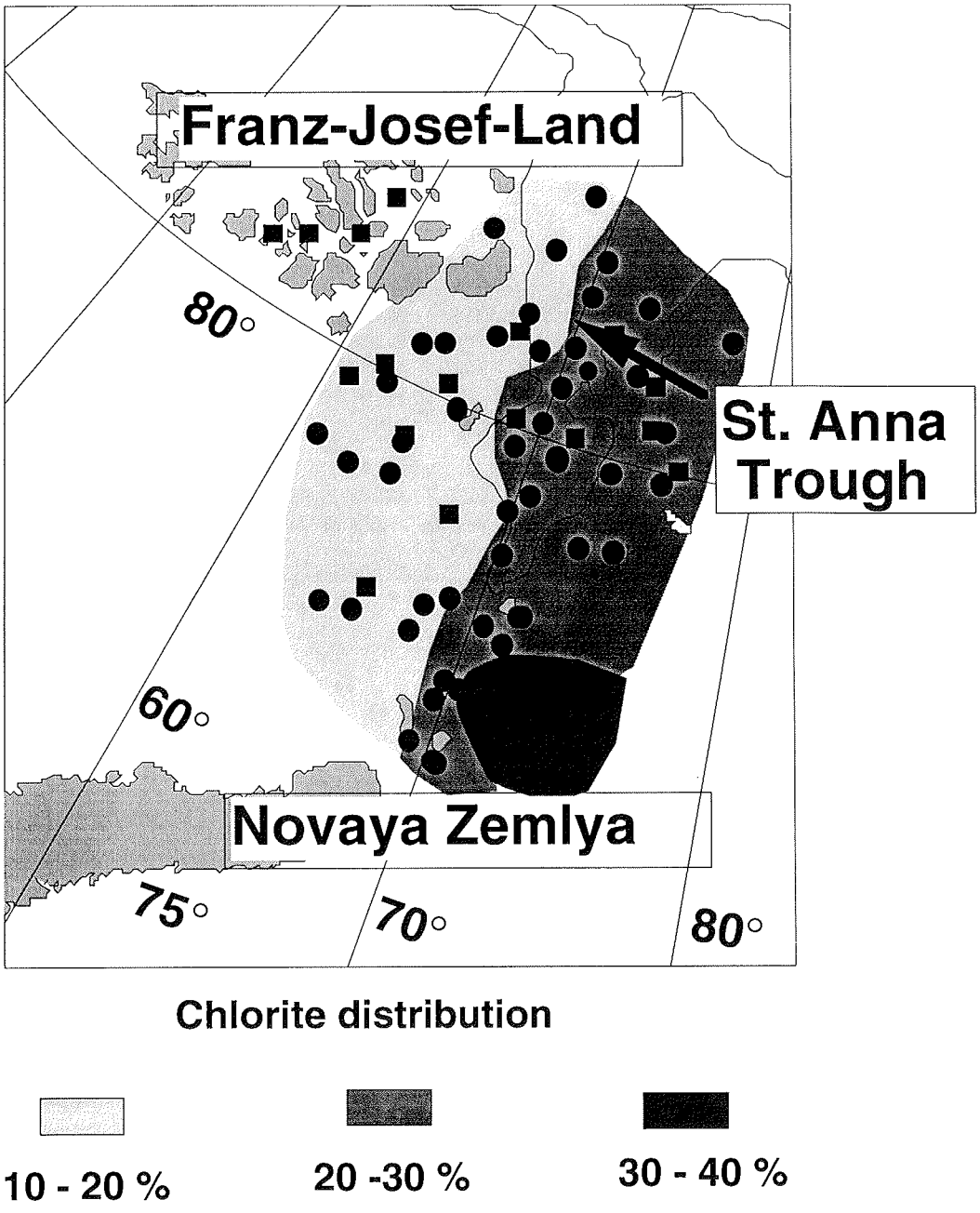

Fig. 4d.: Distribution map of the clay mineral chlorite.

Surface sediments in the eastern part of the trough are characterized by material from the western Kara Sea and Novaya Zemlya represented in higher illite and chlorite occurrences.

Conclusion

These first mineralogical results show that the distribution pattern of the clay minerals depends on different transport and sedimentation processes. Next step is now, (1) to discuss the results with other geological and oceanographic data sets and (2) to complete the distribution maps with data from the Barents and Kara seas.

Acknowledgments

The financial support by the Ministry for Education, Science, Research, and Technology (BMBF) (grant no. 03F08 GUS) is gratefully acknowledged.

References

Biscaye, P. E., 1965. Mineralogy and sedimentation of recent deep-sea clays in the Atlantic Ocean and adjacent seas and oceans. Geol. Soc. Amer. Bull., 76 : 803-832.

Clark, D.L., Whitman, R.R., Morgan, K.A., and Mackay, S.D., 1980. Stratigraphy and glacio-marine sediments of the Amerasian Basin, central Arctic Ocean. Geol. Soc. Amer., Spec. Paper, 181.

Dickson I.R.R, Midttun L.,and Mukhin A.I., 1970. The hydrographic conditions in the Barents Sea in August-September 1965-1968. In: Dragesund O (ed) International O-group fish surveys in the Barents Sea 1965-1968. Int Coun Explor Sea Cooperative Res. Rep., A18: 3-24.

Dalrymple, R.W. and Maass, O.C., 1987: Clay mineralogy of late Cenozoic sediments in the CESAR cores, Alpha Ridge, central Arctic Ocean.- Can. Journ. Earth Sci., 24: 1562 - 1569.

Darby, D. A., Naidu, A. S., Mowatt, T. C., and Jones, G., 1989. Sediment composition and sedimentary processes in the Arctic Ocean. In: Herman, Y. (Ed.), The Arctic Seas - Climatology, Oceanography, Geology, and Biology. New York (van Nostrand Reinhold): 657-720.

Ehrmann, W.E., Melles, M., Kuhn, G., and Grobe, H., 1992. Significance of clay minerals assemblages in the Antarctic Ocean.- Marine Geology 107, 249-273.

Elverhøi, A., Andersen, E. S., Dokken, T., D., H., Spielhagen, R., Svendsen, J. I., Sørflaten, M., Rørnes, A., Hald, M., and Forsberg, C. F., 1995. The growth and decay of the Late Wechselian Ice Sheet in western Svalbard and adjacent areas based on provenance studies of marine sediments. Quaternary Research 44, p. 303-316

Elverhoi, A., Pfirman, S. L., Solheim, A., and Larssen, B. B., 1989. Glaciomarine sedimentation in epicontinental seas exemplified by the Nothern Barents Sea. Mar. Geol., 85 : 225-250.

Nürnberg, D. and Groth, E. 1993. Expedition to Novaja Zemljy and Franz Josef Land with RV "Dalnie Zelentsy". in: Berichte zur Polarforschung 120.

Nürnberg, D., Levitan, M. A., Pavlidis, J. A., and Shelekhova, E. S., 1995. Distribution of clay minerals in surface sediments from the eastern Barents and southwestern Kara seas.- Geol. Rund. 84: 665-682.

Petschik, R., Kuhn, G., and Gingele, F. (in press): Clay mineral distribution in surface sediments of the South Atantic: sources, transport, and relation to the oceanography.- Marine Geology.

Rudels, B., Jones, E.P., Anderson, C.G., and Kattner, G. 1994. On intermediate depth waters of the Arctic Ocean.- in: The Polar Oceans and their role in shaping the global Environment; eds: Johannessen, O.M., Muench, R.D., Overland, J.E., Geophysical Monograph 85: 33-46

Stein, R., Grobe, H., and Wahsner, M., 1994. Organic carbon, carbonate, and clay mineral distributions in eastern central Arctic Ocean surface sediments. in: Thiede, J., Vorren, T. O. and Spielhagen, R. F. (Eds.), Marine Geology, 119: 269-285.

Wahsner, M. and Shelekova, E.S. 1994. Clay-mineral distribution in Arctic deep sea and shelf surface sediments.- Greifswalder Geologische Beiträge, A829: 234 (abstract).

Wahsner, M. 1995. Mineralogical and sedimentological characterization of surface sediments from the Laptev Sea.- Berichte zur Polarforschung 176: 303 - 313.

Wahsner, M., Stein. R., and Vogt, C. 1995. The recent eastern Arctic Ocean sedimentary environment and its change during the Late Quaternary.- Terra Nostra 1/95, Schriften der Alfred-Wegener-Stiftung, p. 48, (abstract, Bremen Februar 1995).

HOLOCENE SEDIMENTS OF THE EAST ARCTIC SEASs

Yashin D.S and Kosheleva V.A.

VNIIOkeangeologiya, Russia

Abstract

Five lithological members are distinguished in late Pleistocene-Holocene sections from the eastern Arctic Seas, which correspond to respective climatic stages. Considered are their paleontological, mineralogical, and geochemical features. The lithostratigraphical and paleogeographical parameters of late Pleistocene-Holocene sediments are presented. Features of the Holocene sedimentogenesis, typical of the Earth's polar areas, are considered.

Introduction

Bottom sediments of the Laptev, East-Siberian and Chuckchi Seas have been regularly studied by AANII and NIIGA since the fifties. All the data obtained mainly for the surficial sedimentary layer were integrated by Semenov (1961, 1965). A new qualitative period of regular investigations covered 1976-1988. The works were carried out by geologists of VNIIOkeangeologiya O.V. Kirillov, O.N. Kuleshova and I.I. Royhdestvenskaya. In this period, the mass aquisition of cores 2 - 3 m length allowed to extend considerably the stratigraphic and age range of sediments sampled and to begin the study of their organic-geochemical components. The ruge amount of diverse data obtained during both investigation stages was integrated in a research work conducted in VNIIkeangeologiya (Yashin et al., 1990). However, investigations of these offshore areas except for some local segments is at the reconnaissance stage today (1 - 2 stations for 1000 km^2). The East-Siberian Sea as well as the marginal shelf and the continental slope within the Laptev and Chuckchi Seas are the least studied.

The Pleistocene stage of the Arctic shelf development was completed by a considerable fall of the World ocean level. The late Cenozoic Laptev-Chuckchi shelf is an area of alluvial and lacustrine-alluvial sediments accumulated under conditions of the flat subdued relief. The landscape was most probably close to the proglacial: dry cold and forestless areas prevailed. Deposits developed at the shelf are similar in grain-size composition to those developed in forests of the northern Yakutiya and Chukotka. Their high density may be explained by the nature of proglacial weathering.

The latest transgression the sediments of which are the subject of the present investigation, began 12 thousand years ago and was the start of a new and yet incompleted cycle of the Arctic shelf development.

A division of Holocene sediments into lithological types is based upon the classification of a dominant fraction, considering in every case combinations of sand (1.0 - 0.1 mm), aleurite (0.1 - 0.01) and pelite (less than 0,.01 mm) fractions. Sediments containing more than 75 % of a certain fraction, are

referred to sands, aleurites or clays, respectively. Mixed sediments (aleuritic sands, clayey aleurites, etc.) contain 50 - 75 % of the main fraction and 25 - 50 % of the additional one.

Results and discussion

A typical feature of the Holocene sedimentogenesis at the East-Arctic shelf is that over a 3000 km stretch and independently of remoteness from the shoreline, a stratum has formed (and now in progress) nearly throughout, built up mainly with aleurite and pelite fractions. Relatively coarse sediments (sand, aleuritic sand) formed locally (Central-Laptev, Alaska shelves) mostly during the inital phases of the transgression.

In the Laptev Sea, certain information of peculiar features of the recent sedimentogenesis is provided by the correlation analysis of grain-size fractions between each other and with the basin depth. The bathymetric control is clearly recorded merely for pelite fraction except for its finest (less than 0.001 mm) component. Grains of sand and aleurite fractions are always absolutely passive to depth variations. A sharp antipode of the sand fraction is not only the pelite but the fine aleurite (0.05 - 0.01 mm) as well. Coarse aleurite (0.1 - 0.05 mm) behaves similarly to the sand relatively to the pelite fraction. However, there is no evidence of a positive correlation between the sand and coarse-aleurite fractions.

In separating fine particles from coarse ones in the coastal zone, the main mass of coarse-aleurite particles does not turn into suspension with the following migration into the deep-water basin part, but remains in the shallow-water zone like the sand. They show an exclusively individual distribution within the shelf and are usually independent of the basin depth. Hence the correlation analysis suggests that processes of mechanical differentiation which are responsible for the sediment distribution in offshore areas of a humid zone, are largely smoothed in the polar area. Together with detritus delivery from land, its significant part arrives at the sea floor due to the melting of ice. Therefore detritus distribution through the shelf depends on neither the basin depth nor the location relative to the shoreline.

Thus, Holocene formations of the East-Arctic seas are mostly presented by a stratum of cryogenic sediments composed by aleurtie and pelite fractions in different proportions. Their distribution curves are close to maximum of contents in proximity of average values. The persistant composition of recent sediments within most of the shelf is indicated by very close average and median values for aleurite (especially) and pelite fractions. The distribution curve of sand fraction is radically different: maximum of contents is sharply shifted toward minimum values, median and average statistic are accordingly very different.

Holocene sediments are of biogenic-terrigenic nature in the central Chuckchi Sea where a 'stagnant' zone forms due to hydrodynamic features. Together with the terrigenous sedimentogenesis there is an intensive accumulation of biogenic opal (up to 14 % of amorphous SiO_2).

Fields of development of sands extend as a narrow band along the coast, and cover shallow-water zones of the central Laptev shelf and the bottom in the vicinity of Wrangel Island and Gerald Bank where they are especially enriched in gravel-pebble products.

The mineral components of the sediments are presented largely by quartz and feldspar. The latter prevails in the light fraction in most parts of the Laptev and East-Siberian Seas. Quartz dominates in sediments of the Chuckchi Sea and in coastal segments of the other seas. Poor-quartz lithologies are rare and observed only in vicinity of the Wrangel Island. In the Chuckchi Sea and near river mouths at the Laptev shelf, grey-wackes are recorded with more than 25 % of rock fragments in the light fraction.

Five histological members are distinguished in sedimentary sections from the Laptev and East-Siberian Seas on the basis of their texture, colour, and consistence. In one section they are rarely recorded because of the wide development of intraformational erosion observed throughout the Holocene section. At the same time, despite of the local remoteness of the sections, they are usually recognizable and comparable.

Member V. Sands, aleuritic and clayey sands, bluish-dark-grey, very dense (over 2,0 g/cm^3), dry. The lack of any inclusions is typical. Penetrated thickness is 0.6 m. A fine-lattice and thinly-lamellar cryogenic structure of sediments that points to their freezing, is occasionally observed.

Member IV. Sandy clays, aleuritic sands, dark-grey, viscous, less dense (1.8 - 1.9 g/cm^3). Mollusk shells, rare black spots, occasionally H_2S odor. Penetrated thickness is 0,8 m.

As supposed by O.F. Baranovskaya, microfauna found in members V and IV (Laptev Sea) shows the extremely unstable composition of associations. It is indicative for the very disalted cold conditions (coastal or deltaic facies). Shallow-water species *Ammotium cassis* (Parker) dominates in the lower member. In the overlaying one *Reophax curtus*, *Haynesina orbicularie*, and *Eggerella advena* are dominant. According to O.F. Baranovskaya sedimentation has changed upward the members' section from alluvial-marine to marine-transgressive conditions as suggested from the paleontological parameters. A similar change took place at the Pleistocene-Holocene boundary.

Member III. Aleurites, clayey and sandy aleurites, aleuritic clays. The density gradually increases down the section from 1.6 g/cm^3 to 1.8 g/cm^3. A typical feature are abundant laminae, inclusions and attachments of black decomposed organics causing the dark-grey colour of sediments. Inclusions contain abundant fragments of mollusk shells and half-decomposed Polychaeta tubes. There is a well-defined sharp contact with sediments of member IV (different composition, colour, consistence). Sediments of this horizon are found in most of the cores and nearly throughout the shelf sediments from a depth of accumulation of more than 30 m. Maximum penetrated thickness is 1.6 m.

Member II. Aleurites, sandy and clayey aleurites; at a depth down to 15 m mostly sands. Colour varies from dark-grey in the basement to greenish-grey

upward the section. Sediments often show the cloudy structure, rare black spots are observed near the base. Density is 1.4 - 1.6 g/cm^3. The horizon is developed occasionally. It overlies dense sands of member IV at a depth down to 15 m. A boundary with sediments of member III is tentatively discerned from the abrupt reduction of black fine-dispersed product. Maximum thickness is 1.0 m.

Member I. Surficial sediments are mostly of aleurite composition, they overlie different Holocene horizons. Semi-fluid consistence. Thickness is 0.1 - 0.5 m.

According to Baranovskaya O.F., sediments of members III - I in the Laptev Sea contain a similar microfauna assemblage which differ from members V and IV assemblages. With rare exception, species *Eggerella advena* dominates in the complex. Widely observed are species *Protconella atlantica*, *Reophax curtus*, *Cunlata arctica* etc. Sediments members I and II are characterized by the lack of plankton and deep-water fauna. Microfauna assemblage member III is more rich and diverse. L.V. Polyak has marked the presence of plankton *Neogloboquadrina pachyderma* and exotiv *Cassidulina teratis*, *Bulimina cullata* that suggests an inflow of Atlantic waters moreover more intensive than at present. On the basis of combined properties, the sediment formation of member III may be referred to the Holocene climatic optimum, the Atlantic stage.

The most continuous Holocene section in the Chuckchi Sea is penetrated in its central part, in the Chuckchi Basin. Four diatom assemblages are recorded by Ye.I. Polyakova in a continuous 4 m-long section of aleurite-clay sediments sampled in the southeastern Chuckchi Basin. She correlates them (upward) with the boreal, atlantic, subboreal, and subatlantic stages of the Holocene (Polyakova, 1984, Vozovik and Polyakova, 1988). The continuous sedimentation in the Chuckchi Basin and a reflection in the section of all the listed climatic epochs of the Holocene were also inferred by Kh.M. Saidova (1982) from microfauna. Holocene sediments of the Chuckchi Basin are over 4,6 m in thickness.

In the Chuckchi Sea, Holocene sediments of the Alaska shelf are sandy and aleurite-sandy, containing dispersed gravel and fragments of broken shells. Holocene sediments vary in thickness from 0.6 to over 2.4 m. Based on diatom assemblages (Polyakova and Vozovik, 1984), gravel and pebble interbeds suggest a discontinuous sedimentation and the presence of hiatuses corresponding to various temporal intervals of the Holocene.

Conclusions

The complex analysis of organic remnants and structural features of the Holocene section indicates that the western (Laptev shelf) and the eastern (Chuckchi shelf) parts of the sea basin were different. In the first instance, Holocene sediments were formed mostly under shallow-sea conditions influenced by continental waters. It is evidenced by the lack of plankton and deep-water fauna. Arctic species of microfauna dominating in the complex suggest relatively stable conditions typical of a zone of the inner shelf of recent polar seas, insignificant variations of main parameters. Another typical feature is a great amount of cryophyllic diatoms in sediments developing through the

sea ice surface that points to the high glaciation of the Laptev Basin. The Chuckchi Basin formed in the Holocene as a marginal sea: it was deeper (down to 50 m), more independent from the land and had a periodical connection with the Pacific Ocean. It is evidenced by the presence of deep-water plankton and much less content of fresh-water diatoms in the Holocene section.

References

Polyakova, Ye.I., Vozovik, Yu.I., 1984. Some problems of the Chuckchi Sea development during the Holocene (from diatom complexes). In: Okeanologiya. V.XXIV. N 5: pp.789-793.

Polyakova, Ye.I., 1988. Diatoms of the USSR Arctic seas and their role in investigation of bottom sediments. In: Okeanologiya. V.XXVIII. N 2: pp. 286-292.

Saidova, Kh.M., 1982. The Holocene stratigraphy and paleogeography of the Chuckchi Sea and Bering Strait as inferred from foraminifera. In: Problema geomorfologii, litologii i litodinamiki shelfa. Moscow: Nauka: pp. 92-114.

Semenov, Yu.P., 1961. Formation conditions of bottom sediments in the Laptev Sea. In: Geologiya morya. V.I. Leningrad: pp. 47-53.

Semenov, Yu.P., 1965. Some features of formation of bottom sediments in the East-Siberian and Chuckchi seas. In: Antropogenovyi period v Arktike i Subarktike. Leningrad: NIGGA. V. 143: pp. 350-352.

ORGANIC GEOCHEMISTRY

ORGANIC MATTER IN BOTTOM SEDIMENTS OF THE WHITE SEA

Artemyev, V.E.[1] and Petrova, V.I.[2]

[1]P.P.Shirshov Institute of Oceanology, Moscow, Russia
[2]VNIIOkeangeologia, Russia

Abstract

Investigations of organic matter (OM) of bottom sediments in upper parts of Dvinsky and Kandalaksha Bays of the White Sea were carried out in 1981-1992. It was shown that levels of concentrations of organic carbon and individual organic compounds (bitumoids-lipids, lignin, polycyclic aromatic hydrocarbons) in bottom sediments depend on both lithological type of sediments (sands, aleurites, muds) and the influence of "natural" or anthropogenous sources of OM.

Introduction

Bays of the White Sea are of great interest for studying biogeochemical processes in areas of the "land-sea" and "river-sea" transitions. They are objects of abundant nutrition supply with riverine waters and the delivery of terrigenous and anthropogenous OM into bottom sediments of coastal zones. Among the greatest bays of the White Sea, Dvinsky and Kandalaksha bays occupy the important place. For surface waters in these bays (Fig. 1-3) the high concentrations of chlorophyll *a* are characteristic (more than 1.5 mg/m; Maximova and Bondarenko, 1985). Bottom sediments of these bays are rich in OM (organic carbon (OC) content is 1-2%) (Beck et al., 1992). The greatest river of the White Sea, Northern Dvina which gives 48% of total riverine discharge, runs into Dvinsky Bay. Clay suspensions and some of sand-aleurite particles are carried out with riverine waters of N. Dvina into Dvinsky Bay (Kalinenko et al., 1976).

The port and town Kandalaksha is in the upper part of Kandalaksha Bay. Therefore the high amounts of industrial pollutants discharge into the Bay parallel with "natural" bioproduction. Though many small streams run into the Bay the role of riverine discharge in Kandalaksha Bay is minor in comparison with Dvinsky Bay. Bottom sediments of Kandalaksha Bay are mainly clay muds and aleurite-clay muds with small admixture of sandy material.

The purpose of this work was to study peculiarities of the composition of OM and their spacial distribution in bottom sediments of upper parts of Dvinsky and Kandalaksha Bays. Exploirations were carried out in 1981-1992 during several expeditions of the Russian Academy of Sciences.

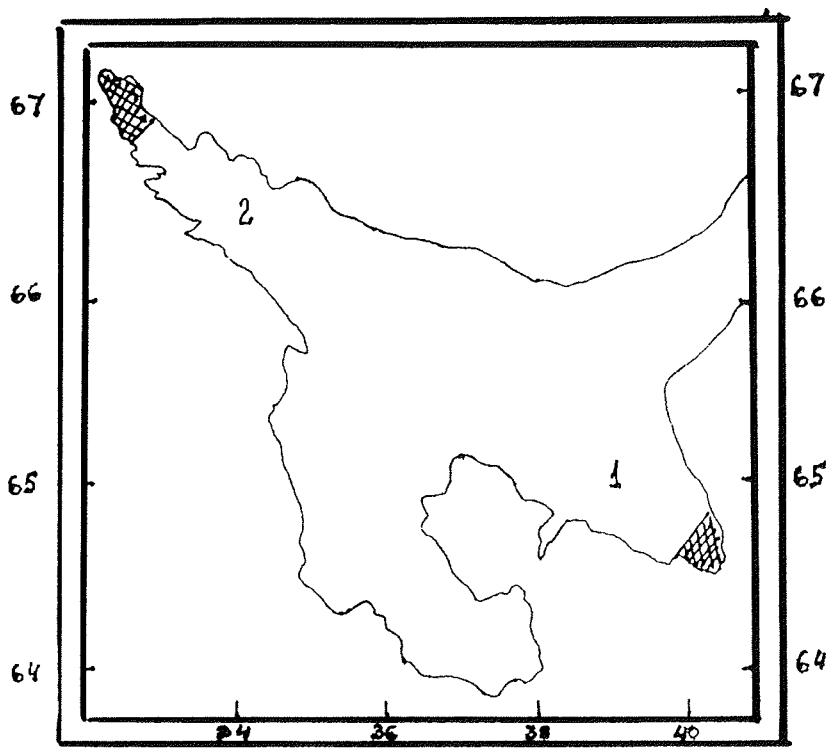

Fig. 1.: Areas of sampling in Dvinsky and Kandalaksha bays of White Sea.

Methods

Organic carbon (OC) in bottom sediments was determined with Knopp method (Uspensky et al., 1966) and lignin by the method of nitrobenzol oxidation with the subsequent determination of oxidation products by GLC (Peresypkin et al., 1989). Analysis of bitumoids (lipids) was carried out using the scheme of Danyushevskaya (1985). Humic acids (HA) were analyzed with the method of Uspensky et al. (1966). Polycyclic aromatic hydrocarbons were determined by HPLC method in a condition of the reverse-phase chromatography with a chromatograph MILICHROM, column Separon SGX RP-18-S (80 x 2 mm) (Petrova, 1990).

Results and discussion

Organic carbon content in bottom sediments of N.Dvina mouth and Dvinsky Bay varies from 0.07 to 1.41%, with an average of about 0.5% (Table 1). Higher content of OC was found in aleurites (1.18 and 1.41%), in sands content of OC is considerably lower (0.07-0.14%) and close to average values for bottom sediments of this type in the White Sea.

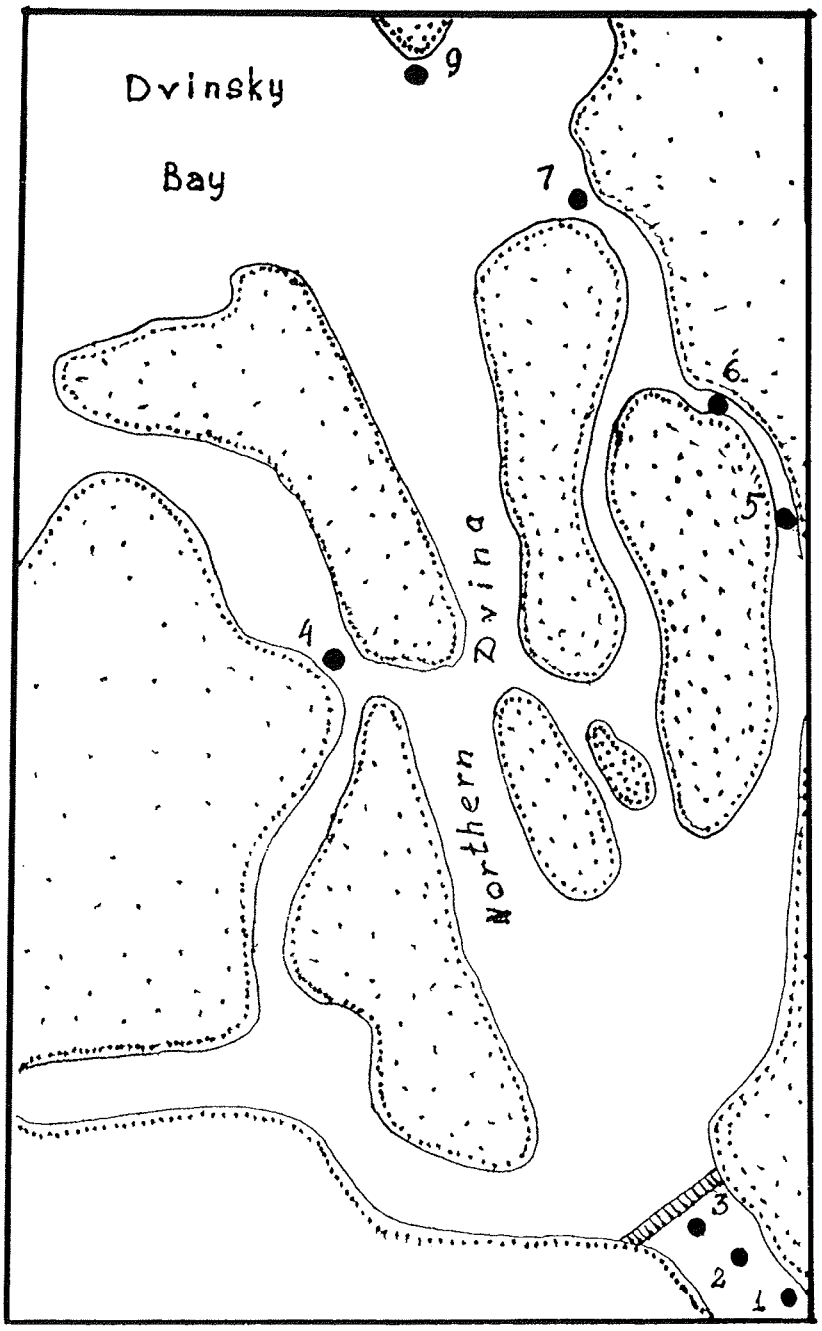

Fig. 2.: Sampling stations in upper part of Dvinsky Bay.

Higher concentrations of OC (1,4-2,97%) are obtained in bottom sediments of Kandalaksha Bay (Table 2) close to the location of great industrial objects and in the aquatory of Kandalaksha port (Fig. 3, Table 2) where the prevailing of thin aleurite-clay muds, absence of great currents, and delivery of authropogenic pollutants lead to quick accumulation and burying of OM into bottom sediments.

Lignin (and its derivatives-phenols) is one of the main components of both natural objects (higher plants, wood) and celluloze-paper industry. Investigations carried out in the southern part of Dvinsky Bay on the cross section N.Dvina river mouth - sea (Peresypkin et al., 1989) showed that a higher content of phenols was found in bottom sediments at stations 2, 4, 5, 6 (Table 1). Higher content of phenols in bottom sediments of station 4, remote from the sources of technogenous pollutions, may be caused by the supply of lignin from wood, floating at the surface of water or stored at river shores, as a result of its washing out with rainwaters. Higher content of lignin in bottom sediments taken at the other three stations is, first of all, connected with the supply of lignin-containing components with sewage waters of neighbouring plants. There is a trend of decreasing quantity of phenols with increased distance from the plants. The lowest concentrations of phenols in bottom sediments were found at the stations remote from the place of sewage discharge.

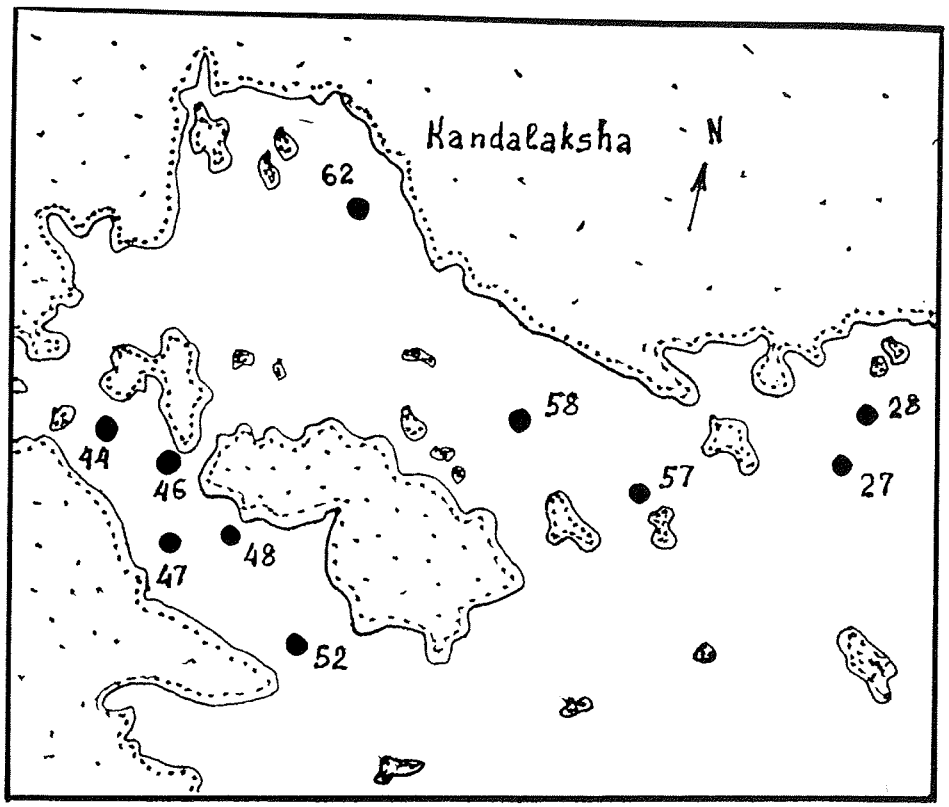

Fig. 3.: Sampling stations in upper part of Kandalaksha Bay.

Among the products of lignin oxidation vaniline aldehydes (VA) as well as benzoic structures predominate (Table 1). Their content in all studied bottom sediment samples of N.Dvina river mouth is considerably higher than that of other components. Higher contents of VA are controlled by the supply from coniferous forests growing on shores of N.Dvina river as well as from sewage products. The source of oxybenzoic structures may be grass as well as macrophytes.

In the Kandalaksha Bay lignin was studied in bottom sediments taken in the upper part of the Bay close to coasts (Fig. 3, Table 2). Total amount of phenol products in the surface layer of bottom sediments varies from 6,3 to 50,0 ng/g of dry sediment (Peresypkin and Shcherbakov, 1992). Higher concentrations of lignin are obtained in bottom sediments of Station 62 (Table 2) close to the port. Apparently the main source of lignin is the waste of wood processing. The other important source of lignin in studied bottom sediments of Kandalaksha Bay are soils. From soils lignin is washed out with rain water and transported into sea water. As a rule p-oxybenzoic structures prevail among studied phenols (Table 2). The source of these structures grass plants.

The comparison of results of lignin studyied in Dvinsky and Kandalaksha Bays obtain the same average content of phenols (20.01 and 17.09 ng/g). The level of concentration of lignin in bottom sediments is controlled by the influence of lignin sources (higher plants, soils, wood, sea grasses, waste of industrial objects). Therefore, higher concentrations of lignin products are often obtained close to the coastal zone, e.g., places of high anthropogenic activity.

Bitumoids-lipids, humic acids, and polycyclic aromatic hydrocarbons

As it was shown earlier (Artemyev, 1993) the typical process of OM transformation of terrigenous sands in the direction river-sea or land-sea is "debituminization" - the decrease of bitumoids (lipids) content in the total amount of OM and the increase of "residual" OM (ROM) or "humines", the OM most stable against transformation and destroying (Table 1, 2). The absence of HA in OM of terrigenous sands (Table 1) testifies that humification of OM does not take place there due to sharply oxidizing conditions helping the destruction of labile OM being a potential base for the formation of geopolymers of HA type (Artemyev, 1993). At the same time the content of HA in OM of aleurite-clay and clay muds is high (Table 1, 2). Another peculiarity of OM of terrigenous riverine and estuarine sands is the prevailing of oils in the composition of chloroform bitumoid "A". At the same time a dominant component of chloroform bitumoid "A" of terrigenous clay and aleurite-clay muds are the resins (Table 1, 2). It was noted (Artemyev, 1993) that this difference in the composition of chloroform bitumoid "A" of terrigenous sands and muds apparently is a global reguliarity. This assumption is confirmed by the example of bottom sediments of Kandalaksha Bay.

Polycyclic aromatic hydrocarbons (PAH) are the minor part of hydrocarbons (Table 1, 2), but they are among the basic pollutants along with heavy metals, radionuclides, oil-products, chlororganic compounds etc. Sources and ways of supply and distribution of PAH in sediments for different areas of the World Ocean, are the subject of a considerable number of investigations. This is explained by the clearly defined mutagenic and cancerogenic activity of a number of PAH which in combination with a considerable molecular

steadyness determines their high importance as markers for the estimation of the ecological condition of water areas.

The strategy for the study of PAH is based on organic-geochemical investigations which include genetic diagnostics and typification in bottom sediments (Petrova, 1990). In some sediments selected in Dvinsky and Kandalaksha Bays (Table 2) the content of PAH exceeds background values in 1-2 orders of magnitude and can be conditioned by the technogenic influence. However investigations of OM have shown that the level of PAH and its spacial distribution was considerably determined by the content of vegetable detritus and products of its biodegradation. This is supported by the data of high contents of HA, lignin and PAH (triphenilene-arene connected genetically with products of lignin degradation) in bottom sediments of some stations of Dvinsky and Kandalaksha Bays (Table 1-3). The extrem contents of PAH and phenols are fixed in the part of the offshore area adjacent to the port of Kandalaksha town. As has been shown a supply of vegetative remains in the Kandalaksha Bay sediments can be both natural and antropogenic at the expense of wastes of the pulp and paper industry.

Contents of pyrogenous PAH (PYR and BAP) in Kandalaksha Bay sediments were considerably lower than in contaminated sediments of the World Ocean where a BAP content can reach 5000 ng/g (Izrael and Tsyban, 1989). However, a PYR/FLA = 1.5-1.9 and high absolute contents of BAP in sediments of the port (238 ng/g) shows a contamination.

References

Artemyev V.E., 1993. Geochemistry of Organic Matter in River-Sea System. Nauka, M., 204 p. (in Russian).

Beck T.A., Sharnaud N.M., Scherbakov F.A., and Potapova L.I., 1992. To the genesis of organic matter of modern sediments of White Sea.- Okeanologiya, v. 32, No. 6, 1131-1138 (in Russian).

Izrael Yu.A. and Tsyban A.V., 1989. Anthropogenic ecology of the Ocean.L., Gydrometeoizdat, 527 p. (in Russian).

Kalinenko V.V., Medvedev V.S., and Nevessky E.N., 1976. Sediments and Facies of White Sea. - In: Lythodynamics, Lithology and Geomorphology of the Shelf. M., Nauka, 111-130 (in Russian).

Maximova M.P. and Bondarenko A.I., 1985. Chlorophyll in waters of White Sea. - Okeanologiya, v. 25, No. 5, 813-818.

Methodical recommendations on the studying of organic matter in bottom sediments of World Ocean. L., Sevmorgeo, 1985, 75 p. (Ed. A.I. Danyushevskaya).

Peresypkin V.I., Kuznetzov V.S., and Artemyev V.E., 1989. Lignin v donnykh osadkakh estuariya r. Sev. Dvina. - Vodnii resursy, No. 5, 96-100 (in Russian).

Peresypkin V.I. and Shcherbakov F.A., 1992. Organic carbon and lignin in the upper layer of the bottom sediments of the Kandalaksha bay of White Sea. - Oceanologya, Vol. 32, No. 6, 1051-1058 (in Russian).

Petrova V.I., 1990. Geochemistry of polycyclic aromatic hydrocarbons of sediments in polar zones of the World Ocean. In: Organic matter of bottom sediments of polar zones of the World Ocean (A.I. Danyushevskaya ed.), p. 70-129, L., Nedra (in Russian).

Uspensky V.A., Rodionova K.Ph., and Gorskaya A.I., 1966. Rucovodstvo po analizu bitumov i rasseyannogo organicheskogo veschestva gornykh porod. L., Nedra, 302 p. (in Russian).

Appendix

Table 1.: Organic compounds in bottom sediments of the upper part of Dvinsky Bay (from Peresypkin et al., 1989; Artemyev, 1993).

Stations	Depth	Type of sediments	OC %	Lignin phenols* mg/g				Composition of OM			Composition of chloroform bitumoid "A", %			HC of oils %	
N	m			P	V	S	Sum	bitumoids -lipids	HA	ROM	oils	resins	asphaltens	Me-Nf	Ar
1	8	Sand, fine-grained, grey-brown	0.07	6.66	9.06	0.65	16.37	15.4	not	84.6	56.3	39.9	3.7	89.5	10.5
2	7	Sand, fine-grained, grey-brown	0.14	12.72	13.78	0.52	27.02	8.0	" "	92.0	41.6	52.7	5.5	84.8	15.2
3	14	Sand, fine-grained, grey-brown	0.12	2.86	2.34	0.30	5.50	9.0	" "	91.0	43.4	48.6	6.0	80.8	19.2
4	7	Sand, fine-grained,	0.08	17.31	15.56	2.22	35.18	13.4	" "	86.6	62.9	33.7	2.5	87.9	12.1
5	1	Aleurite-clayey mud, dark-brown	1.18	15.22	13.93	2.45	31.60	3.8	21.4	74.8	23.1	60.7	11.0	80.2	19.8
6	3	Aleurite-clayey mud, dark-brown	1.41	19.03	10.01	0.85	29.89	4.6	20.2	75.2	20.4	67.9	10.1	79.6	20.4
7	9	Sand, fine-grained with inerbeds of clayey muds	0.48	2.61	2.29	0.40	5.30	4.6	14.9	80.5	49.2	45.3	5.3	86.5	13.5
9	13	Sand, medium-grained with gravel, black	0.96	5.68	10.51	1.06	17.25	3.4	13.1	83.5	61.3	34.1	2.8	86.9	13.1

* Phenols: P-p-oxybenzoic, V-vanillyl, S-syringyl; HA-humic acids; ROM-"residual" OM; HC-hydrocarbons; Me-NF-methane-naphthenous; Ar-aromatic

Table 2.: Organic compounds in bottom sediments of the upper part of Kandalaksha Bay.

Sta-tions	Depth	Type of sediments	OC %	Lignin phenols* mg/g				Composition of OM			Composition of chloroform bitumoid "A", %			HC of oils %	
N	m			P	V	S	Sum	bitumoids -lipids	HA	ROM	oils	resins	asphaltens	Me-Nf	Ar
44		Clayed mud with sand and aleurite	1.62	3.23	1.64	1.41	6.28	2.4	34.8	62.8	15.9	73.4	10.7	-	-
47		Clayed mud with sand and aleurite	1.73	5.58	0.87	0.71	7.17	4.3	26.8	68.9	18.1	75.3	6.6	-	-
48		Clayed mud with sand and aleurite	1.81	8.29	7.64	4.68	20.61	6.9	17.5	75.6	34.2	61.2	4.6	95.7	4.3
52		Clayed mud with sand and aleurite	2.50	5.16	8.68	3.71	17.55	3.6	31.9	64.5	15.1	76.9	8.0	87.1	12.9
57		Aleurite-sandy mud	0.65	6.14	7.95	0.70	14.79	2.4	16.2	81.4	28.5	61.4	10.1	89.7	10.3
58		Aleurite-sandy mud with gravel	1.80	7.05	1.42	0.88	9.35	3.2	19.7	77.1	40.1	56.6	3.3	88.4	11.6
62		Clayey mud with sand and aleurite	29.7	19.63	18.61	11.76	50.00	2.9	35.4	61.7	54.8	41.8	3.4	84.0	16.0
46		Clayey mud	2.33	-	-	-	-	6.4	33.4	60.4	75.8	23.9	0.3	-	-
27		Clayey mud with sand and aleurite	1.91	-	-	-	-	3.8	27.6	68.6	22.4	71.5	6.1	-	-
28		Clayey mud with sand and aleurite	2.46	-	-	-	-	2.0	31.9	66.1	24.2	70.6	5.1	-	-

* from Peresypkin and Shcherbakov, 1992

Table 3.: PAH content (ng/g sediment dry weight) and ratios by sampling for White Sea.

Location	The amount of stations	PAH		Dominante PAH distribution (mean)							PYR	FLA	Alk PHN
		Mean	Range	PHN	FLA	PYR	TRF	CHR	PER	BAR	FLA	FLA+PYR	PHN
White Sea	15	30	8-130	2	2	4	4	3	10	2	2.00	0.33	1.6
Kandalaksha gulf	9	500	300-740	15	34	51	128	80	166	12	1.50	0.40	1.4
Kandalasha port	1	3450	-	380	214	414	825	524	849	238	1.93	0.34	1.0

Abbreviations: PHN-phenanthrene, Alk PHN-alkylated phenanthrene, FLA-fluoranthene, PYR-pyrene, TRF-tryphenilene, CHR-chrysene, PER-perylene.

RIVERINE AND AUTOCHTONOUS CONTRIBUTIONS TO KARA SEA SEDIMENT LIPIDS

Belyaeva N.A.[1], Madureira L.A.S.[2], Eglinton G.[2]

1 P.P. Shirshov Institute of Oceanology, Moscow, Russia
2 University of Bristol, Cantok's Close, Bristol BS8 1TS, England

Abstract

In order to study the controlling factors on selective incorporation and diagenesis of terrestrial, bacterial, and planktonic lipids in sediments in polar environments, 15 samples of Kara Sea sedimentary lipids were examined by means of gas chromatography and mass spectrometry (GC-MS). Terrestrial-derived constituents predominate over autochtonous in alkanes, fatty acid, and fatty alcohol patterns characterized by prevailing high-molecular components. A relative enrichment of planktonic lipids registered by increased portion of short-chain alkanes and odd-over-even predominance index (OEP) for C_{19} of up to 15.0, and lowest long-chain fatty acid content (up to 17.8 % of total acids), was found in the northern part of the transect from the Ob River mouth to the north of the Kara Sea. The highest bacterial input supported by maximum content of bacterial-derived fatty acids (12.5 % of total acids) and low OEP for C_{19} (1.1), occurs nearest to the Ob River mouth. The average content of bacterial fatty acids (9.5 %) in surface sediments suggests intensive bacterial transformation processes in the Kara Sea. The variability of main lipid patterns does not correlate with primary productivity or distance from the Ob River mouth. Instead, factors controlling sedimentation most likely influence the accumulation of various lipids in surface sediments. Diagenetic transformations are reflected in the lipids by an increased proportion of high molecular, i.e. terrestrial compounds such as alkanes, fatty acids, and alcohols. Abietic and dehydroabietic acids derived from terrestrial higher plants, decrease rapidly indicating their diagenetic transformation into final pathway products. Separate analyses of free and total fatty acids provide insights into the mechanism of selective preservation of terrestrial and plankton-derived fatty acids in sedimentation and diagenesis.

Introduction

The assessment of terrestrial, bacterial, and plankton-derived organic matter in sediments of estuarine and shelf areas is a subject of continuing investigations, both for estimation of organic-matter genesis and for studies of its transport and accumulation (Saliot et al., 1988; Bigot et al., 1989; Grimalt and Albaiges, 1990; Yunker et al., 1993). Arctic seas are significantly less intensely studied relatively to temperate parts of the world, though high specificity of biosynthesis and biotransformation in polar environment should be reflected in the organic-matter composition of sea water and sediments. The most important controlling factors in polar marine environment are as follows: the pronounced oscillation of primary productivity caused by the long period of polar night and extrem life conditions of marine organisms under seasonal ice cover. At low temperature, sea water causes various biochemical

adaptations. In addition to these factors, Arctic seas are distinguished from the Antarctic seas by high riverine input. In this regard, the Kara Sea being the most heavily-loaded by riverine runoff (about 1350 km^3 per year), is particularly suitable for the study of the interrelation of organic matter and environmental factors. Therefore, major objectives of this study are the comparison of terrestrial and marine organic matter contributions to bottom sediments and biomarkers of high-latitude environment and related transport and transformation processes.

Material and methods

Seven samples of surface sediments and eight samples of Holocene age (up to 380 cm in subbottom depth) were taken from the 49-th cruise of RV "Dmitry Mendeleev" in 1993 on a transect from the Ob River mouth to the northern part of the Kara Sea up to 76°N. Lipids were extracted from the air-dried sediments in a Soxhlet apparatus with chloroform. One half of lipid extracts was transesterified using 5 % methanolic hydrochloric acid (HCl) and then trimethylsilylated by N,O-bis(trimethylsilyl)-trifluoroacetamid (BSTFA). Free lipids were extracted from the second half after preparative thin layer chromatography (TLC) and trimethilsilylated by BSTFA.

The quantitative analysis of individual lipid compounds was performed by means of GC and GC-MS. GC analyses were carried out using a model 5160 Carlo Erba GC equipped with an on-column injector and 50 m x 0.32 mm i.d. CPSil5CB column (film thickness 0.25 mm, Chrompack). The temperature programme was from 50 - 150°C at 10°C/min and 150 - 300°C at 4°C/min and then held isothermally for 40 minutes. H_2 was used as the carrier gas.

GC-MS analyses were made on a 4500 Finnigan-MAT Mass Spectrometer interfaced to a Model 5160 Carlo Erba GC (EI - 70 eV; 1 scan s^{-1}, scanned from 50 - 600 atomic mass units -amu-) and operated under identical GC conditions except that He was used as carrier gas.

Compounds were quantified from GC peak areas using Minichrom data acquisition/chromatography software (VG Laboratory Systems, UK). Data obtained by GC-MS were processed by INCOS system.

Results and discussion

Total lipid composition.
GC traces of the Kara Sea sedimentary lipids contain 2 - 3 hundred peaks of dissimilar chemical structure. GC-MS analyses allow to identify about 90 compounds. In all samples, fatty acids dominate in the lipid monomer composition varying in the range of 25.54 - 53.56 % of total lipids (average of 39.2 %). The second most abundant lipid fraction are the *n*-alkanes accounting 12.5 % in average. The next important compounds are fatty alcohols, dehydroabietic acid derivatives (D), sterols and their structural analogous, and abietic acid derivatives (A). Diols, hydroxyacids, hopanes, hopanoid acid, and alcohols were identified in a number of samples in minor concentrations.

The spatial distribution of main lipid monomers in surface sediments of the Ob transect (Fig. 1) appears to be independent either from primary productivity of the water column or from the distance of terrestrial organic matter discharge. This result illustrates the complexity of such an environment, where variations in organic-matter transport and accumulation occur in response to changing monomer lipid composition. Therefore, organic-matter genesis is manifested in total lipid composition less distinctly than sedimentation conditions. However, there are two chemical structures in sedimentary lipids closely associated with their genesis; abietic and dehydroabietic acids derivatives (fractions A and D in Fig. 1) strictly derived from terrestrial organic matter (Lafflamme and Hites, 1978). Dehydroabietic acid is considered to be the intermediate product in the diagenetic transformation of abietic acid into diterpenoid and then to polyaromatic hydrocarbons with retene skeleton.

The ratio of dehydroabietic/abietic acids (D/A) in the surface sediments tends to increase from the Ob mouth into the northern direction (Fig. 2). This can be interpreted as continuing transformation process of suspended terrestrial organic matter on its way from the source to the site of burying in the sediment. However, a change in controlling factors of sediment accumulation likely affects both lipid monomer composition and the shift in the D/A ratio in the surface sediments. Therefore, the oxic sand from St. 4395 differs from the anoxic one from next St. 4396 by a two-fold decreased D/A ratio.

Molecular lipid composition

There is growing evidence proven by the last decade of organic geochemical studies, that molecular lipid composition of bottom sediments more definitely reflects the source of organic matter than the lipid group composition (Brassel and Eglinton, 1986; Mar. Org. Geochem., 1992). Thus, *n*-alkane, fatty acid, and fatty alcohol patterns are of particular interest for the assessment of different sources in sedimentary organic matter of the Kara Sea.

The data on indicative parameters of lipid patterns (Fig. 2) show the strong predominance of terrestrial-derived compounds in all analyzed samples of bottom sediments. The evidence for this is provided by alkanes, fatty acids, and fatty alcohols simultaneously. In the surface sediments of the Ob transect, the ratios of low and high molecular weight alkanes C_{17}-C_{19}/C_{23}-C_{33} and C_{17}-C_{22}/C_{23}-C_{35} are averaged at 0.14 and 0.36, respectively, indicating the high input of terrigeneous higher alkanes (Douglas and Eglinton, 1966; Saliot et al., 1988). Similar alkane patterns were also registered in other sites of the Kara Sea (Romankevich et al., 1982).

Terrestrial-derived fatty acids with carbon chains longer than C_{24} (Bigot et al., 1989 and references therein) reach in average 36.2 % of the total fatty acids in surface sediments. The terrigeneous fatty alcohols C_{24}, C_{26}, and C_{28} have a mean value of 30.4 % of total alcohols in surface sediments.

However, the distribution of terrigeneous lipids along the Ob transect is not uniform. There are two samples in the northern part of the transect (St. 4395 and 4396) characterized by lowest accumulation of terrestrial-derived lipids and high amounts of lipids of primary-plankton origin (Fig. 2).

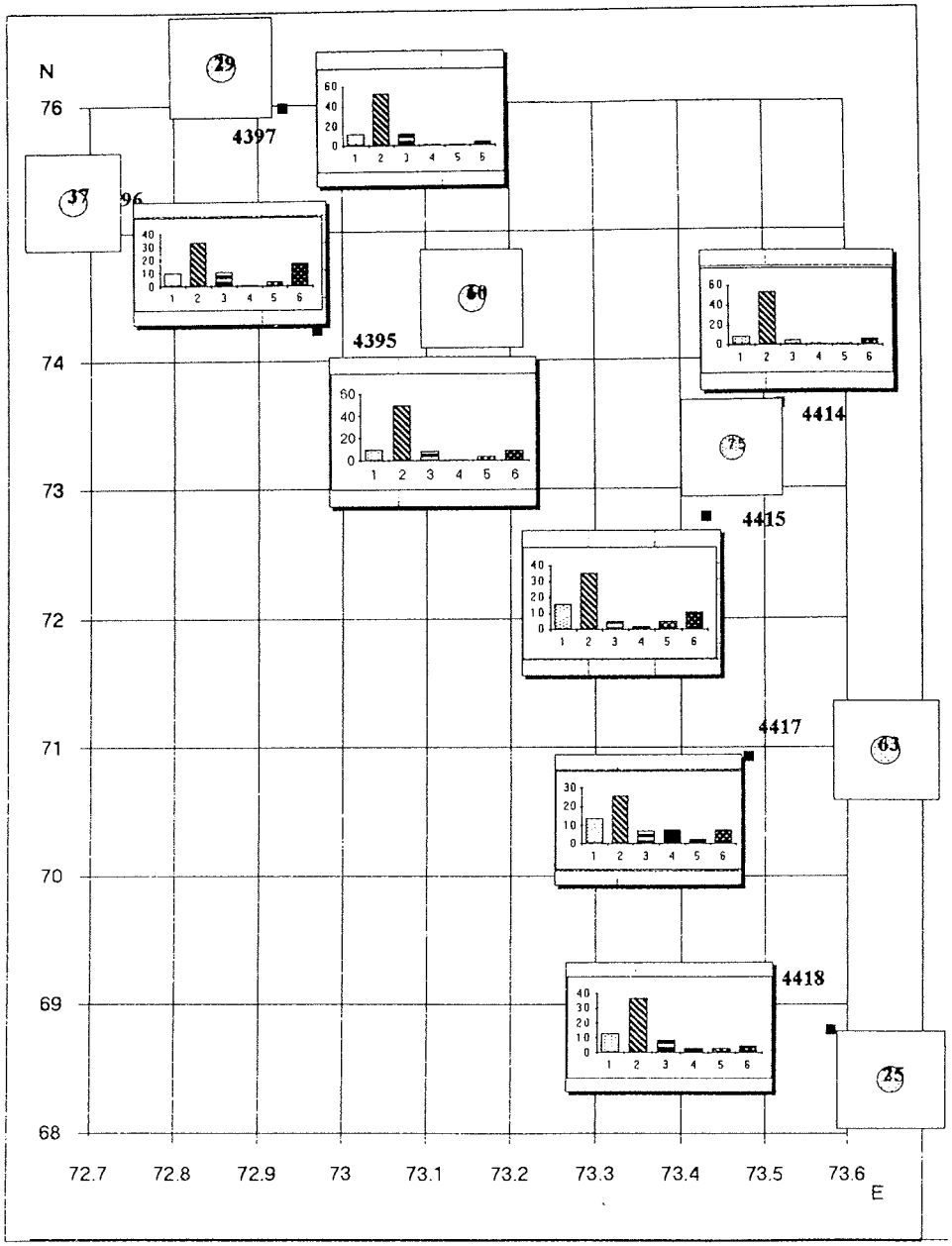

Fig. 1.: Sample sites and lipid monomer composition (% of total): 1 - *n*-alkanes; 2 - fatty acids; 3 - fatty alcohols; 4 - sterols; 5 - abietic acids; 6 - dehydroabietic acids. Numbers in circles - phytoplankton primary productivity, mg/m^2 day.

The plankton origin of lipids is manifested in alkane patterns by the enhanced values of the odd-over-even predominance index (OEP) for C_{19} consistent with the increased ratio of short-chain to long-chain alkanes. Plankton-derived fatty acids (unsaturated acids with different numbers of double bonds 16:1, 18:1(n-9), 18:2, 18:3, 20:5, 22:6) have the highest values of 34.8 - 36.0 % in these samples. They are accompanied by maximum values of the ratio of unsaturated to saturated acids reflecting the "freshness" of organic matter in the sediments (Bigot et al., 1989). Furthermore, the lowest content of terrestrial fatty alcohols (11.5 - 12.3 % of total alcohols) is recorded here. Since the nearby most northern side St. 4397 is characterized by the high input of terrestrial lipids again, the observed accumulation of plankton lipids at St. 4395 and 4396 could be attributed as some sort of "transit" zone for terrigeneous organic matter supply caused by hydrodynamic or other factors driving the sedimentation.

Important is also the distribution of bacterial-derived fatty acids in the Kara Sea surface sediments. The sum of branched iso- and anteisoacis and monounsaturated fatty acid $C_{18:1(n-11)}$ of primary bacterial origin has an average value of 9.5 % of total acids. These data suggest a high microbial activity in organic matter cycling since the overall content of bacterial fatty acids in Kara Sea sediments is comparable to the content of similar acids in Bohai Sea (China) sediments (5.7 to 8.3 % of total fatty acids; Bigot et al., 1989). Therefore, the increased flux of organic matter from the surface to the bottom of the Barents Sea relatively to temperate marine environment (Belyaeva et al., 1989) seems to be not related to supressed bacterial organic-matter transformation.

Moreover, the highest content of bacterial-derived fatty acids (12.54 %) is observerd nearest to the mouth of the Ob River (St. 4418). Increased bacterial input within this sand is also supported by an increased content of short-chain alkanes and low values of OEP for C_{19} (Yunker et al., 1993). These data confirm the conclusions (Peulve et al., 1993) that Arctic Seas estuarine areas are distinguished from marine Arctic shelf areas by more intensive bacterial transformation of organic matter.

The comparison of our data with similar data from other marine environments influenced by river runoff leads to following conclusions. The Ob River input seems to be more important for the sedimentary lipids than the Huanghe River input since the shelf sediments of the Bohai Sea contain just about 17 % of terrestrial fatty acids in the total acids (Bigot et al., 1989). Accordingly, planktonic fatty acids are more abundant in sediments of Bohai Sea relatively to Kara Sea sediments. Secondly, the remarkable variability of various source lipids along the Ob transect makes a difference with the invariant alkane distribution on the Mackenzie River shelf (Yunker et al., 1983). Hence the lipid patterns of the Kara Sea probably reflect the peculiarity of sedimentatary conditions and phytoplankton productivity additionally to genesis features.

Biosynthesis specificity of Arctic environments is reflected in the sedimentary lipids by the occurrence of polyunsaturated fatty acids $C_{16:4}$, $C_{18:4}$ and $C_{16:2}$ identified in minor concentrations (up to 1 %) in the total acids. Additionally, the polyunsaturated fatty acid $C_{20:5}$ is found in sediments of the Ob transect in concentrations averaged at 3.2 % of total acids. This value is remarkably higher than that in sediments of the Bohai Sea (0.7 - 1.3 %). These highly

unsaturated fatty acids are thought to provide lesser specific gravity to cellular membrane lipids in relation to low temperature environments (Prahl and Wakeham, 1987).

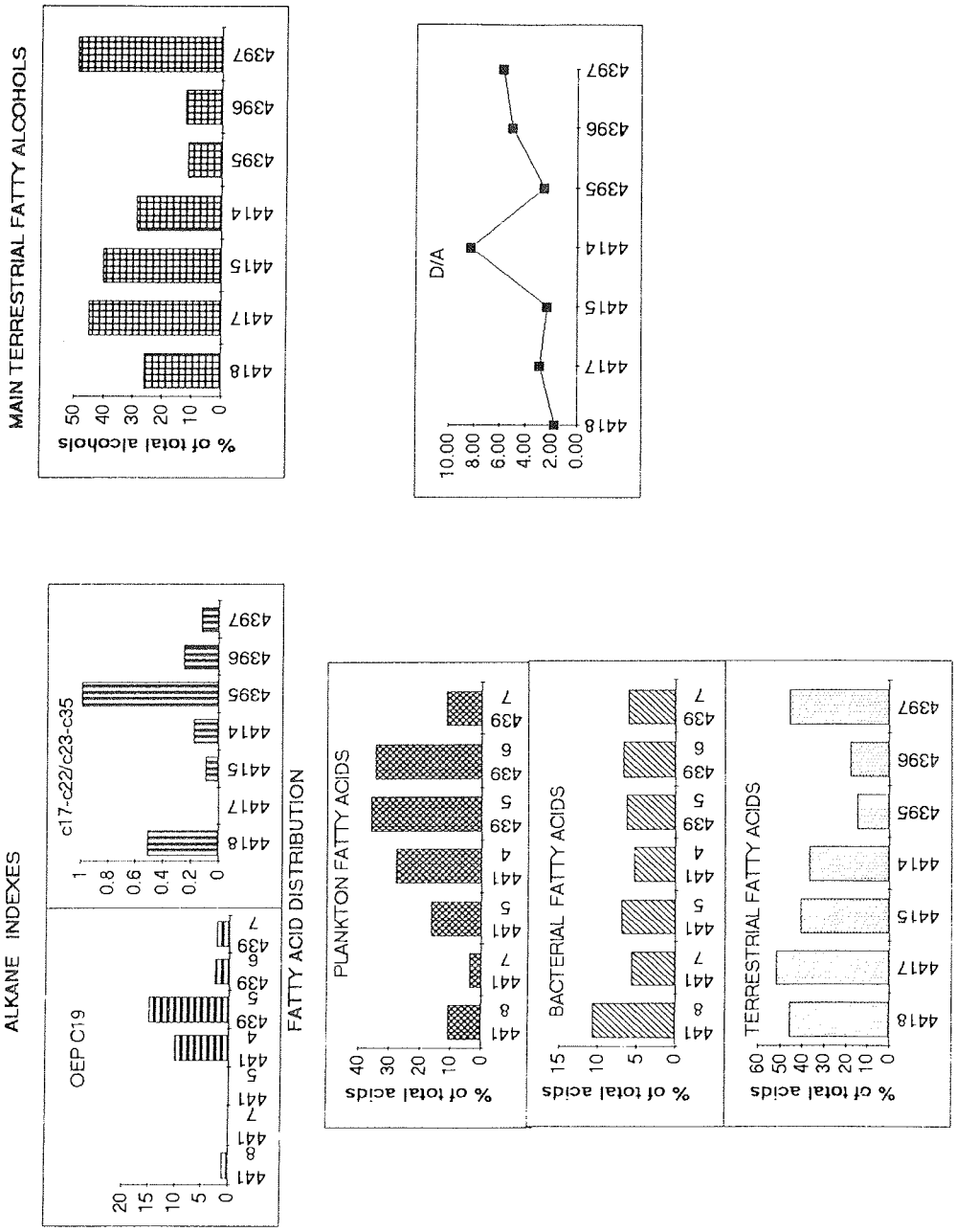

Fig. 2.: Molecular lipid composition parameters (see details in the text).

Diagenetic transformations of lipids can be recognized in fatty acid and alcohol patterns in particular. As shown in Figure 3, fatty acid composition changes in sediment cores with regular and fast decreasing plankton-derived components, more slowly decreasing bacterial fatty acids, and proportionally enhanced content of fatty acids of terrestrial origin. A similar diagenetic alteration of fatty acids was observed in rapidly accumulating coastal sediments and explained by different biogeochemical resistance of various fatty acid structures (Boon et al., 1975; Van Vleet and Quinn, 1979; Lajat et al., 1990; Haddad et al., 1992). The overall diagenetic shift in sedimentary lipids in the direction of increasing portion of terrestrial-derived compounds is also noticeable in fatty alcohol pattern characterized by the rapidly increased content of $C_{24:0}$, $C_{26:0}$, and $C_{28:0}$ (Fig. 3).

During early diagenesis abietic and dehydroabietic acid derivatives decrease regularly with depth (Fig. 3), but the ratio of these components appears to suggest that the initial stage of diagenesis leads predominantely to the formation of dehydroabietic acid. After that, transformation of dehydroabietic acid into final products is more intensive. The increased D/A ratio in the intermediate layers of the sediments relatively to the surface sediments and the decrease of the ratio in the deep layers may indicate such a process. Additional studies are necessary for reliable conclusions on the diagenetic pathway abietic acid - dehydroabietic acid - diterpenoids. These compounds, however, seem to be promising for the better understanding of mechanisms of terrestrial organic matter diagenesis.

Free and bound fatty acids

The alternative existence form of lipid constituents in marine environments can originate from biosynthesis or from specific chemical transformation during sedimentation and early diagensis. Biosynthesis results in the occurrence of free (unbound) sterols, fatty acids or bound ones incorporated into complex membrane lipids via ester, amide, and/or glicosidic linkage. The chemical transformation is mainly based on the formation or cleavage of ester links (Van Vleet and Quinn, 1979; Kawamura and Ishiwatari, 1984) followed by variations in free and bound lipids in particles and sediments. This process is accompanied by a number of physico-chemical reactions such as sorption and quenching driving transfer of free lipids into more resistant and less extractable forms. Therefore, the separate determination of free and bound sedimentary lipids can give insights into the specific rates and mechanisms of selective preservation and/or diagentic alteration of various source lipids.

Figure 4 shows the difference in the behavior of free fatty acids (FFA) and total fatty acids (TFA) in samples of the Ob transect. First of all, the very rapid disappearance of FFA relatively to TFA in the upper part of the cores is noticeable and is similar to that observed in the Santa Barbara Basin (Lajat et al., 1990). Typical changes of unsaturated, branched, and saturated FFA and TFA are shown in Figure 4 and may be applied for testing of different fate of these fractions in diagenesis.

Since unsaturated fatty acids are considered to indicate plankton-derived organic matter, their preservation and transformation in sedimentary lipids is of essential importance. The most striking feature of unsaturated acid distribution is the occurrence of polyunsaturated constituents particularly in bound form. It is difficult to discriminate between a biosynthesis linkage or a

pre-sedimentary incorporation of highly unsaturated fatty acids into the complex lipids. It seems to be likely, however, that just binding provides the capability of these non-resistant compounds to be accumulated in surface sediments escaping from decomposition. This suggestion is consistent with the better preservation of unsaturated sterols in the bound fraction of the sediments (Lajat et al., 1990).

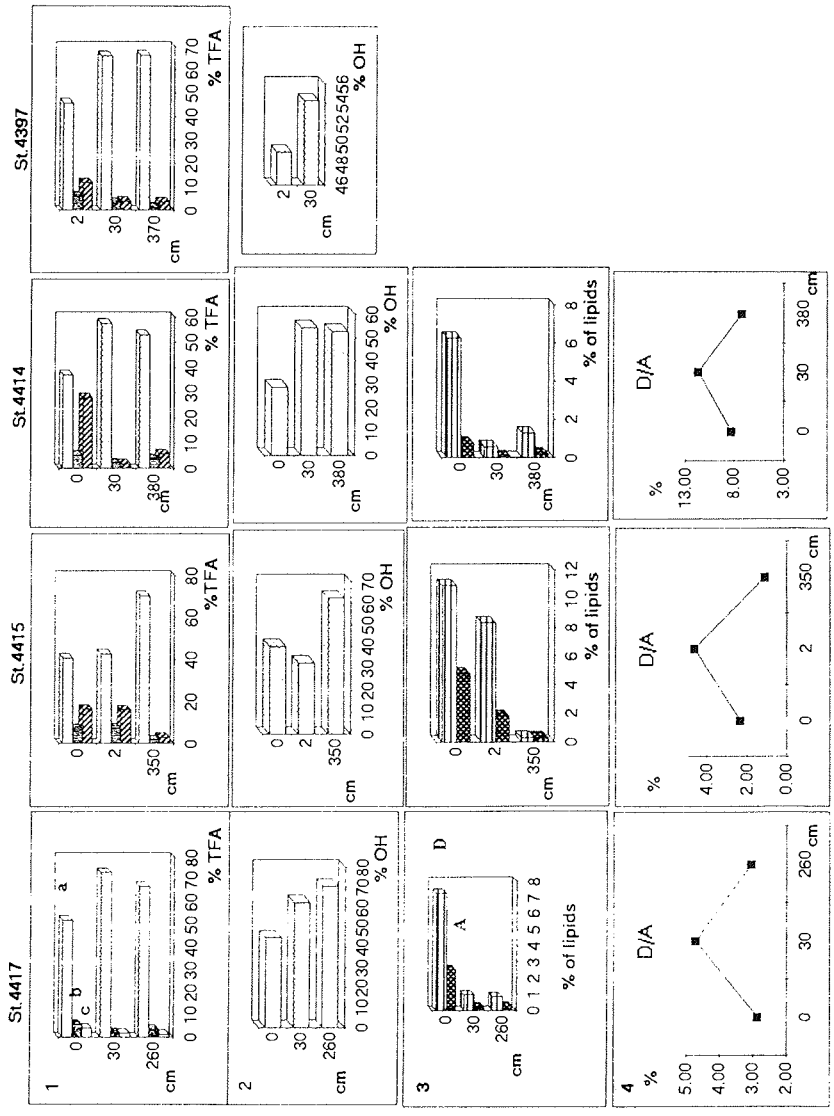

Fig. 3.: Diagenetic alteration of lipid fractions: 1 - fatty acids: a - terrestrial derived; b - abacterial derived; c - plankton derived. 2 - fatty alcohols 24, 26, 28 % of total alcohols. 3 - abietic acids (A) and dehydroabietic acid (D), % of lipids.

Monounsaturated fatty acids are found in sediments in free and bound forms but their ratio changes during diagenesis. Thus, fatty acids $C_{18:1(n-9)}$ and $C_{18:1(n-11)}$ occur predominantly in free form in lipids of surface sediments. In intermediate layers the ratio of free to bound $C_{18:1}$ decreases reflecting more rapid transformation of free fatty acid. The further increase of this ratio in the deep sediment can be related to decomposition of the bound monounsaturated fatty acids.

Branched fatty acids of primary bacterial origin appear to exist particularly in the free fraction of sedimentary fatty acids. However, the variations of free and bound branched fatty in sediment cores reflect the complexicity of the diagenetic behavior of the fatty acid fraction.

Very interesting is the distribution of saturated fatty acids in free and bound forms (Fig. 4). Short-chain fatty acids derived primarily from terrestrial lipids occur mostly in TFA. During diagenesis these bound terrestrial fatty acids appear to be more resistant, significantly increasing their proportion in sedimentary lipids. This may explain the diagenetic shift of the lipid molecular composition mentioned above.

Short-chain fatty acids demonstrate a more irregular behavior in sediment cores. These components tend to decrease in the intermediate layer relatively to the surface one. In the deep layer they occur in concentrations higher than that in the intermediate layer. Such a difference can be explained by preferential consumption of free short-chain fatty acids by bacteria and/or quenching or sorption of these compounds in an early stage of diagenesis. Furthermore, the partial decomposition of the complex lipids could drive the relative enrichment of short- and median-chain saturated FFA in the deep sediments. The upper histograms in Figure 4 suggest that the intensity of the last process may vary in different sites since we can see both a regular decrease of FFA relatively to TFA (St. 4417) or a slight enrichment of the deep layer by FFA (St. 4397).

Conclusion

The data obtained from organic-geochemical investigations of Kara Sea sediments lead to the conclusion that a more accurate assessment of various source lipids in the diagenetically altered sediments can be achieved on the basis of known diagenetic history of various lipid compounds.

In summary, the data obtained on the sedimentary lipids of the Kara Sea appear to confirm the hypothesis on the significance of terrestrial organic matter accumulated in the sediments. Bacterial organic matter transformation in the water-sediment boundary layer, however, seems to be more intensive than it was proposed on the basis of abiotic low temperature controlling factors. Plankton-derived lipids accumulate in surface sediments presumably due to their incorporation into complex lipids less accessible to microbial degradation. The binding of terrestrial-derived fatty acids provide an increased resistance of these fraction during diagenesis.

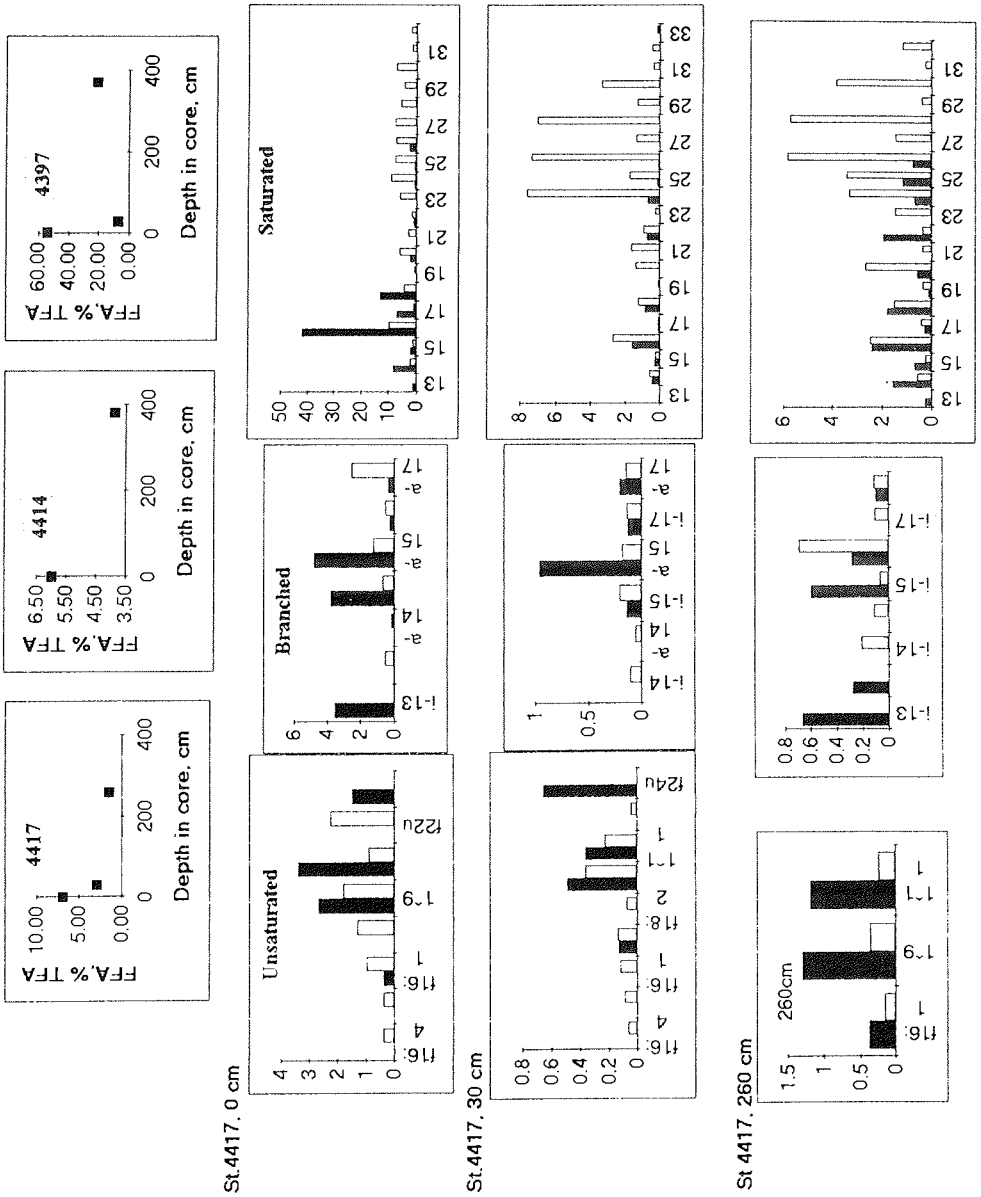

Fig. 4.: Free (FFA, black) and total (TFA, white) fatty acid distribution.

Acknowledgments

The work was funded by Russian Fundamental Science Foundation (grant 93-05-8871) and International Science Foundation (grant M2W00). Additionally, A. Belyaeva is sincerely thankful to The Royal Society of UK for the opportunity to fulfill the experimental study in the Biogeochemical Centre of the University of Bristol.

References

Belyaeva, A.N., Daniushevskaya, A.I., and Romankevich, E.A., 1989. Organic geochemistry of Barents Sea sediments. In: The Arctic Seas. Climatology, Oceanography, Geology, and Biology. (Ed. Y. Herman), Van Nostrand Reinhold Company, N.-Y., p. 761-796.

Bigot, M., Saliot, A., and Cui, X, Li, J., 1989. Organic geochemistry of surface sediments from the Huanghe estuary and adjacent Bohai Sea (China). Chem. Geol., v. 75, p. 339-350.

Brassell, S.C. and Eglinton, G., 1986. Molecular geochemical indicators in sediments. In: Organic Marine Geochemistry (Ed. by M. Sohn), Am. Chem. Soc., Washington, DC, p. 10-32.

Boon, J.J., de Leeuw, J.W., and Schenck, P.A., 1975. Organic geochemistry of Walvis Bay diatomaceous ooze. Occurrence and significance of the fatty acids. Geochim. Cosmochim. Acta, v. 39, p. 1559-1565.

Douglas, A.G. and Eglinton, G., 1966. The distribution of alkanes. In: Comparative phytochemistry (Ed. by T. Swain), Ch. 4. Academic press, N.Y., p. 187-218.

Grimalt, J.O. and Albaiges, J., 1990. Characterisation of the depositional environments of the Ebro Delta (western Mediterranean) by study of sedimentary lipid markers. Mar. Geol., v. 95, p. 207-224.

Haddad, R.I., Martens, C.S., and Farrington, J.W., 1991. Quantifying early diagenesis of fatty acids in a rapidly accumulating coastal marine sediment. Adv. in Org. Geochem. 1992, v. 19, N 1-3, p. 205-216.

Kawamura, K. and Ishiwatari, R., 1984. Fatty acid geochemistry of a 200 m sediment core from Lake Biwa, Japan. Ear5ly diagenesis and paleoenvironmental information. Geochim. Cosmochim. Acta, v. 48, p. 251-266.

Lafflamme, R.E. and Hites, R.A., 1978. The global distribution of polycyclic aromatic hydrocarbons in recent sediments. Geochim. Cosmochim. Acta, v. 42, p. 289-303.

Lajat, M., Saliot, A., and Schimmelman, A., 1989. Free and bound lipids in recent (1835-1987) sediments from Sante Barbara Basin. Adv. in Organic Geochemistry. Org. Geochem., 1990, v. 16, Nos 4-6, p. 793-803.

Marine Organic Geochemistry, 1992. Review and Challenges for the Future. Mar. Chem., v. 39, N 1-3, 242 p.

Peulve, S., Broyelle, I., Sicre, M.-A., Bouloubassi, I., Lorre, A., Saliot, A., de Leeuw, J.W., and Baas, M., 1993. Characterisation of the organic matter in an Arctic delta (Lena River) using biomarkers and macromolecular indicators. In: Organic Geochemistry. Poster Session 16th Int. Meet. Org. Geochem., Stavanger, p. 393-397.

Prahl, F.G. and Wakeham, S.G., 1987. Calibration of unsaturation patterns in long-chain ketone composition for paleotemperature assessment. Nature, v. 330, p. 367-369.

Romankevich, E.A., Daniushevskaya, A.I., Belyaeva, A.N., and Rusanov, V.P., 1982. Biogeochemistry of organic matter in the Arctic Seas. (Eds. I.S. Gramberg, E.A. Romankevich), Nauka, Moscow, 239 p.

Saliot, A., Tronczynski, J., Scribe, P., and Letolle, R., 1988. The application of isotopic and biogeochemical markers to the study of the biochemistry of organic matter in a microtidal estuary, the Loire, France. Estuarine Coastal Shelf Sci., v. 27, p. 645-699.

Van Vleet, E.S. and Quinn, J.G., 1979. Early diagenesis of fatty acids and isoprenoid alcohols in estuarine and coastal sediments. Geochim. Cosmochim. Acta, v. 43, p. 289-303.

Yunker, M.B., Macdonald, R.W., Cretney, W.J., Fowler, B.R., and Mc Laughin, F.A., 1993. Alkane, terpene, and polycyclic aromatic hydrocarbons geochemistry of the Mackenzie River and Mackenzie shelf: riverine contributions to Beaufort Sea coastal sediment. Geochim. et Cosmochim. Acta, v. 57, N 13, p. 3041-3061.

DISTRIBUTION OF PLANT PIGMENTS IN SURFACE SEDIMENTS OF THE EASTERN ARCTIC

Boetius A.*, Grahl C.*, Kröncke I.+, Liebezeit G.# and Nöthig E.-M.*

*Alfred Wegener Institute, Bremerhaven, Germany
+Senckenberg Institute, Wilhelmshaven, Germany
#Research Center Terramare, Wilhelmshaven, Germany

Introduction

Primary production in the eastern Arctic Ocean is controlled by the extreme seasonality in light availability and by low nutrient concentrations. The largest portion of the yearly production of algal biomass develops during a short period in late spring after the ice-melt and the stabilisation of the water-column. Since the low nutrient concentrations are quickly depleted, those processes which support the regeneration of nutrients should strongly influence the primary production in different Arctic regions. Under the ice, primary production is very low due to the reduced light availability. Furthermore, the contribution of the ice-communities is only around 10% of the total phytoplankton production (Subba Rao and Platt, 1984). Thus, the export of marine organic matter from the euphotic zone should largely depend on the size and duration of ice-free areas. At latitudes above 70°N in the Eurasian Arctic, primary production was estimated to be around 5-50 g C m^{-2} y^{-1} and marine organic matter export to range between 0.1-5 g C m^{-2} y^{-1} (Hargrave, 1994; Wassmann and Slagstad, 1993; Wheeler et al., 1996). Only a small fraction thereof is deposited at the sea-floor due to the degradation of the particles during sinking and the relatively strong grazing pressure (Wassmann et al., 1991; Wheeler et al., 1996). Hence, in some parts of the Arctic Ocean, allochtonous fluxes of organic particles might contribute substantially to the accumulation of organic matter in the sediments. Organic matter could be exported from the large productive shelf areas to the deep sea and downslope gravitation flow might enhance particle deposition at the bottom of the continental slope and in the Arctic Basins (Stein et al., 1994; Stein, this vol.). Large amounts of particles are trapped during freezing of sea ice in shallow water, transported with the ice and released during melting (Nürnberg et al., 1994). However, only very few data on carbon flux rates to the sea-floor are available in the ice-covered Arctic Ocean, mainly due to technical and logistical restrictions in the deployment and recovery of sediment traps.

Results and discussion

An indicator of phytodetritus input to marine sediments is the presence of plant pigments. The half-life of chlorophyll pigments in Arctic sediments is around 44 d (Graf et al.,1995). Chlorophyll *a* and its degradation products, the phaeopigments, can be detected fluorometrically as chlorophyll *a* equivalents after their extraction from the sediments (Shuman and Lorenzen, 1975). In this compilation of pigment data from several expeditions to the Eurasian and Central Arctic, we investigated the general relationships between different levels of pigment concentrations in Arctic surface sediments and location,

water depth or distance from the coast. In all samples, total pigments mainly consist of phaeopigments (>90%) except at shallow stations <50 m. Pigment concentrations in the Barents Sea and Central Arctic are demonstrated in Figure 1. The expedition ARK VIII/2 with RV Polarstern in summer 1991 visited the central and northern Barents Sea, where Atlantic and Arctic water masses meet (Rachor, 1992). Study area was the slope around Svalbard, and a profile from the Nansen Basin to the frontal zone in the central Barents Sea was conducted.

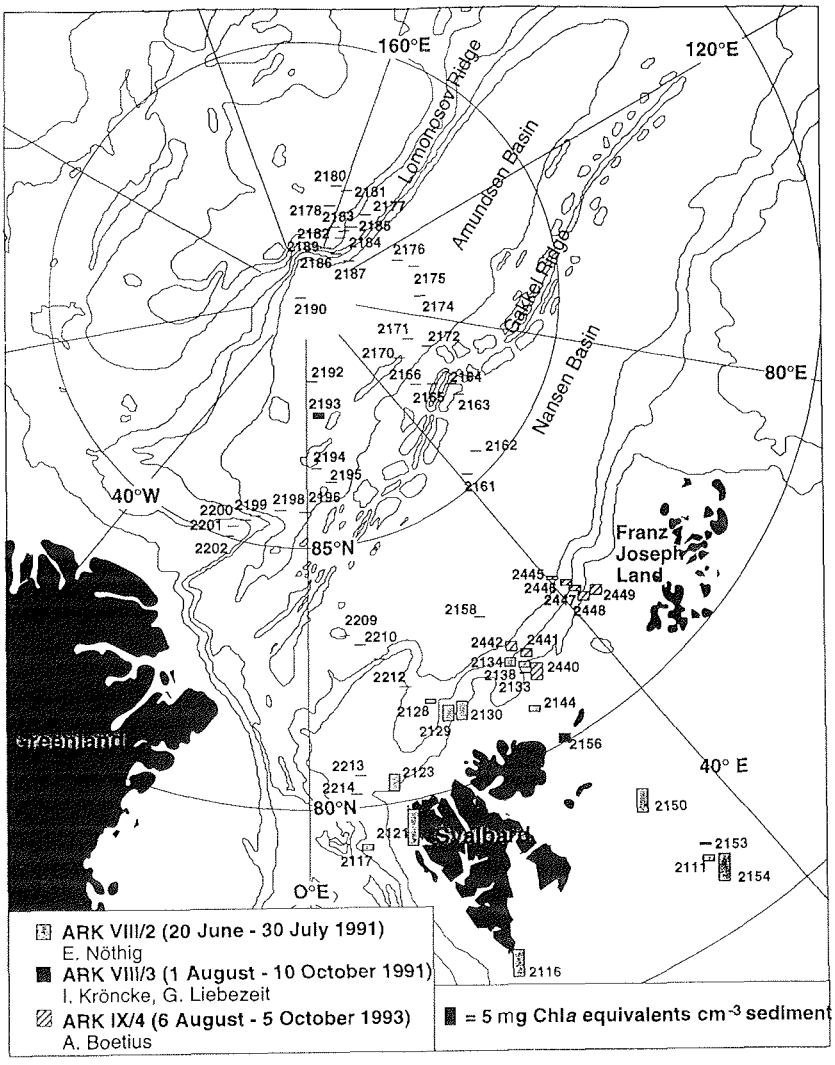

Fig. 1.: Pigment distribution in the Barents Sea and the central Arctic Ocean. Data presented are the levels of pigment concentrations in the surface sediments (0-1 cm), measured as average values (n=5) of chlorophyll *a* equivalents (chlorophyll *a* + phaeopigments). Numbers next to the columns are AWI station numbers (first two chiffres omitted).

Pigment concentrations decrease down the continental slope, from 7-10 mg cm^{-3} at around 200 m water depth to 1-2 mg cm^{-3} at around 2500 m. Along the N-E profile through the Barents Sea, the highest pigment concentration (7.7 mg cm^{-3}) was recorded at the southern-most station (2154, 253 m depth) in an open water area. During the German-Russian expedition ARK IX/4 (Fütterer, 1994), two transects across the continental slope were investigated in the Barents Sea, north of Svalbard and north-east of Franz-Joseph-Land. Again, a strong decrease of pigment concentrations with increasing water-depth was detected, from 3-5 mg cm^{-3} at 250 m to 1.7-2.5 mg cm^{-3} at 3000 m. During the expedition ARK VIII/3 (Fütterer, 1992), the first data on pigment concentrations in the deep Arctic Basin were obtained, including a transect through the Nansen (2158-2162) and the Amundsen Basin (2170-2176, 2190-2196) as well as across the Gakkel Ridge (2163-2166), Lomonosov Ridge (2177-2189) and Morris Jesup Rise (2198-2202). At nearly all stations in the central Arctic, pigment concentrations were below 0.2 mg cm^{-3} sediment. Comparatively high pigment concentrations of >1 mg cm^{-3} were found in the Amundsen Basin at a water depth of >4000 m. In the surface sediments of a few deep stations in the Arctic Basin, no pigments were detected, indicating that some areas under the permanent ice-cover might be completely shut off from any supply of phytoplankton detritus for a year or longer.

The influence of water-depth, ice-cover, and distance from the coast on the input of phytoplankton detritus to the sediment was studied during two cruises to the Laptev Sea, ARK IX/4 in 1993 (Fütterer, 1994) and ARK XI/1 in 1995 (Rachor, in prep.). The distribution of plant pigments (Chl *a* and phaeopigments) was investigated along several transects (76-78°N) extending from the Laptev Sea shelf to the base of the continental slope as well as across the Lomonosov Ridge (Fig. 2). Along the ice-free eastern transect (133°E), highest pigment concentrations in surface sediments were recorded at the shelf edge (100 mg m^{-2} at 30-100 m water depth). These maximum values were related to the sedimentation of a phytoplankton-bloom which had developed along the ice-edge in August 1993. In general, the pigment concentrations in the sediments decrease from the shelf edge (2-13 mg cm^{-3}) to the bottom of the continental slope (0.6-1.0 mg cm^{-3}) by a factor of ten. At comparable water-depths on the upper slope, pigment concentrations are higher at ice-free than at the ice-covered stations.

In Figure 3, the relationship between pigment concentrations and water depth (a) or latitude (b) is demonstrated, including all data of the four cruises. On the shelf edge (30-250 m), values vary by more than one order of magnitude, mainly between 1-10 mg cm^{-3}. Pigment concentrations in the surface sediments of the Eurasian continental slope decrease strongly from the shelf edge to a depth of 1000 m. On the upper slope (250-1000 m), pigment concentrations are generally higher than on the deeper slope (1000-3000 m; 0,2 to 2 mg cm^{-3}). From the bottom of the continental slope towards the central Arctic Basin, concentrations of around 0.5-1 mg cm^{-3} at a water depth of 3000-3500 m drop to <0.1 mg cm^{-3} at a depth of 4000-4500 m. At comparable water depths, samples from the central Arctic ridges are generally lower in pigment concentrations than samples from the Eurasian continental slope. This could indicate that a lateral transport of particles from the shelf contributes substantially to the input of marine organic matter to the slope. In Figure 3b, pigment concentrations are plotted against the station latitude. No distinct trend is present in the distribution of pigment concentrations including all

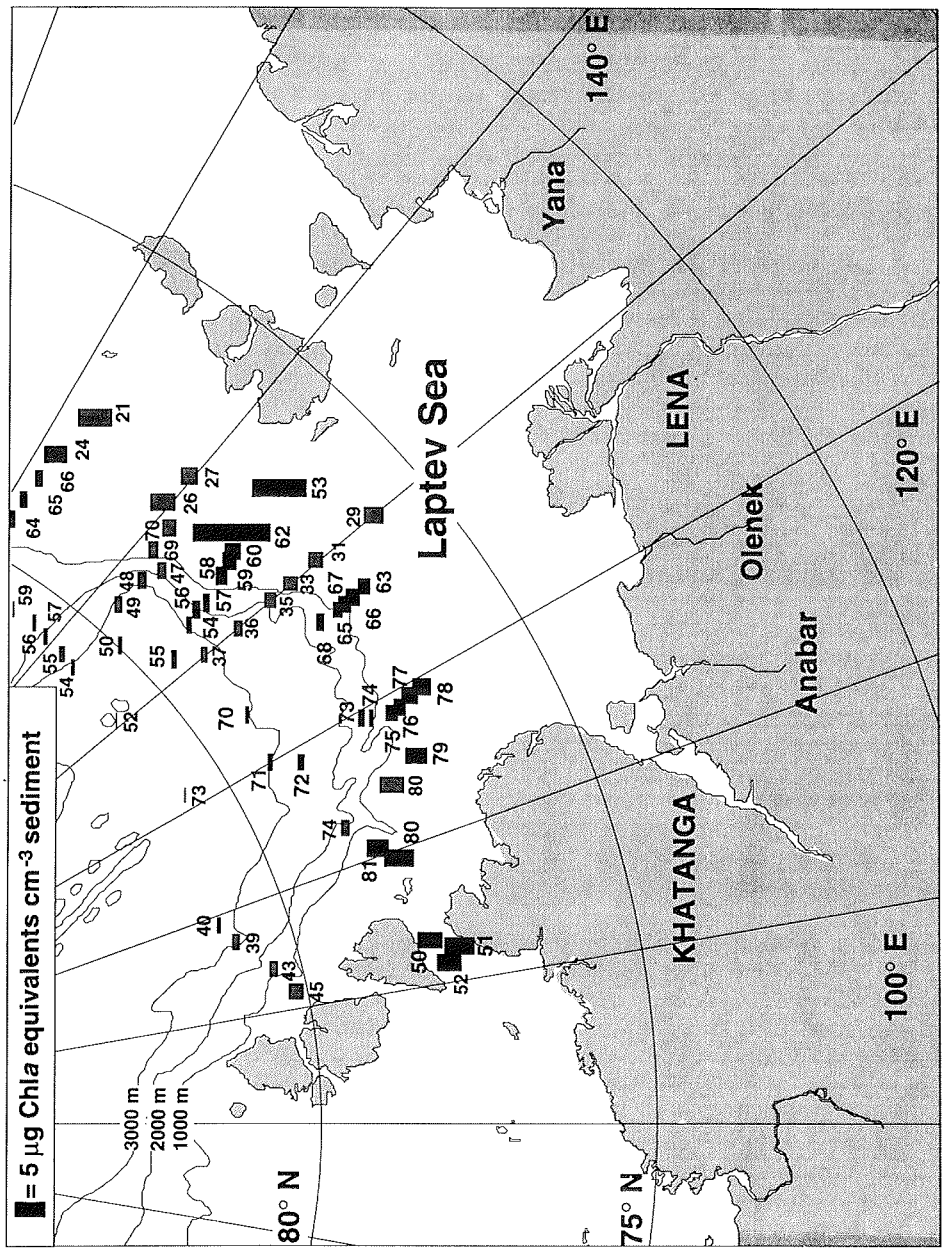

Fig. 2.: Pigment distribution in the Laptev Sea. Black and grey bars represent data from cruises in '93 (ARK IX/4) and '95 (ARK XI/1), respectively. (For further explanation see Figure 1).

No distinct trend is present in the distribution of pigment concentrations including all stations between 76 and 82°N. At latitudes >83°N, values drop to <0.5 mg cm^{-3}. With increasing latitude, the distance from the more productive shelf area and the ice concentrations during spring and summer increase, and both factors tend to reduce the input of phytoplankton detritus to the sediments.

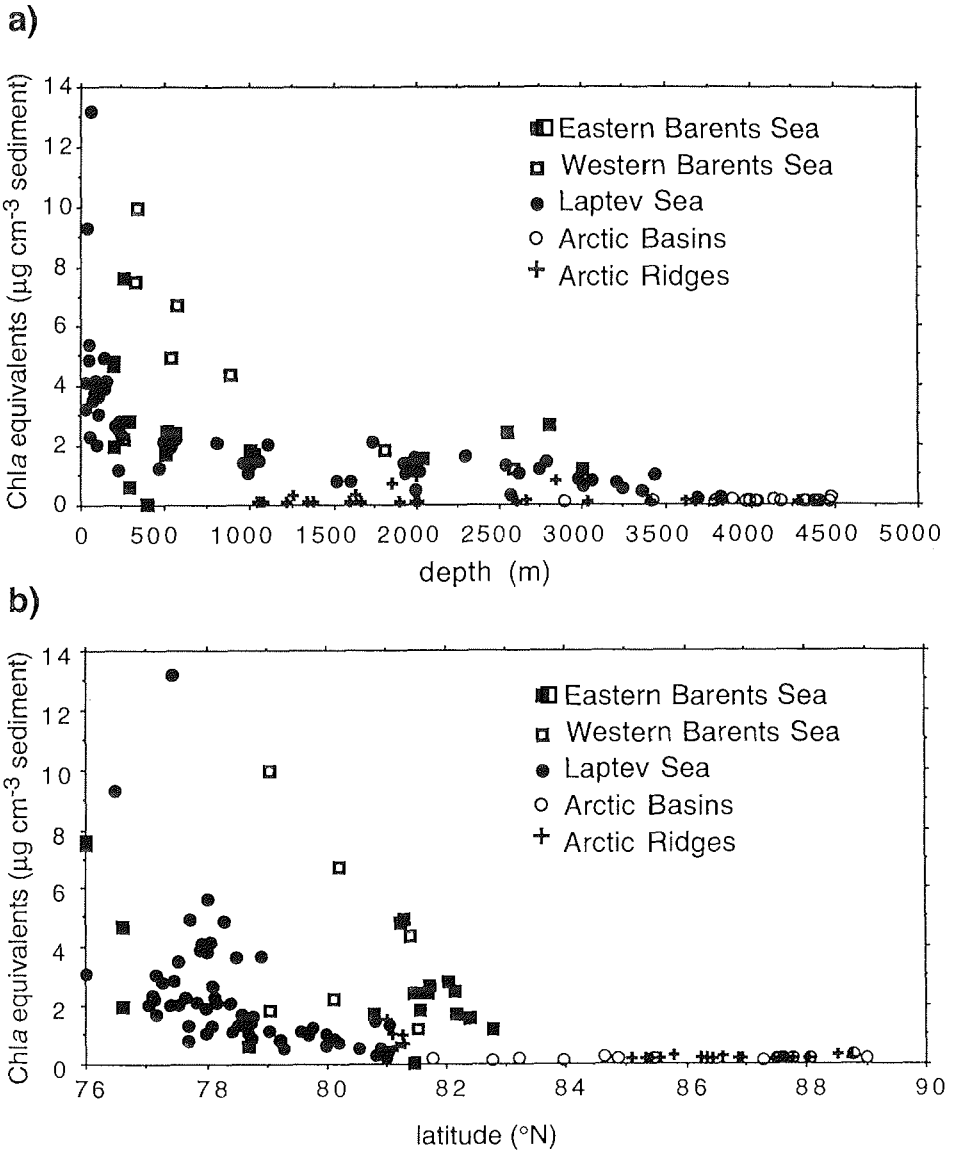

Fig. 3.: Relation between pigment concentrations in the surface sediments and a) water-depth, b) latitude (°N).

References

Fütterer, D. K. (1992): ARCTIC '91: The Expedition ARK-VIII/3 of RV "Polarstern" in 1991. Reports of Polar Research, 107, pp. 267.

Fütterer, D. K. (1994): The Expedition ARCTIC '93: Leg ARK-IX/4 of RV "Polarstern" 1993. Reports of Polar Research, 149, pp. 244.

Graf, G., Gerlach, S. A., Linke, P., Queisser, W., Ritzrau, W., Scheltz, A., Thomsen, L., and Witte, U. (1995): Benthic-pelagic coupling in the Greenland-Norwegian Sea and its effect on the geological record. Geologische Rundschau, 84: 49-58.

Hargrave, B. T. (1994): Seasonal variability in particle sedimentation under permanent ice cover in the Arctic ocean. Continental Shelf Research, 14: 279-293.

Nürnberg, D., Wollenburg, I., Dethle, D., Eicken, H., Kassens, H., Letzig, T., Reimnitz, E., and Thiede, J. (1994): Sediments in Arctic sea-ice: implications for entrainment, transport and release. Marine Geology, 119: 185-214.

Rachor, E. (1992): Scientific cruise report of the 1991 Arctic expedition ARK VIII/2 of RV "Polarstern". Reports of Polar Research, 115, pp.150.

Shuman, F. R. and Lorenzen, C. F. (1975): Quantitative degradation of chlorophyll by a marine herbivore. Limnology and Oceanography, 20: 580-586.

Stein, R., Grobe, H., and Wahsner, M. (1994): Organic carbon, carbonate, and clay mineral distributions in eastern central Arctic Ocean surface sediments. Marine Geology, 119: 333-355.

Subba Rao, D. V. and Platt, T. (1984): Primary production of Arctic waters. Polar Biology, 3: 191-201.

Wassmann, P. and Slagstad, D. (1993): Annual dynamics of carbon flux in the Barents Sea: preliminary results. Norsk Geologisk Tidsskrift, 71: 231-234.

Wassmann, P., Peinert, R., and Smetacek, V. (1991): Patterns of production and sedimentation in the boreal and polar Northeast Atlantic. In: Sakshaug, E., Hopkins, C. C. E., Oritsland, N. A. (eds.) Proceedings of the Pro Mare Symposium on polar marine ecology, Polar Research, 10: 209-228.

Wheeler, P. A., Gosselin, M., Sherr, E., Thibault, D., Kirchman, D. L., Benner, R., and Whitledge, T. E. (1996): Active cycling of organic carbon in the central Arctic Ocean. Nature, 380: 697-699.

POLYCYCLIC ARENES IN BOTTOM SEDIMENTS OF THE BARENTS SEA

Petrova V. and Batova G.

VNIIOkeangeologia, Russia

Abstract

Global contamination of the World Ocean causes the necessarity to estimate an effect of the man-made component and to seek its indication ways. Polar offshore areas undergoing the active oil and gas exploration are considered to be relatively clean but need to be continuously controlled. According to the present knowledge there is a high sensibility of polar zones as caused by the low rate of contaminant degradation and hence by the low assimilation capacity. Unlike the water mass reflecting seasonal and causal processes, bottom sediments show tendencies of geochemical processes to display the real ecological situation in offshore areas.

Among a lot of organic compounds disturbing the natural ecological balance, polycyclic aromatic hydrocarbons (PAH) hold a prominent place (Laflamme and Hites, 1978; Wakeham et al., 1980; Blumer and Voungblood, 1985). Cancerogenic and mutagenic properties of PAH coupled with the molecular stability in time set a dangerous pattern of their accumulation in marine ecosystems. PAH are molecular markers of migrational and transformational processes of the organic component in bottom sediments (Brassel et al., 1987; Venkatesan and Kaplan, 1987, Venkatesan, 1988a).

The estimation of Barents Sea ecology is based on background organic-geochemical criteria and analysis of PAH distribution in bottom sediments.

Method and Material

Figure 1 presents a scheme of the location of stations with organic-geochemical investigations. All organic-geochemical investigations were carried out in the "Laboratory of Organic Geochemistry of VNIIOceangeologia", St. Petersburg, Russia, Analytical procedures were discribed in details elsewhere (Danyushevskaya et al., 1990; Petrova, 1990).

The procedure developed involves: extraction of organic matter from sediments, group fractionation to separate hydrocarbons, and HPLC analysis PAH (Fig. 2).

PAH analyses were performed by HPLC method in a condition of the reverse-phase chromatography with chromatograph MILICHROM, column Separon SGX RP-18-S (80 x 2 mm).

The scanning spectrophotometric detector was applied to get multi-elemental chromatographic spectra and to use supplementary analytical signs during identification.

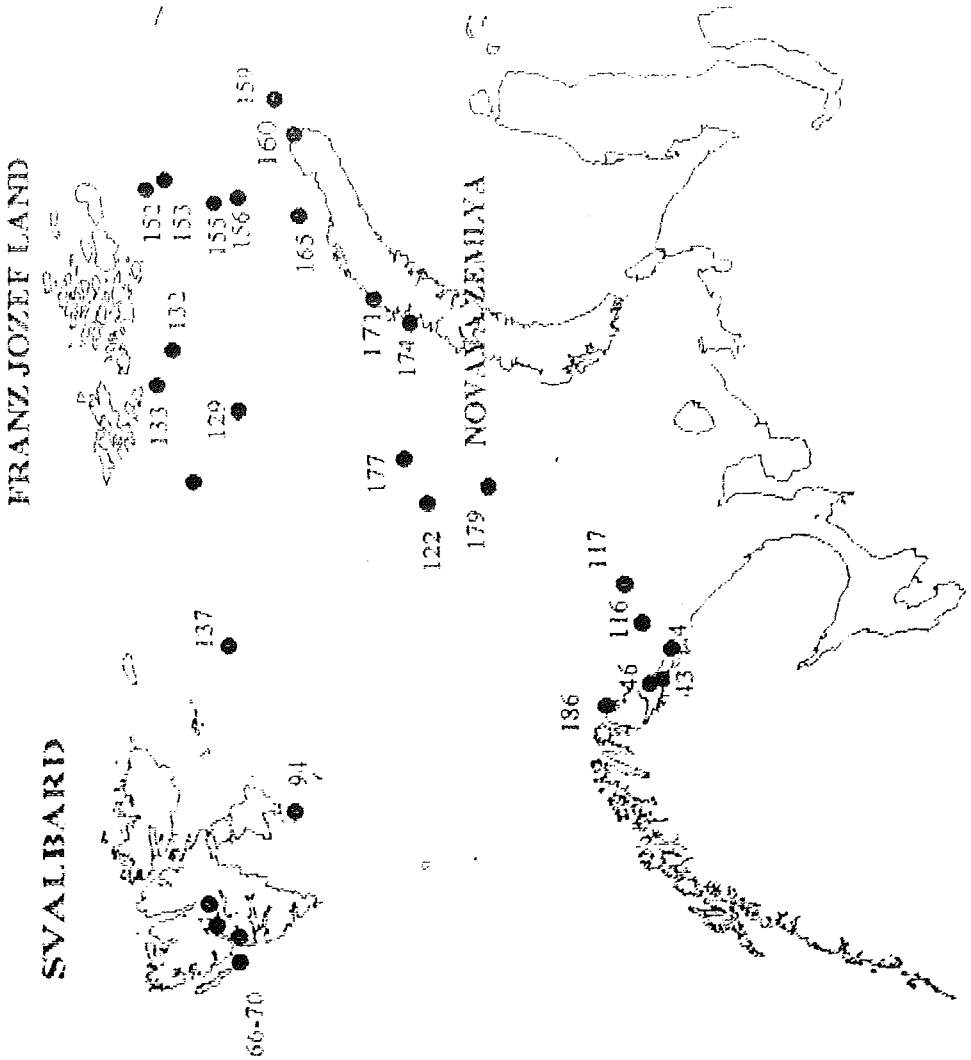

Fig. 1.: Barents Sea study area and sampling locations.

Double-wave detection (254 and 280 nm) was coupled with the record of spectra of all components of the mixture under analysis in the range of 190 - 380 nm. Individual PAH were identified by the correlation of chromatographic (k'), chromato-sepctrophotometric (h 254/h 280) and spectral (max; A max1/A max2) characteristics of real samples and standards.

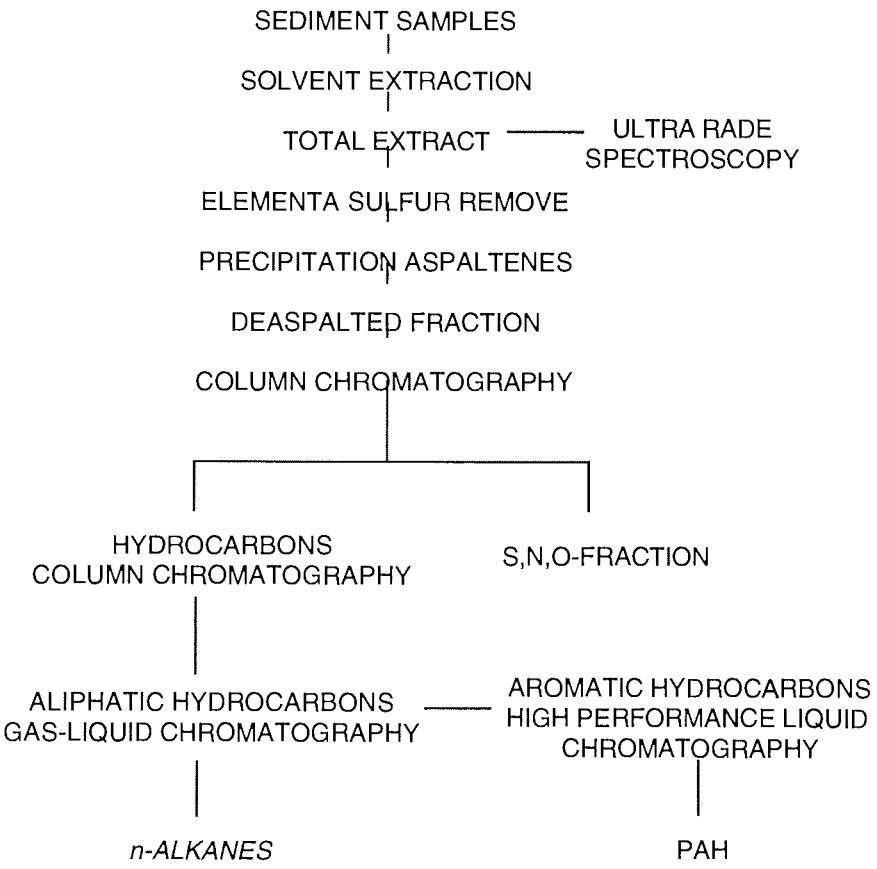

Fig. 2: Analytical scheme.

The individual pattern of spectral characteristics of involved PAH is perfectly evident. Phenanthrene and pyrene were probably identified according to confinement parameters. The correlation of spectral profiles, characteristical maxima, and the relationship of optical densities relationship allowed to reliably verify this suggestion.

The estimation displays that the amount of useful informations increases (in bits) if identified on four analytic signs (k', h 254/ h 280). It marks the greater reliability of identification.

Organic geochemistry characteristics

The Barents Sea is characterized by a predominance of mechanical differentiation processes over chemical and biogenic ones. Accordingly, the composition of bottom sediments is first defined by the geological structure and lithological and petrographical composition of rocks formed at the shore, bottom, and islands (Romankevich et al., 1982).

The complicated relief of the Barents Sea bottom, the active hydrodynamic regime, and the variability of facial conditions of sedimentation are embodied in a wide range of organic matter (OM) content and composition of sediments (Romankevich et al., 1982; Danyushevskaya et al., 1990). We observed the analogical situation in our collection (Table 1, Appendix; Fig. 3). Two fields of data points are clearly obvious is the diagram of the Bit 1 group composition. Samples from the north-western part of the offshore area in the Svalbard archipelago region (NW, Table 1, Appendix), Shtokmanovskayay field (st. 122) as well as coastal samples from Novayay Zemlyay island (st. 171A, 31A, 32A) belong to one of the fields.

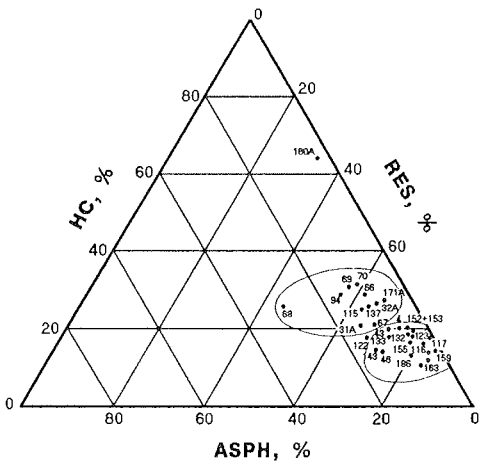

Fig. 3.: Bit1 composition.

The second group of sediments reflects a similar group composition of bitumoids (Bit). However, taking into account distinctions of physical-geographical conditions of regions and lithological-facial features of

sediments, samples from south-western (SW) and north-eastern (NE) parts of the Barents Sea should be considered separately (Table 1, Appendix). The coastal station 160 A (island Novaya Zemlyay) is anomalous in the Bit 1 group composition and outside the two groups.

Stations at the south-western shelf are located in the close vicinity of the continent (Fig. 1) and are represented by a broad spectrum of lithological types: from coarse-wasted mictites to fine-dispersed silty pelites. Accordingly, organic-geochemcial characteristics of sediments also vary widely: total organic carbon (TOC) 0.4 - 1.7 %, Bit1 1 - 4 x 10^{-2} %, humic acids (HA) 5 - 80 x 10^{-2} %, hydrocarbons (HC) 1 - 10 x 10^{-3} %. This is typical for coast-shelf zones of the World Ocean (Romankevich, 1984).

Sediments from the north-eastern part of the Barents Sea are represented mostly by silty pelites. However, OM contents vary over wide limits (TOC 0.6 - 2.0 %) and, distinctly correlate with the bottom morphostructure (Romankevich et al., 1982; Danyushevskaya, 1990). Increased TOC values (1.2 - 2.0 %) are restricted to the sediments of gutters and troughs (st. 159, 152, 153, 133, 165). The OM composition of sediments for this part of the offshore area is more monotonous; Bit 1, HA and HC contents are less than in sediments from the south-western part of the shelf.

In sediments from the north-western part of the Barents Sea selected at the Isfjord profile in the vicinity of Svalbard archipelago, TOC contents vary from 0,9 to 2.2 %; Bit1 and HA contents in the OM composition are 2.4 - 4.5 and 2 - 15 %, respectively. The HC amount in sediments is greater than the average for the Barents Sea 0.006 - 0.025 % (Romankevich et al., 1982). The peculiarity of the Bit1 and HC group composition is characterized by the highest Asph (10 - 30 %) and Ar HC (36 - 46 %) contents in the investigated sediments. IR-spectra reflect the significant role of aromatic compounds with different types of replacement (absorption band 1600, 880, 820, 750 cm^{-1}) and the presence of oxygen-bearing structures - acids of aliphatic ethers, possibly aldehydes, and ketones (absorption band 950, 1170, 1700, 1470 cm^{-1}). The obtained information suggests that the characteristics of OM in the surface sediments of the Isfjord and adjacent offshore area reflect a terrigenous character of organic matter and is connected with the supply of the material of eroded coal-bearing and/or petroleum-containing stratas of the Barentsbourgh suite (Livshits, 1973).

Distribution of Polycyclic Aromatic Hydrocarbons (PAH)
Investigated surface (0 - 10 cm) sediments of the Barents Sea can also be divided into three groups (Table 2, 3, Appendix; Fig. 4) depending on basic organic-geochemical parameters (Table 1, Appendix; Fig. 3) and PAH content and distribution.

Sediments localized in the south-western part (SW) of the Barents Sea shelf are characterized by the lowest PAH content (40 - 190 ng/g). The ratio of individual PAH indicates that the technogenic influence in this region is insignificant. Low contents of BAP (mean 6 ng/g, range ND-15 ng/g, n = 7) and a ratio pyrene/fluoranthene (PYR/FLA) < 1 are typical for low polluted modern sediments (Lipiatou and Saliot, 1991; Rovinsky, 1989; Tan and Heit, 1981; Venkatesan et al., 1987).

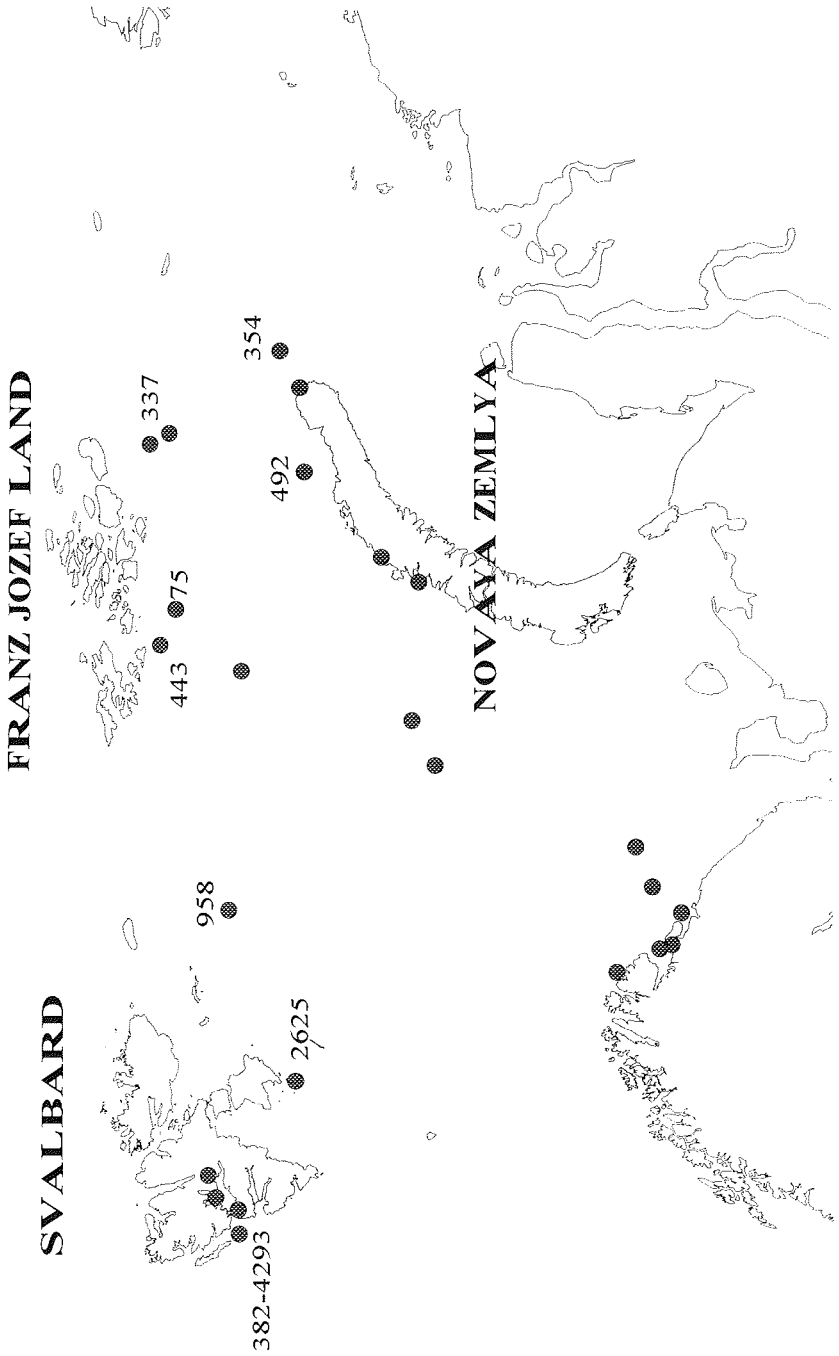

Fig. 4.: Map showing PAH content of surface sample (ng/g).

The exception is the core from station 115 where PYR/FLA = 1.9. Sediments from the White Sea (mean 31 ng/g, range 8 - 134 ng/g, n = 9 and PYR/FLA = 2, 6) are more influenced by the technogenic effects (Petrova, in press). This suggests different sources of the PAH supply in these regions. Evidently, the coastal drift from Kola Peninsula and Nordcape branch of the Gulf Stream are basic sources of sedimentary deposits for the south-western part of Barents Sea shelf.

Sediments collected in the deep-sea north-eastern part of the Barents Sea (Fig. 1) are characterized by relatively higher PAH contents (75 - 490 ng/g) and a different character of distribution of individual components where perylene (PER) is dominating (in the average 27 % of total PAH) (Table 2, 3, Appendix; Fig. 4). For the core from station 132 the PER content comprises 51 % of total PAH. This was also observed in subsurface sediments from station 133 (70 - 80 cm). A PYR/FLA ratio of 0.51 suggests insignificant technogenic influence. The greater rate of deposition (in comparison with the south-western part of the Barents Sea) and the significant thickness of Holocene sediments in St. Ann, Al'banov, and Sedov gutters (Musatov, in press) in combination with the increased bioproductivity (Polyak, in press) identify the regional specifity of genesis. Diagenetic transformations of OM for this region can be embodied in the PAH composition. Erosion and redeposition of the transformed organic material (perhaps Jurassic black shale formations of Franz Josef Land) are also of considerable importance in forming OM of these sediments. This is in line with the data about the dominating role of perilene in the PAH composition of black clays (Venkatsan, 1988a; Danyushevskaya and Petrova, 1991, Danyushevskaya et al., 1993; Petrova, in press).

Samples of sediments collected in the north-western part of the Barents Sea near Svalbard (Fig. 1, Table 2, 3, Appendix) consist of a special group in which the PAH content far exceeds average values for Arctic shelf sediments (Danyushevskaya et al., 1990). High total PAH contents (up to 4000 ng/g) were observed earlier in subsurface sediments (55 - 480 cm) of gutters in the Victoria island area, eastward of Svalbard, where the transformation level reaches protocatagenesis (Danyushevskaya et al., 1984; Danyushevskaya and Petrova, 1991). High PAH contents (up to 2000 ng/g) were also found in Cretaceous deposits (K_1 a; $\prod$K2 - $\prod$K3) revealed by deep drilling at the Barents Sea shelf (Petrova, 1988). In an Upper Jurassic succession from offshore Korea Bay Basin highly pericondensed PAH up to 25 ppm occurs (Killops and Massoud, 1992). In combination with basic organic-geochemical characteristics (Table 1, Appendix), data on PAH distribution suggest a deep degree of transformation of OM of the third group of sediments connected genetically with coaly strata of Svalbard. The dominant role of the terrigenous material in the OM composition and, accordingly, in the PAH distribution for this region is confirmed by the distinctly decreasing content of the latter along the Isfjord profile in the off-shore direction (from 3000 ng/g to 400 ng/g, st. 70 - 66).

The performed investigations showed that the PAH distribution in bottom sediments of different parts of the Barents Sea is defined by variations of the initial OM composition and depth of its transformation (Fig. 5). Accordingly, in zones of intensive supply of terrigenous material and coaly particles (Spitsbergen shelf and Franz Josef Land areas) limits of PAH content considerably increase. The nature of the distribution of individual components indicates the

lack of intensive contamination of sediments in this offshore area. To our opinion, the diagnostics of pollutions must be based on a comprehensive geological information.

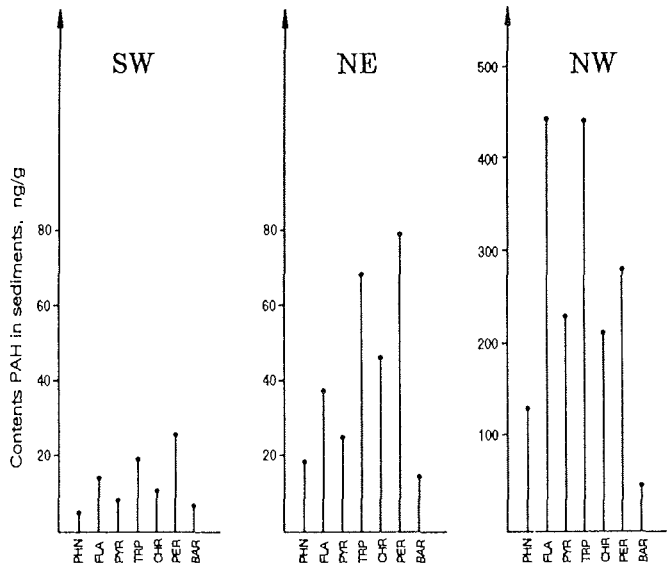

Fig. 5.: PAH distribution in surface sediments of the Barents Sea.

Sediments collected in the central part of Barents Sea at the Shtokmanovskaya field (st. 122 and 177) as well as samples collected in the Novaya Zemlya area (st. 171, 174, 31A, 171A, 160A) were not considered in this investigation due to the non-uniqueness of their organic-geochemical features. Data received during expeditions in 1993 ("Geolog Fersman" cruise) and in 1994 ("Professor Logachev" cruise) will allow to produce more comprehensive investigations of bottom sediments for these regions.

References

Brassell, S., Eglinto, G., and Howell, V., 1987. Paleoenvironment assessment of marine organic-rich sediments using molecular organic geochemistry. In: Brooks, J., Fleet, A., Marine Petroleum Source Rocks, Geological Society Special Publication No. 26, p. 79-98.

Blumer, M. and Voungblood , W., 1985. PAH in soils and resent sediments. Siens, v. 188, No. 4, p. 53-55.

Danyushevskaya, A.I., Kozlova, I.S., and Kirillov, O.V., 1984. Geochemical features of organic matter of bottom sediments in the Barents Sea. Oceanology, v. 29, No. 1, p. 102-111 (in Russian).

Danyushevskaya, A.I., Petrova, V.I., and Batova, G.I., 1990. Organic matter of bottom sediments of polar zones of the World Ocean. L., Nedra, 280 p.

Danyushevskaya, A.I. and Petrova, V.I., 1991. Geochemical features of organic matter of black clays in the Eurasian continental margin. Geochemistry, No. 5, p. 709-714 (in Russian).

Danyushevskaya, A.I., Romankevich, E.A., and Petrova, V.I., 1993. Geochemical features of organic matter of bottom sediments for the Antarctic sector of Atlantics. Oceanology, v. 33, No. 2, p. 10-221.

Killops, S.D. and Massoud, M.S., 1992. PAH of pirolytic origin in ancient sediments: evidence for Jurassic vegetation fires. Org.Gecochem., v. 18, No. 1, p. 1-7.

Laflamme, R.E. and Hites, R.A., 1978. The global distribution of PAH in recent sediments. Geochim. Cosmochim. Acta, V. 42, p. 289-303.

Livshits, Yu.Ya., 1973. Paleogenic deposits and platform structure of Spitsbergen. L., Nedra, 160 p. (in Russian).

Lipiatou, E. and Saliot, A., 1991. Fluxes and transport of antropogenic and natural PAH in the western Mediterranean Sea. Mar. Chem. v. 32, p. 51-71.

Petrova, V.I., 1990. Geochemistry of PAH of sediments for polar zones of the World Ocean. In: Organic matter of bottom sediments of polar zones of the World Ocean, Nedra, p. 70-129 (in Russian).

Petrova, V.I. and Danyushevskaya, A.I., 1988. Katagenic transformations of PAH in bottom sediments of the World ocean. Geochemistry, No. 11, p. 1558-1564 (in Russian).

Rovinsky, F.Ya., Teplitskaya, T.A., and Alexeeva, T.A., 1989. The ocean. M.: Nauka, 256 p. (in Russian).

Romankevich, E.A., 1984. Geochemistry of Organic Matter in the Ocean. Springer Verlag Heidelberg, 334 pp.

Romankevich, E.A., Danyushevskaya, A.I., and Belyaeva, A.N., 1982. Biogeochemistry of organic matter of Arctic seas. M.: Nauka, 240 p. (in Russian).

Tan, Y. and Heit, M., 1981. Biogenic and abiogenic PAH in sediments from two remote Adirondack lakes. Geochim. Cosmochim. Acta, v. 45, p. 2267-2279.

Venkatesean, M. and Kaplan, I., 1987. The lipid geochemistry of Antarctic marine sediments: Bransfield strait. Marine Chemistry, v. 21, N4, p. 347-375.

Venkatesan, M., Ruth, E., Steinberg, S., and Kaplan, I., 1987. Organic geochemistry of sediments from the continental margin off southern New England, USA. Part. 2, Lipids. Marine Chemistry, v. 21, N3, p. 267-299.

Venkatesan, M., 1988a. Occurrence and possible sources of perylene in marine sediments. Marine Chemistry, v. 25, N1, p. 1-27.

Venkatesan, M., 1988b. Organic geochemistry of marine sediments in Antarctic region: marine lipids in McMurdo Sound. Org. Geochem., v. 12, N1, p. 13-27.

Wakeham, S., Schaffner, C., and Giger, W., 1980. PAH in recent lake sediments. Geochim. Cosmochim. Acta, v. 44, p. 403-429.

Appendix

Table 1: Organic-geochemistry characteristics of bottom sediments from the Barents Sea (mean).

Location	Station Numbers	n	TOC	OM	Bit1*	Bit2*	HA*	HC	ReS	Asph	AI	Ar	sed	OM
			Content in sediment (%)											
SW Barents shelf	4, 43, 46, 115, 116, 117, 186	7	0.96	1.75	0.02	0.02	0.41	16.7	4.4	8.9	79.4	20.6	0.004	0.20
NE Franz-Josef Land to Novaya Zemlya	113, 133, 132 152, 153, 155, 159, 165, 129	9	1.10	2.00	0.01	0.02	0.28	14.4	77.6	8.0	6.6	23.4	0.002	0.10
NW Svalbard	66, 67, 68, 69, 70, 94, 137	7	1.49	2.71	0.04	0.04	0.24	27.0	58.3	15.7	64.2	35.8	0.012	0.44

*Bit1-bitumoide C H Cl , Bit2- bitumoide C H OH:C H = 1:1, HA- humic acids

Table 2: PAH concentrations in the Barents Sea (ng/g).

Location	Station Numbers	n	PAH Total Alkyl Mean	Range	Phenanthrene
SW Barents shelf	4, 43, 46, 115, 116, 117, 186	7	100	40-190	20
NE Franz Josef Land to Novaya Zemlya	129, 132, 133, 152 153, 159, 165	7	290	75-490	50
NW Svalbard	66, 67, 68, 69, 70, 94, 137	7	2200	960-4300	400

Table 3: PAH distribution (ng/g) and ratios in the Barents Sea (mean).

Location	Station Numbers	n	PHN	FLA	PYR	TRF	CHR	PER	BAP	PHN+PER	FLA+PYR	FLA
SW Barents shelf	4, 43, 46, 115, 116, 117, 186	7	3	13	8	18	10	26	6	0.10	0.62	0.61
NE Franz Josef Land to Novaya Zemlya	129, 132, 133, 152, 153, 159, 165	7	18	35	18	61	36	65	13	0.22	0.66	0.51
NW Svalbard	66, 67, 68, 69, 70, 94, 137	7	135	450	234	445	208	277	42	0.33	0.66	0.52

PHN-phenantrene, FLA-fluorantene, PYR-pyrene, TRF-tryphenylene,
CHR-crysene, PER-perylene, BAP-benso(a)pyrene

n-ALKANE DISTRIBUTION IN SURFACE SEDIMENTS FROM THE EASTERN CENTRAL ARCTIC OCEAN: PRELIMINARY RESULTS AND PERSPECTIVES

Schubert C.J. and Stein R.

Alfred Wegener Institute, Bremerhaven, Gemany

Abstract

In this paper we present short (C_{17}+C_{19}) and long-chain (C_{27}, C_{29}, C_{31}) *n*-alkane distribution patterns in surface sediments from the central Arctic Ocean. These compounds are used to distinguish between autochthonous marine organic matter and allochthonous terrigenous organic matter supply. Changes in short-chain *n*-alkane contents facilitate a distinction between regions with higher and lower marine productivity. The marine productivity is mainly based on lower sea-ice cover which allows a higher production rate of phytoplankton. Two regions with different mechanisms for a lower sea-ice cover are described. The use of long-chain *n*-alkanes as a general marker for the terrigenous organic carbon supply in the Arctic Ocean seems not to be applicable.

Introduction

The organic carbon content in Arctic Ocean surface sediments is generally high (Stein et al., 1994a, b; Stein, this vol.). High C/N-ratios and low hydrogen indices (HI) characterize the organic matter as material which consists mainly of terrigenous organic matter (Stein et al., 1994a, b; Schubert, 1995; Stein, this vol.). This terrigenous organic matter is derived from the broad shelf areas surrounding the Arctic Ocean. The marine productivity in the central Arctic Ocean is very low due to a virtually permanently closed sea-ice cover (Subba Rao and Platt, 1984 and ref. therein). Exceptions are the shelf areas and areas next to the ice edge, where higher surface water productivity occurs (Heimdal, 1983; Codispotti et al., 1991). To distinguish between marine and terrigenous organic matter detailed organic geochemical investigations were performed. In this study we show the results of *n*-alkane investigations on 22 surface sediment samples (for location of samples see Figure 1).

Methods

During the ARCTIC´91-Expedition aboard the RV "Polarstern", surface sediment samples were recovered along a profile crossing the eastern part of the Arctic Ocean. One to three grams of frozen samples were thawed and homogenized for lipid extraction (for details of the method see Farrimond et al., 1990). Fractionation by column chromatography was used to separate the organic compounds. The column was packed with activated silica (5 cm bed in a 6 mm pasteur pipette) in hexane. Hydrocarbons were then fractionated from the organic extract by elution with hexane (10 cm^3). The *n*-alkanes were analysed using a Hewlett-Packard 5890 fitted with a cold injection system by

Gerstel and an ultra-1 fused silica capillary column (50 m x 0.32 mm internal diameter and a 0.17 µm phase). Analyses were performed using helium as a carrier gas with the following sequence of oven temperatures: 60°C (1min), 60° to 150°C at 15°C/min, 150° to 300°C at 4°C/min and 300°C for 45 min. Data were acquired using a HP Chem-Station.

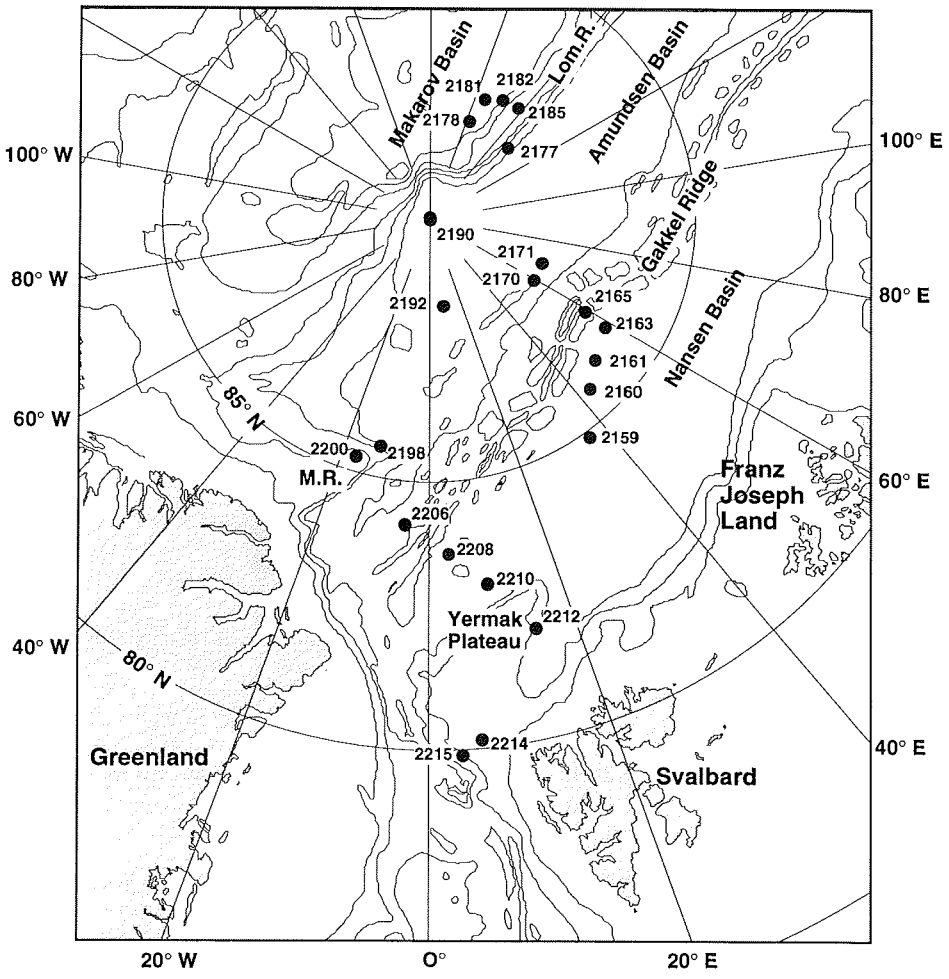

Fig. 1.: Core locations of surface sediments (0-1cm) investigated in this study.

Results

Values of C_{17}+C_{19} *n*-alkanes vary between 11.9 and 191.9 µg/gTOC. The values are generally very low (< 30 µg/gTOC); only on the Lomonosov Ridge and the neighbouring Makarov-Basin, the Morris-Jesup-Rise, and northwest of Spitsbergen higher values occur (up to 191.9 µg/gTOC, Fig. 2a). In Figure 3, short-chain *n*-alkanes are plotted versus water depth to test whether there is an influence of water depth on the decomposition of short-chain *n*-alkanes or not. Higher decomposition of short-chain *n*-alkanes with increasing water depth is not observed, as shown by the independent behaviour of the parameters (Schubert, 1995).

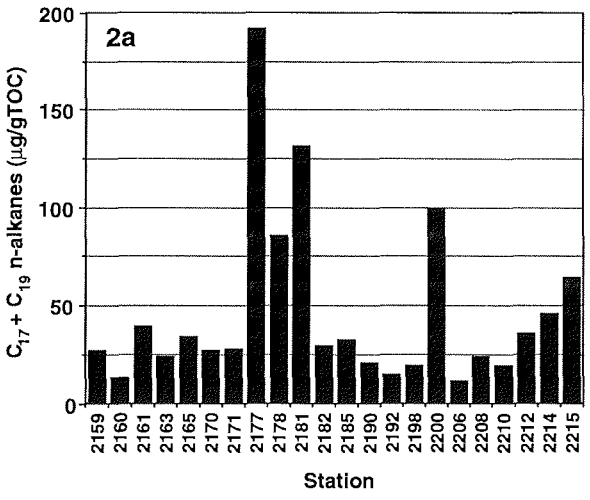

Fig. 2a.: Short-chain *n*-alkane (C_{17}+C_{19}) concentrations of investigated surface sediments.

Values of long-chain *n*-alkanes (C_{27}, C_{29}, C_{31}) vary between 62.1 and 559.1 µg/gTOC (Fig. 2b). The highest long-chain *n*-alkane contents were determined on the Lomonosov Ridge. Higher values also occur on the Gakkel Ridge and northwest of Spitsbergen. The CPI index indicative of the maturity of the organic matter was calculated (index shows the relation of odd to even chain lengths of *n*-alkanes between C_{21} and C_{32}, Bray and Evans, 1961). CPI indices of surface samples from the Arctic Ocean vary from 1.3 to 2.7 (Fig. 2c).

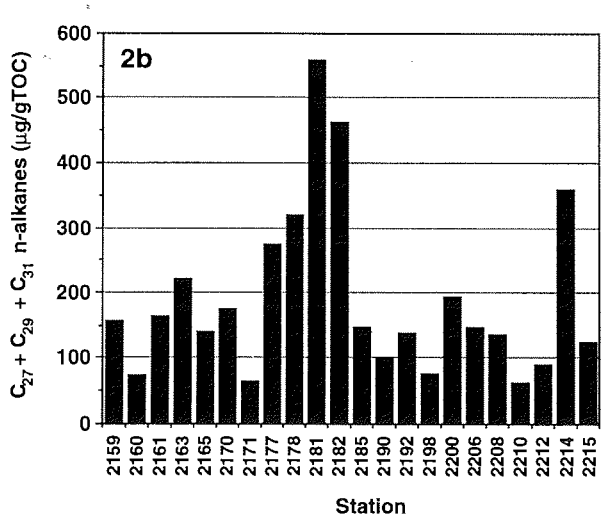

Fig. 2b.: Long-chain *n*-alkane (C_{27}+C_{29}+C_{31}) concentrations of investigated surface sediments.

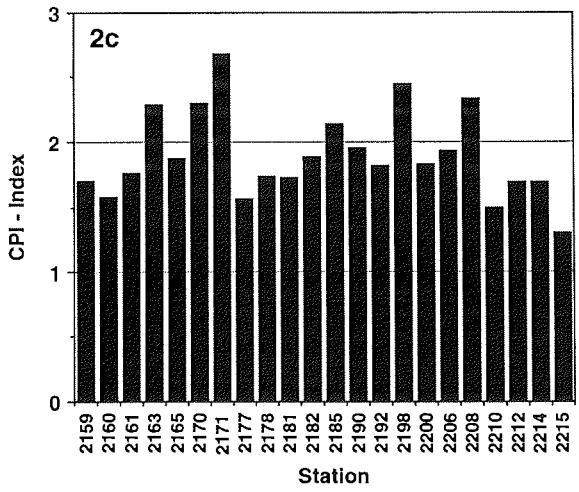

Fig. 2c.: Calculated CPI (index shows the relation of odd to even chain lengths of *n*-alkanes between C_{21} and C_{32}) of investigated surface sediments.

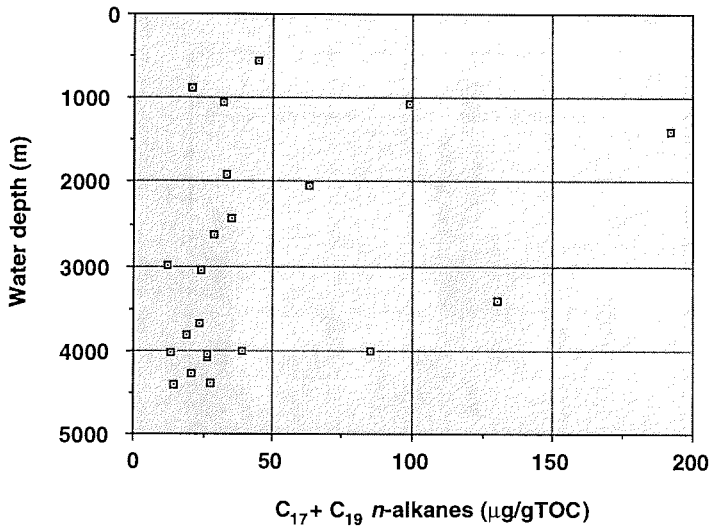

Fig. 3.: Relationship between short-chain *n*-alkane concentrations of surface sediments (0-1cm) and water depth.

Discussion

Stein (this vol.) presents surface sediment distribution maps of TOC and HI values of the Arctic Ocean. The organic carbon values are in general very high (> 0.5 %) in comparison to other open-ocean regions, where mean values of 0.3 % are common (Suess, 1980). Values up to 2.1 % TOC are determined in the Arctic Basin. Regions with an extremly high organic carbon content are shown west of Spitsbergen, at the continental slope of the Barents Sea, in the northern Nansen Basin, and on the western flank of the Lomonosov Ridge. Determination of HI values and calculation of C/N ratios were performed to distinguish on a first look between marine and terrigenous organic matter. The central Arctic Ocean is covered by sea-ice much of the year, reducing productivity in this region (Heimdal, 1983; Subba Rao and Platt, 1984 and ref. therein). Low productivity combined with a well-oxidized water column, result in a very low accumulation of marine organic matter (Stein et al., 1994a,b; Schubert, 1995). Instead, high contents of terrigenous organic material are present, indicated by low HI-values (50-100 mgHC/gC, Stein, this vol.). This is consistent with the calculated CPI indices (1.3 to 2.7) assuming a higher terrigenous input. Fresh terrigenous organic material shows a CPI index of 3 to 10 (Brassel et al., 1978; Hollerbach 1985), whereas fossil material varies around 1 depending on the state of decomposition. Marine organic material shows no predominance of odd-over-even carbon chain lengths of *n*-alkanes. High Tmax values up to 522 °C were measured by using Rock-Eval pyrolysis also support the negligible supply of marine organic material (T_{max} = temperature where the maximum amount of hydrocarbons is released). A reason for these high Tmax values is the presence of coal particles and organic-rich silt stones in the investigated samples (cf. Stein et al., 1994a).

Only in the region west of Spitsbergen higher HI values are determined, indicating sediments with more marine organic matter (Stein et al., 1994a, b; Stein, this vol.). These higher values are a result of the inflow of relatively warm surface water masses (Westspitsbergen Current) into the Arctic Ocean (Vinje, 1977; Quadfasel et al., 1987; Aagaard et al., 1987). This current is responsible for ice-free (i.e. open-water) conditions, allowing a higher primary productivity (Heimdal, 1983; Rachor, 1992), and causing higher marine organic matter content in the underlying sediments.

The investigation of short-chain *n*-alkanes allows a closer look at the organic matter composition. C_{17} and C_{19} *n*-alkanes derived from phyto- and zooplankton (Blumer et al., 1969, 1971; Youngblood and Blumer, 1973) were used as a marker for marine productivity. Figure 4 shows a surface distribution map of short-chain *n*-alkanes in the Arctic Ocean (Schubert, 1995). Four regions with a higher content of short-chain *n*-alkanes could be identified. One of these regions showing the highest concentrations, is the Lomonosov Ridge and neighbouring Makarov Basin area. The high concentrations of short-chain *n*-alkanes in this region indicate a higher marine organic matter input induced by a higher marine productivity in the surface water. Surface water productivity in the Arctic Ocean is not restricted by nutrient supply (Herman, 1983; Andersen, 1989; Heimdal, 1989; Codispotti et al., 1991) but mainly depends on the incoming light to the water surface, which is controlled by sea-ice distribution (Subba Rao and Platt, 1984; Andersen 1989). Thus, higher productivity implies more open water conditions in this region of the Arctic Ocean. It is not clear whether there are absolutely ice-free conditions (polynyas) over a longer timescale or patchy ice-free areas. In the entire Arctic Ocean a combination of ice-drift, wind, and tides is responsible for strongly crushed sea-ice and has been especially described in the region of the Lomonosov Ridge (Gordienko and Laktionov, 1969).

Another important factor allowing open-water conditions could be the divergence of sea-ice floes caused by spreading of the Beaufort Gyre and Transpolar Drift, the two main drift systems in the Arctic Ocean (Gordienko and Laktionov, 1969; cf. Rigor 1992). Ice-free areas up to 100 km^2 were found above the core positions in September, 1991 (Fütterer, 1992), which is consistent with this assumption.

Surface sample PS2185-4 shows a low short-chain *n*-alkane content (32.2 µg/gTOC) in comparison to the other Lomonosov Ridge cores. This core is located at the very top of the ridge, and is therefore strongly influenced by water currents (Rudels et al., 1994). Currents are responsible for winnowing and washing-out the fine-grained light particles including organic matter (cf. Schäper, 1994; Bergmann, 1995). This is also supported by a higher sand content of the sediments (Stein et al., 1994a; Wahsner, pers. com.).

Higher short-chain *n*-alkane contents are also reported in sediments of the Morris-Jesup-Rise (98.8 µg/gTOC). High sea-ice thickness is common in this region (Gloersen et al., 1992). Therefore, the high short-chain *n*-alkane content in this region raises questions. It is well known that Atlantic Intermediate Water (AIW) from the Makarov Basin flows along the continental slope of Greenland crossing the Morris-Jesup-Rise back into the Eurasian Basin (Anderson et al., 1994).

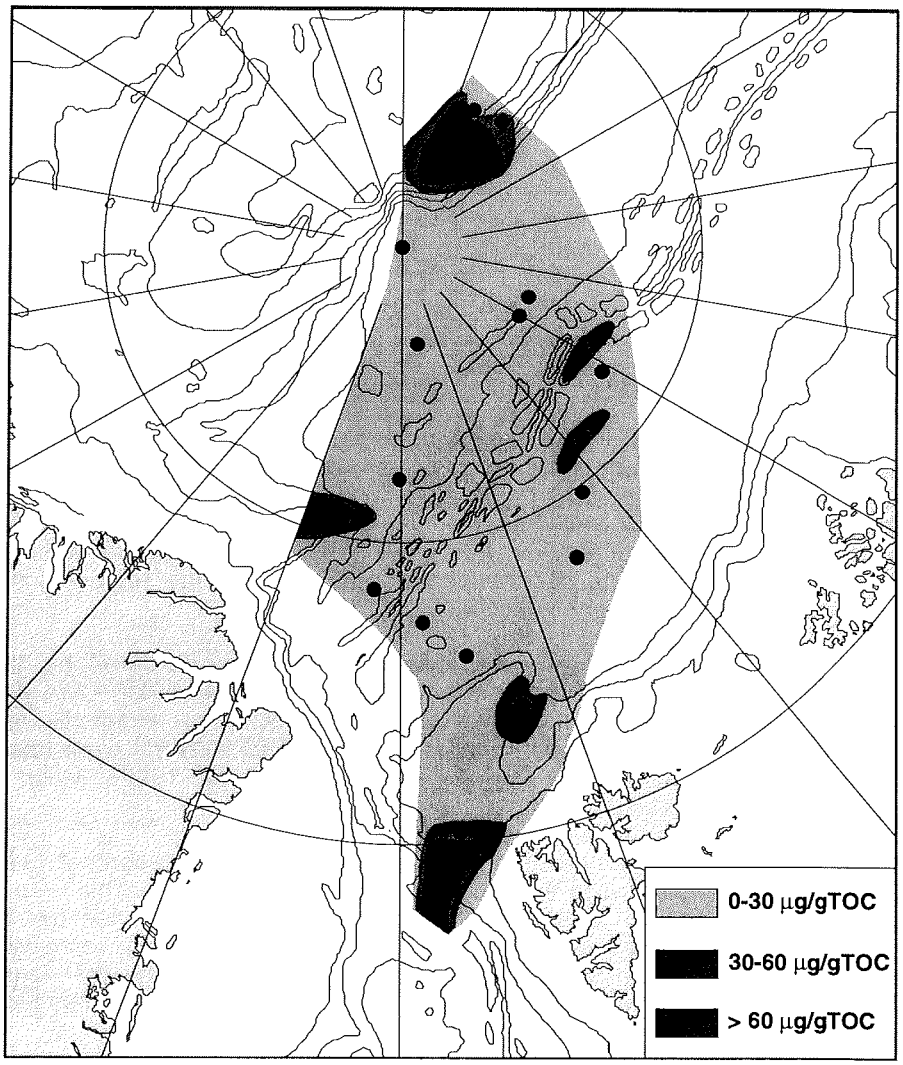

Fig. 4.: Distribution map of short-chain *n*-alkane (C_{17}+C_{19}) concentrations of surface sediments (0-1cm) from the Arctic Ocean.

Relatively large amounts of sediment coarse fraction (Vogt, pers. com.) and restored foraminifers (Wollenburg, 1995) give evidence for high water current flow, leading to very low sedimentation or even erosion at the Morris-Jesup-Rise (Stein et al., 1994b). It is possible that this water current brings resuspended organic material, and therefore, nutrients into this region. This is documented by a higher occurence of benthic foraminifers in the sediments (Wollenburg, 1995). A higher planktonic production in this area could be caused by a higher TOC content in the water column occuring at 20-70 m water depth (Anderson et al., 1994). Higher productivity in this area is also suggested by higher barium concentrations in the sediments (Nürnberg et al., 1995, this vol.). An increased release of sediments, organic matter, and nutrients from sea-ice could be an explanation for the observations in this region. This is also supported by a higher release of terrigenous organic matter indicated by higher long-chain *n*-alkanes concentration (192 µg/gTOC) and a lower HI value (51 mgHC/gTOC, Stein et al., 1994a).

High short-chain *n*-alkane contents in the Yermak Plateau region are related to the higher primary productivity because of the low sea-ice cover in this area. Concentrations are decreasing from the southern to the northern Yermak Plateau. While core position PS2212 in the northern part is at times ice covered, the core positions from the southern part of the Yermak plateau are ice-free throughout the entire year (Gloersen et al., 1992). The ice-free water in this region is caused by the inflow of the relatively warm Westspitsbergen Current into the Arctic Ocean (Vinje, 1977; Quadfasel et al., 1987; Aagaard et al., 1987).

Figure 5 shows a correlation between the short-chain *n*-alkane concentration and the living benthic foraminifers content at core positions PS2190 - PS2215 (foraminifers data from Bergsten, 1994). An excellent correlation is obvious, supporting the application of short-chain *n*-alkanes as a marker for marine organic matter in the Arctic Ocean. Only the surface sample from core position PS2200 does not fit in the correlation. An explanation could be the finding of the highest contents of dead foraminifers (Bergsten, 1994) at this core position, which give evidence for redeposition processes in this region (cf. Stein et al., 1994b).

Long-chain *n*-alkanes (C_{27}, C_{29} and C_{31}) indicative of plant waxes of higher land plants (Eglinton and Hamilton, 1963; Eglinton, 1967; Simoneit, 1978) are commonly used in sediments as a biomarker for terrigenous organic matter supply (Cranwell, 1982; Prahl and Muehlhausen, 1989; Prahl and Pinto, 1987; Simoneit et al., 1977). The investigations in this paper have shown that in Arctic Ocean sediments higher concentrations of long-chain *n*-alkanes do not coincide with higher overall terrigenous organic matter supply as suggested by hydrogen indices and C/N ratios. Figure 6 shows the distribution of long-chain *n*-alkane content in Arctic Ocean surface sediments. The very high concentrations at the Lomonosov Ridge region could be connected to the above mentioned strongly crushed sea-ice in this area (Gordienko and Laktionov, 1969). Crushed sea-ice is responsible for a higher release of sediments from the sea-ice into the Arctic Ocean. The very high concentrations of long-chain *n*-alkanes in this area would suggest a transport of these compounds by sea-ice. This assumption is proved by several indications discussed in the following.

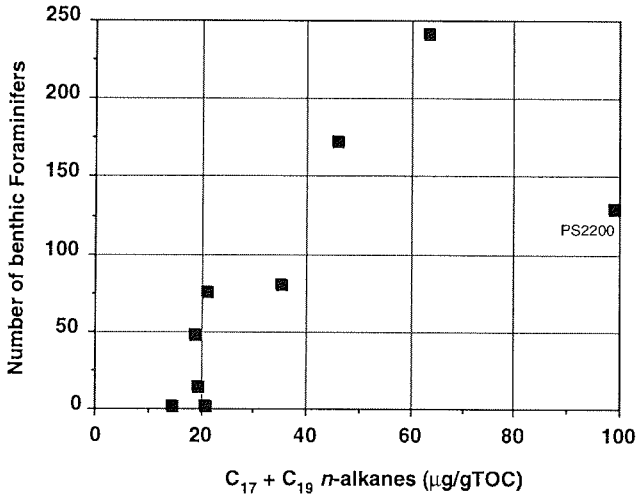

Fig. 5.: Relationship between the short-chain *n*-alkane concentration and the living benthic foraminifers content at core positions PS2190-PS2215 (foraminifers data from Bergsten, 1994).

Stein et al. (1994a) described high smectite contents in Lomonosov Ridge surface sediments. High contents of smectite in sea-ice sediments suggest the Laptev Sea, with high concentrations of smectite in its shelf sediments, as a main source area for sea-ice (Wollenburg, 1993; Nürnberg et al., 1994). Therefore, one source for surface sediments in the Lomonosov Ridge region are sea-ice sediments derived from the Laptev Sea shelf region (Stein et al., 1994a). Surface sediments from the Laptev Sea show long-chain *n*-alkane concentrations up to 450 µg/gTOC (Fahl and Stein, 1996). It is, therefore, possible that the long-chain *n*-alkanes were incorporated within the sediments in the Laptev Sea during the sea-ice build up and released over the Lomonosov Ridge. This, however, cannot be proved with the present data set. Another possibility could be the transport of the long-chain *n*-alkanes from the Canadian Arctic shelf regions into sea-ice sediments with the Beaufort Gyre. Evidence for material from the Canadian Arctic or Greenland which was transported by the Beaufort Gyre and found at the Lomonosov Ridge, are given by detrital carbonates (Nøergaard-Petersen and Spielhagen, 1994; Vogt, this vol.). However, an input from this region is less likely due to the deeper shelfs and the resulting problems of sediment entrainment at the Canadian Arctic or Greenland.

High long-chain *n*-alkane concentrations in surface sediments from the Gakkel Ridge are correlated with higher contents of ice-rafted foraminifers (Wollenburg, 1995), but higher smectite contents are missing (Stein et al., 1994a). Therefore, a correlation to source areas is difficult. Low long-chain *n*-

alkane concentrations in surface sediments from the Amundsen and Nansen Basin could be attributed either to a lower ablation of sea-ice in this region or a dilution by sediments originating from other sedimentation processes (e.g. turbidity currents). A more important role of oceanic or turbidity currents for sedimentation instead of sea-ice transport in the Arctic Ocean basins (Schubert, 1995) is also assumed by Stein et al. (1994a,b) and Nürnberg et al. (1994). Therefore, low long-chain *n*-alkane concentrations in the Arctic Ocean basins are most probably based on dilution effects from sediments transported by other mechanisms than sea-ice transport. The higher long-chain *n*-alkane concentrations of sediments from stations PS2214 and PS2215 are assumed to be related to a direct input from Spitsbergen.

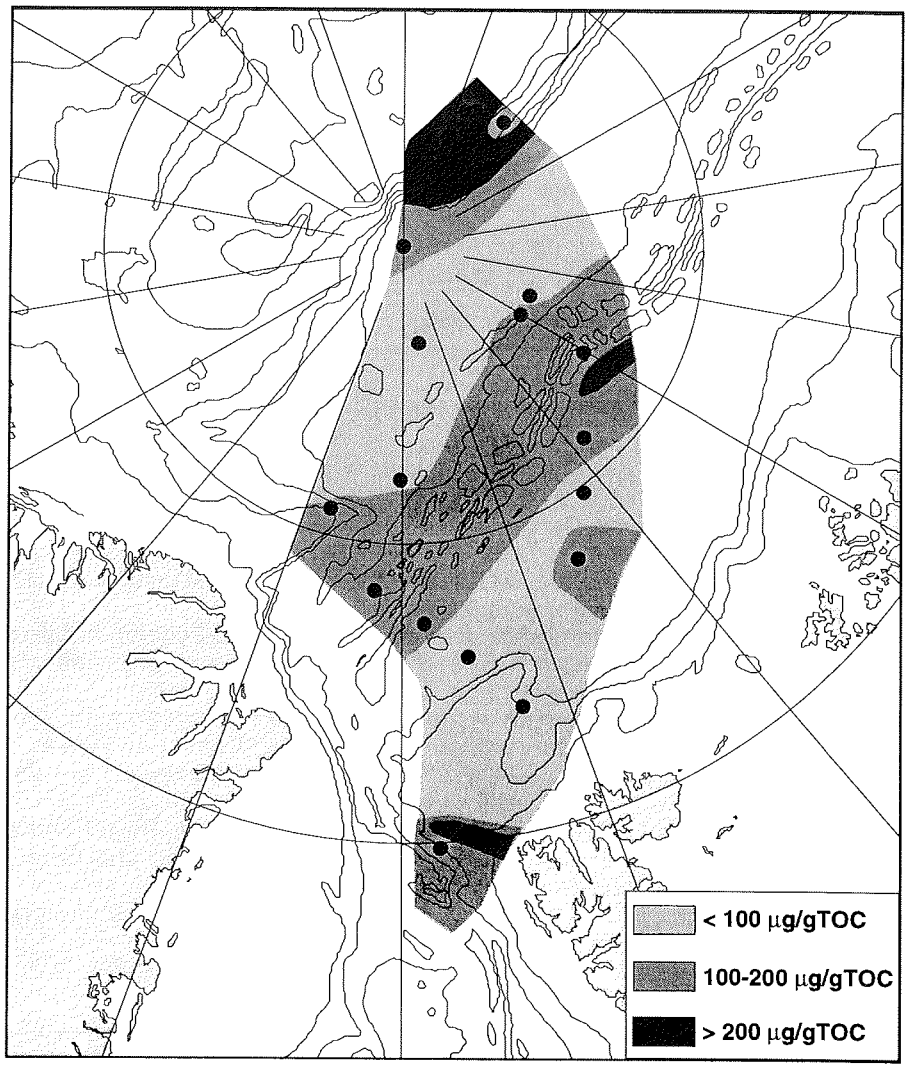

Fig. 6.: Distribution map of long-chain *n*-alkane ($C_{27}+C_{29}+C_{31}$) concentrations of surface sediments (0-1cm) from the Arctic Ocean.

Conclusions

Organic material in Arctic Ocean surface samples is mainly represented by terrigenous organic matter as indicated by high C/N ratios and low hydrogen indices (Stein et al., 1994a,b). This study shows that higher short-chain *n*-alkanes (C_{17} and C_{19}) concentrations in Arctic Ocean sediments could be used as an indicator of an increased marine productivity. Increased concentrations are found in surface sediments from the Lomonosov Ridge and neighbouring Makarov Basin. This is interpreted in terms of a lower sea-ice cover in this area, which could be induced by the Beaufort Gyre and Transpolar Drift surface water and ice drift systems. Higher concentrations in surface sediments of the Spitsbergen area are induced by the Westspitsbergen Current bringing warm surface water from the Atlantic, keeping this region more or less ice-free and allowing a higher surface water productivity. Long-chain *n*-alkanes (C_{27}, C_{29} and C_{31}) could not be used to quantify the terrigenous organic carbon input in Arctic Ocean sediments. This is most probably due to the small long-chain *n*-alkane proportion in the terrigenous organic matter. Therefore, these compounds seem to be not representative for the terrigenous organic matter supply. Further investigations of other organic compounds (e.g. fatty acids, carbohydrates and lignin), however, are necessary to determine the relative contributions of marine productivity and terrigenous supply in Arctic Ocean sediments.

References

Andersen, O. G. N. (1989). Primary Production, Chlorophyll, Light, and Nutrients Beneath the Arctic Sea Ice.- In: Herman, Y. (Ed.), The Arctic Seas. - New York (Van Nostrand Reinhold): 147-193.

Anderson, L. G., Olsson, K. and Skoog, A. (1994b). Distribution of Dissolved Inorganic and Organic Carbon in the Eurasian Basin of the Arctic Ocean.- In: Muench, R. and Johanessen, O. M. (Eds.), The Polar Oceans and Their Role in Shaping the Global Environment. - 85. Washington, D.C. (American Geophysical Union).525pp.

Bergmann, U. (1995). Interpretation digitaler Parasound-Echolot Aufzeichnungen im östl. Arktischen Ozean auf der Grundlage physikalischer Sedimenteigenschaften. - Ber. zur Polarforschung im Druck.

Bergsten, H. (1994). Recent benthic foraminifera of the transect from the North Pole to the Yermak Plateau, eastern central Arctic Ocean. - In: Thiede, J., Vorren, T. O. and Spielhagen, R. F. (Eds.), Marine Geology 119 : 251-267.

Blumer, M., Gordon, J., Robertson, J. C. and Sass, J. (1969). Phytol derived C19 di and triolefinic hydrocarbons in marine zooplankton and fishes. - Biochemistry 8 : 4067-4074.

Blumer, M., Guillard, R. R. L. and Chase, T. (1971). Hydrocarbons of marine phytoplankton. - Marine Biology 8 : 183-189.

Brassell, S. C., Eglinton, G., Maxwell, J. R. and Philip, R. P. (1978). Natural background of alkanes in the aquatic environment.- In: Hutzinger, O., Lelyveld, I. H. and Zoetman, B. C. J. (Eds.), Aquatic Pollutants: Transformation and Biological Effects. - (Pergamon Press) : 69-86.

Bray, E. E. and Evans, E. D. (1961). Distribution of *n*-paraffins as a clue to recognition of source beds. - Geochim. Cosmochim. Acta 22 : 2-15.

Codispoti, L. A., Friederich, G. E., Sakamoto, C. M. and Gordon, L. I. (1991). Nutrient cycling and primary production in the marine systems of the Arctic and Antarctic. - J. of Marine Systems 2 : 359-384.

Cranwell, P. A. (1982). Lipids of aquatic sediments and sedimenting particulates. - Prog. Lipid Res. 21 : 271-308.

Eglinton, G. and Hamilton, R. J. (1963). The distributions of alkanes.- In: Swain, T. (Eds.), Chemical Plant Toxonomy. - New York (Academic Press) : 187-217.

Eglinton, G., Maxwell, J. R. and Philip, R. P. (1975). Organic geochemistry of sediments from contemporary aquatic environments.- In: Tissot, B. and Bienner, F. (Eds.), Advances in Organic Geochemistry : 941-961.

Fahl, K. and Stein, R., 1996. Modern organic-carbon deposition in the Laptev Sea and adjacent continental slope: Surface-water productivity vs. terrigenous input. Organic Geochemistry, submitted.

Farrimond, P., Eglinton, G. and Poynter, J. G. (1990). A molecular stratigraphic study of Peru margin Sediments, HOLE 686B, LEG 112 [1]. - Proc. ODP Sci. Results 112 : 539-546.

Fütterer, D. K. (1992): ARCTIC '91: The Expedition ARK-VIII/3 of RV "Polarstern" in 1991. - Ber. zur Polarforschung 107. 267pp.

Gloersen, P., Campbell, W. J., Cavalieri, D. J., Comiso, J. C., Parkinson, C. L. and Zwally, H. J. (1992). Arctic and Antarctic Sea Ice, 1978-1987: Satellite Passive-Microwave Observations and Analysis. - Washington, D.C. 290pp.

Gordienko, P. A. and Laktionov, A. F. (1969). Circulation and physics of the Arctic Basin waters.- In: (Eds.), Ann. International Geophys. Year. - 46. New York (Oceanogr. Pergamon) : 94-112.

Heimdal, B. R. (1983). Phytoplankton and nutrients in the waters north-west of Spitsbergen in the autumn of 1979. - J. Plankton Res. 5 : 901-918.

Herman, A. W. (1983). Vertical distribution patterns of copepods, chlorophyll, and production in northeastern Baffin Bay. - Limnol. Oceanogr. 28 : 708-719.

Hollerbach, A. (1985). Grundlagen der organischen Geochemie. - Berlin (Springer Verlag). 190pp.

Nürnberg, D., Wollenburg, I., Dethleff, D., Eicken, H., Kassens, H., Letzig, T., Reimnitz, E. and Thiede, J. (1994). Sediments in Arctic sea ice: Implications for entrainment, transport and release.- In: Thiede, J., Vorren, T. O. and Spielhagen, R. F. (Eds.), Marine Geology 119 : 185-214.

Prahl, F. G. and Pinto, L. A. (1987). A geochemical study of long-chain *n*-aldehydes in Washington coastal sediments. - Geochim. Cosmochim. Acta 51 : 1573-1582.

Rigor, I. (1992). Arctic Ocean buoy program. - ARCOS Newsletter 44 : 1-3.

Rudels, B., Jones, E. P., Anderson, L. G. and Kattner, G. (1994). On the Intermediate Depth Waters of the Arctic Ocean.- In: Johannessen, O. M., Muench, R. D. and Overland, J. E. (Eds.), The Polar Oceans and Their Role in shaping the Global Environment. - Geophysical Monograph 85. Washington D.C. (American Geophysical Union): 523pp.

Schäper, S. (1994): Quartäre Sedimentation im polnahen Arktischen Ozean. unveröff. Diplomarbeit, Ruprechts-Karls-Universität Heidelberg. 144pp.

Schubert, C.J. (1995). Organischer Kohlenstoff in spätquartären Sedimenten des Arktischen Ozeans: Terrigener Eintrag und marine Produktivität. Ber. zur Polarforschung 177 : 178pp.

Simoneit, B. R. T. (1978). The organic chemistry of marine sediments.- In: Riley, J. P. and Chester, R. (Eds.), Chemical Oceanography. - 7. New York (Academic Press) : 233-311.

Simoneit, B. R. T., Chester, R. and Eglinton, G. (1977). Biogenic lipids in particulates from the lower atmosphere over the eastern Atlantic. - Nature 267 : 682-685.

Stein, R., Grobe, H. and Wahsner, M. (1994a). Organic carbon, carbonate, and clay mineral distributions in eastern central Arctic Ocean surface sediments.- In: Thiede, J., Vorren, T. O. and Spielhagen, R. F. (Eds.), Marine Geology 119 : 269-285.

Stein, R., Schubert, C., Grobe, H. and Fütterer, D. (1994b). Late Quaternary Changes in Sediment Composition in the Central Arctic Ocean: Preliminary Results of the Arctic '91 Expedition.- In: Thurston, D. K. and Fujita, K. (Eds.), International Conference on Arctic Margins 1992 Proceedings. - MMS 94-0040. Anchorage, Alaska (OCS Study) : 363-368.

Subba Rao, D. V. and Platt, T. (1984). Primary Production of Arctic Water. - Polar Biol. 3 : 191-201.

Suess, E. (1980). Particulate organic carbon flux in the oceans - surface productivity and oxygen utilization. - Nature 288 : 260-263.

Wollenburg, I. (1993). Sedimenttransport durch das arktische Meereis: Die rezente lithogene und biogene Materialfracht. - Ber. zur Polarforschung 127 : 159pp.

Wollenburg, J. (1995). Benthische Foraminiferenfauna als Wassermassen, Produktivität und Eisdriftanzeiger im Arktischen Ozean. - Ber. zur Polarforschung 179.

Youngblood, W. W. and Blumer, M. (1973). Alkanes and Alkenes in Marine Benthic Algae. - Marine Biology 21 : 163-172.

ORGANIC-CARBON AND CARBONATE DISTRIBUTION IN SURFACE SEDIMENTS FROM THE EASTERN CENTRAL ARCTIC OCEAN AND THE EURASIAN CONTINENTAL MARGIN: SOURCES AND PATHWAYS

Stein R.

Alfred Wegener Institute, Bremerhaven, Germany

Abstract

Distribution maps of carbonate, total organic carbon, hydrogen index values, and C/N ratios determined in surface sediments from the eastern central Arctic Ocean and the Laptev, Kara, and Barents Sea areas are presented. The carbonate distribution is mainly controlled by dilution and dissolution processes. In the Arctic Ocean and its marginal seas, the total organic carbon content is generally high, varying between 0.5 and 2.3 %. The source of the organic matter is dominantly terrigenous, as indicated by low hydrogen indices and high C/N ratios. In marginal ice zones of the Eurasian shelf seas (i.e., areas of ice-edge blooms) and, especially, in the ice-free area around Svalbard influenced by the warm Westspitsbergen Current, increased amount of marine organic matter are preserved in the surface sediments, probably related to increased phytoplankton productivity.

Introduction

The Arctic Ocean is rather low-productive due to the permanent ice-cover (Subba Roa & Platt, 1984). In marginal seas (such as the Laptev Sea and the Kara Sea), however, characterized by an increased fluvial nutrient supply, near ice edges, and at local/regional upwelling cells, however, significantly raised primary production rates are expected. The mapping of sedimentological and organic-geochemical proxies reflecting the surface water productivity in surface sediments, and the subsequent comparison to recent oceanographic and biological parameters will allow to decipher processes most important for primary production in the Arctic Ocean. Besides nutrients, the major Arctic rivers (Lena, Khatanga, Ob, and Yenisey) also transport large amounts of dissolved and particulate material (i.e., chemical elements, siliciclastic and organic matter) onto the shelves (Martin et al., 1993) where it is accumulated or further transported by different mechanisms (sea-ice, icebergs, turbidity currents, etc.) towards the open ocean (e.g., Pfirman et al., 1989; Nürnberg et al., 1994; Stein and Korolev, 1994). Thus, river-derived (terrigenous) organic material contribute in major proportions to the organic carbon content in the sediments of the Eurasian shelf seas and the adjacent continental slope and deep-sea areas.

Data on amount and composition (i.e., marine vs. terrigenous) of the organic carbon fraction in marine sediments can yield important information about the depositional environment, oceanic circulation, and surface-water productivity (e.g., Berger et al., 1989; Stein, 1991 and further references therein).

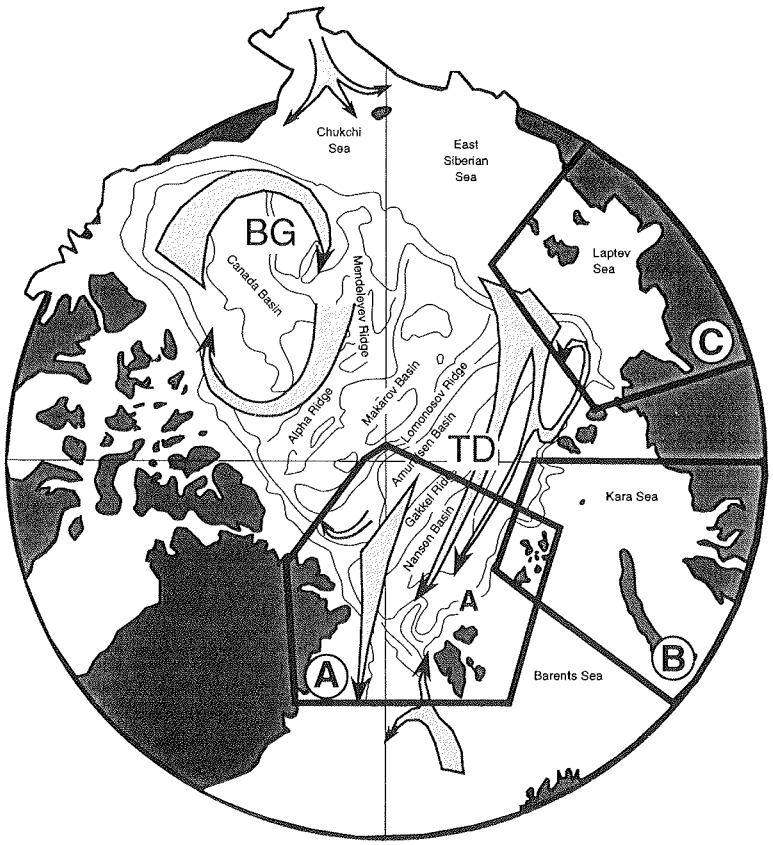

Fig. 1.: Overview map of the Arctic Ocean with major surface-water circulation systems and study areas. (A) central Arctic Ocean, Fram Strait, and East Greenland and Svalbard continental margin (Figs. 2 - 4); (B) Kara Sea and St. Anna Trough area (Figs. 5 - 7), and (C) Laptev Sea and adjacent continental slope (Figs. 8-11).

In the central Arctic Ocean, this kind of data is rare. Thus, the major goal of this paper is to summarize the distribution of organic carbon and carbonate in surface sediments from the Eurasian shelf seas and the adjacent continental slope and deep-sea areas (Fig. 1), and to identify the main mechanisms controlling the organic carbon deposition (i.e., surface-water productivity vs. terrigenous input; Fig. 2). Part of the data including a more detailed discussion, is already published elsewhere (Stein et al., 1994; Stein and Nürnberg, 1995).

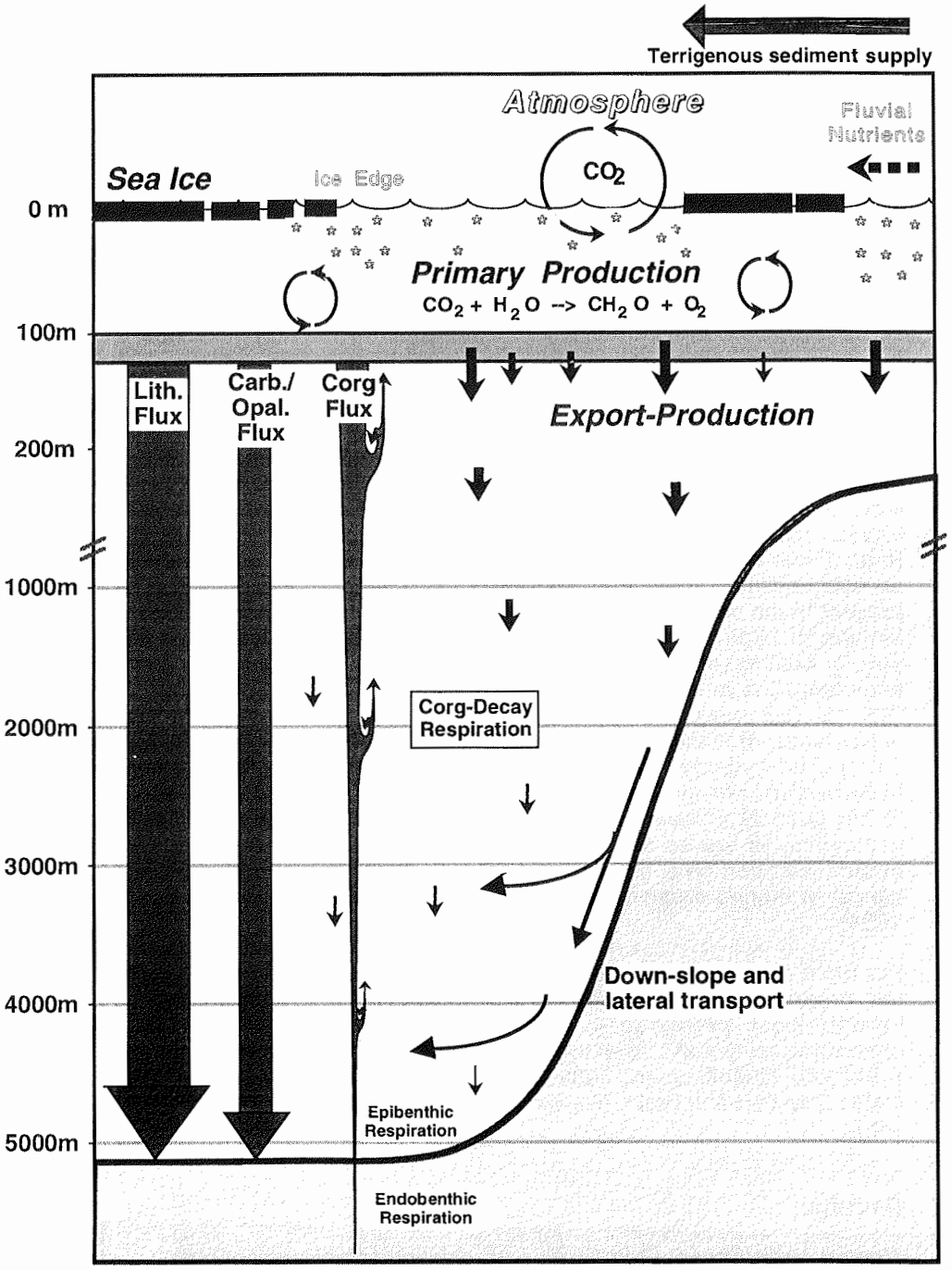

Fig. 2.: Scheme indicating processes controlling the organic carbon flux (as well as fluxes of lithogenic, carbonate, and opal components) in the Arctic Ocean and adjacent deep-sea areas.

Methods

Total carbon, sulfur, nitrogen, and organic carbon were determined on ground bulk samples and carbonate-free sediment samples by means of a Heraeus CHN-analyzer and/or a LECO-CS- analyzer. The carbonate content was calculated as

$$CaCO_3 = (TC - TOC) * 8.333$$

where TC = total carbon and TOC = total organic carbon (both in wt% of the bulk sample). C/N ratios, as indicator for the composition of the organic carbon, were calculated as "total organic carbon / total nitrogen ratios". C/N ratios of marine organic matter (mainly phytoplankton and zooplankton) are around 6, whereas terrigenous organic matter (mainly from higher plants) has C/N ratios of > 15 (e.g., Bordowskiy, 1965; Scheffer and Schachtschabel, 1984).

In organic-carbon-rich (TOC > 0.5 %), immature sediments, Rock-Eval pyrolysis parameters (S2 peak, hydrogen and oxygen indices) are also useful indicators for the characterization of the composition of the organic-carbon fraction (i.e., to estimate the amount of terrigenous and marine proportions) (e.g., Tissot and Welte, 1984; Stein, 1991). The pyrolysis was conducted out on bulk sediment samples to determine the amount of hydrocarbons already present in the sample (S1 peak in mg hydrocarbons per gram sediment), the amount of hydrocarbons generated by pyrolytic degradation of the kerogen during heating of up to 550°C (S2 peak in mg hydrocarbon per gram sediment), the amount of carbon dioxide generated during heating of up to 390 °C (S3 peak in mg carbon dioxide per gram sediment), and the temperature of maximum pyrolysis yield (Tmax value in °C) (Espitalié et al., 1977). The hydrogen index (HI) corresponds to the quantity of pyrolyzable hydrocarbons per gram TOC (mgHC/gC), the oxygen index (OI) corresponds to the quantity of carbon dioxide per gram TOC ($mgCO_2/gC$). In immature sediments, HI values of < 100 mgHC/gC are typical of terrigenous organic matter (kerogen type III), whereas HI values of 300 to 800 mgHC/gC are typical of marine organic matter (kerogen types I and II) (Tissot and Welte, 1984).

For more precise determinations of the marine and terrigenous proportions of the organic-carbon fraction, other more sophisticated methods such as kerogen/coal petrography and gas chromatography (GC) and gas chromatography/mass spectrometry (GC/MS) techniques are required (e.g., Prahl and Muehlhausen, 1989; for Arctic Ocean sediments see Schubert, 1995; Schubert and Stein, this vol.; Fahl and Stein, 1996; Belyaeva et al., this vol.).

Results

Central Arctic Ocean, Fram Strait, and Svalbard continental margin

In general, the carbonate content of the central Arctic Ocean surface sediments is relatively low; most values are less than 10 % (Fig. 3, Table 1, Appendix 1).

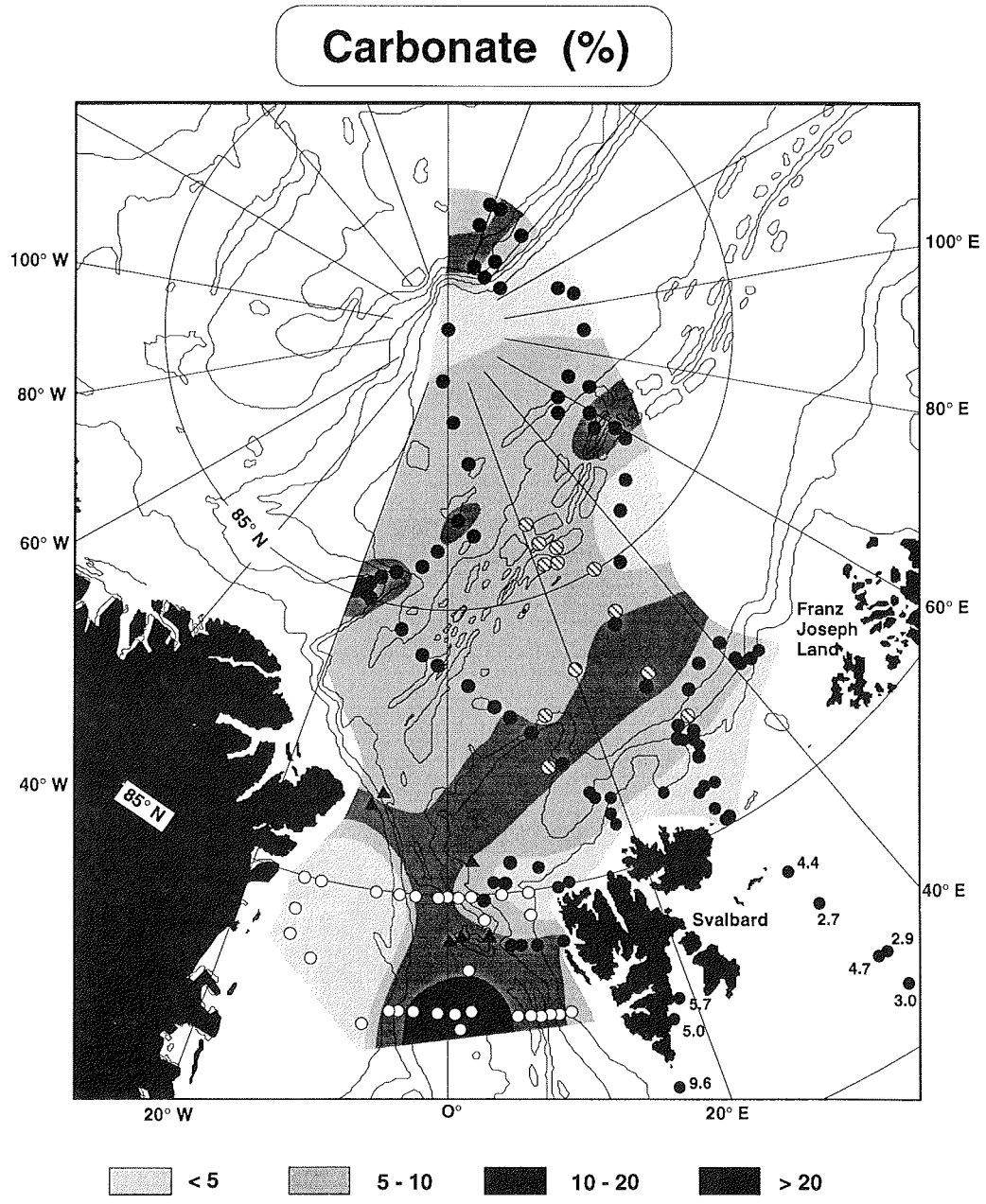

Fig. 3.: Distribution map of carbonate content in surface sediments from the eastern central Arctic Ocean, Fram Strait, and the East Greenland and Svalbard continental margin (data produced on sediments taken during RV "Polarstern" expeditions ARK-VIII/2 and ARK-VIII/3; Fütterer (1992), Rachor (1992)). In the distribution map, data from Hebbeln and Berner (1993) (open circles), Boström and Thiede (1984) (black triangles), and Pagels (1991) (hatched circles) are included.

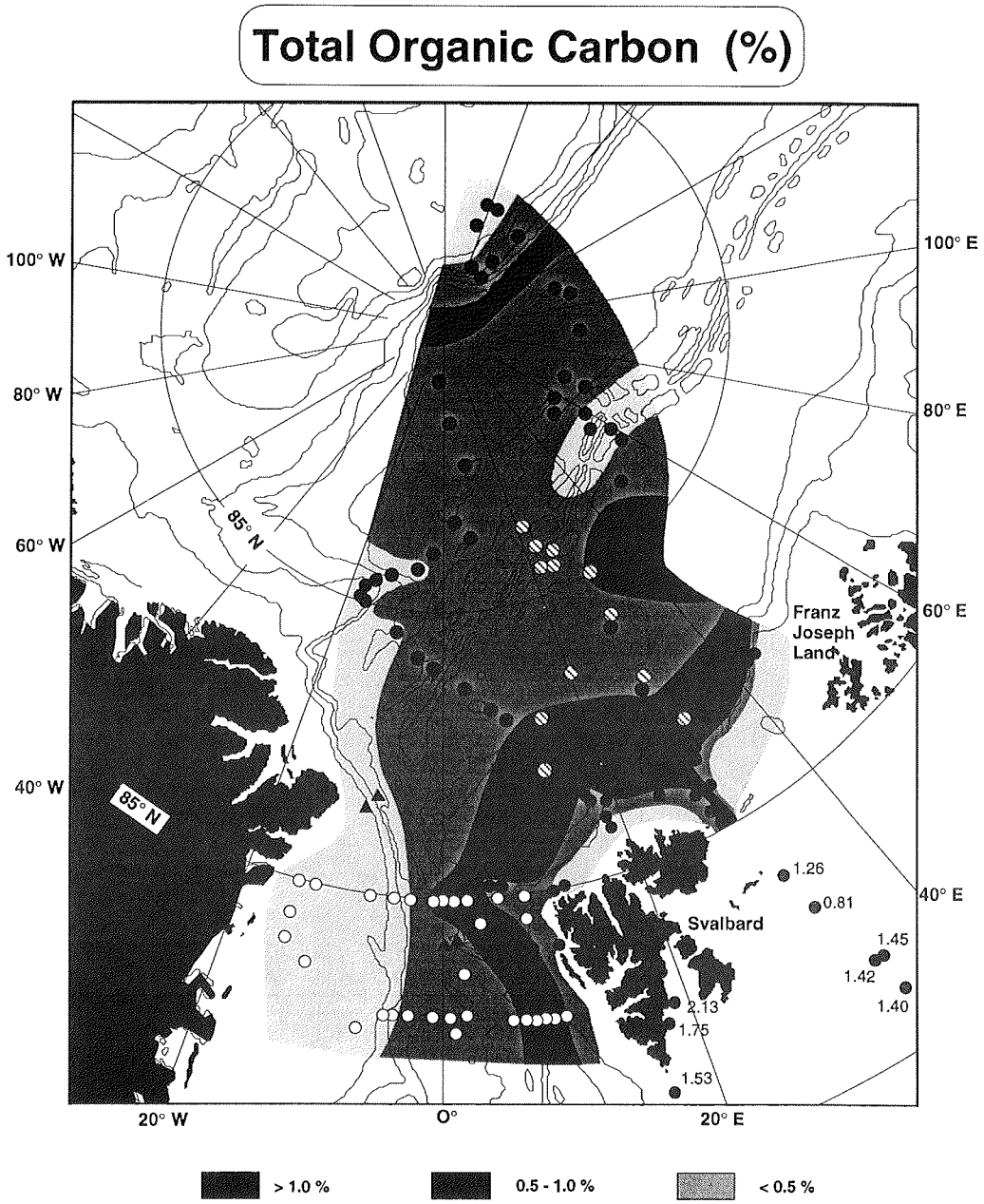

Fig. 4.: Distribution map of total organic carbon content in surface sediments from the eastern central Arctic Ocean, Fram Strait, and the East Greenland and Svalbard continental margin (data produced on sediments taken during RV "Polarstern" expeditions ARK-VIII/2 and ARK-VIII/3; Fütterer (1992), Rachor (1992)). In the distribution map, data from Hebbeln and Berner (1993) (open circles), Boström and Thiede (1984) (black triangles), and Pagels (1991) (hatched circles) are included.

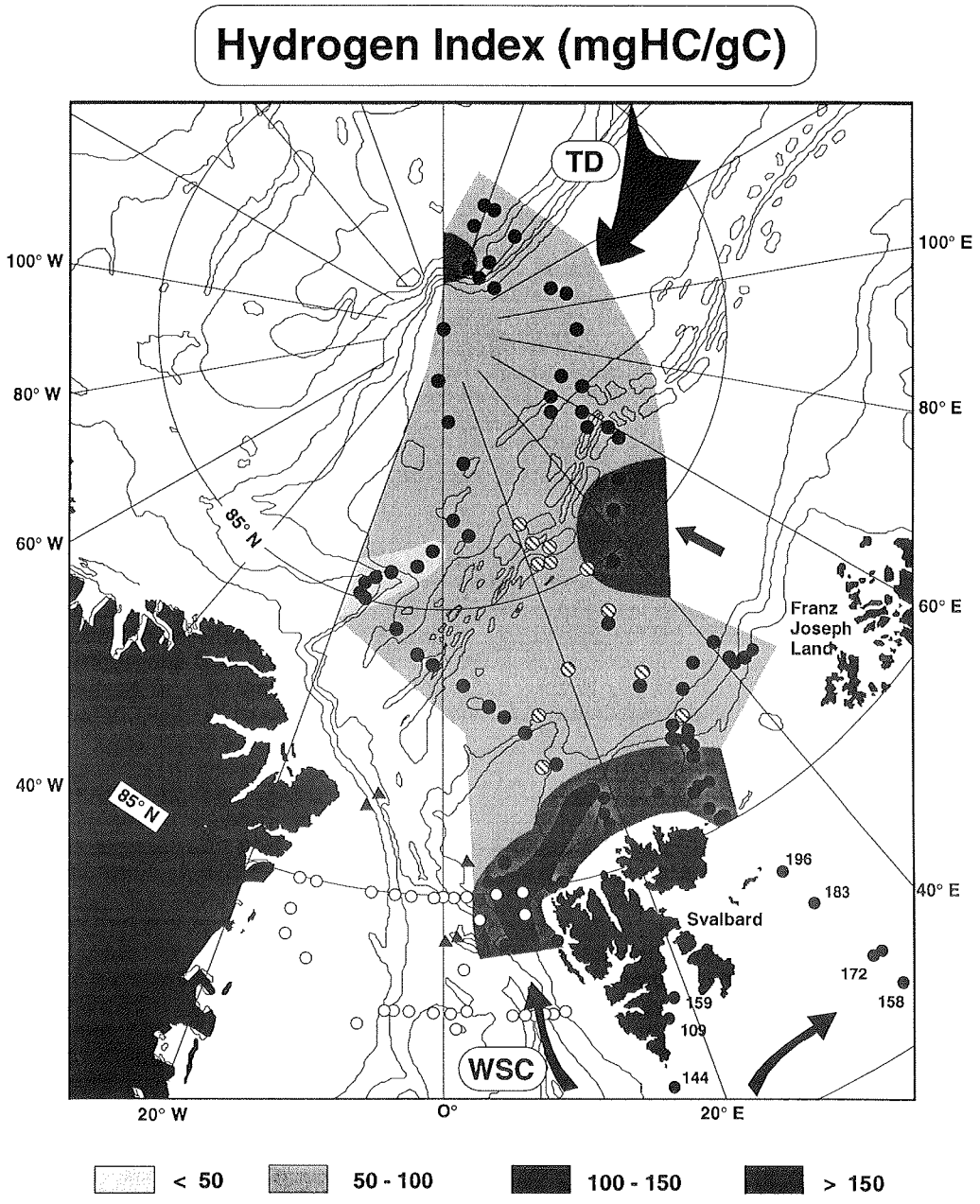

Fig. 5.: Distribution map of hydrogen index values (mgHC/gC) in surface sediments from the eastern central Arctic Ocean and the Svalbard continental margin (data produced on sediments taken during RV "Polarstern" expeditions ARK-VIII/2 and ARK-VIII/3; Fütterer (1992), Rachor (1992)). TD = Transpolar Drift; WSC = Westspitsbergen Current.

Minimum values of less than 5 % occur in the central Amundsen and Nansen Basins as well as directly north and east of Svalbard and along the northern East Greenland continental margin. Carbonate contents of 10 to 20 % are common on the Yermark Plateau, the Gakkel Ridge, and the eastern flank of the Lomonosov Ridge, as well as in the central Fram Strait area. Maximum carbonate contents of up to 30 % are recorded on the Morris-Jesup-Rise and the central northern Greenland-Norwegian-Sea.

Almost all of the surface sediment samples have relatively high total organic carbon (TOC) values ranging between about 0.5 and 2.1 % (Fig. 4, Table 1, Appendix 1). Maximum values of > 1 % occur in the Fram Strait, at the northern Svalbard continental slope, and in parts of the Nansen and Amundsen Basins. A couple of TOC measurements of sediments from the Barents Sea and the Storfjorden also display high values of 1.3 to 2.1 % (Fig. 4). Low values of < 0.5 % are recorded directly north of Svalbard, the Gakkel Ridge, the eastern flank of the Lomonosov Ridge, the Morris-Jesup-Rise, and along the northern East Greenland continental margin. In general, TOC values are higher in the deep-sea basins than on the ridges. There is, however, no simple linear correlation between TOC content and water depth (Stein et al., 1994).

Based on low hydrogen index values of < 100 mgHC/gC, the organic carbon fraction of the central Arctic Ocean surface sediments is clearly dominated by terrigenous material (kerogen type III) (Fig. 5). This is also corroborated by dominantly high C/N ratios (Stein et al., 1994). Sediments from the northern Svalbard Continental Margin, Storfjorden, the Barents Sea, and the central Nansen Basin show some higher hydrogen index values of 100 to 250 mgHC/gC suggesting the presence of some higher amounts of marine organic material (Fig. 5).

Kara Sea

Carbonate contents of the sediments from the inner Kara Sea as well as from the St. Anna Trough area are very low throughout (0 - 4 %; Table 1, Appendix 1).

Total organic carbon values vary between 0.6 and 2.2 % (Fig. 6, Table 1, Appendix 1). Similar organic carbon values in Kara Sea sediments were also recorded by Romankevich et al. (1982). In the inner Kara Sea, maximum values of 1.7 to 2.2 % are recorded in the Yenisey estuary. In the St. Anna Trough area, the maximum values occur in the vinicity of Franz-Josef-Land, north of Novaya Zemlya, and in the central part of the trough. The minimum TOC values of < 0.75 % are obvious along the eastern margin of the St. Anna Trough (Fig. 6).

Hydrogen indices vary between about 70 and 150 mgHC/gC (Fig. 7). Low hydrogen indices < 100 mgHC/gC corresponding to maximum TOC values, occur in the Yenesey estuary and clearly indicate the dominance of terrigenous organic matter. This is also corroborated by elevated C/N ratios of 9 to 13 (Fig. 8). A couple of samples with HI values 120 to 150 mgHC/gC and C/N ratios of about 5 point to the preservation of some higher amount of marine organic matter. In the St. Anna Trough area, most of the C/N ratios are between 5 and 7 (Table 1, Appendix) suggesting the presence of significant

amount of marine organic carbon. Southeast of Franz-Josef-Land, C/N ratios of 8 - 12, corresponting to significantly increased TOC values, indicate the terrigenous origin of the organic matter. This has to be proved, however, by other techniques (Rock-Eval pyrolysis, kerogen microscopy, and GC analysis)

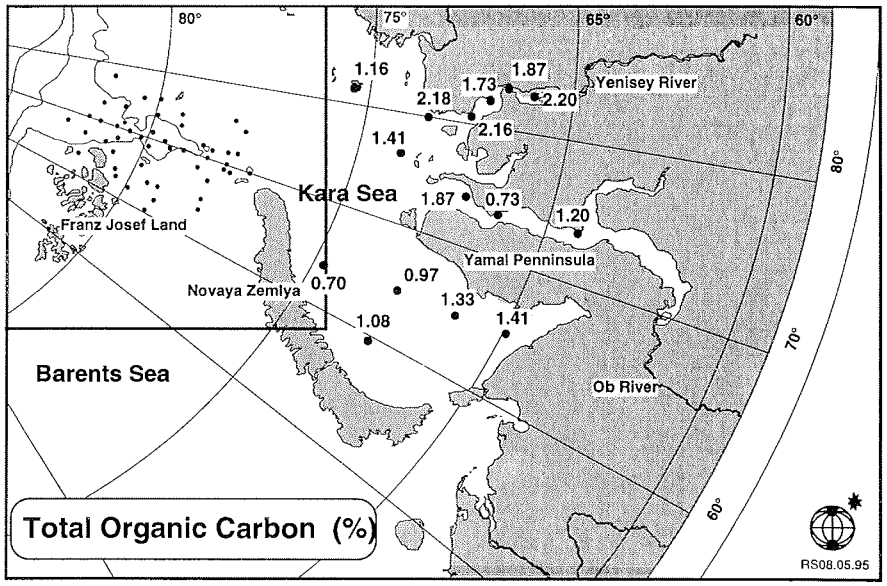

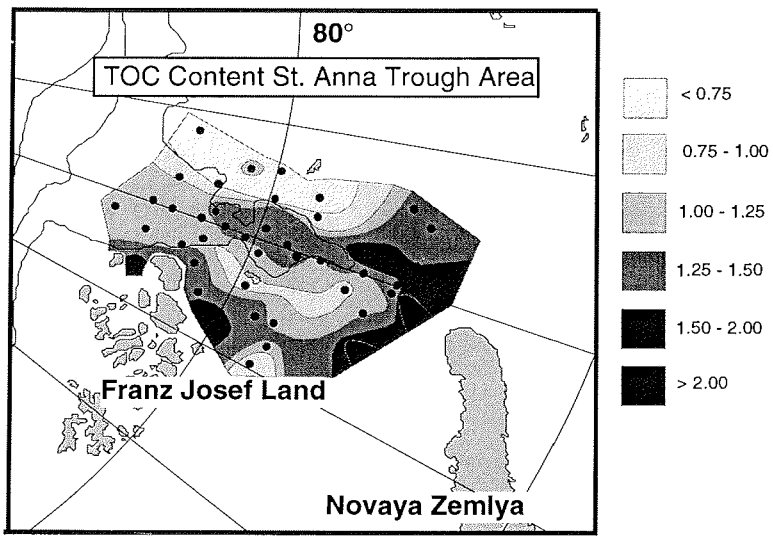

Fig. 6.: Distribution map of total organic carbon content in surface sediments from (A) the inner Kara Sea (samples taken during the RV "Mendeleev" Expedition 1993), and (B) the St. Anna Trough area (samples taken during the RV "Prof. Logachev" Expedition 1994).

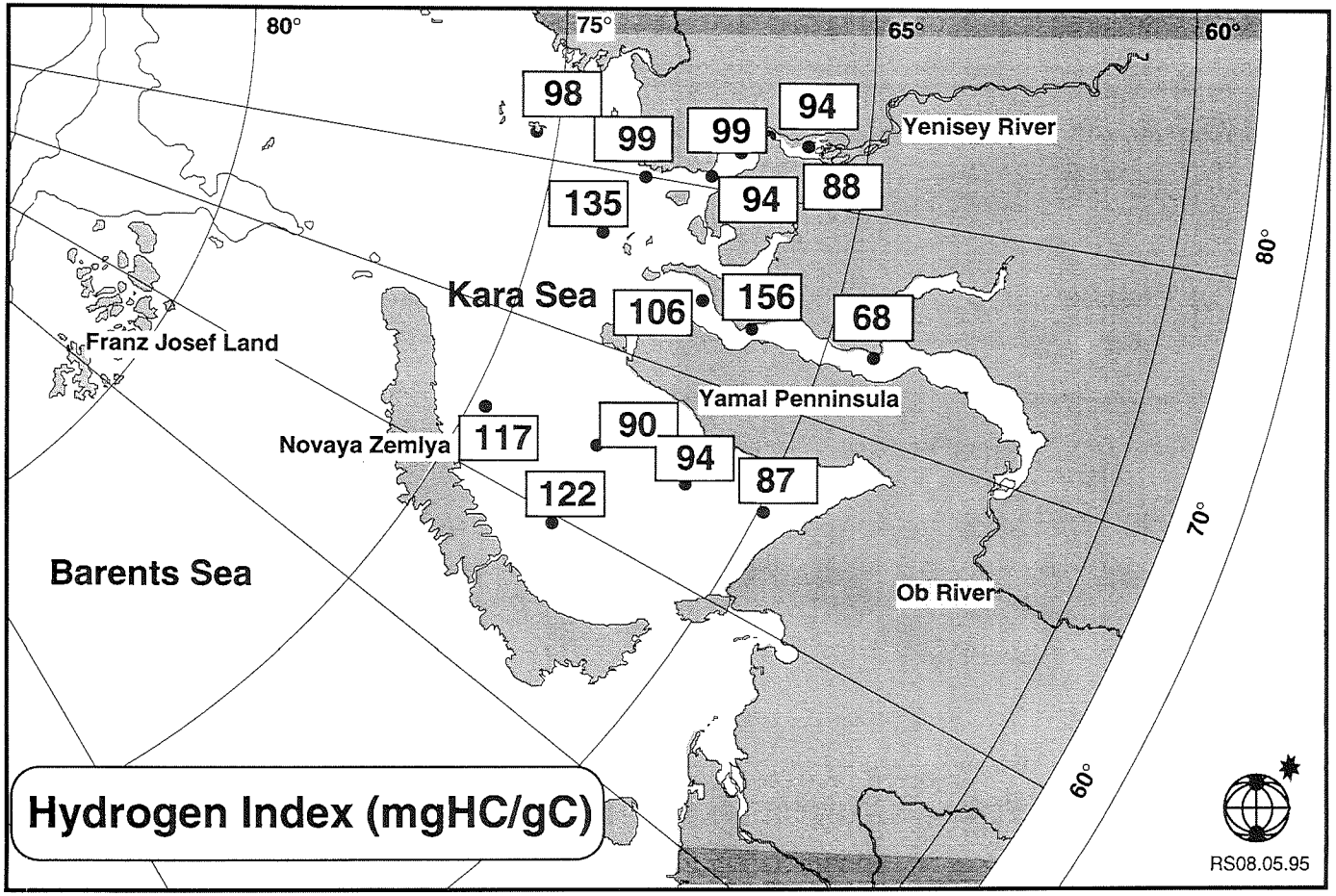

Fig. 7.: Distribution of hydrogen index values (mgHC/gC) in surface sediments from the inner Kara Sea (samples taken during the RV "Mendeleev" Expedition 1993)

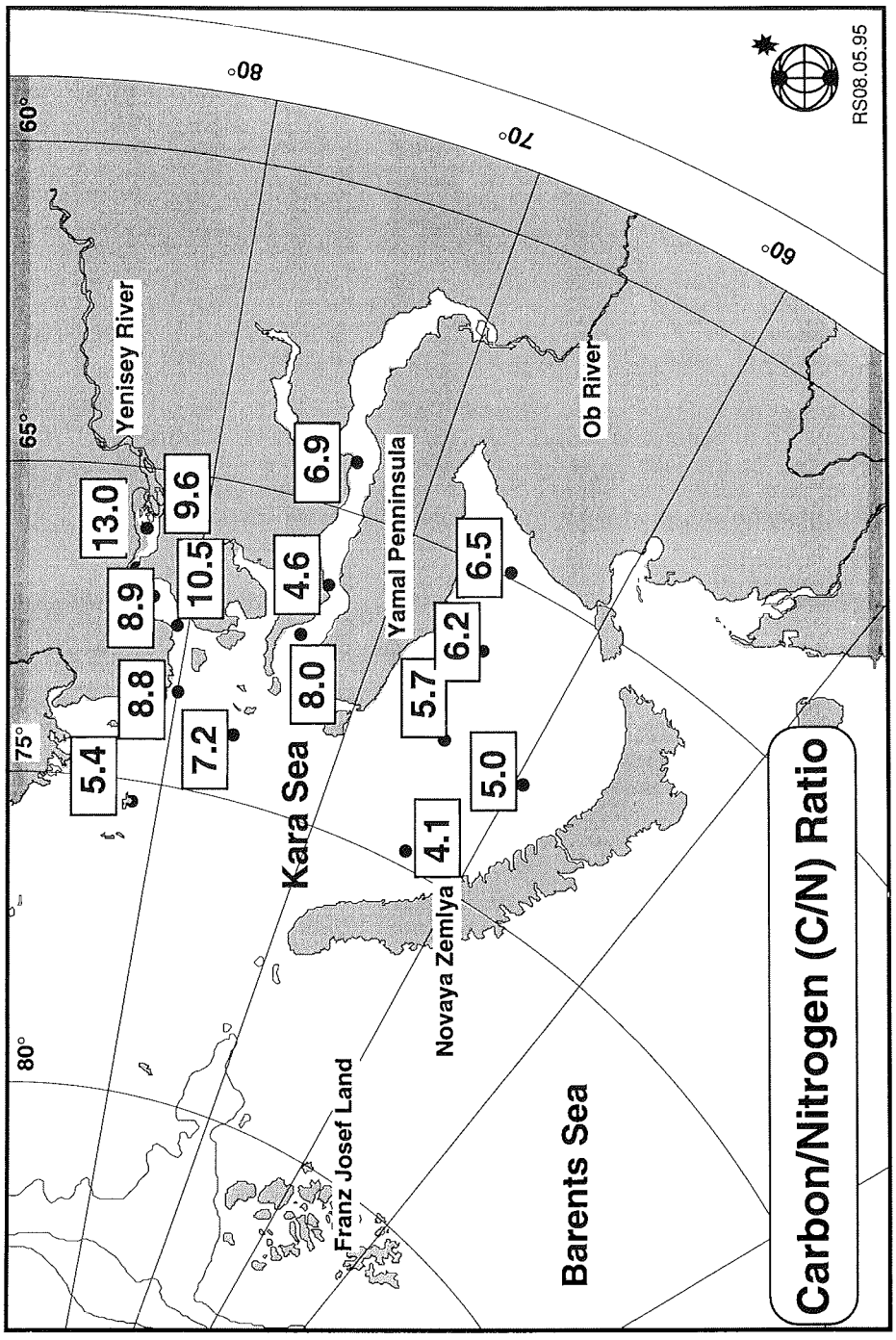

Fig. 8.: C/N ratios in surface sediments from the inner Kara Sea (samples taken during the RV "Mendeleev" Expedition 1993)

Laptev Sea and adjacent continental slope

The carbonate content of sediments from the inner Laptev Sea and its adjacent continental slope are very low, ranging between 0 and 2.6 % (Table 1, Appendix 1).

TOC values vary between 0.3 and 2.3 % (Fig. 9, Table 1, Appendix 1). Maximum TOC values occur off the eastern Lena Delta, southwest of the New Siberian Islands, and in the central part of the lower Laptev Sea continental slope. In general, areas of high TOC concentrations commonly correspond to low HI values (< 100 mgHC/gC) and high C/N ratios (> 7.5) indicating the dominance of terrigenous organic matter (Figs. 10 and 11). In the central part of the Laptev Sea and along the upper continental slope, hydrogen indices reach values > 100 mgHC/gC and C/N ratios are generally < 7.5, suggesting the presence of significant concentrations of marine organic matter.

The total sulfur content varies between 0.07 and 0.36 % (Fig. 12, Table 1, Appendix 1). In general, elevated sulfur values correspond to increased TOC values, i.e., in the vicinity of the river mouths, south of the New Siberian Islands, and along the Laptev Sea continental slope (cf., Fig. 9). The maximum sulfur values of > 0.2 % occur along the continental slope.

Discussion

Variations in carbonate content: Dilution vs. dissolution

In pelagic sediments, variations in biogenic carbonate content are mainly controlled by dissolution, dilution, and/or productivity changes. Based on coarse fraction data, the carbonate in the modern eastern central Arctic Ocean sediments (Fig. 3) is mainly of biogenic origin; detrital carbonate is only of minor importance. Planktonic foraminifers are dominant throughout, whereas benthic foraminifers, bivalves, and ostracodes occur in minor amounts on the ridges and plateaus (Fütterer, 1992). Coccoliths are also present in significant amounts in the surface sediments (Gard, 1993). The occurrence of planktonic foraminifera and coccoliths suggests at least seasonal open-ice conditions.

Only in the Morris-Jesup-Rise area, i.e., relatively close to the North Greenland continental margin, major proportions of detrital calcite and dolomite grains were recorded (Vogt, this vol.; Vogt, 1996). This may support the transport of terrigenous (carbonate) sediments from northern Greenland and the Canadian Arctic onto the Morris-Jesup-Rise, the source area of which are probably the Paleozoic carbonate rocks in North Greenland (Peel, 1982) and the Canadian Arctic Islands.

In the central Arctic Ocean, the good preservation of foraminifera tests in all surface sediment samples from about 200 to almost 4500 m water depth suggests that carbonate dissolution has not dominantly controlled the carbonate variations shown in Figure 3; instead, dilution by siliciclastics seems to be more important (cf., Pagels, 1991). In the Yermak Plateau and Fram Strait areas the high carbonate values may additionally reflect the influence of the warm Westspitsbergen Current causing increased carbonate production (cf., Pagels, 1991; Hebbeln and Berner, 1993).

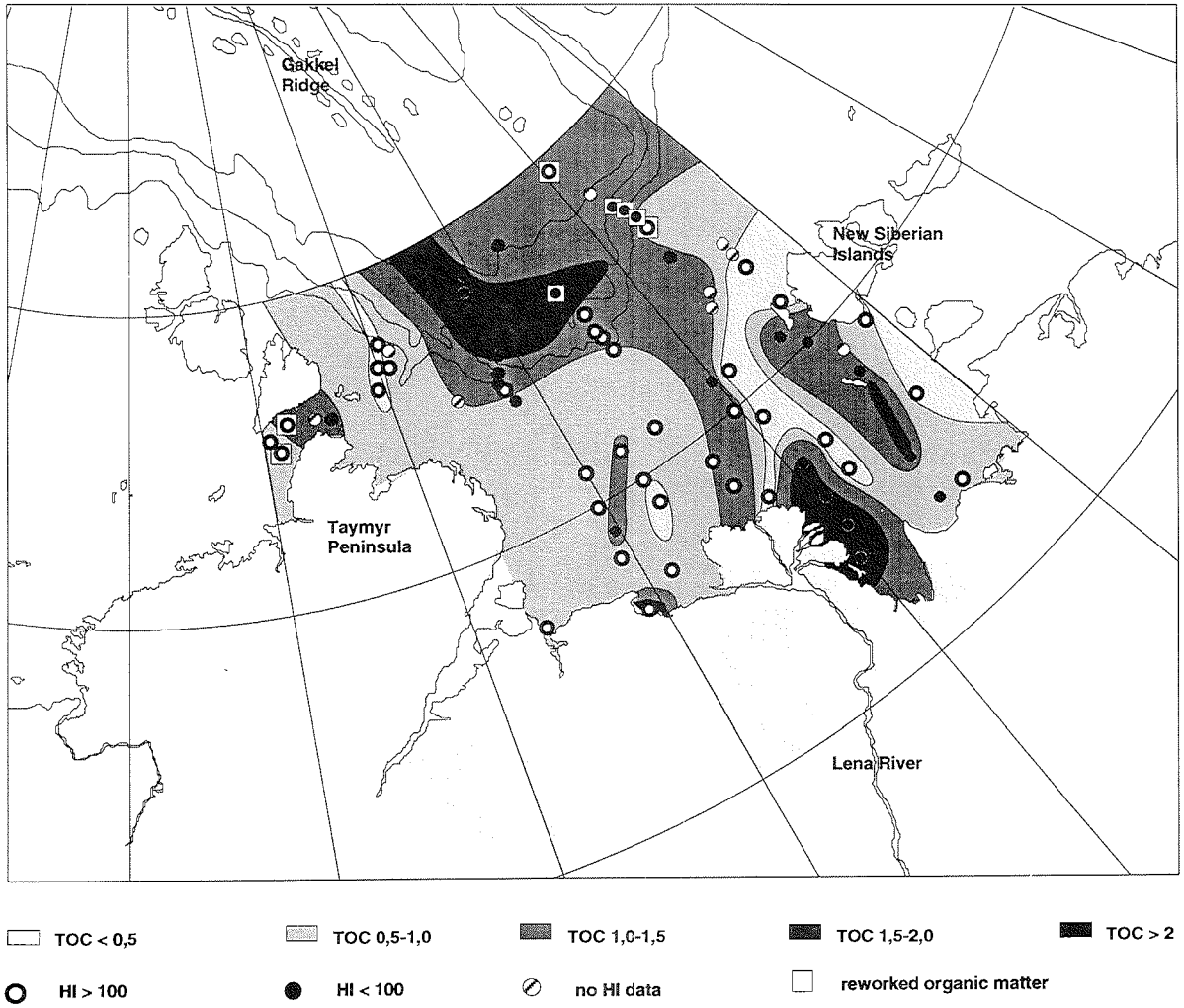

Fig. 9.: Distribution map of total organic carbon content in surface sediments from the inner Laptev Sea (samples taken during the RV "Kireev" Expedition 1993; Kassens and Karpiy, 1994), and the adjacent continental margin (samples taken during the RV "Polarstern" Expedition 1993; Fütterer,1994)

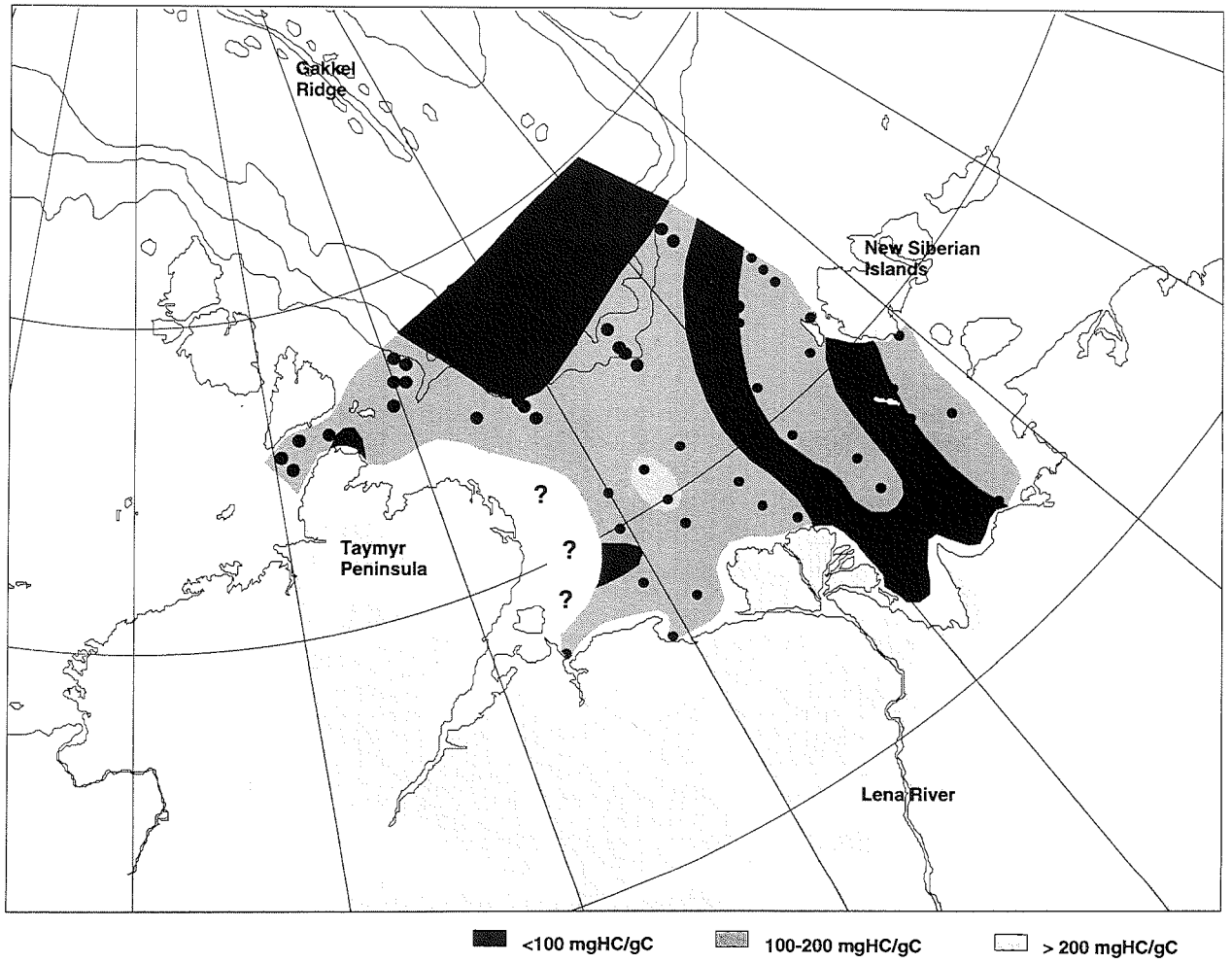

Fig. 10.: Distribution map of hydrogen index values (mgHC/gC) in surface sediments from the inner Laptev Sea (samples taken during the RV "Kireev" Expedition 1993; Kassens and Karpiy, 1994), and the adjacent continental margin (samples taken during the RV "Polarstern" Expedition 1993; Fütterer,1994)

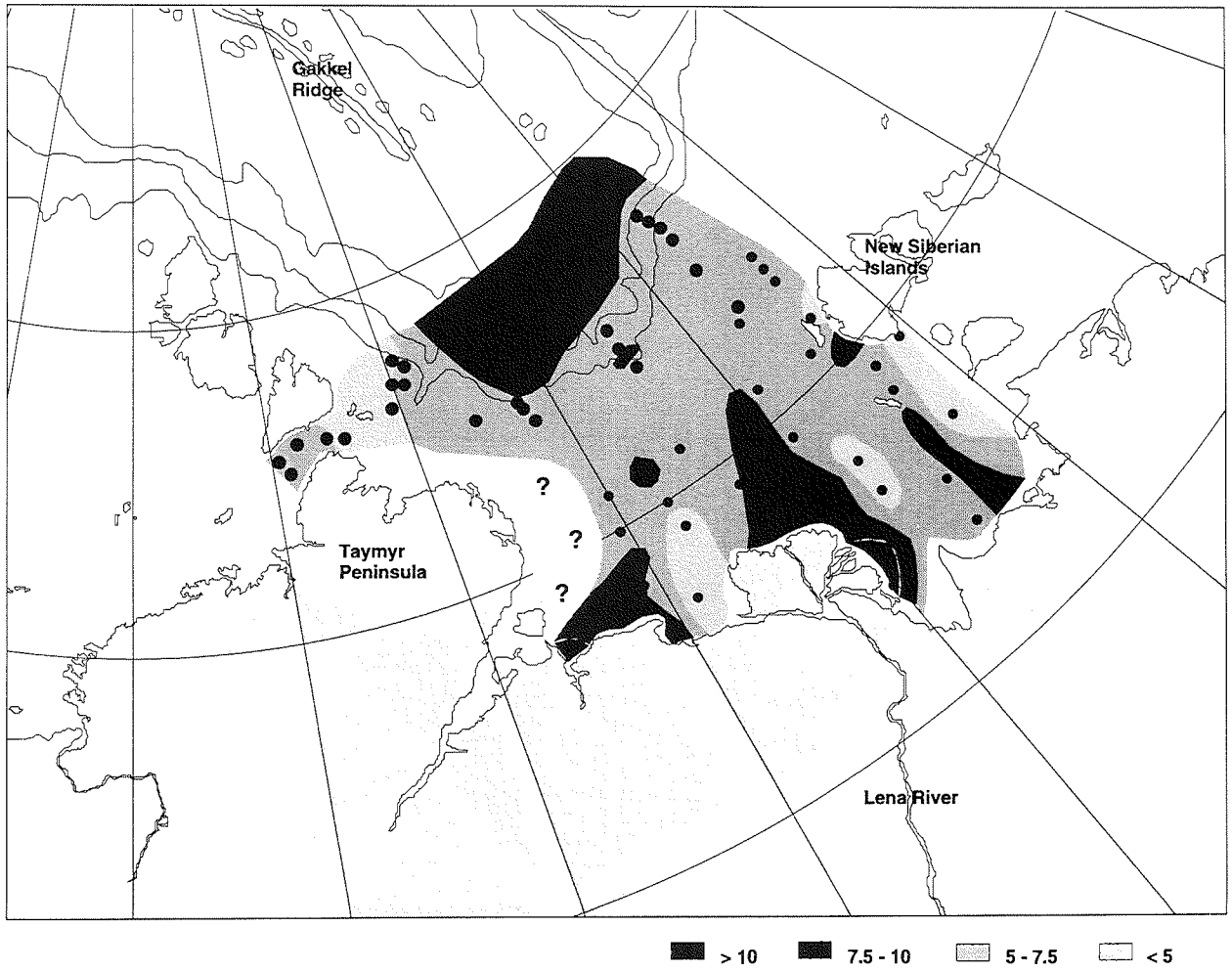

Fig. 11.: Distribution map of C/N ratios in surface sediments from the inner Laptev Sea (samples taken during the RV "Kireev" Expedition 1993; Kassens and Karpiy, 1994), and the adjacent continental margin (samples taken during the RV "Polarstern" Expedition 1993; Fütterer,1994)

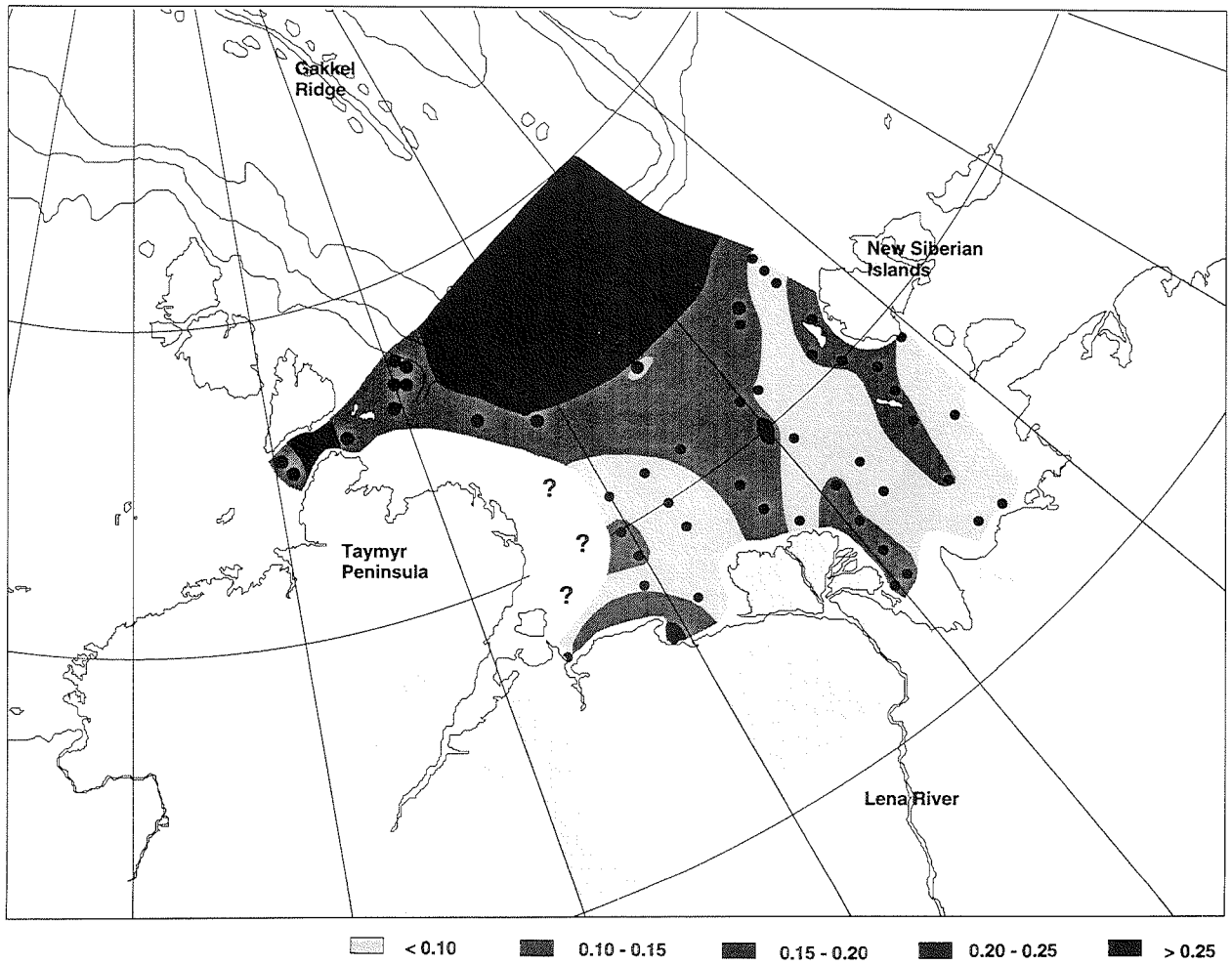

Fig. 12.: Distribution map of total sulfur content in surface sediments from the inner Laptev Sea (samples taken during the RV "Kireev" Expedition 1993; Kassens and Karpiy, 1994), and the adjacent continental margin (samples taken during the RV "Polarstern" Expedition 1993; Fütterer,1994).

In the marginal seas (i.e., Barents, Kara, and Laptev Seas), the very low carbonate values of << 3 % are probably controlled by dilution and/or dissolution processes. Especially in the inner Kara and Laptev Seas where huge amounts of fluvial suspension are supplied by the major rivers Ob, Yenesei, Khatanga, and Lena, dilution by fine-grained siliciclastic material is the most important factors causing the extremely low carbonate contents of the surface sediments. In the Barents Sea and outer Kara Sea, calcium carbonate dissolution may become the dominant factor. The existence of cold saline dense bottom water enriched in CO_2 produced by the decay of organic matter, may have favoured carbonate dissolution in these regions (Steinsund and Hald, 1994; Hald and Steinsund, this vol.).

Organic carbon record: Productivity indicator vs. terrigenous supply

In general, the modern central Arctic Ocean is a low-productivity environment because of its sea-ice coverage (Subba Rao and Platt, 1984). This, together with the well-oxygenated deep-water sphere, results in the very low flux and preservation of marine organic matter in the surface sediments. However, the occurrence of significant amount of biogenic carbonate (see above) as well as the occurrence of detectable amounts of unsaturated alkenones (Schubert, 1995) which are biomarker produced by prymnesiophytes (e.g., Marlowe et al., 1984), indicate at least seasonally open-ice or ice-free conditions and some bioproductivity.

The relatively high organic carbon contents, i.e., values which are distinctly higher than those recorded in modern normal open-marine environments, are certainly caused by the supply of terrigenous organic matter. This is clearly indicated by the low hydrogen index values (Fig. 5) and generally high C/N ratios (Table 1, Appendix 1). Part of the organic carbon measured in ground bulk sediments derives from black organic-carbon-rich silt stones (up to 4 % TOC) and coal fragments which were identified as IRD in the coarse fraction (Stein et al., 1994). These particles as well as the other terrigenous organic material were probably derived from the Siberian shelf areas and were transported by sea ice (via the Transpolar Drift) and/or currents (cf., Pfirman et al., 1989; Wollenburg, 1991; Bischof et al., 1992). Terrigenous organic carbon is also dominant in the inner Kara and Laptev Sea areas (Figs. 6 to 11). River-derived terrigenous organic material from the Siberian hinterland probably contribute in major proportions to the organic carbon content in the sediments of the Eurasian shelf seas. This is especially obvious in the surface sediments off the Lena river mouth (Figs. 9 to 11). Franz-Joseph-Land and Novaya Zemlya are important source areas for the organic matter deposited in the St.-Anna Trough area (Fig. 6). In the central St. Anna Trough, a couple of samples with high TOC values and C/N ratios of about 6 also show relatively high biogenic opal values of 3 - 5 % (Nürnberg, this vol.) which may suggest some increased surface-water productivity.

Elevated amounts of marine organic carbon are recorded in the sediments around Northwest Svalbard, as indicated by both increased organic carbon contents and increased hydrogen index values (Figs. 4 and 5). These higher marine organic carbon values are probably caused by increased (ice-edge) surface-water productivity due to reduced sea-ice cover and increased nutrient supply, both triggered by the inflow of warm Atlantic Ocean water masses, i.e., the Westspitsbergen Current.

In the Laptev Sea, hydrogen indices are > 100 mgHC/gC observed in upper continental slope sediments in 500 - 1000 m water depth (and corresponding to high TOC values of 1 - 2 %), suggest some increased amounts of marine organic matter (Figs. 9 and 10). This is also supported by high concentrations of short-chain unsaturated fatty acids (Fahl and Stein, 1996). At the same sites, a distinct opal maximum of about 3-5% is recorded (Stein and Nürnberg, 1995; Nürnberg, this vol.). These sites are situated directly below the ice edge, which is relatively stable during summer over years as inferred from satellite imagery (H. Eicken, pers. com. 1995). Surface waters overlying these sites showed drastically enhanced chlorophyll A and phaeopigment concentrations during summer 1993, whereas nutrients (NO3, PO4) are significantly depleted indicating a plankton bloom at the ice edge (Boetius et al., this vol.). Due to the relatively stable position of the ice edge during summer, repeated plankton blooms are apparently providing enough biogenic silica and marine organic matter to be reflected in the surface sediments.

Detailed organic-geochemical investigations (i.e., GC and GC/MS measurements as well as kerogen microscopy) of the surface sediments from the Eurasian shelf seas and the adjacent continental margin and deep-sea areas are in progress to get more precise informations about modern mechanisms controlling the organic-carbon flux (Fahl and Stein, 1996). The transfer of the knowledge on modern processes to similar data sets derived from studies on sediment cores will then allow to reconstruct the paleo-situation. Since surface-water productivity may affect the concentration of atmospheric CO_2 (i.e., in areas and at times of high production rate of organic matter, the ocean may act as a sink for CO_2; cf. Fig. 2) which is an important factor controlling the global climate, the quantification of the organic carbon budget in the Arctic Ocean and its change through time may yield important insights into the role of the Arctic Ocean during global climate change.

Acknowledgments

For technical assistance and data discussion, I thank K. Fahl, C. Schubert, M. Seebeck, M. Siebold, and R. Stax. The financial support by the Ministry for Education, Science, Research, and Technology (BMBF) and by the "Deutsche Forschungsgemeinschaft" (DFG) (grant no. STE 412/6) is gratefully acknowledged. Samples taken during the RV *Mendeleev* Expedition 1993 and the RV *Prof. Logachev* Expedition 1994 were provided by M. Levitan (Shirshov Institute of Oceanology Moscow) and G. Ivanov (VNIIO St. Petersburg), respectively.

References

Berger, W.H., Smetacek, V., and Wefer, G., 1989. Productivity of the Ocean: Past and Present. Life Sciences Research Report, Vol. 44, Wiley & Sons, New York, 471p.

Bischof, J., Koch, J., Kubisch, M., Spielhagen, R.F., and Thiede, J., 1990. Nordic Seas surface ice drift reconstructions: evidence from ice rafted coal fragments during oxygen isotope stage 6. In: Dowdeswell, J.A. and Scourse, J.D. (Eds.), Glacimarine Environments: Processes and Sediments., Geol. Soc. Spec. Publ., 53, p. 235-251.

Bordowskiy, O.K., 1965. Sources of organic matter in marine basins. Mar. Geol., 3, p. 5-31.

Boström, K. and Thiede, J., 1984. YMER-80. Swedish Arctic Expedition Cruise Report. Meddel. Stockholms Univ. Geol. Inst., 260, 123 pp.

Espitalié, J., Laporte, J.L., Madec, M., Marquis, F., Leplat, P., Paulet, J., and Boutefeu, A., 1977. Méthode rapide de characterisation des roches-mere, de leur potential petrolier et de leur degre d´évolution. Rev. Inst. Tranc. Petrol., 32, p. 23-42.

Fahl, K. and Stein, R., 1996. Modern organic-carbon deposition in the Laptev Sea and adjacent continental slope: Surface-water productivity vs. terrigenous input. Organic Geochemistry, submitted.

Fütterer, D.K. , 1994: The Expedition ARCTIC´93 Leg ARK IX/4 of RV "Polarstern" 1993. Ber. Polarforsch., 149/94, 244 pp.

Fütterer, D.K., 1992. ARCTIC´91: The Expedition ARK-VIII/3 of RV "Polarstern" in 1991. Berichte zur Polarsternforschung, 107, 267 pp.

Gard, G., 1993. Late Quaternary coccoliths at the North Pole: Evidence of ice-free conditions and rapid sedimentation in the central Arctic Ocean. Geology, 21, p. 227-230.

Hebbeln, D. and Berner, H., 1993. Surface sediment distribution in the Fram Strait. Deep-Sea Res., 40/9, p. 1731-1745.

Kassens, H., and Karpiy, V.Y., 1994. Russian-German Cooperation: The Transdrift I Expedition to the Laptev Sea. Ber. Polarforsch., 151/94, 168 pp.

Marlowe, I.T., Green, J.C., Neal, A.C., Brassell, S.C., Eglinton, G., and Course, P.A., 1984. Long chain alkenones in the Prymnesiophyceae. Distribution of alkenones and other lipids and their taxonomic significance. Br. J. Phycol., Vol. 19, p. 203-216.

Marlowe, I.T., Green, J.C., Neal, A.C., Brassell, S.C., Eglinton, G., and Course, P.A., 1984. Long chain alkenones in the Prymnesiophyceae. Distribution of alkenones and other lipids and their taxonomic significance. Br. J. Phycol., Vol. 19, p. 203-216.

Martin, J.M., Guan, D.M., Elbaz-Poulichet, F., Thomas, A.J., and Gordeev, V.V., 1993. Preliminary assessment of the distributions of some trace elements (As, Cd, Cu, Fe, Ni, Pb and Zn) in a pristine aquatic environment: the Lena River estuary (Russia). Marine Chemistry, Vol. 43, 185-199.

Nürnberg, D., Wollenburg, I., Dethleff, D., Eicken, H., Kassens, H., Letzig, T., Reimnitz, E., and Thiede, J., 1994. Sediments in Arctic sea ice - Implications for entrainment, transport, and release. Mar. Geol., 119: 185-214.

Pagels, U., 1991. Sedimentologische Untersuchungen und Bestimmungen der Karbonatlösung in spätquartären Sedimenten des östlichen Arktischen Ozeans. PhD. Thesis, Kiel University, 106 pp.

Peel, J.S., 1982. The lower Paleozoic of Greenland. In: Embry, A.F. and Balkwill, H.R. (Eds.), Arctic Geology and Geophysics, Can. Soc. Petrol. Geol., Memoir 8, p. 309-330.

Pfirman, S., Lange, M.A., Wollenburg, I.,, and Schlosser, P., 1989. Sea ice characteristics and the role of sediment inclusions in deep-sea deposition: Arctic-Antarctic comparison. In: Bleil, U., and Thiede, J. (Eds.), Geological History of the Polar Oceans: Arctic versus Antarctic, NATO ASI Ser., C308, p. 187-211.

Prahl, F.G. and Muehlhausen, L.A., 1989. Lipid Biomarkers as Geochemical Tools for Paleoceanographic Study. In: Berger, W.H., et al. (Eds.),

Productivity of the Ocean: Past and Present, Life Sci. Res. Rep., Vol. 44, Wiley & Sons, p. 271-290.
Rachor, E., 1992. Scientific Report of RV "Polarstern" Cruise ARK-VIII/2. Berichte zur Polarforschung, 115, 150 pp.
Romankevich, E. A., Dayushevskaya, A.I., Belyaeva, A.N., and Rusanov, V.P., 1982. The biogeochemistry of organic matter of the Arctic Seas, Nauka, Moscow, 240 pp (in russian).
Sakshaug, E. and Skjoldal H.R., 1989. Life at the ice edge. Ambio, 18, p. 60-67.
Scheffer, F. and Schachtschabel, P., 1984. Lehrbuch der Bodenkunde. Enke Verlag Stuttgart, 442 pp.
Schubert, C., 1995. Organischer Kohlenstoff in spätquartären Sedimenten des Arktischen Ozeans: Terrigener Eintrag und marine Produktivität, PhD Thesis, Bremen University.
Schubert, C. and Stein, R., 1996. Deposition of organic carbon in Arctic Ocean sediments: Terrigenous supply and marine productivity. Organic Geochemistry, in press.
Stein, R. and Korolev, S., 1994. Shelf-to-basin sediment transport in the eastern Arctic Ocean. Berichte zur Polarforschung, 144: 87-100.
Stein, R. and Nürnberg, D., 1995. Productivity proxies: Organic carbon and biogenic opal in surface sediments from the Laptev Sea and the adjacent continental slope. In: Kassens, H., et al. (Eds.), Second Workshop on "Russian-German Cooperation in and around the Laptev Sea", St. Petersburg, November 1994, Berichte zur Polarforschung, 176, p. 286-296.
Stein, R., 1991. Accumulation of organic carbon in marine sediments : Lecture Notes in Earth Sciences 34, Springer, Heidelberg, 217 pp..
Stein, R., Grobe, H., and Wahsner, M., 1994. Organic carbon, carbonate, and clay mineral distributions in eastern central Arctic Ocean surface sediments. Mar. Geol., Vol. 119, p. 269-285.
Steinsund, P.I. and Hald, M., 1994. Recent calcium carbonate dissolution in the Barents Sea, Paleoceanographic implications. Mar. Geol., 117: 303-316.
Subba Rao, D.V. and Platt, T., 1984. Primary Production of Arctic Waters. Polar Biol., 3, p. 191-201.
Thiede, J., 1988. Scientific Cruise Report of Arctic Expedition ARK-IV/3. Ber. Polarforschung, 43, 237 pp.
Tissot, B.P. and Welte, D.H., 1984. Petroleum Formation and Occurrence, Springer Verlag Heidelberg, 699 p..
Vogt, C., 1996. Gesamt- und Tonmineralogie in Sedimenten des Arktischen Ozeans: Indikator für Sedimentationsprozesse und paläo-ozeanographische Verhältnisse im Spätquartär, PhD thesis, Bremen University.
Wollenburg, I., 1991. Sedimenttransport durch das arktische Meereis - Die rezente lithogene und biogene Materialfracht. PhD. Thesis, Kiel University, 189 pp.

Appendix

Table 1: Summary table of carbonate contents, total organic carbon contents, C/N ratios, hydrogen index values, and sulfur contents of investigated surface sediments

Core/Station Number	CaCO3 (%)	TOC (%)	C/N	HI (mgHC/gC)	Sulfur (%)
"Polarstern" ARK VIII/3 (Central Arctic Ocean and Barents Sea)					
2111	2.9	1.45			
2113	3.0	1.40		158	
2114	5.7	2.13		159	
2115	5.0	1.75		109	
2116	9.6	1.53		144	
2117	12.1	1.02		113	
2119	8.0	1.00		183	
2120	14.0	1.41		174	
2121	11.2	1.75		133	
2122	4.2	1.17		147	
2123	4.4	1.41		147	
2124	5.0	0.17			
2125	38.3	0.42		247	
2127	5.5	0.35		137	
2128	9.0	0.81		135	
2129	3.4	0.75		174	
2130	8.0	1.57		132	
2131	3.7	0.35		122	
2132	7.7	0.63		106	
2133	7.8	0.73		100	
2134	9.0	1.41		117	
2136	6.5	0.82		110	
2137	5.0	0.91		118	
2138	6.3	1.08		108	
2142	13.4	0.43		155	
2143	4.8	0.89		161	
2144	5.7	1.36		143	
2147	5.4	0.80		131	
2148	5.6	1.30		148	
2149	3.1	0.48		185	
2150	4.4	1.26		196	
2151	2.7	0.81		183	
2153	4.7	1.42		172	
2156	6.2	1.19		138	
2157	11.3	1.33	10	89	
2158	12.1	0.88		57	
2159	10.4	0.75	26	62	
2160			28	120	
2161	2.6	0.78	28	97	
2162	2.9	0.76		142	
2163	8.3	0.47	19	55	
2164	8.3	0.33	13	46	
2165	8.9	0.26	23	62	
2166	6.3	0.52	20	73	

Core/Station Number	CaCO3 (%)	TOC (%)	C/N	HI (mgHC/gC)	Sulfur (%)
"Polarstern" ARK VIII/3 (Central Arctic Ocean and Barents Sea)					
2167	2.7	0.31	21	108	
2168	4.7	0.45	22	76	
2170	5.8	0.55	24	47	
2171	6.2	0.60	19	71	
2172	6.4	0.54	18	75	
2174	4.1	0.63	21	84	
2175	4.3	0.66	27	76	
2176	3.8	0.74	22	88	
2177	6.2	0.63	16	79	
2178	5.8	0.40	15	60	
2179	5.9	0.54	16	88	
2180	6.3	0.40		72	
2181	9.8	0.32	9	57	
2182	15.3	0.30	17	55	
2183	6.7	0.23	11	80	
2184	11.7	0.25	7	44	
2185	8.6	0.49	12	60	
2186	10.0	0.58	10	65	
2187	3.1	1.00	10	81	
2189	10.7	0.37	13	129	
2190	3.3	0.91	11	75	
2191			20	57	
2192	10.0	0.56	19	52	
2193	6.4	0.67	19	64	
2194	11.8	0.52		57	
2195	7.8	0.61		63	
2196	8.0	0.64	6	49	
2198	8.9	0.57	10	47	
2199	12.2	0.30			
2200	23.3	0.31	8	51	
2202	29.0	0.25	5	44	
2204			7	77	
2205	6.9	0.40	7	74	
2206			7	67	
2208			9	70	
2209	13.3	0.95		64	
2210	13.5	0.89	11	58	
2212	13.7	1.15		63	
2213	3.4	1.16	10	147	
2214	3.4	0.83	11	208	
2215	4.9	0.65	10	136	
"Polarstern" ARK IX/4 (Barents Sea Continental Margin)					
2439	1.7	1.78	9	122	
2440	3.9	0.59	8	181	
2441	3.4	1.74	11	76	
2442	6.3	1.85	10	65	
2443	6.6	1.83	10	53	
2444	6.7	1.81	11	67	
2445	8.8	1.69	10	65	
2446	7.1	1.63	10	66	

Core/Station Number	CaCO3 (%)	TOC (%)	C/N	HI (mgHC/gC)	Sulfur (%)
"Polarstern" ARK IX/4 (Barents Sea Continental Margin)					
2447	6.3	1.54	7	83	
2448	9.1	2.01	8	71	
2449	2.9	0.40	4	146	
"Polarstern" ARK IX/4 (Laptev Sea Continental Margin)					
2450	1.0	1.03	7	127	0.19
2451	1.6	0.52	5	174	0.10
2452	1.7	0.51	6	128	0.10
2453	1.5	1.20	7	98	0.28
2455	1.0	1.02	7	116	0.22
2456	0.3	1.29	8	92	
2457	1.3	0.33	5	78	
2458	1.2	1.19	7	83	
2459	0.5	1.18	7	90	0.19
2460	1.8	0.81	6	115	0.15
2461	1.0	0.87	7	112	0.20
2462	0.5	1.31	7	86	0.19
2463	0.6	0.34	5	125	0.07
2465	0.0	1.40	9	68	0.19
2466	1.1	1.00	7	100	0.17
2467	1.1	0.29	5	178	0.07
2468	2.3	1.10	6	101	0.20
2469	0.4	1.60	8	84	0.24
2470	2.0	1.22	8	59	0.17
2471	0.9	1.52	9	52	
2472	0.7	1.66	8	69	0.22
2473	0.0	1.65	9	77	0.36
2474	0.0	1.36	8	68	
2475	0.0	1.18	7	79	0.20
2476	0.0	1.10	7	97	0.19
2477	1.4	0.57	7	112	0.15
2478	1.0	0.68	7	94	0.11
2480	1.2	0.26	4	237	
2481	1.1	0.56	5	140	0.10
2483	1.9	0.45	5	128	0.11
2484	0.3	0.66	6	120	0.14
2485	2.2	1.02	3	85	0.19
2486					0.12
"Kireev" (Laptev Sea)					
9301	1.7	0.74	5	91	0.07
9306	1.2	1.74	9	72	0.13
9307	0.5	2.27	10	84	0.13
9309	0.8	1.48	7	68	0.10
9313	1.1	0.31	3	120	0.05
9315	1.0	0.39	3	128	0.06
9316	1.5	1.97	8	98	0.15
9318	0.0	1.77	8	99	0.12
9320	0.7	0.18	1	189	0.04
9321	0.9	1.63	8	95	0.16
9323	1.6	0.49	6	129	0.07
9324	1.9	0.68	4	139	0.09

Core/Station Number	CaCO3 (%)	TOC (%)	C/N	HI (mgHC/gC)	Sulfur (%)
"Kireev" (Laptev Sea)					
9327	1.9	0.74	7	121	0.09
9330	2.6	1.44	8	123	0.14
9334	1.6	1.18	7	100	0.10
9338	0.0	1.22	10	83	0.14
9340	0.6	0.11	2	226	0.04
9342	1.5	1.01	8	127	0.12
9344	0.8	0.40	5	158	0.06
9348	0.0	0.57	7	120	
9349	0.0	0.55	4	109	0.09
9350	0.4	1.05	9	85	0.11
9353	1.3	1.70	8	101	0.24
9356	0.3	0.52	6	203	0.08
9358	2.6	0.88	6	103	0.13
9365	1.2	0.49	6	127	0.08
9367	0.3	1.05	8	116	0.09
9368	2.1	0.71	6	133	0.11
9370	0.8	1.25	9	86	0.13
9371	1.4	0.30	5	152	0.07
9373A-6	0.7	0.99	9	122	0.12
9373-8	1.5	1.19	9	39	
9382	0.0	0.34	7	199	0.05
9384					0.07
93Z2-8	1.1	0.91	13	112	0.07
93Z3-2	7.4	2.28	10	108	0.18
93Z4-4	1.7	1.81	15	88	
93Z5-3	2.3	0.80	9	103	0.05
IK93 Kir1-1	0.8	0.34	2	146	
"Mendeleev" (Inner Kara Sea)					
4380	2.4	1.08	5	122	
4382	1.8	0.70	4	117	
4386	1.3	0.97	6	90	
4388	0.3	1.32	6	94	
4391	0.7	1.41	7	87	
4399	2.1	1.16	5	98	
4403	0.0	2.18	9	99	
4409	0.7	2.20	10	88	
4410	0.4	1.87	13	94	
4411	0.0	2.16	11	94	
4413	0.0	1.73	9	110	
4414	0.0	1.41	7	135	
4416	0.0	1.87	8	106	
4417	1.2	0.73	5	156	
4418	0.7	1.20	7	68	
"Logachev" (St. Anna-Trough-Area)					
1	0.8	1.01	6		0.18
2	0.0	1.38	7		0.24
3	0.0	1.33	12		0.12
4	0.3	1.51	9		0.16
5	1.0	1.02	6		0.19
7	3.9	1.09	6		0.21

Core/Station Number	CaCO3 (%)	TOC (%)	C/N	HI (mgHC/gC)	Sulfur (%)
"Logachev" (St. Anna-Trough-Area)					
7	3.5	1.10	6		0.19
8	3.3	1.12	6		0.24
9	0.0	1.61	7		0.24
9	0.1	1.61	7		0.23
10	2.5	1.07	6		0.21
11	1.1	1.15	6		0.20
12	1.4	1.15	6		0.22
13	1.5	0.95	5		0.16
13	0.9	0.89	6		0.16
16	1.1	0.58	6		0.10
16	2.9	0.92	7		0.18
18	2.2	1.17	6		0.22
19	0.9	0.68	8		0.07
20	1.5	1.44	6		0.24
22	0.8	1.08	6		0.21
23	1.2	1.32	6		0.27
25	1.9	0.63	5		0.15
26	1.3	0.61	5		0.14
28	1.4	1.50	6		0.28
30	1.0	1.34	7		0.22
31	0.8	1.12	6		0.22
32	8.0	0.64	3		0.26
32	0.0	1.45	7		0.16
35	1.4	0.66	5		0.13
37	0.4	1.19	6		0.23
38	0.0	1.26	7		0.20
39	1.0	1.23	6		0.19
40	1.0	1.02	6		0.19
41	0.5	0.91	5		0.16
42	0.4	1.41	7		0.20
44	0.9	0.85	5		0.15
46	0.0	1.61	8		0.22
50	1.2	1.24	5		0.18
51	0.7	0.84	6		0.18
53	0.0	1.47	6		0.25
54	0.0	1.44	7		0.23
55	0.4	1.59	7		0.22
56	0.8	1.41	6		0.22
57	0.8	1.30	6		0.20
58	0.0	1.44	7		0.20
62	1.1	1.62	6		0.24
63	0.5	1.42	6		0.21
64	0.0	2.06	7		0.34
65	0.1	1.45	6		0.22
67	0.9	1.26	6		0.15
68	1.2	1.23	6		0.27
69	0.0	1.81	8		0.29
70	0.0	1.33	6		0.22

MICROPALEONTOLOGY

DISTRIBUTION OF DEEP-SEA OSTRACODA IN THE ARCTIC OCEAN

Cronin T.M.

970 U.S. Geological Survey, Reston, Virginia 22091

Introduction

Ostracoda are bivalved Crustacea that constitute an important biogenic component of surface sediments in the Arctic Ocean. Ostracodes have excellent potential for reconstructing Quaternary bottom water environmental history because many species have specialized ecology and are limited by factors such as salinity, temperature, nutrients and dissolved oxygen. Until recently, most studies of Arctic ostracodes concentrated on faunas from shallow water areas on continental shelves (see Cronin et al., 1991), with the important exception of Joy and Clark (1977), who demonstrated that ostracodes were common in deep-sea cores from the Canada Basin. Little was known of faunas from the Eurasian Basin until recent cruises obtained new cores with abundant ostracode material.

This paper is a synthesis of the distribution of eleven of the most common deep-sea ostracode species that occur in the Arctic Ocean and have paleoceanographic significance for inferring deep Arctic circulation changes that have occurred during Quaternary glacial/interglacial cycles. A number of recent studies have demonstrated that ostracodes are common in Quaternary sediments (Clark et al. 1990; Mostafawi, 1990; Pak et al., 1992; Cronin et al., 1993, 1995), but reliable paleoceanographic inferences can only be made with extensive ecological and zoogeographic data on common species. The primary goal is to illustrate the geographic and bathymetric distribution of these eleven species in the Arctic based on their proportions of the total assemblage in coretop and surface sediment samples from numerous cruises from the Arctic and adjacent Nordic Seas (Greenland, Iceland, and Norwegian Seas). In addition, species census data are presented for the first time for transects of surface samples collected during the 1993 cruise of the *Polarstern* to the Laptev and Barents Sea.

Material and Methods

The distribution maps for deep-sea Arctic ostracode species were constructed using the species census data from more than 400 modern coretop samples that have been compiled into a large Arctic ostracode database; the location of most of these samples is shown in Figure 1 (a few are off the map area). Latitude, longitude and depth data and species census data are available electronically from the U.S. National Geophysical Database Center (NGDC) or over anonymous ftp from geochange.er.usgs.gov. The ostracode data were derived from several sources. First, most shallow water faunal data came from the Modern Arctic Ostracode Database (MAOD, Cronin et al., 1991), which consisted of a compilation of data from several researchers (W.M. Briggs, Jr., E. Brouwers, R. Whatley, A. Wood, T.M. Cronin). Second, the *Polarstern* in

1991 ARKTIS VIII/3 cruise to the Amundsen, Nansen, and Makarov Basins, the Lomonosov and Gakkel Ridges, and the Morris Jesup Rise and Yermak Plateaus (Fütterer, 1992) provided some of the first quality material from the deep Eurasian Basin (Cronin et al., 1993). Supplementing the 1991 *Polarstern* material, additional samples have been included from *Meteor* cruises to the Nordic Seas (provided by R. Spielhagen, GEOMAR, and J. Wollenberg, AWI) and the 1992 *Polar Star* cruise to the Northwind Ridge in the Canada Basin (provided by R.Z. Poore, USGS); the ostracodes from the latter are reported in Cronin et al. (1995).

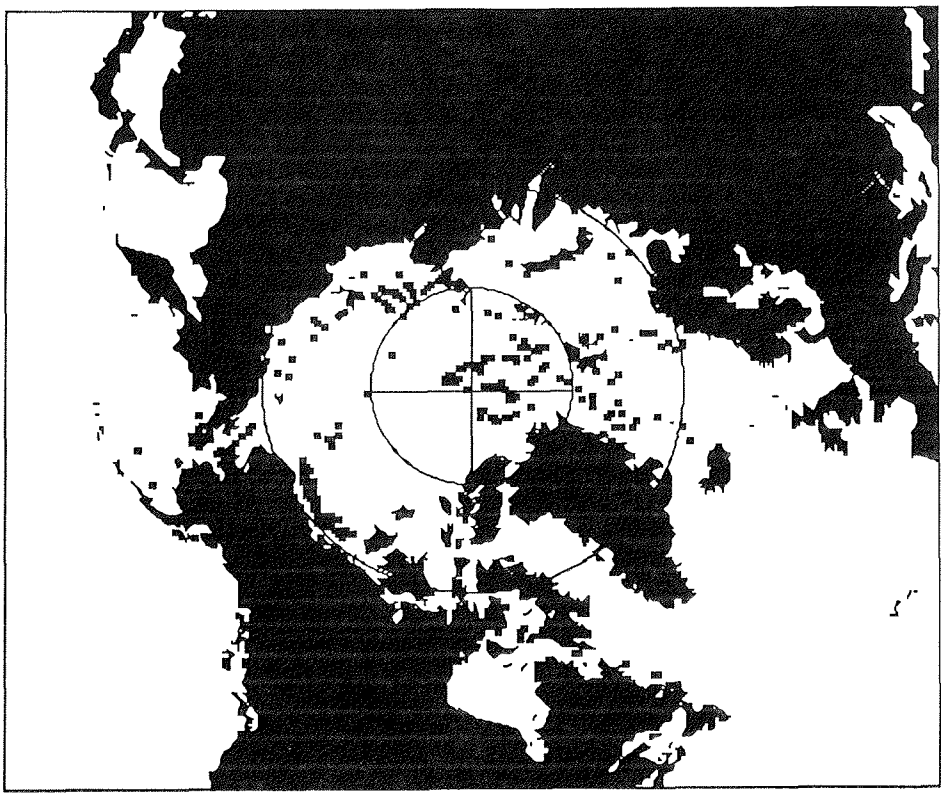

Fig. 1.: Map of Arctic region sites used in modern ostracode occurrence database.

Finally, the 1993 ARKTIS IX/4 *Polarstern* cruise to the Laptev and Barents Seas (Fütterer, 1994) provided new material from previously poorly known areas and is published here for the first time. The station data for 43 surface samples from ARKTIS IX/4 (provided by D. Nurnberg, R. Stein, D. Fütterer, AWI) and the species census counts for 57 species are given here in Table 1 (Appendix). Figure 2 shows the location of these sites. These samples were processed for ostracodes by washing through a 63 μm sieve, and specimens were picked from the size fraction >180 μm.

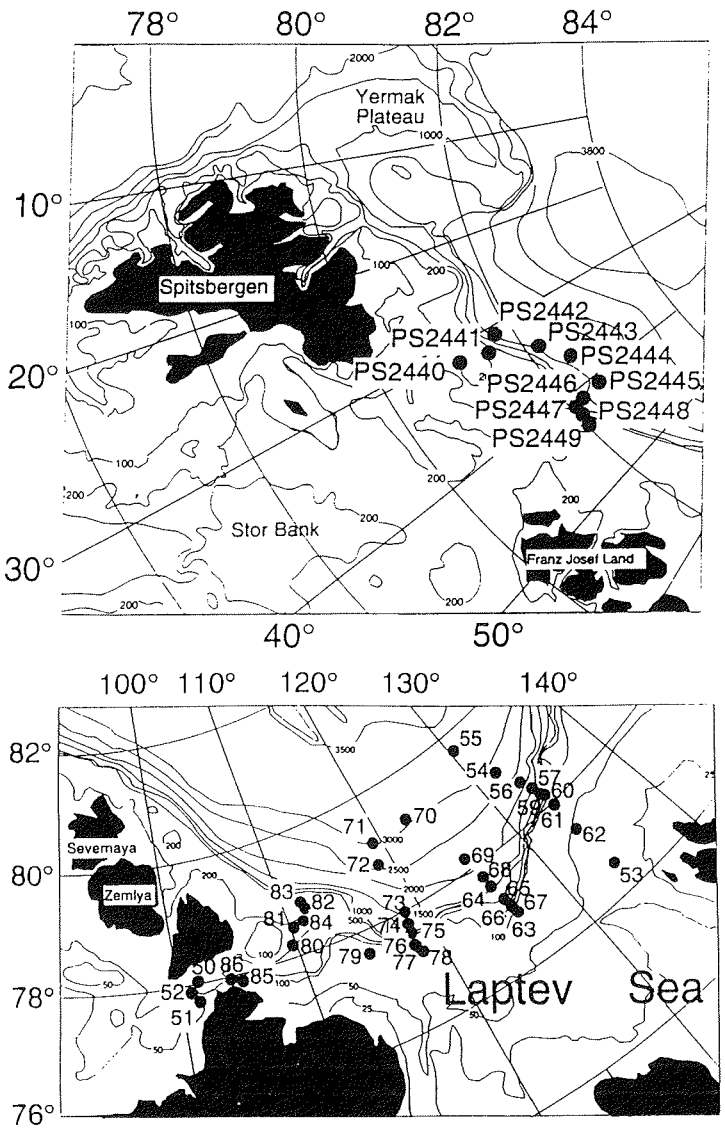

Fig. 2.: Map of Laptev and Barents Seas sample stations.

Many specimens had appendages and soft parts preserved (see bold numbers in Table 1, Appendix), indicating they contained near life assemblages, and thus provide an excellent transect from the shelf to the deep Arctic Basin (from 51 to 3429 m water depth). Figure 3 shows the depth distribution of the major species occurring in the transect across the Laptev Sea.

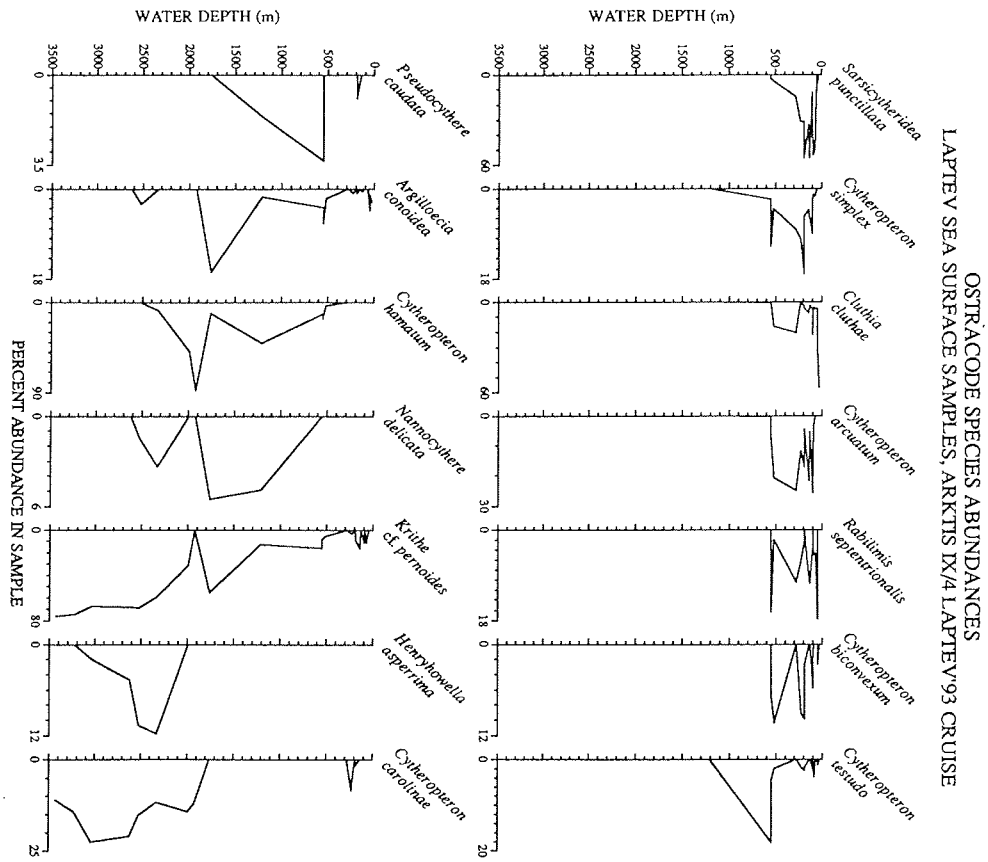

Fig.3.: Depth distribution of major ostracode species across transect in Laptev Sea.

Distribution of Deep-Sea Arctic Ostracode Species

Figures 4-14 show the distribution of 11 common ostracode species found in surface samples. These species were chosen for highlighting also because they occur commonly in Quaternary sediments in the Arctic and show significant changes in their downcore proportions, which indicate paleoceanographic changes in bottom water environments (Cronin et al., 1995). In this section, brief descriptions of each the taxonomic affinities, zoogeography, and ecology of each species is given.

Acetabulastoma arcticum Schornikov, 1970 (Fig. 4a). This species occurs primarily in low percentages (1-10%) at mid-depths on the ridges and plateaus of the Arctic, but not in the deepest basins below 3000 m water depth, nor on Arctic continental shelves. *A. arcticum* lives as a parasite on amphipods that live at the sea-ice/water interface (*Paradoxostoma rostratum* Sars of Baker and Wong, 1968), and thus this species has potential as an indicator of sea-ice conditions. It is closely related to shallow water intertidal species of *Acetabulastoma* from the Arctic and surrounding areas (Schornikov, 1970; Whatley, 1982).

Argilloecia conoidea Sars, 1923 (Fig. 4b). Most occurrences of *Argilloecia* in the Arctic probably represent *A. conoidea* Sars, 1923, although it is possible additional studies will show more than one species inhabit the Arctic. Little previous information exists on its distribution in the Arctic, but the data presented here show it is common (>0-10%) throughout the Eurasian and Canada Basins at mid-depths about 500-2500 m water depth.

Cytheropteron alatum Sars, 1865 (Fig. 5a). This species predominates in the deepest parts of the Eurasian and Greenland Sea basins and is more limited in distribution and abundance in the Canada Basin. The Lomonosov Ridge appears to act as a partial barrier to its distribution into the Makarov Basin but the opposite situation exists in the Fram Strait area where *C.alatum* inhabits the Eurasian Basin and Greenland Sea (see also Whatley and Eynon, 1995). *C. alatum* commonly occurs with *Cytheropteron bronwynae* and *Cytheropteron carolinae* in the Nansen and Amundsen Basins.

Cytheropteron bronwynae Joy and Clark, 1977 (Fig. 5b). This species appears to be the only podocopid ostracode species endemic to the Arctic Ocean proper and is a dominant component of assemblages from the deepest Canada and Eurasian Basins. Whatley and Jones (in prep.) provide stereo-atlas scanning electron photomicrographs of *C. bronwynae*.

Cytheropteron carolinae Whatley and Coles, 1987 (Fig. 6a). This species originally was described from Leg 94 Deep-Sea Drilling Project (DSDP) cores from the deep North Atlantic, and it is also a major component of deep-water assemblages of the Arctic Ocean. There are two slightly different morphotypes of *C. carolinae*; and future work may indicate these are different species.

Cytheropteron hamatum Sars, 1869 (Fig. 6b). *C. hamatum* characterizes mid-depths (1000-2500 m water depth) mainly in the Canada Basin, in the western Fram Strait area and the Laptev Sea. Its distribution appears to be correlated generally with boundary currents along Arctic margins and specifically with Canada Basin deep water that flows out of the Arctic Ocean near the southwestern Lomonosov Ridge, the Morris Jesup Rise along northern Greenland and into the Greenland Sea. It is not yet clear what hydrologic, nutrient, or resource (food) factors limit it to these environments.

Henryhowella asperimma (Ruess, 1850) (Fig. 7a). This is a member of a species-complex that occurs commonly throughout the world's oceans in deep and mid-depth environments (see discussion by Dingle et al., 1990). It occurs in greatest proportions in highly oxygenated (about 6ml/l) water below the oxygen minimum layer off SW Africa (Dingle et al., 1990) and in the Nordic Seas in areas of deep-water production (Fig. 7a).

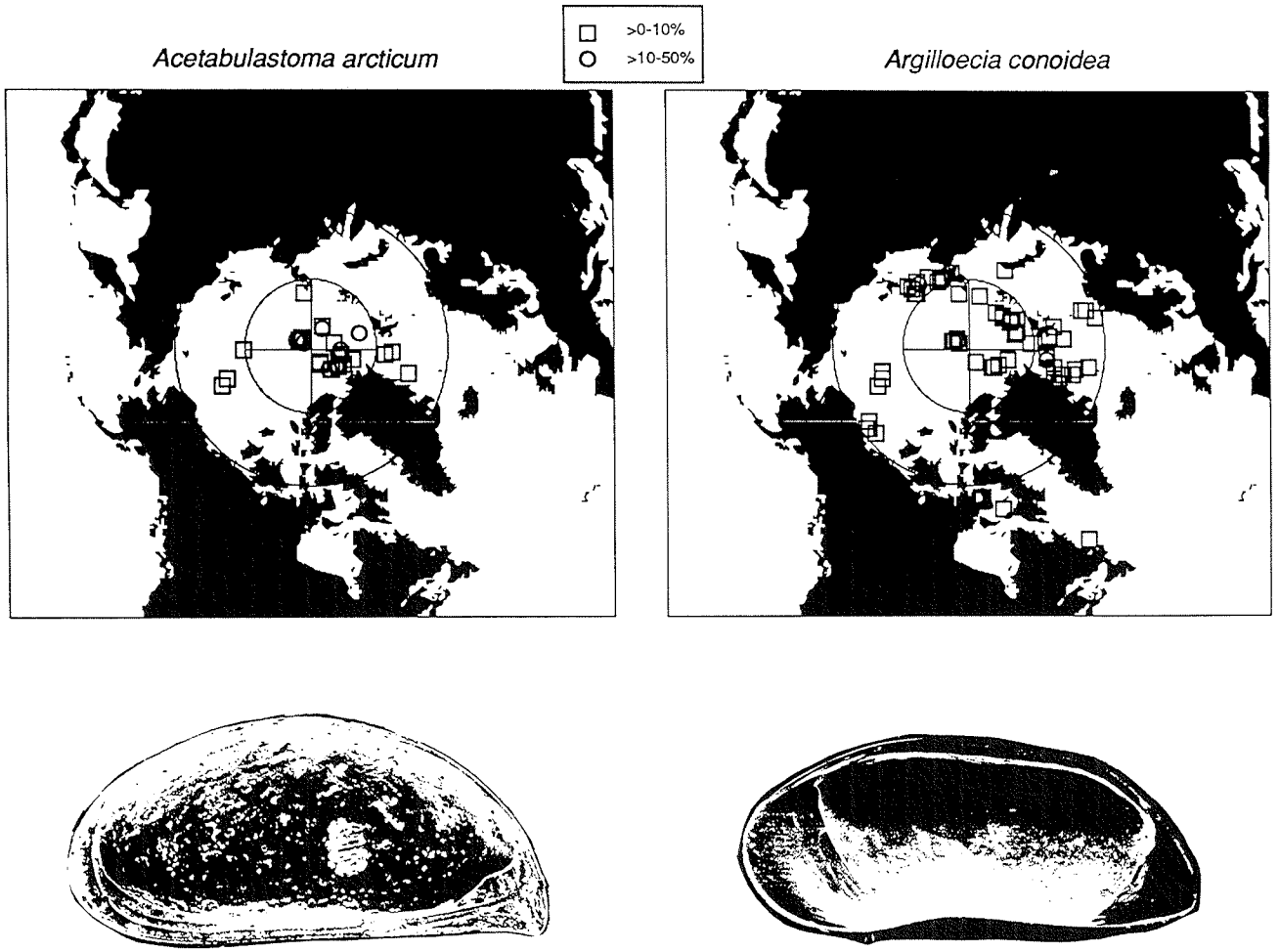

Fig. 4a.: Map of percent occurrence of *Acetabulastoma arcticum* in modern Arctic ostracode samples (above) and scanning electron micrograph (SEM) of *A. arcticum* (below). 4b.: Map of percent occurrence of *Argilloecia conoidea* in modern Arctic ostracode samples (above) and SEM of *A.conoidea* (below).

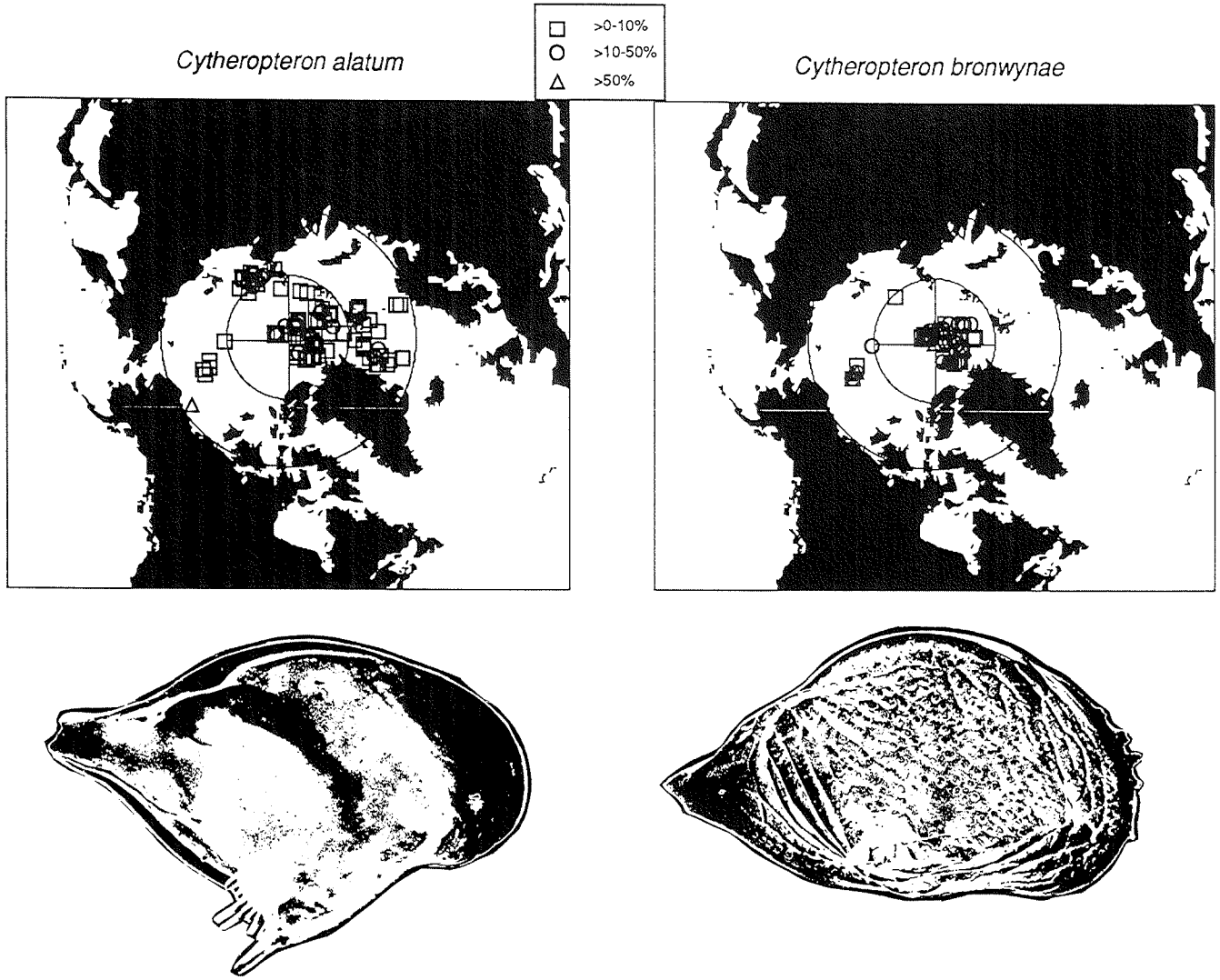

Fig. 5a.: Map of percent occurrence of *Cytheropteron alatum* in modern Arctic ostracode samples (above) and SEM of *C. alatum* (below). 5b.: Map of percent occurrence of *Cytheropteron bronwynae* in modern Arctic ostracode samples (above) and SEM of *C. bronwynae* (below).

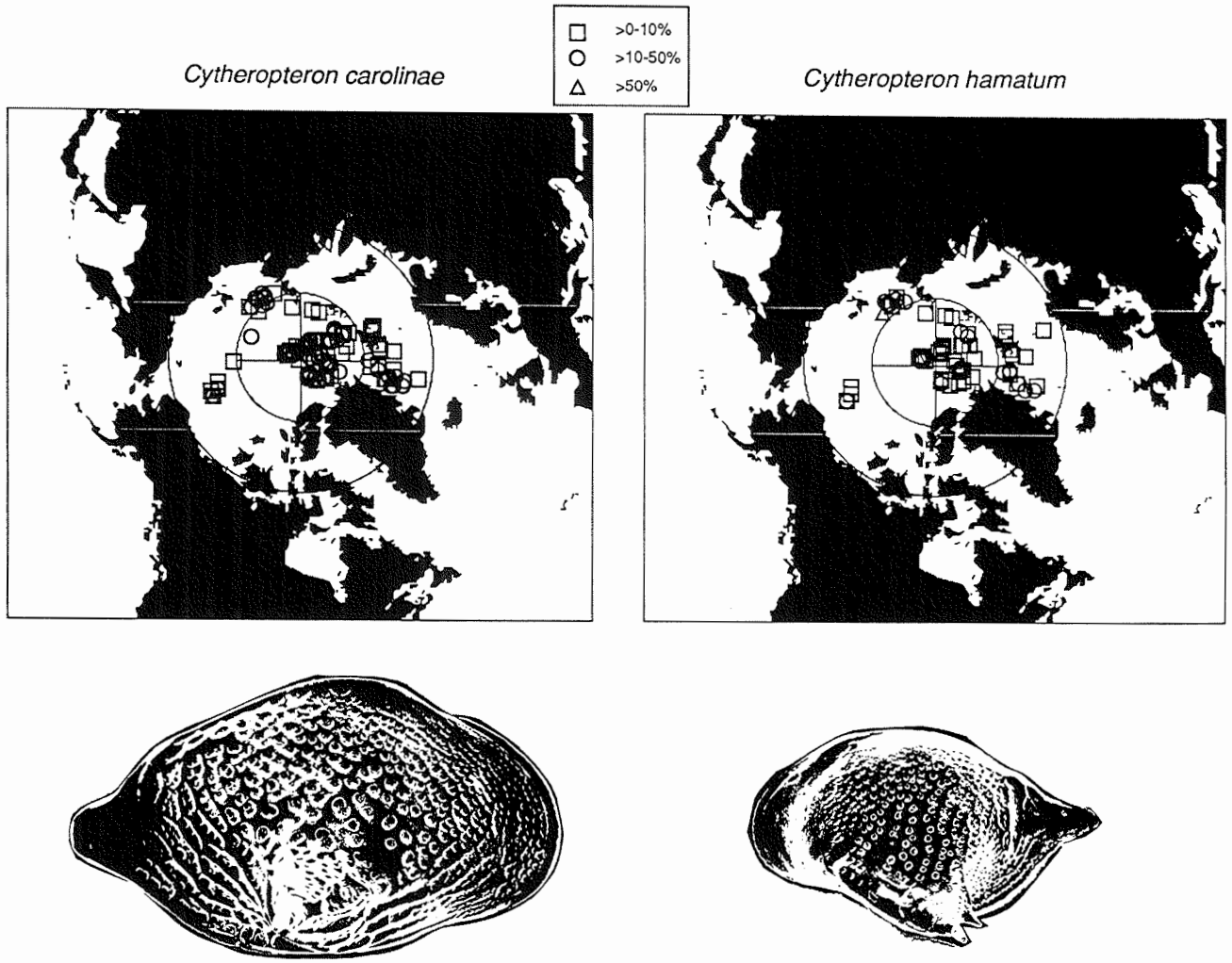

Fig. 6a.: Map of percent occurrence of *Cytheropteron carolinae* in modern Arctic ostracode samples (above) and SEM of *C. carolinae* (below). 6b.: Map of percent occurrence of *Cytheropteron hamatum* in modern Arctic ostracode samples (above) and SEM of *C. hamatum* (below).

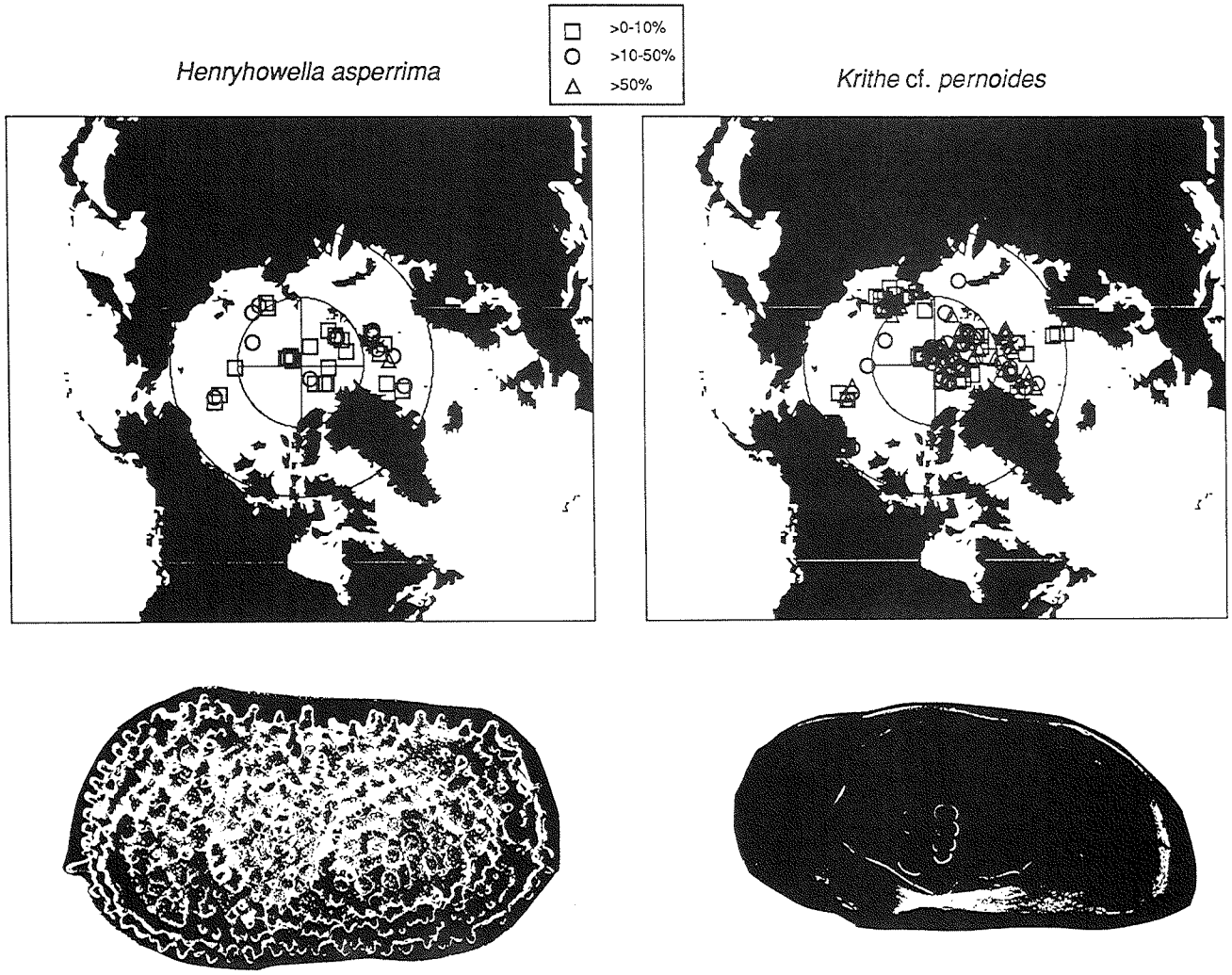

Fig.7a.: Map of percent occurrence of *Henryhowella asperrima* in modern Arctic ostracode samples (above) and SEM of *H. asperrima* (below). 7b.: Map of percent occurrence of *Krithe* cf. *pernoides* in modern Arctic ostracode samples.

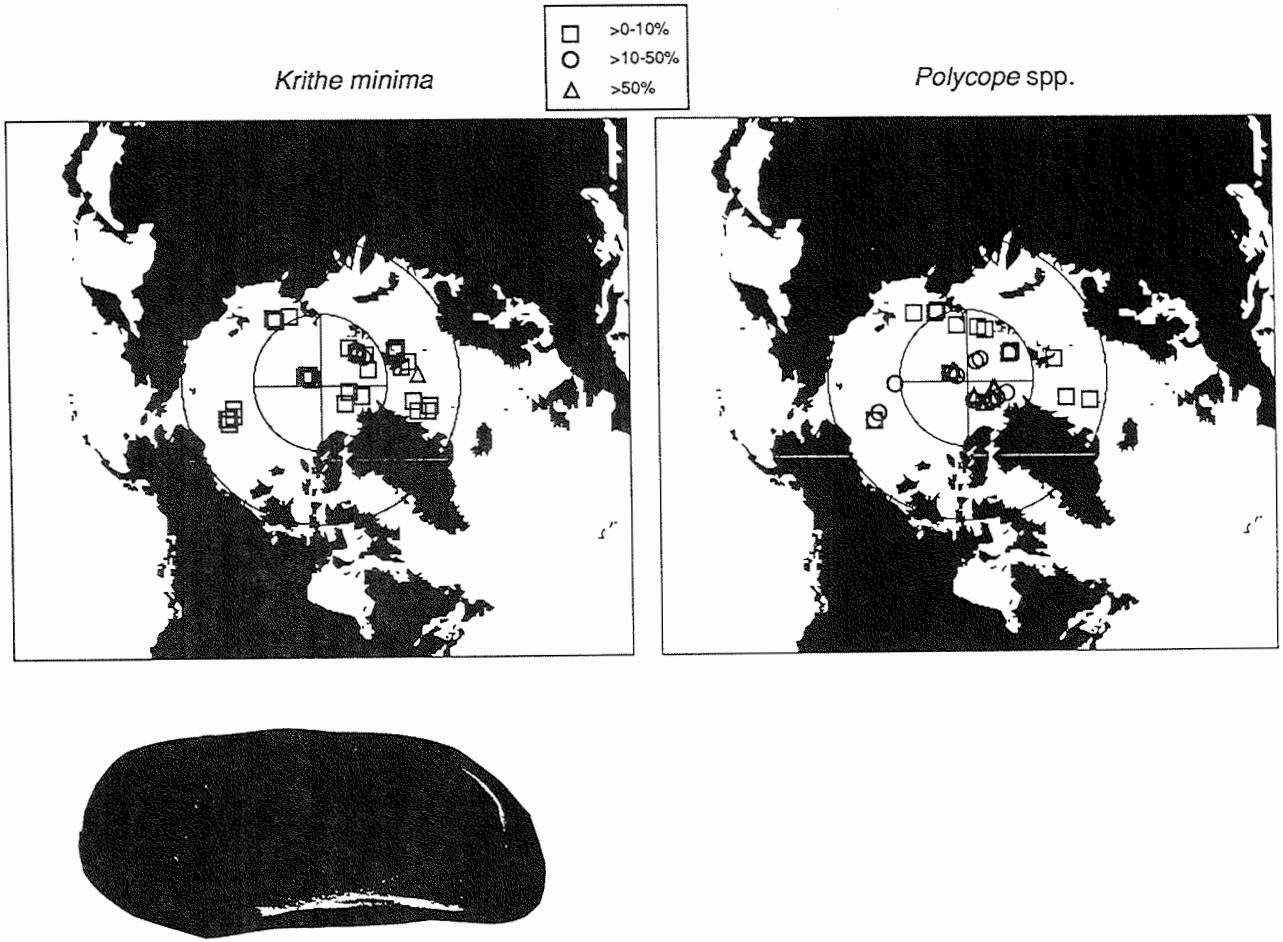

Fig. 8a.: Map of percent occurrence of *Krithe minima* in modern Arctic ostracode samples. 8b.: Map of percent occurrence of *Polycope* spp. in modern Arctic ostracode samples.

Krithe cf. *pernoides* (Bornemann, 1855) (Fig. 7b). This species is the most abundant podocopid to inhabit the Arctic and Nordic Seas, often comprising >50 % of assemblages from deep Eurasian and Nordic Sea basins. It has been recorded as *K. glacialis* (Brady, Crosskey and Robertson, 1874) and *K. "bartonensis"* Jones by various authors, but it has vestibule size and shape and radial pore distribution that are intermediate between *K. pernoides* and *K. morkhoveni* groups as described in a recent detailed revision of Atlantic Ocean *Krithe* by Coles et al. (1993). In the Arctic it is easily distinguished from *K. minima* by its much larger size and its large, mushroom-shaped anterior vestibule. This deep arctic species is clearly distinct in vestibule size and shape from *K. praetexta* of Sars, 1923 which occurs in shallow waters of Scandinavia in water temperatures up to 10-12°C (Penney, 1993).

Krithe minima Coles et al. 1993 (Fig. 8a). This species is more common in Nordic Sea deep water assemblages than within the Arctic proper, where is occurs rarely in low percentages on ridges and plateaus. *K. minima* is also common in the North Atlantic and it has potential for documenting deep-water and mid-depth exchange through the Nordic Seas and the Fram Strait.

Polycope spp. (Fig. 8b). Joy and Clark (1977) recorded 8 species of *Polycope* in the Canada Basin sediments, and Cronin et al. (1993, 1995) found this genus comprised up to 70-80% of deglacial ostracode assemblages obtained from cores from the Lomonosov Ridge. The abundance of *Polycope* is tentatively interpreted as indicating high organic matter typical of fine grained Arctic sediments and its abundance may be related to seasonally ice-free, high productivity, surface water conditions leading to high inputs of phytodetritus in benthic environments.

Pseudocythere caudata Sars, 1865 (Fig. 9). This eurythermal species is especially common along the margins of the Arctic and Nordic Sea at mid-depths and seems to be most characteristic of relatively warm, inflowing Atlantic water, which can be +2-3°C. The affinities between Arctic and Mediterranean *Pseudocythere* were noted by Elofson (1941). Cronin et al. (1993) suggested that several Arctic bathyal species have affinities with Mediterranean taxa indicating a possible migration along mid-depth environments of Nordic Seas in relatively warm water of Atlantic/Mediterranean origin. This hypotheses must be examined further through comparative study of living species from the Norwegian Sea, the Arctic and the Mediterranean.

Summary

In summary, ostracodes are an important metazoan microfaunal group in surface sediments throughout the Arctic Ocean and adjacent seas. The bathymetric and geographic distributions of the most common Arctic and Nordic Sea ostracode species indicate there are a variety of factors that control the occurrence and relative abundance of species. These factors include physical barriers like the Lomonosov Ridge, the presence of sea-ice and surface water productivity, bottom water temperature and dissolved oxygen, and availability of food and nutrient resources and other as yet unknown biotic factors such as competition and predation. Generally, however, the modern stratified Arctic Ocean appears to have produced a clear

water-depth-related zonation of ostracode species from the shelf to the deep basins that reflects a first order control of species depth distributions by physico-chemical and/or resource-related characteristics of Arctic water masses. Additional coretop and downcore studies are needed to test the hypothesized paleoceanographic significance of each ostracode indicator species described here.

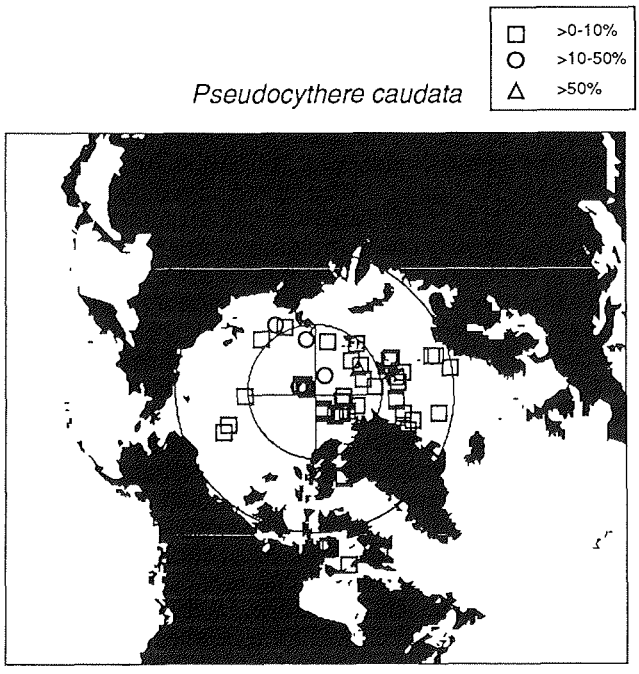

Fig. 9: Map of percent occurrence of *Pseudocythere caudata* in modern Arctic ostracode samples.

Acknowledgments

I am especially grateful to Drs. R. Stein, G. Ivanov, and M. Levitan for inviting this paper and to Prof. D. Fütterer and Dr. D. Nürnberg for obtaining *Polarstern* samples from the Laptev and Barents Seas. This work was improved through many conversations with Dr. W.M. Briggs, Jr. This study was funded by the U.S. Geological Survey Global Change and Climate History Program. Drs. D.A. Willard and T. R. Holtz, Jr. kindly read early drafts and improved the paper substantially.

References

Baker, J.H., and J.W. Wong. (1968): *Paradoxastoma rostratum* Sars (Ostracoda, Podocopida) as a commensal on the Arctic gammarid amphipods *Gammaracanthus loricatus* (Sabine) and *Gammarus wilkitzkii* Birula, Crustaceana 14: 307-311.

Clark, D.L., L.A. Chern, J.A. Hogler, C.M. Mennicke, *E.D. Atkins* (1990): Late Neogene climate evolution of the central Arctic Ocean. Marine Geology 93: 69-94.

Coles, G., R.C. Whatley, and A. Moguilevsky. (1994): The ostracod genus *Krithe* from the Tertiary and Quaternary of the North Atlantic. Paleontology 37(1): 71-120.

Cronin, T.M., W.M. Briggs, Jr., E.M. Brouwers, R.C. Whatley, A. Wood, M.A.Cotton. (1991): Modern Arctic Podocopid Ostracode Database. US Geological Survey Open-file Report OF: 91-385.

Cronin, T.M., T.R. Holtz, Jr., and R.C. Whatley (1994): Quaternary paleoceanography of the deep Arctic Ocean based on quantitative analysis of Ostracoda, Marine Geology, 119: 305-332.

Cronin, T.M., T.R. Holtz, Jr., R. Stein, R. Spielhagen, D. Fütterer, J. Wollenberg (1995): Late Quaternary paleoceanography of the Eurasian Basin, Arctic Ocean. Paleoceanography, 10: 259-281.

Dingle, R.C., A.R.Lord, and I.D. Boomer (1990): Deep-water Quaternary Ostracoda from the continental margin off south-western Africa (SE Atlantic Ocean), Annals of the South African Museum, 99(9): 245-366.

Elofson, O. (1941): Zur Kenntnis der marinen Ostracoden Schwedens, mit besonderer Berücksichtigung des Skagerraks. Uppsala Univ. Zool. Bidrag. 19: 215-534.

Fütterer, D. *(ed.)* (1992): Arctic'91: The expedition ARK-VIII/3 of RV "Polarstern" in 1991, Berichte zur Polarforschung, 107: 1-267, .

Fütterer, D. (ed.) (1994): The expedition ARCTIC '93 Leg IX/4 of RV "Polarstern" 1993. Berichte zur Polarforschung, 149: 1-244.

Joy, J.A., and D.L. Clark. (1977): The distribution, ecology, and systematics of the benthic Ostracoda of the central Arctic Ocean, Micropalaeontology, 23(2): 129-154.

Mostafawi, N. (1990): Ostracods in late Pleistocene and Holocene sediments from the Fram Strait, eastern Arctic. In, R.Whatley and C. Maybuty, (Eds.), Ostracoda and Global Events. Chapman and Hall, London, pp. 489-494.

Pak, D.K., Clark, D.L., and Blasco, S.M. (1992): Late Pleistocene stratigraphy and micropaleontology of a part of the Eurasian Basin (=Fram Basin), central Arctic Ocean. Marine Micropaleontology, 20: 1-22.

Penney, D.N. (1993): Northern North Sea benthic Ostracoda: modern distribution and palaeoenvironmental significance. The Holocene 3(3): 241-254.

Schornikov, E.I., (1970):*Acetabulastoma*, a new genus of ostracodes. Zool. Zhurn., 49: 1132-1143.

Whatley, R.C. (1982): Littoral and sublittoral Ostracoda from Sisimiut, West Greenland, in Report of the 1979 Greenland White-fronted Goose Study Expedition to Eqalungmint Nunal, West Greenland, edited by A.D.Fox and D.A. Stroud (Eds.), pp. 269-284, Univ. Wales Press.

Whatley, R.C. and G. Coles. (1987): The late Miocene to Quaternary Ostracoda of Leg 94, Deep Sea Drilling Project, Revista Espanola de Micropaleontologicia, 19 (1): 33-97.

Whatley, R.C. and M. Eynon. (1995): Ostracoda from the Greenland Sea, Micropalaeontology, (in press).

Appendix

Table 1.: Ostracode occurrences from ARCTIC `93 ARK-IX/4, "Polarstern"

Station	Depth	Lat (°)	Lat (')	Long (°)	Long (')	Acanthocythereis dunelmensis	Argilloecia conoidea	Baffinicythere howei	Bythoceratina scaberrima	Bythocythere sp.	Cluthia cluthae	Cytheropteron alatatum	Cytheropteron angulatum	Cytheropteron arcuatum	Cytheropteron bronwynae	Cytheropteron carolinae	Cytheropteron cronini	Cytheropteron hamatum	Cytheropteron inflatum	Cytheropteron spp.	Cytherop. pseudomontorosiense	Cytheropteron testudo	Cytheropteron biconvexa	Cytheropteron champlainum	Cytheropteron elaeni	Cytheropteron n. sp. B	Cytheropteron nodosoalatum	Cytherop. paralatissimum
2439-2	459	73	38.8	22	55.4						1																	
2442-3	2876	81	42.3	30	19.8														33									
2442-4	2915	81	43	30	20.9																							
2443-2	2462	82	12.2	34	37.9																							
2444-1	2566	82	29.2	37	44.4											3												
2445-3	2995	82	45.8	40	14.6							8																
2446-3	2025	82	24	40	53.6		1					10				11		14										
2447-4	1024	82	9.6	42	2.7		14		1			13				17	4	6			1							
2448-3	534	82	7.4	42	32.3																							
2450-2	148	78	1.8	102	18.3						1			1							1							
2451-2	143	77	42.4	102	17.3						5			15							1							
2452-2	132	77	53.5	101	35.5		1				4	2	1	8			2		4		14					2		
2453-2	38	76	30.5	133	21.3	5	1			2	21						1								6			
2455-3	3429	79	39.1	130	32.1							2			4	6												
2456-2	2520	78	29	133	0.1		2									10												
2458-3	981	78	10	133	23.7													1										
2459-2	517	78	5.9	133	30.8						1					1						5						
2460-3	191	78	4.3	133	36.5		1				5	10		5		2				3		2	3					
2461-2	73	77	54.6	133	33.3	3					8																2	5
2462-3	54	77	24.3	133	33.4	4	2				2									1								
2463-3	92	77	1.8	126	24.8			1		2	9			8			3		11			9			10			
2464-2	1760	77	28.8	125	54.2		3					1						2										
2465-3	1026	77	11	126	13.4						2																	
2466-3	552	77	8.1	126	21.2		3					4		3				7	1	1		2	3					
2467-3	284	77	5	126	13.4						10			12										3	1			1
2468-3	1991	77	41.6	125	53.6											5		17		1								
2469-3	2332	78	3.6	125	0							1				7		5										
2470-4	3233	79	13	122	54.4							14				19												
2471-3	3048	79	9.3	119	46.9							11				45												
2472-3	2620	78	40	118	44.3							4				18												
2473-3	1927	77	58.9	118	34.3											3		22										
2474-2	1497	77	40.2	118	34.5							2				1		1										
2475-1	1108	77	32	118	27.5													1				4						
2476-3	524	77	23.5	118	11.5		1				8	6		10				2	1	5		1	5					
2477-3	193	77	14.8	118	33.2						4			21					1	1		3	12					4
2478-3	101	77	10.3	118	42.6					1	7	1		30					1			3	7	1	1			3
2480-2	51	78	15.7	109	14.7	5	1	1		1	21											1	2	5	4			1
2481-2	100	78	28.3	110	47.5						19			22									2					1
2482-2	557	78	42	112	30.9		7		3		2	23		1				22		10		33						
2483-2	1216	78	45.7	112	42.2		1					16						25		2								
2484-2	235	78	34.9	111	23.2		1					12		13		9						2	10					1
2485-1	229	77	54	105	5																							2
IRO=Ice-rafted ostracodes (continental shelf taxa transported by ice)																												
Bold numbers = specimens with appendages preserved																												

Station	Cytheropteron paraarcticumc	Cytheropteron pseudoinflatum	Cytheropteron sedovi	Cytheropteron simplex	Cytheropteron sulense	Cytherura sp.	Elofsonella concinna	Eucytherura delineata	Eucythere sp.	Eucythere declivis	Henryhowella asperrima	Heterocyprideis fascis	Heterocyprideis sorbyana	Krithe cf. pernoides	Krithe minima	Loxoconcha venepidermoidea	Microcythere medistriatum	Nannocythere ? sp.	Palmenella limicola	Paracyprideis pseudopunctillata	Paradoxostoma	Propontocypris sp.	Polycope spp.	Paracytheroischuckchiensis	Pseudocythere caudata	Rabilimis septentrionalis	Robertsonites tuberculatus	Roundstonia globulifera	Sarsicytheridea bradii	Sarsicytheridea punctillata	Semicytherura complanata	Semicytherura spp.	Other	IRO	total
2439-2																																			1
2442-3		39						3									1					3	45	28	235								2		389
2442-4														4																					4
2443-2											3				3																				6
2444-1											2			3	3																				11
2445-3														12																				1	21
2446-3									1		2			15	1																			1	56
2447-4		2						5						49	33			5			1			3	4								1	3	162
2448-3																																			0
2450-2				2										1												4				2					12
2451-2				3						3				11					1							7				23					69
2452-2				9		2		1																		16				83					149
2453-2																															1				37
2455-3					1									41					2	9									6						71
2456-2											7			45				1																	65
2458-3																																			1
2459-2														3												7									17
2460-3				6										10											1					59					107
2461-2				3								25		20						10						8				85					169
2462-3							6					1		1												8			12		8				45
2463-3	5		10	3						2			9										6			12			3	125	2	2			232
2464-2									1					10				1																	18
2465-3														3																					5
2466-3				5					1					4										1		7				1					43
2467-3				4								3								1						5		1		7					48
2468-3														11	1																				35
2469-3											7			35	1	1		2																	59
2470-4														99																					132
2471-3									4		4			135																					199
2472-3									1		4			58																					85
2473-3																																			25
2474-2																																			4
2475-1																		2							2										9
2476-3				2				1						3												1				2					48
2477-3				21								4														3		10		38					122
2478-3			2	11								5		12						3						4		6		14	8	1			121
2480-2			2				5					2							2								6		10	6					75
2481-2				2						2		3		10														5		20					86
2482-2		2		4				7	5					30	9						4		4	8	6										180
2483-2										2				8				3					1	2	1										61
2484-2				11								3		4									1	1		7				34					109
2485-1																													4		10				16

IRO=Ice-rafted ostracodes (continental shelf taxa transported by ice)

Bold numbers = specimens with appendages preserved

BENTHIC FORAMINIFERA AND CARBONAT DISSOLUTION IN THE SURFACE SEDIMENTS OF THE BARENTS AND KARA SEAS

Hald M. and Steinsund P.I.

Department of Geology, IBG, University of Tromsø, N-9037 Tromsø, Norway

Introduction

Benthic foraminifera are sensitive environmental indicators and have been widely used to describe modern as well as ancient marine environments. On the continental shelf off Norway and in the Barents Sea several studies reconstruct late Quaternary environments using foraminifera as a paleoenvironmental and stratigraphical tool (see for example Feyling-Hanssen 1964, Vorren et al. 1978, Løfaldli and Rokoengen 1980, Nagy and Ofstad 1980, Østby and Nagy 1981, Hald and Vorren 1987, Nagy and Qvale 1985 and Hald et al. 1989, 1994, Knudsen and Sejrup 1993, Sejrup and Knudsen 1993). In order to improve these reconstructions it is of great importance to know the recent distribution patterns of species and the factors controlling these. The last few years there has been an increase in the information, especially from European Arctic margin with respect to: a) assemblage distribution patterns, b) correlation of these patterns to various physical, chemical and biological factors and c) foraminifera as indicator for carbonate dissolution (Hald and Steinsund, 1992; Hald et al., 1994; Steinsund and Hald, 1994; Steinsund et al., in press). The political changes in Europe has made possible active cooperation between Norwegian and Russian scientists, that has resulted in the establishment of a large data base of surface sediment benthic foraminifera in the Barents and Kara Seas.

Hydrography

Water masses in the Barents and Kara Seas are represented by Atlantic, Arctic, Polar, coastal, and locally formed waters (Treshnikov, 1985; Carmack, 1990; Loeng, 1991; Hopkins, 1991) (Fig. 1). Warm (>2°C) and high saline (35‰) Atlantic Water is brought by the Norwegian Current, originating from the Gulf Stream. When entering the Barents Sea from the south-west, it splits into the North Cape and West-Spitsbergen Currents. The main branch of the North Cape Current flows counterclockwise along the southern and eastern margin of the Barents Sea, while two other branches follow those of the Bear Island Trough. The West-Spitsbergen Current flows northward along the Barents Sea slope and enters the Arctic Ocean through the Fram Strait. The continuation of this current moves along the northern slope of the Arctic Eurasian shelf underneath the lighter Polar Water at depths below 200 m, and enters the Barents and Kara Seas from the north through the marginal troughs, Franz Victoria-, St. Anna-, and Voronin troughs. While flowing, Atlantic Water gradually mixes with other water masses and losing its heat supply. The mixture of transformed Atlantic and Polar waters forms the local Barents Sea Water (Hopkins,1991), typically with temperatures around 0°C and salinity 34.4-35‰. Only 30% of the waters brought by the North Cape Current reach the Kara Sea (Nikiforov and Shpajher, 1980).

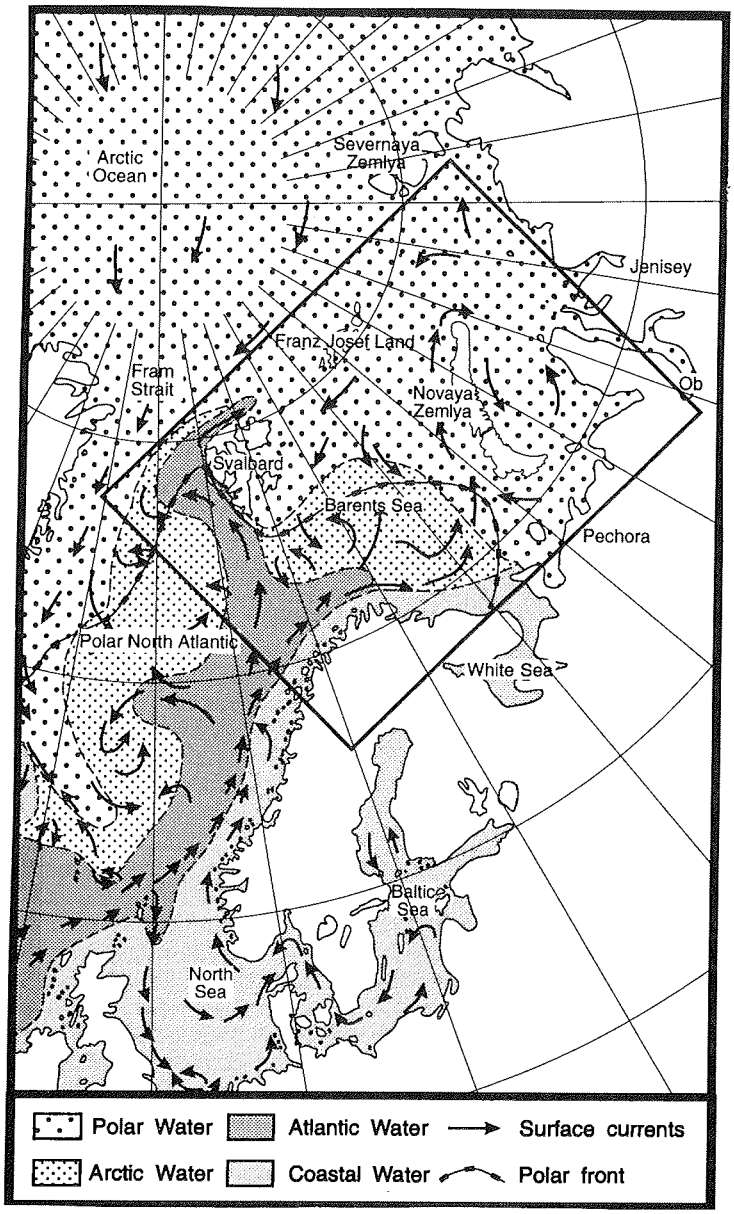

Fig. 1.: Map showing surface waters in the Norwegian Sea and adjoining areas (from Mosby, 1968; Hopkins, 1991). The study area is framed.

The Polar Water is being formed in the Arctic Ocean under the influence of low solar radiation balance, freshwater discharge of Siberian rivers, and perennial sea ice cover. This water is characterized by low temperature and salinity, typically of <0°C and <34.5‰, and occupies the topmost level in the multi layer hydrographical structure of the Arctic Ocean. In summer, owing to sea ice melting, its surface temperature might increase to 2-3°C, while salinity decreases to <32‰. The Polar Water is exported into the Barents Sea by southwestwards flowing surficial currents, while much of the Kara Sea itself is part of the site for the Polar Water formation.

The interaction between the Atlantic and Polar waters produces strong hydrological fronts. The most prominent is the Polar front, separating the Polar waters from those brought by the Norwegian Current.

Main features of coastal waters are shaped by river discharge. Relatively warm (>2°C) Norwegian Coastal Current flows along the Norwegian coast above denser Atlantic Water. It is fed by the input from the North and Baltic Seas as well as local run off, which maintain its low salinity of <34.7‰ (Sætre and Ljøen, 1971). Much more significant is the discharge of Pechora, Ob and Jenisej rivers, which contribute respectively 130, 530, and 603 km^3/yr of water (Treshnikov, 1985). Due to their influence in the Kara and southeastern Barents Seas salinities might be as low as 22-25‰, while temperatures fluctuate from <0°C in winter to 4-8°C in summer. Another impact of river discharge is high turbidity of coastal waters.

Dense bottom waters are formed during the fall and winter period from the mixture of transformed Atlantic and Polar waters. Their formation is initiated by the cooling of the uppermost water layer, and is completed by rejection of brines during the sea ice freezing (Midttun, 1985). The combination of salinity near 35‰ and temperature close to the freezing point provides extremely high density of these waters. They sink to the sea floor to fill the depressions in its topography, and contribute to the bottom waters of the Arctic Ocean and Norwegian-Greenland Sea. Their main gateways are Bear Island and Storfjord troughs in the west, and Franz Victoria, St. Anna and Voronin troughs in the north (Sarinina, 1972; Nikiforov and Shpajher, 1980; Quadfasel et al., 1988). While flowing along these troughs, winter bottom waters follow their northern/eastern flanks and partially mix with subsurface Atlantic waters.

The winter limit of sea ice is mainly controlled by the distribution of surficial Polar Water (Treshnikov, 1985; Vinje, 1977). West of 30°E sea ice reaches a maximum extent south to 74°N, while at 35°E it already has a maximum extent to 71°N (Madden and Loeng, 1987). In the eastern Barents Sea the winter sea ice boundary turns southwards to reach the Russian coast. In summer the sea ice limit typically retreats to the northernmost part of the Barents Sea and northeastern Kara Sea.

The data base

Steinsund et al. (in press) have compiled a data base consisting of 600 samples of surface sediment foraminiferal countings in the Barents and Kara Seas. For this purpose all available relevant sources were used: Basov and Slobodin (1965); Stoll (1968); Digas (1969, 1971); Slobodin and Tamanova

(1972); Østby and Nagy (1982); Stenløkk (1984); Polyak (1985); Khousid (1989); Hald and Steinsund (1992); and Steinsund et al. (in press). Sample locations are shown in Figure 2. Most of the samples were obtained by box-corers and grabs. Sixty four samples from Østby and Nagy (1982), Stenløkk (1984), and 40 Russian samples from the eastern Barents and Kara Seas are from core tops.

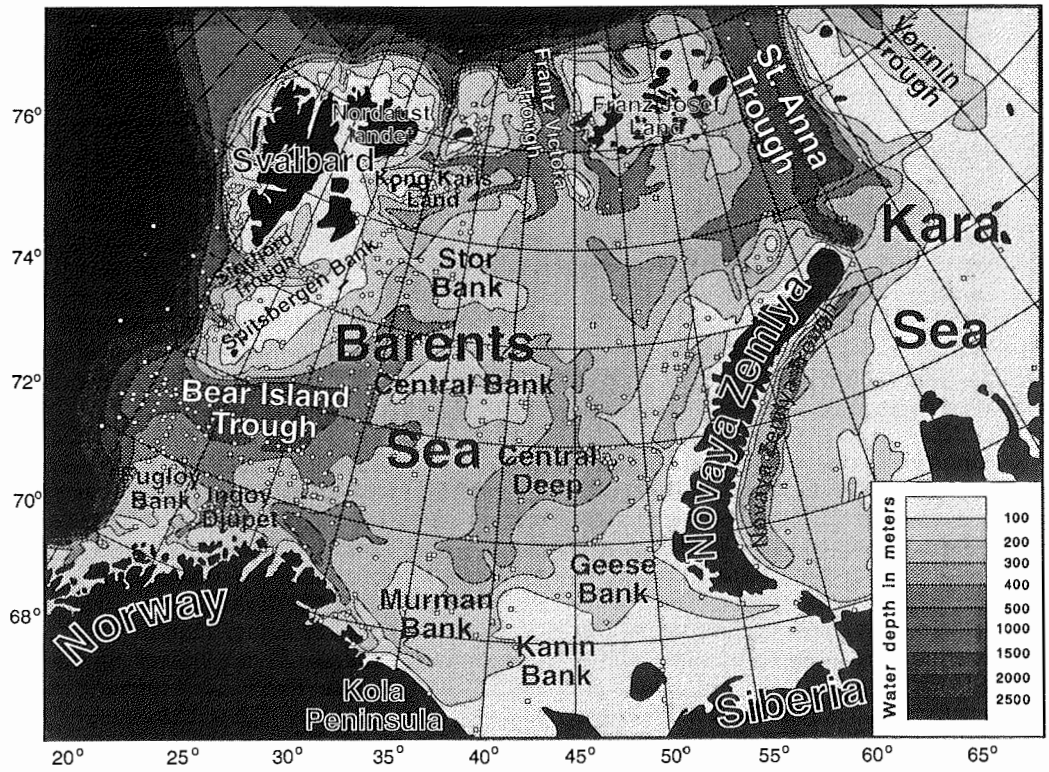

Fig. 2.: The bathymetry and location of the samples in the Barents and Kara Seas.

In order to distinguish modern from relict surficial sediments the following indices were used: presence of living foraminifera and other organisms, lithology, physical properties, and diagenetic conditions of sediment samples. However, tests redeposited from relict Pleistocene deposits may be present in some samples, especially in erosional areas such as the shallow banks. Judging from generally low modern sedimentation rates in the Barents and Kara Seas, surficial samples of 1-3 cm thick used in the study must represent an averaged record for the last several hundred years.

Surface sediments, holocene sedimentation and turbidity

A surface sediment distribution map of the Barents and Kara Seas (Fig. 3) has been compiled by GeoGruppen as. from several sources (Dahle et al. 1993, Elverhøi et al., 1989, Fredriksen et al. 1992, Hald and Steinsund 1992, Klenova 1960, Lien and Myhre 1977, Solheim and Elverhøi 1983, Vassmyr and Vorren 1990, Vinogradovna and Litvin 1960, Vorren et al. 1978, 1984, Wensaas 1986). A major part of the surface sediments are of clastic origin and to a large degree controlled by bottom water currents. In line with this is the concentration of the coarser sediments on the shallower banks, while the deeper banks and troughs show finer surface sediments. The biogenic component is mainly represented by benthic foraminifera (see discussion below). Major present sources of sediments are concentrated along the southern coast of the Kara and eastern Barents Seas. They include erosion of Quaternary coastal deposits and the discharge of Ob, Jenisej and Pechora rivers, and the White Sea. Most of the sediments are deposited in the proximity of the river estuaries and fjords.

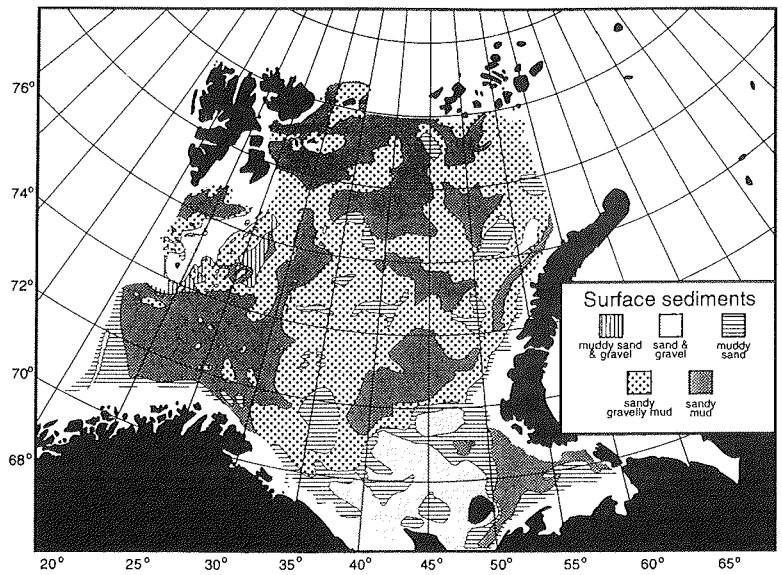

Fig. 3.: The surface sediment distribution in the Barents Sea. The map is compiled by Geogruppen a.s. from several sources (Dahle et al., 1993; Elverhøi et al., 1989; Forsberg, 1983; Fredriksen and others 1992; Hald and Steinsund, 1992; Klenova, 1960; Lien and Myhre, 1977; Solheim and Elverhøi, 1983; Vassmyr and Vorren, 1990; Vinogradovna and Litvin, 1960; Vorren et al., 1978; Vorren et al., 1984; Wensaas, 1986).

During the last decade, several stratigraphical studies of close to 100 gravity cores from the southwestern Barents Şea have been undertaken (Vorren et al., 1978; Hald et al., 1989; Thomsen, 1989; Vassmyr and Vorren, 1990; Dokken, 1991, Hald and Steinsund 1992). Based on these, Hald and Steinsund (1992) mapped the Holocene sediment thickness of the

southwestern Barents Sea (Fig. 4). The Holocene/Pleistocene boundary is defined based on various methods: foraminiferal stratigraphy, radiocarbon, lithostratigraphy, oxygen isotopes or macrofossils. A large part of the banks are characterized by a relatively thin Holocene sediment cover resting on sediments of glacigenic origin (Vorren et al., 1978; Vassmyr and Vorren, 1990). Contamination of older (glaciomarine) faunas into the modern fauna may occur due to bioturbation or during sampling.

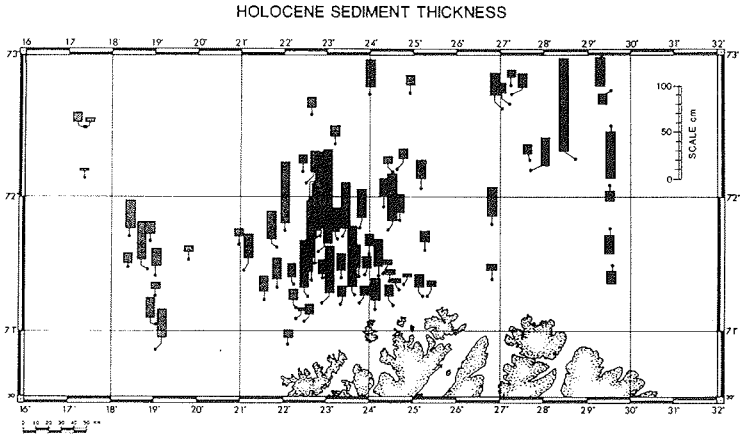

Fig. 4.: Holocene sediment thickness in the SW Barents Sea.

Generally, the coarsest surface sediments correspond to the lowest Holocene sediment thicknesses. Vorren et al. (1978) and Hald and Vorren (1984) concluded that similar coarse sediments on the banks and towards the continental shelf edge off northern Norway were *palimpsests* (cf. Swift et al., 1971) which have characteristics derived from an earlier glacigenic environment as well as from the modern environment. Thus, the sands on the banks, the flanks of Ingøydjupet and towards the coast is interpreted by Hald and Steinsund (1992) as material winnowed from the underlying glacigenic deposits. This winnowing probably is caused by strong bottom currents. For example, in the Tromsøyflaket area, bottom currents up to 48 m/s have been measured (Tryggestad, 1981). Ingøydjupet and local depressions on the banks probably represent local depocenters in which part of the winnowed sediments from the banks are deposited as soft, sandy mud.

Measurements of turbidity at the bottom in the Barents Sea show large variations (Gurevich et al.,1993) (Fig. 5). The highest values are found in the Pechora Sea and around Franz Josef Land. Generally there is higher turbidity in areas were rivers and glaciers terminate into the sea. High turbidity also correlate well to the areas with the highest sedimentation rate trough the Holocene. The lowest turbidity is found along the western flank of St. Anna Trough. Lower turbidity is also found along the continental margin and in the

troughs. An exception of this is the area along the Norwegian cost, which has a low turbidity, probably since the sediments are trapped in the fjords.

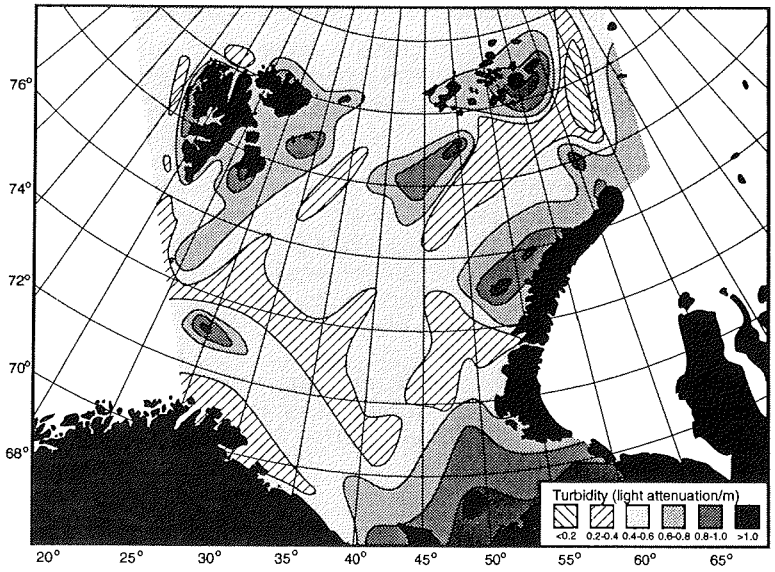

Fig. 5.: Measurements of turbidity at the bottom in the Barents Sea (from Gurevich et al.,1993).

Calcareous benthic foraminifera

Most arenaceous foraminifera disintegrate easily after their death, thus leaving a highly variable amounts of their tests in the sediment samples depending on the geochemical environment, sedimentation rates, and sample processing techniques. Typically, downcore sediments from the Arctic shelf are devoid of arenaceous foraminifera because of their disintegration during early diagenetic processes. To make the model of modern foraminiferal distribution more comparable with the fossil record, Steinsund et al. (in press) excluded all arenaceous foraminifera from the countings and based the study solely on calcareous species. Their amount is not always sufficient for quantitative analysis of species distribution due to calcium carbonate dissolution. To avoid biased models, samples containing less than 25 benthic calcareous specimens were excluded. Usually this number is too low, but in this case it is probably sufficient, since there usually are several samples from the same area.

As the data base comprises foraminiferal countings from many scientists, some taxonomic discrepancies were faced and it was necessary to combine certain closely related species. In particular, the following widely defined species or groups of species were combined:

Buccella spp. includes: *B. frigida, B. tenerrima, B. hannai arctica;*
Cibicides lobatulus includes: *C. lobatulus, C. pseudoungerianus, C. refulgens, C. rotundatus*;
Elphidium subarcticum includes: *E. subarcticum, E. frigidum, E. magellanicum;*
Islandiella norcrossi includes: *I. norcrossi, I. helenae;*
Nonion labradoricum includes: *Nonion labradoricum, Nonionella auricula;*
Stainforthia loeblichi includes: *S. loeblichi, S. schreibersiana.*

Before performing these modifications the data base consisted of 237 calcareous benthic foraminifera species. Based on mean values, the 20 most common shelf species were selected along with *Elphidium incertum* and *Haynesina orbiculare* because of the significance of the two latter species with respect to brackish environment, for further analysis. For a description and interpretation of all 20 species distribution see Steinsund et al. (in press). Together these species compose 90% of specimens in the analyzed samples.

To discriminate the samples and species between different assemblages the Q-mode factor analysis program Cabfac was used. This program was originally written by Klovan and Imbrie (1971), and rewritten for Microsoft Windows by P. I. Steinsund.

General features

The abundance of calcareous benthic foraminifera has maximum values (reaching over 6,000 specimens per gram sediment) on the banks in the southwestern Barents Sea, where there is a high primary production coupled with a good preservation of $CaCO_3$ in the sediment (Hald and Steinsund 1992, Steinsund et al., in press). Lower, but still significantly high abundances over 10 sp./g, are typical for areas influenced by riverine input, which also promotes marine biological production. Calcium carbonate dissolution is probably responsible for the extremely low foraminiferal abundance in the St. Anna Trough. The low abundance of foraminifera east of Svalbard is probably a result of a glacial influence (high turbidity), depressing organic productivity rather than calcium carbonate dissolution as there is a high calcareous to arenaceous foraminiferal ratio in the area (Fig. 6).

The concentration of calcareous foraminiferal tests (Fig. 7) follows the expected trends of calcium carbonate preservation on the sea-floor (Korsun, 1991; Steinsund and Hald, 1994). The dominance of calcareous forms (over 50% of total benthic assemblage) is typical for the western Barents Sea covered by warm Atlantic Water, and for shallow areas subjected to high hydrodynamic activity. Lowest calcareous ratio <25% is mostly observed in areas occupied by cold water (winter bottom water).

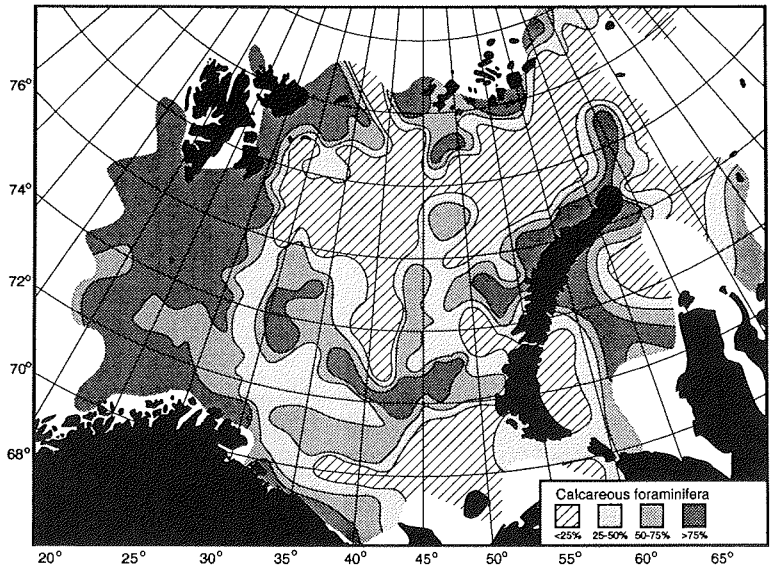

Fig. 6.: The ratio calcareous/arenaceous benthic foraminifera in the Barents and Kara Seas.

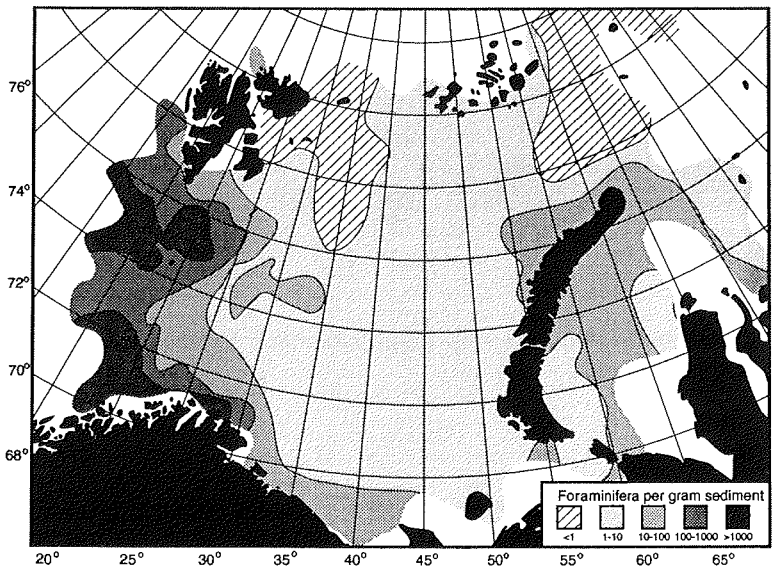

Fig. 7.: Number of calcareous benthic foraminifera per gram bulk, dry sediment.

Planktic foraminifera (Fig. 8) are mainly found in the areas influenced by the Atlantic waters, which penetrate the shelf from the southwest and through marginal troughs from the north (Steinsund et al., in press). This dependence of planktic foraminifera on the Atlantic Water distribution is recorded all over the Arctic shelf and in the Arctic Ocean water column (Tamanova, 1973; Lagoe, 1979; Thiede, 1988). It probably reflects the transportation of nutrients by the subsurface Atlantic Water into the Arctic Ocean. In addition there is a striking correlation between water depth and the ratio of planktic to benthic foraminifera. This is of course also related to Atlantic Water, but such a rapid decrease of planktic foraminifera eastward in the Barents Sea only due to Atlantic Water is not expected. However, carbonate dissolution could explain this rapid decrease of planktic foraminifera.

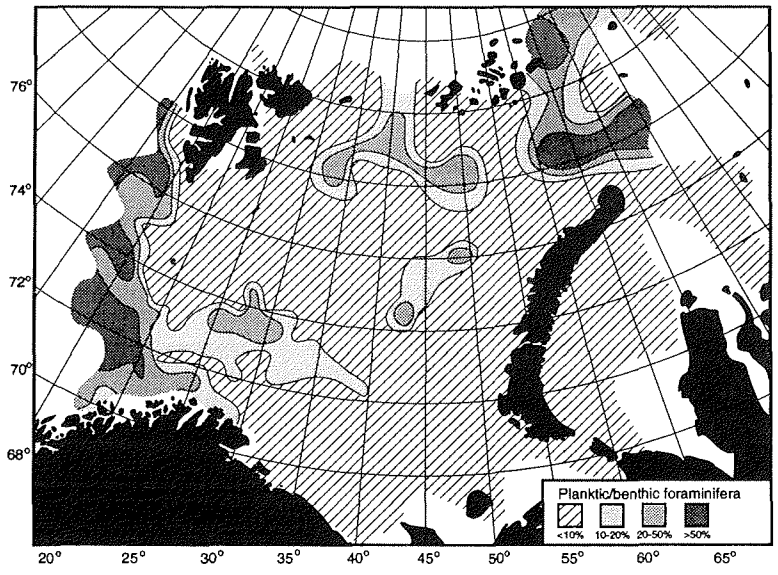

Fig. 8.: Distribution of calcareous benthic/planktic foraminifera-ratios in the Barents and Kara Seas.

Factor analysis

The results of the factor analysis define six factors explaining 82.4% of the variance in 544 samples (Fig. 9a-f). Communality values on the result are fairly good; only four samples show values below 0.25 and only 33 are below 0.5. Each factor is considered to represent a foraminiferal assemblage named after its most important species. Distributions of factor loadings show distinct geographic patterns, which is a sign of a reasonable result.

Nonion barleeanum (Factor 1, Fig. 9a)

This factor explains the largest part of the total variation; 20.9%. It is strongly dominated by *N. barleeanum*, with *Epistominella nipponica* and *Pullenia bulloides* as common species. Its distribution in the Barents Sea mainly follows the troughs with a bottom sediment characterized by a soft, organic rich mud. In the Kara Sea, Factor 1 is also found in areas with muddy sediments, but not close to the low saline waters of the Siberian coast. Temperature does not seem to significantly limit the distribution of this assemblage, but low salinity is apparently a restricting parameter.

Cibicides lobatulus (Factor 2, Fig. 9b)

This factor explains 18.0% of the variation, and is clearly dominated by the *Cibicides lobatulus*. The factor loadings show high values for the shallow areas at the banks and along the coasts all over the region, although somewhat less for the Siberian coast which has strong riverine influence.

Such a distribution is apparently controlled by the availability of coarse sediments and high hydrodynamic activity. Temperature does not seem to be a restricting parameter for this assemblage, but low salinity does. Some of the species that are found in small numbers in this assemblage may be reworked from underlying older sediments.

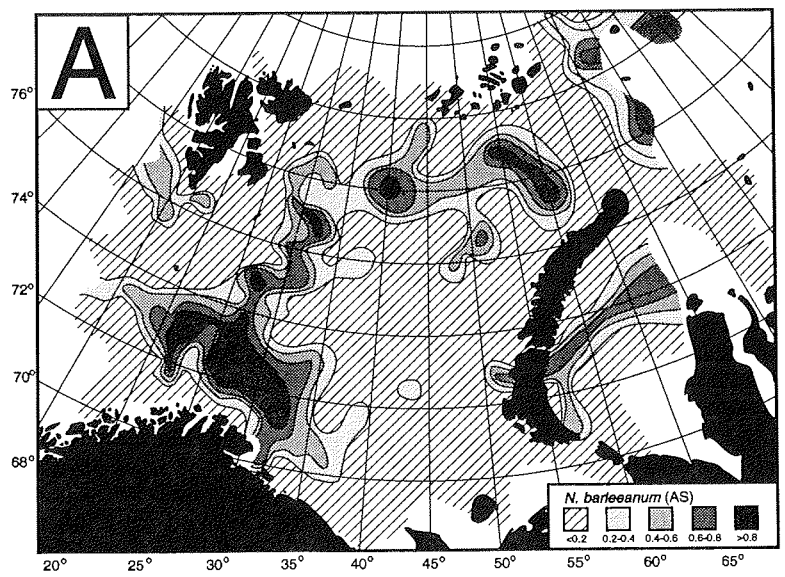

Fig. 9a.: Distribution of benthic calcareous foraminifera assemblages in the Barents and Kara Seas: *Nonion barleeanum* .

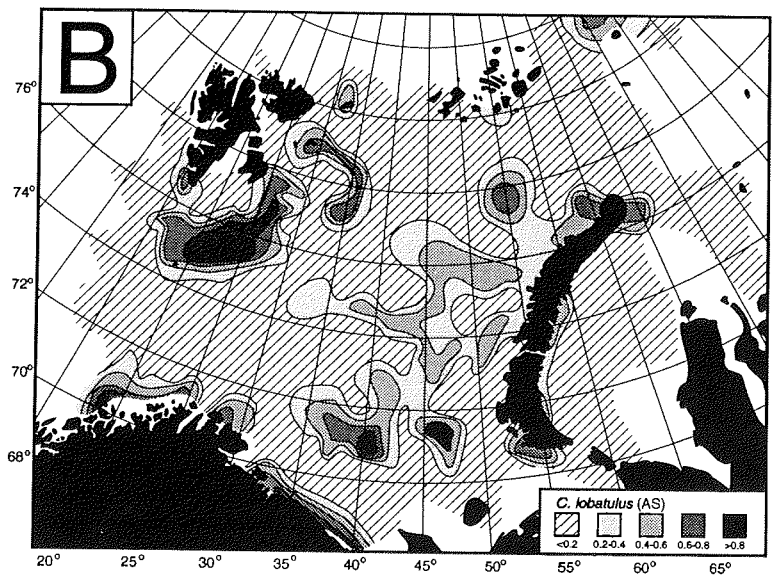

Fig. 9b.: Distribution of benthic calcareous foraminifera assemblages in the Barents and Kara Seas: *Cibicides lobatulus* assemblage.

Elphidium excavatum f. clavatum (Factor 3, Fig. 9c)

This factor explains 16.0% of the total variation. *E. excavatum* f. *clavatum* strongly dominates this assemblage. Other common other species are *C. reniforme* and *E. subarcticum*. Its highest loadings are found in the deeper parts of the northern Barents Sea, and along the Siberian and Novaya Zemlya coasts at depths <100 m. An additional area of high loadings is the Central Bank of the Barents Sea.

The northern maximum is apparently related to parameters such as cold water, sea-ice cover during most of the year, high turbidity due to proximity of glaciers and/or a combination of these. Riverine influence causes variable, but generally low temperature and salinity, and turbid environments in the shallow area along the Siberian cost. The Central Bank of the Barents Sea is also influenced by cold and relatively low saline Polar Water. High values of the factor loadings here may also be connected with redeposition of glacial sediments, which yield high concentrations of *E. excavatum* f. *clavatum*. A detailed discussion of the European Arctic recent and late Quaternary distribution of the species *E. excavatum* f. *clavatum* is given by Hald et al. (1994).

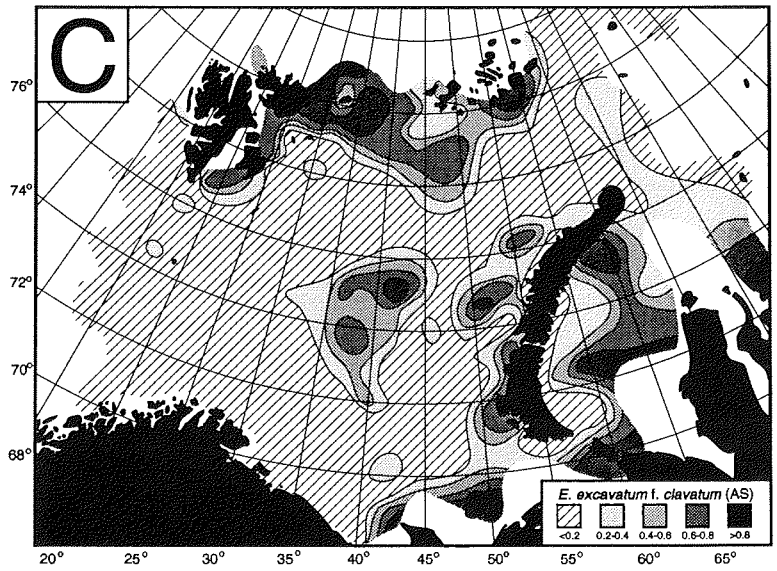

Fig. 9c: Distribution of benthic calcareous foraminifera assemblages in the Barents and Kara Seas: *Elphidium excavatum* f. *clavatum* assemblage.

Buccella spp./Islandiella norcrossi (Factor 4, Fig. 9d)

This factor explains 11.4% of the variance. It is dominated by *Buccella spp.*, *Islandiella norcrossi* and *Trifarina fluens*, with *Nonion labradoricum* also being common. Its main distribution follows a broad band from Svalbard to the southeastern Barents Sea, but there are also some spots near Franz Josef Land and in the Kara Sea. The broad band corresponds to the area of seasonal sea-ice cover, where an ice-edge productivity bloom occurs during the spring/summer period. It is suggested that the food availability from the high productivity pulses primarily controls the distribution of this assemblage. Its temperature, salinity and substrate type ranges are fairly wide, although in general it prefers relatively low temperatures and only slightly reduced salinities.

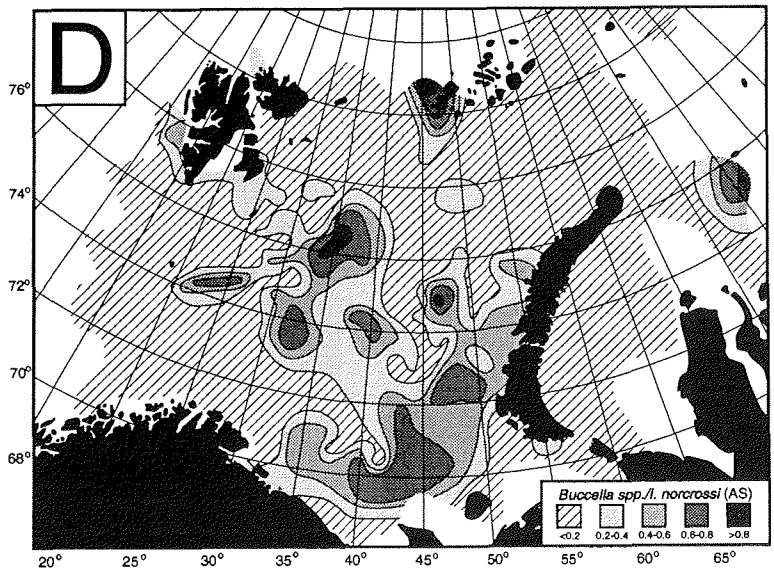

Fig. 9d.: Distribution of benthic calcareous foraminifera assemblages in the Barents and Kara Seas: *Buccella spp./Islandiella norcrossi* assemblage.

Cassidulina teretis/reniforme (Factor 5, Fig. 9e)

9.2% of the variation is explained by this factor. It is dominated by the combination of *Cassidulina teretis* and *Cassidulina reniforme*. Its highest abundance is found along the shelf slopes, particularly along the western margin of the Barents Sea and the St. Anna Through. These are the deepest parts of the study area, occupied by the chilled Atlantic Water with low turbidity. Similar patterns of distribution are also shown by planktic foraminifera (Fig. 8). This assemblage contains the highest abundance of *Cibicides wuellerstorfi*, which is considered as a deep sea species. Temperatures over 5°C and low salinity restrict the distribution of this assemblage. Patches of increased factor loadings in the eastern Barents and Kara Seas are connected with *C. reniforme* alone.

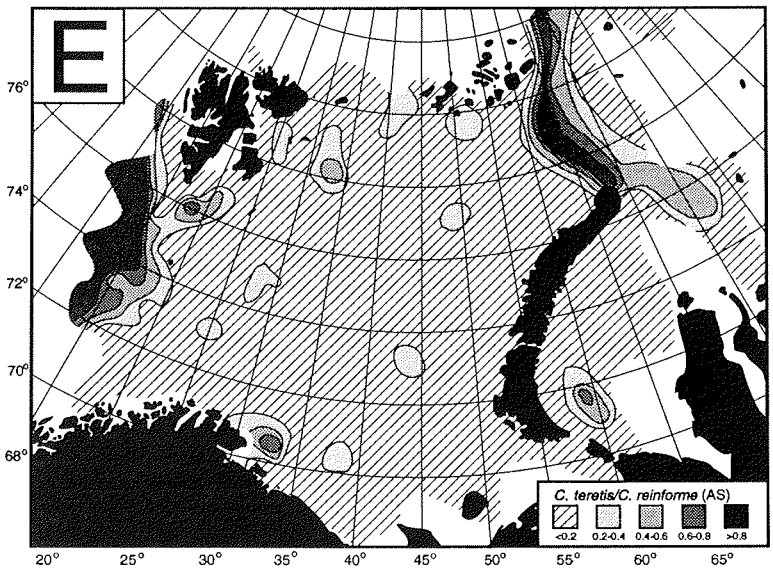

Fig. 9e.: Distribution of benthic calcareous foraminifera assemblages in the Barents and Kara Seas: *Cassidulina teretis/C. reniforme* assemblage.

Epistominella nipponica/Trifarina angulosa (Factor 6, Fig. 9f)

This factor explains 6.8% of the variance. It is dominated by *Epistominella nipponica* and *Trifarina angulosa*, with some minor influence of *Cassidulina teretis* and *Cibicides lobatulus. Cassidulina obtusa, Cassidulina laevigata* and *Discorbinella sp* are found almost exclusive in this assemblage. Its distribution is limited only to the southwestern Barents Sea and is most common on the central Fugløy Bank, the warmest part of the study area. A detailed discussion of the SW Barents Sea assemblages is given in Hald and Steinsund (1992).

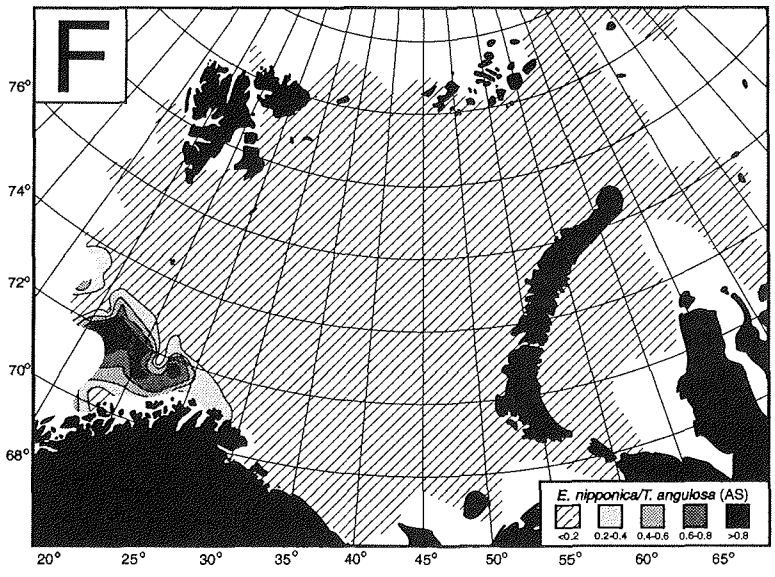

Fig. 9f.: Distribution of benthic calcareous foraminifera assemblages in the Barents and Kara Seas: *Epistominella nipponica* assemblage.

Carbonate dissolution

Studies from the southwestern Barents Sea (Hald and Steinsund, 1992; Steinsund and Hald, 1994), shows several signs of carbonate dissolution in the surface sediments. The main indicators are: 1) Broken and corroded calcareous foraminiferal tests. 2) Decreasing carbonate values 3) Nearly pure arenaceous foraminiferal assemblages 4) Living/dead-, benthic/planktic- and arenaceous/calcareous ratios.

Test preservation

The sediment in the eastern and northern part of the study area contains many broken and fragile calcareous foraminiferal tests, with a dull and mealy surface. For the species *Cibicides lobatulus*, parts of the organic lining were often visible. Whole organic linings without any calcium carbonate were also frequently found in areas with dissolution, which is a clear sign of dissolution.

Carbonate and foraminiferal assemblages

The carbonate distribution in surface sediments decrease from 25-30% in the southwest to 1-3% in the northeastern part of the area. Two of the benthic foraminifera assemblages (*Reophax* and *Nonion* assemblage zones) are influenced by calcium carbonate dissolution. The *Reophax* assemblage zone, comprising a nearly pure arenaceous fauna is most affected by dissolution. The *Nonion* assemblage zone west of the *Reophax* assemblage zone is partly dissolved. This fauna shows relatively high values of arenaceous foraminifera and most of the calcareous foraminifera shows signs of dissolution. The dominance of *Nonion barleeanum* is probably related to larger resistance to carbonate dissolution for this species as it lives in a pelitic microenvironment (Corliss, 1985) which protect it from corrosive water.

Living/dead-, benthic/planktic- and arenaceous/calcareous ratios

Carbonate dissolution indicators such as the ratio of living/dead, benthic/planktic and arenaceous/calcareous foraminifera increases strongly towards the northeast. Comparing these ratios with percentage calcium carbonate in the surface sediment shows a high correlation. Data from the Barents- and Kara Seas (Steinsund et al., in press) shows that the trend with high ratio of arenaceous/calcareous foraminifera continues further east and north in the Barents Sea. More than 75% of arenaceous foraminifera are commonly found on the banks in the northern Barents Sea and in the troughs leading into the Arctic Ocean (Fig. 6).

Causes of carbonate dissolution

Dissolution of calcium carbonate depends on several factors such as the partial pressure of CO_2, temperature, salinity and hydrostatic pressure. In the Barents Sea, which is no deeper than 500 m, hydrostatic pressure can be eliminated as a cause of dissolution. According to Edmond and Gieskes (1970), the solubility of calcium carbonate increases with decreasing temperature, increasing salinity and increasing concentrations of CO_2. One or more of these conditions have to exist for calcium carbonate to dissolve.

The dissolution can take place either in the sediment or at the sediment-water interface. Plots of grain size versus percentage calcium carbonate show no obvious correlation between grain size and percentage calcium carbonate (plot not shown here). There are indications that benthic foraminiferal species living in the sediment (*Nonion barleeanum*) are less dissolved than species living at the sediment water-interface. Both of these observations supports the idea that dissolution takes place at the sediment-water interface.

Dense bottom water has high salinity and very low temperature, which both are factors favouring dissolution. Dissolution of calcium carbonate and distribution of dense bottom water seem to correlate. Most of the dissolution is found in areas where dense bottom water is produced. Furthermore, the southwestward extent of the dissolution follows troughs and depressions, which are the natural pathways for dense bottom water (McClimans and Nilsen, 1990). This may suggest that the dissolution is related to presence of dense bottom water. Although dense bottom water has high salinity and low

temperature, it may also be enriched in CO_2. Production of CO_2 requires oxygen and organic matter. The polar front area has a high organic production peak during the spring and summer. Downward transport by brines could provide CO_2 to the seafloor. A possible source for CO_2 is the decay of organic matter in the upper water column. CO_2 which would be trapped under the sea-ice, preventing exchange with the atmosphere. During winter, sea-ice formation produces brines which generate downward currents to the sea bed (Fig. 10). This process creates well-oxygenated conditions at the sediment-water interface. Owing to the polar night and sea-ice cover, this condition occurs when photosynthesis is strongly reduced and leads to the production of CO_2 when there is no biological process to deplete it.

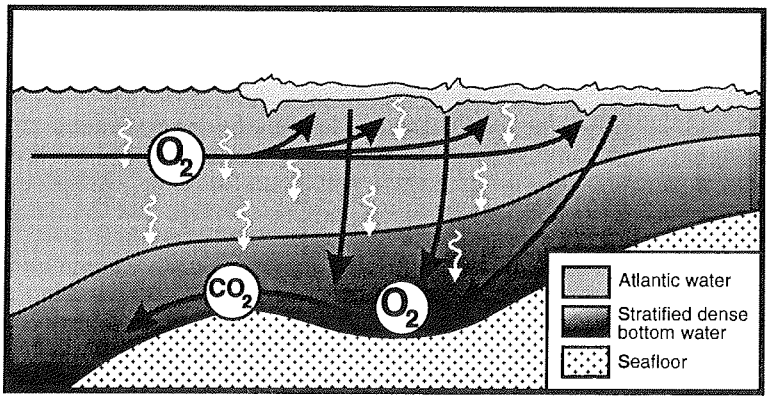

Fig. 10.: Model for transport of oxygen-rich water down to organic-rich sediment at the seafloor. Downward currents indicate the formation of dense bottom water. At the sediment-water interface, organic carbon oxidizes and forms CO_2 which, in combination with low temperature and high salinity, dissolve calcium carbonate. White arrows=organic flux, black arrows=water currents.

Formation of CO_2 at the sediment-water interface is probably the most effective way of dissolving calcium carbonate. This process concentrates CO_2 where the dissolution takes place, while transport of CO_2 through the water column will dilute the concentration of CO_2. If the CO_2 is produced by oxidation at the sediment-water interface, CO_2 production will continue until all the oxygen or organic matter is depleted. This will give a much higher capacity to dissolve calcium carbonate, compared to if the CO_2 is formed in the water column. Without a continuous supply of CO_2, dissolution will cease when all the CO_2 is used.

According to maps of calcium carbonate distribution in surface sediments (Lisitzin, 1971), areas containing less than 1% calcium carbonate can be found in polar regions and in areas below the CCD. Comparing these low calcium carbonate areas in polar regions with seasonal sea-ice distribution shown by Maykut (1985). This shows that areas in Arctic regions with less

than 1% calcium carbonate are mostly covered by seasonal sea-ice. Several reports of calcium carbonate dissolution from the Antarctic shelf support the assumption that dissolution removes calcium carbonate from the sediment (Anderson, 1975; Osterman and Kellogg, 1979). Also, frequent reports of arenaceous foraminiferal faunas in Arctic areas suggest that neither low production nor high sediment input cause the low calcium carbonate content (Schröder-Adams et al, 1990; Hald and Steinsund, 1992; Hunt and Corliss, 1993). Low calcium carbonate content in polar regions is therefore probably caused by dissolution. The process which causes the dissolution on other polar shelves could be the same as in the Barents Sea.

Conclusions

-Based on a large data base (600 samples) of benthic foraminifera that has been assembled from the Barents and Kara seas, the following conclusions can be made:

-Judging from generally low modern sedimentation rates in the area, surficial samples of 1-3 cm thick used in the study must represent an averaged record for the last several hundred years.

-The observed distribution of calcareous benthic foraminifera in the Barents and Kara Seas is largely controlled by their microhabitat, feeding preferences and water mass properties.

-Six major assemblages are distinguished by means of factor analysis: *E. excavatum* f. *clavatum* assemblage exemplifies an opportunistic fauna, able to survive at highly variable environments with prevailing low salinities and/or temperatures, and high turbidity. *N. barleeanum* assemblage is restricted to areas with soft muddy sediments and normal salinity; temperature doesn't seem to control its distribution. *C. lobatulus* assemblage populates shallow areas with coarse substrate and high hydrodynamic activity. It covers wide temperature range, but prefers normal salinity. *C. teretis/C. reniforme* assemblage mainly follows chilled Atlantic Water with normal salinity and low turbidity, which penetrates the Barents and Kara Seas through the marginal troughs at bathyal depths. *Buccella spp./I. norcrossi/T. fluens* assemblage occupies the area of seasonal sea-ice distribution, which suggest it is dependent on ice-edge blooms of organic productivity. *E. nipponica/T. angulosa* assemblage is restricted to the south-eastern part of the Barents Sea, which is affected by warm (>4^{o}C) and saline Atlantic Water.

-Surface sediment calcium carbonate is being dissolved in the area indicated by: Traces of dissolution on calcareous foraminiferal tests, visible on both SEM photographs and under light microscope. The distribution of benthic foraminifera faunas; foraminifera more resistant to dissolution are more common in areas with dissolution. High ratios of benthic/planktic, agglutinating/calcareous, and living/dead foraminifera.

The calcium carbonate dissolution may be favoured by the existence of cold saline dense bottom water, produced by sea-ice formation in the Barents sea. Decay of organic matter may cause a relatively high concentration of CO_2 at the sediment-water interface. Such conditions probably exist along the

oceanic polar front. Calcium carbonate dissolution on other polar shelves may be caused by the same process as in the Barents Sea.

References

Anderson, J.B., 1975. Ecology and distribution of foraminifera in the Weddell Sea of Antarctica. Micropaleontology, 21: 69-96.

Basov, V. A. and Slobodin, V.Ya. 1965, Kompleksy foraminifer iz sovremennyh i pozdnekajnozojskih otlozhenij zapadnoj chasti Sovetskoj Arktiki (Foraminiferal assemblages from recent and Late Cenozoic deposits of the western Soviet Arctic). In: Antropogenovyi Period v Arktike i Subarktike: Nauchno-Issled. Inst. Geologii Arktiki Trudy, 143, 190-210. (in Russian).

Carmack, E. C. 1990, Large-scale physical oceanography of Polar oceans. In, W.O. Smith, Jr. (Ed.), Polar oceanography: Part A. Physical science, 171-222.

Corliss, B. H. 1985, Microhabitats of benthic foraminifera within deep-sea sediments: Nature, 314, 6010, 435-438.

Dahle, S., Denisenko, S., Fredriksen, K. R. and Larsen, L. H., 1993, Field report, environmental survey in the Kara Sea and the estuaries of Ob and Jenesei: Report to the Norwegian Ministry of Environmental protection. Report No. 391.01.01, Akvaplan-niva and Geogruppen as., 15 pp.

Digas, L. A. 1969, Raspredelenie foraminifer v sovremennyh osadkah Barentseva morya i pogranichnyh s nim uchastkov Grenlandsko-Norvezhskogo bassejna (Distribution of foraminifera in recent sediments of the Barents Sea and adjacent areas of the Norwegian-Greenland Sea): Unpubl. dissertation, Saratov (in Russian).

Digas, L. A. 1971, Fauna foraminifer Central'noj vozvyshennosti i severo-vostochnoj chasti Zapadnogo zheloba Barenceva morya (Foraminiferal fauna of the Central Bank and northeastern part of the Bear Island Trough of the Barents Sea). Voprosy Geologii Yuzhnogo Urala i Povolzh'ya (Problems of geology of the Southern Urals and Volga Region): Saratov University, 4, part 2 (Cenozoic), 179-194 (in Russian).

Dokken, T., 1991, Sen-kvartær lito-og biostratigrafi fra det sørlige Barentshavet: Unpublished thesis, University of Tromsø. (In Norwegian).

Edmond, J.M. and Gieskes, J.M.T.M., 1970. On the calculation of the degree of saturation of sea water with respect to calcium carbonate under in situ conditions. Geochimica et Cosmochimica Acta, 35: 1261-1291.

Elverhøi, A., Pfirman, S. L., Solheim, A. and Larssen, B.B. 1989, Glaciomarine sedimentation in epicontinental seas exemplified by the northern Barents Sea: Marine Geology, 85, 225-250.

Feyling-Hanssen, R.W., 1964, Foraminifera in Late Quaternary deposits in the Oslofjord area: Norges Geologiske Undersøkelse, v. 225, p. 383.

Forsberg, C. F., 1983, Thickness of Holocene sediments in the southeastern Barents Sea: Master Thesis, University of Oslo, Norway. 120 pp.

Fredriksen, K. R., Dahle, S., Danielsen, T. K., Costello, J. and Frogh, M., 1992, Field report, environmental survey in Isfjordren, Svalbard and in the northern Barents Sea, August 1992: Report to the Norwegian ministry of Environmental Protection. Report No. 242.01.03. Akvaplan-niva and Geogruppen as., 14 pp.

Gurevich, V.I., Yakovlev, A.V., Kijko, O.A., Yakovleva, T.V., Musatov, Ye.Ye., Petrova, V.I., Bondarenko, S.A. and Potakhina, T.A. 1993, Geo-ecology of

the Western Arctic shelf of Eurasia. Unpublished report, VNII Okeangeologia, St.Petersburg.

Hald, M. and Vorren, T.O., 1984, Modern and Holocene foraminifera and sediments on the continental shelf of Troms, North Norway: Boreas, v. 13, p. 133-154.

Hald, M. and Vorren, T.O., 1987, Foraminiferal stratigraphy and environments of Late Weichselian deposits on the continental shelf off Troms, Northern Norway: Marine Micropaleontology, v. 12, p. 129-160.

Hald, M., Danielsen,T.K. and Lorentzen, S., 1989, Late Pleistocene and Holocene benthic foraminiferal distribution in the southwestern Barents Sea: paleoenvironmental implications: Boreas, v. 18, p. 367-388.

Hald, M., and Steinsund, P. I., 1992, Distribution of surface sediment benthic foraminifera in the southwestern Barents Sea: Journal of Foraminiferal Research, 22, 347-362.

Hald, M., Steinsund, P. I., Dokken, T., Korsun, S., Polyak, L. and Aspeli, R, 1994, Recent and Late Quaternary distribution of *Elphidium excavatum* f. *clavatum* in Arctic seas: Cushman Foundation Special Publication No. 32, 141-153.

Hopkins, T. S., 1991, The GIN Sea - A synthesis of its physical oceanography and literature review 1971-1985: Earth Science Review, 30, 175-318.

Hunt, A. S. and Corliss, B. H. 1993, Distribution and microhabitats of living (stained) benthic foraminifera from the Canadian Arctic Archipelago: Marine Micropaleontology, 20, 321-345.

Imbrie, J. and Kipp, N.G., 1971, A new micropaleontological method for quantitative paleoclimatology: application to a late Pleistocene Caribbean core. In "The Late Cenozoic Glacial Ages." (K.K. Turekian, ed.). Yale University Press, New Haven, v. 3, p. 71-181.

Khousid, T. A. 1989, Paleoekologia Barentseva morya v pozdnechetvertichnoe vremya po foraminiferam (Late Quaternary paleoecology of the Barents Sea based on benthic foraminifera). Byul: Komissii po Izucheniyu Chetvertichnogo Perioda (INQUA Bull.), 58, 105-116 (in Russian).

Klenova, M. V., 1960, Geology of the Barents Sea: Academika Nauk SSR, Moscow, 355 pp.

Klovan, J.E., and Imbrie, J., 1971, An algorithm and fortran-IV program for large-scale Q-Mode factor analysis and calculations of factor scores: Journal of The International Association for Mathematical Geology, v. 3, p. 61-77.

Knudsen, K.L. and Sejrup, H.P., 1993, Pleistocene stratigraphy in the Devils Hole area, central North Sea: foraminiferal and amino-acid evidence. Journal of Quaternary Science, 8, 1, 1-14.

Korsun, S.A., 1991, Solution of biogenic carbonate in sediments of the Barents Sea: Oceanology, 31, 5, 547-550.

Lagoe, M. 1979, Recent benthonic foraminiferal biofacies in the Arctic Ocean: Micropaleontology, 25, 2, 214-224.

Lien, R. and Myhre, L., 1977, Undersøkelser av overflatelaget på kontinentalsokkelen utenfor Troms og vest Finnmark: Institutt for kontinentalundrsøkelser, 92, (In Norwegian). 33 pp.

Lisitzin A. P. 1971. Distribution of carbonate microfossils in suspension and in bottom sediments. In: Funnel B. M. and Riedel W. R. (Editors), The Micropaleontology of oceans. Cambridge University Press, London: 197-218.

Loeng, H. 1991, Features of the physical oceanographic conditions of the Barents Sea: Polar Research, 10, 5-18.

Løfaldli, M. and Rokoengen, K., 1980. Late-and post-glacial foraminifera and sediments on Viknaryggen and Haltenbanken off Mid. Norway: Continental Shelf Institute Publications no. 109, 102 pp.

Maycut G. A., 1985. The ice environment. In: Horner R. A. (Editor), Sea ice biota. CRC Press Inc. Boca Raton Florida.

McClimans, T.A. and Nilsen, J.H., 1990. A laboratory simulation of the ocean currents of the Barents Sea during 1979-1984. NHL Report STF60 A90018: 59 pp.

Midttun. L., 1985, Formation of dense bottom water in the Barents Sea: Deep Sea Research, 32, 1233-1241.

Mosby, H., 1968, Surrounding Seas, *in* A. Sømme (ed.), Geography of Norden: J. W. Cappelens Forlag, Oslo, Norway, 18-26, map 7.

Nagy, J. and Ofstad, K., 1980, Quaternary foraminifera and sediments in the Norwegian Channel: Boreas v. 9, p. 39-52.

Nagy, J. and Qvale, G., 1985, Benthic foraminifers in Upper Quaternary Skagerrak deposits: Norsk Geologisk Tidsskrift v. 65, p. 107-113.

Nikiforov, Ye. G. and Shpajher, A. O. 1980, Zakonomernosti formirovaniya krupnomasshtabnyh kolebanij gidrologicheskogo rezhima Severnogo Ledovitogo Okeana (Regular features controlling the large-scale variations in hydrological regime in the Arctic Ocean): Gidrometeoizdat, Leningrad, (in Russian). 269 pp.

Osterman, L. and Kellogg, T.B., 1979. Recent benthic foraminiferal distributions from the Ross Sea, Antarctica: Relation to ecologic and oceanographic conditions. Journal of Foraminiferal Research, 9: 250-269

Østby, K.L. and Nagy, J., 1981, Foraminiferal stratigraphy of Quaternary sediments in the Western Barents Sea. In: "Microfossils from recent and fossil shelf seas" (J.Neale and M.D.Braiser eds.). Ellis Horwood, Chichester, 260-273 pp.

Østby, K. L. and Nagy, J. 1982, Foraminiferal distribution in the western Barents Sea, Recent and Quaternary: Polar Research, 1, 53-87.

Polyak, L. V. 1985, Foraminifery donnyh otlozhenij Barentseva i Karskogo morej i ih stratigraficheskoe znachenie (Foraminifera of bottom sediments of the Barents and Kara Sea and their stratigraphic significance): Unpubl. dissertation, Leningrad (in Russian).

Quadfasel, D., Rudels, B. and Kurtz, K., 1988, Outflow of dense water from a Svalbard fjord into the Fram Strait: Deep-Sea Research, 35, 1143-1150.

Sarinina, R. N., 1972, Conditions of origin of cold deep-sea waters in the Bear Island Channel. In," Proceedings of a Symposium held in Dublin." (Lee and Charnock, eds.): International Council for the Exploration of the Sea, 300-301.

Schröder-Adams, C. J., Cole, F. E., Medioli, F. S., Mudie, J. P., Scott, D. B. and Dobbin, L. 1990. Recent Arctic shelf foraminifera: seasonally ice covered vs. perennially ice covered areas. Journal of Foraminiferal Research, 20: 8-36.

Sejrup, H. P. and Knudsen, K.L., 1993, Paleoenvironments and correlations of interglacial sediments in the North Sea. Boreas, 22, 223-235.

Slobodin, V. Ya. and Tamanova, S. V. 1972, Kompleksy foraminifer iz donnyh otlozhenij Karskogo morya i ih znachenie dlya izucheniya rezhima novejshih dvizhenij (Foraminiferal associations from bottom sediments of the Kara Sea, and their significance for the study of modern tectonics). In, Novejshaya tektonika i paleogeografiya Sovetskoj Arktiki v svyazi s

ocenkoj mineral'nyh resursov: Published by NIIGA, Leningrad, 23-35 (in Russian).

Solheim, A. and Elverhøi, A., 1983, Physical environment western Barents Sea, 1:1,500,000. Surface sediment distribution: Norsk Polar Institutt, 179, 14pp.

Steinsund, P. I. and Hald, M., 1994, Recent calcium carbonate dissolution in the Barents Sea, Paleoceanographic applications: Marine Geology, 117, 303-316.

Steinsund, P. I., Polyak, L., Hald, M., Mikhaylov, V. and Korsun, S., (in press), Distribution of calcareous benthic foraminifera in recent sediments of the Barents and Kara Seas. *Journal of Foraminiferal Research.*

Stenløkk, J. A. 1984, En mikropaleontologisk undersøkelse av recent ostrakode- og foraminiferfauna fra NV-Barentshavet: Master Thesis, University of Oslo, Norway. (In Norwegian). 131 pp.

Stoll, S. J. 1968, A foraminiferal study of the Kara Sea north of 76 degrees North latitude: Unpublished Master Thesis, University of Wisconsin, 86 pp.

Swift, D.J.P., Stanley, D.J. and Curray, J.R., 1971, Relict sediments on continental shelves: a reconsideration: J. Geology, v. 79, p. 322-346.

Sætre, R. and Ljøen, R., 1971, The Norwegian Coastal Current: Proc. from the first international conference on port and ocean engineering under arctic condition. University of Trondheim.

Tamanova, S. V. 1973, Foraminifery sovremennyh osadkov Arkticheskogo bassejna (Foraminifera of recent sediments of the Arctic Ocean). In, Geologiya Morya (Geology of the Sea), 2: Published by NIIGA, Leningrad, 59-66 (in Russian).

Thiede, J. 1988, Scientific cruise report of Arctic Expedition ARK IV/3: Reports on Polar Research, 43, 237 pp.

Thomsen, E., 1989, Aspects of macrofaunal preservation stratigraphy and palaeoecology in Late Quaternary continental shelf sediments off northern Norway: Dr. scient.thesis, University of Tromsø.

Treshnikov, A. F. (ed.) 1985, Atlas Arktiki (Atlas of the Arctic): Published by AANII, Moscow (in Russian).

Tryggestad, S., 1981, Environmental conditions 71 ^{o} 30'N 19^{o} 00'E. Currents and waves. Report 4: Current and Waves at Tromsøflaket 1978 and 1979. Norwegian Petroleum Directorate, Stavanger, 63 pp.

Vassmyr, S. and Vorren, T.O. (1990), Clast petrography and stratigraphy in Late Pleistocene sediments in the southwestern Barents Sea: Norsk Geologisk Tidsskrift, v. 70, p. 95-110.

Vingradovna, P. S. and Litvin, V. N., 1960, Studies of bottom relief and sediments in the Barents and Norwegian Seas: Poljarny Naucuno-Issledovatelskij Institute, 101-110.

Vinje, T. E., 1977, Sea ice conditions in the European sector of the marginal seas in the Arctic, 1966-75: Årbok Norsk Polarinstitutt 1975, 163-174.

Vorren, T.O., Strass, I.F. and Lind-Hansen. O.-W., 1978, Late Quaternary sediments and stratigraphy on the continental shelf off Troms and West Finnmark, Northern Norway: Quaternary Research, v. 10, p. 340-365.

Vorren, T. O., Hald, M. and Thomsen, E., 1984, Quarternary sediments and environments on the continental shelf off northern Norway: Marine Geology, 57, 229-257.

Wensaas, L., 1986, Sedimentologiske og sedimentpetrografiske studier av kvartære sedimenter i det nordlige Barentshav: Master Thesis, University of Oslo, Norway. (In Norwegian). 178 pp.

MODERN BENTHIC FORAMINIFERAL ASSEMBLAGES IN THE KARA SEA.

Khusid T.K. [1]and Korsum S.A.[2]

[1] P.P. Shirshov Institute of Oceanology, Moscov, Russia
[2] Murmansk Marine Biological Institute, Murmansk, Russia

Abstract

The distribution of modern benthic foraminifera was studied in 37 samples of surface sediments from the Kara Sea. The analysis allows to delineate three assemblages and a barren zone. The assemblages are discriminated on the basis of dominant species composition. The assemblages with a dominance of arenaceous foraminifera *Cribrostomoides subglobosum* and *Tritaxis nana* occupy the deeper (70 - 380 m) section of the study area. The brown mud sediments as well as the cold stagnant bottom water are characteristics of the zone. The assemblage dominated by calcareous taxa *Elphidium clavatum* and *Cassidulina reniforme* occupies the shallow (30 to 90 m) southeastern section of the Kara Sea. Low salinity (about 3 ‰) of the bottom water is the main environmental characteristic of the zone. The inner estuaries of Ob and Yenisei rivers are barren of foraminifera. Low salinity (13 to 27 ‰) is most likely to be the environmental parameter preventing foraminifera to inhabit this area.

Introduction

The Kara Sea performs a peculiar function in the water system of the Arctic Ocean. Two great Siberian rivers, Ob and Yenisei, run into the Kara Sea. The fresh-water discharge into the Kara Sea is 1290 km^3/yr that comprises 55% of the freshwater income in all Arctic Siberian Seas. This tremendous fresh-water inflow forms the brackish surface layer that causes haline stratification of the water column and, hence, inhibits vertical mixing. The brackish surface layer is the main source of sea - ice formation. A significant portion of the Arctic pack ice is formed in the Kara Sea (Dobrovolsky and Zalogin, 1982). The bottom water salinity in the Kara Sea is 34.5 to 35.0 ‰, and the bottom water temperature varies from 1.7 to 1.0 °C (Dobrovolsky and Zalogin, 1982). The sediments in the Kara Sea are terrigenous. The organic carbon content of the sediments is 0,01 to 3%, and the values higher than 1% are observed close to the coast. The $CaCO_3$ content ranges from 0.09 to 1.15% (Gorshkova, 1975; Romankevich et al, 1982). Schedrina (1938), Basov and Slobodin (1965), Slobodin and Tamanova (1972), and Todd and Low (1980) have studied benthic foraminiferal fauna of the Kara Sea. The main aims of this study are: (1) to describe benthic foraminiferal distribution in the Kara Sea and (2) to relate the observed distribution to environmental parameters. This new data will give insight into modern foraminiferal ecology that can be used in paleoceanography reconstructions.

Materials and Methods

Thirty seven surface sediment samples were used in this study. Two samples (1405 and 1407) were retrieved by R/V Prof. Shtokman, cruise No.49 in autumn 1993 (Fig. 1). Samples were taken from undisturbed surface layer of sediment (0 - 2 through 0 - 5 cm) retrieved by a corer and grab sampler "Ocean 50". The samples were washed through a 0.05 mm sieve. One sample from the Yenisei estuary was preserved in Rose Bengal stained alcohol. Data are expressed in number of specimens per 1g of dry sediment.

Results and Discussion

A total of 70 foraminiferal taxa were identified for samples from the Kara Sea (Table 1). 31 of those are arenaceous taxa, and the other 39 have calcareous tests. Three assemblages of benthic foraminifera were distinguished in the Kara Sea. Discrimination of the assemblages is based on composition of dominant species. One barren zone was also found (Fig. 1).

This assemblage is restricted to Novaya Zemlya Trough and adjacent regions - in the western part of the study area. The depth range of the samples is 70 to 380 m. The bottom water temperature and salinity generally vary between -1.7 and -1.5 °C and between 34.4 and 34.6 ‰, respectively. The assemblage occupies the area where bottom sediment is brown mud. The assemblage consists of 27 arenaceous and 9 calcareous species. Each sample contains 10 to 18 species (Table1). The number of foraminifera ranges from 1 to 30 tests/g. Arenaceous taxa prevail in the assemblage. The most abundant species are *Cribrostomoides subglobosum* (5 - 38%) and *Tritaxis nana* (4 - 42 %). Both species are characteristic of all abyssal foraminiferal assemblages of the ocean (Saidova, 1975; Burmistrova, 1977; Bernstein et al., 1978; Corliss, 1979; among others). Scarce calcareous fauna mainly consists of typical Arctic shelf species *Elphidium clavatum*, *Elphidium albiumbilicatum*, *Cassidulina reniforme*, and *Bucella frigida*. Most of the calcareous tests are partly dissolved. The occurence of the calcareous forms is 0 to 13% in the majority of the samples. Only in two samples 4377 and 4394 situated in the very southwestern region of the sea, the abundance of the calcarous tests is higher, 38 and 43%, respectively. The presence of the transformed Atlantic Water in the region coming in from the Barents Sea through the Kara Gates (Dobrovolsky and Zalogin, 1982) is the most possible cause of the increase in the calcareous test content. The *Cribrostomoides subglobosum* - *Tritaxis nana* assemblage is associated with stagnant waters in the western deep-water of the Kara Sea.

Elphidium clavatum - *Cassidulina reniforme* assemblage
The assemblage occupies the eastern Kara Sea. The depth limits are 30 and 90 m. Sediments are silt, clay, and sand. The bottom water in this region is more agitated compared to the western deeper region of the Kara Sea. Salinity of the bottom water generally ranges from 34,0 to 34,5 ‰, and temperature is about -1.5°C (Dobrovolsky and Zalogin, 1982). The assemblage consists of 11 arenaceous and 37 calcareous species. Each sample contains 6 to 15 species (Table 1). The number of foraminifera ranges from 1 - 124 tests/g. The calcareous specimen comprise more than 90% of the total fauna. The most abundant taxa are *Elphidium clavatum* (17 - 51) and

Cassidulina reniforme (12 - 37%). These two species have been reported to be typical of polar and subpolar shelves. Both species dominate particularly in areas characterized by rapid sedimentation (>1 cm/ka) of terrigenous material (Feylimg - Hanssen et al., 1971; Sejrup et al., 1981; Mackensen et al., 1981; among others). Arenaceous foraminifer *Eggerella advena* is abundant at two stations (4391 and 4395) where sediment is sand. Korsun et al. (1994) found a similar pattern in the Barents Sea. The highest standing crop of living *E. advena* occurs in sandy sediments of shallow areas. Schafer et al. (1991) suggest that a high occurence of the species in Saguenay Fjord, Quebec, reflects a consequence of pollution stress. A very low pollution level in the Kara Sea does not allow to verify this conclusion for the study area.

Elphidinium clavatum - Haynesina orbiculare assemblages
This assemblage occupies the outer estuaries of Ob and Yenisei rivers and the adjacent area of the southern Kara Sea. The depth range of the samples is 18 to 29 m. The sediment is olive mud. The bottom water salinity is 27 to 33 ‰. The brackish surface layer causes stagnant conditions at the bottom (Dobrovolsky and Zalogin, 1982). The number of foraminifera is low, less than 1 test/g (Table 1). There is a general decrease in number of foraminifera upstream in the estuaries. The assemblage includes only four calcareous species. *Elphidinium clavatum* and *Haynesina orbiculare* prevail; *Elphidinium albiumbilicatum* and *<Buccella frigida* are accessor forms. These foraminifera are able to survive in low-salinity environment. All tests are corroded due to probably $CaCO_3$ dissolution. One sample from the Yenisei estuary (st. 4411) is stained with Rose Bengal. The results of staining seem to confirm the dissolution effect. All the specimens in this sample contain cytoplasm; there are no dead foraminifera. The calcareous foraminifera are probably able to build the test in this calcite aggressive environment, but post-mortem dissolution of the test is rapid. The presumable undersaturation of the pore water with calcite is likely caused by a high organic carbon content in the sediment (Dobrovolsky and Zalogin, 1982). Aerobic oxidization of the organic matter results in pH decreasing and consequent calcite dissolution.

Barren zone
Benthic foraminifera are absent in the inner estuaries of Ob and Yenisei rivers (Table 1). The depth range of the samples is 14 to 23 m. The sediment is sand and silt of different color. The bottom water salinity is 15 to 27 ‰. Probably this low salinity is the physiological limit for the Kara Sea foraminifera and prevents them to inhabit the inner estuaries of Ob and Yenisei rivers.

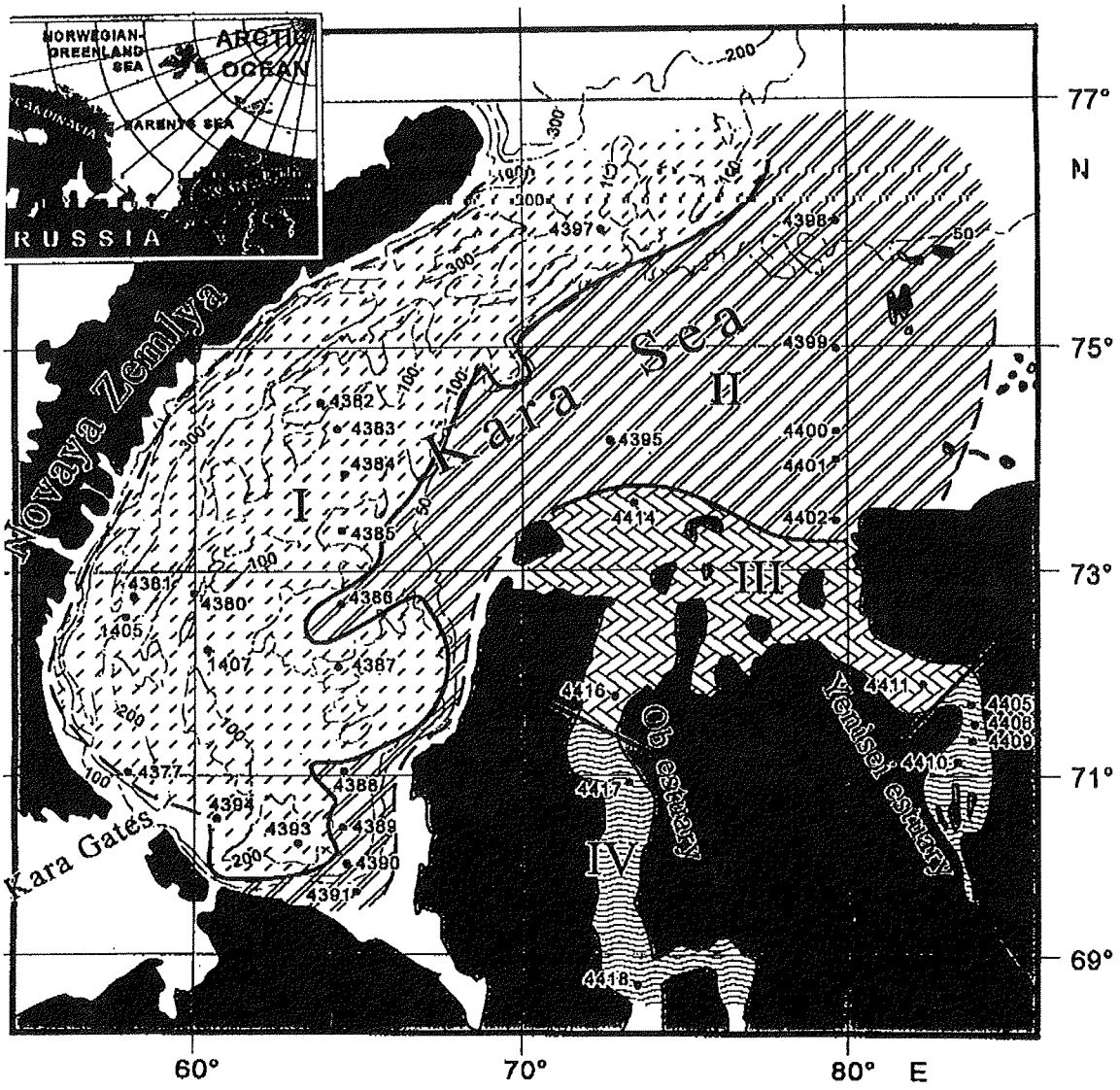

Fig.1.: Assemblages of modern benthic foraminifera in the Kara Sea: I.*Cristrobrostomoides subglobosum - Tritaxis nana* assemblage; II.*Elphidium clavatum - cassidulina reniforme* assemblage; III.*Elphidium clavatum - Haynesina orbiculare* assemblage; IV.The barren zone *Cribrostomoides subglobosum - Tritaxis nana* assemblage.

Table 1: Taxa of tree assemblages of benthic foraminifera.

Textulariina	
Saccammina sphaerica	G.O.&M.Sars, 1872
Sorosphaera sp.	
Thurammina sp.	
Astrorhiza arenaria	Norman, 1892
Rhabdammina abyssorum	M. Sars, 1868
Rhabdammina discreta	Brady, 1881
Hyperammina elongata	Brady, 1878
Hyperammina subnodosa	Brady, 1884
Saccorhiza ramosa	Brady, 1879
Ammodiscus sp.	
Glomospira charoiges	Jones & Parker, 1860
Hormosina globulifera	Brady, 1879
Reophax arctica	Brady, 1881
Reophax curtus	Cushman, 1920
Reophax dentaliniformis	Brady, 1884
Reophax scorpiurus	Montfort, 1808
Ammotium cassis	Parker, 1970
Ammobaculites agglutinans	Brady, 1884
Alveolophragmium crassimargo	Norman, 1892
Cribrostomoides jeffreysi	Williamson, 1858
Cribrostomoides subglobosum	G.O. Sars, 1872
Cyclammina sp..	
Adercotryma glomerata	Brady, 1878
Recuvoides turbinatus	Brady, 1881
Recurvoides trochamminiforme	Höglund, 1947
Trochammina inflata	Montagu, 1808
Trochammina sp..	
Tritaxis nana	Brady, 1881
Spiroplectammina biformis	Parker & Jones, 1865
Textularia torquata	Parker 1952.
Eggerella advena	Cushman, 1922.
Miliolina	
Quiqueloculina arctica	Cushman, 1933.
Quiqqueloculina seminula	Linne, 1758
Quinqueloculina stalkeri	Loeblich & Tappan, 1953
Miliolinella subrtunda	Montagu, 1803
Triloculina trichedra	Loeblich & Tappan, 1953
Triloculina trigonula	Lamark, 1804
Pyrgo williamsoni	Silvestri, 1923
Rotaliina	
Cibicides lobatulus	Walker & Jacob, 1798
Rosalina vilardeboana	d'Orbigny, 1839.
Bucella frigida	Cushman, 1922
Bucella tenerrima	Bandy, 1950
Nonion umbilicatulum	Walker & Jacob, 1798
Nonionella auricula	Heron-Allen & Earland, 1930
Nonionellina labradorica	Dawson, 1960
Haynesina orbiculare	Brady, 1881
Elphdiella hannai	Cushman & Grant, 1927
Elphidium subarcticum	Cushman, 1944
Elphidium subarcticum	Weiss, 1954
Elphidium bartletti	Cushman, 1933
Elphidium clavatum	Cushman, 1930
Cassidulina reniforme	Norvang, 1945
Islandiella norcrossi	Cushman, 1933
Islandiella helenae	Feyling-Hanssen&Buzas, 1976
Bolivina pseudopunctata	Hoeglund, 1947
Trifarina fluens	Todd, 1947
Stainforthia loeblichi	Feyling - Hanssen, 1954
Polymorphina suboblonga	Cushman & Ozawa, 1930
Esosyrinx curta	Cushman & Ozawa, 1930
Guttulina problema	d'Orbigny, 1826
Dentalina baggi	Galloway & Wissler, 1927
Lagena gracillima	Seguenza, 1862
Oolina melo	d'Orbigny, 1839
Oolina setigera	Millet, 1901
Oolina sp..	
Fissurina marginata	Montagu, 1803
Fissurina orbignyana	Seguenza, 1862
Fissurina spp.	
Fissurina ventricosa	Wiesner, 1931
Parafissurina sp.	

Conclusions

Three foraminifera assemblages are distinguished in the Kara Sea based on dominant taxa. The assemblage with a dominance of arenaceous foraminifera *Cribrostomoides subglobosum* and *Tritaxis nana* occupies the Novaya Zemlya Trough and the adjacent deeper region (70 - 380 m) of the study area. The dominant species are typical of the abyssal zone of the ocean. The brown mud sediment as well as the cold stagnant bottom water are characteristic of the trough. The assemblage dominated by calcareous taxa *Elphidium clavatum* and *Cassidulina reniforme* occupies the shallow southeastern section of the open shelf. The dominant species are typical of polar and subpolar shelves. *Elphidium clavatum - Haynesina orbiculare* assemblage occupies the outer estuaries of Ob and Yenisei rivers and the adjacent area of the southern Kara Sea. Both diversity and number of foraminifera are low. The assemblage consists entirely of calcareous foraminifera, and post-mortem dissolution of the calcareous tests is rapid. Low salinity (about 30 ‰) is the main environmental characteristic of the assemblage. The inner estuaries of Ob and Yenisei rivers are barren of foraminifera. Low salinity of 13 to 27 ‰ is most likely to be the environmental parameter preventing foraminifera to inhabit this area.

Acknowledgments

A.P. Lisitzin and M.A. Levitan planned and organized collecting of the samples. M.A. Levitan and I.I. Buristrova carefully reviewed the manuscript. The authors thank the persons mentioned. This paper is Grant No. 94-05-17071a from Russian Foundation of Basic Researchers.

References

Basov V.A. and Slobodin V.Ja., 1965. Forminiferal assemblages from Recent and Late Cenozoic deposits of the western Soviet Arctic.Trudy NIIGA, 143; 190 - 200 (Russian).

Bernstein B.B., Hessler R.R., Smith R., and Jumass P.A., 1978. Spatial dispersion of benthic foraminifera in the abyssal central North Pacific.Limnol. Oceanogr, 23 (3); 401 - 406.

Burmistrova I.I., 1977. Distributional ranges of deep-sea benthic foraminifera distributions in the southern Indian Ocean.Biologija morja, 3; 3 - 11 (Russian, English abstract).

Corliss B.H., 1979. Recent deep-sea foraminifera distributions in the southern Indian Ocean: inferred botttom-water routes and ecological implications.Mar. Geol., 31(1/2); 115 - 138.

Dobrovolsky A.D. and Zalogin B.S., 1982. Seas of the USSR. Moscow, 192 pp.

Feyling - Hanssen R.W., Jorgensesn J.A., Knudsen K.L., and Andersen A.L., 1971. Late Quaternary Foraminifera from Vensyssei, Denmark and Sandnes.Norway. Bul. Geol. Soc. Denm., 21; 317 pp.

Gorshkova T.I., 1957. Sediments of the Kara Sea.Trudy Vsesojuznogo Gidrobiologicheskogo Obschestva, 8;66 - 72 (Russian).

Korsun S.A., Pogodina I.A., Tarasov G.A., and Matishov G.G., 1994. Foraminifera of the Barents Sea (Hydrobilogy and Paleoecology).Apatity, Kola Sci. Center Publ;140 pp (Russian, English abstract).

Mackensen A., Sejrup H.P., and Jansen E., 1985. The distribution of living benthic foraminifera on the continental slope and rise off southwest Norway.Mar. Micropaleontol., 9; 275 - 306.

Romankevich E.A., Danjushevskaya A.I., Belyaeva A.N., and Rusanov V.P., 1982. Organic Matter Biogeochemistry in the Arctic Seas.Moscov, Nauka; 240 pp (Russian, English abstract).

Saidova Kh. M., 1975. Benthic foraminifera of the Pacific Ocean. Moskow, Academy of sciences Publishers & Inst. of Oceanology;875 pp (Rusiian, English abstract).

Schafer C.T., Collins E.S., and Smith J.N., 1991. Relationship of Foraminifera and thecamoebian distribution to sdeiments contaminated by pulp mill effluent: Saguenay Fiord, Quebec, Canada.Mar. Micropaleontol., 17; 225 - 283.

Schedrina Z.G., 1938.On foraminiferal distribution in the Kara Sea.Doklady Akademii Nauk, XIX (4); 321 - 324 (Russian).

Sejrup H.-P., Fjæran T., Hald M., Beck L., Hagen J., Miljeteig I., Morvik I., and Norvik O., 1981. Benthonic foraminifera in surface samples from the Norwegian continental margin between 62°N and 65°N.N. J. Foraminiferal Res., 11 (4): 277 - 295.

Slobodin V.Ja. and Tamanova S.V., 1972. Foraminiferal assemblages from deositional records of the Kara Sea and their significance for (interpretation of) modern tectonics regime.In: Novejshaja tektonika i paleogeografija Sovetskoj Arktiki v svjazi s otsenkoj mineral'nykh resursov.Leningrad, Trudy NIIGA; 23 - 35 (Russian).

Todd R. and Low D., 1980. Foraminifera from the Kara and Greenland Seas and review of Arctic studies.Geol. Surv. Profess. Pap., 1070; 1 - 30.

DIATOMS OF THE EURASIAN ARCTIC SEAS AND THEIR DISTRIBUTION IN SURFACE SEDIMENTS

Polyakova Y.I.

Geographical Department, Moscow State University, Moscow, Russia

Abstract

Analysis of about 300 surface sediment samples of the Chukchi, East Siberian, Laptev, Kara and Barents Seas define main characteristic features of diatom thanatocoenoses in surface sediments of the Eurasian Arctic seas. According mainly to phytoplankton productivity, sedimentological conditions, and concentration of dissolved silica in the water, the total number of diatom valves per gram of dry sediment varies from a few or no valves up to several millions, with number increasing from west to east. Distribution patterns of marine planktonic diatom species in the phytoplankton and sediments depend upon the extension of different water masses in the Arctic seas; the most diverse being in the Barents and Chukchi Seas. Abundance of cryophilic species in surface sediments indicating sea-ice position, varies from a few valves up to 43% of the total valve number. Abundance of planktonic and cryophilic diatoms is limited in some regions under unfavourable depositional conditions and lack of dissolved silica in the water. Freshwater species are brought into the Arctic seas with river influx and river ice and became the most abundant (to 94%) in the surface sediments of the southeastern Laptev Sea and southeastern Kara Sea.

Introduction

Diatoms are the main producers of organic matter in the Arctic seas. They were studied for more than 100 years, but our knowledge about the modern diatom flora of the region is far from complete. There is some information about the planktonic diatom flora of the Eurasian Arctic Seas, summarized by Proshkina-Lavrenko (1974). During the last thirty years planktonic diatoms mainly of the coastal zones were studied by Bursa (1963), Okolodkov (1988 a,b), Koltzova and Ilyash (1982), Makarova and Polyakova (1990), Ryzhov et al. (1984), and some others. More than 160 planktonic diatom species were reported in these works (Polyakova, 1988, 1989). Cryophilic diatom species present on sea ice attracted the attention of early polar investigators, but Usachev (1938, 1949) was the first who summarized the information. More recently, taxonomical, ecological and physiological informations were obtained, e.g. Meguro et al. (1967), Horner (1976, 1989), and Melnikov (1980, 1989). Sea-ice diatoms were also used for indication of the ice drift (Abelmann, 1992). Literature on the benthic diatom flora is fragmentary and usually of an inventory nature. Research on the formation of diatom thanatocoenoses, their species composition, and the number of diatoms in Arctic seas was accomplished by the author for the past years (Polyakova, 1988, 1989, and others).

Material and Methods

Almost 300 surface sediment samples (upper 1 to 2 cm of cores of surface grabs) from the Eurasian Arctic seas were examined. Sources of the material include cores and grabs from the Institute of Oceanology of the Russian Academy of Sciences and the Geographical Department of Moscow State University, collected over three periods from 1982 to 1984 in July and August. The diatoms were concentrated by treatment with HCL and H_2O_2 followed by heavy liquid (KDL and KJ) separation accordig to Jouse et al. 1974. Subsequently, they were mounted on glass slides using a mounting medium having a high index of refraction (1,68). The valves were examined under a light microscope at 1000 x magnification. Counts were made and abundance estimated per sample (number of valves per gram of dry residue).

Results

For the characteristic of diatom thanatocoenoses the common abundance of diatom valves per one gram of dry sediments is the most significant index. The results of the study of the uppermost sediment samples of the Eurasian Arctic seas show that the total number of valves were per gram of dry sediment varies from a few or no valves up to several millions with the numer increasing from west to east (Fig. 1). The main factors of diatom accumulation in sediments of the Erasian Arctic seas are the planktonic productivity, hydrochemical and hydrobiological conditions as well sedimentation on the shelf. Surface sediments of the Chukchi Sea are characterized by the greatest number of diatom valves among the Eurasian Arctic seas. Clayey-silt sediments of the Central Chukchi depression and Central Cukchi canyon with an amorphous SiO_2 content of 10 - 13 % (Logvinenko and Ogorodnikov, 1980; Pavlidis, 1982), contain the greatest number of diatom valves - up to 13,6 million per gram. This is mainly due to the high phytoplankton productivity of the Bering Sea water masses penetrating into these regions. The genetic basis of these water masses are the Northern Pacific waters which are formed in the deep part of the Bering Sea and enter the Bering Strait and Chukchi Sea by upwelling. The rise of the deep water masses causes the high concentrations of the biogenic elements in the regions of their extention, particularly dissolved silicic acid up to 35 µgat Si l^{-1} and phosphates up to 75 µgat P l^{-1}. This is the cause of the high phytoplankton producivity - up to 25 - 30 cells per litre (Rhyzhov et al., 1984). In the eastern part of the Chukchi Sea influenced by the Alaskian branch of the Bering Sea current, the number of diatom valves is 9 - 8,2 million per gram in fine silts and gravels of the Alaskian coast. In the fine and coarse silts of the Long Strait and the Chukchi Peninsula coast, the number of valves is up to 1,5 million and 13 - 37 thousands of valves per gram, respectively.

The diversity of hydrological and depositional environments on the East Siberian Sea and outheastern Laptev Sea shelf produces a variety of diatom thanatocoenoses. The total diatom amount varies from 570 valves per gram to 5,9 million valves per gram, increasing eastward. The main factor limiting diatom accumulation in sediments of the East Siberian Sea is the amount of terrigenous material in the shelf zone, mainly supported by river influx and active coastal thermobrasion.

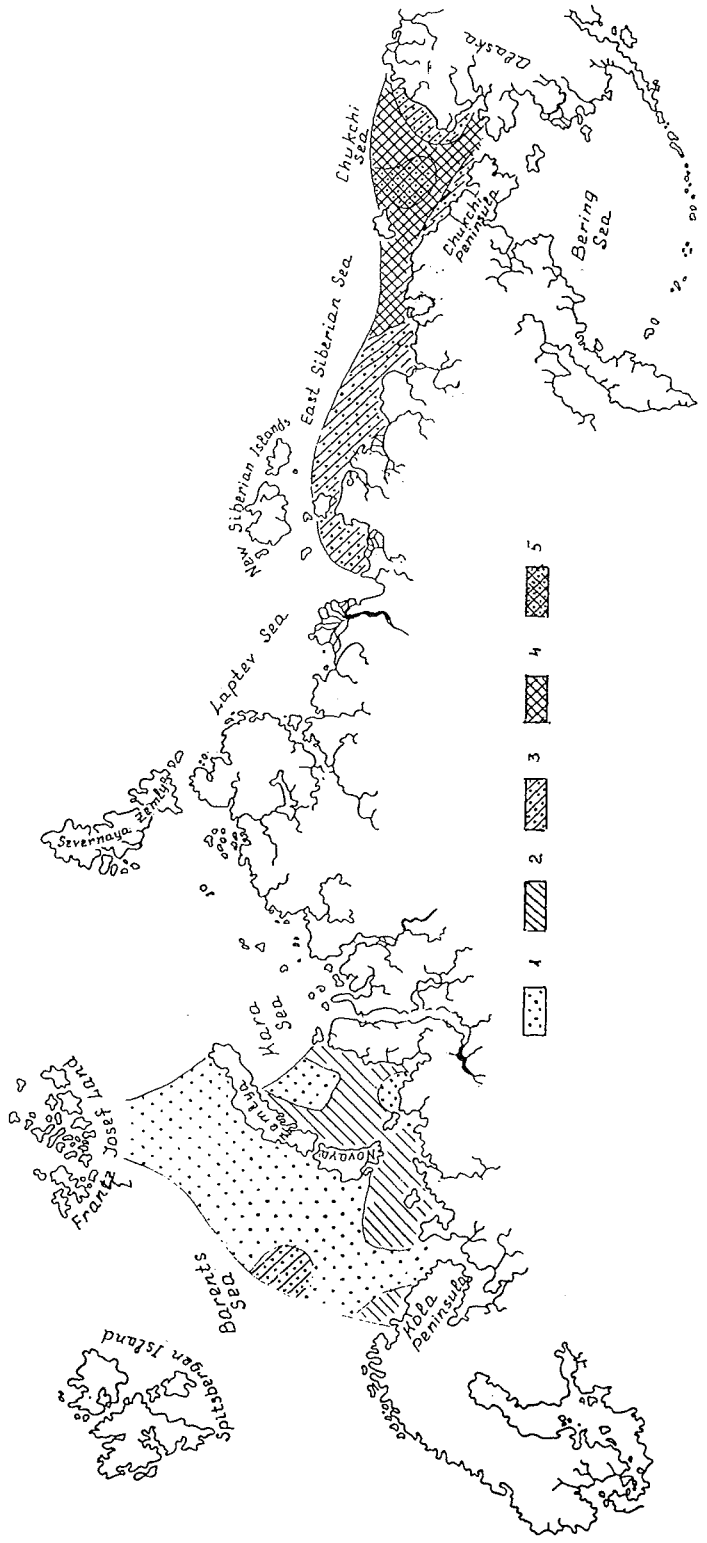

Fig. 1.: Abundances of diatoms in surface sediments of the Eurasian Arctic Seas (1: less than 10 diatom numbers per gram of dry sediment; 2: 10-100; 3: 100-1000; 4: 1000-1000000; 5: more than 1000000).

The diatom thanatocoenoses of the Barents Sea and the studied western part of the Kara Sea are characterized by the extremely low number of valves in sediments. Nearly half of the studied sediment samples of the Barents Sea involve recent diatoms, while 30% of the samples contain only a few valves per gram of sediment, 9% of the samples contain 10 - 100 valves per gram, and only 13% of samples include more than 100 valves. The same results were obtained in the Kara Sea and corresponding indices were 14%, 36%, 25%, and 25%. Although the phytoplankton abundance of the Barents Sea is high (Rouhijajnen, 1960; Ryzhov, 1980; and others) the abundance of planktonic diatoms in the surface layer is low, and samples usually include only a few valves of planktonic species. At the same time the sublittoral froms with predominance of *Paralia sulcata* were traced in 46% of the studied sample of the Barents Sea and in 86% of the samples of the Kara Sea. This ratio of planktonic and sublittoral diatoms in deep - sea (to 100 - 200 m) thanatocoenoses indicates dissolution of valves during sinking caused by the low concentration of dissolved silica (less than 10 μgat Si l^{-1} in the water of the studied regions of the Barents and Kara Seas).

The prevalance of the arctic waters in the Northern Eurasian seas causes the predominance of coldwater arctic - boreal and bipolar species as in the phytoplankton and in the diatom thanatocoenoses (Fig. 2). In the Siberian Seas - the largest parts of the Kara Sea, Laptev and East Siberian Sea - these cold-water species contain 59% of the known planktonic diatom taxa. The most comon species in sediments of these areas are: *Thalassiosira antarctica, Thalassiosira gravida, Thalssiosira nordenskiöldii, Thalassiosira hyalina, Bacerosira fragilis, Rhizosolenia hebetata, Coscinodiscus oculus-iridis*; as well as species of genus *Chaetoceros*, (*Chaetoceros mitra, Chaetoceros furcellatus, Chaetoceros ingolfianus, Chaetoceros subsecundus*, and others). Spores of *Chaetoceros* are the most abundant in sediments of southeastern part of the Siberian Sea, where their total number is up to 50 - 96 %.

Planktonic diatom flora of the Chukchi Sea penetrated by the Bering Sea waters includes: predominant coldwater arctic boreal and bipolar species (45% sum total), as well as the boreal - tropical (6%) and tropical (5%) species (*Chaetoceros didymus, Belleroches malleus* and others), whose habitats in the Chukchi Sea coincide with the Bering Sea waters. Relatively warmwater species (*Coscinodiscus radiatus, Coscinodiscus asteromphalus, Coscinodiscus perforatus, Proboscia alata*, and others) comprising only 0.5%, are rarely found in the plankton and sediments of the Chukchi Sea, being restricted to the Berig Sea Current waters close to the Bering Strait. The single valves of these species were found in sediments near the Barrow Cap and Gerald Bank.

Diatom plankton of the Barents Sea and the farmost southwestern regions of the Kara Sea which are influenced by the North Atlantic current, is characterized by the predominance of cosmopolitan and arctic-boreal-tropical (more than 50%) species with large ecological amplitude allowing them to live in different water masses. Only coldwater arctic-boreal and bipolar species (35% sum total) such as *Thalassiosira antarctica*, *Thalassiosira gravida*, *Coscinodiscus oculus-iridis* have been found in the sediments of the northeastern regions of the Barents Sea mainly covered by the arctic water mass. The most diverse planktonic species composition is characteristic for

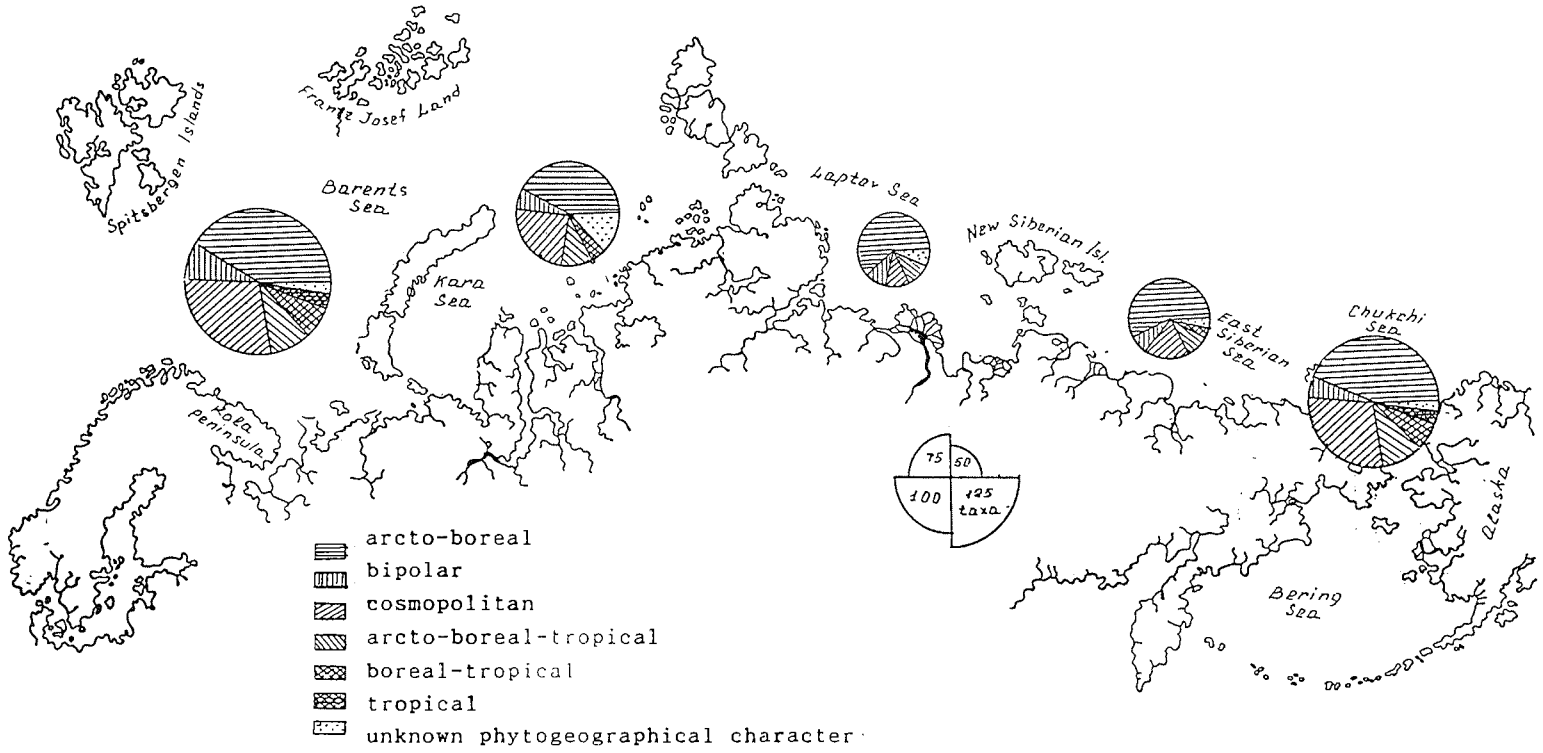

Fig. 2.: Phytogeographical composition of the planktonic diatoms in the Eurasian Arctic Seas.

the southwestern part of the sea - where both coldwater species (*Thalassiosira antarctica, Thalassiosira gravida* and others) and warmwater ones (*Coscinusdiscus asteromphalus, Coscinusdiscus radiatus, Rhizosolenia styliformis* and others) brought by the North Cape Current from the Atlantic Ocean, have been found. Northward and eastward - North Atlantic species disappear from the Phytoplankton and thanatocoenoses. With the Western Novaya Zemlya Current some of them reach the latitude of the Cape Zhelaniye and with the Murmansk branch of the North Atlantic Current, the extreme south-western region of the Kara Sea, where their valves were found in the sediment samples.

Sea-ice biocenoses, mainly formed by cryophilic diatom species, are an important source of diatoms for Arctic marine sediments. For example, sea-ice algae are able to produce up to 5 μg C m^{-2} y^{-1} which constitutes about 25 - 30% of the annual primary production in source areas (Alexander, 1974). Sea-ice diatoms are usual component of the diatom thanatocoenoses and their abundance in sediments correlates with ice conditions. Among diverse cryophilic diatoms studied in the biocenosesof the arctic sea-ice, the following species *Nitzschia grunowii, Nitzschia cylindrus, Chaetoceros septentrionalis, Navicula vanhoeffenii, Detonula confervacea*, are the most common in the diatom thanatocoenoses. Their abundance changes within vast limits (Fig. 3). In the Chukchi Sea sea-ice diatoms constitute from 4 to 51% of the total number of diatom valves in the sediment samples reaching their maximum near the northeastern coast of Alaska and in the region to the north from the Bering Strait. Distribution of cryophilic diatoms in the East Siberian and Laptev Sea is limited by the warming and freshing effects of the river influx. That is why in the region of the Indigirka River mouth cryophilic diatoms are represented by only a few valves, and in the southeastern part of the Laptev Sea their abundance is only 8 - 10% of the total number of valves. Near the Kolyma River mouth cryophilic diatoms are less than 31%. In the eastern part of East Siberian Sea which has the most ice covered area on the arctic shelf, the cryophilic diatom content is always high reaching 27 - 43%. In the northern regions of the Barents and Kara Sea where cryophilic diatoms predominate in the spring bloom of arctic waters, the number of cryophilic as well as planktonic species is low due to unfavourable depositional conditions and the lack of dissolved silica in the water. They are rarely found in sediments in these regions being present as only few valves per gram. In the Kara Sea they reach their maximum abundance on the northwestern coast of Yamal Peninsula, correlating with the greatest number of planktonic diatoms in sediments. In the Barents Sea their maximum abundance is characteristic feature of the zone where arctic and atlantic water masses meet.

Distribution patterns of freshwater diatom species brought in with river influx and river ice correlate with the spreading of river waters in the coastal zones of arctic seas. Usually in Chukchi Sea surface sediments only few valves of the freshwater species were found and only in the coastal zone near the river mouth their content reaches 42 - 68%. In the East Siberian Sea the number of freshwater diaroms reaches its maximum to the north of the Indigirka River mouth (to 74 - 83%) and the Kolyma River mouth (15 - 21%), decreasingdown to 1-3% in the Chauna Bay region and less than 1% to the east from it (Fig. 4). In the southeastern part of the Laptev Sea river influx results in the high number of freshwater diatoms (up to 94%) decreasing steadily down to 15% at the distance of 200 km from the Lena River mouth. In the western part of the

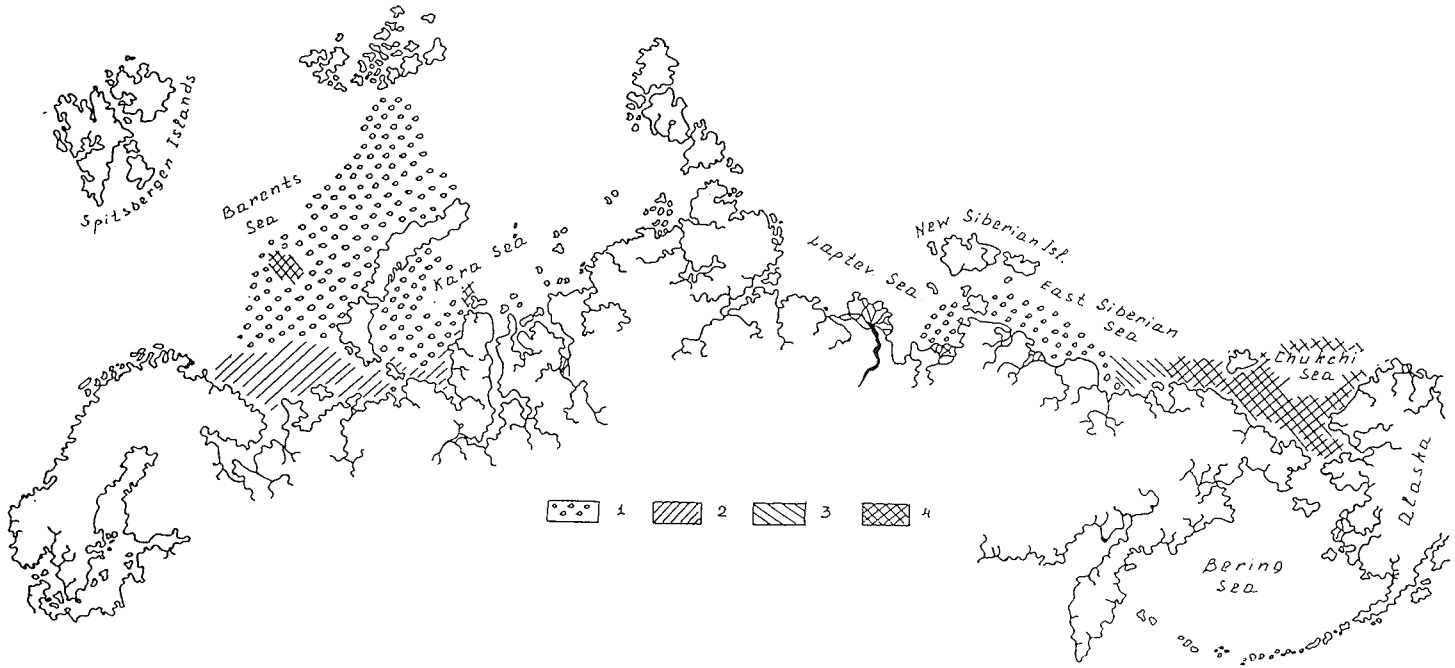

Fig. 3.: Abundances of cryophilic diatoms in surface sediments of the Eurasian Arctic Seas (1: less than 10 diatom numbers per gram of dry sediment; 2: 10-100; 3: 100-1000; 4: 1000-1000000; 5: more than 1000000).

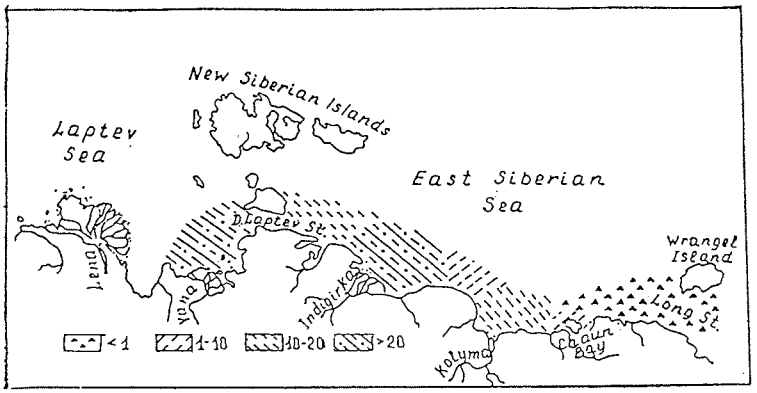

Fig. 4.: Distribution of freshwater diatoms as percentage of total diatom assemblage in surface sediments of the East-Siberian and Laptev Seas.

Kara Sea freshwater diatoms included in the river ice, are carried out to the north with the strong Ob - Yenisei Current and reach 78 - 79°N. They were found in the 25% of the studied sediment samples but their usual abundance in the northwestern region is never more than 1% of the total number increasing steadily to the south. Along the coast of the Yamal Peninsula freshwater diatoms are the common component of diatom thanatocoenoses (up to 2 - 22%), and the diatom thanatocoenoses of the Ob Bay are represented by only freshwater diatoms. In the Barents Sea freshwater diatoms occur in the southeastern regions being carried out by the Pechora River influx; their usual abundance in diatom assemblages beeing less than 1%. Few valves of freshwater species were found in sediments of the fjords along the western coast of the Novaya Zemlya.

Summary and conclusions

1. The total number of valves per gram of dry sediments in the Eurasian Arctic seas varies from a few or no valves up to several millions with the number increasing from west to east. This is mainly due to phytoplankton productivity, sedimentological conditions and concentration of dissolved silica in the water.

2. Distribution patterns of marine planktonic diatom species in the sediments correlate with their modern natural habitats and depends on the extension of different water masses in the Arctic Seas.

3. Sea - ice biocenoses mainly formed by cryophilic diatom species, are an important source of diatoms for Arctic marine sediments. Distribution patterns of cryophilic species in the surface sediment layer mainly correlate with ice conditions varying from a few valves up to 43% of total number of diatom valves. Their abundance is limited in some regions by unfavourable depositional conditions and lack of dissolved silica in the water.

4. Freshwater diatom species are brought into Arctic seas with river influx and river ice. Ice influx results in a high abundance of freshwater diatoms in sediments of the coastal zones (up to 94%) decreasing steadily in the vicinity of river mouths. Abundant freshwater diatoms are the common component of diatom thanatocoemoses of the southeastern Laptev Sea and southwestern East Siberian Sea.

Acknowledgments

I am grateful to Dr. Yu. Pavlidis from the Institute of Oceanology of the Russian Academy of sciences who provided me with the sediment samples from the Arctic Seas. This publication was supported by Russian State Scientific TEchnical Programm"Biological Diversity".

References

Abelmann A., 1992. Diatom assemblages in Arctic sea ice - indicator for ice drift pathways. Deep -Sea Research, 39 (Suppl. 2); 525 - 538.

Alexander V., 1974. Primary productivity regimes of te nearshore Beaufort Sea with references to potential roles of ice biota. In: The coast and shelf of the Beaufort Sea. Arlington: The Arctic Institute of North America; 609 - 635 Editors: Reed J.C. and Saree J.R.

Bursa A., 1963. Phytoplankton incoastal waters of the Arctic Ocean at the Point Barrow, Alaska. Arctic, Vol 16, No. 4; p. 3239 - 263

Horner R.A., 1976. Sea ice organisms. Oceanogr. Mar. Biol. Ann. Rev., 14; p. 167 - 182

Horner R.A., 1989. Arctic sea ice biota. In: The Arctic seas. Climatology, Oceanography, Geology and Biology. ew York: Van Nostrand Reinhold. p. 123 - 146.

Jouse A.P., Proshkina - Lavrenko A.I., and Sheshukova - Poretskaya V.S., 1974 Methods of investigations. In: Diatoms of the USSR. Fossil and recent. Editors: Gleser Z.I., Jouse A.P., Makarova L.V. et al.. Leningrad, Nauka; 50 - 79; Russian

Koltzova T.I. and Ilyash L., 1982. Distribution of phytoplankton in the coastal zone of Taymir Peninsula in dependence on hydrological conditions. Water resources, No. 4; 158 - 165, Russian

Logvinenko N.V. and Ogorodnikov V.I., 1980. Recent bottom sediments on the Chukchi Sea shelf. Okeanologiya, Vol. 20, No. 4; 691 - 687, Russian

Makarova I.V. and Polyakova Ye.I., 1990. Species of genus Thalassiosira Cl., new for the East Siberian Sea. News in the systematic of primary plants, Vol 27; p. 9 - 14, Russian.

Meguro H., Ito K., and Fukushima H., 1967. Ice flora (bottom type): A mechanism of primary production in polar seas and the growth of diatoms in sea ice. Arctic, 20; p. 114 - 133.

Melnikov I.A., 1980. Ecosystem of the Arctic drift ice. In: Biology of the Central Arctic basin. Editors: Vinogradov M.E., Melnikov I.A., Moscow, Nauka, p. 61 - 98, Russian.

Melnikov I.A., 1989. Ecosystem of the Arctic sea ice. Moscov, Akademy of Sciences of the USSR, Institue of Oceanology; p. 191.

Okolodkov Yu. B., 1988 a. Parasitic and epiphytic planktonic algae of the Chukchi Sea. News in the systematic of primary plants, 25; p. 53 - 54, Russian.

Okodlov Yu.B., 1988 b. To plankton flora of the East Siberian Sea. News in the systematic of primary plants, 25; 53 - 54, Russian.

Pavlidis, Yu. A., 1982. Sedimentological conditions in the Chukchi Sea and facies - sedimentological zones on the shelf. In: The problems of geomorphology and lithodynamics of the shelf. Editors: Aksyonov A.A..

Polyakova Ye. I., 1989 Diatoms in Arctic shallow seas of the USSR and their importance for stratigraphy of bottom sediments. Okeanologya, 25, No. 5., p. 789 - 793, Russian

Polyakova Ye.I., 1989. Diatoms in Arctic shallow seas sediments. In: Climatology, Oceanology and Biology. Editors: Herman Y.. New York, Van Nostrand Reinhold Company, p. 481 - 496.

Proshkina - Lavrenko A.I., 1974. Diatoms of the recent seas and lakes. In: Diatoms of the USSR. Fossil and recent. Editors: Glezer Z.I., Jouse A.P., Makarova L.V. et al.. Leningrad, Nauka; ; p. 274 - 351, Russian

Ryzhov V.M., 1988. Ecology and geography of the Barents Sea phytoplankton. Author's abstract of Cand. Thesis, Moscov, 20 pp., Russian

Ryzhov V.M., Rusanov V.P., and Latishev V.S., 1984. Chemical - biological indication of the Chukchi Sea water masses. Proc. Arctic and Antarctic Res. Inst., Vol. 368, p. 26 - 40, Russian.

Rouhijajnen M.I., 1960. The character of phytoplankton development in May - June 1958 at the southern parts of the Barents Sea. Trudy Murmansk Biol. Stat. Vol. 4, No. 8, p. 11 - 18, Russian.

Usachev P.I., 1938. Biological analysis of the ice. Doklaady Akademii Nauk USSR, Vol. 19, No. 8, p. 643 - 646, Russian.

Usachev P.I., 1949. Microflora of polar ice. Trudy Inst. Oceanol. USSR, Vol. 3, p. 216 - 259, Russian.